

Rapp

328 pg's
MSC-PA-R-68-15



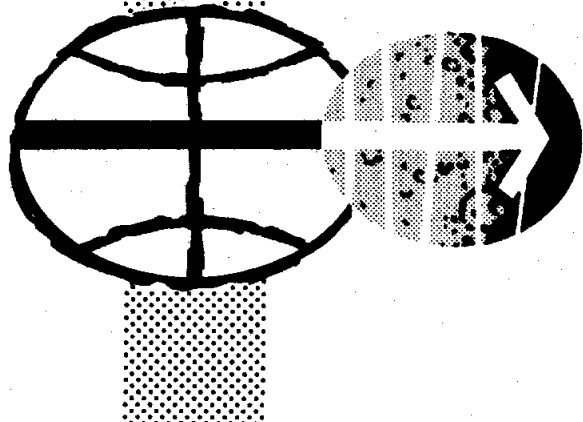
NATIONAL AERONAUTICS AND SPACE ADMINISTRATION

MSC-PA-R-68-15

Apollo 7 Mission Report

DISTRIBUTION AND REFERENCING

This paper is not suitable for general distribution or referencing. It may be referenced only in other working correspondence and documents by participating organizations.



MANNED SPACECRAFT CENTER
HOUSTON, TEXAS
DECEMBER 1968

APOLLO SPACECRAFT FLIGHT HISTORY

<u>Mission</u>	<u>Spacecraft</u>	<u>Description</u>	<u>Launch date</u>	<u>Launch site</u>
PA-1	BP-6	First pad abort	Nov. 7, 1963	White Sands Missile Range, N. Mex.
A-001	BP-12	Transonic abort	May 13, 1964	White Sands Missile Range, N. Mex.
AS-101	BP-13	Nominal launch and exit environment	May 28, 1964	Cape Kennedy, Fla.
AS-102	BP-15	Nominal launch and exit environment	Sept. 18, 1964	Cape Kennedy, Fla.
A-002	BP-23	Maximum dynamic pressure abort	Dec. 8, 1964	White Sands Missile Range, N. Mex.
AS-103	BP-16	Micrometeoroid experiment	Feb. 16, 1965	Cape Kennedy, Fla.
A-003	BP-22	Low-altitude abort (planned high- altitude abort)	May 19, 1965	White Sands Missile Range, N. Mex.
AS-104	BP-26	Micrometeoroid experiment and service module RCS launch environment	May 25, 1965	Cape Kennedy, Fla.
PA-2	BP-23A	Second pad abort	June 29, 1965	White Sands Missile Range, N. Mex.
AS-105	BP-9A	Micrometeoroid experiment and service module RCS launch environment	July 30, 1965	Cape Kennedy, Fla.
A-004	SC-002	Power-on tumbling boundary abort	Jan. 20, 1966	White Sands Missile Range, N. Mex.
AS-201	SC-009	Supercircular entry with high heat rate	Feb. 26, 1966	Cape Kennedy, Fla.
AS-202	SC-011	Supercircular entry with high heat load	Aug. 25, 1966	Cape Kennedy, Fla.

(Continued inside back cover)

APOLLO 7 MISSION REPORT

PREPARED BY

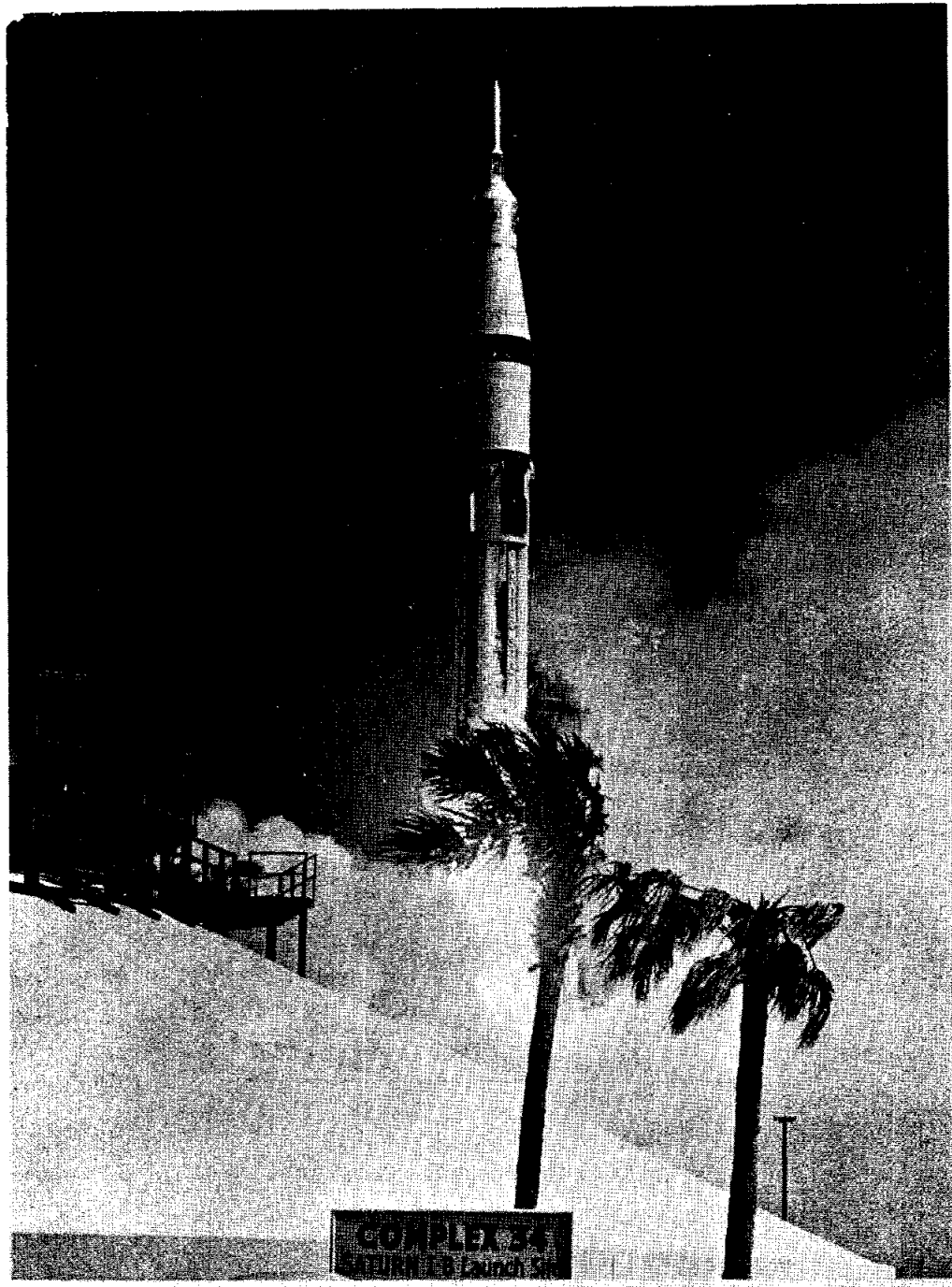
Apollo 7 Mission Evaluation Team

APPROVED BY

George M. Low

George M. Low
Manager
Apollo Spacecraft Program

NATIONAL AERONAUTICS AND SPACE ADMINISTRATION
MANNED SPACECRAFT CENTER
HOUSTON, TEXAS
December 1968



Apollo 7 lift-off.

CONTENTS

Section	Page
1.0 <u>SUMMARY</u>	1-1
2.0 <u>MISSION DESCRIPTION</u>	2-1
3.0 <u>TRAJECTORY</u>	3-1
3.1 LAUNCH	3-1
3.2 EARTH ORBIT	3-2
3.2.1 Rendezvous Maneuvers	3-2
3.2.2 Service Propulsion Maneuvers	3-3
3.3 ENTRY	3-5
3.4 S-IVB AND SERVICE MODULE ENTRY	3-5
4.0 <u>LAUNCH VEHICLE PERFORMANCE SUMMARY</u>	4-1
5.0 <u>COMMAND AND SERVICE MODULE PERFORMANCE</u>	5-1
5.1 STRUCTURES	5-1
5.1.1 Structural Loads Analysis	5-1
5.1.2 Vibration	5-2
5.2 AERODYNAMICS	5-16
5.3 THERMAL CONTROL	5-20
5.4 THERMAL PROTECTION	5-24
5.5 EARTH LANDING	5-37
5.6 MECHANICAL SYSTEMS	5-37
5.7 ELECTRICAL POWER DISTRIBUTION	5-38

Section	Page
5.8 FUEL CELLS AND BATTERIES	5-39
5.8.1 Fuel Cells	5-39
5.8.2 Batteries	5-40
5.9 CRYOGENICS	5-55
5.10 SEQUENTIAL	5-64
5.11 PYROTECHNIC DEVICES	5-64
5.12 LAUNCH ESCAPE	5-64
5.13 EMERGENCY DETECTION	5-64
5.14 COMMUNICATIONS	5-64
5.14.1 Command and Service Module Equipment	5-65
5.14.2 Command and Service Module/Manned Space Flight Network	5-66
5.14.3 Spacecraft/Apollo Range Instrumentation Aircraft	5-68
5.15 INSTRUMENTATION	5-89
5.15.1 Operational Instrumentation	5-89
5.15.2 Flight Qualification Instrumentation	5-89
5.16 GUIDANCE, NAVIGATION, AND CONTROL SYSTEMS . . .	5-92
5.16.1 Mission Related Performance	5-93
5.16.2 Guidance and Navigation System Performance	5-101
5.16.3 Stabilization and Control System Performance	5-103
5.16.4 Entry Monitor System	5-103

Section	Page
5.17 REACTION CONTROL SYSTEMS	5-149
5.17.1 Service Module Reaction Control System	5-149
5.17.2 Command Module Reaction Control System	5-150
5.18 SERVICE PROPULSION	5-158
5.18.1 Engine Performance	5-158
5.18.2 Propellant Utilization and Gaging System	5-159
5.18.3 Propellant Thermal Control	5-159
5.19 CREW SYSTEMS	5-168
5.19.1 Pressure Suit and Cabin Circuits . . .	5-168
5.19.2 Oxygen Distribution Circuit	5-169
5.19.3 Thermal Control System	5-170
5.19.4 Water Management	5-171
5.19.5 Waste Management	5-172
5.19.6 Postlanding Ventilation	5-173
5.20 CREW STATION	5-183
5.20.1 Crew Provisions	5-183
5.20.2 Displays and Controls	5-185
5.20.3 Windows	5-185
5.20.4 Lighting	5-185
5.20.5 Equipment Stowage	5-186
5.20.6 Intravehicular Activity	5-186

Section	Page
5.21 CONSUMABLES	5-186
5.21.1 Service Propulsion System Propellants	5-186
5.21.2 Reaction Control System Propellants	5-187
5.21.3 Cryogenics	5-188
5.21.4 Water	5-189
6.0 <u>FLIGHT CREW</u>	6-1
6.1 FLIGHT CREW PERFORMANCE	6-1
6.1.1 Training	6-1
6.1.2 Flight Activities	6-1
6.1.3 Human Factors	6-4
6.1.4 Operational Equipment Evaluation . . .	6-4
6.2 FLIGHT CREW REPORT	6-21
6.2.1 Mission Description	6-21
6.2.2 Systems Operation	6-23
7.0 <u>BIOMEDICAL EVALUATION</u>	7-1
7.1 INFILIGHT	7-1
7.1.1 Bioinstrumentation Performance	7-1
7.1.2 Physiological Data	7-2
7.1.3 Medical Observations	7-3
7.1.4 Oxygen Enrichment Procedure	7-6
7.2 PHYSICAL EXAMINATIONS	7-6

Section	Page
8.0 <u>MISSION SUPPORT PERFORMANCE</u>	8-1
8.1 FLIGHT CONTROL	8-1
8.1.1 Prelaunch Operations	8-1
8.1.2 Powered Flight	8-1
8.1.3 Orbital	8-2
8.1.4 Entry Phase	8-9
8.2 NETWORK	8-10
8.3 RECOVERY OPERATIONS	8-11
8.3.1 Landing Areas and Recovery Force Deployment	8-11
8.3.2 Command Module Location and Retrieval	8-11
8.3.3 Direction Finding Equipment	8-13
8.3.4 Command Module Postrecovery Inspection	8-14
8.3.5 Command Module Deactivation	8-15
9.0 <u>EXPERIMENTS</u>	9-1
9.1 EXPERIMENT S005 — SYNOPTIC TERRAIN PHOTOGRAPHY	9-2
9.2 EXPERIMENT S006 — SYNOPTIC WEATHER PHOTOGRAPHY	9-11
10.0 <u>ASSESSMENT OF MISSION OBJECTIVES</u>	10-1
10.1 GUIDANCE AND NAVIGATION ATTITUDE CONTROL (P1.12)	10-1
10.2 MIDCOURSE NAVIGATION (P1.15)	10-2

Section	Page
10.3 STABILIZATION AND CONTROL ATTITUDE DRIFT CHECKS (P2.7)	10-2
10.4 SEXTANT/HORIZON SIGHTINGS	10-3
11.0 <u>ANOMALY SUMMARY</u>	11-1
11.1 LOSS OF S-BAND SUBCARRIERS	11-1
11.2 BIOMEDICAL INSTRUMENTATION	11-2
11.3 WATER GUN TRIGGER STICKING	11-2
11.4 SHIFT ON FLIGHT DIRECTOR ATTITUDE INDICATOR . . .	11-3
11.5 MOMENTARY FAILURE OF ROTATION HAND CONTROLLER	11-3
11.6 ENTRY MONITOR SYSTEM MALFUNCTIONS	11-4
11.7 ADAPTER PANEL DEPLOYMENT	11-5
11.8 COMMAND MODULE WINDOW FOGGING	11-6
11.9 FLIGHT QUALIFICATION COMMUTATOR FAILURE	11-6
11.10 WATER NEAR WASTE WATER DISCONNECT	11-7
11.11 MOMENTARY LOSS OF AC BUSES	11-7
11.12 BATTERY CHARGING	11-8
11.13 UNDERTHRESHOLD INDICATION ON DC BUSES A AND B . .	11-8
11.14 FUEL CELL EXIT TEMPERATURE INCREASE	11-9
11.15 INADVERTENT PROPELLANT ISOLATION VALVE SWITCHING	11-9
11.16 VOICE COMMUNICATIONS DURING LAUNCH PHASE	11-10
11.17 ERRATIC OPERATION OF WATER EVAPORATOR	11-11
11.18 CONDENSATION IN CABIN	11-11

Section	Page
11.19 FOOD	11-11
11.20 BATTERY MANIFOLD LEAK	11-12
11.21 FAILED FLOODLIGHTS	11-12
11.22 CRACKED GLASS ON MISSION EVENT TIMER	11-12
11.23 WATER IN DOCKING TUNNEL	11-13
11.24 VHF RECOVERY BEACON OPERATION	11-13
11.25 APPARENT FREE WATER IN SUIT SUPPLY HOSE	11-13
11.26 ELECTROMAGNETIC INTERFERENCE PROBLEMS	11-14
12.0 CONCLUSIONS	12-1

APPENDIX A

<u>SPACE VEHICLE DESCRIPTION</u>	A-1
A.1 COMMAND AND SERVICE MODULES	A.3
A.1.1 Structures	A-3
A.1.2 Emergency Detecting System	A-4
A.1.3 Sequential Events Control System	A-4
A.1.4 Communications System	A-5
A.1.5 Environmental Control System	A-6
A.1.6 Guidance and Control System	A-7
A.1.7 Electrical Power System	A-9
A.1.8 Service Propulsion System	A-11
A.1.9 Reaction Control Systems	A-11
A.1.10 Instrumentation System	A-12

Section		Page
A.1.11	Pyrotechnics	A-14
A.1.12	Crew Provisions	A-15
A.1.13	Recovery System	A-17
A.2	LAUNCH ESCAPE SYSTEM	A-41
A.3	SPACECRAFT/LAUNCH-VEHICLE ADAPTER	A-43
A.4	LAUNCH VEHICLE	A-44
A.4.1	S-IB Stage	A-44
A.4.2	S-IVB Stage	A-44
A.4.3	Instrument Unit	A-45
A.5	MASS PROPERTIES	A-46
<u>APPENDIX B</u>		
<u>SPACECRAFT HISTORY</u>		B-1
<u>APPENDIX C</u>		
<u>POSTFLIGHT TESTING</u>		C-1
<u>APPENDIX D</u>		
<u>DATA AVAILABILITY</u>		D-1

TABLES

Table		Page
2-I	SEQUENCE OF EVENTS	2-3
2-II	ORBITAL ELEMENTS BEFORE AND AFTER MANEUVERS . . .	2-5
3-I	DEFINITION OF TRAJECTORY AND ORBITAL PARAMETERS	3-7
3-II	TRAJECTORY PARAMETERS FOR LAUNCH AND PARKING ORBIT	3-8
3-III	TRAJECTORY PARAMETERS FOR MANEUVERS	3-11
3-IV	RENDEZVOUS MANEUVERS	3-18
3-V	SERVICE PROPULSION MANEUVERS	3-19
3-VI	TRAJECTORY PARAMETERS FOR ENTRY	3-20
5.1-I	MAXIMUM SPACECRAFT LOADS AT LIFT-OFF	5-4
5.1-II	SPACECRAFT LOADS AT MAXIMUM $q\alpha$	5-4
5.1-III	MAXIMUM SPACECRAFT LOADS AT END OF FIRST STAGE BOOST	5-4
5.14-I	COMMUNICATION SYSTEM PERFORMANCE DURING EARTH ORBIT PHASE	5-69
5.16-I	SUMMARY OF INERTIAL MEASUREMENT UNIT ALIGNMENTS	5-104
5.16-II	RENDEZVOUS SOLUTION COMPUTATIONS	5-106
5.16-III	TERMINAL PHASE INITIATION	5-107
5.16-IV	TERMINAL PHASE BRAKING	5-108
5.16-V	CONTROL MODE USAGE	5-109
5.16-VI	GUIDANCE AND CONTROL MANEUVER SUMMARY	5-110

Table		Page
5.16-VII	ENTRY NAVIGATION AND GUIDANCE RECONSTRUCTION	5-111
5.16-IX	INERTIAL COMPONENT PREFLIGHT HISTORY	5-112
5.16-X	INERTIAL SUBSYSTEM ERRORS USED IN FIT OF BOOST VELOCITY ERRORS	5-113
5.16-XI	COMPUTER PROGRAMS USED	5-114
5.17-I	SECONDARY TANK SWITCHOVER	5-152
5.18-I	STEADY-STATE PERFORMANCE	5-161
5.18-II	STEADY-STATE PRESSURES	5-162
5.18-III	SHUTDOWN TRANSIENT SUMMARY	5-163
5.18-IV	MINIMUM IMPULSE FIRINGS	5-164
5.19-I	WATER CHLORINATION	5-174
7-I	SUMMARY OF BIOMEDICAL INSTRUMENTATION PROBLEMS	7-7
7-II	DESCRIPTIVE STATISTICS OF HEART RATES	7-8
7-III	DESCRIPTIVE STATISTICS OF RESPIRATION RATES	7-8
7-IV	CIRCADIAN VARIATION IN HEART RATES	7-9
8.3-I	RECOVERY SUPPORT	8-16
9.2-I	EXPERIMENT S006 PHOTOGRAPHY	9-13
10-I	DETAILED TEST OBJECTIVES	10-4
A.1-I	EQUIPMENT LIST	A-19
A.5-I	SPACECRAFT MASS PROPERTIES	A-47
C-I	POSTFLIGHT TESTING SUMMARY	C-2
D-I	DATA AVAILABILITY	D-2

FIGURES

Figure		Page
3-1	Ground track	
	(a) Rendezvous	3-21
	(b) Entry	3-22
3-2	Trajectory parameters during the launch phase	
	(a) Latitude, longitude, and altitude	3-23
	(b) Space-fixed flight-path angle and velocity	3-24
	(c) Earth-fixed flight-path angle and velocity	3-25
	(d) Mach number and dynamic pressure	3-26
3-3	Relative motion of command and service module in S-IVB curvilinear system	
	(a) Corrective combination maneuver to rendezvous	3-27
	(b) Coelliptic maneuver to rendezvous, expanded	3-28
3-4	Apogee and perigee altitudes	3-29
3-5	Trajectory parameters during the entry phase	
	(a) Geodetic latitude, longitude, and altitude	3-30
	(b) Space-fixed velocity and flight-path angle	3-31
	(c) Earth-fixed flight-path angle and velocity	3-32
	(d) Load factor	3-33
3-6	Command module and service module entry trajectories	
	(a) Space-fixed velocity	3-34
	(b) Altitude	3-34

Figure		Page
3-7	Command module and service module separation range and velocity	
	(a) Relative velocity	3-35
	(b) Relative range	3-35
5.1-1	Speed and direction of peak ground winds at 60-foot level at lift-off	5-5
5.1-2	Command module acceleration at lift-off	5-6
5.1-3	Scalar winds at lift-off	
	(a) Velocity	5-7
	(b) Direction	5-7
5.1-4	Command module accelerations at S-IB cutoff and staging	5-8
5.1-5	Service module helium pressurization panel tangential vibration at lift-off (-1 to +1 second)	5-9
5.1-6	Service module helium pressurization panel, X-axis vibration	
	(a) Lift-off (-1 to +1 second)	5-10
	(b) Transonic (58 to 60 seconds)	5-11
	(c) Maximum dynamic pressure (77 to 79 seconds)	5-12
5.1-7	Service module forward bulkhead vibration at lift-off (-1 to +1 second)	5-13
5.1-8	Helium pressurization panel instrumentation . . .	5-14
5.1-9	Helium pressurization panel vibration at lift-off (typical for launch phase)	5-15
5.2-1	Command module hypersonic entry aerodynamics . . .	5-18
5.2-2	Aerodynamic torquing effects	5-19
5.3-1	Temperatures on service module reaction control system helium tanks and service propulsion propellant tanks	5-21

Figure		Page
5.3-2	Temperature of service module reaction control system helium tank and primary fuel and oxidizer tank outlets	5-22
5.3-3	Temperatures of command module reaction control system helium tanks and service propulsion propellant tanks and feedlines	5-23
5.4-1	Char condition of aft heat shield	5-25
5.4-2	Aft heat shield temperatures	
	(a) Distance from center = 69.4 in.; angle from +Y = 91 deg	5-26
	(b) Distance from center = 0 in.; angle from +Y = 2.2 deg	5-27
	(c) Distance from center = 50 in.; angle from +Y = 268 deg	5-28
	(d) Distance from center = 63 in.; angle from +Y = 101 deg	5-29
	(e) Distance from center = 75 in.; angle from +Y = 268 deg	5-30
5.4.3	Maximum temperatures measured in depth and comparison of char with 1000° F isotherm	5-31
5.4-4	Crew compartment heat shield temperature	
	(a) Distance along +X axis = 27 in.; angle from +Y axis = 89 deg	5-32
	(b) Distance along +X axis = 85 in.; angle from +Y axis = 85 deg	5-33
	(c) Distance along +X axis = 78 in.; angle from +Y axis = 176 deg	5-34
	(d) Distance along +X axis = 78 in.; angle from +Y axis = 268 deg	5-35
5.4-5	Temperature on forward hatch	5-36
5.8-1	Performance of three fuel cell systems	5-43
5.8-2	Voltage degradation for 18-ampere loads	5-44

Figure		Page
5.8-3	Thermal performance of fuel cells	
(a)	Fuel cell 1	5-45
(b)	Fuel cell 2	5-46
(c)	Fuel cell 3	5-47
5.8-4	Response to second fuel cell oxygen purge	5-48
5.8-5	Reactant flow rates	5-49
5.8-6	Voltage timeline	5-50
5.8-7	Entry battery performance following deorbit maneuvers	5-51
5.8-8	Entry battery charging characteristics	5-52
5.8-9	Battery charger characteristic	5-53
5.8-10	Battery capacity remaining	5-54
5.9-1	Cryogenic system heat leak	5-57
5.9-2	Typical hydrogen tank pressure history with automatic fan and heater cycles	5-58
5.9-3	Typical oxygen pressure history with automatic heater cycles	5-59
5.9-4	Hydrogen stratification tests	5-60
5.9-5	Oxygen stratification tests	5-61
5.9-6	Hydrogen quantity profile	5-62
5.9-7	Oxygen quantity profile	5-63
5.14-1	Received S-band carrier power and telemetry performance, Merritt Island, launch	5-73
5.14-2	Received S-band carrier power and telemetry performance, Grand Bahama, launch	5-74
5.14-3	Received S-band carrier power and telemetry performance, Bermuda, launch	5-75

Figure		Page
5.14-4	Received S-band carrier power and telemetry performance, USNS Vanguard, revolution 1	5-76
5.14-5	Received S-band carrier power, Canary Island, revolution 1	5-77
5.14-6	Launch-phase voice communications	5-78
5.14-7	Received VHF/AM signal power, launch phase	5-79
5.14-8	Received S-band carrier power and telemetry performance, Carnarvon, revolution 17	5-80
5.14-9	Received S-band carrier power and telemetry performance, Carnarvon, revolution 18	5-81
5.14-10	Received S-band carrier power and telemetry performance, Texas, revolution 33	5-82
5.14-11	Received S-band carrier power and telemetry performance, Carnarvon, revolution 46	5-83
5.14-12	Received S-band carrier power and telemetry performance, Carnarvon, revolution 48	5-84
5.14-13	S-band total received power (FM) and television photographs, Merritt Island, revolution 60/61	5-85
5.14-14	Received S-band carrier power and telemetry performance, Merritt Island, revolution 104/105	5-86
5.14-15	Received S-band carrier power and telemetry performance, Antigua, revolution 151	5-87
5.14-16	Received S-band carrier power and telemetry performance, Hawaii, revolution 163	5-88
5.16-1	Attitude error displayed during launch phase . . .	5-115
5.16-2	Gimbal angle comparison during launch phase, instrument unit minus command module computer	5-116

Figure		Page
5.16-3	Spacecraft dynamics during spacecraft/S-IVB separation	5-117
5.16-4	Sextant star count geometry	5-118
5.16-5	Digital autopilot automatic maneuver (typical) . .	5-119
5.16-6	Spacecraft dynamics during Y-axis accelerometer test	5-120
5.16-7	Spacecraft dynamics during first service propulsion maneuver	5-121
5.16-8	Spacecraft dynamics during second service propulsion maneuver	5-122
5.16-9	Spacecraft dynamics during third service propulsion maneuver	5-123
5.16-10	Spacecraft dynamics during fourth service propulsion maneuver	5-124
5.16-11	Spacecraft dynamics during fifth service propulsion maneuver	5-125
5.16-12	Spacecraft dynamics during sixth service propulsion maneuver	5-126
5.16-13	Spacecraft dynamics during seventh service propulsion maneuver	5-127
5.16-14	Spacecraft dynamics during eighth service propulsion maneuver (deorbit)	5-128
5.16-15	Velocity to be gained during first service propulsion maneuver	5-129
5.16-16	Velocity to be gained during second service propulsion maneuver	5-130
5.16-17	Velocity to be gained during third service propulsion maneuver	5-131
5.16-18	Velocity to be gained during fourth service propulsion maneuver	5-132

Figure	Page
5.16-19 Velocity to be gained during fifth service propulsion maneuver	5-133
5.16-20 Velocity to be gained during sixth service propulsion maneuver	5-134
5.16-21 Velocity to be gained during seventh service propulsion maneuver	5-135
5.16-22 Velocity to be gained during eighth service propulsion maneuver	5-136
5.16-23 Attitude errors during fifth service propulsion maneuver	5-137
5.16-24 Gimbal angles during roll passive thermal control test	5-138
5.16-25 Gimbal angles during pitch passive thermal control test	5-139
5.16-26 Spacecraft dynamics during entry	
(a) 259:43:30 to 259:45:45	5-140
(b) 259:45:45 to 259:56:00	5-141
(c) 259:56:00 to 260:02:15	5-142
(d) 259:02:15 to 260:08:30	5-143
5.16-27 Entry sequence attitude and range	5-144
5.16-28 Roll command plotted against actual roll	5-145
5.16-29 Landing point data	5-146
5.16-30 Velocity comparison during launch phase, command module computer minus launch vehicle instrument unit	5-147
5.16-31 Scroll from entry monitor system	5-148
5.17-1 Total propellant expended from service module reaction control system	5-153

Figure		Page
5.17-2	Propellant consumed from quads	
(a)	Quads A and B	5-154
(b)	Quads C and D	5-155
5.17-3	Propellant expended from command module reaction control system	
(a)	System A	5-156
(b)	System B	5-157
5.18-1	Chamber pressure during fifth service propulsion maneuver	5-165
5.18-2	Start and shutdown transients for fifth service propulsion maneuver	5-166
5.18-3	Chamber pressure during minimum impulse firings	
(a)	Fourth maneuver	5-167
(b)	Sixth maneuver	5-167
5.19-1	Cabin and suit pressures and oxygen flow during launch phase	5-175
5.19-2	Oxygen content of total cabin pressure	5-176
5.19-3	Cabin pressure and temperature during entry . . .	5-177
5.19-4	Partial pressure of carbon dioxide	5-178
5.19-5	Relative humidity survey	5-179
5.19-6	Primary evaporator operation during launch	5-180
5.19-7	Coolant loop operation during entry	5-181
6.1-1	Summary flight plan	
(a)	0 to 10 hours	6-6
(b)	10 to 30 hours	6-7
(c)	30 to 50 hours	6-8
(d)	50 to 70 hours	6-9
(e)	70 to 90 hours	6-10
(f)	90 to 110 hours	6-11

Figure		Page
(g)	110 to 130 hours	6-12
(h)	130 to 150 hours	6-13
(i)	150 to 170 hours	6-14
(j)	170 to 190 hours	6-15
(k)	190 to 210 hours	6-16
(l)	210 to 230 hours	6-17
(m)	230 to 250 hours	6-18
(n)	250 to 262 hours	6-19
7-1	Crew rest cycles	7-10
7-2	Oxygen enrichment sequence for 24 hours	7-11
7-3	Oxygen enrichment sequence for 7 days	7-12
8.3-1	Launch abort areas and recovery force deployment . .	8-18
8.3-2	Recovery zones, aircraft staging bases, and recovery force deployment	8-19
8.3-3	Predicted entry trajectory and recovery force deployment	8-20
8.3-4	Command module in flotation collar	8-21
8.3-5	Command module aboard recovery ship	8-22
9.1-1	Mexico, Gulf of California, central Baja California, mainland north of Guaymas	9-5
9.1-2	Iran, Persian Gulf coast	9-6
9.1-3	Brazil, Uruguay, Atlantic coast, Lajoa dos Patos, Lagoa Mirim	9-7
9.1-4	United Arab Republic, Gilf Kebir Plateau	9-8
9.1-5	Mexico, Bahia de Petacalco, Balsas River	9-9
9.1-6	Sinai Peninsula, Gulf of Suez, Gulf of Aqaba	9-10
9.2-1	Hurricane Gladys, centered off the West Coast of Florida, at 1531 G.m.t. on October 17, 1968 . . .	9-14
9.2-2	Hurricane Gladys photographed from ESSA-7 (meteorological satellite) on October 17, 1968 . .	9-15

Figure	Page
9.2-3 Eye of typhoon Gloria (western Pacific Ocean) taken at 0026 G.m.t. on October 20, 1968	9-16
9.2-4 Typhooon Gloria photographed from ESSA-7 at 0505 G.m.t. on October 20, 1968	9-17
9.2-5 Northerly view of Oahu in the Hawaiian Islands taken at 0001 G.m.t. on October 15, 1968	9-18
9.2-6 Supiori and Biak Islands in Indonesia are surrounded by the sun's reflection on October 22, 1968, 0219 G.m.t.	9-19
A.0-1 Apollo 7 space vehicle	A-2
A.1-1 Spacecraft 101 configuration	A-20
A.1-2 Inner structure	A-21
A.1-3 Command module heat shields	A-22
A.1-4 Service module	A-23
A.1-5 Emergency detection system	A-24
A.1-6 Sequential event control system	A-25
A.1-7 Communications	A-26
A.1-8 Environmental control	A-27
A.1-9 Guidance and navigation	A-28
A.1-10 Stabilization and control system	A-29
A.1-11 Electrical power system	
(a) dc	A-30
(b) ac	A-31
A.1-12 Cryogenic oxygen storage system	A-32
A.1-13 Fuel cell schematic	A-33
A.1-14 Control for service propulsion propellants	A-34

Figure	Page
A.1-15 Flow of service propulsion propellants	A-35
A.1-16 Service module reaction control system	A-36
A.1-17 Command module reaction control system	A-37
A.1-18 Instrumentation	A-38
(a) Operational	A-38
(b) Flight qualification	A-39
A.1-19 Uprighting system	A-40
A.2-1 Launch escape system	A-42
B-1 Command and service module checkout at contractor facility	B-2
B-2 Spacecraft checkout history at Kennedy Space Center	B-3

1.0 SUMMARY

The Apollo 7 space vehicle was launched from Cape Kennedy, Florida, at 11:02:45 a.m. e.d.t. on October 11, 1968. After a nominal boost phase, the spacecraft and S-IVB combination was inserted into an orbit of 123 by 153 nautical miles. Prior to separation of the command and service module from the S-IVB, the crew manually controlled the spacecraft/S-IVB combination. After separation, a transposition and simulated docking exercise was completed. Phasing maneuvers were later executed in preparation for a successful rendezvous with the S-IVB. During the 10.8-day flight, eight planned maneuvers using the service propulsion system were completed, and all major mission objectives were satisfied.

Almost without exception, spacecraft systems operated as intended. All temperatures varied within acceptable limits and essentially exhibited predicted behavior. Consumable usage was always maintained at safe levels and permitted introduction of additional flight activities toward the end of the mission. Communications quality was generally good, and live television was transmitted to ground stations on seven occasions. A test of the rendezvous radar transponder was completed in support of later flights with the lunar module. Manual control of the spacecraft by the crew was good. Even though somewhat hampered by head colds and upper respiratory congestion, the crew satisfactorily performed all flight-plan functions and completed the photographic experiments.

A normal deorbit, entry, and landing sequence was completed, with all parachutes operating properly. The vehicle landed at 260:09:03 in the Atlantic Ocean southeast of Bermuda. The crew was retrieved by helicopter, and the spacecraft and crew were taken aboard the prime recovery ship, *USS Essex*.

2.0 MISSION DESCRIPTION

The Apollo 7 mission followed the planned mission in almost all respects. The spacecraft was launched at 11:02:45 a.m. e.d.t. on October 11, 1968, from launch complex 34, Cape Kennedy, Florida. The launch phase was nominal, and the spacecraft was inserted into a 123- by 153-n. mi. orbit. Table 2-1 contains a sequence of events for the launch phase.

The crew performed a manual takeover of the S-IVB attitude control during the second revolution, and the control system responded properly. The spacecraft separated from the S-IVB at 02:55:02, followed by spacecraft transposition, simulated docking, and station-keeping with the S-IVB.

At 03:20:10, a phasing maneuver was performed with the service module reaction control system to establish the conditions required for the rendezvous scheduled for approximately 1 day later. The maneuver was targeted to place the spacecraft approximately 75 n. mi. ahead of the S-IVB at 26:25:00. During the next 6 revolutions, however, the orbit of the S-IVB decayed more rapidly than anticipated, and a second phasing maneuver was performed to obtain the desired initial conditions. Table 2-II lists the orbital elements prior to and after each maneuver.

The first service propulsion maneuver was a corrective combination maneuver for the rendezvous and was targeted to achieve the proper phase and height offset so that the second maneuver would result in an orbit coelliptic with that of the S-IVB. The two maneuvers resulted in terminal-phase-initiation conditions very close to those planned.

The terminal-phase-initiation maneuver, performed at 29:16:45, used an onboard computer solution based on sextant tracking of the S-IVB. A small midcourse correction was made, followed by braking and final closure to within 70 feet of the S-IVB at approximately 30 hours. Station-keeping was performed for about 20 minutes. Final separation consisted of a 2 ft/sec posigrade maneuver with the reaction control system.

The 24-hour period following separation was devoted to a sextant calibration test, a rendezvous navigation test, an attitude control test, and a primary evaporator test. The crew used the sextant to visually track the S-IVB to distances of 320 n. mi.

The third service propulsion maneuver, which used the stabilization and control system, was performed at 75:48:00 and lasted 9.1 seconds. The maneuver was performed earlier than planned in order to increase the backup deorbit capability of the service-module reaction control system and resulted in moving the orbital perigee to a lower altitude over the northern hemisphere.

The test of the rendezvous radar transponder was performed later than planned, during revolution 48, and lock-on with a radar at White Sands Missile Range was accomplished at 76 hours 27 minutes at a range of 415 n. mi.

A test to determine whether the radiator in the environmental control system had degraded was successfully conducted during the period from 92-1/2 to 97 hours, and operation of the system was validated for lunar flight.

The fourth service propulsion maneuver was initiated at 120:43:00 for a duration of 0.5 second to evaluate the minimum-impulse capability of the service propulsion engine. The test was successfully performed and resulted in a velocity change of 12.9 ft/sec.

At approximately 161 hours, an increase was noted in the temperature at the condenser exit in fuel cell 2, and as a precautionary measure, this unit was taken off-line until just prior to the next service propulsion maneuver.

The fifth service-propulsion maneuver was conducted at 165:00:00. To assure verification of the propellant gaging system, the firing duration was increased from that originally planned. The 67.6-second maneuver produced the largest velocity change during the mission and incorporated a manual thrust-vector-control takeover approximately half-way through the maneuver. The maneuver was targeted to position the spacecraft for an optimum deorbit maneuver at the end of the planned orbital phase.

The sixth service propulsion maneuver was performed during the eighth day and was a second minimum-impulse maneuver. This firing lasted 0.5 second, as planned, and resulted in a velocity change of 15.4 ft/sec.

The seventh service propulsion maneuver was performed on the tenth day at 239:06:12 and lasted for 7.6 seconds. This maneuver was targeted to place the perigee at the proper longitude for eventual spacecraft recovery. Hydrogen stratification and optics degradation tests were also conducted during the tenth day.

The eleventh, and final, day of the mission was devoted primarily to preparation for the deorbit maneuver, which was performed at 259:39:16. The service module was jettisoned, and the entry was performed using both automatic and manual guidance modes.

The parachute system effected a soft landing at 260:09:03 in the Atlantic Ocean near the recovery ship, USS Essex. Upon landing, the spacecraft turned over to an apex-down flotation attitude, but was successfully returned to the normal flotation position by the inflatable bag uprigting system. The crew was retrieved by helicopter, and the spacecraft was later taken aboard the recovery ship.

TABLE 2-I.- SEQUENCE OF EVENTS

Event	Time, hr:min:sec	
	Planned ^a	Actual
Launch Phase		
Range zero (15:02:45 G.m.t.)		
Lift-off (15:02:45.36 G.m.t.)	00:00:00.2	00:00:00.4
Maximum dynamic pressure	00:01:15.6	00:01:18.5
S-IB inboard engine cutoff	00:02:20.3	00:02:20.7
S-IB outboard engine cutoff	00:02:23.3	00:02:24.3
S-IB/S-IVB separation	00:02:24.6	00:02:25.6
S-IVB engine ignition	00:02:26.0	00:02:27.0
Escape tower jettison	00:02:43.3	00:02:46.5
S-IVB engine cutoff	00:10:14.8	00:10:16.8
Orbital Phase		
Orbital insertion	00:10:24.8	00:10:26.8
S-IVB safing start	01:34:27.0	01:34:29.0
S-IVB safing terminate	01:46:28.0	01:46:30.0
S-IVB takeover	02:29:55	02:30:49.1
Spacecraft/S-IVB separation	02:54:55.2	02:55:02
First phasing maneuver start	03:20:00	03:20:09.9
First phasing maneuver cutoff	03:20:16.3	03:20:26.7
Second phasing maneuver start	15:52:00	15:52:00.9
Second phasing maneuver cutoff	15:52:18.5	15:52:18.5
First service propulsion ignition	26:24:55.2	26:24:55.7
First service propulsion cutoff	26:25:04.7	26:25:05.7
Second service propulsion ignition	28:00:56.0	28:00:56.5
Second service propulsion cutoff	28:01:03.8	28:01:04.3
Terminal phase initiate start	29:18:34.0	29:16:33

^aPlanned times for the launch phase are those calculated prior to the mission; planned times after orbital insertion are the last updated time prior to the event.

TABLE 2-I.- SEQUENCE OF EVENTS - Concluded

Event	Time, hr:min:sec	
	Planned ^a	Actual
Orbital Phase - Concluded		
Begin braking	29:43:34	29:43:55
End braking, begin station-keeping	29:53:34	29:55:43
Separation maneuver start	30:20:00	30:20:00
Separation maneuver cutoff	30:20:05.4	30:20:05.4
Third service propulsion ignition	75:47:58.6	75:48:00.3
Third service propulsion cutoff	75:48:07.8	75:48:09.3
Fourth service propulsion ignition	120:43:00	120:43:00.5
Fourth service propulsion cutoff	120:43:00.4	120:43:00.9
Fifth service propulsion ignition	165:00:00	165:00:00.5
Fifth service propulsion cutoff	165:01:05.9	165:01:07.6
Sixth service propulsion ignition	210:08:00	210:08:00.5
Sixth service propulsion cutoff	210:08:00.4	210:08:01.0
Seventh service propulsion ignition	239:06:11	239:06:12.0
Seventh service propulsion cutoff	239:06:18.8	239:06:19.7
Eighth service propulsion ignition	259:39:15.9	259:39:16.3
Eighth service propulsion cutoff	259:39:27.9	259:39:28.2
Entry Phase		
Command module/service module separation	259:43:33.8	259:43:33.8
Entry interface (400 000 feet)	259:53:26	259:53:27
Enter blackout	259:56:17	259:54:58
Leave blackout	259:59:14	259:59:46
Drogue deployment	260:03:17	260:03:23
Main parachute deployment	260:04:14	260:04:13
Landing	260:08:58	260:09:03

^aPlanned times for the launch phase are those calculated prior to the mission; planned times after orbital insertion are the last updated time prior to the event.

TABLE 2-II.- ORBITAL ELEMENTS BEFORE AND AFTER MANEUVERS

Maneuver	Condition	Before maneuver		After maneuver	
		Planned	Actual	Planned	Actual
Insertion	Apogee, n. mi.	--	--	151.5	153.7
	Perigee, n. mi.	--	--	123.0	123.3
	Period, min	--	--	89.66	89.70
	Inclination, deg	--	--	31.57	31.58
S-IVB venting	Apogee, n. mi.	15.15	153.7	166.8	167.5
	Perigee, n. mi.	123.0	123.3	123.2	123.4
	Period, min	89.66	89.70	89.95	89.96
	Inclination, deg	31.57	31.58	31.57	31.58
Spacecraft/S-IVB separation	Apogee, n. mi.	166.8	167.5	166.9	167.0
	Perigee, n. mi.	123.2	123.4	122.9	125.3
	Period, min	89.95	89.96	89.94	89.99
	Inclination, deg	31.57	31.58	31.64	31.61
First rendezvous phasing	Apogee, n. mi.	166.9	167.0	164.1	165.2
	Perigee, n. mi.	122.9	125.3	122.4	124.8
	Period, min	89.94	89.99	89.88	89.95
	Inclination, deg	31.64	31.61	31.62	31.62
Second rendezvous phasing	Apogee, n. mi.	164.0	165.1	164.4	164.7
	Perigee, n. mi.	122.0	124.7	120.2	120.8
	Period, min	89.87	89.95	89.84	89.86
	Inclination, deg	31.62	31.62	31.61	31.62
Corrective combination (first service propulsion)	Apogee, n. mi.	164.0	164.6	196.1	194.1
	Perigee, n. mi.	120.0	120.6	125.2	123.0
	Period, min	89.83	39.86	90.55	90.57
	Inclination, deg	31.62	31.62	31.62	31.62

TABLE 2-II.-- ORBITAL ELEMENTS BEFORE AND AFTER MANEUVERS - Continued

2
6

Maneuver	Condition	Before maneuver		After maneuver	
		Planned	Actual	Planned	Actual
Coelliptic (second service propulsion)	Apogee, n. mi.	196.1	194.1	153.4	153.6
	Perigee, n. mi.	125.2	123.0	113.9	113.9
	Period, min	90.55	90.57	89.52	89.52
	Inclination, deg	31.62	31.62	31.63	31.63
Terminal phase initiate	Apogee, n. mi.	153.4	153.6	153.9	154.1
	Perigee, n. mi.	113.9	113.9	121.7	121.6
	Period, min	89.52	89.52	89.68	89.68
	Inclination, deg	31.63	31.63	31.62	31.61
Terminal phase finalize (braking)	Apogee, n. mi.	153.9	154.1	160.9	161.0
	Perigee, n. mi.	121.7	121.6	121.8	122.1
	Period, min	89.68	89.68	89.81	89.82
	Inclination, deg	31.62	31.61	31.62	31.61
Separation	Apogee, n. mi.	160.9	161.0	161.7	161.0
	Perigee, n. mi.	121.8	122.1	122.0	122.2
	Period, min	89.81	89.82	89.83	89.82
	Inclination, deg	31.62	31.61	31.64	31.61
Third service propulsion	Apogee, n. mi.	159.5	159.4	160.1	159.7
	Perigee, n. mi.	121.5	121.3	90.3	89.5
	Period, min	89.76	89.77	89.19	89.17
	Inclination, deg	31.61	31.61	31.26	31.23
Fourth service propulsion	Apogee, n. mi.	150.7	149.4	156.3	156.7
	Perigee, n. mi.	88.9	87.5	90.1	89.1
	Period, min	88.99	88.94	89.12	89.11
	Inclination, deg	31.24	31.25	31.22	31.24

TABLE 2-II.- ORBITAL ELEMENTS BEFORE AND AFTER MANEUVERS - Concluded

Maneuver	Condition	Before maneuver		After maneuver	
		Planned	Actual	Planned	Actual
Fifth service propulsion	Apogee, n. mi.	147.3	146.5	240.6	244.2
	Perigee, n. mi.	89.1	87.1	89.8	89.1
	Period, min	88.93	88.88	90.72	90.77
	Inclination, deg	31.25	31.25	30.09	30.08
Sixth service propulsion	Apogee, n. mi.	232.1	234.8	236.0	234.6
	Perigee, n. mi.	90.1	88.5	90.2	88.4
	Period, min	90.58	90.59	90.64	90.58
	Inclination, deg	30.07	30.08	30.05	30.07
Seventh service propulsion	Apogee, n. mi.	230.4	228.3	230.3	229.8
	Perigee, n. mi.	90.2	88.4	90.0	88.5
	Period, min	90.53	90.24	90.52	90.48
	Inclination, deg	30.07	30.07	29.88	29.87
Eighth service propulsion	Apogee, n. mi.	227.8	225.3	--	--
	Perigee, n. mi.	90.0	88.2	--	--
	Period, min	90.48	90.39	Entry	Entry
	Inclination, deg	29.88	29.88	--	--

3.0 TRAJECTORY

The planned trajectory parameters for the phase from lift-off to spacecraft/S-IVB separation are based on preflight-calculated trajectories; after separation, the planned parameters are real-time predictions generated by the Real Time Computer Complex in the Mission Control Center. The actual trajectories are based on mission data from the Manned Space Flight Network. The Marshall Space Flight Center provided the trajectory data for the phase from lift-off to spacecraft/S-IVB separation; a detailed analysis of these data is presented in reference 1. The orbital trajectory analysis is based on the best-estimate trajectory generated 21 days after the end of the mission.

The earth model for all trajectory analysis contained geodetic and gravitational constants representing the Fischer ellipsoid. The state vectors for orbital events, based on analysis in section 3.2, are in the geographic coordinate system defined in table 3-I. The ground track of the rendezvous sequence and the locations of the tracking network sites are shown in figure 3-1.

3.1 LAUNCH

The launch-phase trajectory (fig. 3-2) was nominal during S-II stage flight. Planned and actual trajectory parameters agreed well, as shown in figure 3-2. The actual cutoff times for the inboard and outboard engines were within 1.0 second of the planned times. At outboard engine cutoff (table 3-II), the velocity, flight-path angle, and altitude were low by 11.2 ft/sec, 0.05 degree, and 99 feet, respectively.

The S-IVB stage trajectory parameters were also nominal (fig. 3-2). S-IVB cutoff was 2 seconds later than predicted; velocity and altitude were low by 1 ft/sec and 463 feet, respectively, and flight-path angle was high by 0.01 degree (table 3-II). At orbital insertion (S-IVB cutoff plus 10 seconds), the velocity, flight-path angle, and altitude were high by 4 ft/sec, 0.01 degree, and 568 feet, respectively. Trajectory conditions for the S-IVB stage liquid oxygen dump and for spacecraft/S-IVB separation are shown in table 3-II.

3.2 EARTH ORBIT

The trajectory for the command and service module was reconstructed from spacecraft/S-IVB separation to entry interface (400 000 feet) using low-speed S-band tracking data. Low-speed skin tracking data were also utilized when available. The quality of the S-band data was generally good. For a representative fit, the maximum value of the residuals was 5-Hz for doppler, 400 feet for range, and 0.08 degree for X and Y angles. More important, the comparison showed a difference in total position of less than 1500 feet and a difference in total velocity of less than 1.5 ft/sec. For off-range periods where propagation times beyond the fit interval were large, the differences in total position and total velocity were on the order of 3000 feet and 3.0 ft/sec, respectively. A few selected vectors from the Real Time Computer Complex were compared with the postflight vectors, and the comparison was satisfactory.

Approximately 80 passes of S-band data, representing all stations, contained anomalous data; this number was less than 10 percent of the total and did not compromise the trajectory reconstruction. In the fits where the amount of data and the corresponding data interval were large, drag was included in the solution vector, which substantially improved the fits, especially during the period of low perigee. Even though the skin tracking data were noisy, as expected, the quality was good, and the data were consistent with the S-band data.

3.2.1 Rendezvous Maneuvers

Conditions and parameters during the rendezvous sequence are presented in table 3-III. The lack of tracking information during the terminal-phase-initiate maneuver prevented obtaining any valid vector solutions at cutoff. Table 3-IV contains a comparison of rendezvous maneuver velocities, figure 3-1 presents a ground track of the revolutions during rendezvous, and figure 3-3 illustrates the relative motion between the command and service modules and the S-IVB.

At 3:20:09.9, the first phasing maneuver (table 3-IV) was performed with the reaction control system so that by 26:25:00, the spacecraft would lead the S-IVB by about 75 n. mi. The retrograde velocity change of 5.7 ft/sec placed the spacecraft in a 165 by 124.8 n. mi. orbit. After the first phasing maneuver, the S-IVB orbit decayed more rapidly than expected, and a second phasing maneuver was performed at 15:52:00.9. The resulting retrograde velocity change of 7 ft/sec was about 0.5 ft/sec greater than planned and caused the spacecraft to lead by about 84 n. mi. instead of by the intended 75 n. mi., although this had little effect on the ensuing targeting. The resultant orbit was 164.7 by 120.8 n. mi.

The first service propulsion maneuver, a corrective combination maneuver, was initiated at 26:24:55.7 and lasted for 9.5 seconds to achieve the 1.3-degree phasing and 8-n. mi. height offset required for the co-elliptic maneuver planned for 1 hour 36 minutes later. The maneuver was executed as planned, and the resultant ellipse was 194.1 by 123 n. mi.

The second service propulsion maneuver (table 3-IV, fig. 3-3) was initiated at 28:00:56 when the spacecraft was approximately 80 n. mi. behind and 7.8 n. mi. below the S-IVB stage. This 7.9-second firing was targeted to achieve a coelliptic orbit with the S-IVB, but minor dispersions in the actual orbit determination and in the maneuver execution caused the coellipticity to vary by about 1 n. mi. As a result, terminal phase initiation occurred about 4.5 minutes earlier than had been targeted but still well within the maximum of 12 minutes.

The terminal phase initiation maneuver (table 3-IV) was performed at 29:16:33, and was based on the onboard computer solution, using data from sextant tracking of the S-IVB. The 46-second maneuver, performed with the reaction control system, provided a velocity change of 17.7 ft/sec.

The first midcourse correction was performed at 39:30:42 and was based on the onboard solution and the backup chart. The reaction control system was used to achieve a velocity change of 2 ft/sec aft and 0.5 ft/sec up. A second midcourse correction was computed but was very small and consequently was not performed.

The braking phase (table 3-IV) was initiated at 29:43:55 with visual line-of-sight rate correction. At 7 minutes 51 seconds before theoretical intercept, braking was started at a range of 1.2 n. mi. Range-rate control was initiated at a range of 0.6 n. mi. as compared with the nominal of 0.5 n. mi. for this rendezvous. The total change in velocity during the braking phase was 49.1 ft/sec. Braking was completed at 29:55:43, and the spacecraft and S-IVB were in a 161.0 by 122.2 n. mi. orbit.

3.2.2 Service Propulsion Maneuvers

Six additional service propulsion maneuvers were performed after the two required for rendezvous. The conditions at ignition and cutoff for each of these maneuvers are shown in table 3-III, and the planned and actual velocity changes and maneuver times are compared in table 3-V. The velocity magnitudes were determined from platform accelerometer data and do not include velocity changes from the reaction control plus X translations prior to each maneuver. The differences between the planned and actual conditions for the first six maneuvers (table 3-V) resulted

from the unpredictable tail-off characteristics exhibited by the service propulsion engine. Figure 3-4 shows the resulting apogee and perigee altitudes for each maneuver.

To improve the backup deorbit capability of the service module reaction control system, the time of initiation for the third service propulsion maneuver was advanced approximately 16 hours from the original flight plan. The maneuver was targeted to lower the perigee point to 90 n. mi. and place it in the northern hemisphere. The in-plane velocity required to satisfy this orbit was not sufficient to produce a valid test of the stabilization and control system; therefore, 200 ft/sec in additional velocity was directed out-of-plane to the south during the maneuver. Ignition occurred at 75:48:00.3, and the orbit resulting from the 9-second firing was a 159.7 by 89.5 n. mi. ellipse.

The fourth service propulsion maneuver was a 0.5-second, minimum impulse, posigrade, in-plane maneuver which was initiated at 120:43:00.4 and resulted in a 156.7 by 89.1 n. mi. ellipse.

The fifth service propulsion maneuver was targeted for a desired end-of-mission ground track such that the deorbit maneuver (eighth service propulsion maneuver) would have at least 2 minutes of Hawaii tracking and such that if another revolution was required, the service module reaction control system could provide a deorbit capability from apogee to a landing at latitude 29 degrees north and longitude 60 degrees west. The required shift in the orbital plane was accomplished by a large out-of-plane velocity component in combination with an orbital-period adjustment. The 67-second maneuver was initiated at 165:00:00.5 and resulted in a change in velocity of 1691 ft/sec and an elliptical orbit of 244.2 by 89.1 n. mi. Because of a late cutoff, the velocity change was 49 ft/sec greater than planned, but the trajectory was not significantly perturbed.

The sixth service propulsion maneuver lasted 0.5 second, and was the second minimum-impulse firing. This maneuver was initiated at 210:08:00.5 and was directed out-of-plane because no change in the orbit was desired.

The seventh service propulsion maneuver was targeted to place the perigee for revolution 163 at longitude 45 degrees west to provide an optimal deorbit capability. The 8.2-second maneuver was initiated at 239:06:12.0 and succeeded in rotating the line of apsides approximately 30 degrees to the west. A 100 ft/sec velocity change, directed out-of-plane to the north, increased the firing time and provided a more valid test of the stabilization and control system. The orbit resulting from this maneuver was 229.8 by 88.5 n. mi.

The eighth service propulsion system maneuver was performed to deorbit the spacecraft. This 12.4-second maneuver was initiated at 259:39:16.3. As shown in table 3-III, the actual conditions agreed well with the planned conditions at cutoff.

3.3 ENTRY

The planned entry trajectory was based upon the state vector obtained by the Honeysuckle tracking site but with a nominal deorbit maneuver and integration to drogue deployment added. The planned trajectory differed from the actual because the lift vector was held at a 55-degree roll-right attitude 60 seconds longer than planned. The actual trajectory values shown in figure 3-5 were obtained from the best-estimate vector based on radar tracking after the deorbit maneuver and included corrections for known inertial measurement unit errors in the guidance and navigation platform accelerometer data. Table 3-VI presents the planned and actual conditions at entry interface. The onboard guidance system indicated a 1.0 n. mi. undershoot at drogue deployment compared with a 2.2 n. mi. overshoot indicated by the reconstructed trajectory.

3.4 S-IVB AND SERVICE MODULE ENTRY

The point of impact for the S-IVB stage was latitude 8.9 degrees south and longitude 81.6 degrees east (in the Indian Ocean); impact was at 168:27:00.

At command module/service module separation, the minus X reaction control engines of the service module should have ignited to impart a velocity change of about 290 ft/sec posigrade to the service module. At 2 seconds after separation, the plus roll engines should have ignited for 5.5 seconds to spin-stabilize the service module. Under these conditions, the service module would have remained ahead of and above the command module during entry, as shown in figure 3-6. Tracking data and visual observations indicate that the service module may have been tumbling after separation. Because of the apparent separation velocity and the momentary thrust impingement disturbances noted on the command module at separation, the minus X thrusters fired. The redundancy in the circuits which control the firing of these thrusters also suggests that an electrical failure is very unlikely.

However, the trajectory reconstruction of the service module and the analysis of the dynamics show that a velocity change of only about 25 to 30 ft/sec occurred, which would be consistent with a failure of

the roll engines in the service module reaction control system. Without the roll engines firing, the vehicle would become unstable, and the subsequent tumbling reduces the effective velocity change to the levels observed. There are no indications available which can either confirm or deny roll-engine operation.

Figure 3-7 shows that the two vehicles had different velocities, and the separation distance was always increasing. The time accuracy of the trajectory reconstruction was poor; consequently, the actual path of the service module, shown in figure 3-6, could have been more critical (that is, closer to the command module) than shown. The time of the thermal and dynamic disturbances noted in the data from body rates, calorimeters, and thermocouple measurements in the heat shield are also indicated on the figure. Proximity of the command module and service module to each other was such that shock wave and flow disturbances caused by the service module could explain the thermal and dynamic responses noted. Furthermore, the disturbances were at approximately the time the crew reported hearing a loud noise.

During the entry period, three objects — the command module, the service module, and a 12-foot insulation disk from between the two modules — were tracked simultaneously and also sighted visually. The trajectory reconstruction indicates the service module impacted at approximately 260:03:00 in the Atlantic Ocean at latitude 29 degrees north and longitude 72 degrees west.

TABLE 3-I.- DEFINITION OF TRAJECTORY AND ORBITAL PARAMETERS

<u>Trajectory parameters</u>	<u>Definition</u>
Geodetic latitude	Spacecraft position measured north or south from the equator to the local vertical vector, deg
Longitude	Spacecraft position measured east or west from the Greenwich meridian to the local vertical vector, deg
Altitude	Perpendicular distance from the reference ellipsoid to the point of orbit intersect, ft
Space-fixed velocity	Magnitude of the inertial velocity vector referenced to the earth-centered, inertial reference coordinate system, ft/sec
Space-fixed flight-path angle	Flight-path angle measured positive upward from the geocentric local horizontal plane to the inertial velocity vector, deg
Space-fixed heading	Angle of the projection of the inertial velocity vector onto the local geocentric horizontal plane, measured positive eastward from north, deg
Apogee	Maximum altitude above the oblate earth model, n. mi.
Perigee	Minimum altitude above the oblate earth model, n. mi.
Period	Time required for spacecraft to complete 360 degrees of orbit rotation (perigee to perigee, for example), min
Inclination	Angle between the orbit plane and the equator, deg

TABLE 3-II.- TRAJECTORY PARAMETERS FOR LAUNCH AND PARKING ORBIT

Condition	Planned	Actual
Inboard Engine Cutoff		
Time, hr:min:sec	00:02:20.3	00:02:20.6
Geodetic latitude, deg North	28.67	28.67
Longitude, deg West	80.03	80.67
Altitude, ft	188 349	186 088
Altitude, n. mi.	31.0	30.6
Space-fixed velocity, ft/sec	7440	7394
Space-fixed flight-path angle, deg	27.28	27.09
Space-fixed heading angle, deg E of N	75.77	75.87
Outboard Engine Cutoff		
Time, hr:min:sec	00:02:23.3	00:02:24.3
Geodetic latitude, deg North	28.69	28.69
Longitude, deg West	79.98	79.98
Altitude, ft	198 657	198 558
Altitude, n. mi.	32.7	32.6
Space-fixed velocity, ft/sec	7628	7617
Space-fixed flight-path angle, deg	26.60	26.55
Space-fixed heading angle, deg E of N	75.80	75.78
S-IVB Cutoff		
Time, hr:min:sec	00:10:14.8	00:10:16.8
Geodetic latitude, deg North	31.53	31.53
Longitude, deg West	61.99	61.98
Altitude, ft	747 837	748 374
Altitude, n. mi.	123.0	123.0
Space-fixed velocity, ft/sec	25 527	25 526
Space-fixed flight-path angle, deg	-0.01	0.00
Space-fixed heading angle, deg E of N	85.90	85.91

TABLE 3-II.- TRAJECTORY PARAMETERS FOR LAUNCH AND PARKING ORBIT - Continued

Condition	Planned	Actual
Insertion (S-IVB Cutoff + 10 Seconds)		
Time, hr:min:sec	00:10:24.8	00:10:26.8
Geodetic latitude, deg North	31.58	31.58
Longitude, deg West	61.99	61.98
Altitude, ft	747 871	748 439
Altitude, n. mi.	123.0	123.0
Space-fixed velocity, ft/sec	25 549	25 553
Space-fixed flight-path angle, deg	0.00	0.01
Space-fixed heading angle, deg E of N	86.31	86.32
S-IVB Venting Initiate		
Time, hr:min:sec	01:34:27	01:34:29
Geodetic latitude, deg North	27.84	27.77
Longitude, deg West	107.20	107.39
Altitude, ft	750 373	752 413
Altitude, n. mi.	123.4	123.7
Space-fixed velocity, ft/sec	25 548	25 560
Space-fixed flight-path angle, deg	-0.09	-0.09
Space-fixed heading angle, deg E of N	74.09	74.38
S-IVB Venting Terminate		
Time, hr:min:sec	01:46:28	01:46:30
Geodetic latitude, deg North	29.39	29.43
Longitude, deg West	54.22	55.24
Altitude, ft	769 203	767 308
Altitude, n. mi.	126.5	126.1
Space-fixed velocity, ft/sec	25 554	25 555
Space-fixed flight-path angle, deg	0.19	0.18
Space-fixed heading angle, deg E of N	102.59	102.47

TABLE 3-II.- TRAJECTORY PARAMETERS FOR LAUNCH AND PARKING ORBIT - Concluded

Condition	Planned	Actual
Spacecraft/S-IVB Separation		
Time, hr:min:sec	02:54:55	02:55:02
Geodetic latitude, deg North	12.99	13.00
Longitude, deg West	164.41	164.42
Altitude, ft	788 136	819 762
Altitude, n. mi.	129.63	134.83
Space-fixed velocity, ft/sec	25 524	25 500
Space-fixed flight-path angle, deg	-0.28	-0.30
Space-fixed heading angle, deg E of N	60.87	60.86

TABLE 3-III.- TRAJECTORY PARAMETERS FOR MANEUVERS

Condition	Ignition		Cutoff	
	Planned	Actual	Planned	Actual
First phasing maneuver (reaction control system)				
Time, hr:min:sec	03:20:00.0	03:20:09.9	03:20:16.3	03:20:26.2
Geodetic latitude, deg	25.07	24.96	24.68	24.46
Longitude, deg	-61.72	-61.39	-60.62	-60.02
Altitude, ft	789 581	789 997	790 031	791 756
Altitude, n. mi.	129.95	130.01	130.00	130.31
Space-fixed velocity, ft/sec	25 532.2	25 531.7	25 526.9	25 525.0
Space-fixed flight-path angle, deg	0.234	0.236	0.239	0.244
Space-fixed heading angle, deg E of N	110.11	110.26	110.60	110.87
Second phasing maneuver (reaction control system)				
Time, hr:min:sec	15:52:00.0	15:52:00.9	15:52:18.5	15:52:18.5
Geodetic latitude, deg	-31.70	-31.70	-31.74	-31.73
Longitude, deg	-116.36	-119.41	-115.10	-117.10
Altitude, ft	1 004 151	1 002 632	1 004 169	1 002 090
Altitude, n. mi.	165.26	165.00	165.26	164.92
Space-fixed velocity, ft/sec	25 281.3	25 283.1	25 274.8	25 277.4
Space-fixed flight-path angle, deg	0.0	0.0	-0.006	-0.007
Space-fixed heading angle, deg E of N	92.26	92.29	91.59	91.19

TABLE 3-III.-- TRAJECTORY PARAMETERS FOR MANEUVERS - Continued

Condition	Ignition		Cutoff	
	Planned	Actual	Planned	Actual
First service propulsion maneuver				
Time, hr:min:sec	26:24:55.2	26:24:55.7	26:25:04.7	26:25:05.1
Geodetic latitude, deg	-29.55	-29.56	-29.41	-29.42
Longitude, deg	106.8	107.7	107.5	107.5
Altitude, ft	990 459	990 253	988 920	988 518
Altitude, n. mi.	163.01	162.98	162.75	162.69
Space-fixed velocity, ft/sec	25 289.4	25 289.9	25 354.2	25 354.0
Space-fixed flight-path angle, deg	-0.110	-0.130	-0.557	-0.556
Space-fixed heading angle, deg E of N	77.79	77.81	77.43	77.45
Second service propulsion maneuver				
Time, hr:min:sec	28:00:56.0	28:00:56.5	28:01:03.8	28:01:04.3
Geodetic latitude, deg	-22.42	-22.41	-22.19	-22.21
Longitude, deg	106.77	106.76	107.27	107.24
Altitude, ft	902 496	902 269	901 015	901 050
Altitude, n. mi.	148.53	148.49	148.29	148.29
Space-fixed velocity, ft/sec	25 446.7	25 446.5	25 354.7	25 357.2
Space-fixed flight-path angle, deg	-0.529	-0.516	-0.196	-0.196
Space-fixed heading angle, deg E of N	66.94	66.94	66.74	66.75

TABLE 3-III.- TRAJECTORY PARAMETERS FOR MANEUVERS - Continued

Condition	Ignition		Cutoff	
	Planned	Actual	Planned	Actual
Terminal phase initiate				
Time, hr:min:sec	29:18:34.0	29:16:33.0		
Geodetic latitude, deg	-31.74	-31.14		
Longitude, deg	35.66	26.45		
Altitude, ft	934 904	931 769		
Altitude, n. mi.	153.86	153.35		
Space-fixed velocity, ft/sec	25 323.4	25 327.1		
Space-fixed flight-path angle, deg	0.043	0.086		
Space-fixed heading angle, deg E of N	91.55	96.63		
Station-keeping initiate				
Time, hr:min:sec	29:53:34.0	29:55:43.0		
Geodetic latitude, deg	23.00	26.06		
Longitude, deg	162.54	171.29		
Altitude, ft	775 469	764 351		
Altitude, n. mi.	127.62	125.80		
Space-fixed velocity, ft/sec	25 531.7	25 546.1		
Space-fixed flight-path angle, deg	0.238	-0.206		
Space-fixed heading angle, deg E of N	67.54	71.22		

TABLE 3-III.- TRAJECTORY PARAMETERS FOR MANEUVERS - Continued

Condition	Ignition		Cutoff	
	Planned	Actual	Planned	Actual
Separation maneuver				
Time, hr:min:sec	30:20:00.0	30:20:00.0	30:20:05.4	30:20:05.4
Geodetic latitude, deg	12.79	12.81	12.63	12.64
Longitude, deg	-88.60	-88.63	-88.32	-88.34
Altitude, ft	786 642	786 598	787 157	784 351
Altitude, n. mi.	129.46	129.45	129.55	129.09
Space-fixed velocity, ft/sec	25 514.1	25 514.1	25 515.0	25 515.1
Space-fixed flight-path angle, deg	0.270	0.270	0.271	0.257
Space-fixed heading angle, deg E of N	119.21	119.21	119.28	119.28
Third service propulsion maneuver				
Time, hr:min:sec	75:47:58.6	75:48:00.3	75:48:07.8	75:48:09.3
Geodetic latitude, deg	-16.97	-16.95	-16.69	-16.68
Longitude, deg	105.52	105.57	106.06	106.08
Altitude, ft	944 885	944 663	944 297	943 708
Altitude, n. mi.	155.51	155.47	155.41	155.31
Space-fixed velocity, ft/sec	25 326.2	25 326.1	25 272.2	25 273.9
Space-fixed flight-path angle, deg	-0.140	-0.144	-0.238	-0.237
Space-fixed heading angle, deg E of N	62.84	62.84	63.46	63.12

TABLE 3-III.- TRAJECTORY PARAMETERS FOR MANEUVERS - Continued

Condition	Ignition		Cutoff	
	Planned	Actual	Planned	Actual
Fourth service propulsion maneuver				
Time, hr:min:sec	120:43:00.0	120:43:00.4	120:43:00.4	120:43:00.9
Geodetic latitude, deg	31.38	31.38	31.38	31.39
Longitude, deg	-102.75	-102.78	-102.73	-102.79
Altitude, ft	609 937	610 161	609 948	609 848
Altitude, n. mi.	100.38	100.42	100.38	100.36
Space-fixed velocity, ft/sec	25 658.9	25 661.2	25 671.9	25 670.6
Space-fixed flight-path angle, deg	-0.383	-0.383	-0.381	-0.382
Space-fixed heading angle, deg E of N	90.77	90.75	90.76	90.75
Fifth service propulsion maneuver				
Time, hr:min:sec	165:00:00.0	165:00:00.5	165:01:05.9	165:01:07.6
Geodetic latitude, deg	28.57	28.56	29.47	29.41
Longitude, deg	-91.09	-91.12	-85.82	-86.24
Altitude, ft	720 774	720 388	701 234	700 249
Altitude, n. mi.	118.62	118.56	115.41	115.24
Space-fixed velocity, ft/sec	25 518.9	25 519.3	25 707.4	25 714.9
Space-fixed flight-path angle, deg	-0.482	-0.482	-0.902	-0.912
Space-fixed heading angle, deg E of N	75.46	76.46	81.52	82.70

TABLE 3-III.- TRAJECTORY PARAMETERS FOR MANEUVERS - Continued

Condition	Ignition		Cutoff	
	Planned	Actual	Planned	Actual
Sixth service propulsion maneuver				
Time, hr:min:sec	210:08:00.0	210:08:00.5	210:08:00.4	210:08:01.0
Geodetic latitude, deg	24.41	24.40	24.42	24.44
Longitude, deg	-82.77	-82.81	-82.74	-82.70
Altitude, ft	994 614	995 944	994 225	993 943
Altitude, n. mi.	163.69	163.91	163.63	163.58
Space-fixed velocity, ft/sec	25 354.1	25 354.7	25 354.5	25 354.6
Space-fixed flight-path angle, deg	-1.169	-1.169	-1.168	-1.168
Space-fixed heading angle, deg E of N	71.67	71.67	71.73	71.73
Seventh service propulsion maneuver				
Time, hr:min:sec	239:06:11.0	239:06:12.0	239:06:18.8	239:06:19.7
Geodetic latitude, deg	15.06	15.05	14.82	14.80
Longitude, deg	-66.20	-66.16	-65.72	-65.68
Altitude, ft	545 506	545 503	545 583	544 535
Altitude, n. mi.	89.78	89.78	89.79	89.62
Space-fixed velocity, ft/sec	25 864.5	25 864.6	25 865.7	25 866.4
Space-fixed flight-path angle, deg	-0.224	-0.207	-0.239	-0.242
Space-fixed heading angle, deg E of N	116.38	116.38	116.30	116.31

TABLE 3-III.- TRAJECTORY PARAMETERS FOR MANEUVERS - Concluded

Condition	Ignition		Cutoff	
	Planned	Actual	Planned	Actual
Eighth service propulsion maneuver				
Time, hr:min:sec	259:39:15.9	259:31:16.3	259:39:27.9	259:39:28.2
Geodetic latitude, deg	13.84	13.83	14.20	14.19
Longitude, deg	-148.63	-148.65	-147.96	-147.98
Altitude, ft	1 143 422	1 143 579	1 138 667	1 137 041
Altitude, n. mi.	188.18	188.21	187.40	187.13
Space-fixed velocity, ft/sec	25 152.8	25 155.3	24 966.7	24 966.5
Space-fixed flight-path angle, deg	-0.985	-0.988	-1.652	-1.643
Space-fixed heading angle, deg E of N	63.21	63.20	63.38	63.38

TABLE 3-IV.- RENDEZVOUS MANEUVERS

Maneuver	Local horizontal velocity components, ft/sec												Resultant	
	Nominal			Expendeed ^a			Effective ^b			Ground solution			Velocity change, ft/sec	Time, sec
	X	Y	Z	X	Y	Z	X	Y	Z	X	Y	Z		
First phasing (reaction control)	-6.8	0	0	-5.8	0	0	-5.7	0	0	-5.7	0	0	5.7	16.3
Second phasing (reaction control)	--	--					-7.0	0	0	-6.5	0	0	7.02	18.5
Corrective combination (service propulsion) ^c	55.5	-1.3	200.1	64.3	-3.0	204.4	61.5	-1.5	196.5	62.5	-1.3	196.7	204.1	9.4
Circularization (service propulsion) ^c	-87.9	0.3	-161.0	-94.9	2.9	-156.4	-91.0	1.2	-149.8	-92.0	1.3	-149.0	175.3	7.8
Terminal phase initiate	14.2	1.1	-8.8	(d)			15.5	2.9	-7.3	15.1	2.8	-7.5	17.4	43.4
Terminal phase finalize (braking)	13.0	0.2	11.5	14.2	14.7	32.0	13.0	4.6	11.8	12.8	2.0	11.3	18.2	708.0

^aExpendeed velocity includes ΔV required to null residuals.^bEffective velocity is resultant ΔV required to satisfy target conditions.^cVelocity components do not include +X translation prior to maneuver.^dData not recorded.

TABLE 3-V.- SERVICE PROPULSION MANEUVERS

No.	Firing time, sec		Total velocity, ft/sec		Reaction control +X translation velocity, ft/sec
	Planned	Actual	Planned	Actual	
1	9.5	9.4	202.1	204.1	4.3
2	7.8	7.8	171.3	173.8	3.8
3	9.2	9.0	206.5	209.7	4.9
4	0.5	0.5	9.8	12.3	3.1
5	65.9	67.0	1642.7	1691.3	3.7
6	0.5	0.5	11.1	14.2	4.3
7	7.8	8.2	219.3	220.1	6.1
8	11.9	12.4	343.4	343.6	6.6

TABLE 3-VI.- TRAJECTORY PARAMETERS FOR ENTRY

Condition	Planned	Actual
Entry Interface (400 000 ft)		
Time, hr:min:sec	259:53:26	259:53:27
Geodetic latitude, deg North	29.92	29.92
Longitude, deg West	92.63	92.62
Altitude, n. mi.	65.79	65.79
Space-fixed velocity, ft/sec	25 844	25 846
Space-fixed heading angle, deg E of N	87.44	87.47
Maximum Conditions		
Maximum entry velocity, ft/sec	25 955	25 953
Maximum entry deceleration, g	3.37	3.33
Drogue Deployment Coordinates		
Time, hr:min:sec	260:03:28	260:03:25
Geodetic latitude, deg North	27.61	^a 27.64
Longitude, deg West	64.17	^a 64.15

^aBased on the best estimated trajectory; onboard guidance indicated drogue deploy at latitude 27.63 deg North and longitude 64.18 deg West, and USS Essex indicated drogue deploy at latitude 27.54 deg North and longitude 64.07 deg West.

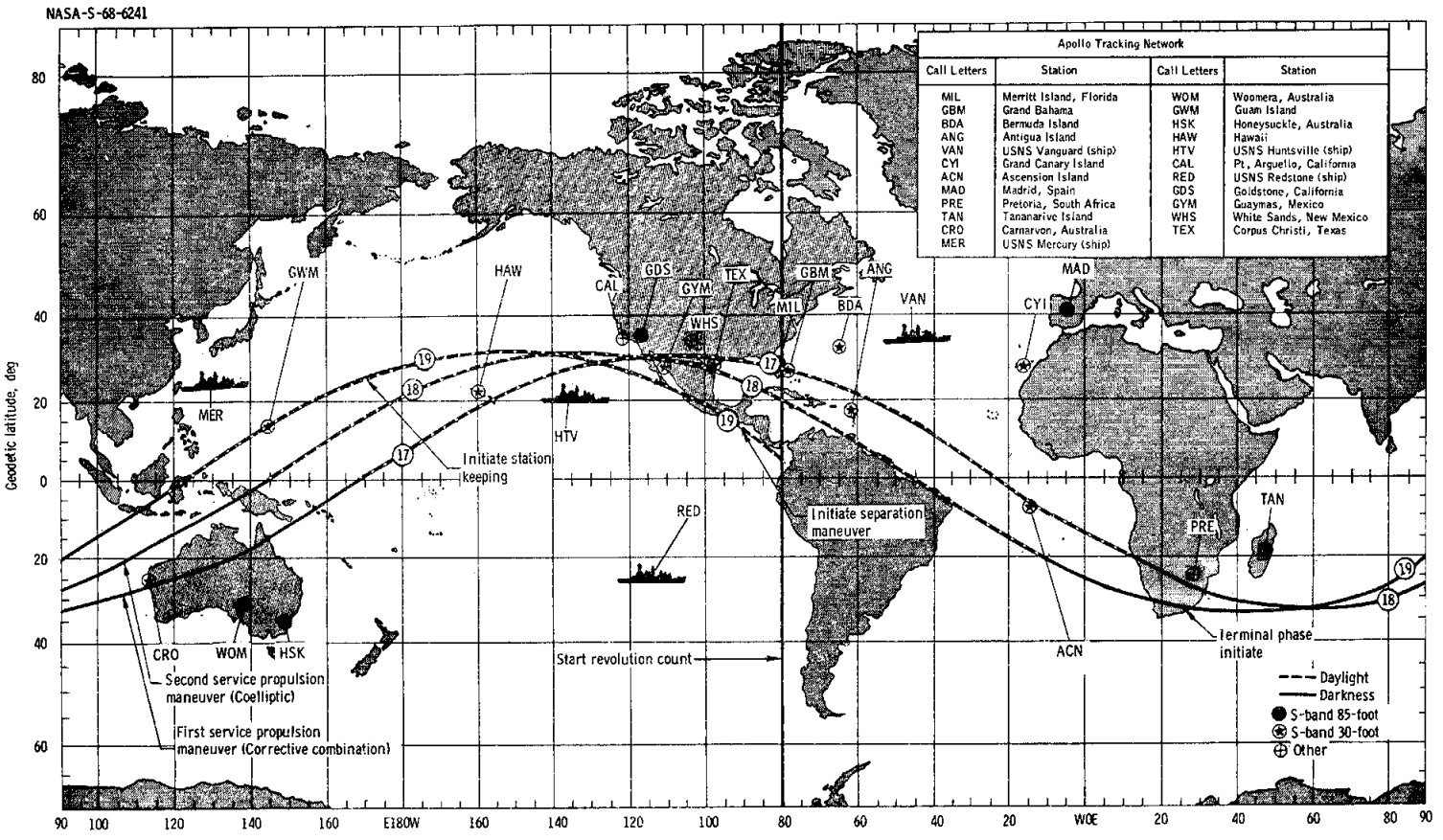
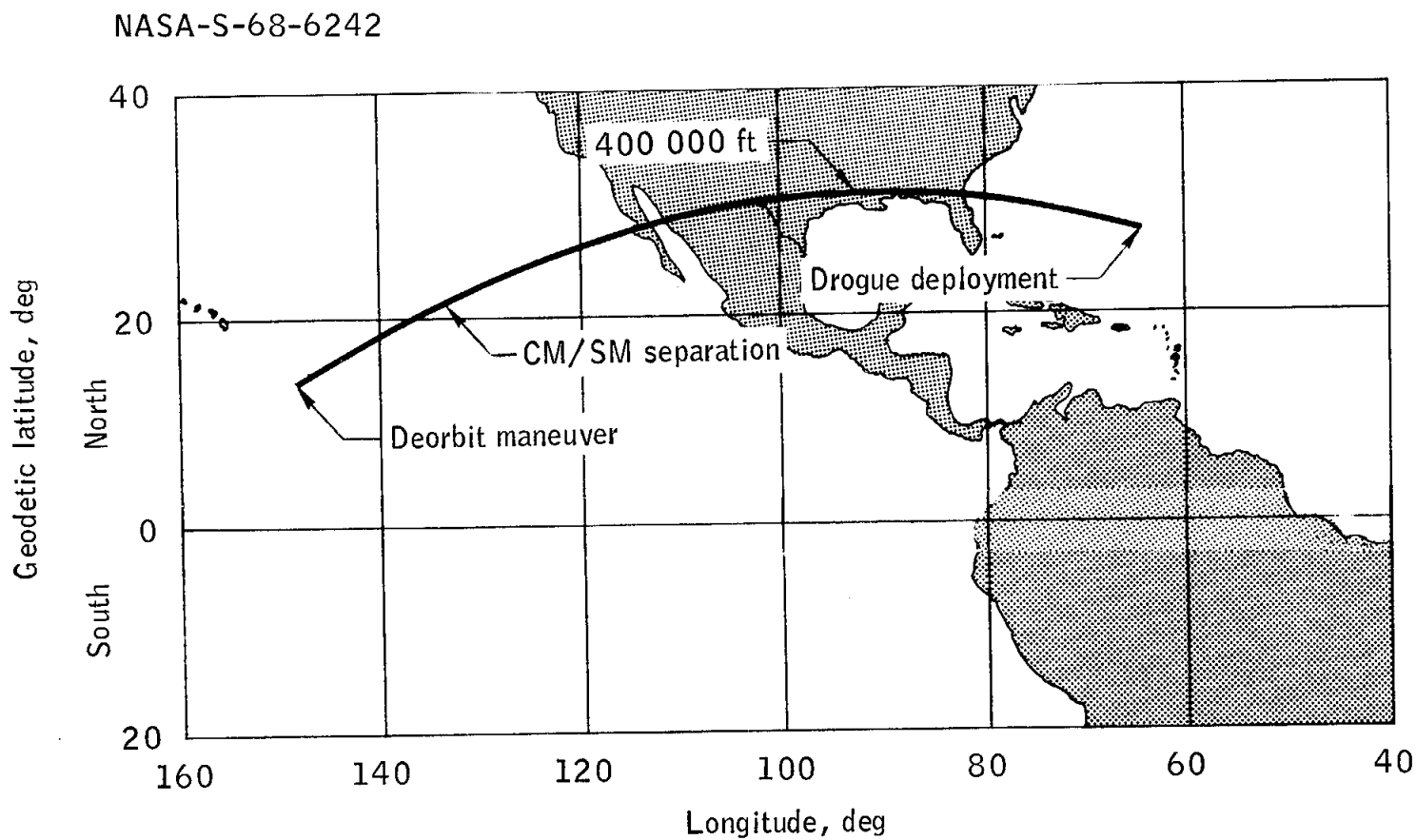
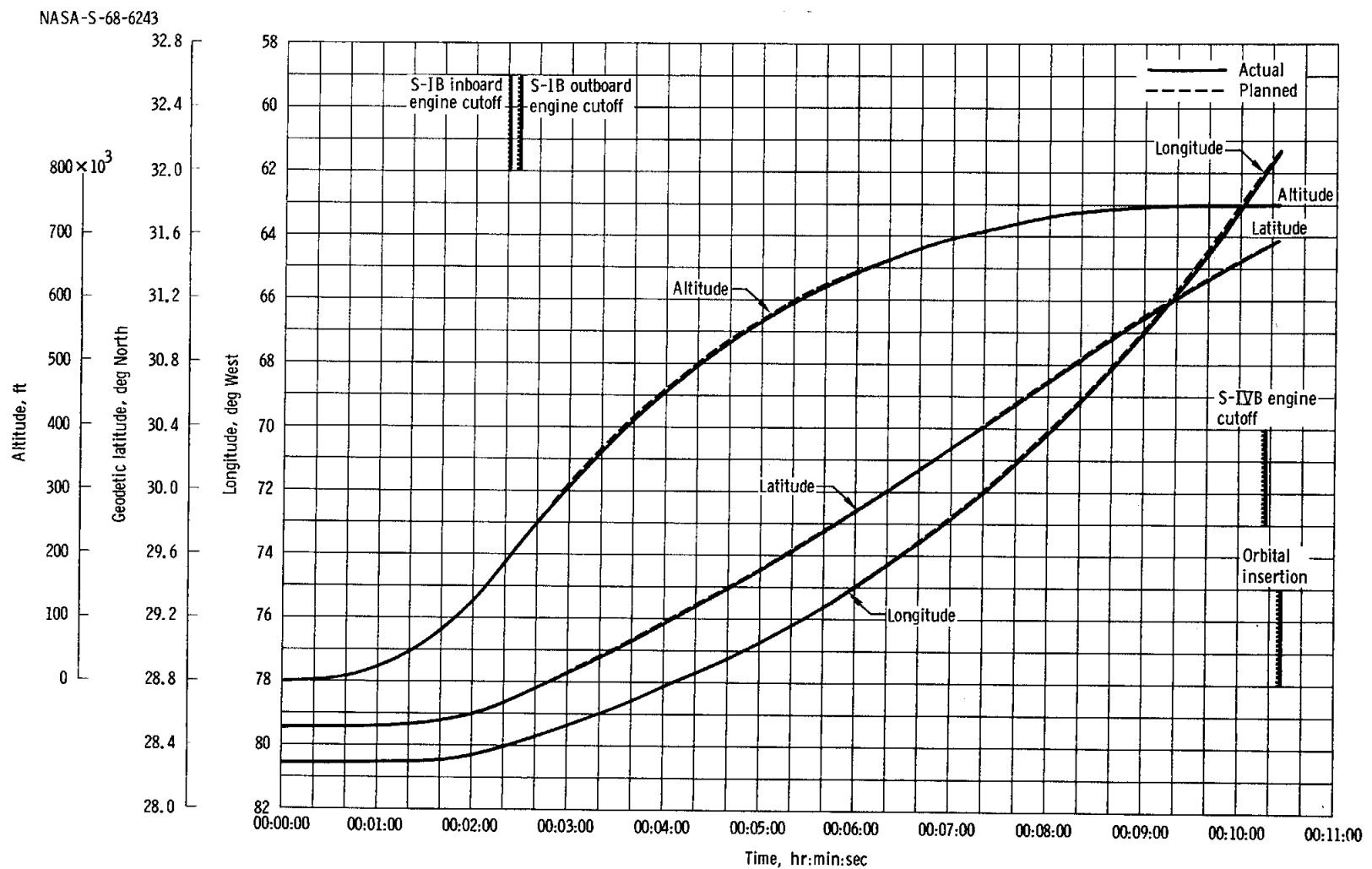


Figure 3-1. - Ground track.



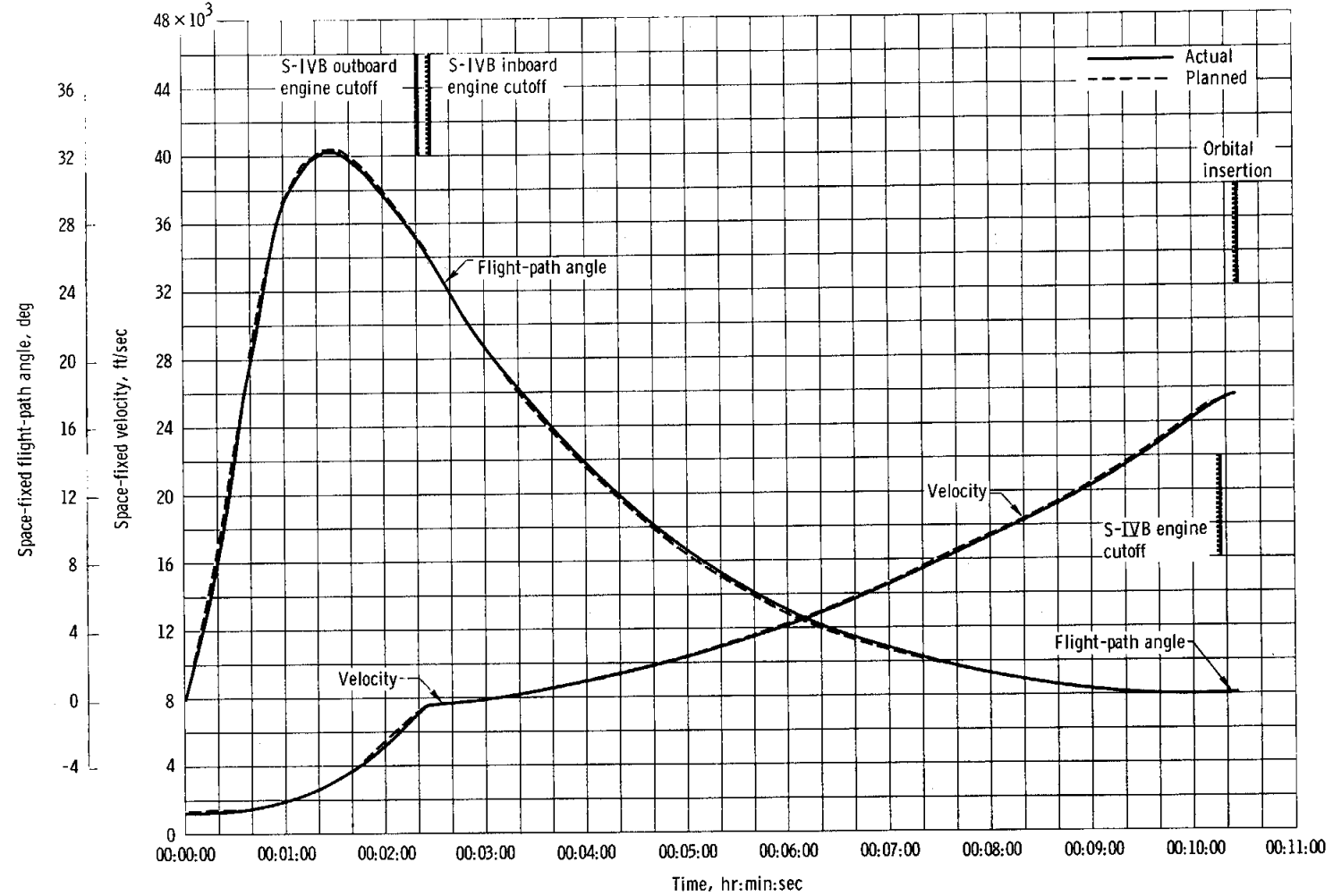
(b) Entry.

Figure 3-1. - Concluded.



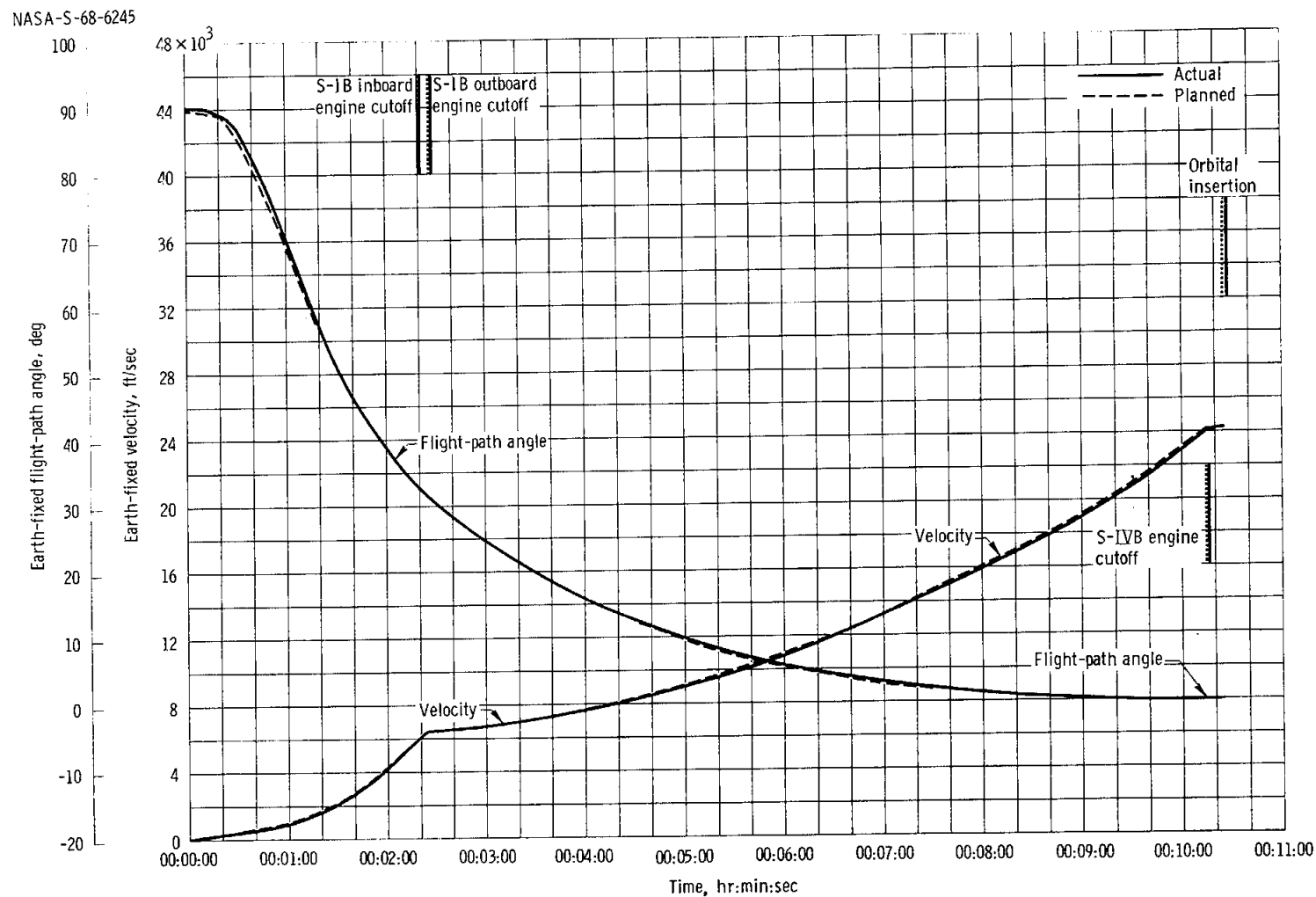
(a) Latitude, longitude, and altitude.

Figure 3-2.-Trajectory parameters during the launch phase.



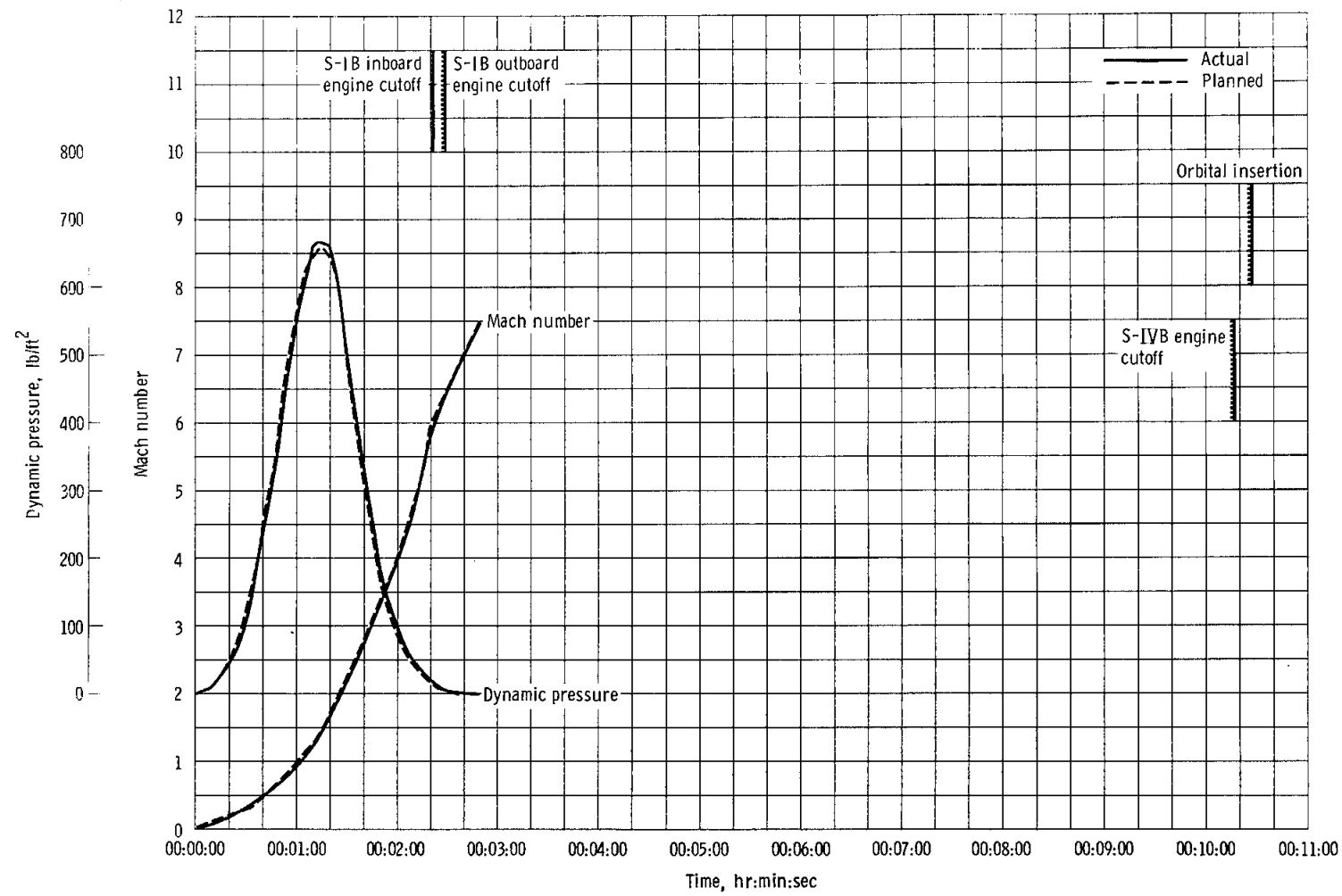
(b) Space-fixed flight-path angle and velocity.

Figure 3-2.- Continued.



(c) Earth-fixed flight-path angle and velocity.

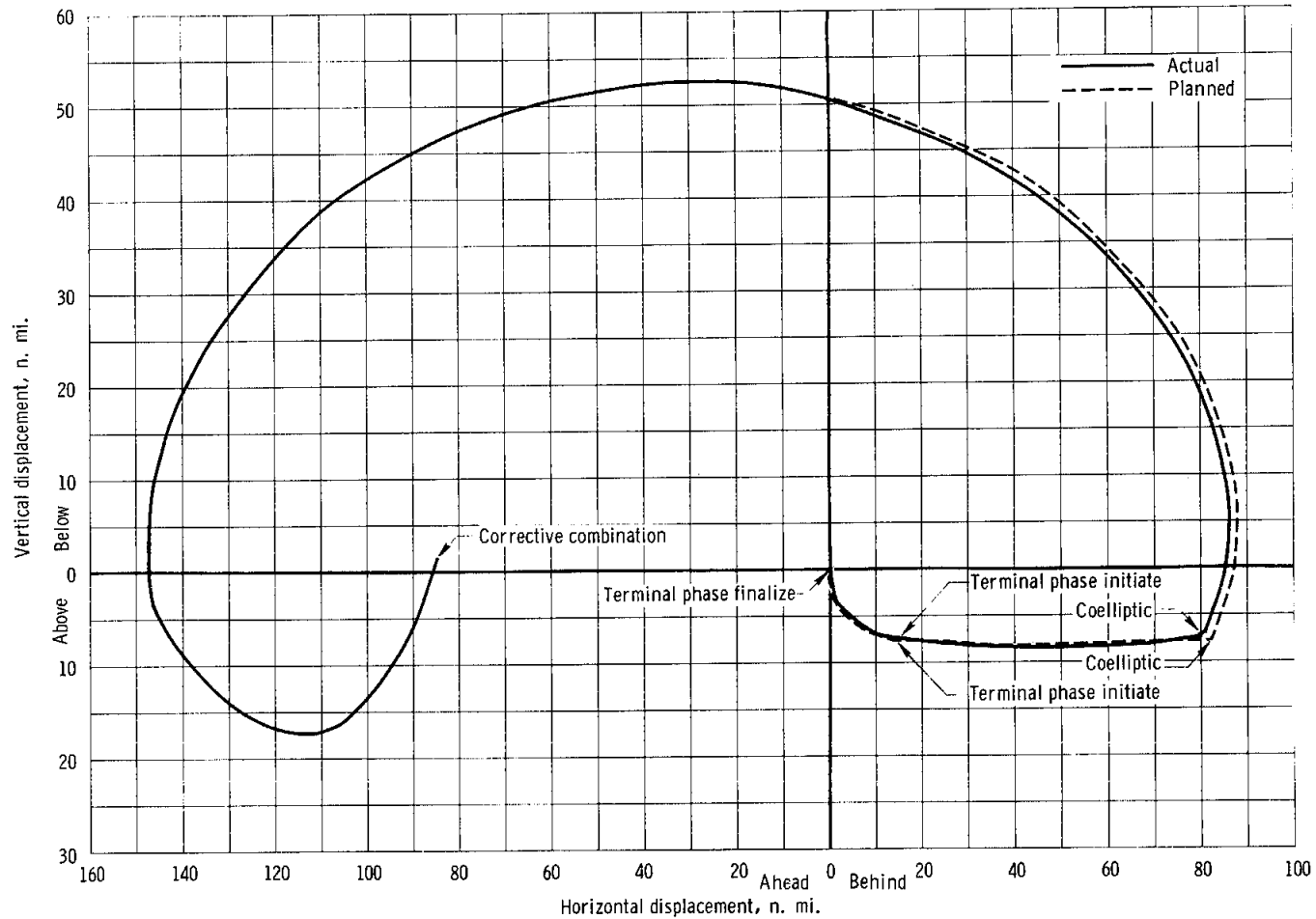
Figure 3-2.- Continued.



(d) Mach number and dynamic pressure.

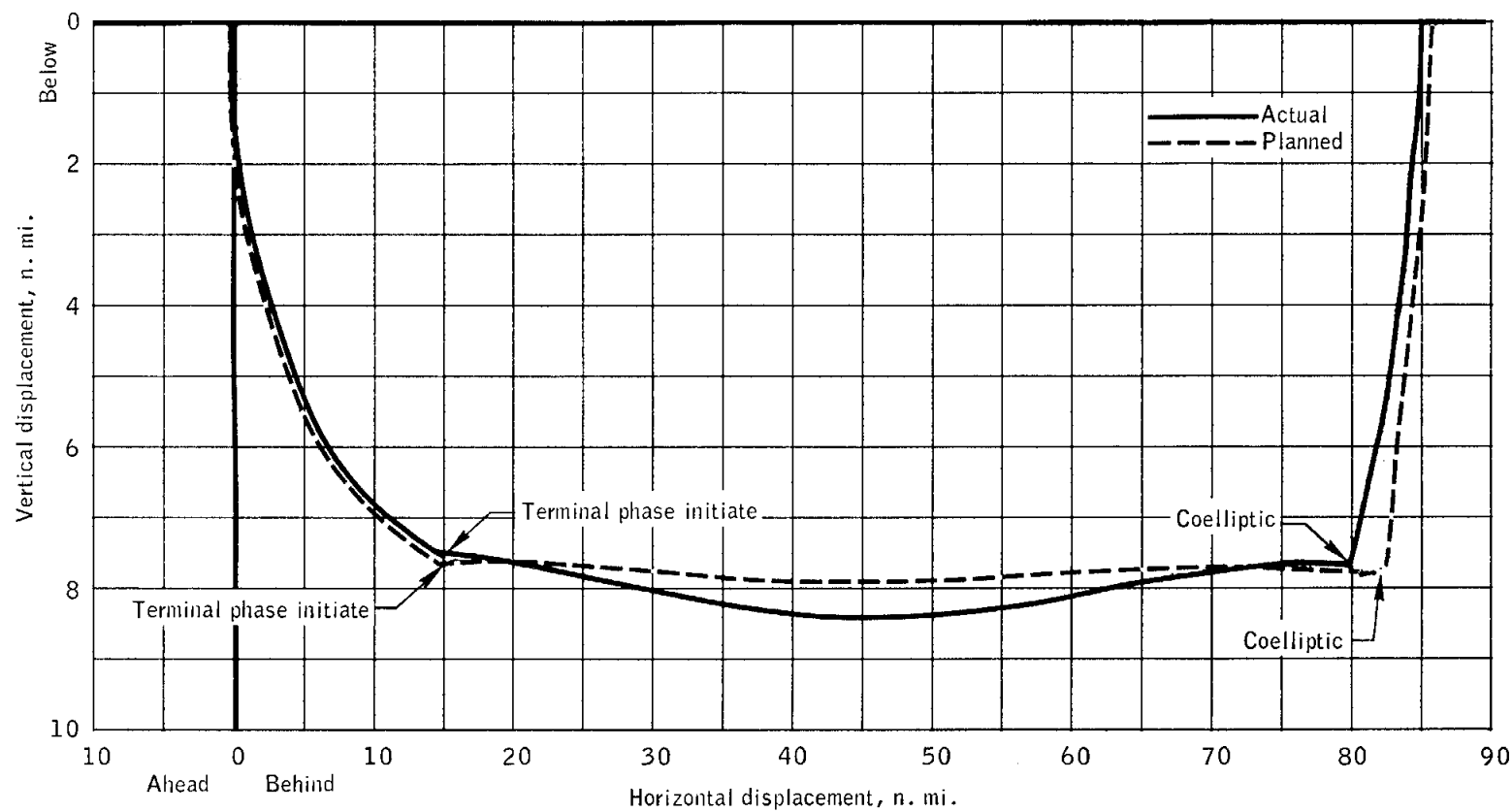
Figure 3-2.- Concluded.

NASA-S-68-6247



(a) Corrective combination maneuver to rendezvous.

Figure 3-3. - Relative motion of command and service module in S-IVB curvilinear system.



(b) Coelliptic maneuver to rendezvous, expanded.

Figure 3-3.- Concluded.

NASA-S-68-6249

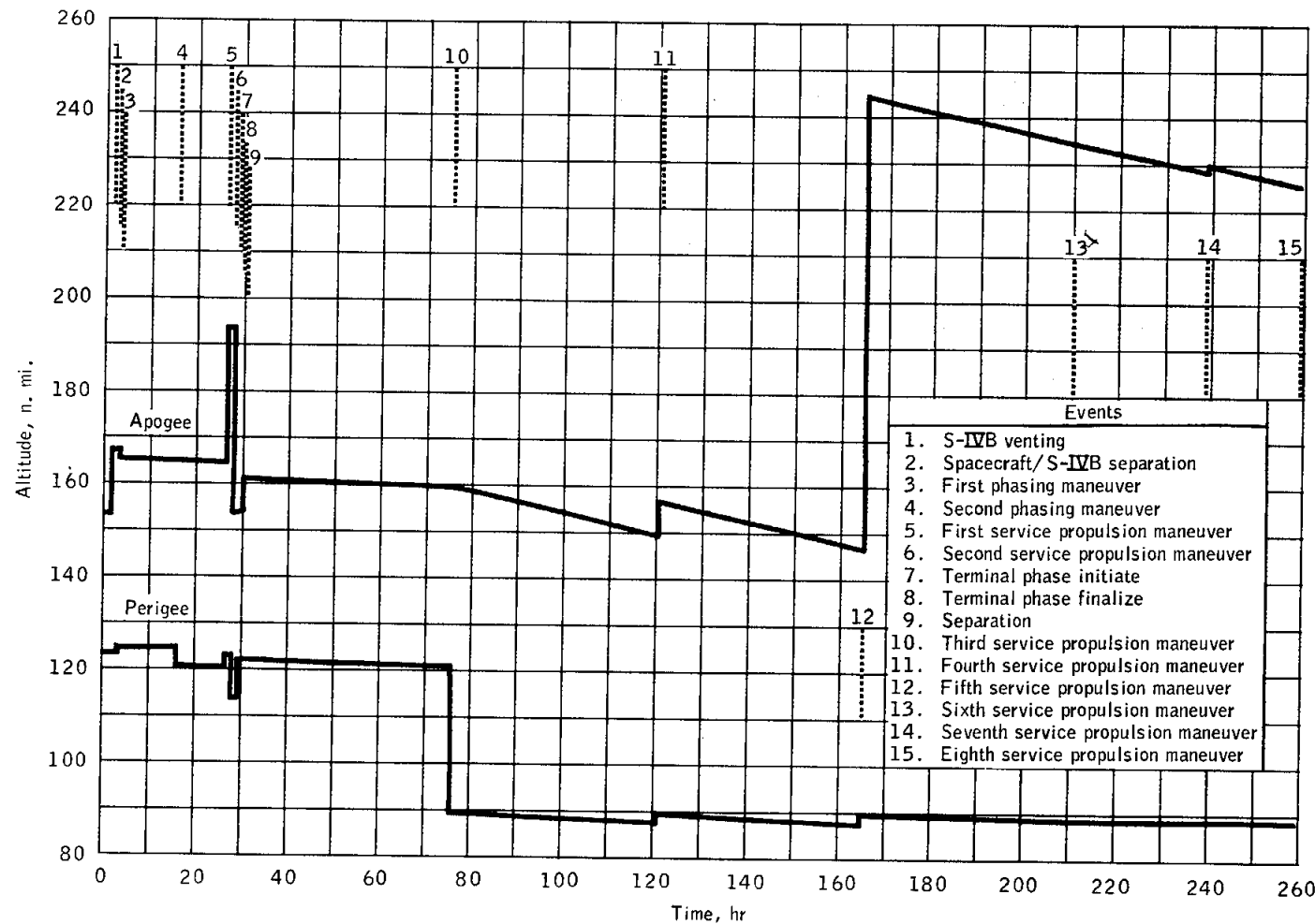
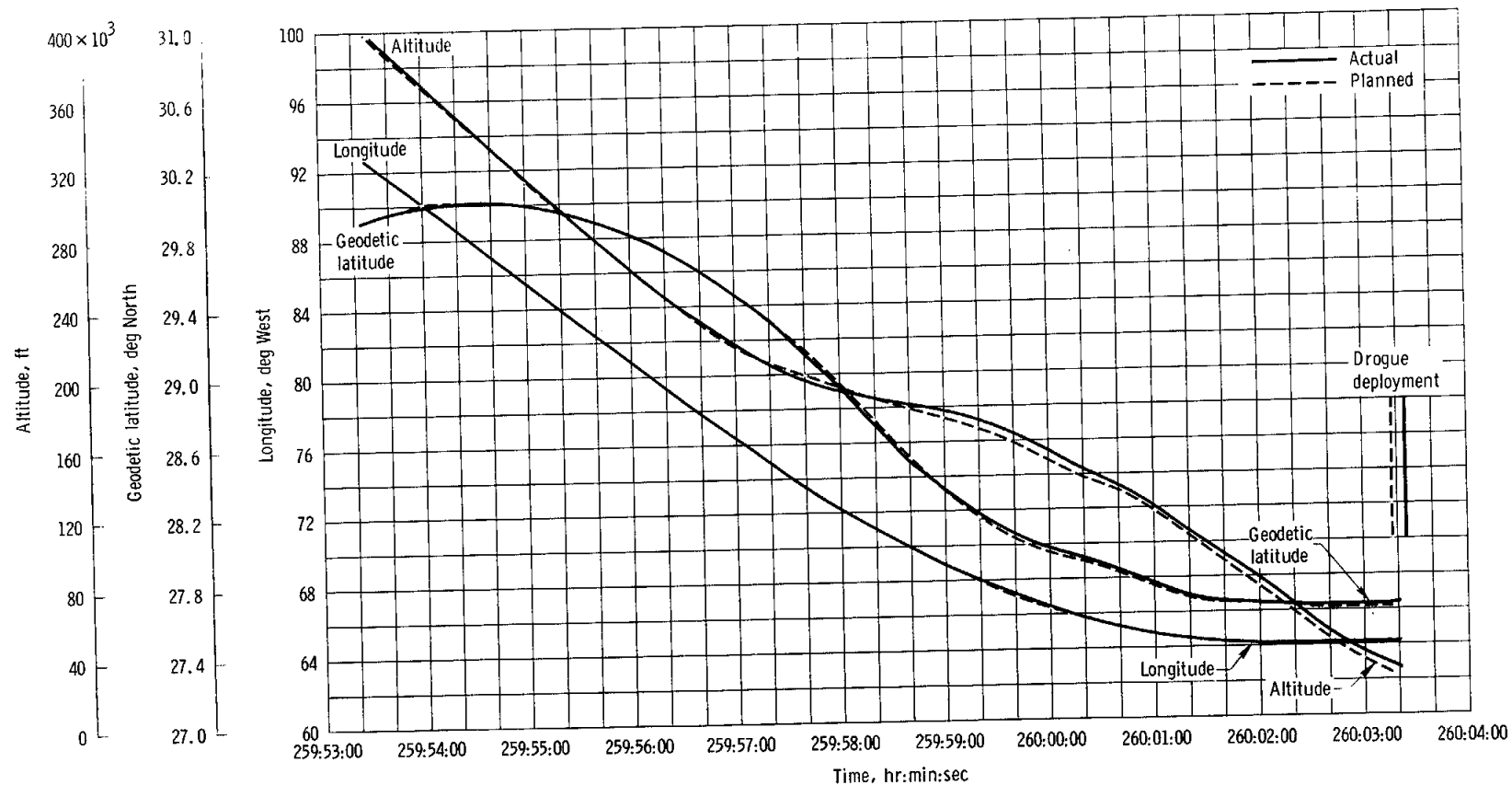


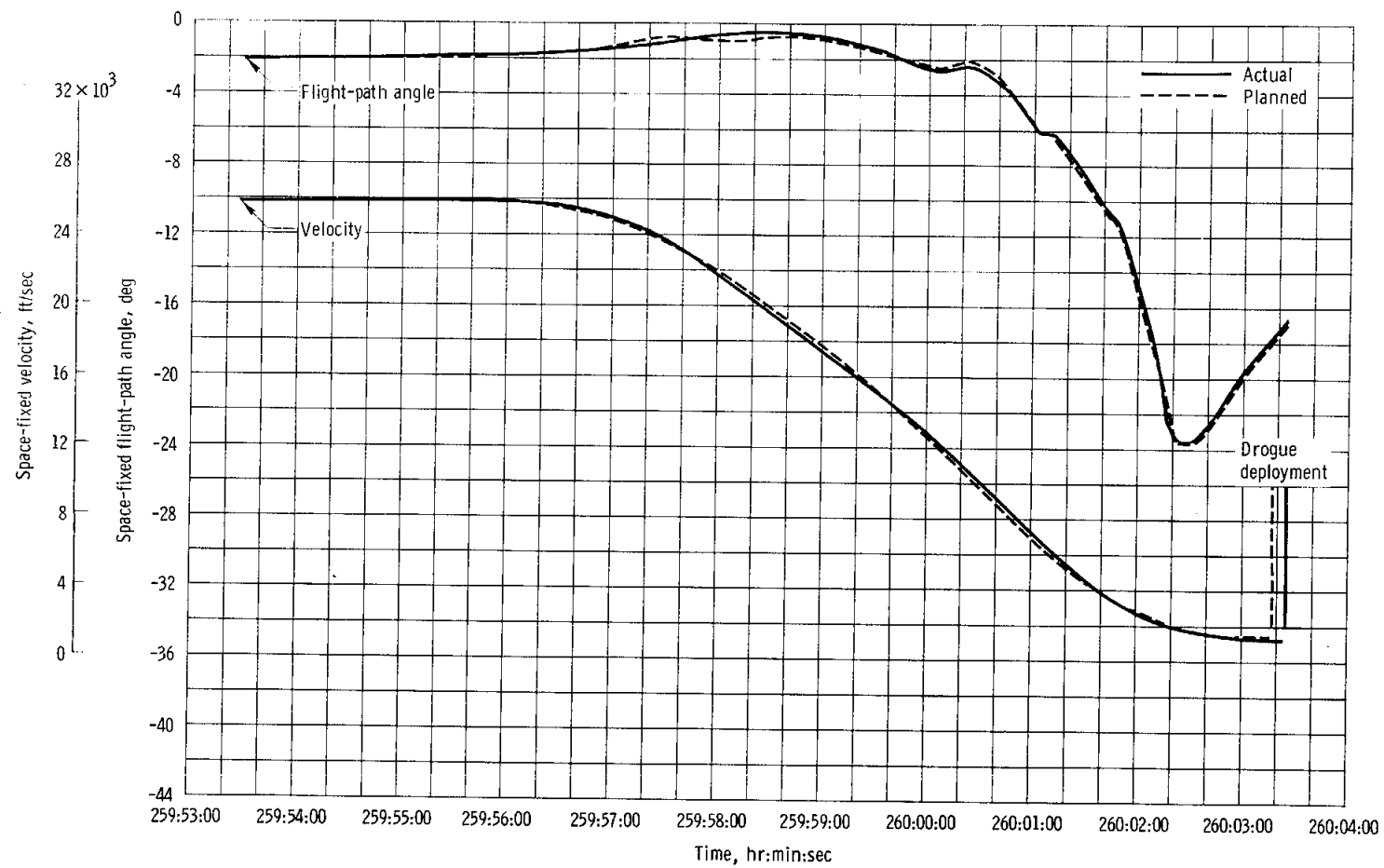
Figure 3-4. - Apogee and perigee altitudes.



(a) Geodetic latitude, longitude, and altitude.

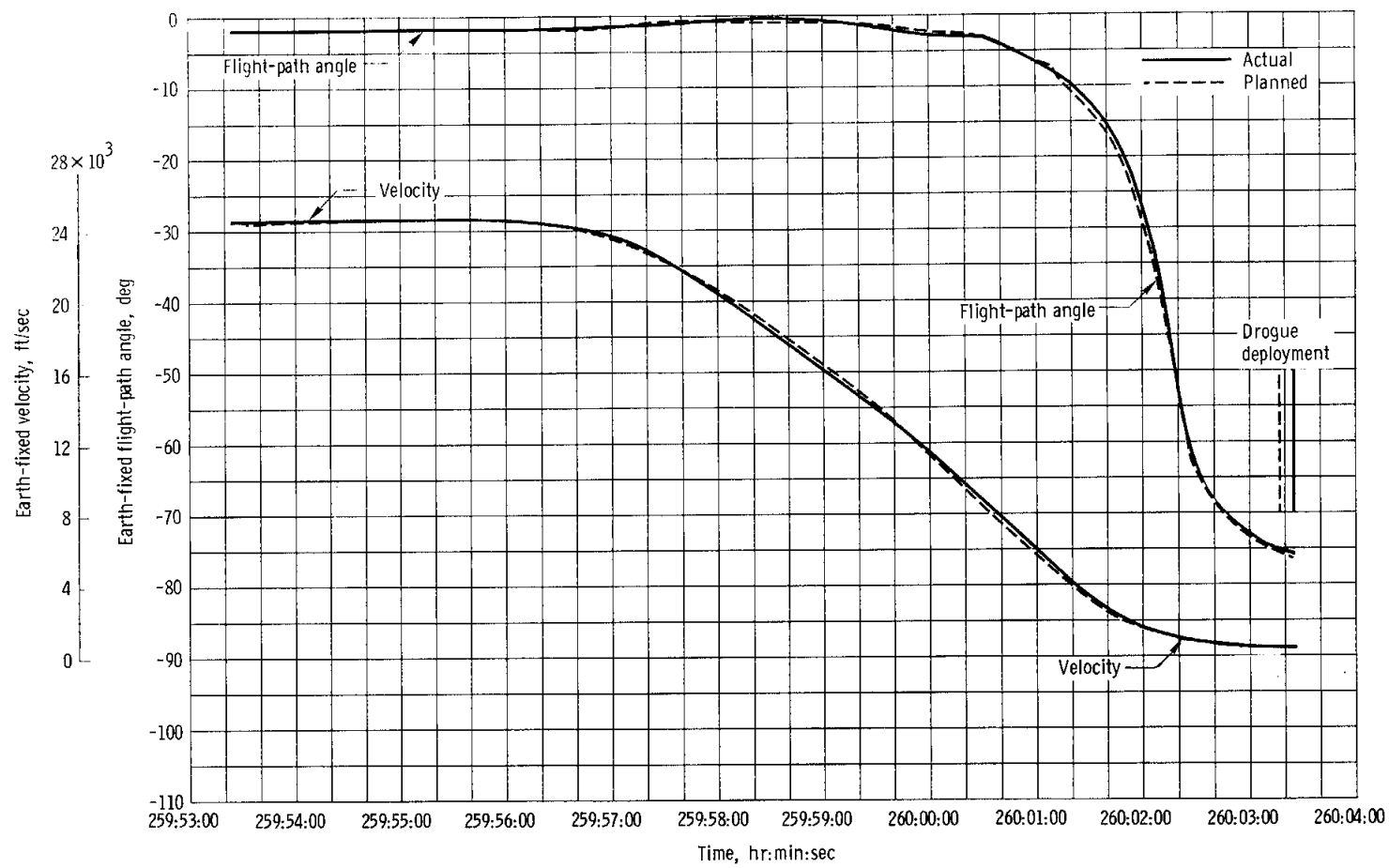
Figure 3-5. Trajectory parameters during the entry phase.

NASA-S-68-6251



(b) Space-fixed velocity and flight-path angle.

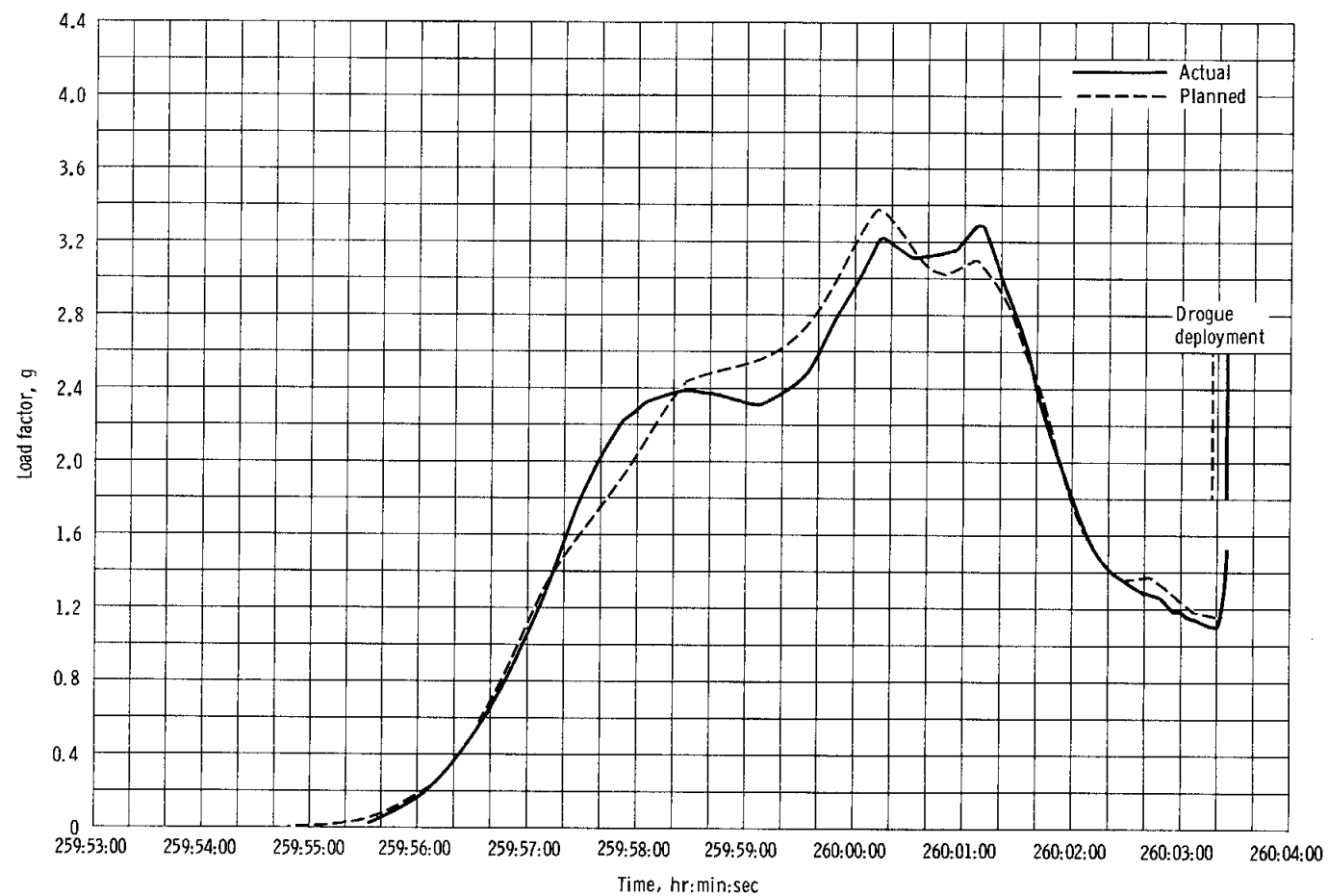
Figure 3-5. - Continued.



(c) Earth-fixed flight-path angle and velocity.

Figure 3-5. - Continued.

NASA-S-68-6253



(d) Load factor.

Figure 3-5. - Concluded.

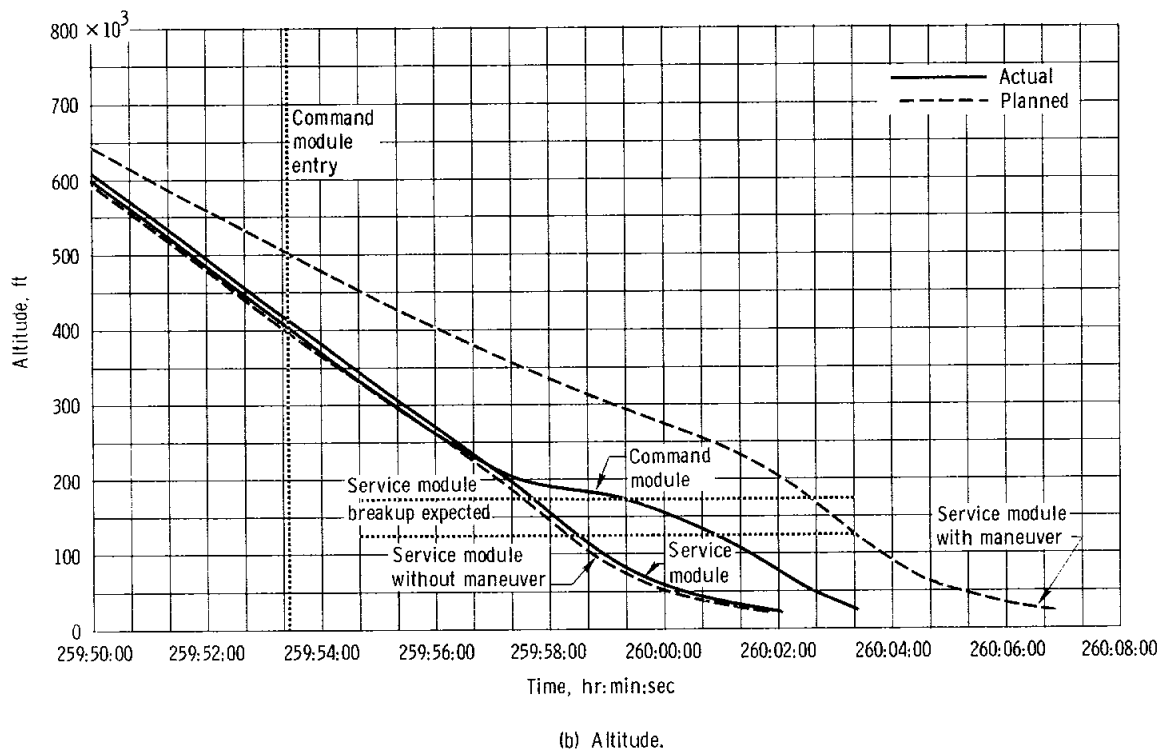
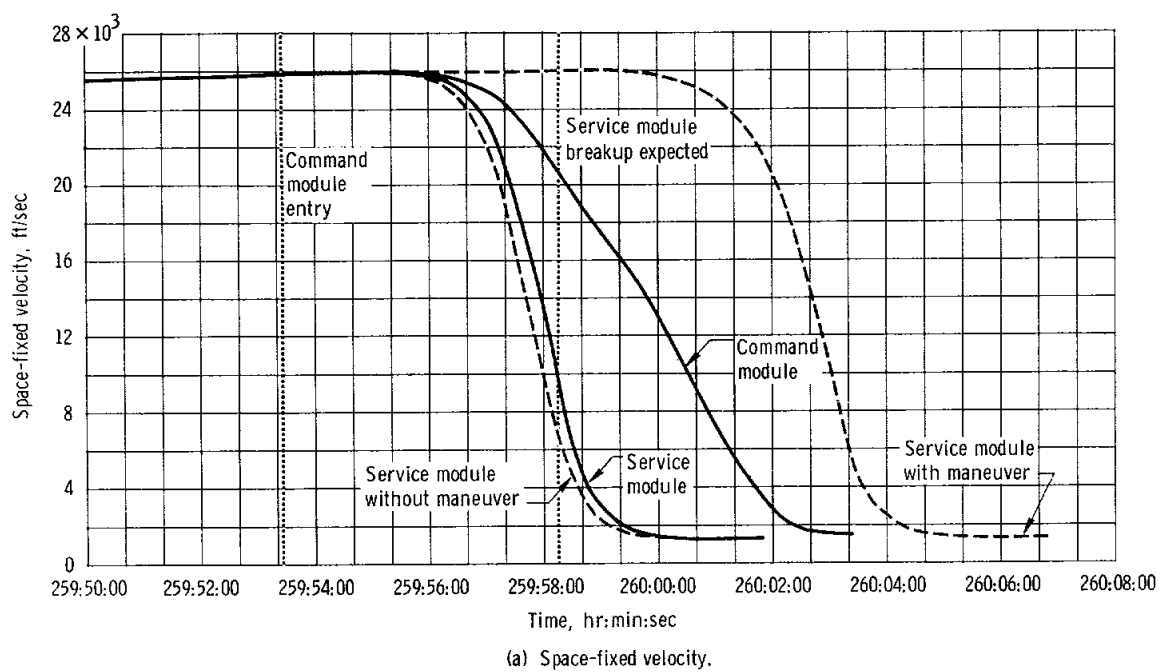
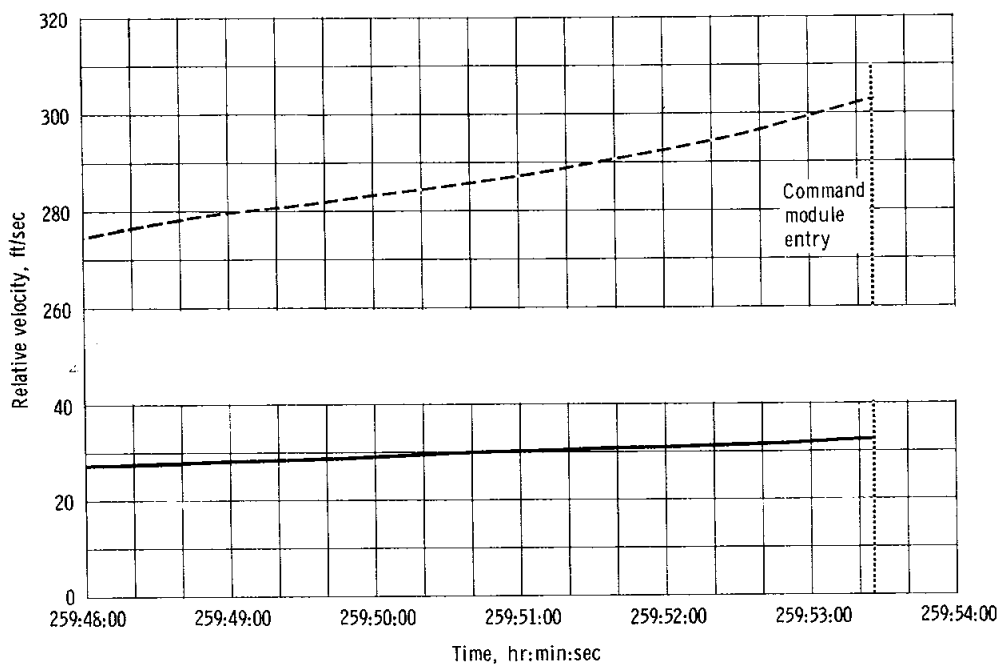
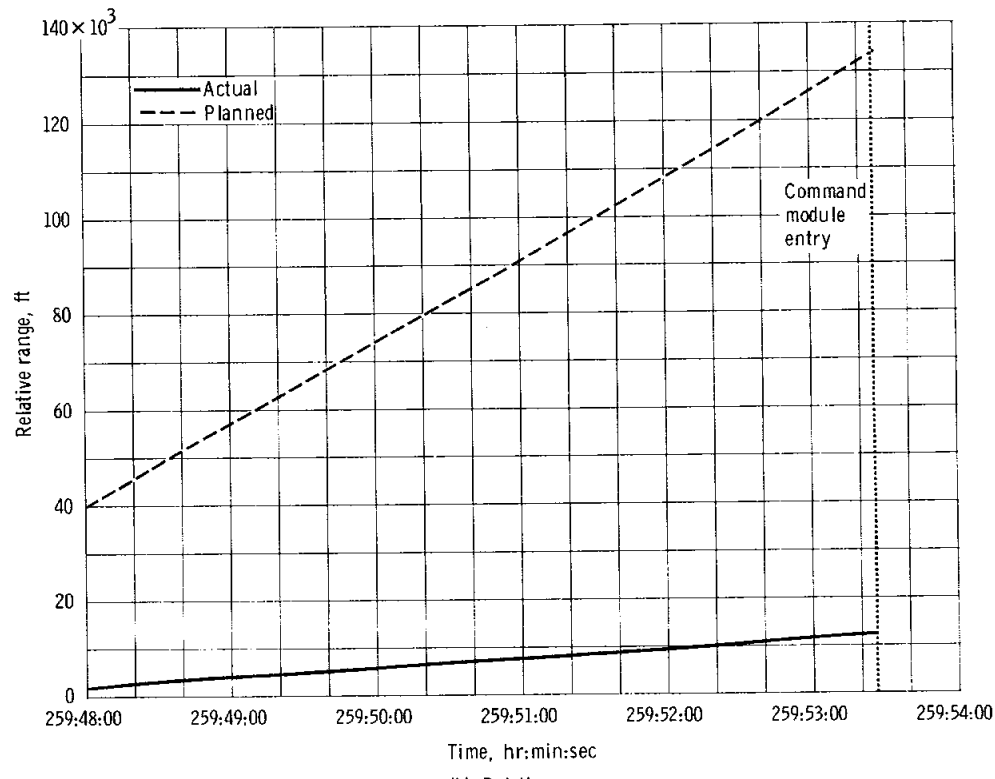


Figure 3-6. - Command module and service module entry trajectories.

NASA-S-68-6255



(a) Relative velocity.



(b) Relative range.

Figure 3-7. - Command module and service module separation range and velocity.

4.0 LAUNCH VEHICLE PERFORMANCE SUMMARY

The launch vehicle, AS-205, satisfactorily placed the Apollo 7 spacecraft into orbit. All assigned mission objectives were met, and no flight anomalies occurred affecting mission accomplishment. A detailed analysis of launch vehicle performance is contained in reference 1.

After launch, the vehicle rolled from 100 to 72 degrees between 00:00:10.3 and 00:00:38.5. The programmed pitch attitude profile was accomplished between 00:00:10.3 and 00:02:14.0, at which time an essentially constant pitch attitude was maintained until the initiation of active guidance 25.3 seconds after separation of the S-IB/S-IVB stages. Shutdown of the S-IB stage engine occurred at 00:02:24.3 (1.0 second earlier than predicted). At S-IB stage engine cutoff, the actual trajectory parameters compared with nominal were 11.2 ft/sec low in space-fixed velocity, 0.02 n. mi. low in altitude, and 0.21 n. mi. long in range.

Separation of the S-IB/S-IVB stages occurred at 00:02:25.6, followed 1.4 seconds later by ignition of the S-IVB stage. S-IVB stage engine cutoff occurred at 00:10:16.8 (2.0 seconds later than predicted).

At S-IVB stage engine cutoff, the actual trajectory parameters compared with nominal were 1.3 ft/sec low in space-fixed velocity, 0.1 n. mi. high in altitude, and 0.6 n. mi. short in range.

Orbital safing of the S-IVB stage was performed successfully, including propellant venting, propellant dump, and stage/engine pneumatic supply dump.

The S-IVB/spaceship combination responded as expected during the period of manual control by the crew. The spaceship/S-IVB separation sequence was initiated at 02:55:02.

5.0 COMMAND AND SERVICE MODULE PERFORMANCE

5.1 STRUCTURES

5.1.1 Structural Loads Analysis

The spacecraft structural loads, as derived from a command module triaxial linear accelerometer, the angle of attack indicator (q-ball) atop the launch escape system, and S-IB engine deflections, were less than the design values for all phases of flight.

Launch release.- Before lift-off, spacecraft lateral loads result from steady-state winds, gusts, unsymmetrical S-IB thrust buildup, and vortex shedding. These external forces cause a large constraining moment and shear at the base of the launch vehicle. Spacecraft loads immediately after lift-off are caused primarily by the sudden release of the spacecraft from this constraining moment and shear.

Calculated interface loads during the launch release phase were compared with predictions (table 5.1-I); the predicted loads were based on maximum expected unsymmetric thrust buildup and on actual launch vehicle bending moments measured prior to launch, including the effects of the 20 to 24-knot peak ground winds measured at the 60-foot level (fig. 5.1-1). Each pair of diametrically opposed S-IB outboard engines, the usual source of unsymmetric thrust buildup excitation, ignited almost simultaneously; therefore, the calculated loads were less than predicted. Vortex shedding was neither predicted nor indicated by the vehicle response at the measured ground wind speeds. Also shown in the table for comparison are the spacecraft design limit for saturn-V launch release.

Maximum dynamic pressure region.- Large values of spacecraft interface loads occur where the product of dynamic pressure and angle of attack is maximum (maximum $q\alpha$). The interface loads (table 5.1-II) were caused primarily by wind-shear induced body bending. The measured winds in this region were light but with large shears (fig. 5.1-3). For comparison, the predicted values and the design limit loads for a Saturn V launch are also included in the table.

End of first stage boost.- The maximum axial acceleration and compression loads in the spacecraft during a Saturn IB launch are normally experienced immediately prior to inboard engine cutoff. Spacecraft interface loads for this condition are compared with predicted values (based on maximum expected axial and lateral accelerations) and design limit loads for Saturn V in table 5.1-III. Axial and lateral accelerations during this period are shown in figure 5.1-4.

S-IB/S-IVB staging.— The S-IB/S-IVB staging operation was accomplished smoothly, and the structural loads were of no consequence. Accelerations during this period are shown in figure 5.1-4.

S-IVB powered flight.— Although the crew reported a slightly "bumpy" S-IVB stage flight, structural loading was insignificant and oscillatory accelerations did not exceed 0.06g in any direction.

Spacecraft operation.— Loads during the service propulsion maneuvers were low, as expected, and structural performance was satisfactory. The maximum steady-state axial acceleration during any maneuver was 0.85g, during the eighth service propulsion maneuver.

Entry.— The peak acceleration during entry was 3.41g, well below the 20g structural design limit.

5.1.2 Vibration

Sufficient flight vibration data were obtained during launch and during a service propulsion maneuver to permit a comparison between the flight vibration environment and the design criteria. Power spectral density analyses were made on all vibration measurements for selected times and were compared with the design criteria. The measured vibrations were less than the criteria except for the service propulsion helium pressurization panel and the service module forward bulkhead (see figs. 5.1-5, 5.1-6, and 5.1-7). The data at the lower frequencies are not shown in the figures because they are invalid. This conclusion is based on an analysis of the power spectral density data during quiescent periods prior to first stage ignition.

Helium pressurization panel vibration measurements were made in three axes: X, radial, and tangential (fig. 5.1-8). The tangential vibration at lift-off (fig. 5.1-5) exceeded the criteria at 190 Hz; however, a 10-second test at a level 4 dB greater than the criteria shown is conducted on Apollo systems to simulate transonic flight and covers the 190 Hz peak.

The X-axis measurement (fig. 5.1-6) on the helium pressurization panel showed characteristics completely different from the radial and tangential data and exceeded the criteria by significant margins. Throughout atmospheric flight, the X-axis measurement produced unusual data, typically shown in figure 5.1-9, with a strong 45 Hz oscillation which periodically became assymetrical. Note in figure 5.1-9 that the frequency content in the X-axis is greatly different than that in the radial and tangential directions (figs. 5.1-5 and 5.1-6). Typically, the frequency content in the X, radial, and tangential directions would be expected to be similar. The data suggest structural deflections at the

X-axis transducer of about 0.20-inch at lift-off. Deflections of this magnitude and frequency along the X-axis could produce damage to the structure or the pressurization system. However, pressurization system operation, including the high-pressure valves and plumbing mounted on the panel, operated normally throughout the 10.8-day flight. Furthermore, no other flight data exhibited this response at 45 Hz with magnitudes near the level observed for the one transducer. For example, the X-axis transducer located on the hydrogen tank shelf (see fig. 5.1-8) did not have this type of response. The 45 Hz response is therefore unique to this one measurement. The examination of ground test data and structure showed no mechanism that could produce the motion shown in figure 5.1-9. Postflight tests on similar panels are inconclusive as to the source of this disturbance. However, a structurally sound panel does not exhibit the noted vibration characteristics. Because of this and the fact that the helium system did not exhibit a malfunction or leakage, the panel is considered to be structurally sound for the vibration environment. The cause of the noted characteristics in the data can not be explained. In any event, either the data are not valid, or the panel and/or its attached items were not proper.

As a result of this unusual response, all subsequent service modules will be examined for proper helium panel installation. During postflight tests conducted to determine the cause of this response, improper clearance between three tubing clamps on the back side of this panel and the radial beam shear web was discovered. This situation has been corrected on subsequent spacecraft by bonding a rubber bearing pad on the radial beam web at each tubing clamp location to attenuate any impact vibrations.

Vibration of the service module forward bulkhead exceeded the qualification level by significant margins (fig. 5.1-7). As a result, the vibration criteria for this bulkhead were reviewed, and ground test results were utilized to revise these criteria where appropriate. The revision encompassed the measured amplitude with the exception of the peak at about 325 Hz. Equipment in this area will be requalified by subjecting a 180-degree segment of a service module to an acoustic field.

Vibration levels during the service propulsion engine operation and entry were low, as expected.

TABLE 5.1-I.- MAXIMUM SPACECRAFT LOADS AT LIFT-OFF

Interface	Load	Predicted	Calculated from flight data	Design limit
Launch escape system/command module	Bending moment, in-lb	1 430 000	1 260 000	3 100 000
	Axial force, lb*	-14 300	-12 600	-16 200
Command module/service module	Bending moment, in-lb	1 710 000	1 490 000	4 100 000
	Axial force, lb*	-30 900	-30 200	-36 700

*Negative sign indicates compression.

TABLE 5.1-II.- SPACECRAFT LOADS AT MAXIMUM q_a

Interface	Condition	Predicted using measured winds aloft	Calculated from flight data	Design limit
Launch escape system/command module	Flight time, sec	73.5	72.8	75.6
	Mach no.	1.4	1.4	1.3
	Dynamic pressure, psf . . .	654	663	686
	Angle of attack, deg	1.2	1.7	10.5
	Maximum q_a , psf-deg	785	1127	7200
	Bending moment, in-lb	450 000	700 000	1 100 000
	Axial force, lb*	-22 000	-21 000	-32 000
	Bending moment, in-lb	620 000	930 000	2 200 000
	Axial force, lb*	-81 000	-81 000	-96 100
	Bending moment, in-lb	1 700 000	1 500 000	9 310 000
Service module/adapter	Axial force, lb*	-121 000	-121 000	-204 000
	Bending moment, in-lb	4 100 000	3 800 000	29 010 000
Adapter/instrument unit	Axial force, lb*	-151 000	-147 000	-295 000

*Negative sign indicates compression

TABLE 5.1-III.- MAXIMUM SPACECRAFT LOADS AT END OF FIRST STAGE BOOST

Interface	Load	Maximum predicted	Calculated from flight data	Design limit
Launch escape system/command module	Axial acceleration, g	4.41	4.3	5.0
	Lateral acceleration, g	0.1	0.04	0.11
	Bending moment, in-lb	214 000	87 000	235 000
	Axial force, lb	-39 500	-38 500	-44 700
Command module/service module	Bending moment, in-lb	690 000	484 000	773 000
	Axial force, lb	-99 000	-96 500	-112 000
Service module/adapter	Bending moment, in-lb	1 717 000	1 182 000	3 574 000
	Axial force, lb	-188 000	-183 000	-370 000
Adapter/instrument unit	Bending moment, in-lb	3 200 000	1 708 000	6 712 000
	Axial force, lb	-207 000	-202 000	-551 000

NASA-S-68-6256

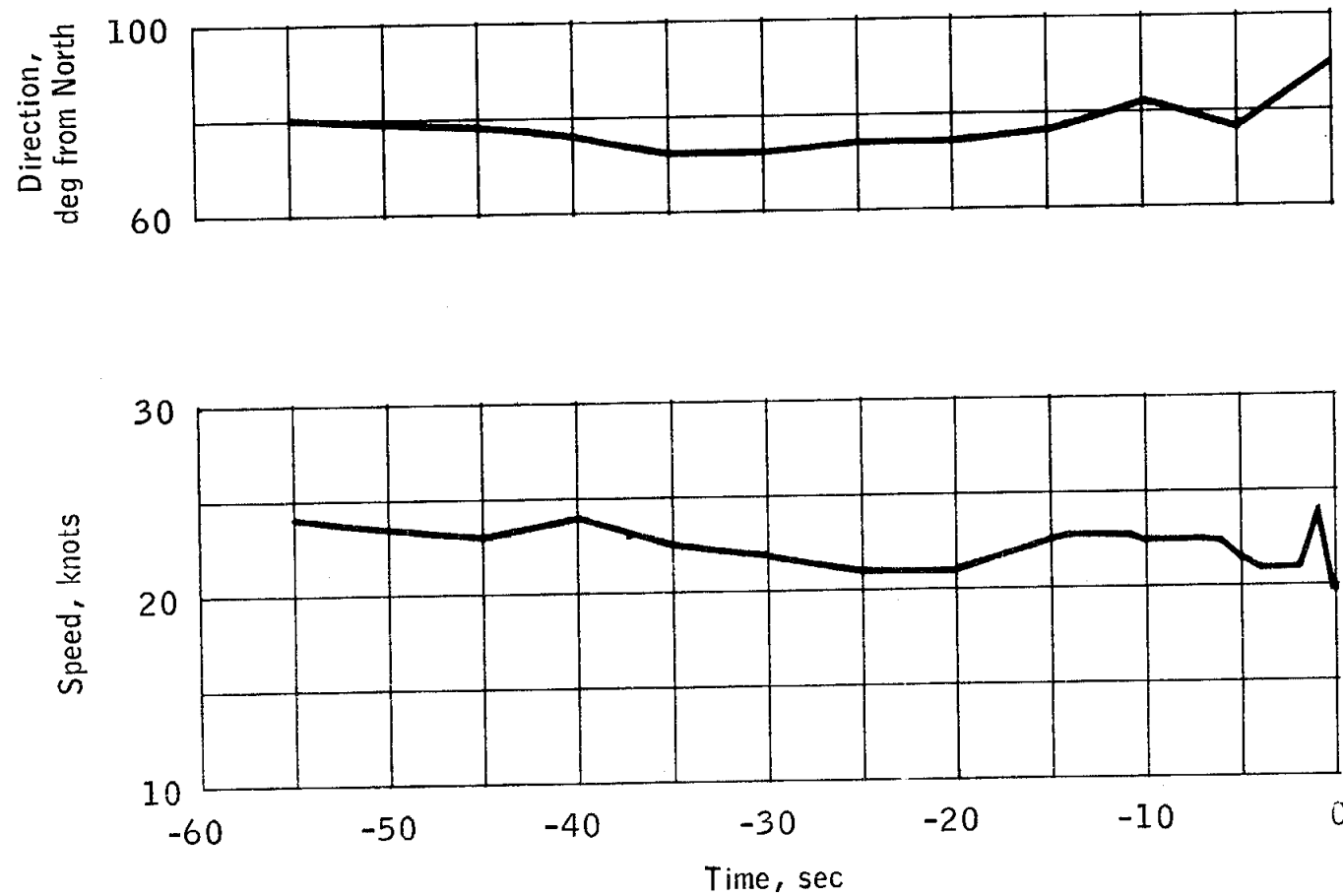


Figure 5.1-1.- Speed and direction of peak ground winds
at the 60-foot level at lift-off.

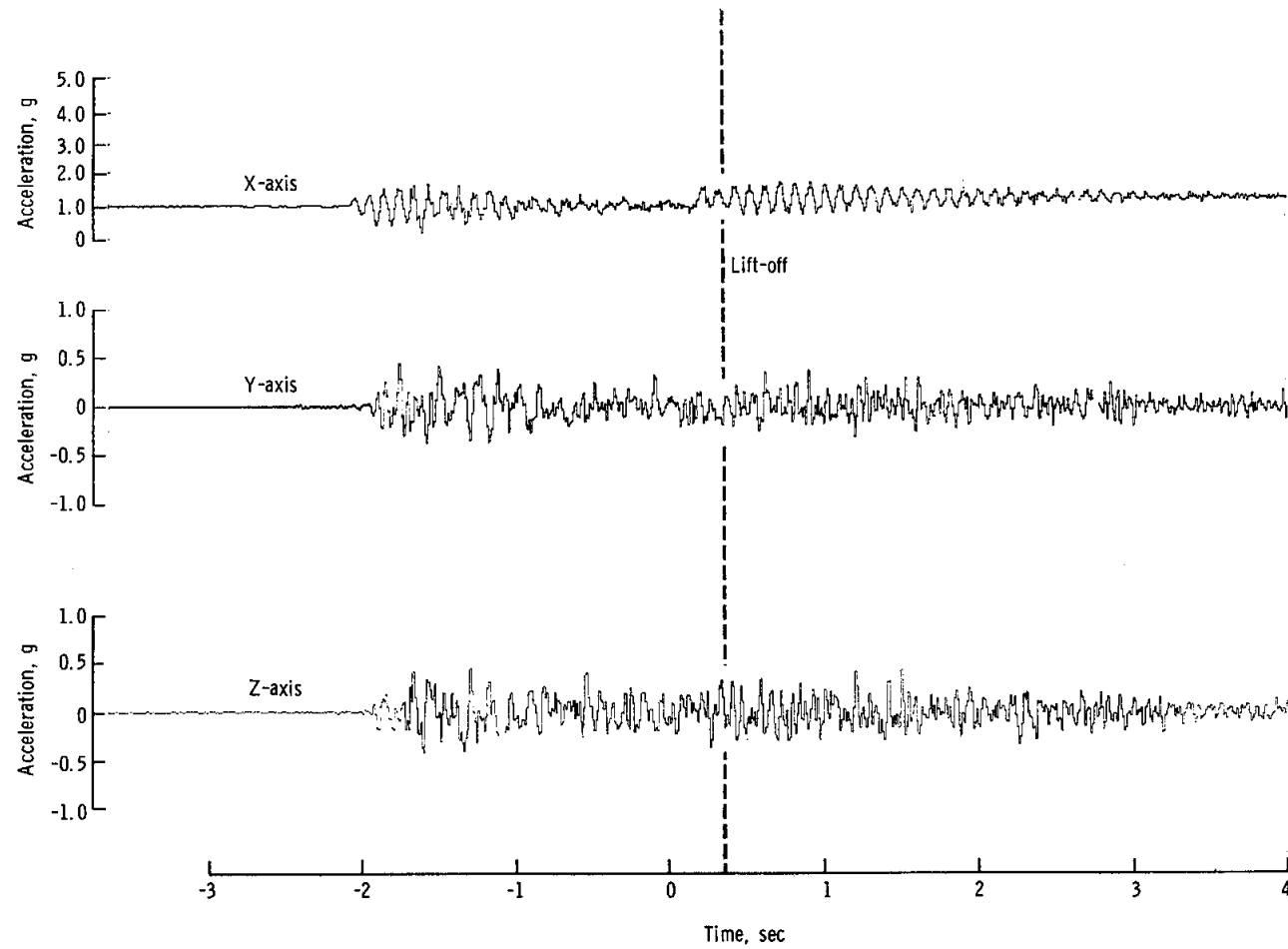
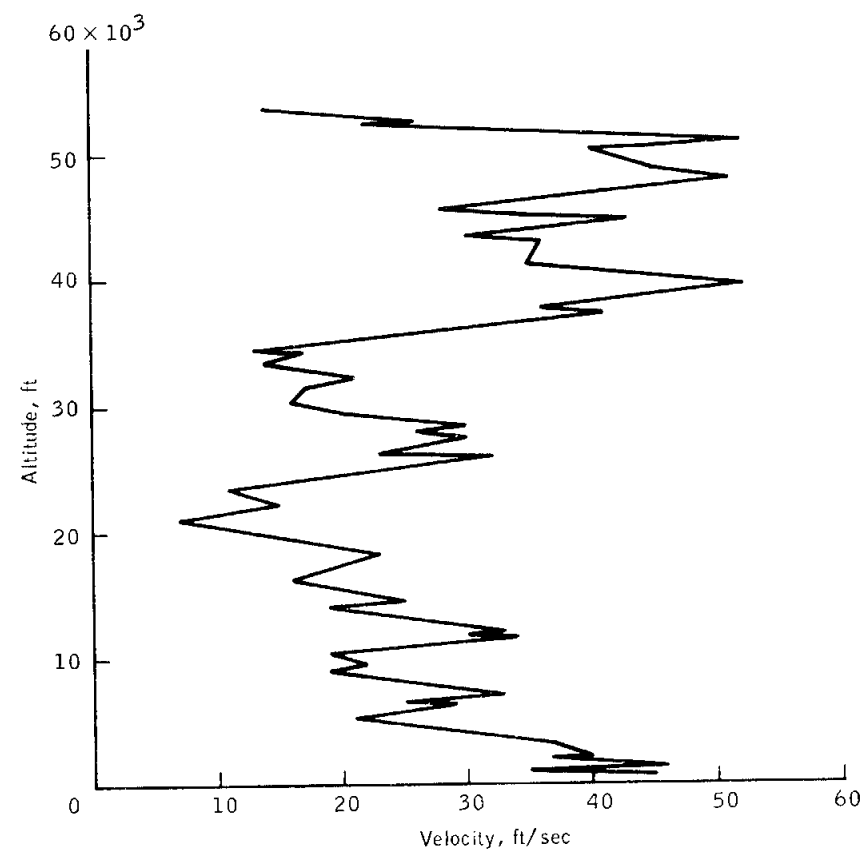
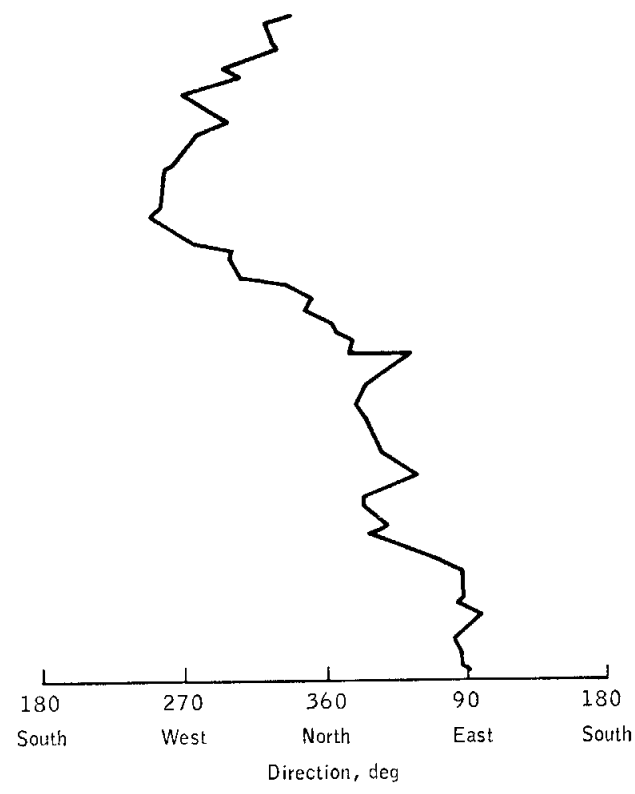


Figure 5.1-2. - Command module acceleration at lift-off.

NASA-S-68-6258



(a) Velocity.



(b) Direction.

Figure 5.1-3.- Scalar winds at lift-off.

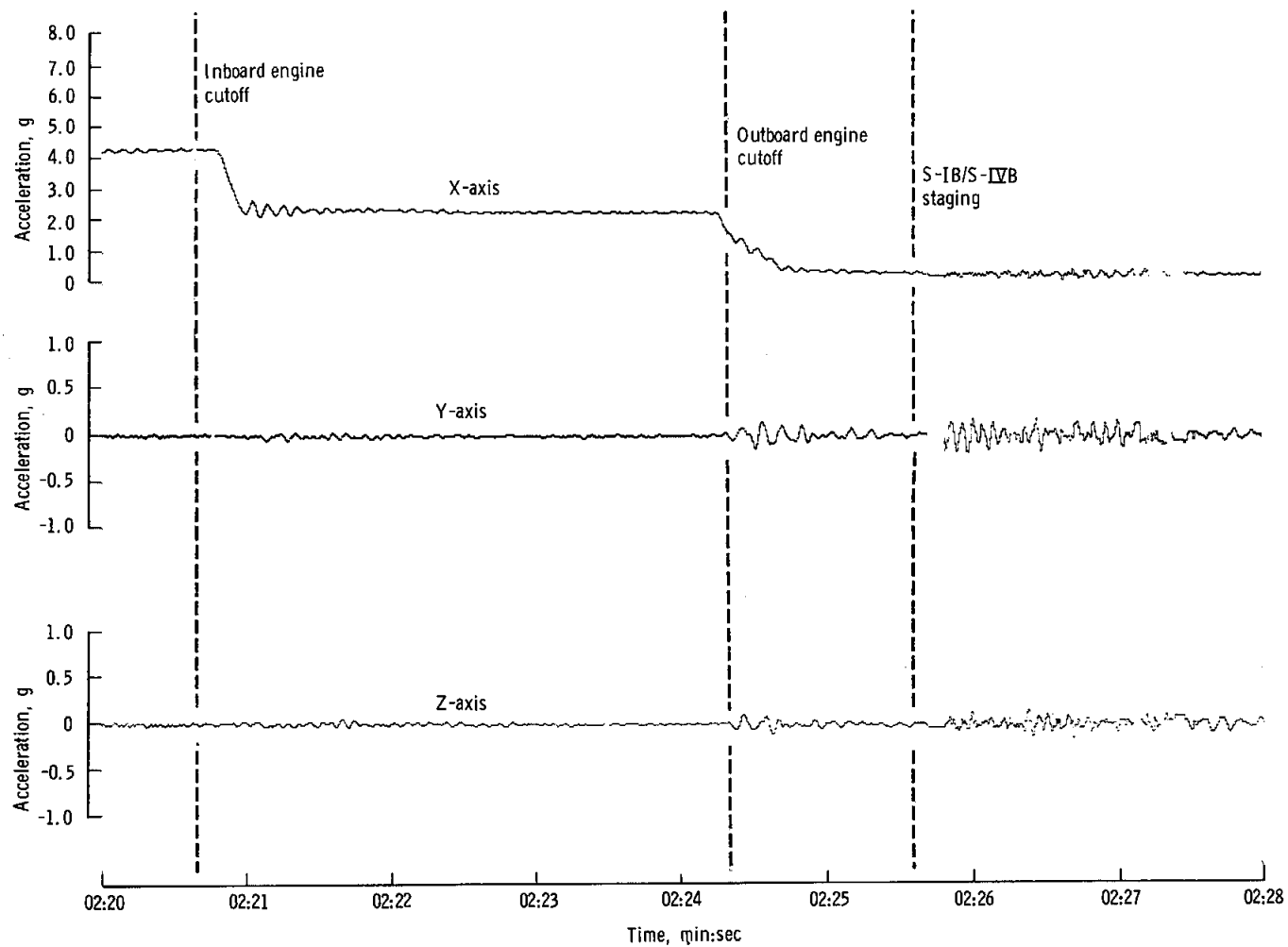


Figure 5.1-4. - Command module accelerations at S-IB cutoff and staging.

NASA-S-68-6260

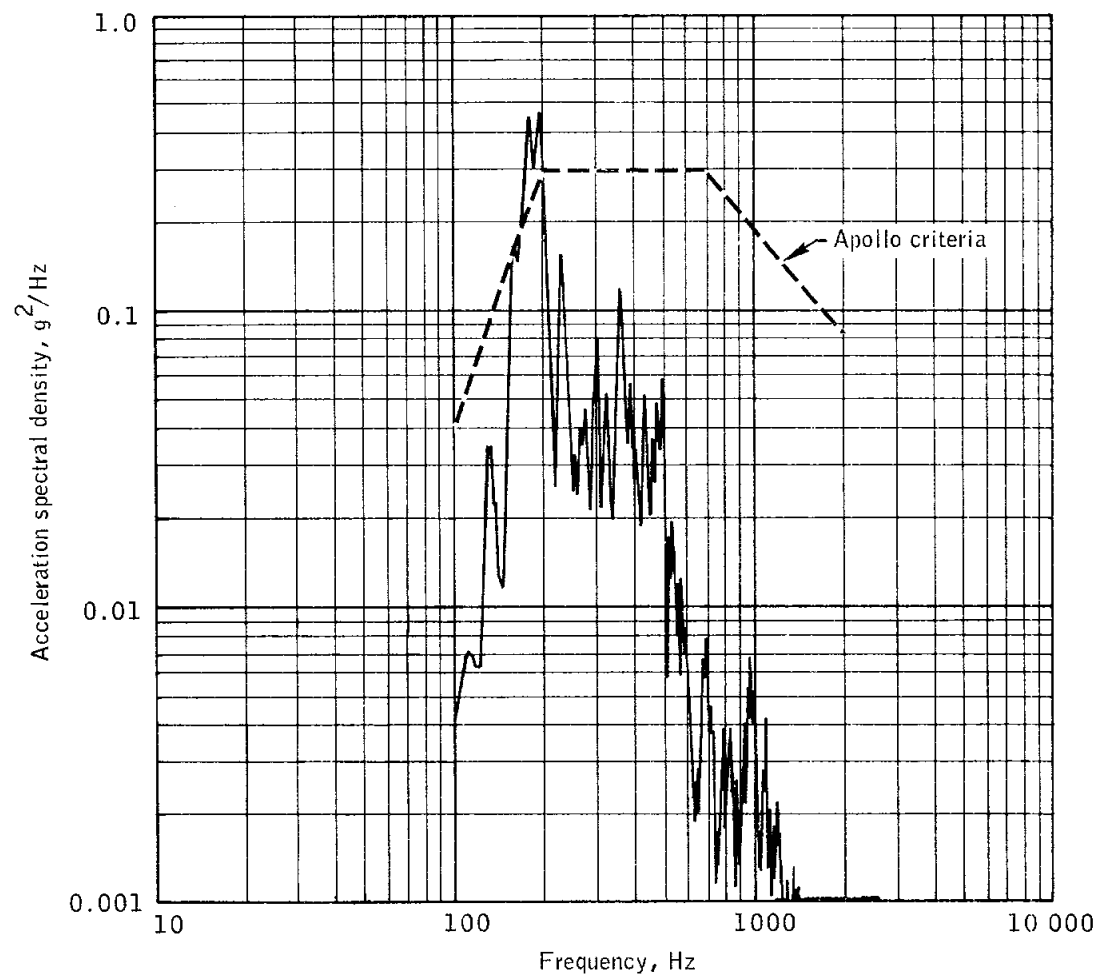
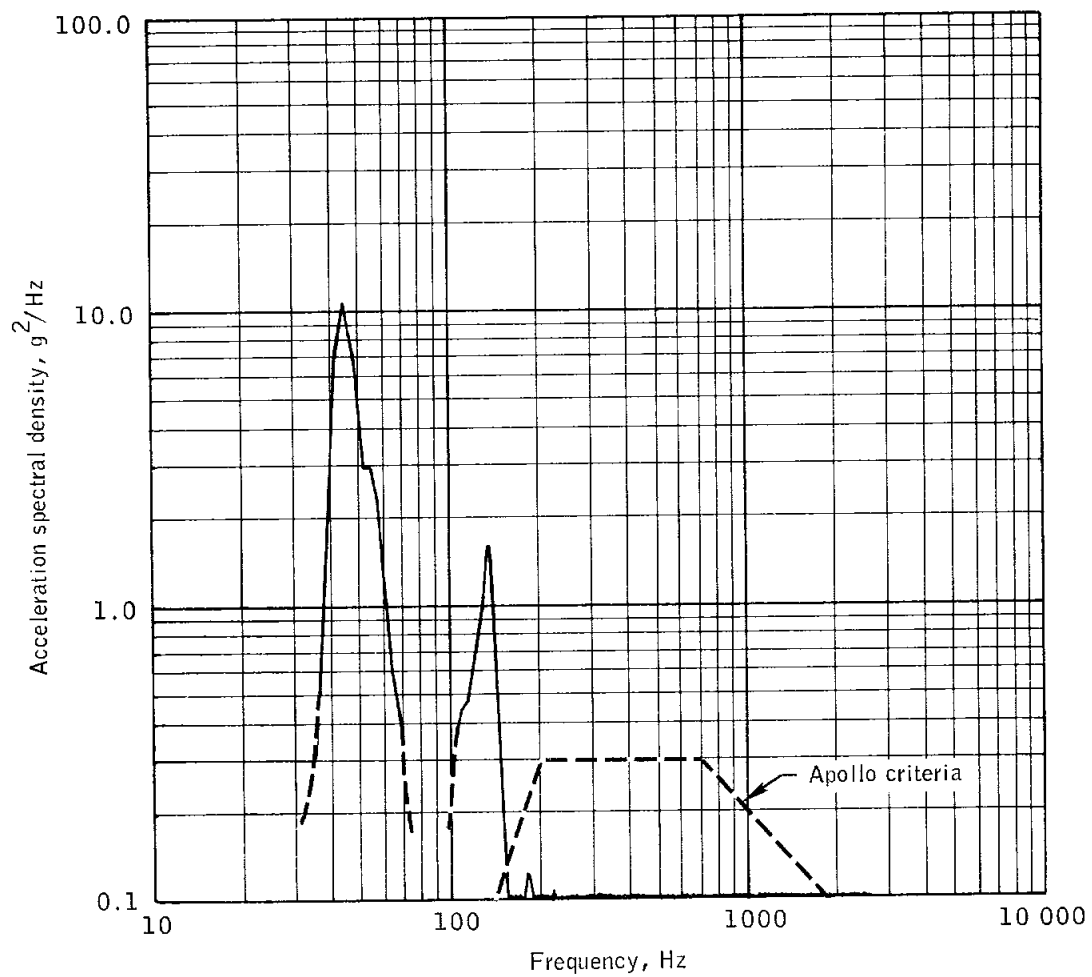


Figure 5.1-5.- Service module helium pressurization panel tangential vibration at lift-off (-1 to +1 second).

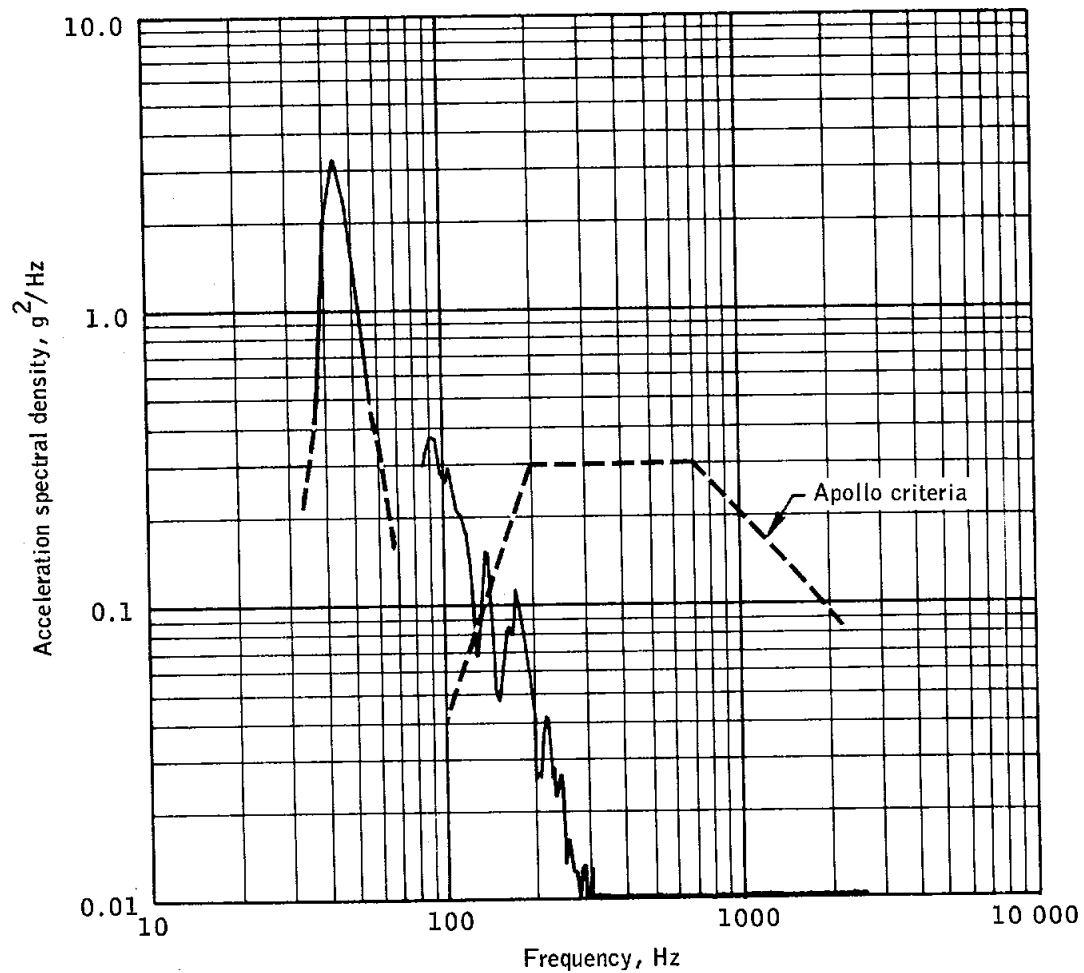
NASA-S-68-6261



(a) Lift-off (-1 to +1 second).

Figure 5.1-6.- Service module helium pressurization panel, X-axis vibration.

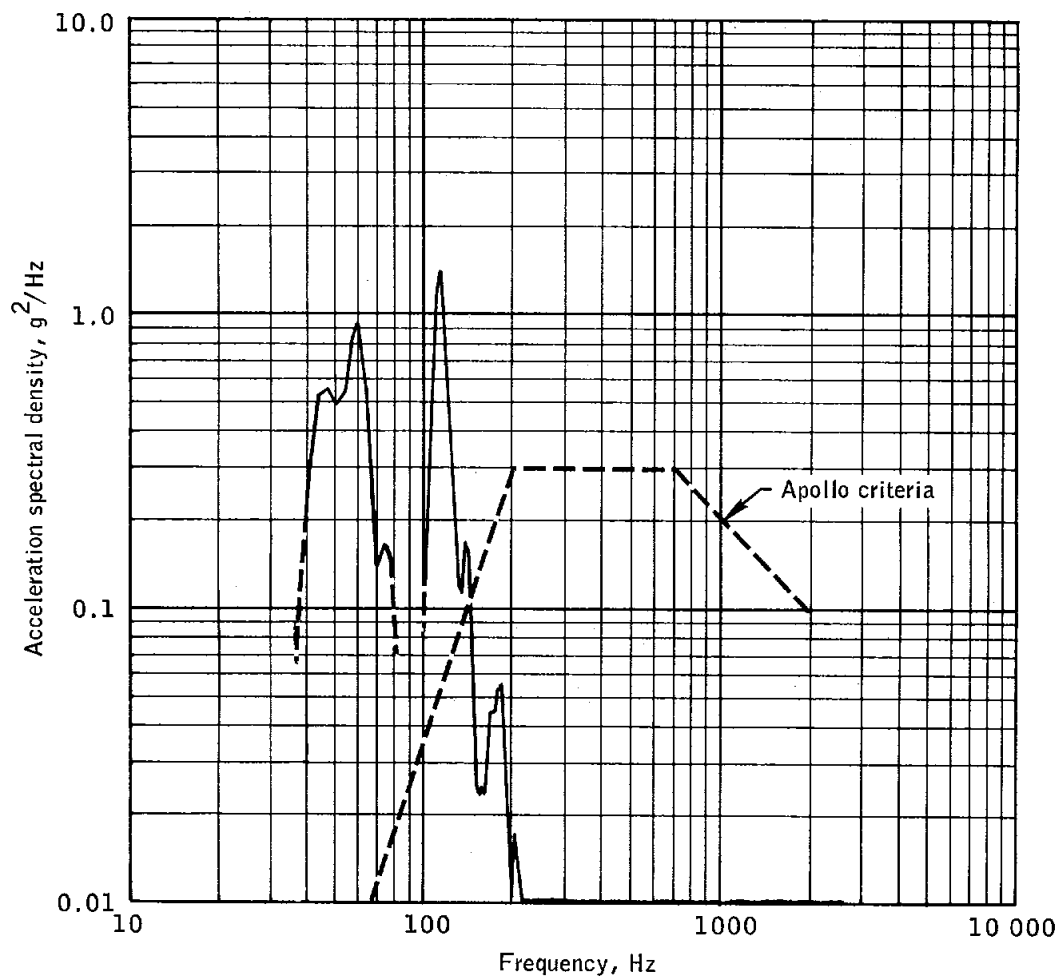
NASA-S-68-6262



(b) Transonic (58 to 60 seconds).

Figure 5.1-6.- Continued.

NASA-S-68-6263



(c) Maximum dynamic pressure (77 to 79 seconds).

Figure 5.1-6.- Concluded.

NASA-S-68-6264

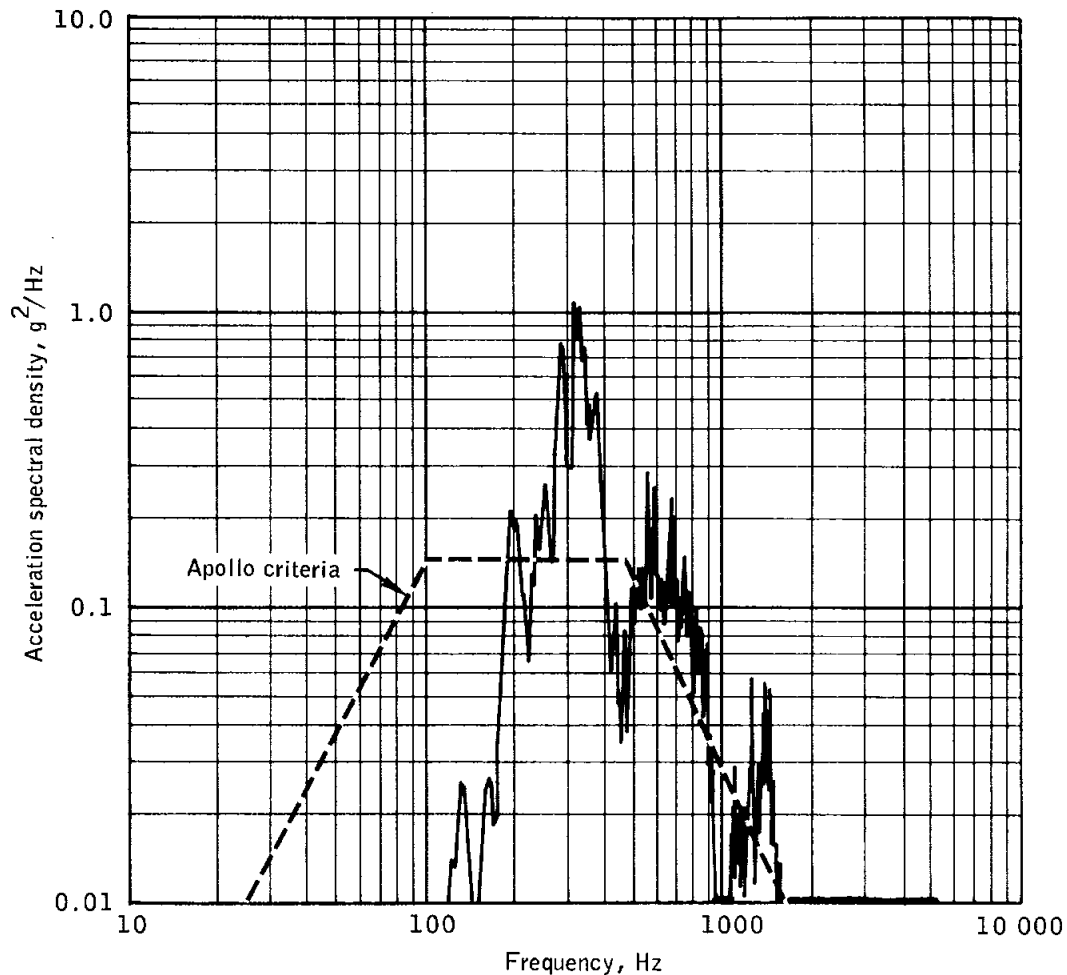


Figure 5.1-7.- Service module forward bulkhead vibration
at lift-off (-1 to +1 second).

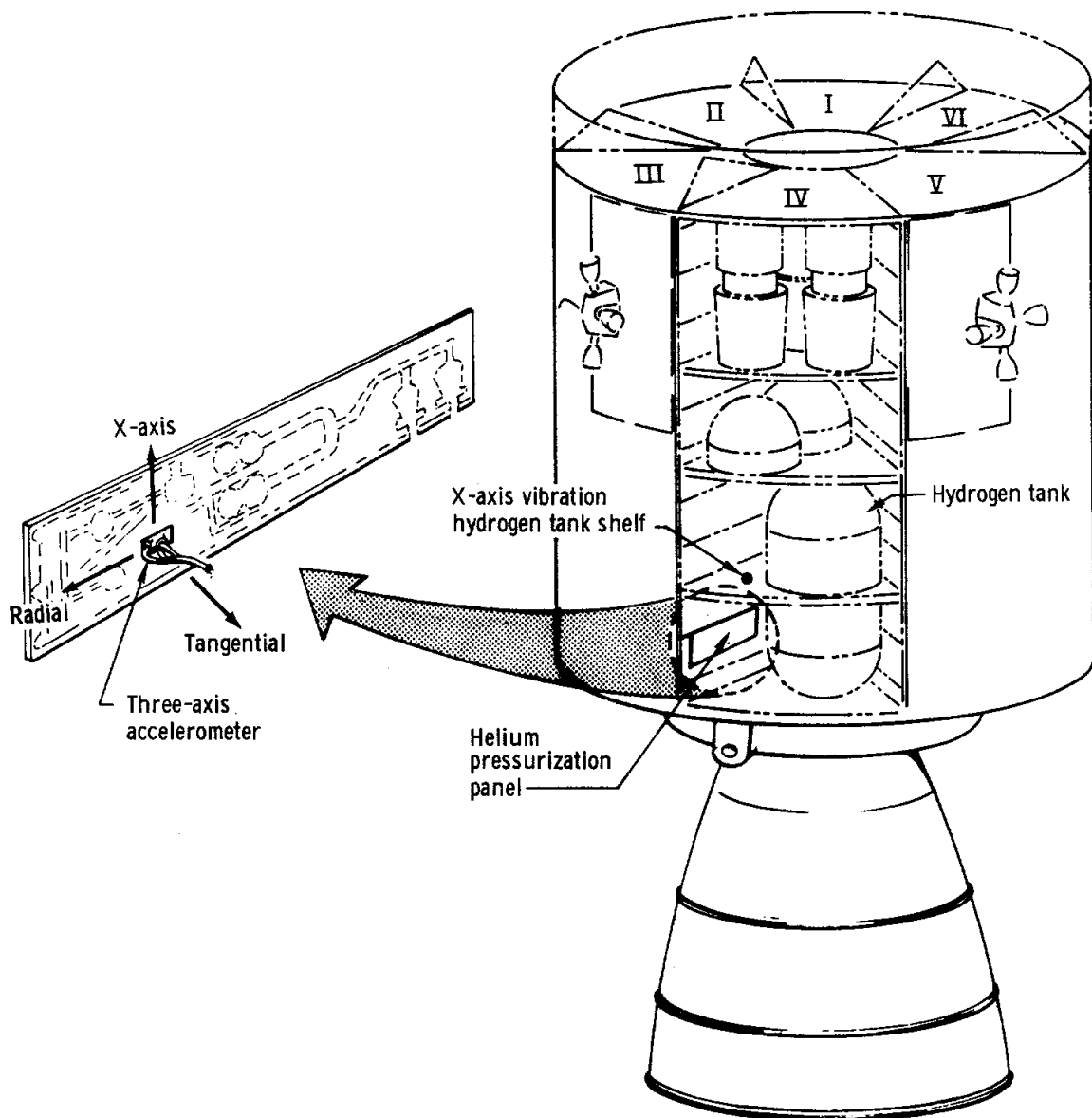


Figure 5.1-8. - Helium pressurization panel instrumentation.

NASA-S-68-6427

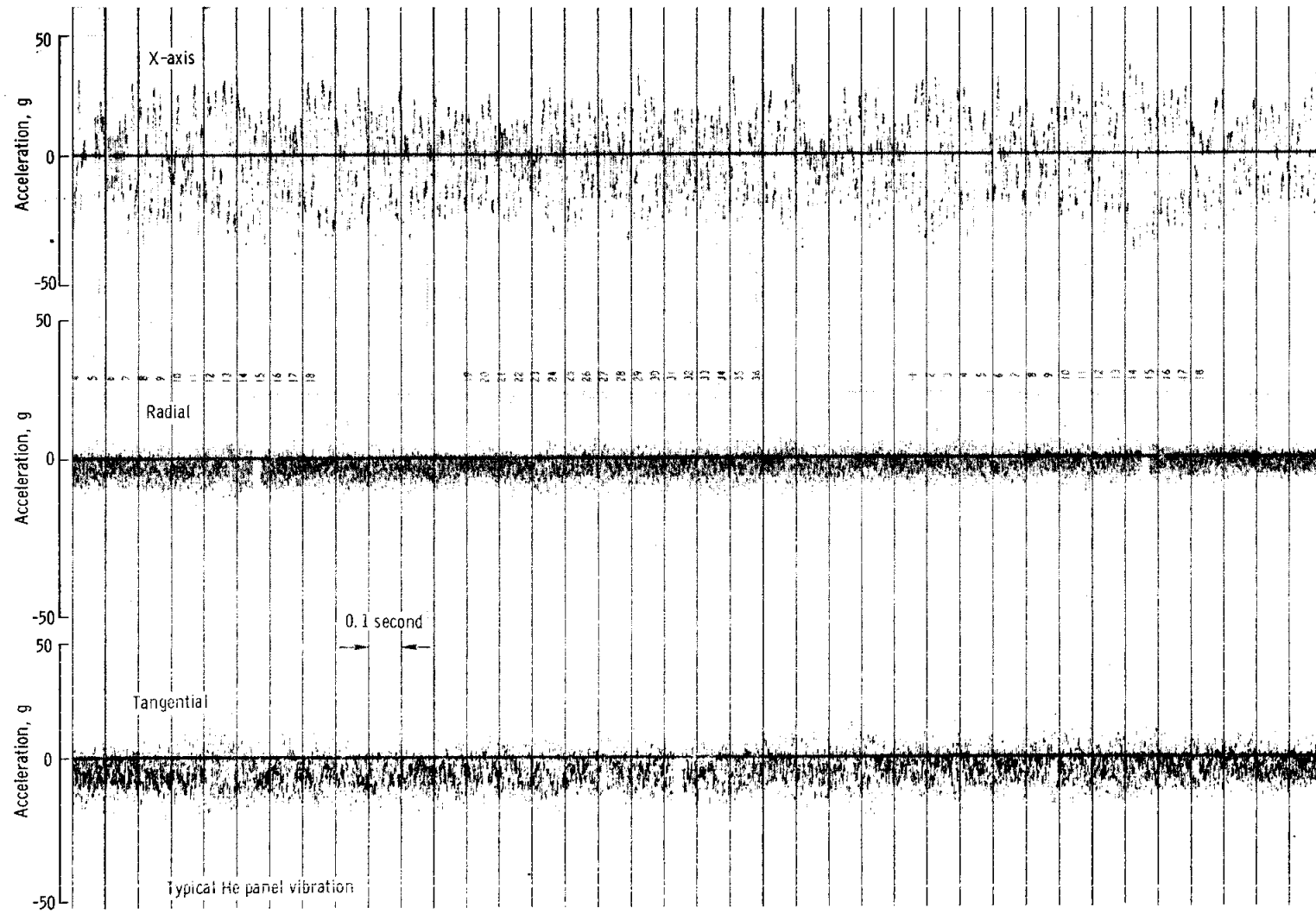


Figure 5.1-9. - Helium pressurization panel vibration at lift-off (typical for launch phase).

5.2 AERODYNAMICS

As noted in all previous flights, the trend for the hypersonic trim lift-to-drag ratio to increase with decreasing Mach number was observed for this flight. The flight-derived lift-to-drag ratio was within the predicted uncertainty band of ± 0.03 from the beginning of entry to a Mach number of 4.0.

The predicted and flight-derived lift-to-drag ratios and the estimated trim angle of attack are shown in figure 5.2-1.

Accelerometer data and entry position and velocity information were used to obtain the flight lift-to-drag ratios. The accelerometer data were corrected for known preflight bias and scale factor errors. The estimated trim angle of attack was obtained from the flight-derived lift-to-drag ratio and wind-tunnel variation of lift-to-drag ratio with angle of attack.

The third service propulsion maneuver established an orbit with a perigee altitude of 90.3 n. mi. At 98:39:00, the Commander reported an external torquing of the spacecraft at an attitude with the +X axis vertical (assumed to be a 90 degree angle-of-attack). Oscillograph data indicate a pitch rate of -0.15 deg/sec at 98:39:15 and -0.32 deg/sec at 98:42:45 (see fig. 5.2-2). The state vector at 98:39:15 was:

Latitude, deg north	26.2
Longitude, deg west	89.2
Altitude, n. mi.	89.5
Velocity, ft/sec	25 739.9
Flight-path angle, deg	-0.08
Heading angle, deg	107.9

An evaluation of these effects was made using the preflight predicted free-molecular-flow aerodynamic data and a Jacchia dynamic, non-rotating atmospheric model (see ref. 2) in a six degree-of-freedom computer program to predict the vehicle rates.

Propagating the state vector forward using approximated center-of-gravity and inertia data resulted in a peak aerodynamic torque of 1.3 ft-lb, and the predicted rate time history is presented in figure 5.2-2. The close correlation between the predicted and the measured rates indicates that the free-molecular-flow aerodynamic model is reasonably valid.

The maximum aerodynamic torque which can occur at this altitude is approximately 2.2 ft-lb, which can produce pitch rates on the order of 1 deg/sec.

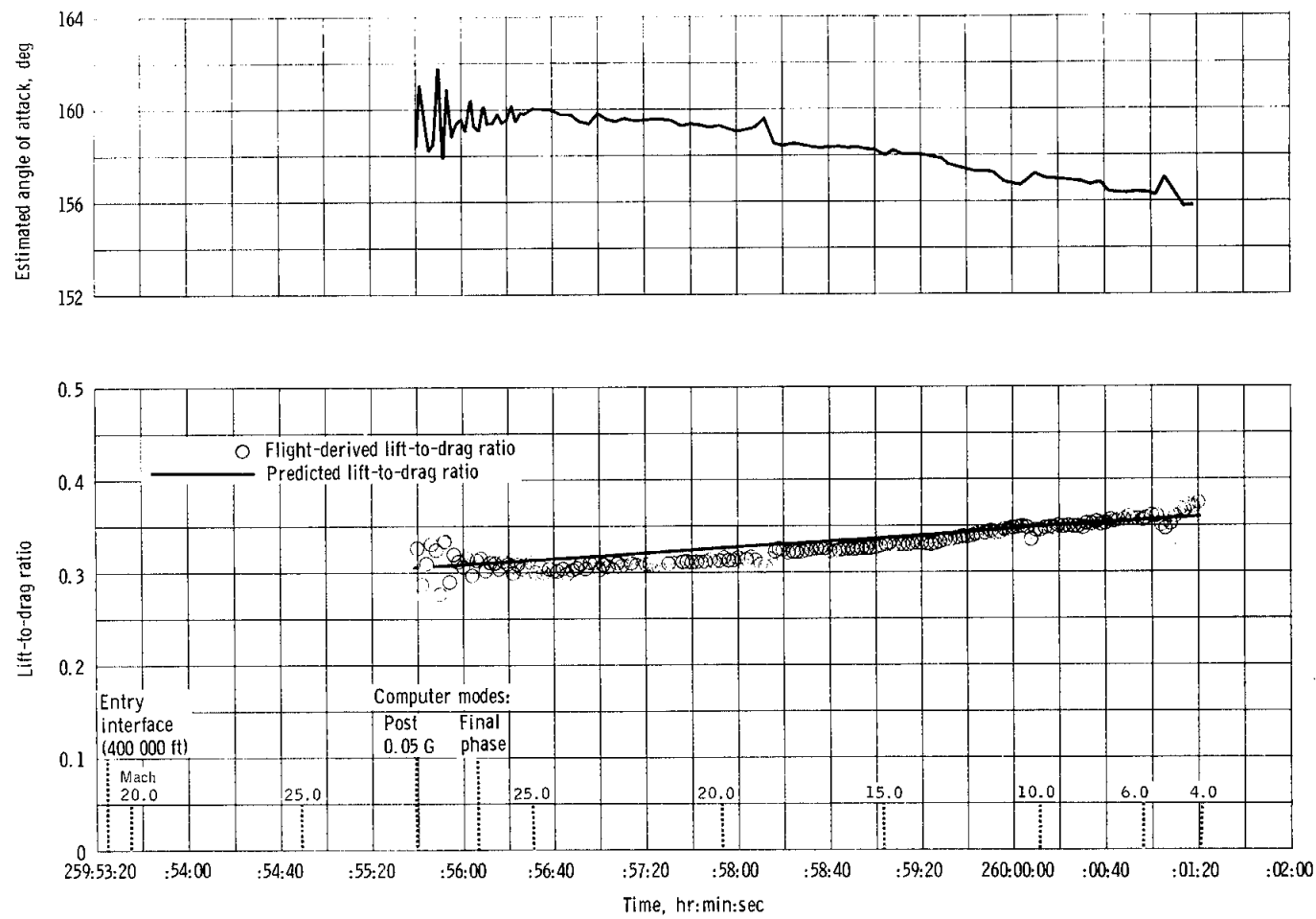


Figure 5.2-1. - Command module hypersonic entry aerodynamics.

NASA-S-68-6266

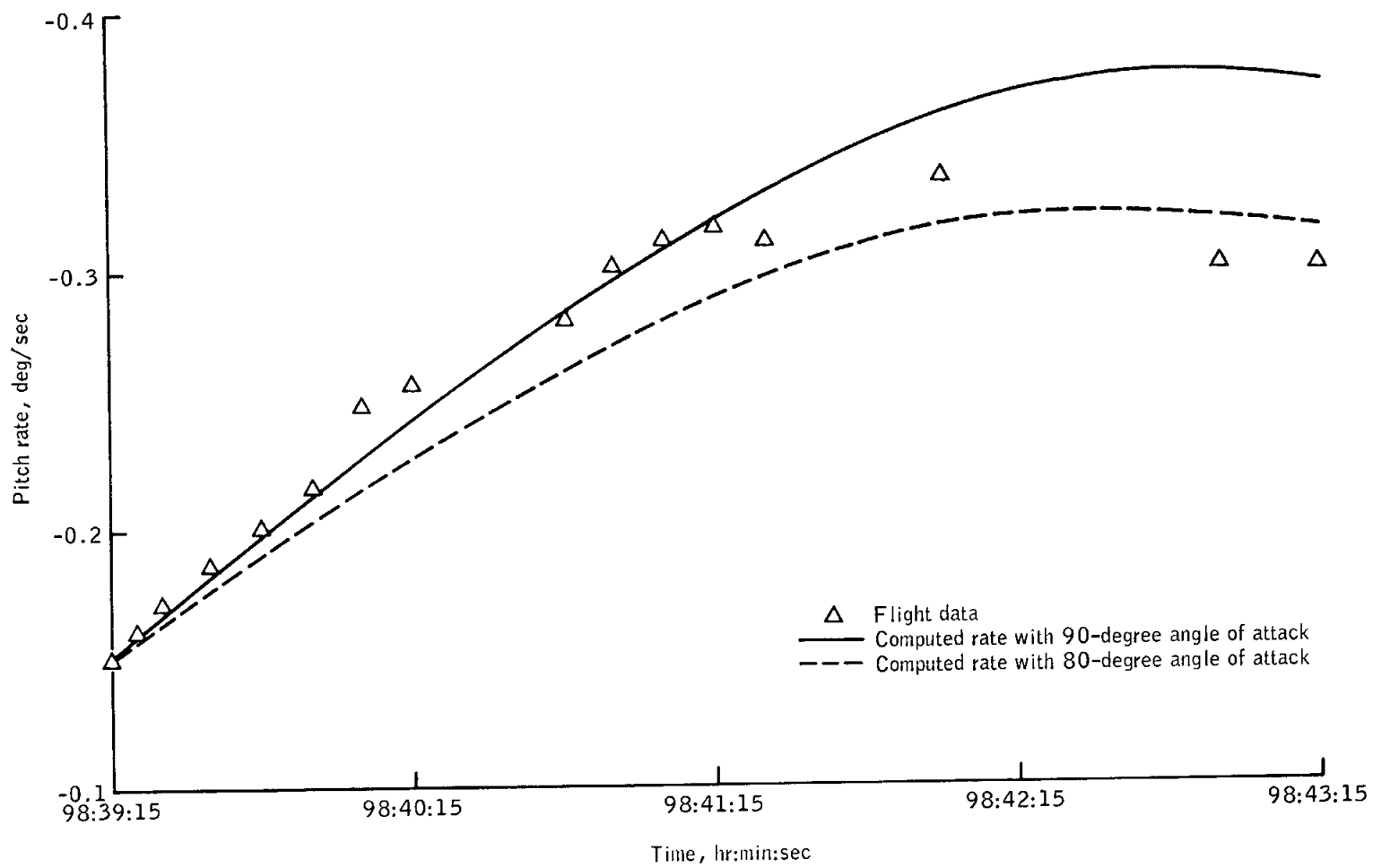


Figure 5.2-2.- Aerodynamic torquing effects.

5.3 THERMAL CONTROL

This section discusses thermal response for those areas which lacked active temperature control. The spacecraft orientation during the mission produced a thermal environment which resulted in a general cooling trend. Measured temperatures of passive elements are shown in figures 5.3-1, 5.3-2, and 5.3-3.

The temperature response for the service propulsion tank and reaction-control helium tank for each bay is shown in figure 5.3-1. The service-propulsion propellant sump tanks remained partially filled throughout the mission and had less temperature fluctuation than the storage tanks because of the damping effect of the propellant. The temperature response for the helium tank in each reaction control quad is shown in figure 5.3-2. The helium tanks in bays 3 and 5 were affected by the heat from the fuel cells, as expected; the primary fuel tanks in bays 3 and 5 were also affected by the fuel cell heat but to a lesser degree. The primary oxidizer tank temperatures for bays 2 and 5 were higher than those for bays 3 and 6 because of the effects of propellant in the service propulsion tanks (see fig. 5.3-2).

A general cooling trend was followed throughout the mission (figs. 5.3-1 and 5.3-2) and the spacecraft orientation with respect to tank bays appeared to vary randomly as indicated by the changes in temperature (increases and decreases at any one time). During the cold-soak orientation from 168 to 172 hours, all tank temperatures decreased. Overall, the incremental changes were about as anticipated, indicating proper performance of service module insulation.

The service propulsion feedline temperatures (fig. 5.3-3) remained relatively stable during the mission and showed a general cooling trend except for the time from 221 to 227 hours when the service propulsion feedline and engine heaters were operated for a relatively long period. The heater operation affected only the engine feedlines and not the distribution lines.

The helium tanks for the command module reaction control system, which were strongly influenced by the temperate cabin environment, maintained a moderate environment (fig. 5.3-3). The command module ablator temperatures remained between 3° and 91° F; this range was slightly warmer than expected.

NASA-S-68-6267

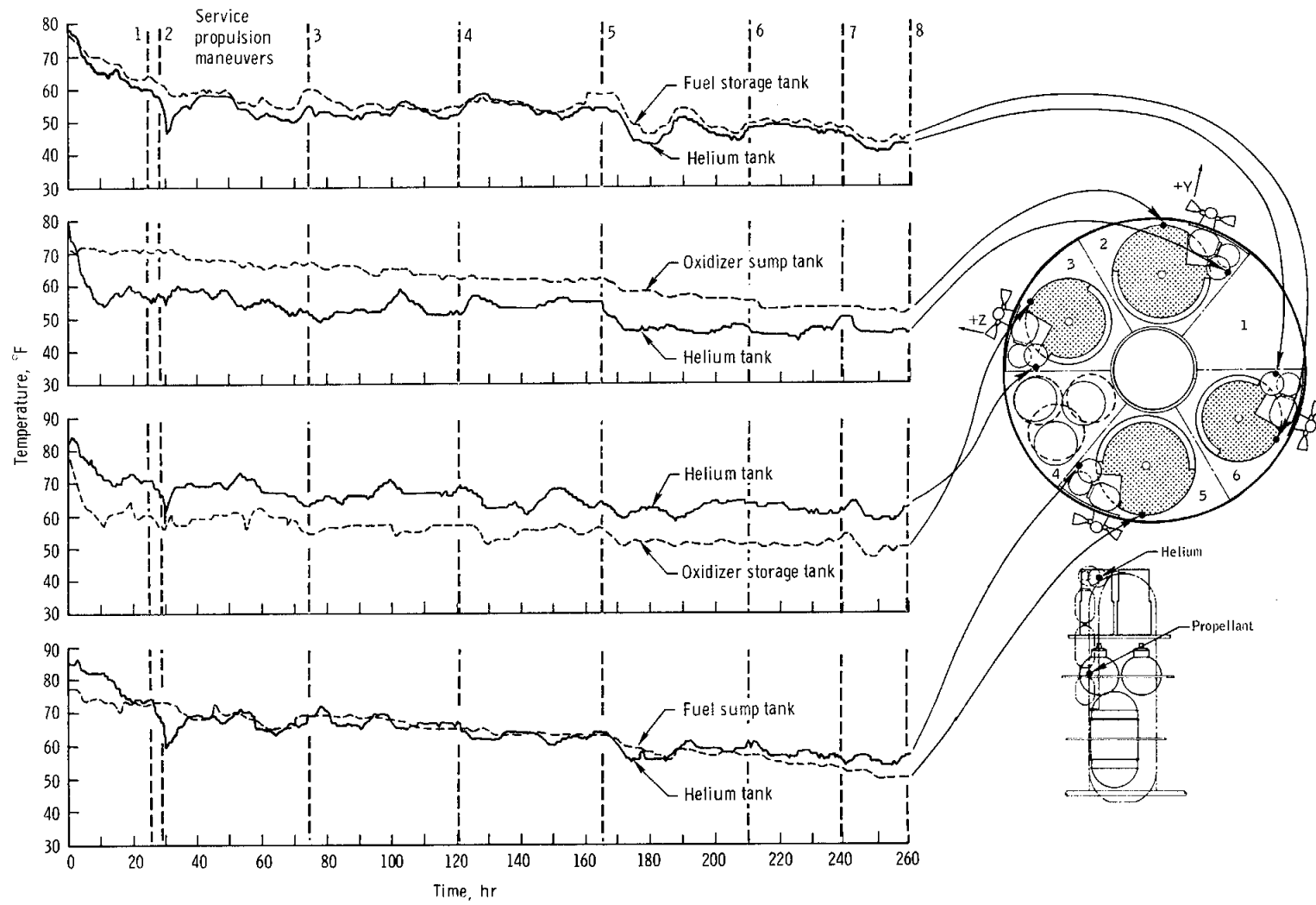


Figure 5.3-1. - Temperatures on service module reaction control system helium tanks and service propulsion propellant tanks.

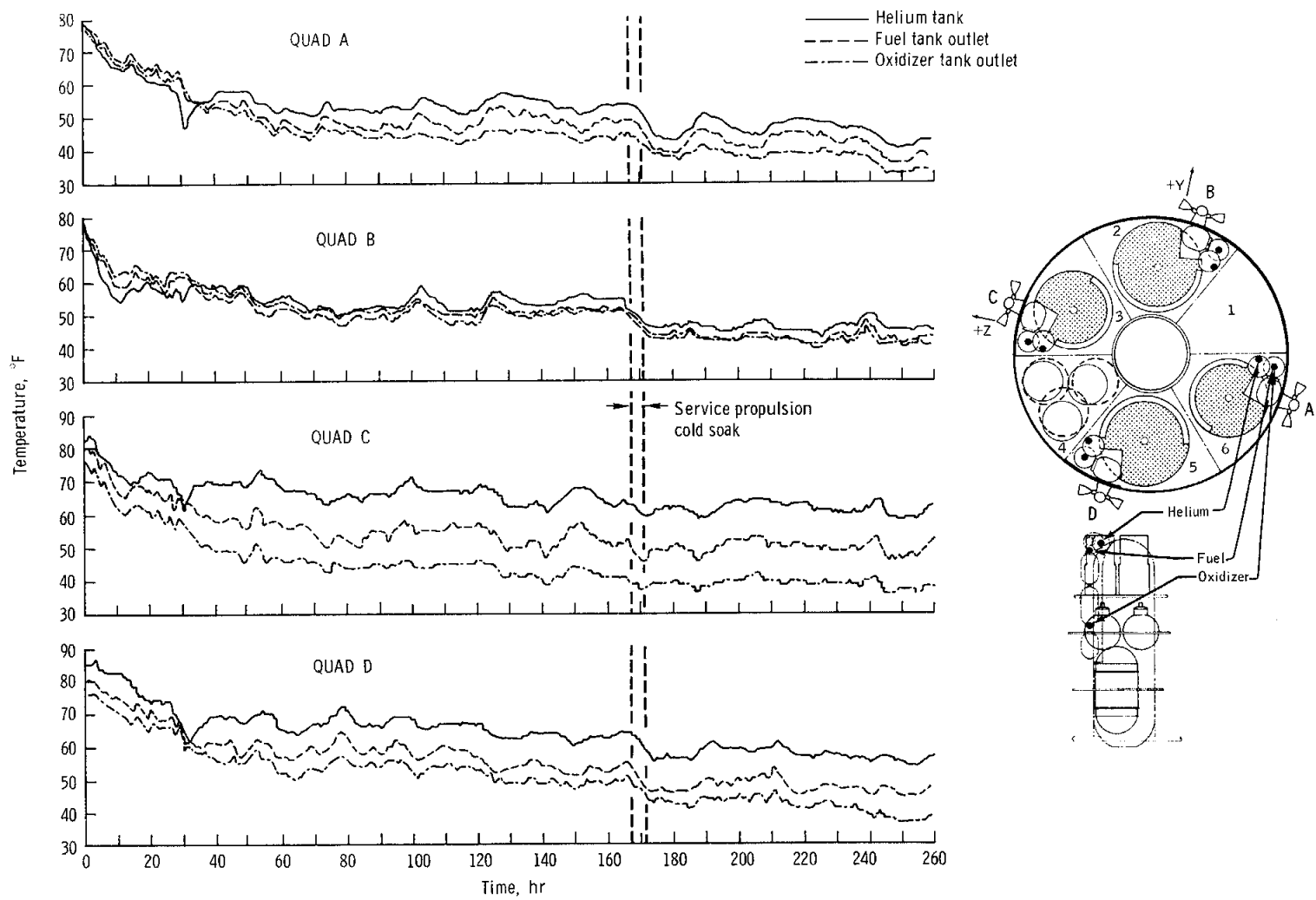


Figure 5.3-2. - Temperatures of service module reaction control system helium tank and primary fuel and oxidizer tank outlets.

NASA-S-68-6269

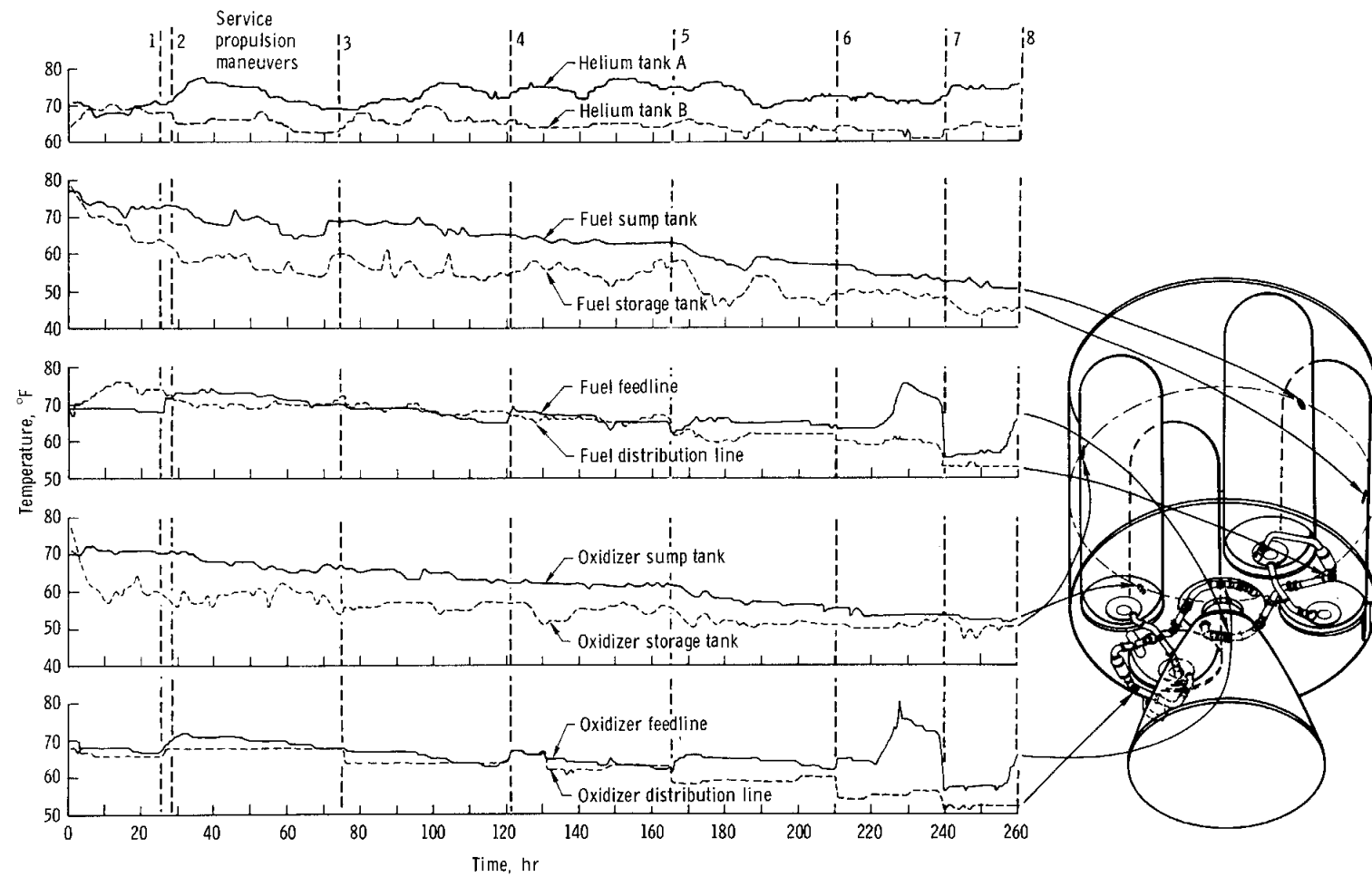


Figure 5.3-3. - Temperatures of command module reaction control system helium tanks and service propulsion propellant tanks and feedlines.

5.4 THERMAL PROTECTION

The forward compartment thermal environment would have been satisfactory for a lunar return mission, based on preliminary integrated heating data. The forward heat shield was not recovered, preventing examination of the temp-plates (temperature indicators), and prior to forward heat shield jettison, the flat apex temperature data were lost because the tape recorder reached the end of usable tape.

The aft heat shield (fig. 5.4-1) was charred to a depth of approximately 0.6 inch from the original surface at the stagnation point, and ablative surface loss was estimated to be 0.05 inch. The center and downstream side of the aft heat shield charred approximately 0.4 inch in depth with an estimated 0.07-inch surface loss. The depth of the 1000° F isotherm closely agrees with the char interface measurements. The temperatures measured in depth at five locations from the geometric center of the aft heat shield are shown in figure 5.4-2. The erratic temperature data are indicative of spacecraft oscillations. The maximum temperatures measured at three locations, as a function of depth, are shown in figure 5.4-3. By extrapolation of these temperatures to the apparent surface, an approximate surface temperature can be obtained.

The crew compartment heat shield experienced low heating, as expected for an earth orbital entry. The thermal control coating on the plus-Z windward side was burned off and slightly charred. The coating remained attached to the lee side with no signs of hot spots. The white paint on the forward hatch was yellowed, and the two nylon handles were fused and partially disintegrated. The temperatures measured in depth on the crew compartment heat shield are shown in figure 5.4-4 and on the forward hatch in figure 5.4-5. Because the thermocouples in a given stack are at various depths in the ablator, they indicate the temperature gradient through the ablator prior to entry. In figure 5.4-5(a), the thermocouple 0.5 inch from the ablator surface rises to 250° F and then drops to about 25° F before rising again. This region on the windward side of the spacecraft experienced separated flow and reduced heating for a short time, and the thermocouple was cooled by the colder ablator in depth.

The thermal protection system performed well during the mission. The responses of the thermocouples and the calorimeters indicate a very erratic motion of the spacecraft during entry; the entry is discussed in more detail in section 3.0 and 5.16.

NASA-S-68-6270

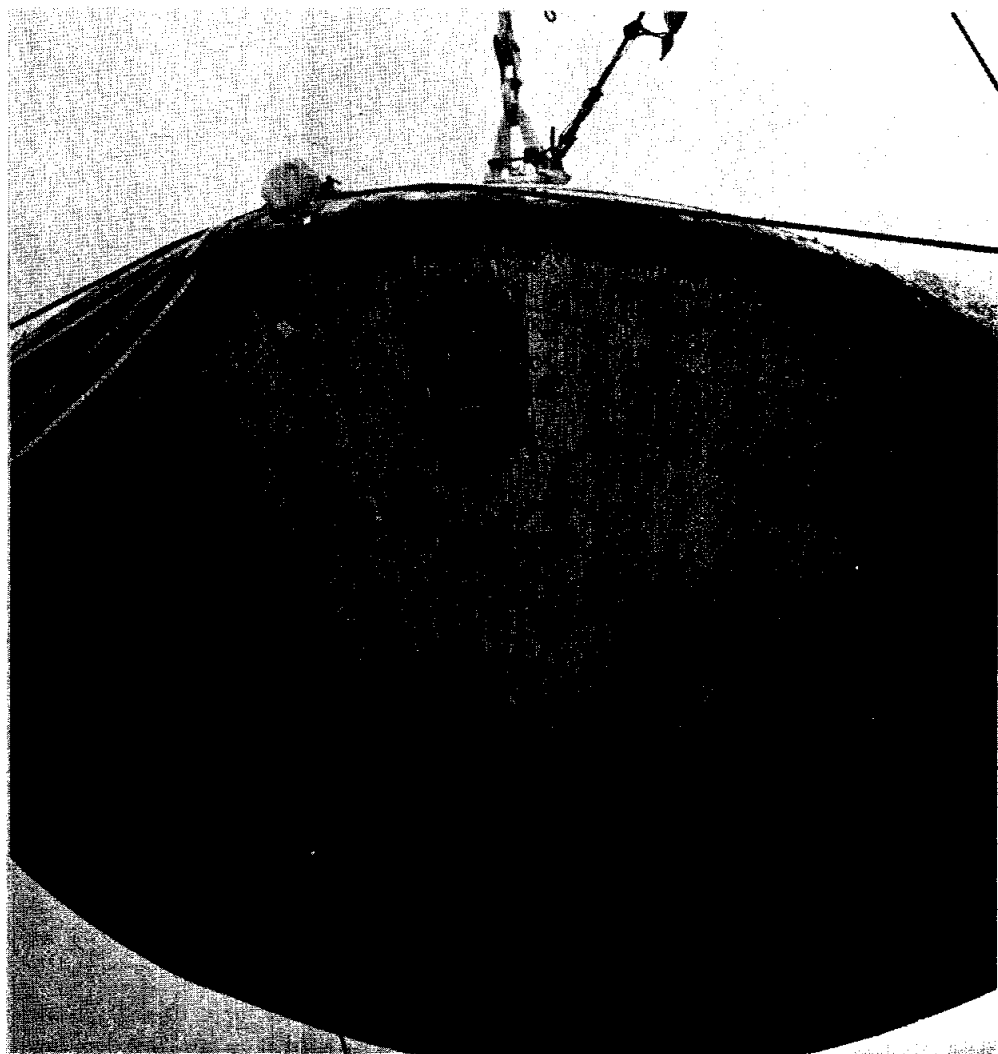
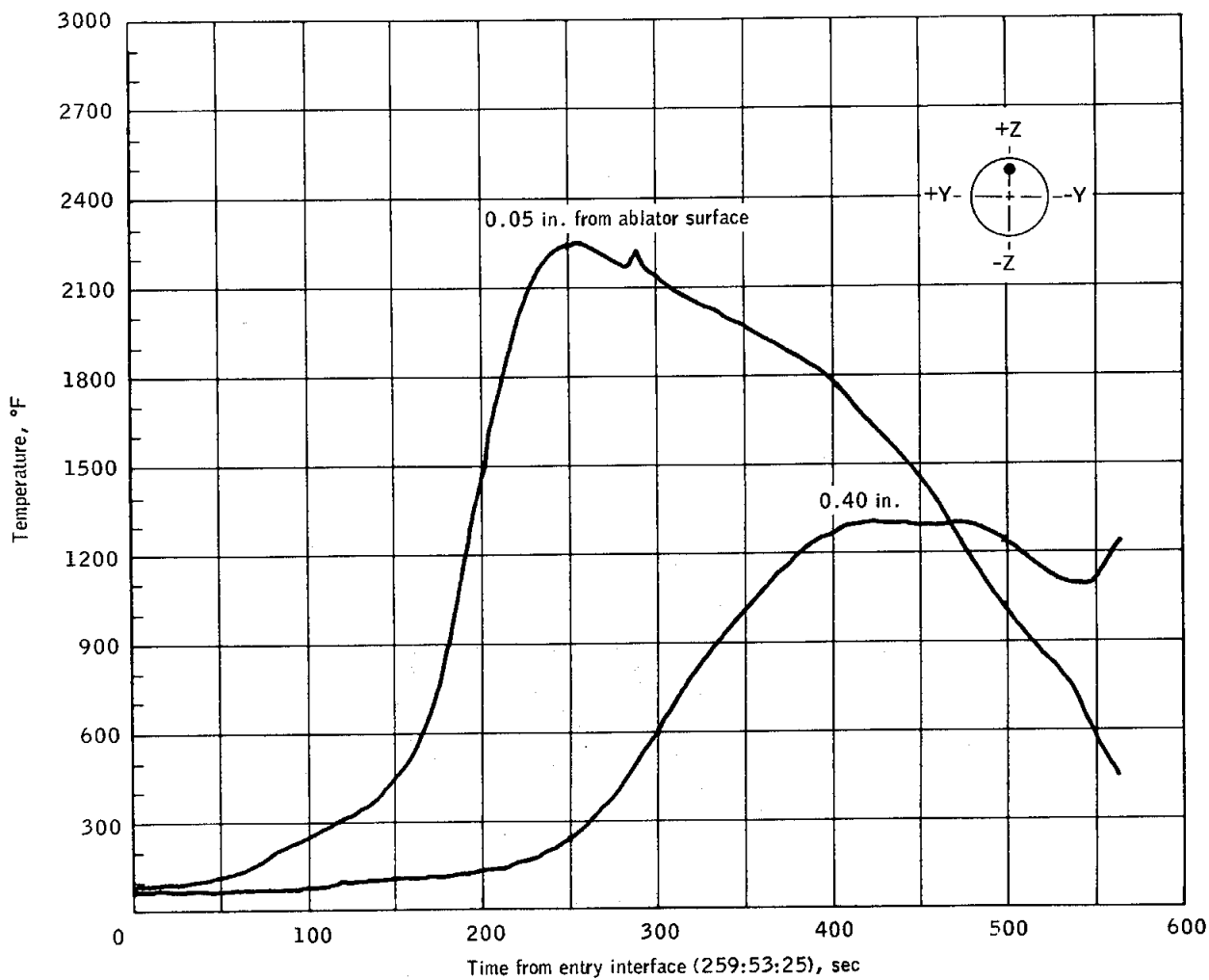


Figure 5.4-1.- Char condition of aft heat shield.

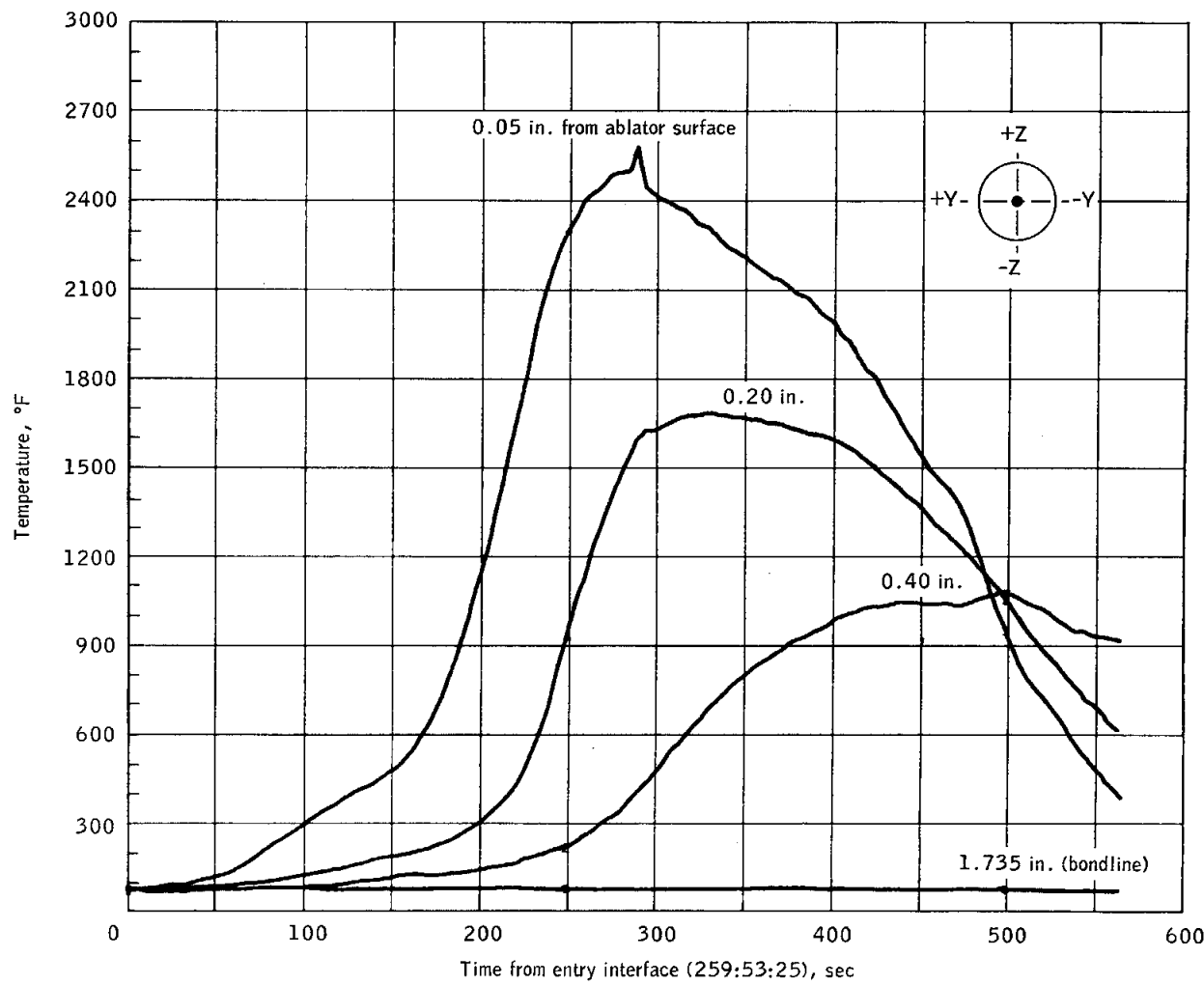
NASA-S-68-6271



(a) Distance from center = 69.4 in.; angle from +Y = 91 deg.

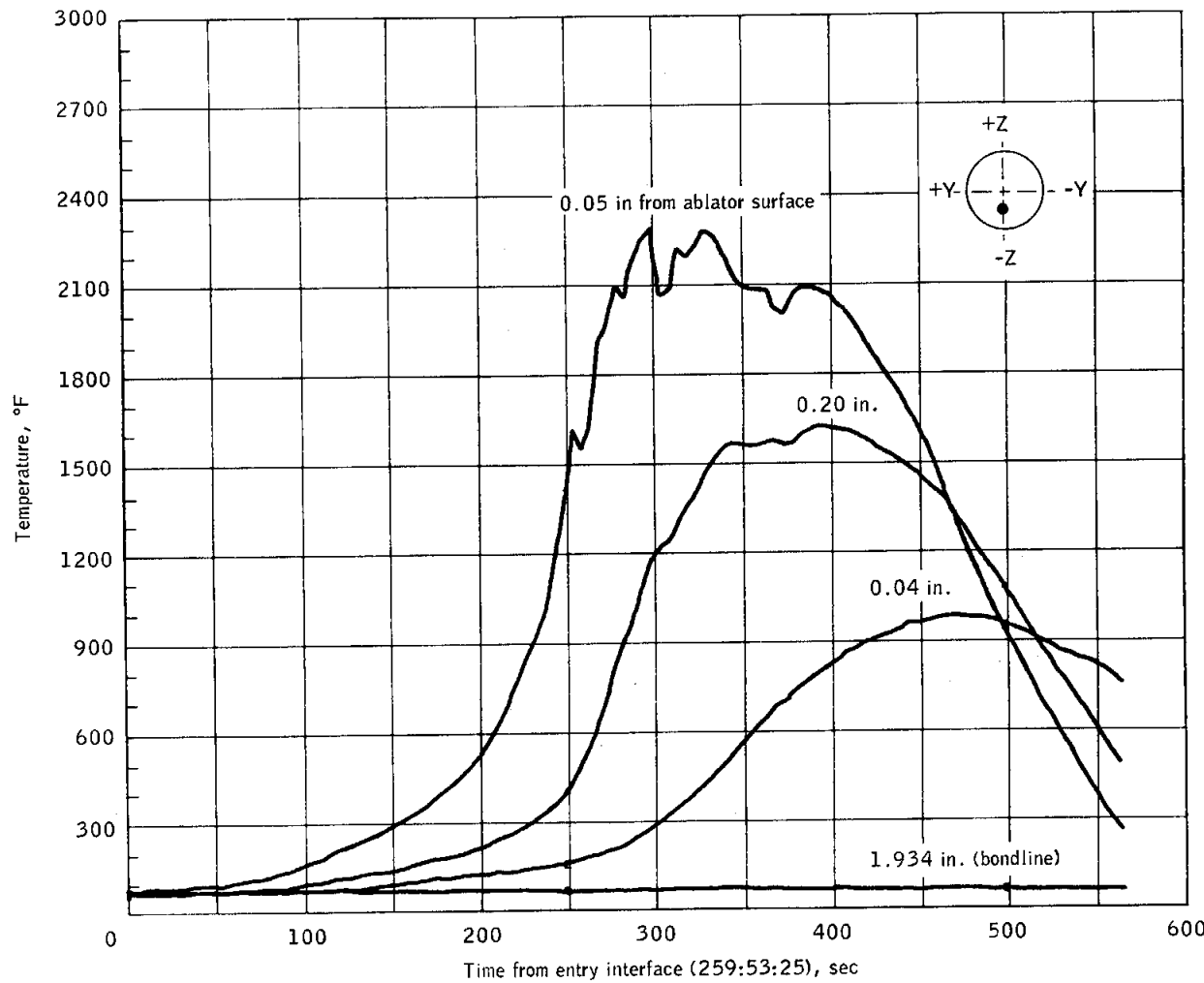
Figure 5.4-2.- Aft heat shield temperatures.

NASA-S-68-6272



(b) Distance along +X = 0 in.; angle from +Y = 0 deg.

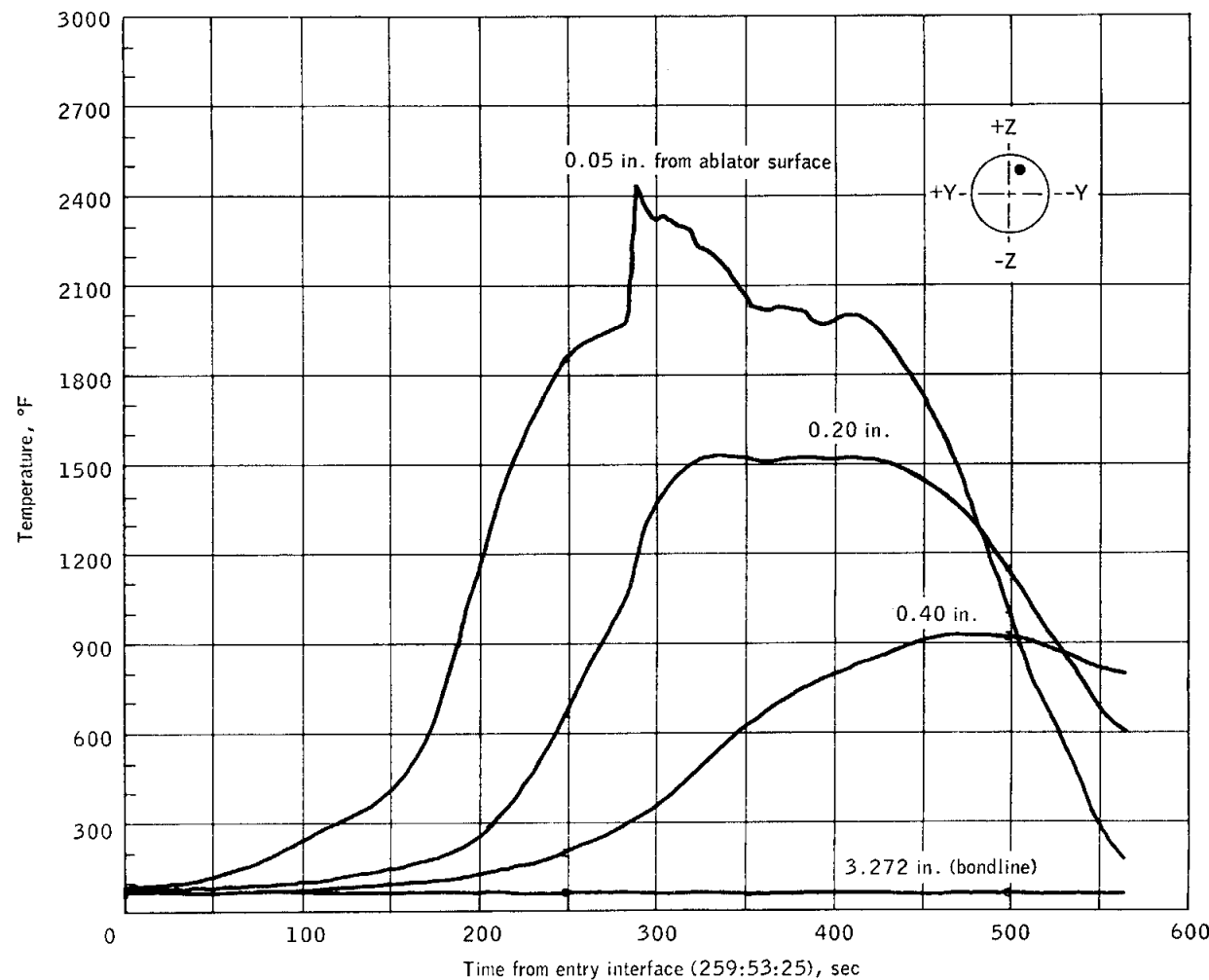
Figure 5.4-2.- Continued.



(c) Distance along +X = 50 in.; angle from +Y = 268 deg.

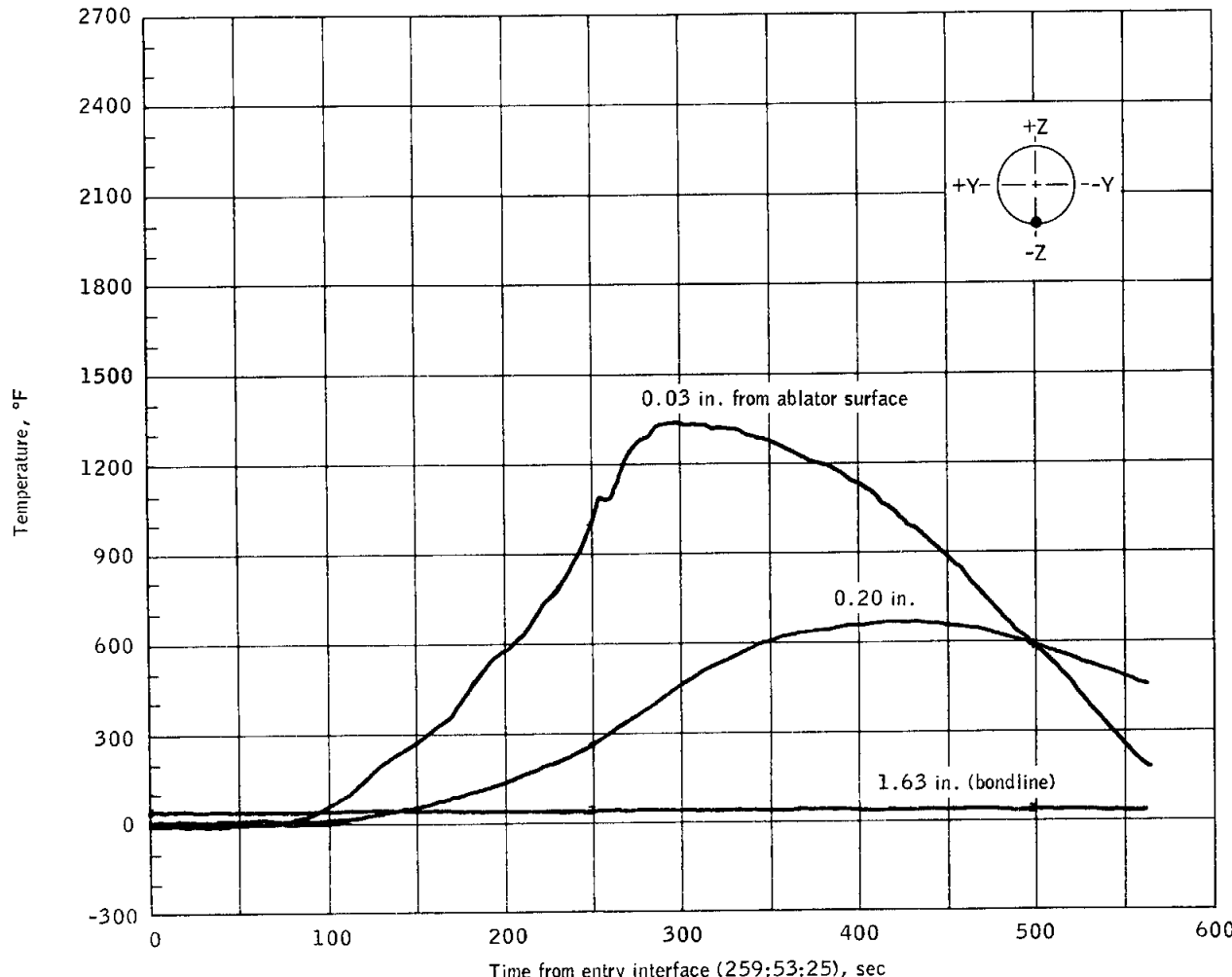
Figure 5.4-2-- Continued.

NASA-S-68-6274



(d) Distance along +X = 63 in.; angle from +Y = 101 deg.

Figure 5.4-2.- Continued.



(e) Distance along +X = 75 in.; angle from +Y = 268 deg.

Figure 5.4-2.- Concluded.

NASA-S-68-6276

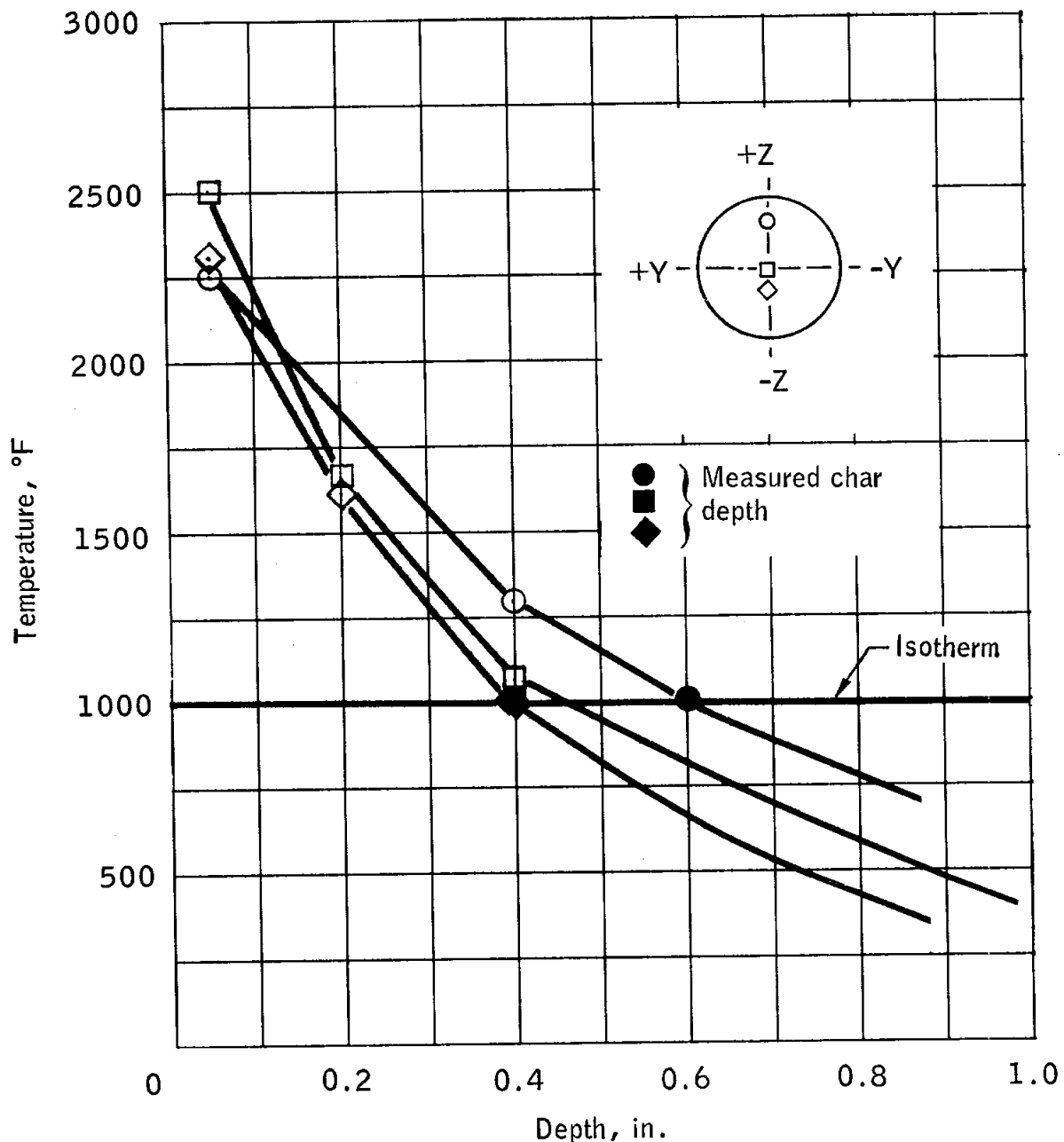
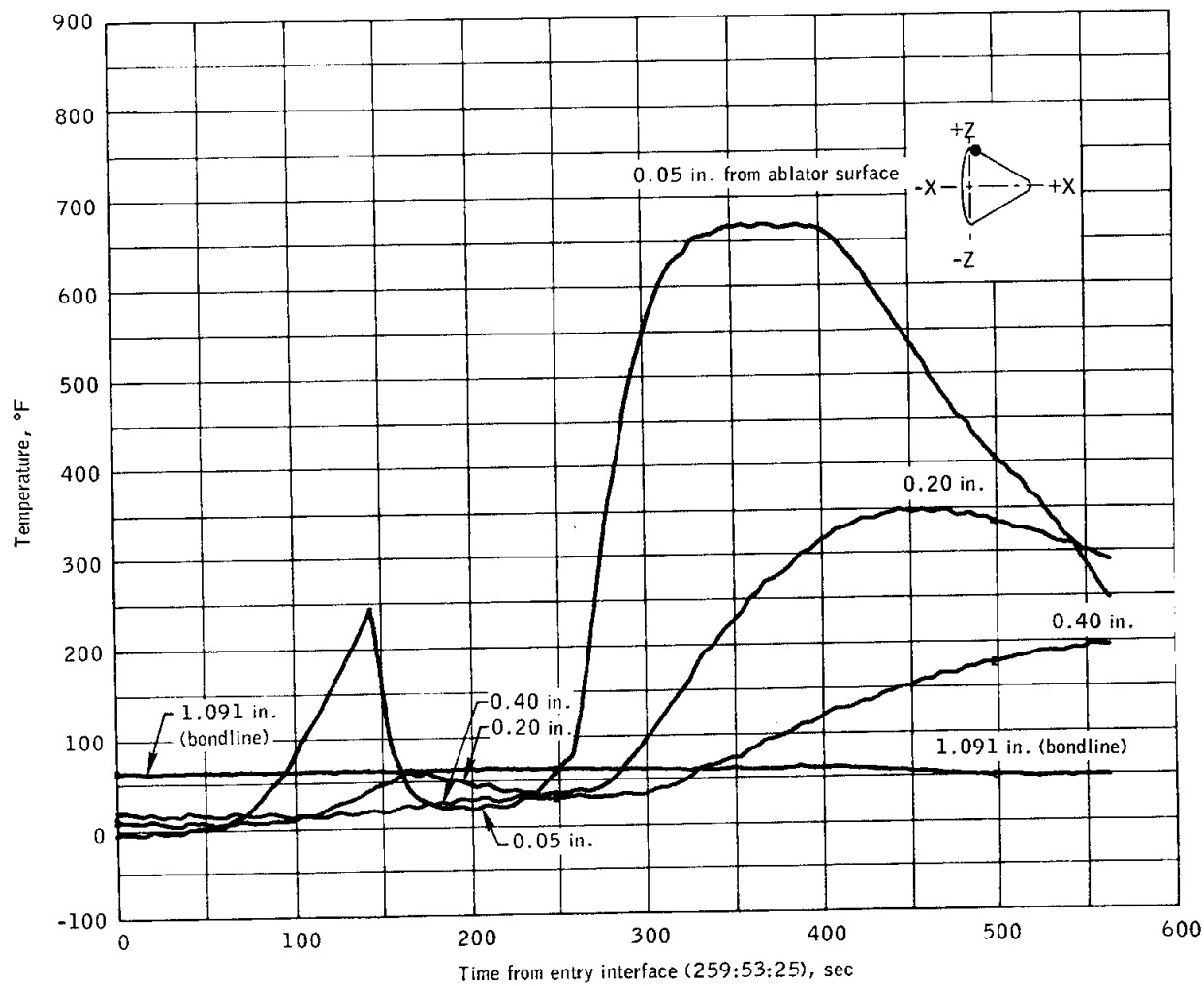


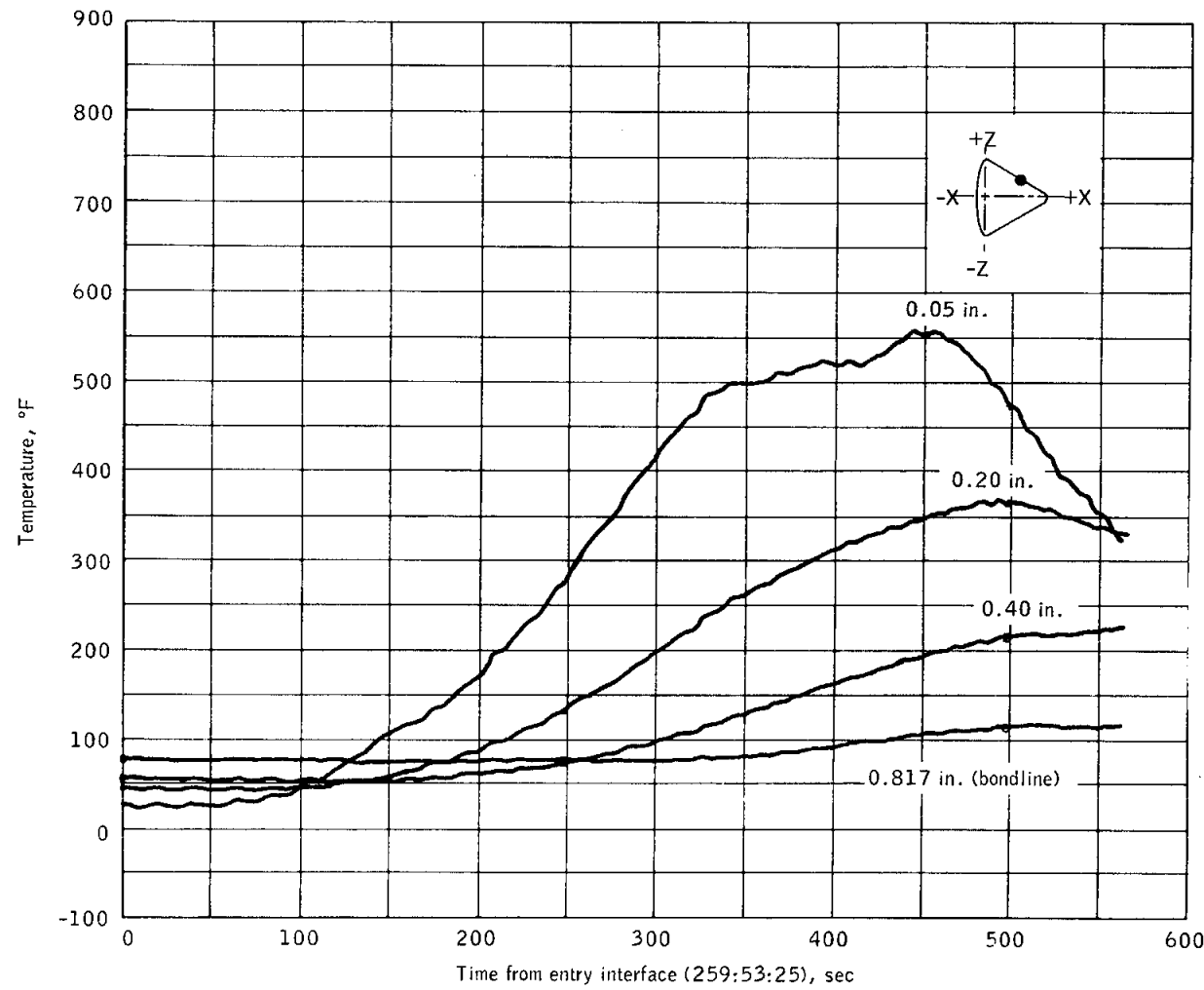
Figure 5.4-3.- Maximum temperatures measured in depth and comparison of char with 1000° F isotherm.



(a) Distance along +X = 27 in.; angle from +Y = 89 deg.

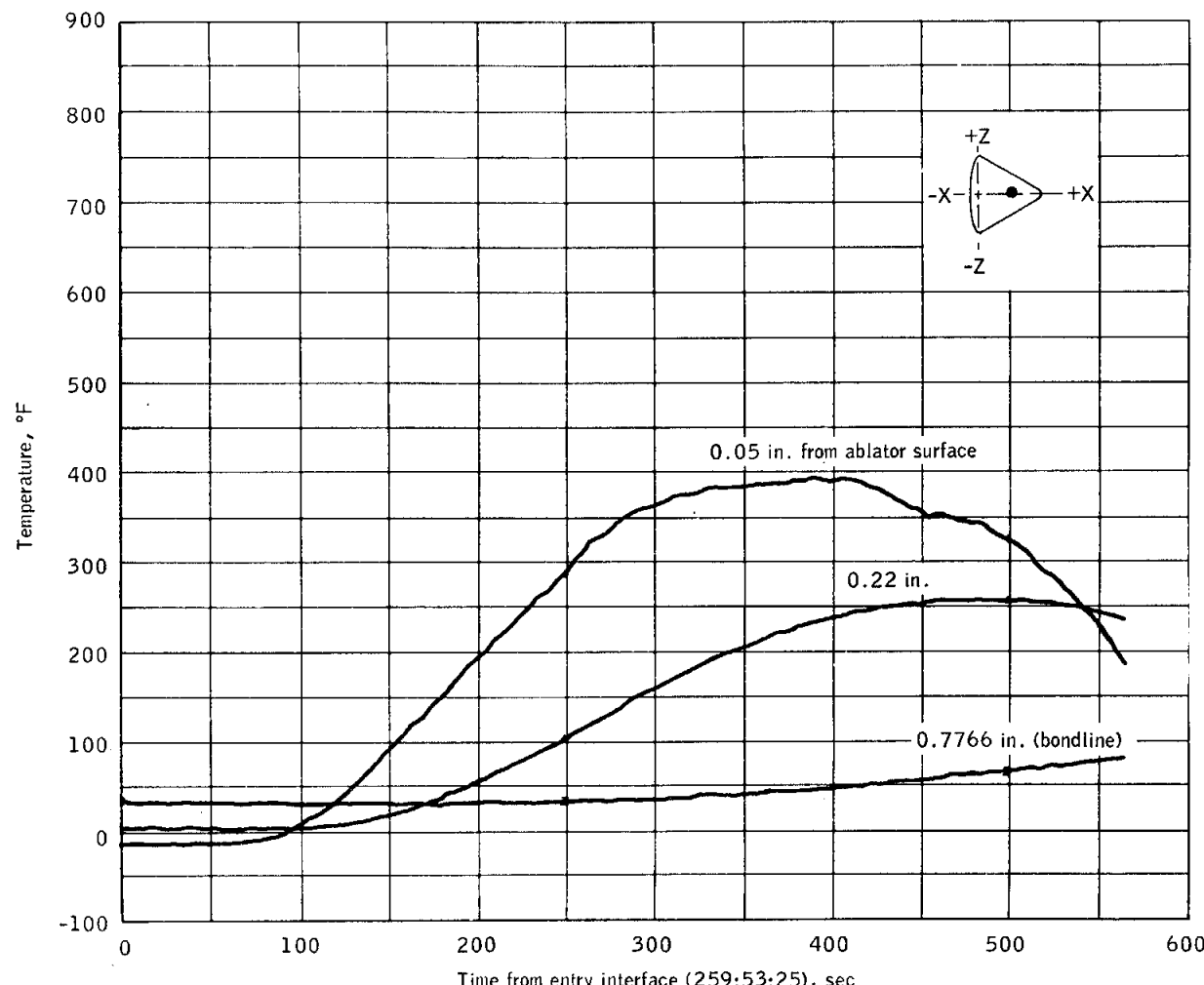
Figure 5.4-4.- Crew compartment heat shield temperatures.

NASA-S-68-6278



(b) Distance along +X = 85 in.; angle from +Y = 85 deg.

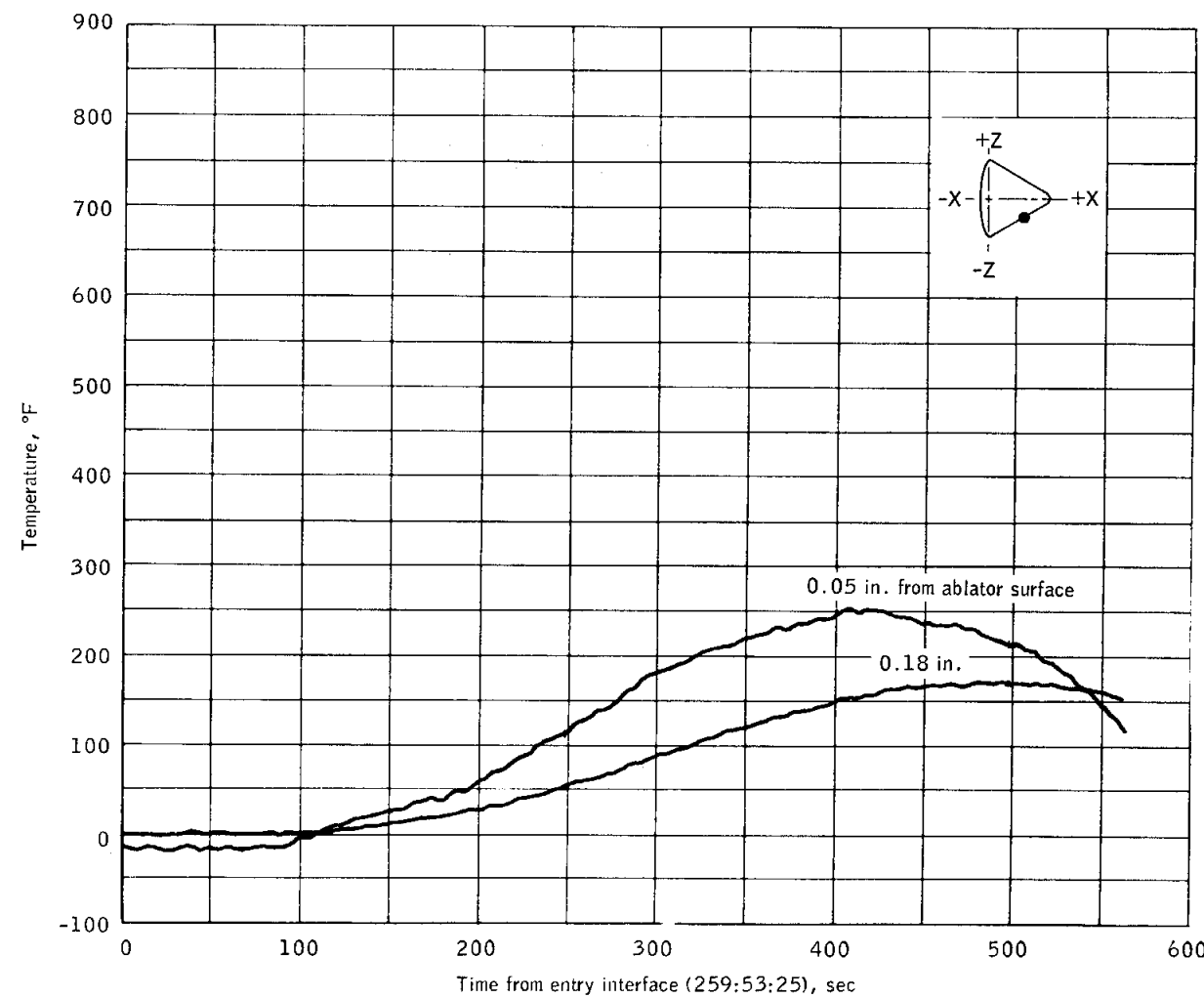
Figure 5.4-4.- Continued.



(c) Distance along +X = 78 in.; angle from +Y = 176 deg.

Figure 5.4-4.- Continued.

NASA-S-68-6280



(d) Distance along +X = 78 in.; angle from +Y = 268 deg.

Figure 5.4-4.- Concluded.

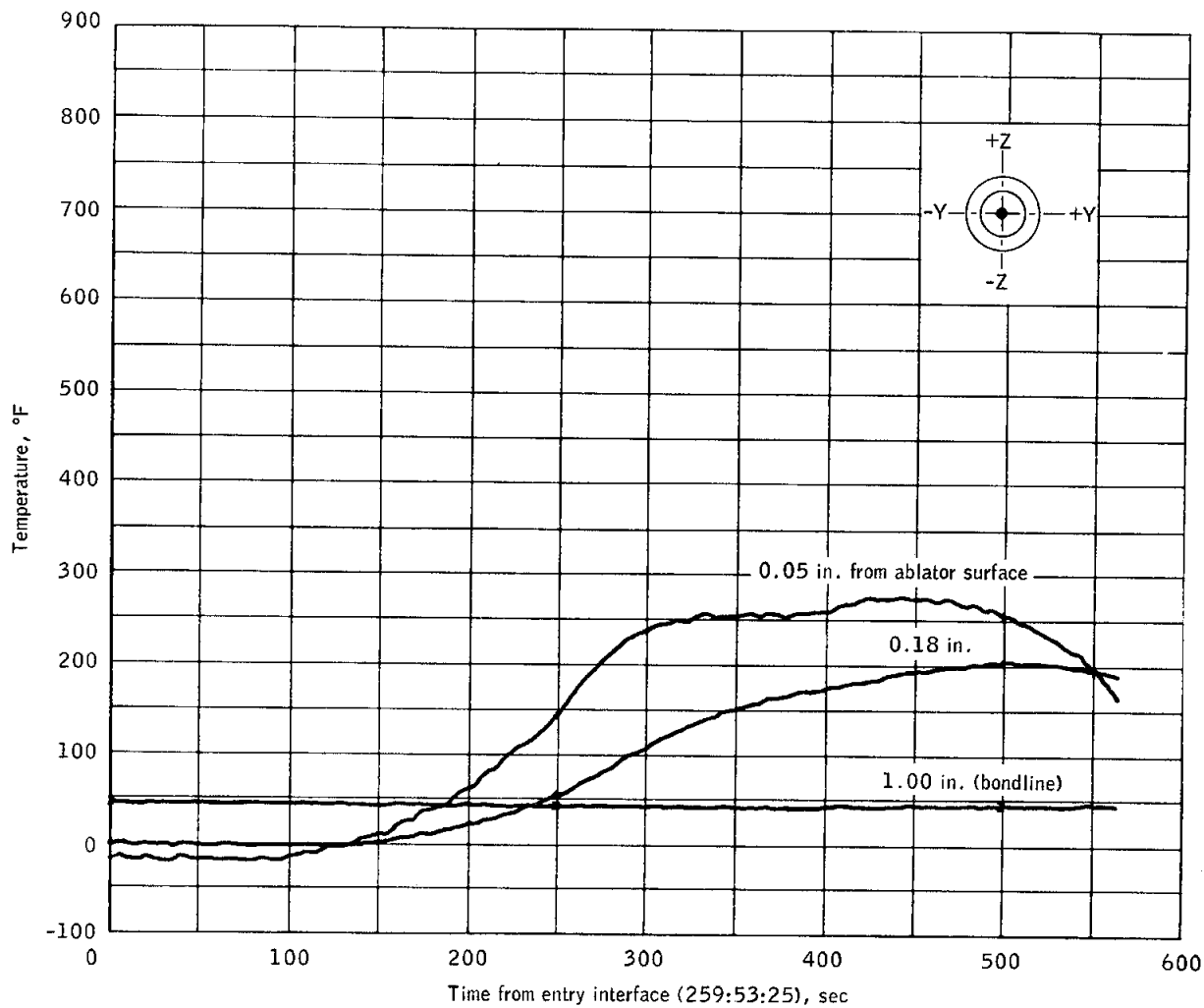


Figure 5.4-5.- Temperature on forward hatch.

5.5 EARTH LANDING

The earth landing sequence was performed automatically and all components functioned as planned with the system performing well within its capabilities. No damage to any component was noted.

The first discrete event in the earth landing operational sequence was forward heat shield jettison, at an altitude of approximately 23 500 feet. Drogue mortar fire was initiated 1.6 seconds later. The peak total load exerted on the command module structure by the reefed drogues was approximately 21 000 pounds at 1.3 seconds after drogue mortar fire. The predicted total load for Apollo 7 was 19 150 pounds. The load exerted by the disreefed drogues (10 seconds after deployment) was approximately 19 000 pounds. The crew reported that the drogues operated normally and were very stable. Postflight examination of the upper deck showed no evidence of drogue riser contact with the command module structure. Examination of the parachute disconnect housing ("flowerpot") indicated that drogue riser motion was minor.

Drogue disconnect and pilot parachute mortar fire were initiated by closure of the baroswitches at approximately 10 300 feet. The pilot parachutes deployed as planned, and all three main parachutes were deployed into the first reefed stage of inflation. The peak total load exerted by the main parachutes in the first stage of reefed inflation was approximately 28 000 pounds (predicted total reefed load was 32 600 pounds). The peak total load in the second reefed stage was approximately 23 000 pounds, and the full-open load was about 20 300 pounds.

The command module landed at 260:09:03. The crew reported that the landing was soft (no accelerometer data were available). Consequently, the eight attenuation struts for the crew couches did not stroke. The main parachute disconnect system separated the parachutes from the command module after landing, and the crew observed the main parachutes sinking.

5.6 MECHANICAL SYSTEMS

The spacecraft mechanical systems include the canard system, the uprigting system, the deployment mechanisms for the recovery aids, and the hatch-operating mechanisms (unified-side, forward-pressure, forward-ablator, and boost-protective-cover hatches). All components operated properly.

The deployment mechanisms for the flashing light and the antennas operated satisfactorily. The crew did not deploy the sea dye marker.

The uprighting system was activated by the crew about 8 minutes after the command module turned over to the stable II attitude (apex down). The vehicle was uprighted by the inflated bags within 4-1/2 minutes, as expected, even though about 200 pounds of water had flowed into the docking tunnel, reducing the net uprighting moment.

The unified side hatch was used for egress after landing. The hatch counterbalance was recharged with the backup nitrogen bottle before the hatch was opened. The initial charge had bled below acceptable pressure because the valve was left in the charge position during the mission.

5.7 ELECTRICAL POWER DISTRIBUTION

The electrical power distribution system functioned normally throughout the mission.

At launch, the voltages on both pyrotechnic buses were 37.2 V dc. Just prior to landing, these voltages were 36.8 and 35.3 V dc on pyrotechnic buses A and B, respectively.

At command module/service module separation, the dc bus voltages were below the alarm level. This problem is discussed in section 5.8.

At approximately 32-1/2 hours, a dc bus undervoltage alarm was caused by switching the 15-ampere load of suit compressor 2 to the bus for a component redundancy check; the fuel cells were operating at a degraded voltage output just prior to a purge. The characteristic load voltage of the fuel cells under these conditions was such that an undervoltage alarm could be expected with the additional 15-ampere load.

The ac power was supplied by inverters 1 and 2 connected to ac buses 1 and 2, respectively, throughout the mission. During overvoltage fluctuations at 19:46:38, approximately 56:00:00, and 61:12:50, the ac sensors reacted normally by disconnecting the inverters from the buses. Two dropouts of ac bus 1 and one dropout of both ac buses were concluded to have been caused by an overvoltage resulting from arcing inside a motor switch (see section 11.0).

5.8 FUEL CELLS AND BATTERIES

5.8.1 Fuel Cells

The fuel cells and radiators performed satisfactorily during the prelaunch and flight phases. The three fuel cells were activated 35 hours prior to launch and thereafter shared the spacecraft electrical loads with the ground support equipment until 2 hours prior to launch, when they assumed the full spacecraft power load.

During the mission, the fuel cells provided approximately 493 kilowatt-hours of energy at an average current of 22.1 amperes per fuel cell and an average command module bus voltage of 28.8 V dc. The command module bus voltage was maintained between 26.2 and 30.7 V dc during all mission phases when fuel cell power was being used, with one exception discussed in section 5.7. Figure 5.8-1 shows that the actual performance agreed well with predicted performance. The maximum deviation from equal load sharing among individual fuel cells was 4 amperes, which was acceptable. The slight overall degradation of the fuel cell performance with time shown in figure 5.8-2 was as expected. The variation for specific increments of time was caused by the state of the fuel cell with respect to the purge period.

The thermal performance of all three fuel cells as a function of load current is summarized in figure 5.8-3. Condenser exit temperatures for each of the fuel cells were outside the nominal range (155° to 165° F) at different times during the flight. The condenser exit temperature on fuel cell 2 reached 180° F between 161 hours and 163-1/2 hours during the high-power phase preparatory to the fifth service propulsion maneuver. Fuel cell 2 was then disconnected from the bus by the crew and allowed to cool for about 1 hour. At that time, the condenser exit temperature was 154° F and the fuel cell was reconnected to the bus for the fifth service propulsion maneuver. This fuel cell exhibited the same anomalous behavior during subsequent power-up phases of the flight.

The temperature on fuel cell 1 reached 175° F at 164 hours when fuel cell 2 was open-circuited and the 80-ampere spacecraft load was being shared by fuel cells 1 and 3. The condenser exit temperature on fuel cell 3 was frequently 5° F below normal at low power levels and concurrent low radiator exit temperatures. These problems associated with abnormal condenser exit temperatures were probably caused by contaminants in the water/glycol; such contamination could have affected the valve that controlled condenser exit temperature (see section 11).

Fuel cell skin temperatures were maintained between 399° and 439° F and agreed favorably with predictions. The skin temperatures of fuel cell 2 were consistently higher than those of fuel cells 1 and 3. This condition could have resulted from fuel cell 2 being physically located inboard of fuel cells 1 and 3 and therefore unable to radiate as much heat to bay 4 as the other two fuel cells. Similar characteristics were also observed during ground testing of spacecraft 2TV-1. The radiator outlet temperatures ranged from 50° to 100° F during the flight and agree favorably with predicted values.

Typical performance of the fuel cells in response to oxygen purge activity is shown in figure 5.8-4. This response, after approximately 700 ampere-hours of operation per fuel cell since the previous purge, shows that the oxygen purity of 99.97 percent was lower than that of the pre-launch samples, which measured 99.995 percent. The fuel cell response to hydrogen purging was not measurable, indicating that high-purity hydrogen was being supplied to the fuel cells from the cryogenic tanks.

Calculations based on total ampere-hours generated by the fuel cells indicate a total consumption of 44.25 pounds of hydrogen and 350.15 pounds of oxygen, including purges. These quantities agree well with measured cryogenic quantities and the estimated oxygen usage by the environmental control system. However, figure 5.8-5 shows that the flow meter readings were consistently higher than the actual usage. Based on total ampere-hours generated, the fuel cells produced 394.4 pounds of water during the mission. No high pH indications were noted.

5.8.2 Batteries

Three entry and postlanding batteries (A, B, and C) and two pyrotechnic batteries (A and B) were onboard. Except for a period of low voltage on the entry batteries after command module/service module separation at 259:43:33, the voltages and currents delivered by all batteries remained within the normal range (fig. 5.8-7). Battery C was isolated shortly after launch and was not utilized again until initiation of the deorbit phase.

During service propulsion maneuvers, battery A and B voltages and current-sharing with the fuel cells were within nominal limits; however, on the later maneuvers, the batteries exhibited lower ratios of power-sharing as the states of charge decreased (see fig. 5.8-7). Voltages on batteries A and B declined in accordance with a normal slope for a load of 0.021 ampere per battery, caused by the small loads which are continuously tied to battery relay buses. When the total spacecraft electrical load was imposed on the batteries at command module/service module separation, the voltage on battery buses A and B decreased to 26.4 volts,

resulting in main bus voltages of about 25 volts. Consequently, the low-voltage indication (26.2 volts) came on. The voltage slowly increased above the alarm level about 12 minutes later. All equipment, however, operated satisfactorily during this period. The performance of the entry batteries is presented in figure 5.8-8. These conditions were caused by both the cool temperatures and the states of charge of the batteries. A more detailed discussion is given in section 11.

Another flight discrepancy was the inability to fully recharge entry batteries A and B because the lower charge rate limit of 0.4 ampere was reached sooner than expected. Figure 5.8-9 indicates charging current decrease with time, and figure 5.8-10 shows the charger current/voltage characteristics. The condition resulted from the particular characteristics of the charger, coupled with the normal line resistance between the charger and the batteries. Further details are presented in section 11.

A third discrepancy, but of less consequence, was leakage of the entry battery manifold vent line. Onboard measurements of the manifold pressure, made before and after the battery vent valve was opened, indicate that cabin air was leaking into the manifold. During postflight procedures, the batteries were inadvertently removed from the spacecraft before the source of leakage could be determined.

Battery C open-circuit voltages from 36.0 to 36.5 V dc (37.0 expected) were obtained from onboard readouts. The lower open-circuit voltage is attributed to the cooler temperature of battery C (50° to 60° F, estimated).

The usage timeline is shown in figure 5.8-12 as a total for all three batteries. Energy replaced by recharging of batteries A and B was:

	Discharge, A-h	Recharge, A-h
Battery A	9.3	4.5
Battery B, first charge	11.7	2.3
Battery B, second charge	16.0	2.2

The batteries contained the following residual capacities postflight:

	<u>Capacity, A-h</u>
Battery A	18
Battery B	17
Battery C	37

These numbers include 10 A-h per battery, reserved for postlanding use, although this additional 30 A-h is not shown in figure 5.8-10.

The pyrotechnic batteries performed normally, with a no-load pyrotechnic bus voltage of 36.9 V dc.

NASA-S-68-6282

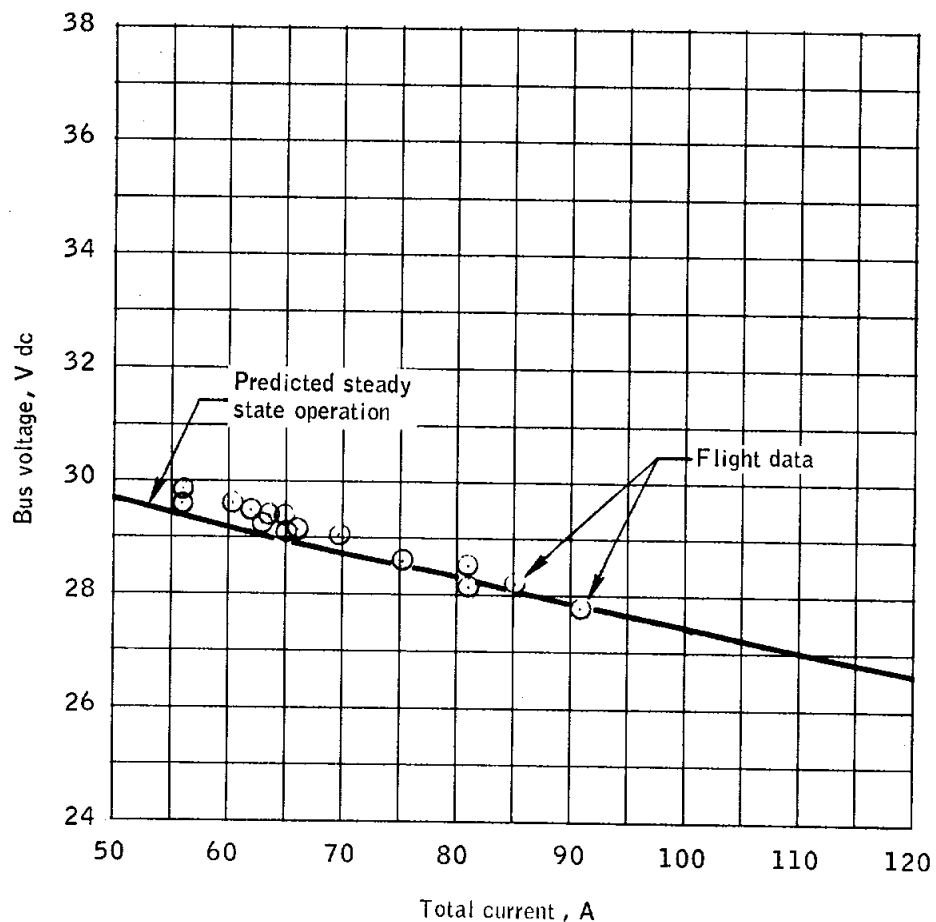


Figure 5.8-1.- Performance of three fuel cell systems.

A

NASA-S-68-6283

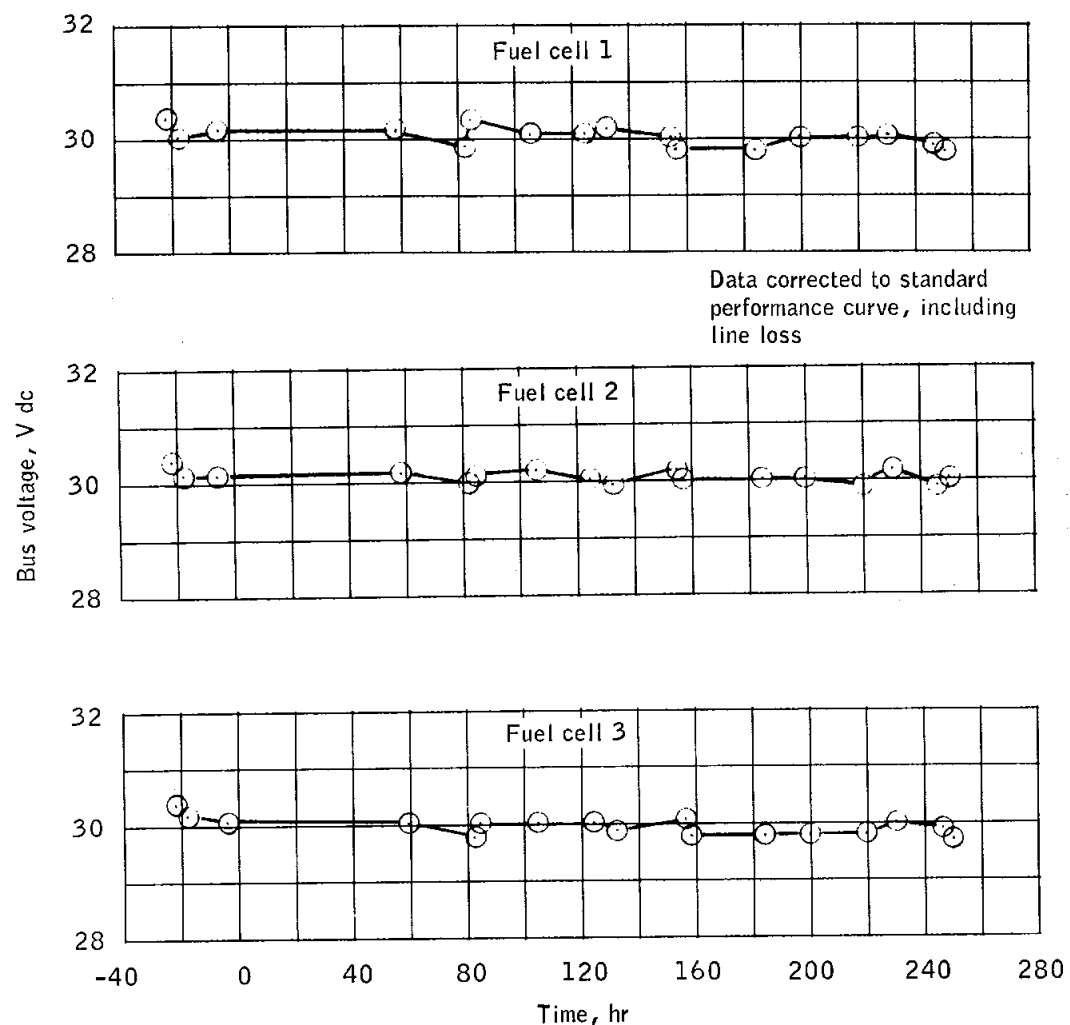


Figure 5.8-2.- Voltage degradation for 18-ampere loads.

NASA-S-68-6284

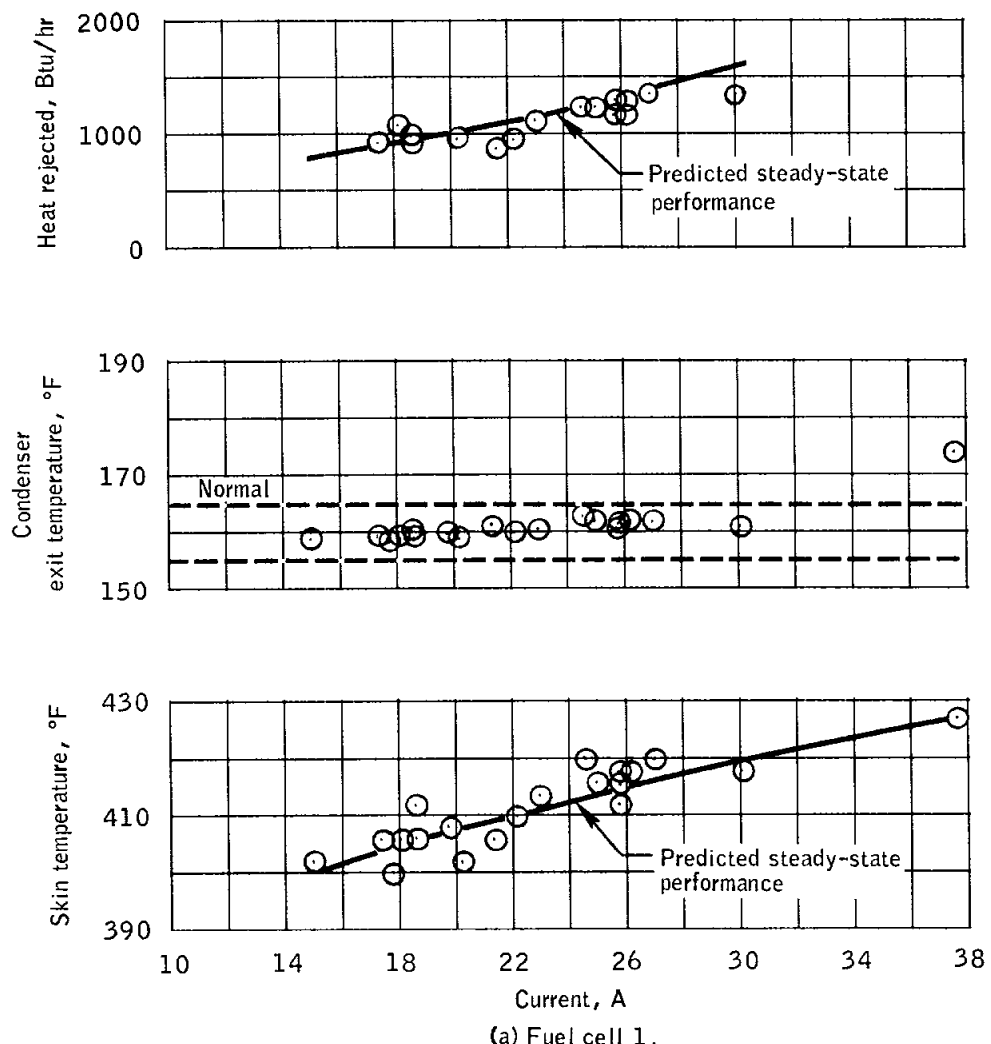
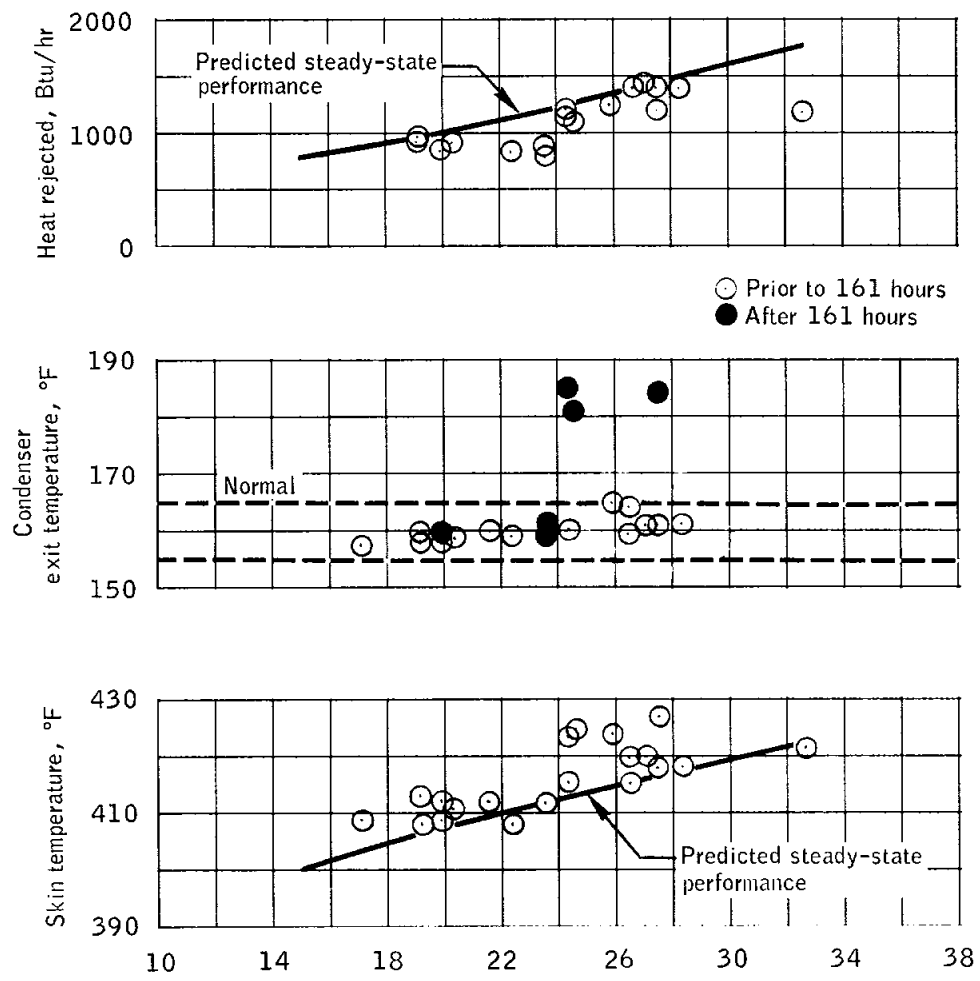


Figure 5.8-3.- Thermal performance of fuel cells.

NASA-S-68-6285



(b) Fuel cell 2.

Figure 5.8-3.- Continued.

NASA-S-68-6286

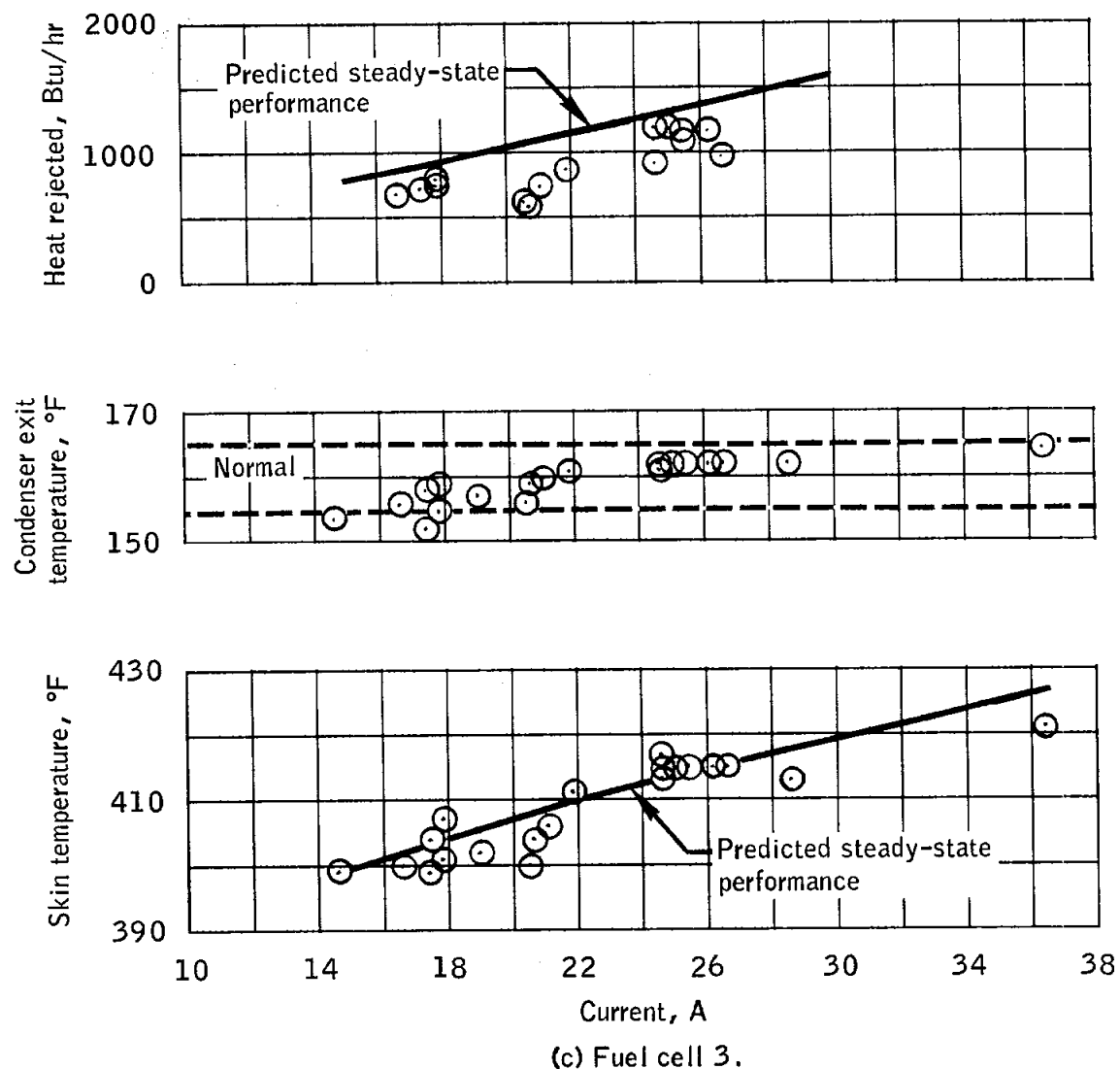


Figure 5.8-3.- Concluded.

NASA-S-68-6287

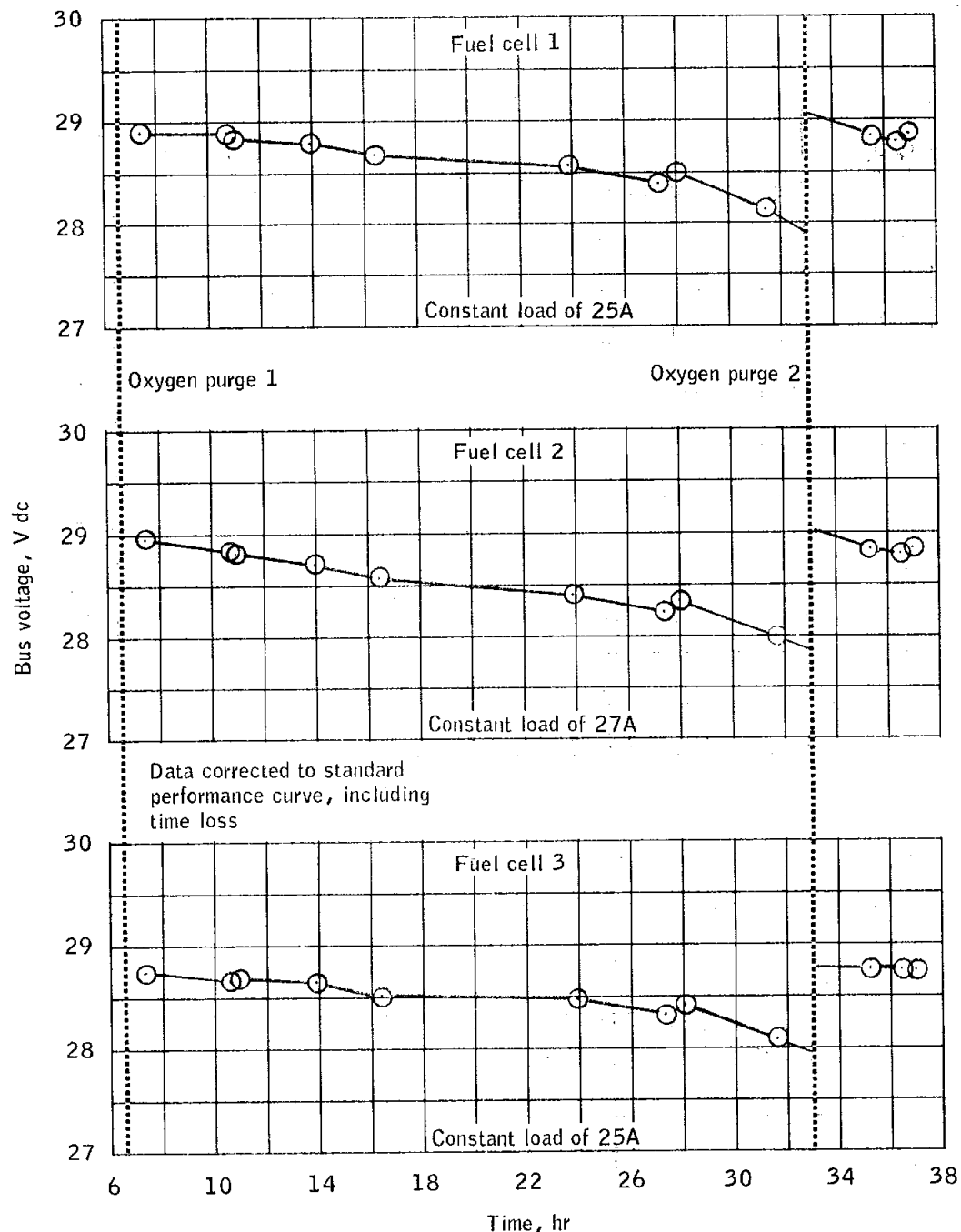


Figure 5.8-4.- Response to second fuel cell oxygen purge.

NASA-S-68-6288

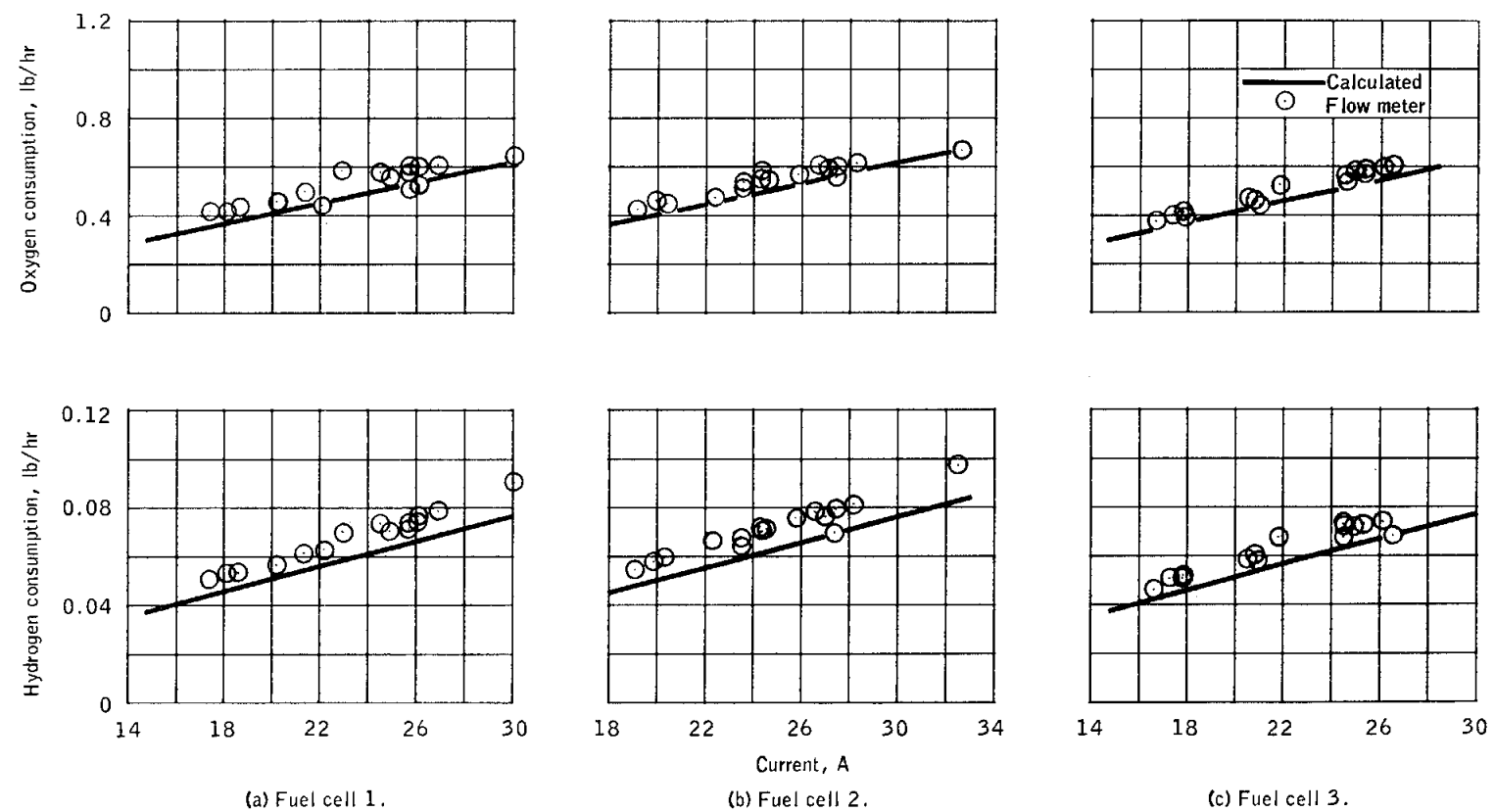


Figure 5.8-5.- Reactant flow rates.

NASA-S-68-6289

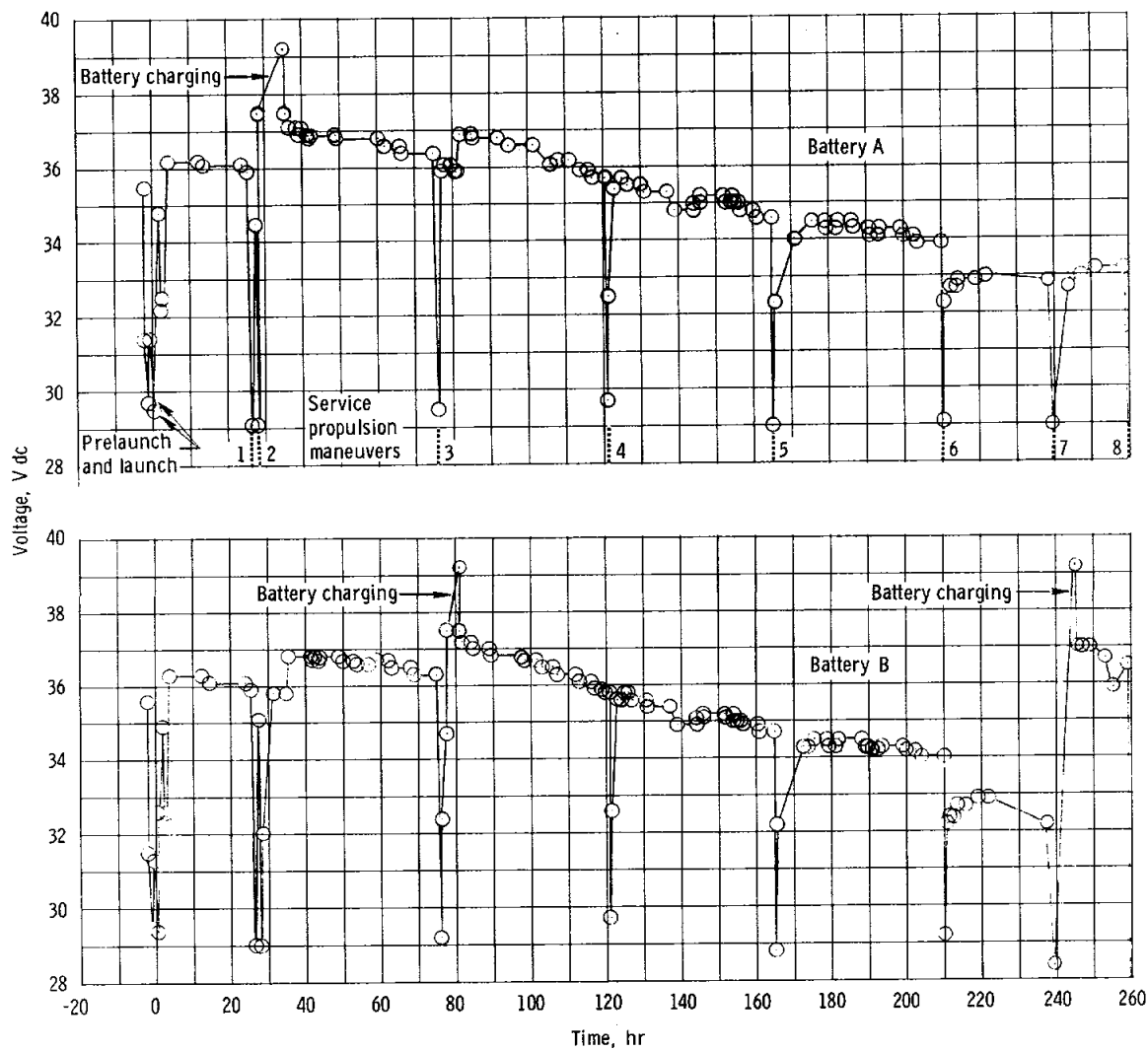


Figure 5.8-6. - Voltage timeline.

NASA-S-68-6290

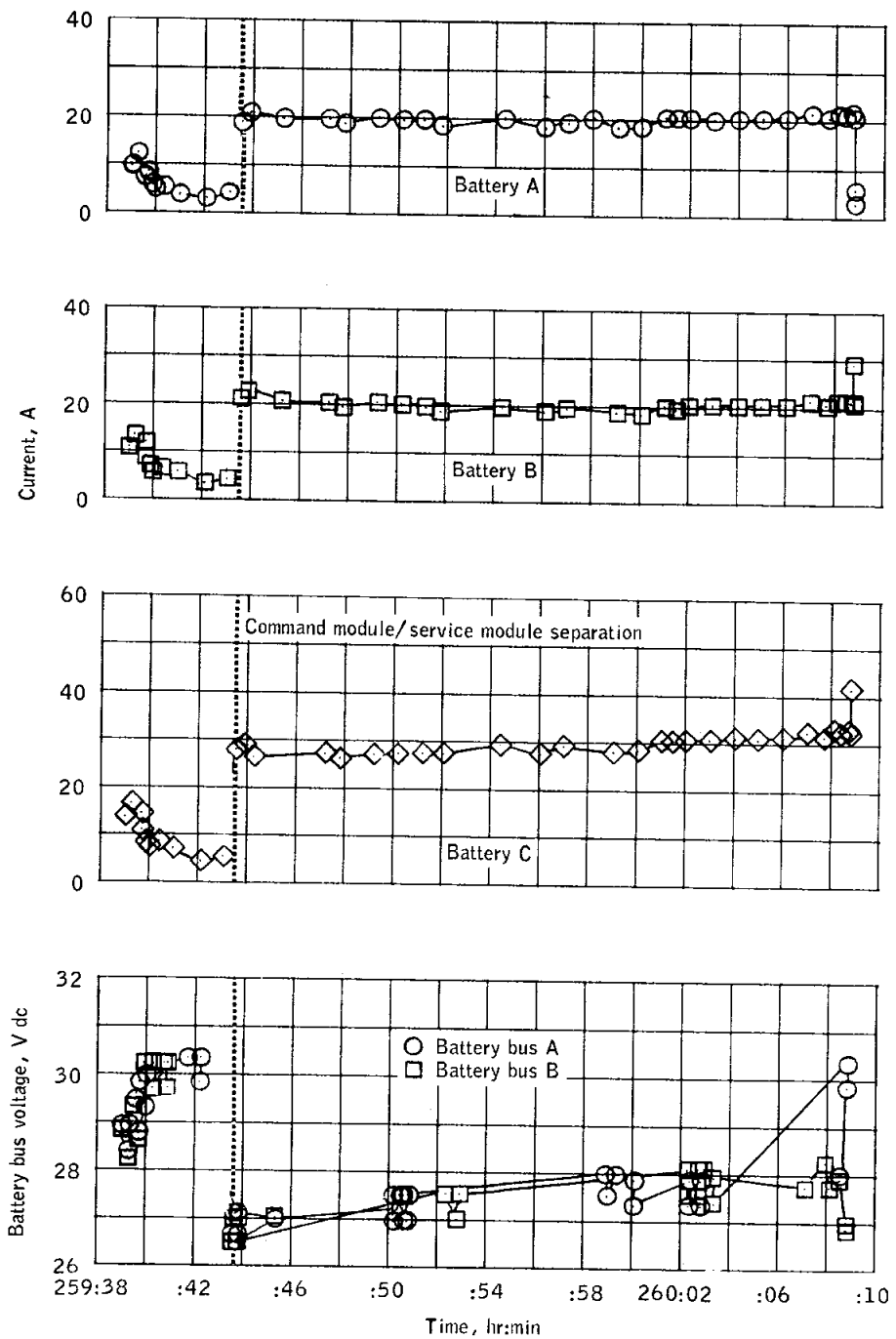


Figure 5.8-7.- Entry battery performance following deorbit maneuvers.

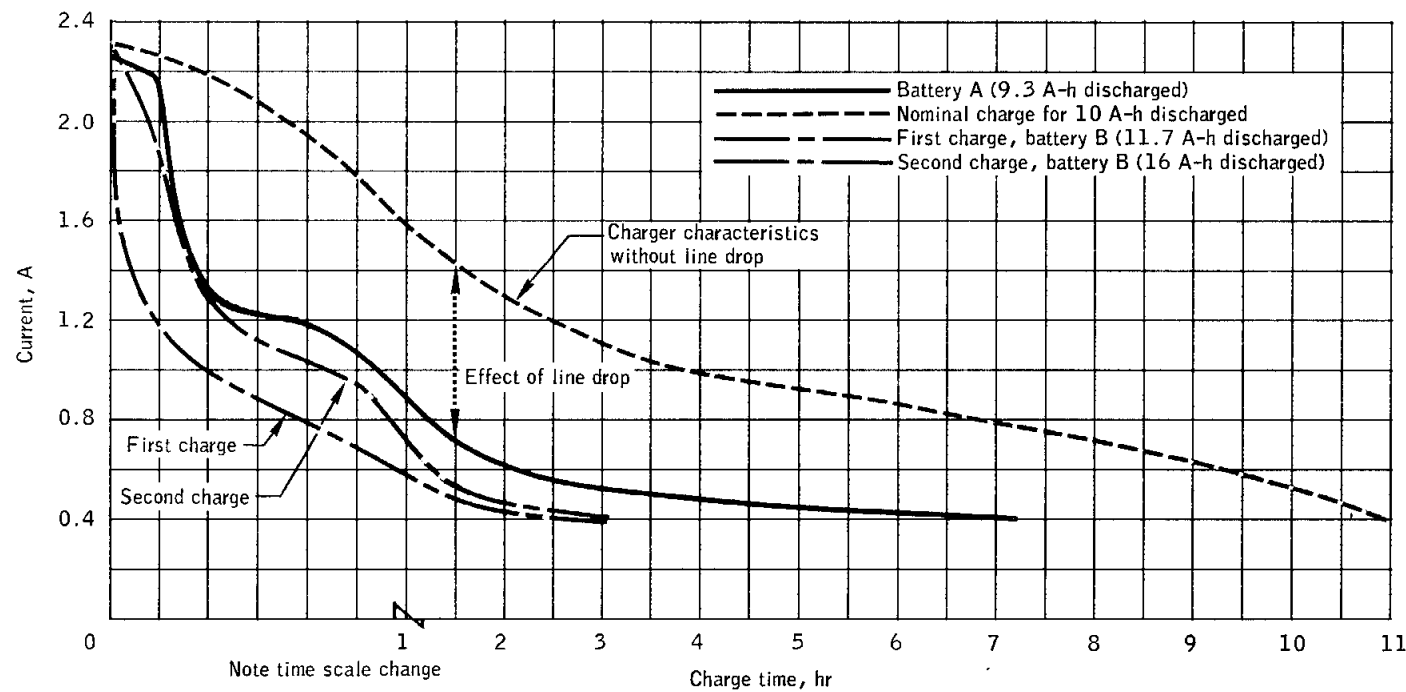


Figure 5.8-8.- Entry battery charging characteristics.

NASA-S-68-6292

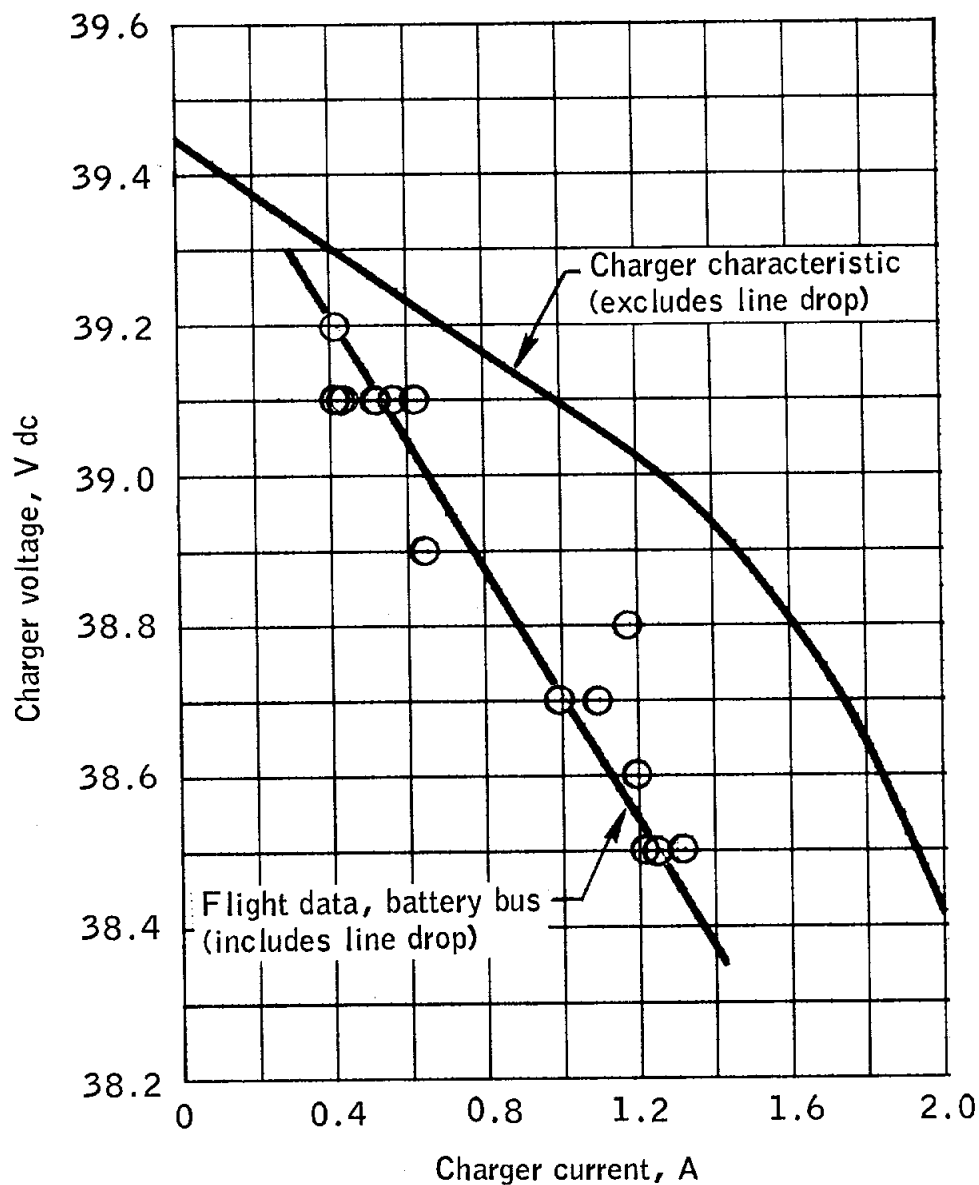


Figure 5.8-9.- Battery charger characteristic.

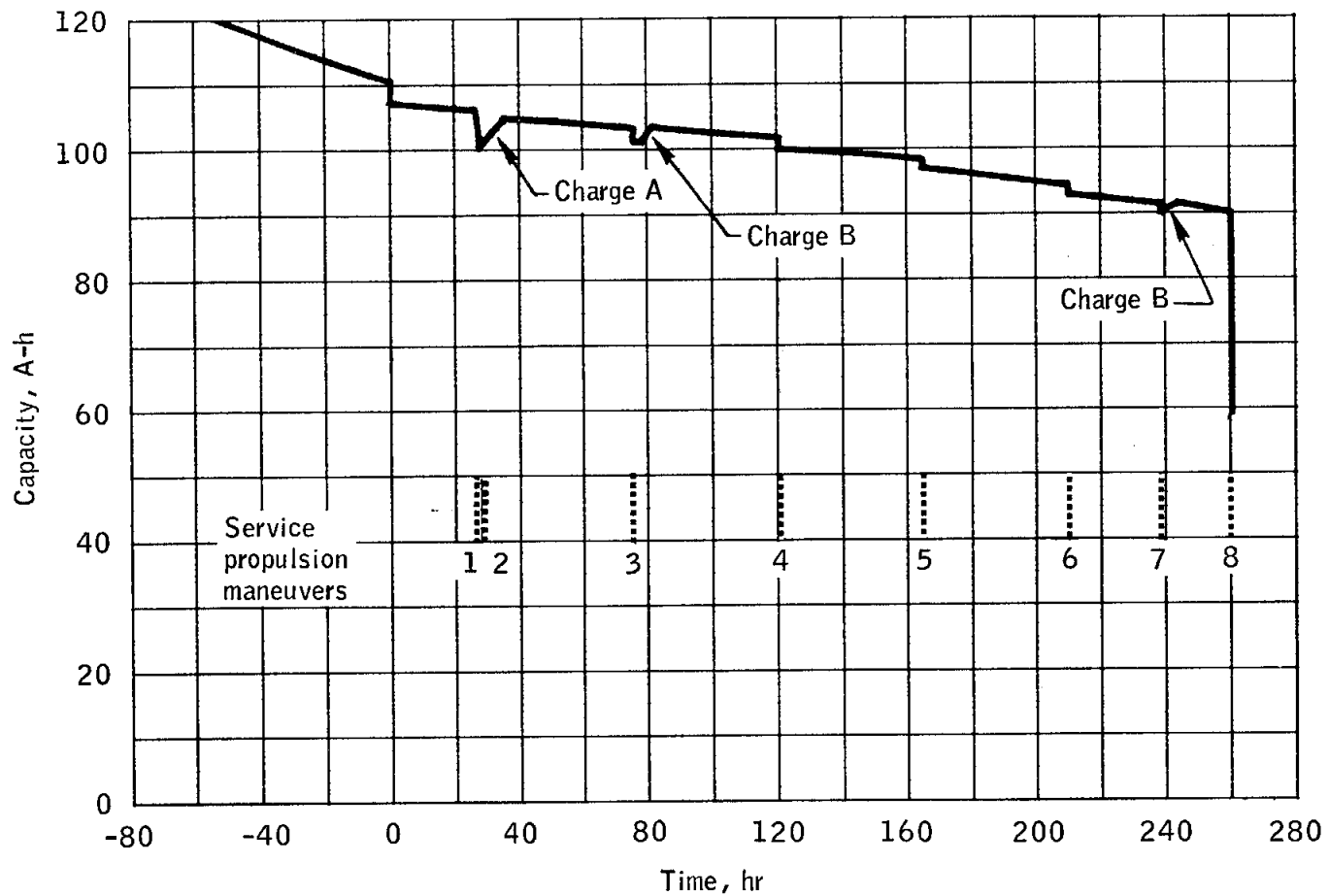


Figure 5.8-10.- Battery capacity remaining.

5.9 CRYOGENICS

The cryogenic storage system satisfactorily supplied reactants to the fuel cells and metabolic oxygen to the environmental control system. At launch, the total oxygen quantity was 635 pounds (42.7 pounds above the minimum red-line limit), and the total hydrogen quantity was 52.2 pounds (0.7 pound above the minimum red-line limit). The overall consumption from the system was less than predicted during the flight.

The VAC-ION pumps, which are connected to the vacuum annulus surrounding the cryogenic storage tank, were not used during the mission to maintain annulus vacuum. As expected, the heat leaks increased at launch, apparently because of outgassing in the vacuum annulus during launch vibration. However, the subsequent decrease in heat leak, as shown in figure 5.9-1, was not expected. This phenomenon will be analyzed to determine the cause. This reduced heat leak precluded the anticipated oxygen venting.

Continuous cryogenic quantity balance between pairs of oxygen tanks and hydrogen tanks was demonstrated. The two oxygen tanks remained within the 4 percent (12.9 pounds) quantity balance criterion throughout the mission without manual balancing. At 167:53:00, the hydrogen tank quantities exceeded the 3 percent (0.84 pound) requirement by 0.4 percent, and a manual balancing was performed by turning off the heaters in the tank with the lower quantity (tank 2). Tank 1 then supplied most of the flow. About 10 hours later, the two hydrogen tanks were equalized, and they subsequently remained within 0.5 percent.

The automatic pressure control system maintained tank pressures at an acceptable level. Typical pressure cycling is shown in figures 5.9-2 and 5.9-3 for hydrogen and oxygen, respectively.

Thermal gradients within a cryogen produce stratification and could result in two-phase fluid conditions if the gradients are severe enough. To eliminate these thermal gradients, fans (mixers) are used in the space-craft cryogenic tanks to stir the fluid. Tests were performed in flight to determine the severity of the stratification. For these tests, the heaters in the tanks were turned on, raising the tank pressure; the heaters were then turned off, pressure readings taken, and the fans turned on. Further pressure readings were taken over the next 4 to 5 minutes. The test data (figs. 5.9-4 and 5.9-5) obtained from the crew log show that under normal conditions, stratification does not adversely affect the tank pressures at quantities of less than 60 percent; consequently, the fans are not required at the lower values.

At 76:58:00, the fan-motors in oxygen tank 2 were deenergized because of an electrical circuit problem, as discussed in section 5.7; these fan-motors were cycled manually approximately every 12 hours for the remainder of the mission. Pressure data during these cycles indicate that the tanks may be operated in this mode with no problems.

The following table indicates that the quantities of hydrogen and oxygen used during the mission and the calculated usage by the environmental control system and fuel cells agree to within 0.7 pound of hydrogen and 3.5 pounds of oxygen, both within instrumentation accuracy. The hydrogen and oxygen quantity profiles are shown in figures 5.9-6 and 5.9-7.

<u>Item</u>	<u>Oxygen, lb</u>	<u>Hydrogen, lb</u>
Predicted usage prior to flight	558.6	48.8
Actual quantity used	454.0	45.0
Calculated usage from fuel cells and environmental control system	450.5	44.3

NASA-S-68-6294

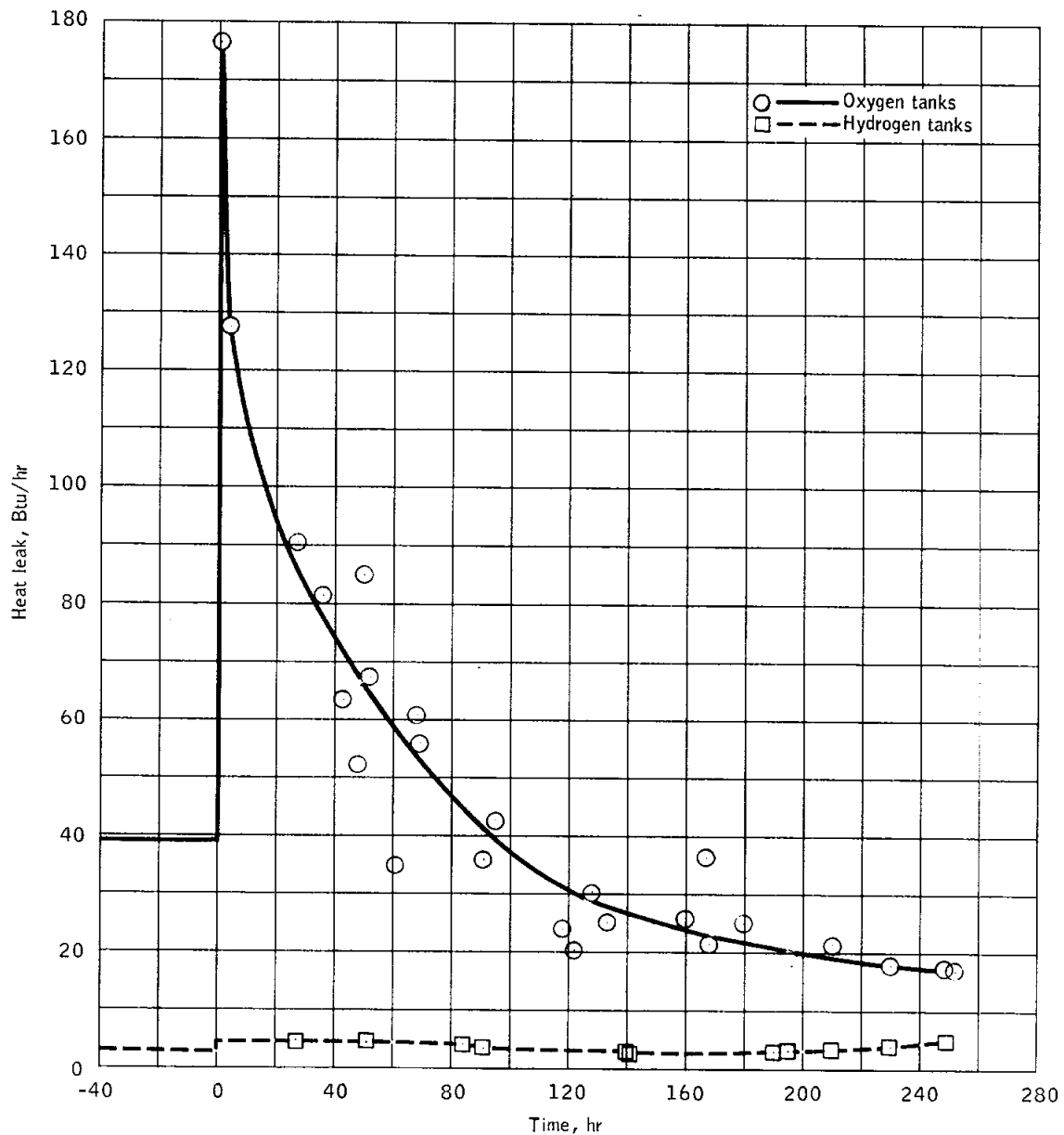


Figure 5.9-1.- Cryogenic system heat leak.

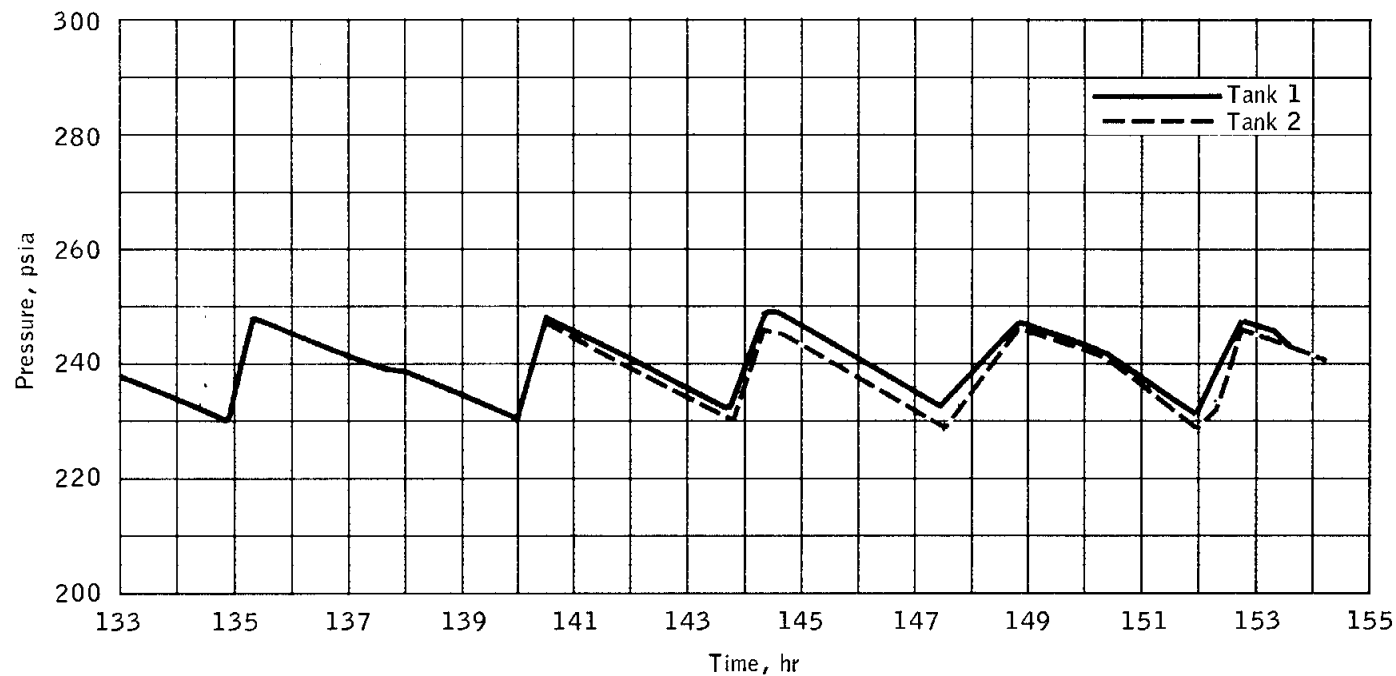


Figure 5.9-2.- Typical hydrogen tank pressure history with automatic fan and heater cycles.

NASA-S-68-6296

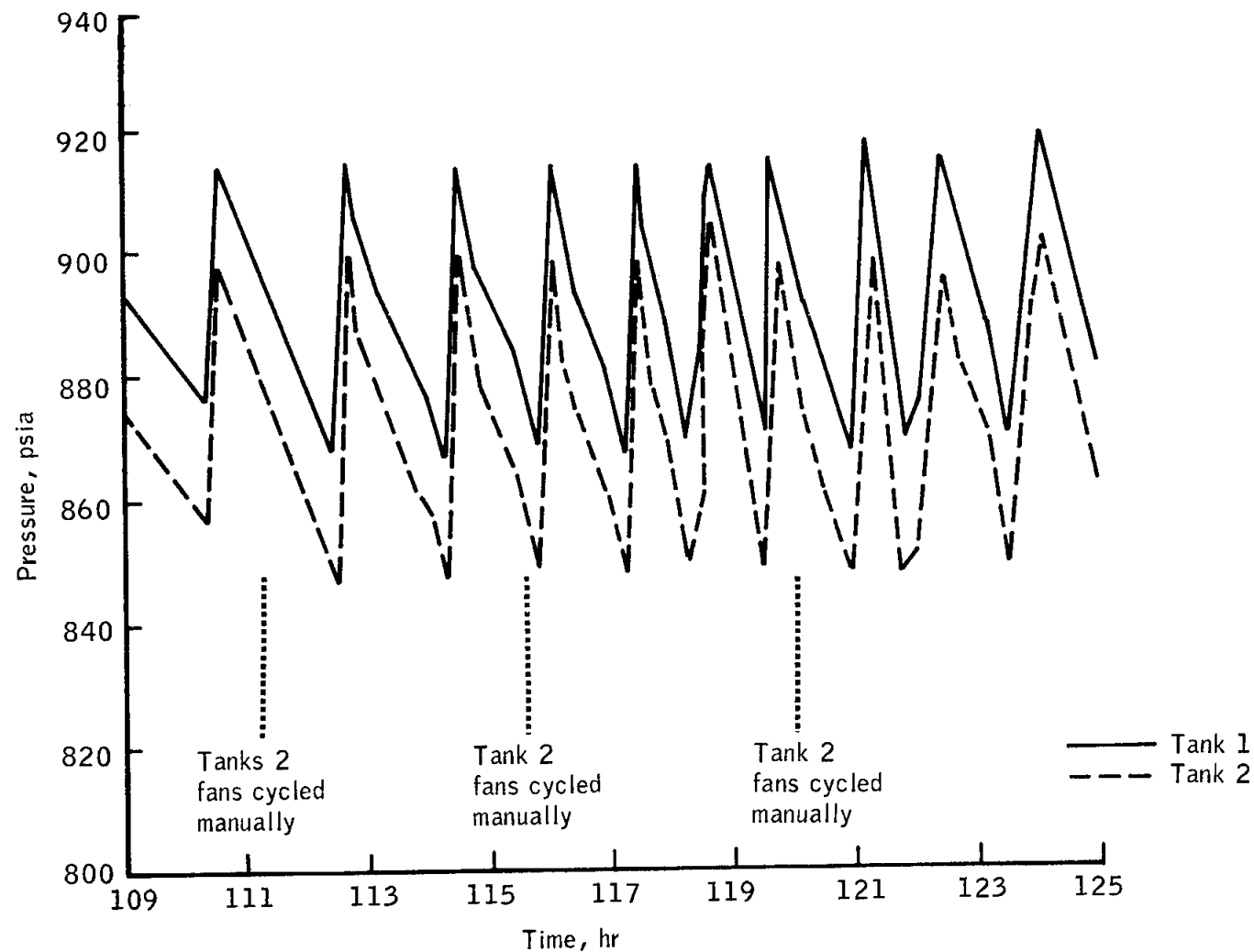


Figure 5.9-3.- Typical oxygen pressure history with automatic heater cycles.

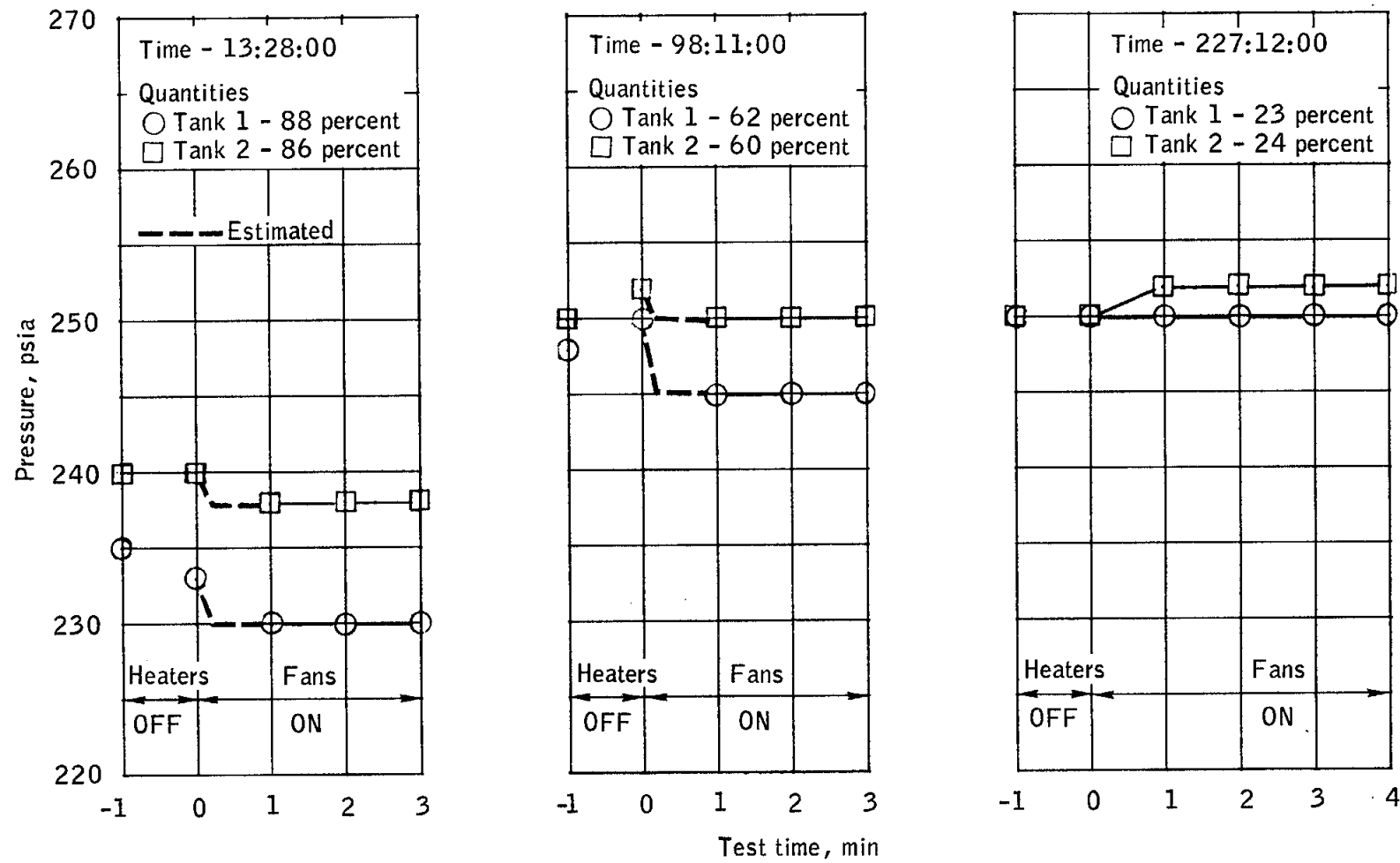


Figure 5.9-4.- Hydrogen stratification tests.

NASA-S-68-6298

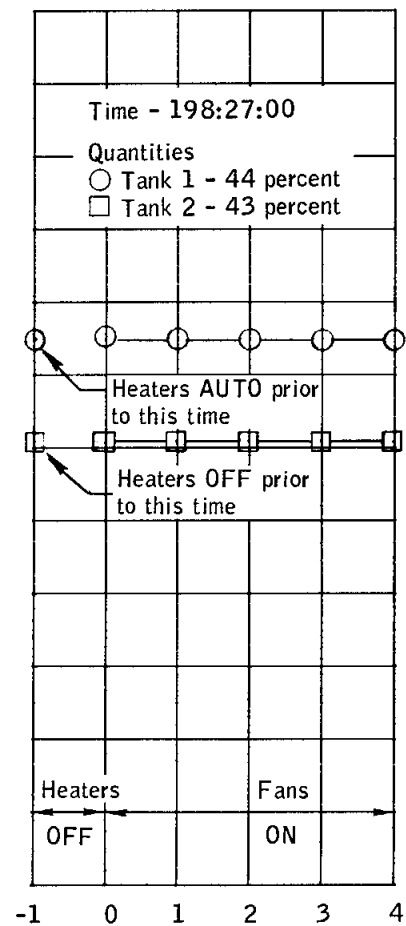
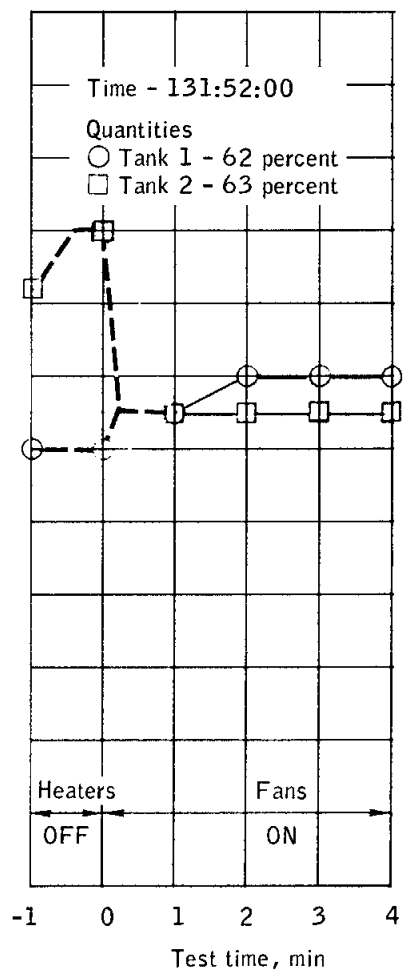
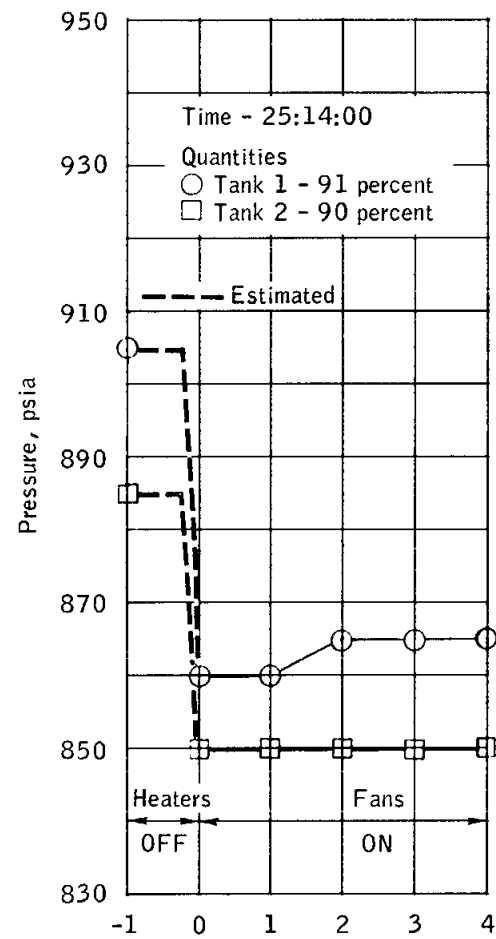


Figure 5.9-5.- Oxygen stratification tests.

NASA-S-68-6299

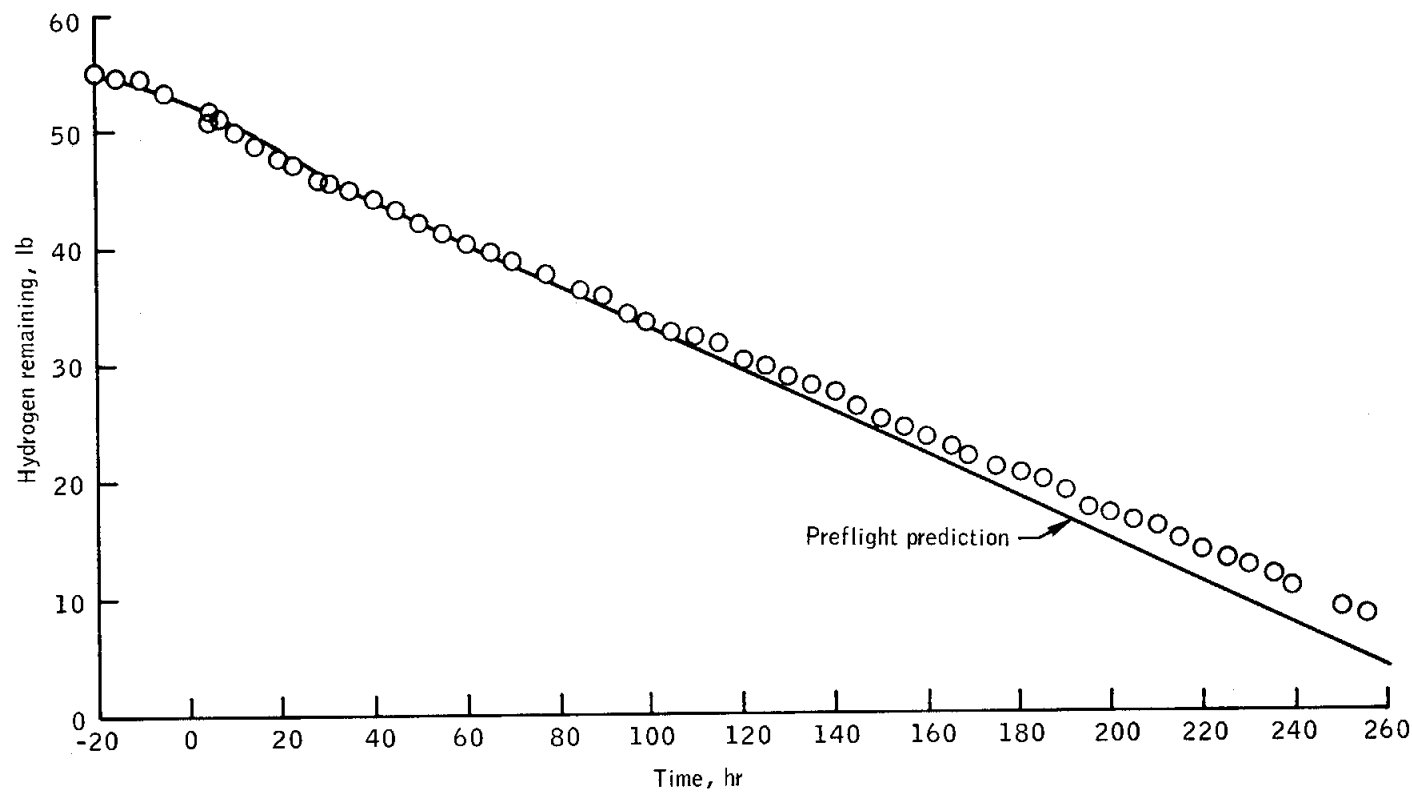


Figure 5.9-6.- Hydrogen quantity profile.

NASA-S-68-6300

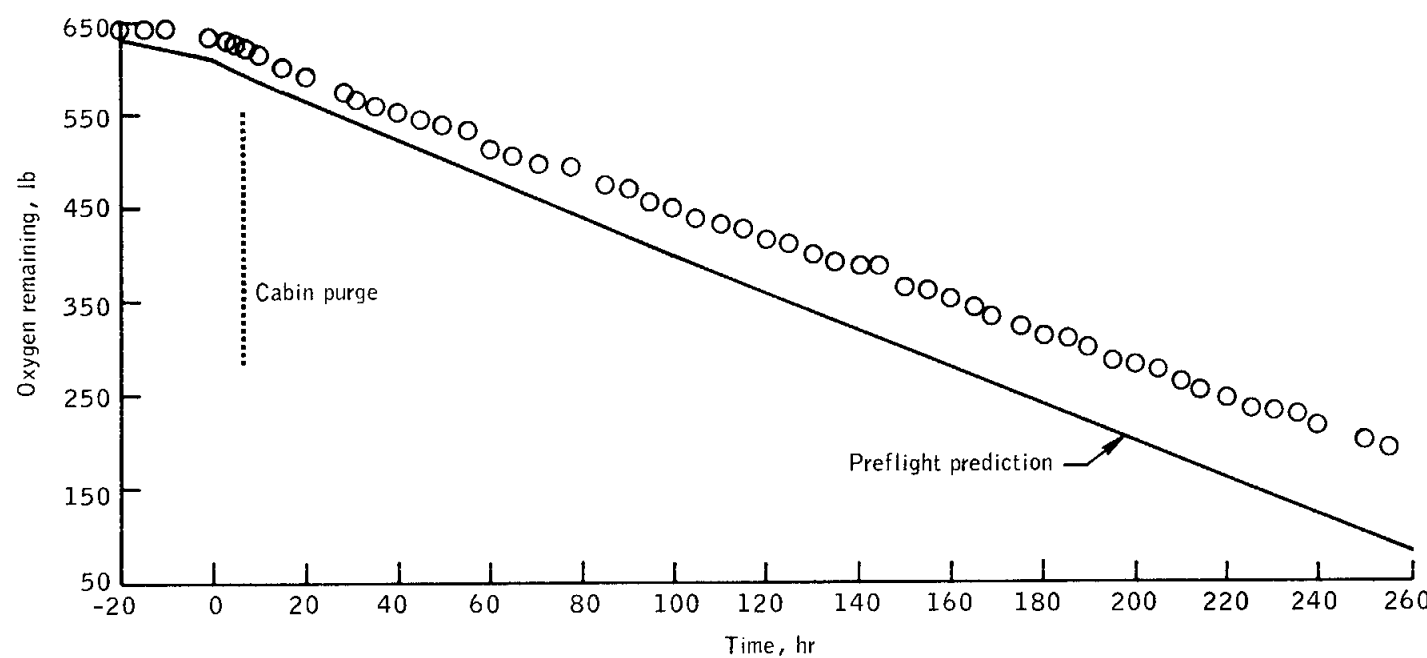


Figure 5.9-7.- Oxygen quantity profile.

5.10 SEQUENTIAL

The sequential system performed satisfactorily.

5.11 PYROTECHNIC DEVICES

All pyrotechnic devices functioned as expected.

5.12 LAUNCH ESCAPE

Performance of the launch escape system was satisfactory. The tower jettison motor fired as programmed to remove the launch escape system, including the boost protective cover, from the command module.

5.13 EMERGENCY DETECTION

The emergency detection system performed satisfactorily. The crew reported that the applicable indications from the launch vehicle were properly displayed and that there were no indications of excessive launch vehicle rates or attitude reference failure. The angle-of-attack dynamic pressure measured by the q-ball sensor system located on the launch escape system was lower than in any previous Saturn/Apollo flight (5 percent was indicated; 100 percent is abort limit). The launch vehicle pressure display meters were checked against telemetry data and were adequate for use by the crew as an abort cue.

5.14 COMMUNICATIONS

The communication system satisfactorily supported the mission, and the applicable mission objectives were achieved. The S-band and VHF links provided good quality voice communications except during the launch phase, when the crew failed to receive certain uplink transmissions and the down-voice was garbled because of improper procedures and/or malfunctioning receivers at the ground stations. The quality of the dumped (recorded) voice ranged from poor to good. The performance of the real-time and dumped telemetry channels was consistent with the received signal strengths. The quality of television pictures during the seven broadcasts ranged from fair to excellent. More than 94 percent of the commands transmitted were

verified by the spacecraft updata link equipment; in each instance, the unverified commands had been transmitted during a period of weak signal strength.

The S-band carrier phase modulation by voice and telemetry subcarriers was interrupted at 65:13:58, and real-time telemetry was then transmitted on the S-band FM link. Full S-band communications capability was restored at 72:36:32 when the crew selected the alternate S-band transponder.

5.14.1 Command and Service Module Equipment

The spacecraft S-band communications system performed satisfactorily, except for the loss of S-band PM subcarriers from 65:13:58 to 72:36:32. Real-time telemetry and television were time-shared on the backup S-band FM mode until the crew switched to the PM alternate transponder, restoring normal operation. (See section 11 for a further discussion of the discrepancy.)

An excessive audible noise is a characteristic of the loss of phase lock with the ground. The crew effectively controlled this noise level by adjusting the volume control to a minimum setting whenever the slow buildup of background noise was noted and used this change in noise level as a convenient indication of impending loss of phase lock. Quieting of the background noise when the volume controls were set at a minimum provided an indication that phase lock with the ground had been established.

Because the crew could not determine which S-band antenna provided optimum performance, the antennas were generally switched on request from the ground; however, switching was requested so frequently that the task became objectionable to the crew.

The quality of the VHF voice communications was generally very good. The periods of garbled or fading voice were near the times of acquisition or loss of signal. The VHF voice (duplex-B mode) was satisfactory during the countdown and launch phase until approximately 00:07:00 when the voice communications received at the Mission Control Center became garbled and did not completely clear until the simplex-A mode was selected. Satisfactory operation of the duplex-B mode was verified at about 07:30:00 (see section 11 for further discussion of the discrepancy).

The recovery forces did not receive the VHF recovery beacon signal while the spacecraft was on the parachutes. (See section 11 for a further discussion of this discrepancy.)

A successful track of the onboard rendezvous radar transponder was achieved with a ground-based radar during the 48th revolution. Frequency track was maintained for 57.5 seconds while the spacecraft line-of-sight velocity passed through the interval bounded by approximately ± 6500 ft/sec; this exceeds the range rate requirement for a lunar mission. Range acquisition occurred 8 seconds after AUTO-TRACK ENABLE was commanded manually at initial frequency lock. The RANGE GOOD data period lasted for 49.5 seconds and terminated upon loss of frequency track, and the radar range to the spacecraft varied between 396 and 414 n. mi. during the entire tracking period. The transponder frequency track was reported by the crew to have lasted about 3 minutes, based on onboard computer indications.

5.14.2 Command and Service Module/Manned Space Flight Network

S-band RF two-way phase lock with the spacecraft S-band transponder was established by the Manned Space Flight Network prior to launch and was successfully maintained until the handover from the Bermuda Island site to USNS Vanguard (figs. 5.14-1, 5.14-2, and 5.14-3). At that time, downlink communications were interrupted for approximately 1 minute (fig. 5.14-4). The duration of the interruption may have been increased because the spacecraft omnidirectional antennas were switched 21 seconds after initiation of handover. Transfer of the uplink from USNS Vanguard to the Canary Island site resulted in a 5-second loss of downlink communications (figs. 5.14-4 and 5.14-5). The received carrier powers at all network sites agreed with premission predictions.

The VHF duplex-B (ground-to-spacecraft on a 296.8 MHz carrier and spacecraft-to-ground on a 259.7 MHz carrier) was the prime voice communications link; however, simultaneous transmissions via S-band provided immediate backup (fig. 5.14-6).

From 00:07:06 to 00:08:05, both the Grand Bahama Island and Bermuda Island sites were transmitting voice to the spacecraft on the VHF link. Voice transmissions to the spacecraft from the Bermuda site via VHF were terminated at 00:09:50 and were not resumed until 00:11:57. As shown in figure 5.14-6, the MODE IV MARK, which the crew did not hear, was transmitted on S-band only. The results of a qualitative evaluation of the ground voice receiver outputs are also presented in the figure. Although the received VHF signal power at Bermuda (fig. 5.14-7) was sufficient to support good voice communications, the receiver output was garbled from acquisition to 00:09:50. The output of the receiver cleared up after it was removed from NETWORK 1. The garbled voice at the output of the Bermuda VHF receiver also degraded the outputs of the S-band and VHF receivers at Grand Bahama during the time that the two sites were simultaneously connected to NETWORK 1. The output of the VHF receiver at the Canary Island site was also garbled until the simplex-A mode was selected

at 00:19:17. The failure of the crew to receive certain uplink transmissions resulted from improper procedures at the ground station, and the garbled voice resulted from improper procedures and/or malfunctioning receivers at the Bermuda and Canary Island sites.

During the launch phase, good telemetry data were received except during short intervals when the performance was perturbed by the launch vehicle plume, launch events, or S-band handovers (figs. 5.14-1 through 5.14-4). Each of the three commands transmitted were verified by the spacecraft updata link equipment.

The performance of the communications system during the earth-orbit phase is highlighted in figures 5.14-8 through 5.14-15 and summarized by station pass in table 5.14-I. S-band communications during most of the earth-orbit phase were maintained by the crew switching between opposite omnidirectional antennas when required by ground cue, when the performance of the telemetry and/or voice channels was marginal, or when the onboard display indicated weak uplink carrier power.

The performance of the S-band PM system was nominal except for the period from 65:13:58 to 72:36:32, as previously discussed. In general, the telemetry channel performance was consistent with the received carrier power. The crew reported receipt of clear voice communications each time the S-band system was utilized. The overall performance of the S-band downvoice channel was good, and in general, was better than that of the VHF voice.

A total of 3793 commands, including 55 computer loads and two central timing equipment updates, were transmitted during the earth-orbit phase. The onboard updata link equipment did not verify 241 commands that were transmitted during periods of weak signals.

The S-band FM system was successfully utilized for television transmissions, numerous dumps of data and voice that had been recorded on the data storage equipment, and real-time telemetry backup to the PM system.

The VHF simplex-A mode was utilized as the prime voice communications link for the first half of the earth-orbit phase. During the second half, the VHF link provided the uplink voice, and the S-band system the downvoice. The VHF link was adequate in both cases.

Coverage of the eighth service propulsion system maneuver (deorbit maneuver) was provided by the network site at Hawaii. The average downlink carrier power during the maneuver was minus 85 dBm (fig. 5.14-16), and telemetry channel performance was nominal. After the handover from Hawaii to USNS Huntsville at 259:41:09, two-way communication between the spacecraft and USNS Huntsville was intermittently lost from 259:42:50 until

loss of signal at 259:45:23. S-band communications blackout occurred at 259:54:58 and lasted for 5 minutes 2 seconds. The final loss of signal, by the Bermuda site, occurred at 260:02:13. The performance of the voice and telemetry channels was normal during the deorbit and entry phase.

5.14.3 Spacecraft/Apollo Range Instrumentation Aircraft

Several checks of the communications link between the spacecraft and the aircraft were conducted and included relay of VHF and S-band voice, receipt and recording of real-time and dump telemetry, and receipt and recording of dump voice. In general, the S-band voice relays were more successful than the VHF relays. The real-time and dump telemetry data recorded during portions of the aircraft coverage were subsequently dumped to the network sites.

TABLE 5.14-I.- COMMUNICATION SYSTEM PERFORMANCE DURING EARTH ORBIT PHASE

Site	Rev	Event	AOS	LOS	Remarks
MIL	1/2		01:36:31	01:44:50	The first dump of voice and telemetry data recorded on space-craft data storage equipment was effected during this station pass. The dump was accomplished using the S-band FM link and a tape speed 32 times faster than the record speed. The quality of voice was degraded by background noise and ranged from poor to good. The quality of the dumped telemetry data was good. The received S-band PM link carrier power compared favorably with permission predictions.
GWM	5	Communications check			Correct operation of the VHF duplex-B voice communications link was reverified. The speech-to-noise ratio of the received downlink voice averaged +20 dB and the intelligibility was good.
HAW	7	Communications check			Operation of the VHF duplex-A voice communications link was checked. The intelligibility of the received downlink voice ranged from fair to good.
ACN	9	Communications check			A check of the VHF simplex-B voice communications link was performed. The downlink speech intelligibility was degraded by a tone on the site recording and ranged from fair to good.
CRO	17	First service propulsion maneuver	26:23:03	26:31:03	The performance of the communication system was nominal. The received S-band carrier power corresponded to premission predictions (see fig. 5.14-8).
CRO	18	Second service propulsion maneuver	27:57:37	28:06:04	As shown in figure 5.14-9, the average received S-band downlink carrier power was -78 dBm. The performance of the command, telemetry, and voice channels was nominal. The speech-to-noise ratio of the recorded S-band downvoice averaged +11 dB, and the downvoice quality and intelligibility were good.

TABLE 5.14-I.-- COMMUNICATION SYSTEM PERFORMANCE DURING EARTH ORBIT PHASE - Continued

Site	Rev	Event	AOS	LOS	Remarks
TEX	19	Formation-flying with S-IVB	30:12:55	30:19:17	The site provided communications support for approximately 6 minutes while the command and service module was flying in formation with the S-IVB. A 40 dB increase in received carrier power was noted when omnidirectional antenna C was selected at 30:16:20. The line-of-sight to the spacecraft entered the south keyhole of the Texas antenna at 30:17:00 and emerged at approximately 30:18:20. Considering the weak carrier power received during this pass, the telemetry channel performance was nominal.
TEX	33	Communications check	52:21:41	52:39:06	The S-band uplink signal combination consisting of voice and updata operating in conjunction with the downlink combination of backup voice and low bit rate telemetry was checked. The quality and intelligibility of the backup downvoice ranged from fair to good. Each of the three commands transmitted were accepted by the spacecraft updata link equipment. As expected, the telemetry frame synchronization was interrupted by backup voice modulation (fig. 5.14-10). Tests have shown that these interruptions can be minimized by selection of the MSFN receiver 50-Hz carrier tracking loop (inflight doppler rates necessitated use of the 700-Hz loop). Since the doppler rates during the translunar coast, lunar orbit, and transearth coast phases of future Apollo missions will not require use of the 700 Hz loop, Goddard Space Flight Center has been requested to utilize the 50 Hz loop when the spacecraft is in one of the above mission phases and backup downvoice and low bit rate telemetry are transmitted.
RED	41				Transmission of the S-band telemetry and voice subcarriers on the PM carrier was interrupted at approximately 65:13:58. See section 11 for description of this anomaly.

TABLE 5.14-I.- COMMUNICATION SYSTEM PERFORMANCE DURING EARTH ORBIT PHASE - Continued

Site	Rev	Event	AOS	LOS	Remarks								
TEX MIL	45	Television transmission	71:41:14	71:48:40	Coverage of the first television broadcast from an Apollo spacecraft was provided by the Texas and Merritt Island sites. Even though performance was somewhat limited by weak signal strength, the picture quality ranged from fair to excellent.								
CRO	46		72:35:05	72:44:21	Full capability of the S-band PM link was restored during this pass by selecting the primary S-band transponder (see fig. 5.14-11 and section 11).								
CRO	48	Third service propulsion maneuver	75:44:58	75:50:19	As shown in figure 5.14-12, the performance of the S-band RF system and the telemetry channel were nominal								
TEX MIL	60	Television transmission	95:25:27	95:33:12	The communication system performance was nominal. As shown in figure 5.14-13, the total received signal power during the majority of the Merritt Island coverage was -75 dBm. This received signal power provided excellent television picture quality as evidenced by the photographs in figure 5.14-13, and resulted in a video signal-to-noise ratio greater than 16 dB.								
HAW	63	Communications check	99:53:57	99:57:04	S-band signal combination check: <table style="margin-left: auto; margin-right: auto;"> <tr> <td style="text-align: center;"><u>Uplink</u></td> <td style="text-align: center;"><u>Downlink</u></td> </tr> <tr> <td style="text-align: center;">Carrier</td> <td style="text-align: center;">Carrier</td> </tr> <tr> <td style="text-align: center;">Voice</td> <td style="text-align: center;">Voice</td> </tr> <tr> <td style="text-align: center;">Updata</td> <td></td> </tr> </table> Seven commands were transmitted. Two which were transmitted near loss-of-signal were not verified. The speech-to-noise ratio of the recorded downvoice averaged +23 dB during the evaluation period. Voice quality and intelligibility were good.	<u>Uplink</u>	<u>Downlink</u>	Carrier	Carrier	Voice	Voice	Updata	
<u>Uplink</u>	<u>Downlink</u>												
Carrier	Carrier												
Voice	Voice												
Updata													

TABLE 5.14.-I.- COMMUNICATION SYSTEM PERFORMANCE DURING EARTH ORBIT PHASE - Concluded

Site	Rev	Event	AOS	LOS	Remarks
TEX	76	Fourth service propulsion maneuver	120:42:30	120:47:55	The average S-band received downlink carrier power was -83 dBm. The command and telemetry channels performed nominally.
MIL	104/105	Fifth service propulsion maneuver	164:59:10	165:05:02	As shown in figure 5.14-14, received downlink carrier power variations as large as 15 dB were observed. Three commands were transmitted and accepted by the spacecraft. The telemetry channel performance was consistent with the received carrier power.
CYI	118	Communications check	186:11:38	186:18:56	Crew confirmed receipt of very clear voice during the check of the S-band backup voice.
GDS	120	Communications check	190:36:06	190:43:01	The message "THIS IS A TEST OF EMERGENCY KEY" was transmitted in Morse code utilizing the emergency key capability. A clear 1-KHz tone was audible each time the transmitter was keyed.
GYM	121	Communications check	192:13:01	192:19:50	A check of the spacecraft voice relay capability was conducted between 192:15:41 and 192:16:18 by relaying the voice output of the spacecraft VHF receiver to the Guaymas site on the S-band link. The quality of the relayed voice varied from fair to good.
MIL	132/133	Sixth service propulsion maneuver	210:04:15	210:13:29	The received downlink carrier power during the maneuver was approximately -82 dBm. The voice quality was good during the majority of the pass. The spacecraft updata link equipment accepted each of the three commands which were transmitted.
ANG	151	Seventh service propulsion maneuver	239:04:24	239:10:24	As shown in figure 5.14-15, the received downlink carrier power increased from -100 to -90 dBm during the maneuver. The performance of the voice and telemetry channels was consistent with the received carrier power. Each of the three commands transmitted was accepted and verified by the spacecraft updata link equipment.

NASA-S-68-6301

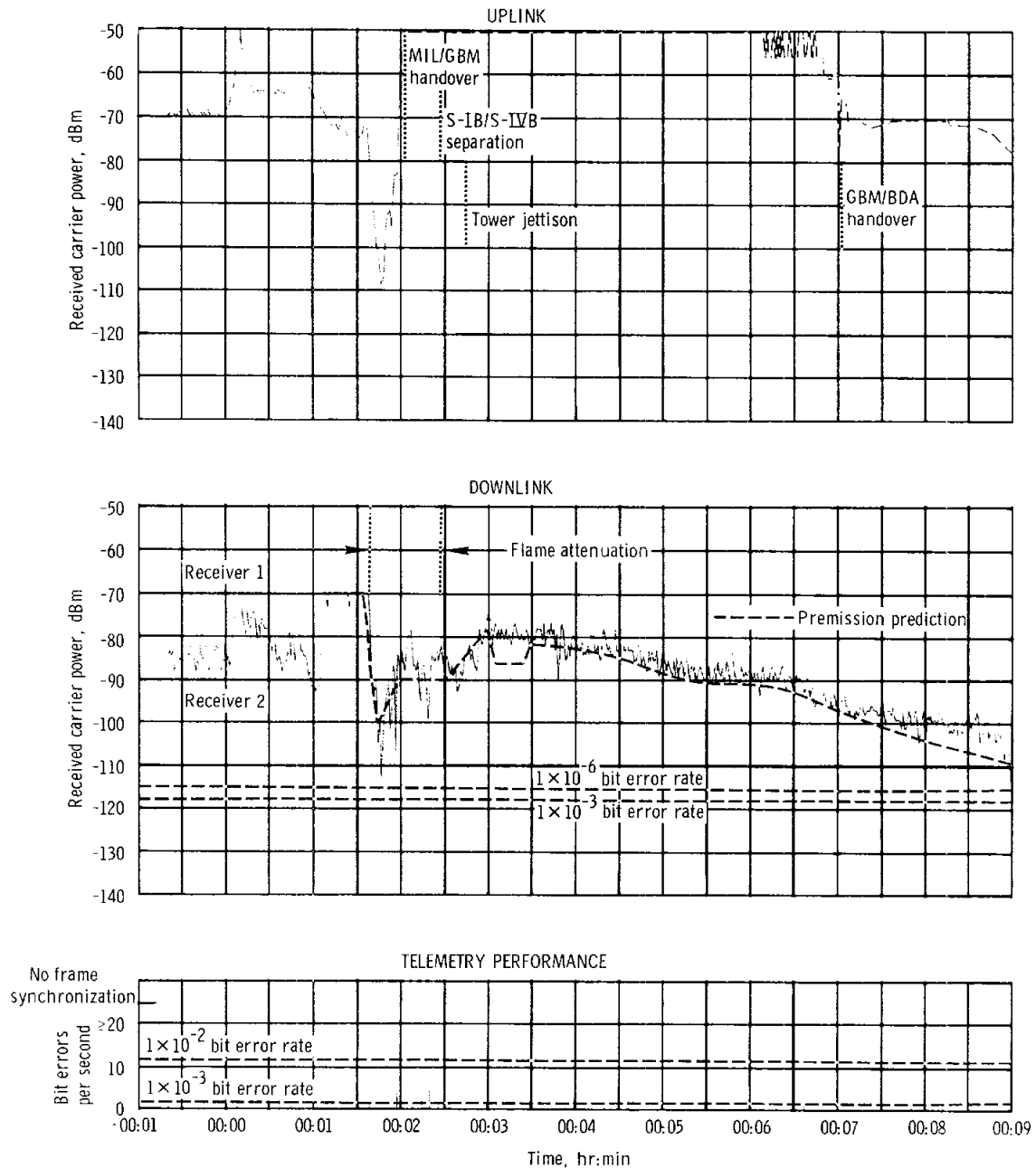


Figure 5.14-1. - Received S-band carrier power and telemetry performance, Merritt Island, launch.

NASA-S-68-6302

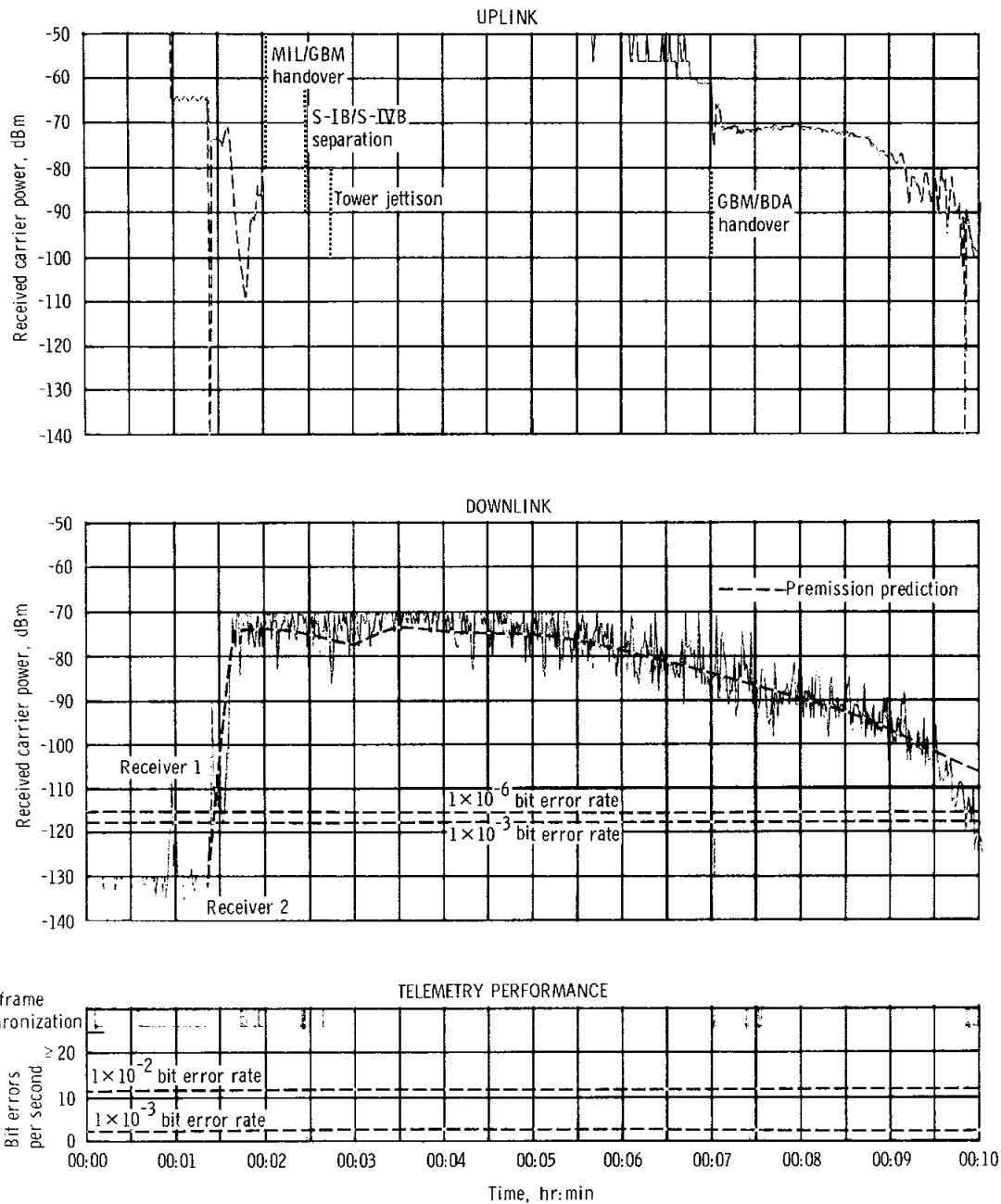


Figure 5.14-2. - Received S-band carrier power and telemetry performance, Grand Bahama, launch.

NASA-S-68-6303

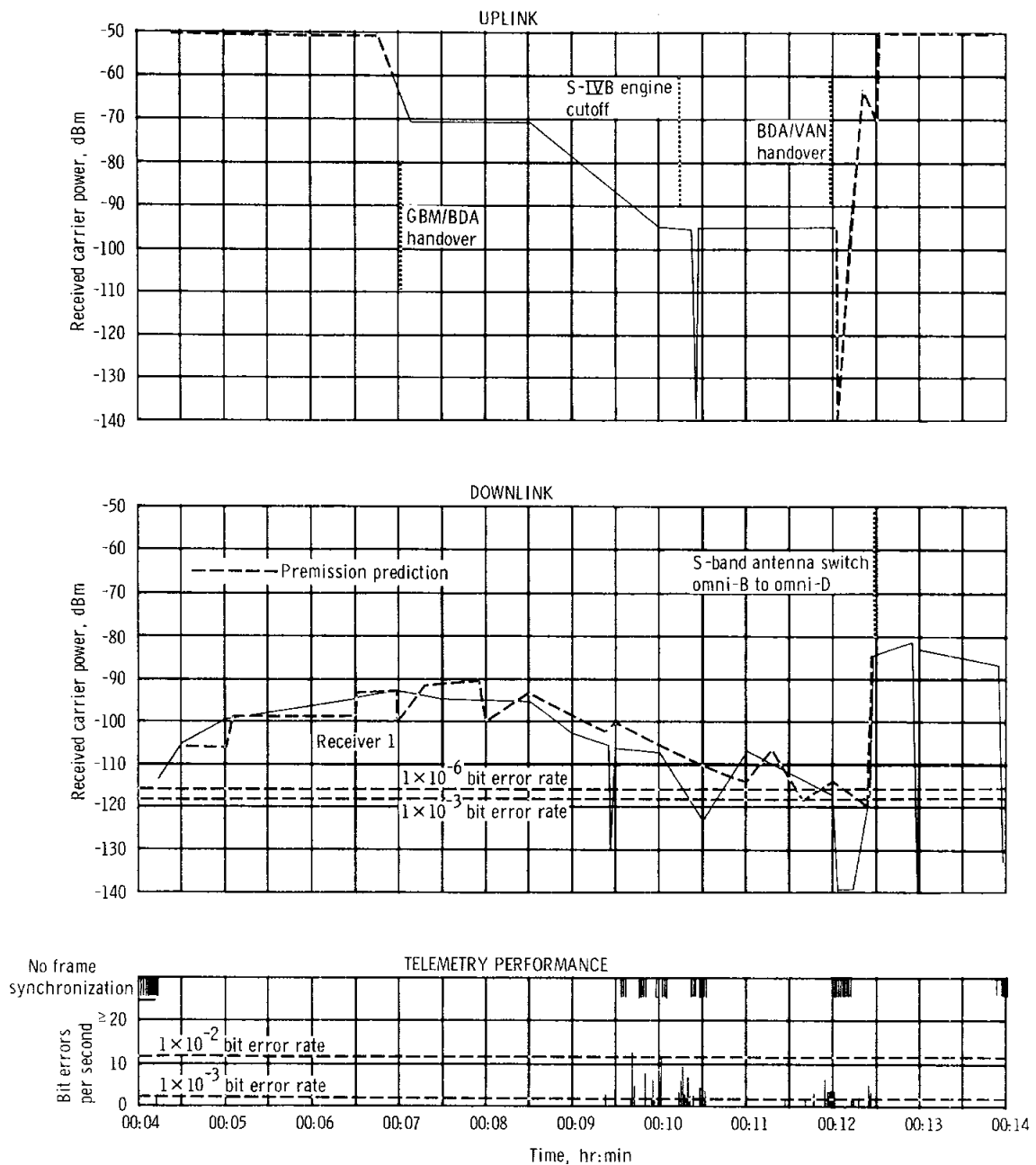


Figure 5.14-3. - Received S-band carrier power and telemetry performance, Bermuda, launch.

NASA-S-68-6304

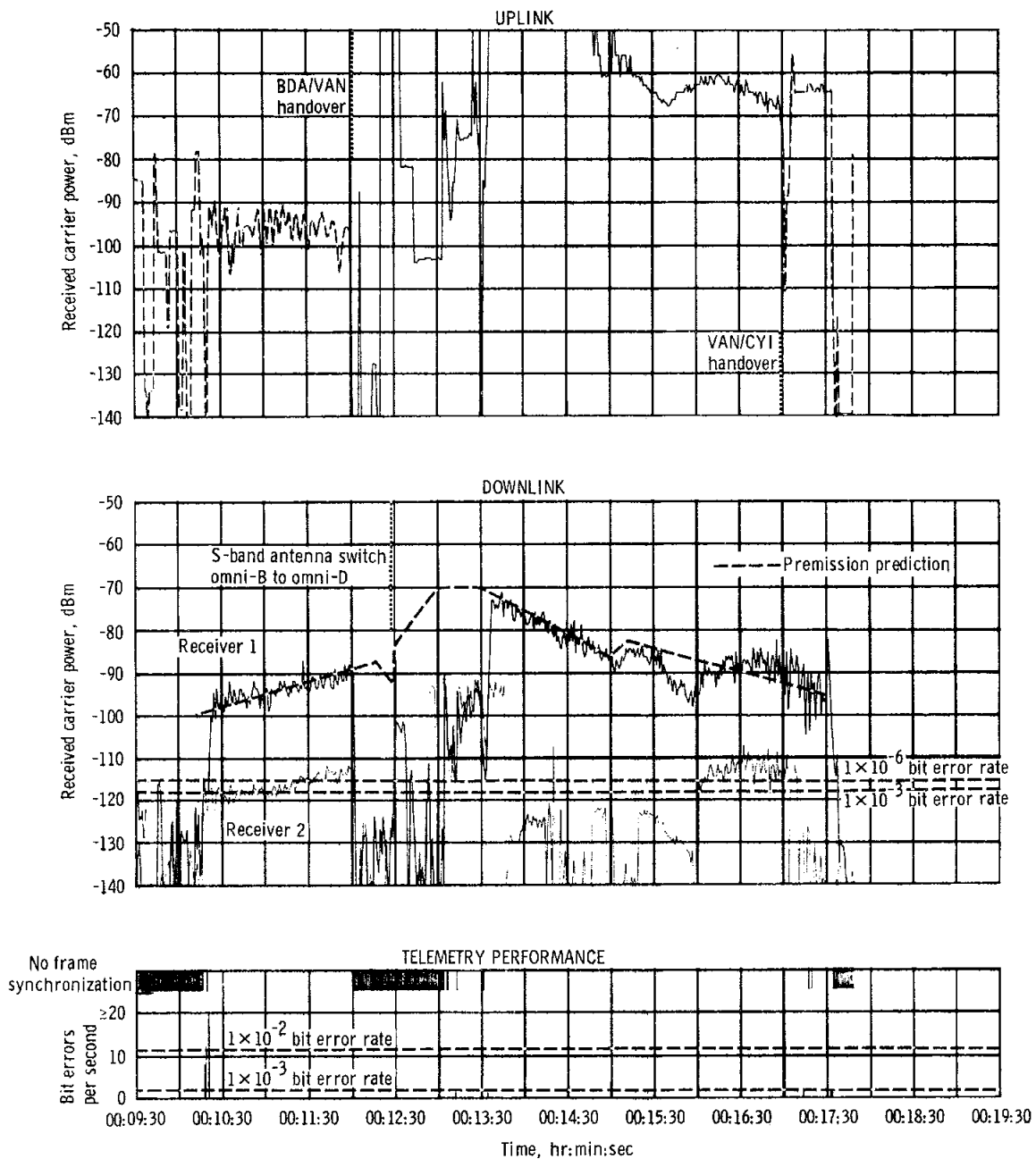


Figure 5.14-4. - Received S-band carrier power and telemetry performance,
USNS Vanguard, revolution 1.

NASA-S-68-6305

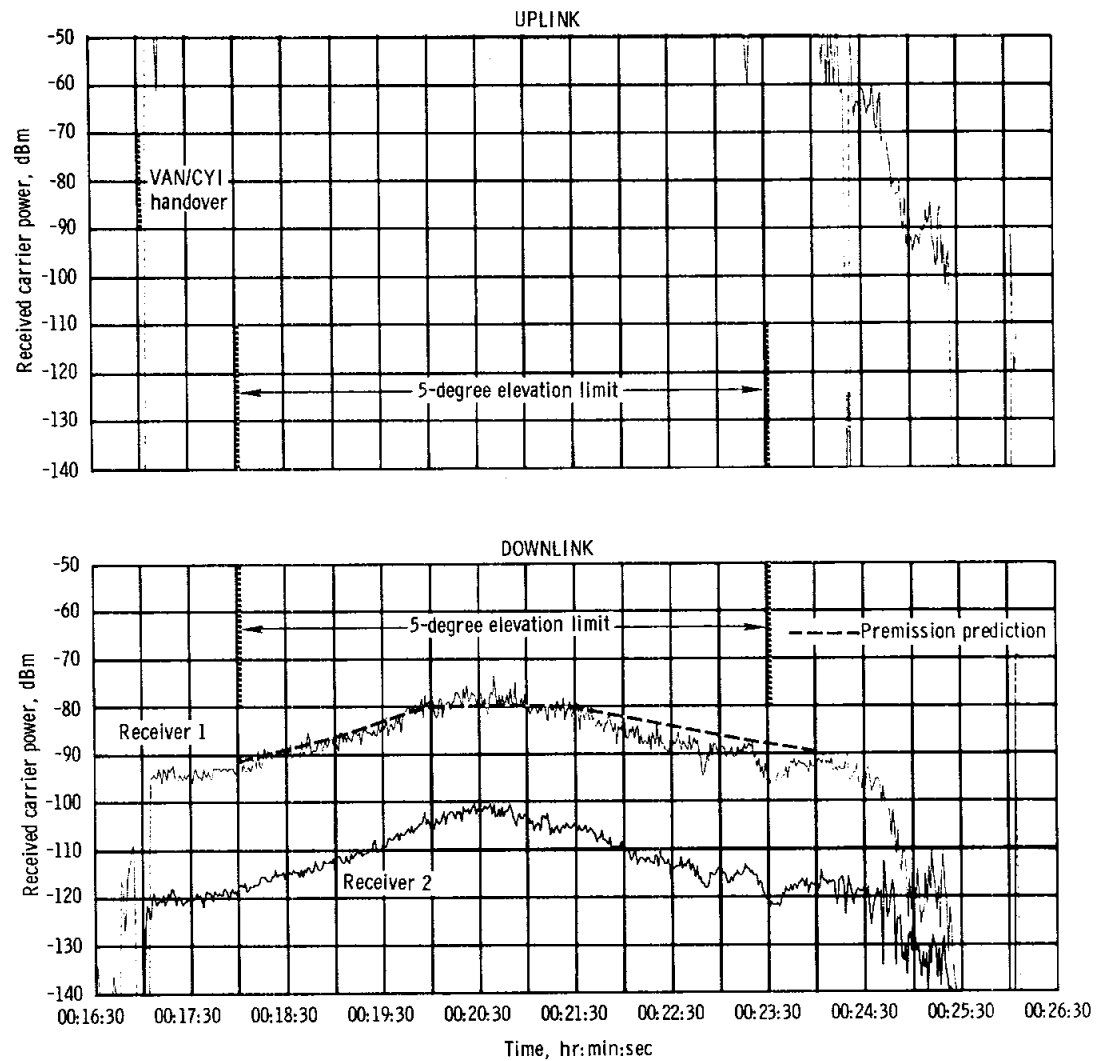


Figure 5.14-5. - Received S-band carrier power, Canary Island, revolution 1.

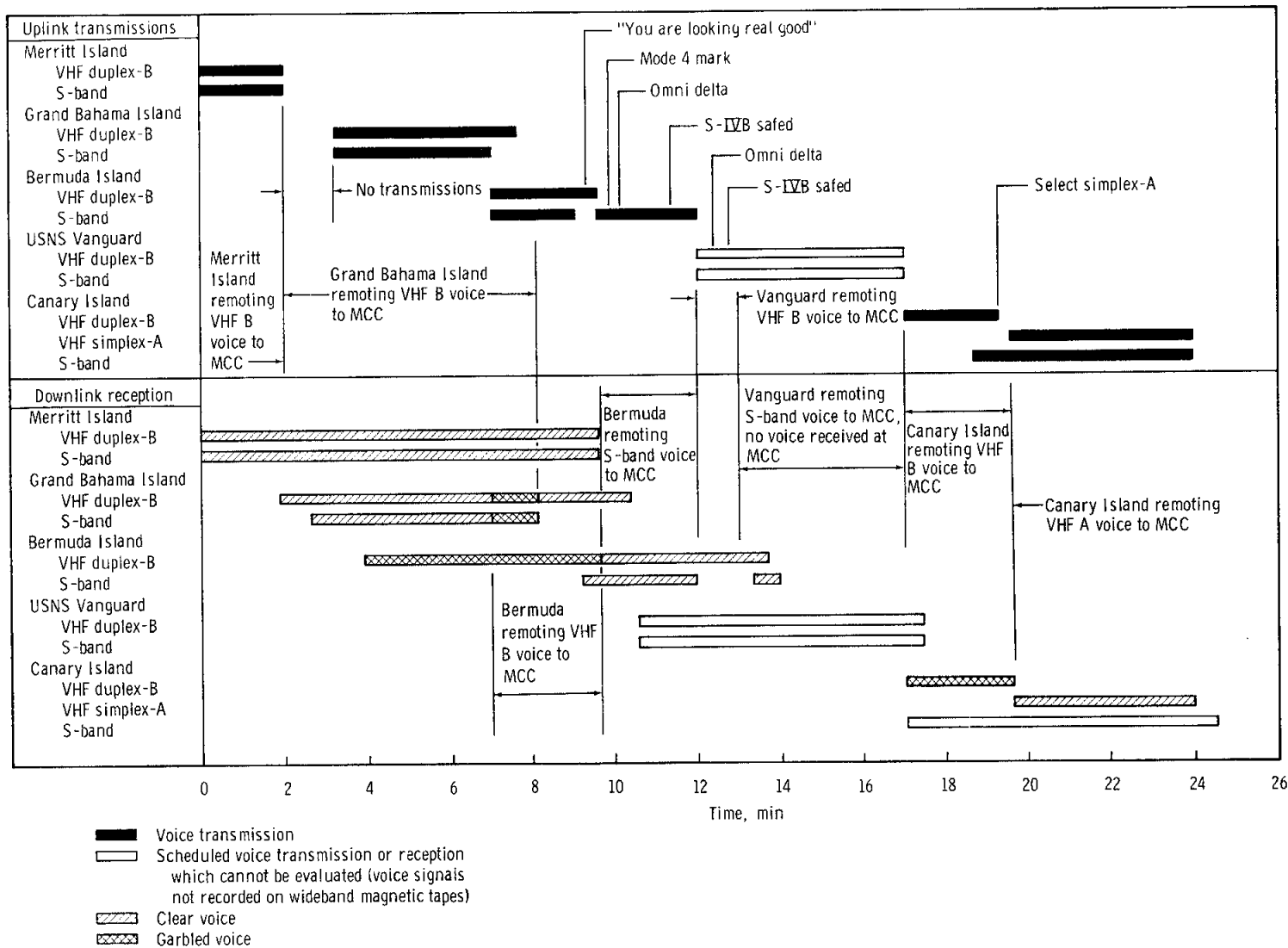


Figure 5.14-6. - Launch-phase voice communications.

NASA-S-68-6307

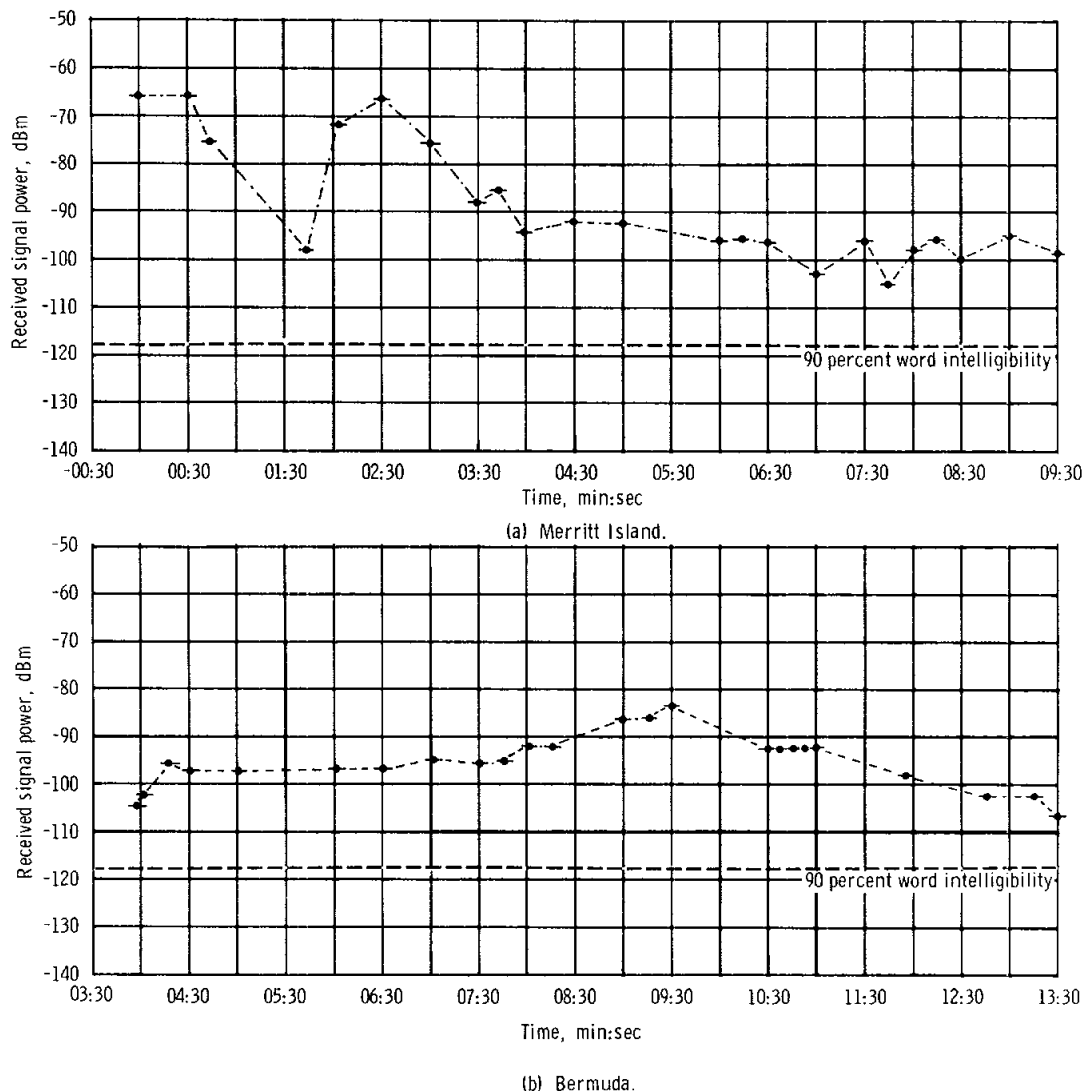


Figure 5.14-7. - Received VHF/AM signal power, launch phase.

NASA-S-68-6308

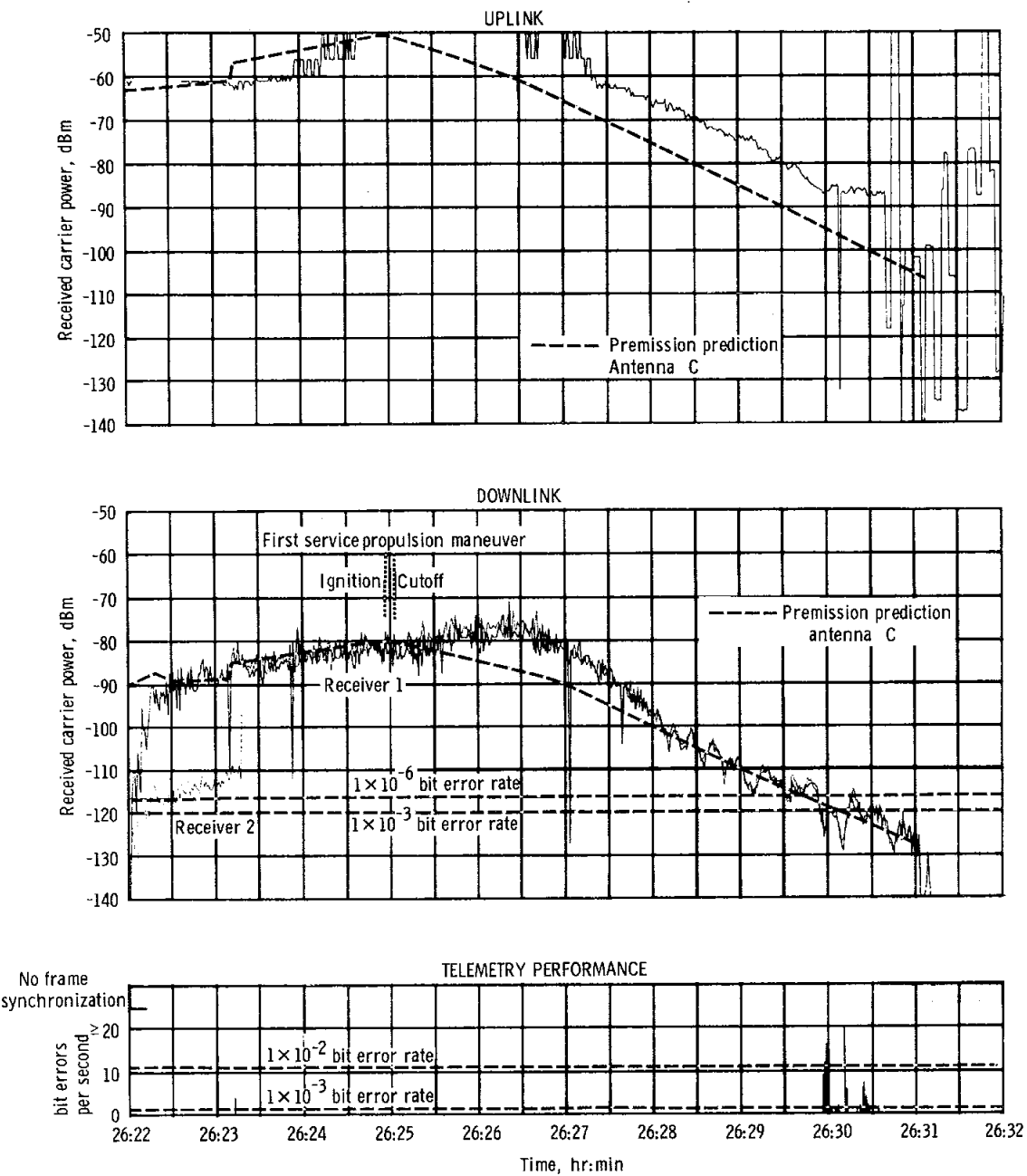


Figure 5.14-8. - Received S-band carrier power and telemetry performance,
Carnarvon, revolution 17.

NASA-S-68-6309

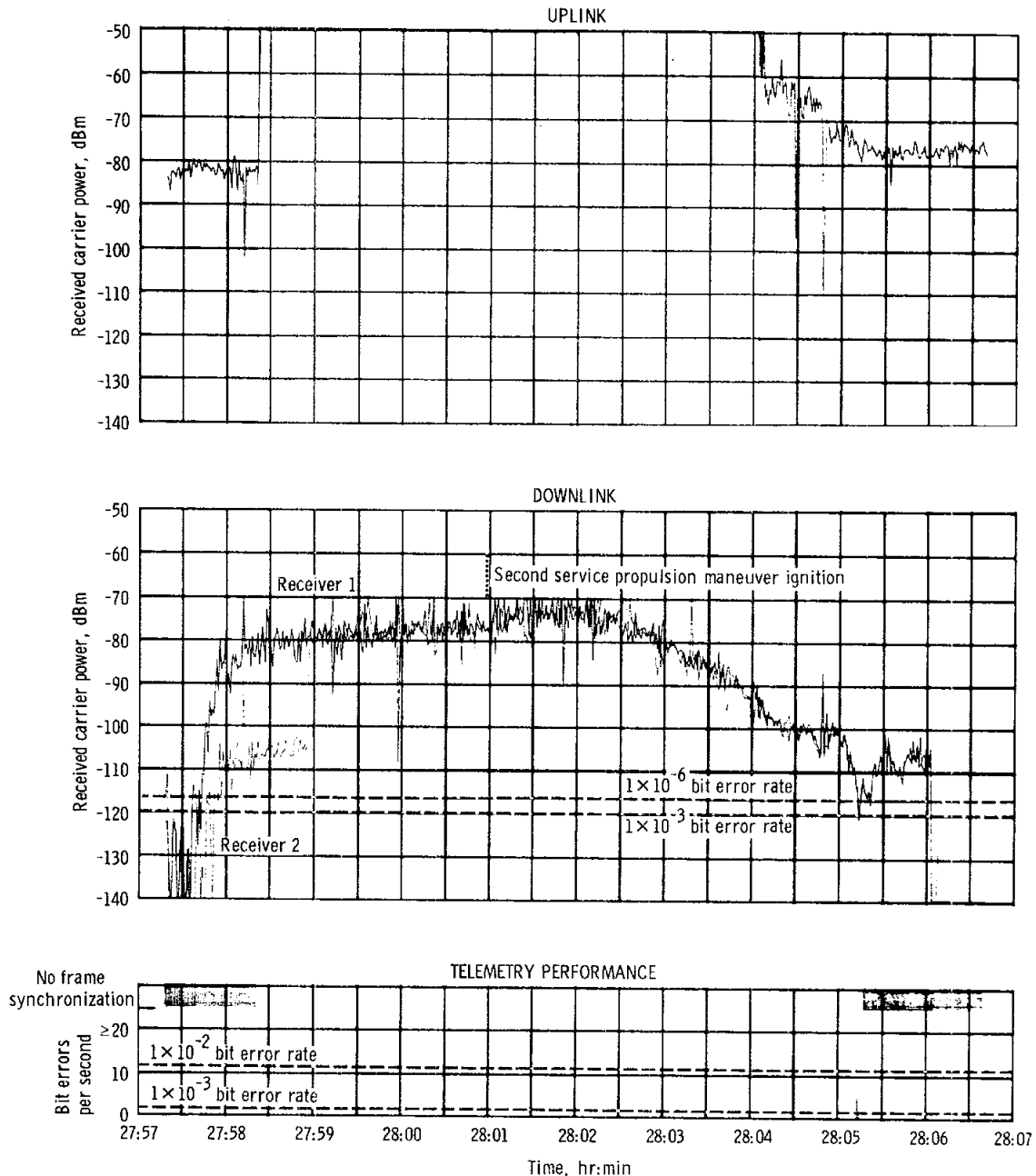


Figure 5.14-9. - Received S-band carrier power and telemetry performance,
Carnarvon, revolution 18.

NASA-S-68-6310

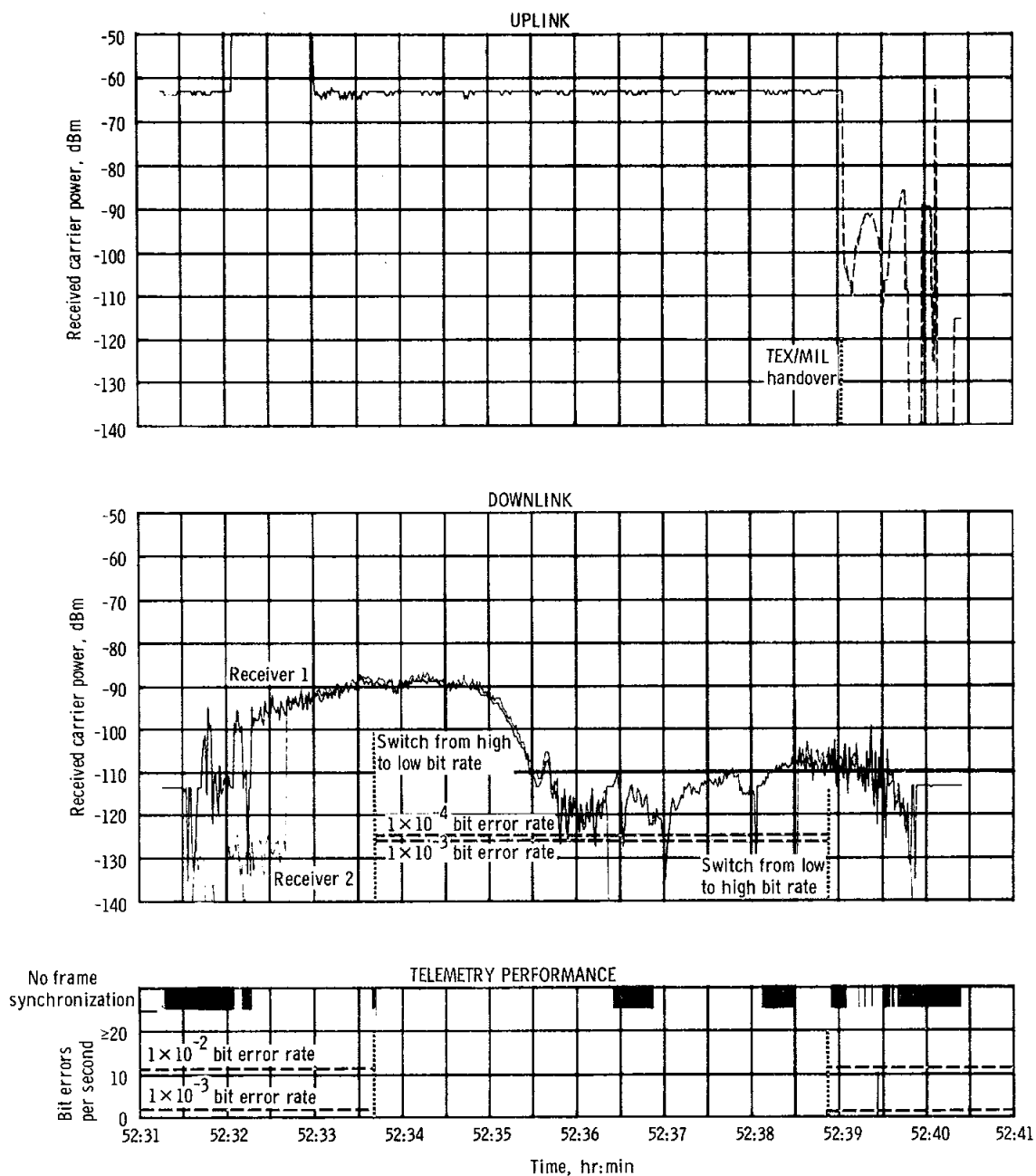


Figure 5.14-10. - Received S-band carrier power and telemetry performance,
Texas, revolution 33.

NASA-S-68-6311

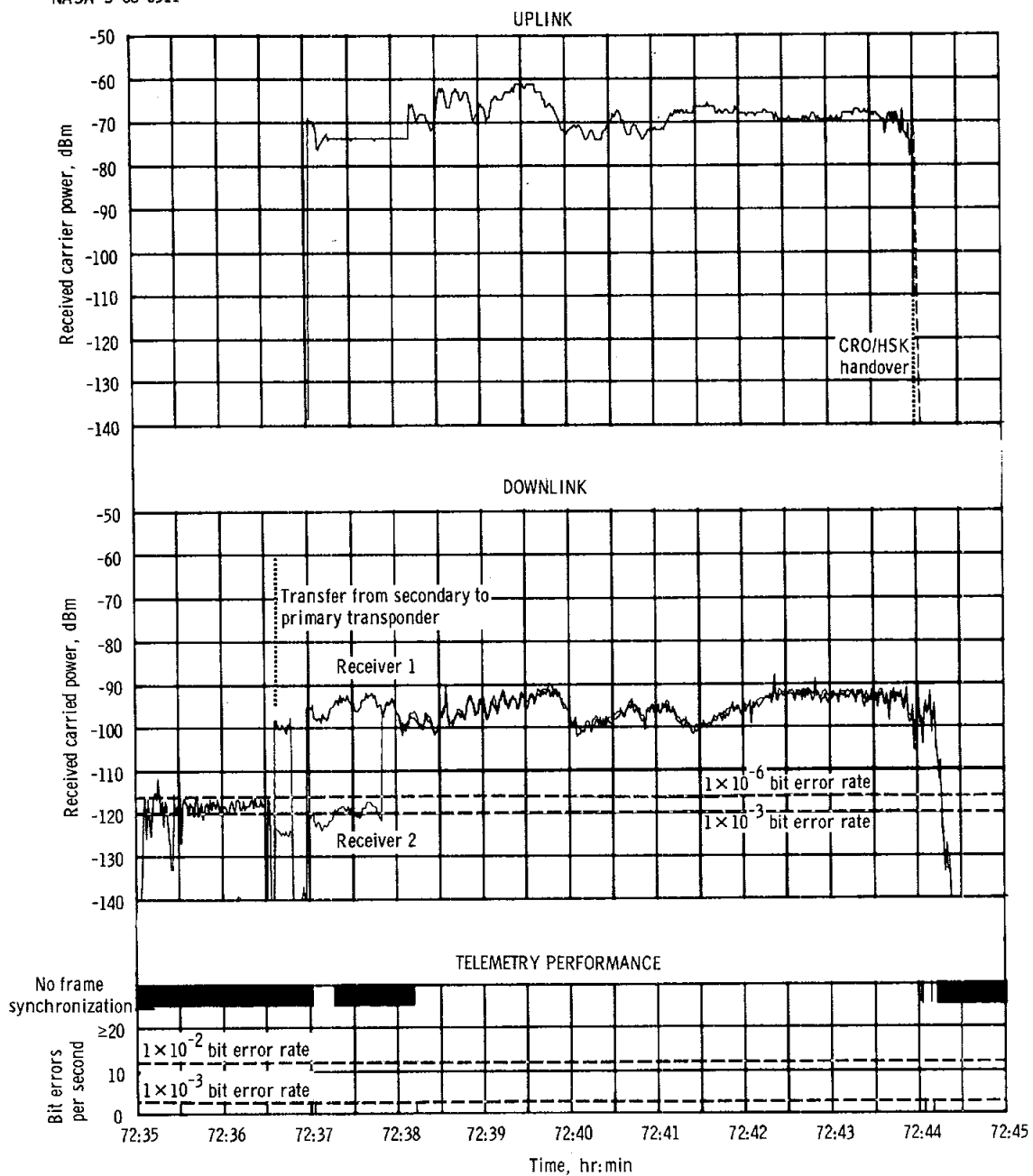


Figure 5.14-11. - Received S-band carrier power and telemetry performance, Carnarvon, revolution 46.

NASA-S-68-6312

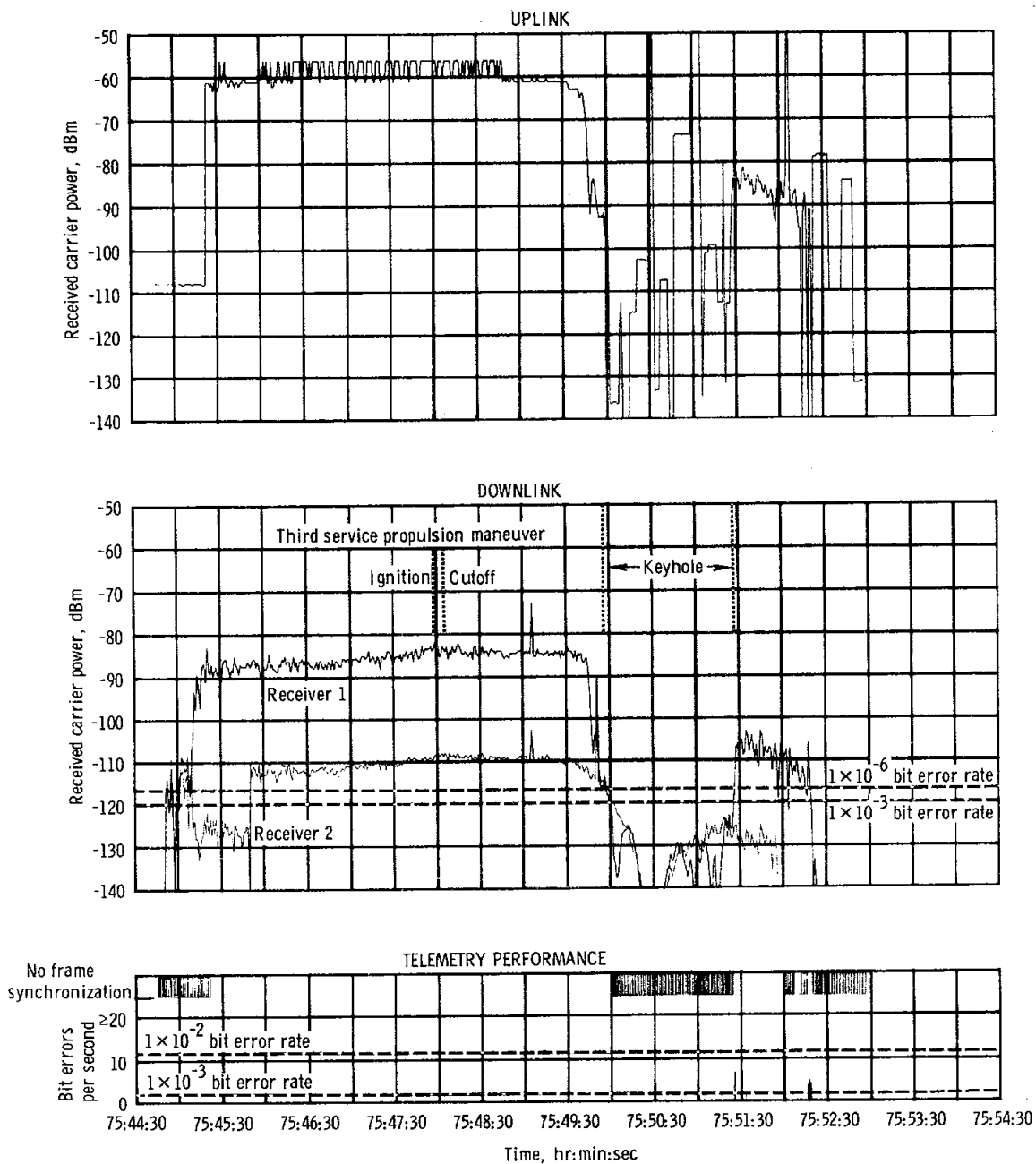


Figure 5.14-12. - Received S-band carrier power and telemetry performance,
Carnarvon, revolution 48.

NASA-S-68-6313

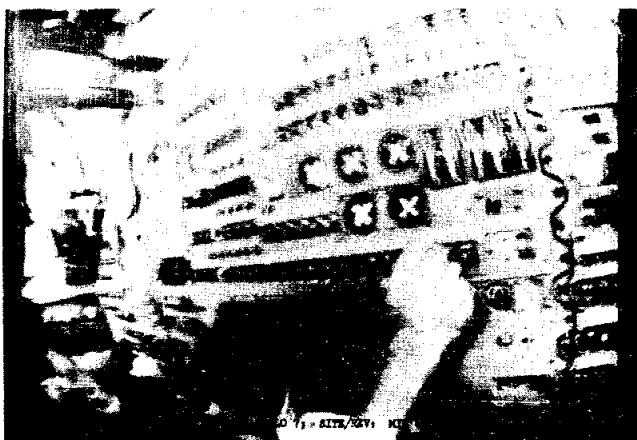


Photo 1



Photo 2

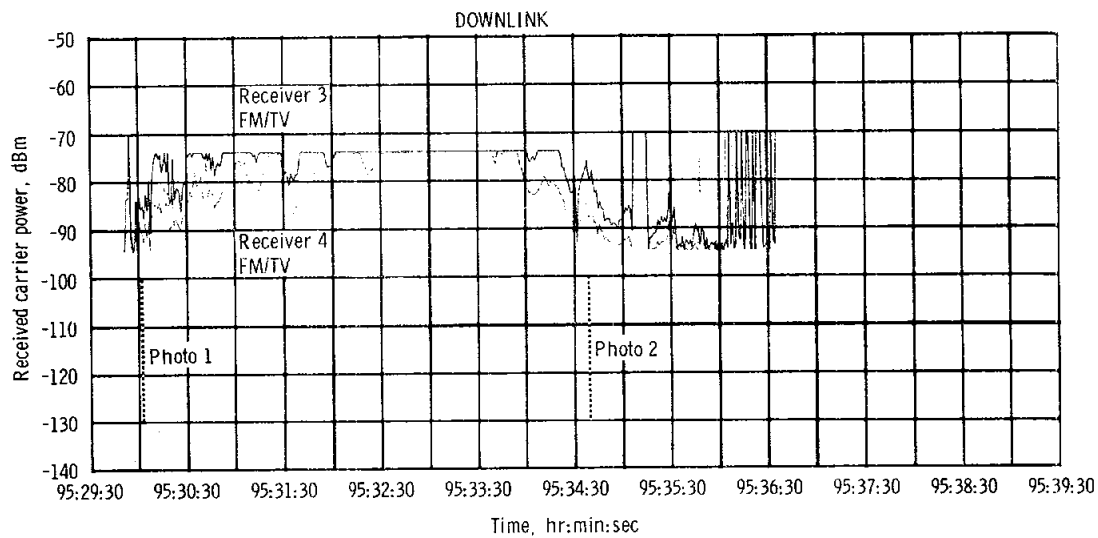


Figure 5.14-13. - S-band total received power (FM) and television photographs, Merritt Island, revolution 60/61.

NASA-S-68-6314

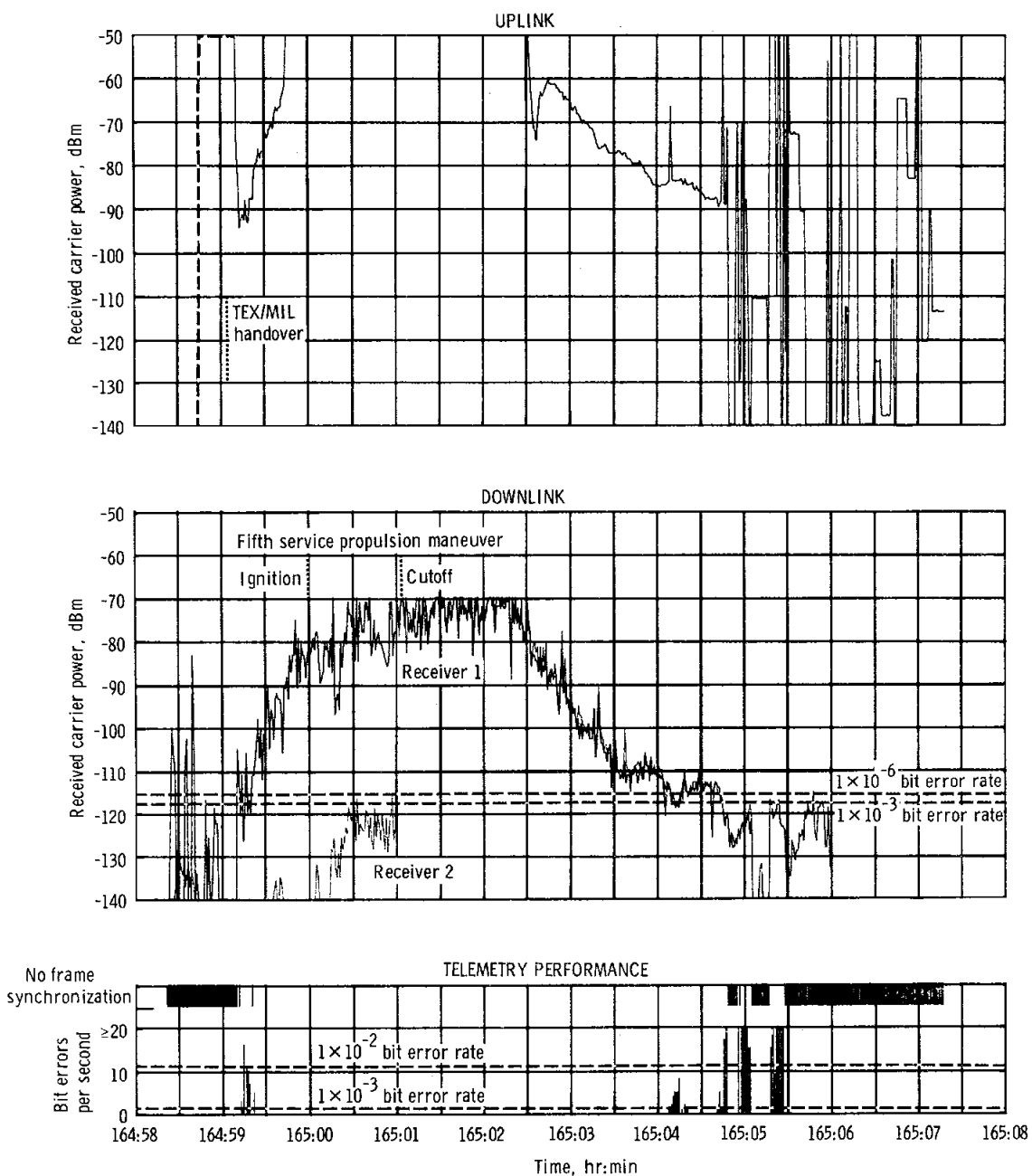


Figure 5.14-14. - Received S-band carrier power and telemetry performance,
Merritt Island, revolution 104/105.

NASA-S-68-6315

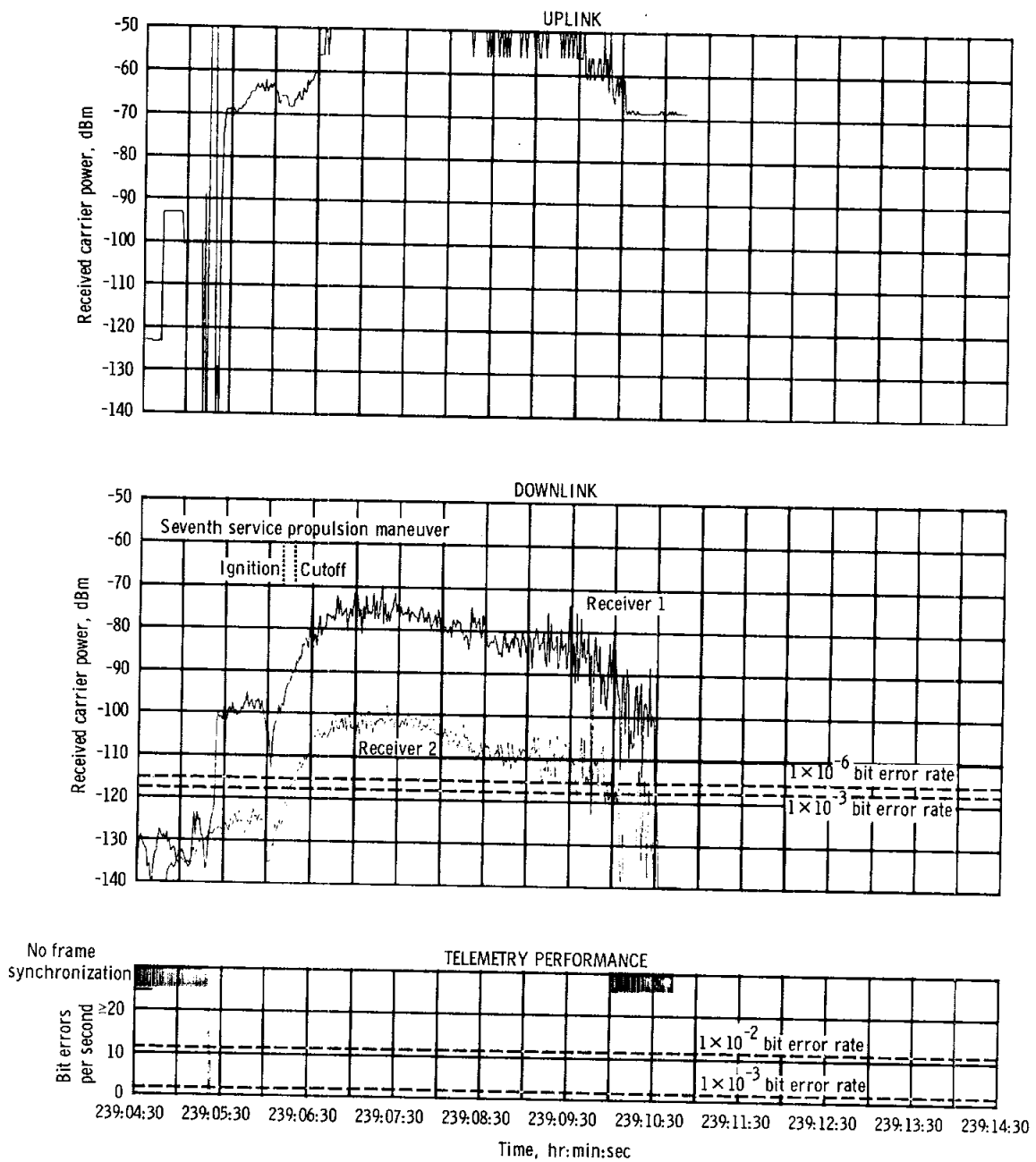


Figure 5.14-15. - Received S-band carrier power and telemetry performance, Antigua, revolution 151.

NASA-S-68-6316

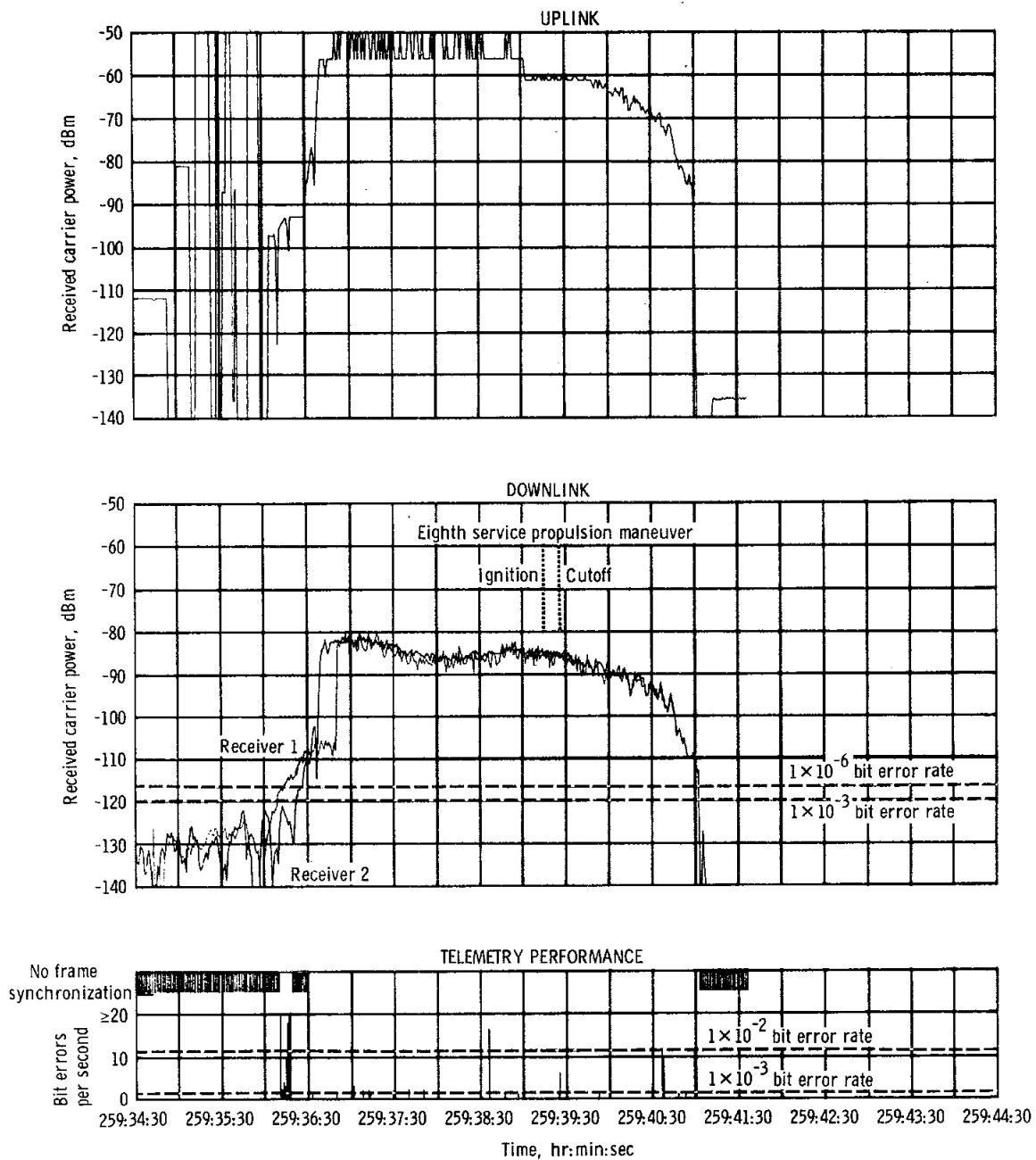


Figure 5.14-16. - Received S-band carrier power and telemetry performance,
Hawaii, revolution 163.

5.15 INSTRUMENTATION

The spacecraft instrumentation system adequately supported the mission and provided satisfactory data for postflight mission analysis.

5.15.1 Operational Instrumentation

The general operation of the 298 operational measurements and the associated equipment was good. Only four measurements required waivers prior to the mission. After lift-off, all operational instrumentation measurements operated satisfactorily except for two biomedical instrumentation parameters, discussed in section 5.19. Twelve of fifteen temp-plates (passive temperature indicators) were lost because the forward heat shield was not recovered. Of the three remaining temp-plates, one of the two located on the forward hatch of the command module was lost, while the other indicated a nominal temperature rise. The third temp-plate, mounted on the inside of the hatch, showed no response, as expected.

A launch hold of 2 minutes 45 seconds caused the central timing equipment to be in error at launch. This error was corrected by an update over Carnarvon during the first revolution. The central timing equipment continued to operate satisfactorily until the eighth revolution when at 12:07:26, it read 00:42:09, indicating that a reset had occurred at 11:25:17. The timing equipment was updated at 12:26:20 over Hawaii and continued to read correctly for the remainder of the mission. The cause of the reset is attributed to electrical interference discussed in section 11.

The data storage equipment, which recorded data for 130 hours of the flight, worked well, recording and dumping both high- and low-bit data. However, time required for phasing the rewinding and playback with ground stations left much to be desired because of the short time available over a station. On a lunar mission, the time over a station would be sufficient to preclude such a problem. During entry, the recorder operated until the end-of-tape limit was reached at 260:08:48, approximately 20 seconds prior to landing.

5.15.2 Flight Qualification Instrumentation

The flight qualification instrumentation operated satisfactorily except for high-level commutator 1, which became erratic during entry at 259:43:49.6. This commutator processed forward and aft heat shield pressure and temperature measurements and two structural measurements. The commutator performed satisfactorily during the first 5 minutes of

the entry phase, then exhibited nonsynchronous operation for approximately 6 seconds, and finally provided good data for an additional 1 minute 30 seconds. Thereafter, except for one period of approximately 3 seconds, the commutator processed only 18 channels of data until the end of recorded data. The commutator problem is further discussed in section II.

The flight qualification tape recorder operated satisfactorily and recorded data during the launch phase from lift-off minus 32 seconds to 00:03:12, during the fifth service propulsion maneuver (164:59:31.7 to 165:01:56.5), and during entry from 259:39:56.6 until the end-of-tape limit was reached at 260:02:55.1 (approximately 6 minutes 39 seconds prior to landing).

The 167 flight qualification measurements and associated equipment operated satisfactorily. Three measurements were waived prior to lift-off, six measurements failed during the mission, and ten measurements provided questionable data.

Five of seven low-range heat-flux calorimeter measurements located in the aft heat shield failed during entry. These calorimeters measured the initial heating of entry but then failed either because the increasing heat load exceeded the heat capacity or because the transducer bond was weak and the transducer was dislodged by ablator outgassing. These five sensors were missing from the heat shield at recovery.

The crew compartment heat shield bond line temperature at location 3 exhibited normal data through lift-off but indicated open-circuit at the start of the fifth service propulsion maneuver.

Nine thermocouple temperature measurements were questionable during entry. Six of these thermocouples exhibited characteristics indicative of improper installation of wire splices, such as were found on the Apollo 6 spacecraft. These splices create additional thermocouple junctions, and the data become meaningless during a heat pulse.

The X-axis vibration measurement on the helium pressure panel was erratic during the launch phase in that the data were unsymmetrical and greater in amplitude than anticipated. Tests are being conducted on similar instrumentation in an attempt to reconstruct the questionable data.

5.16 GUIDANCE, NAVIGATION, AND CONTROL SYSTEMS

Performance of the guidance, navigation, and control systems was satisfactory throughout the mission. Launch monitoring, manual attitude control, and all other functions required while the spacecraft was attached to the S-IVB were nominal. Spacecraft attitude and translation control during separation, transposition, and the simulated docking exercise were proper. The crew satisfactorily used the sextant to perform many inertial measurement unit (platform) alignments. Several times, the system was brought up from a powered-down condition and an inertial reference established using the scanning telescope for constellation recognition. Data were obtained on daylight star visibility through both instruments. Several landmark tracking exercises provided sufficient data to assess the feasibility and determine the accuracy of the technique.

The guidance, navigation, and control system used sextant tracking data to calculate the rendezvous maneuvers. All significant attitude control modes were exercised and performed properly. The primary and backup thrust vector control systems performed satisfactorily. Manual takeover of one maneuver was successfully accomplished. Attempts to define an earth horizon locator for star/horizon sightings were not successful; however, star/lunar landmark measurements were easily made. Passive thermal control initiation procedures were demonstrated, and information concerning use of the technique in cislunar space was obtained. The command module/service module separation sequence was nominal, as were the subsequent maneuvers to entry attitude. Entry guidance and control were performed automatically after 202 000 ft.

Three hardware problems occurred, but none reduced the operational capability. The rotational hand controller minus-pitch breakout switch inadvertently remained closed during a manual attitude maneuver. The trouble cleared itself and the controller operated properly for the remainder of the flight. The Commander's attitude indicator exhibited abnormal behavior in that it did not indicate properly when the backup attitude reference was displayed; performance was normal with the primary system. The entry monitor system ΔV /RANGE counter behaved abnormally in both ΔV and ENTRY modes; this behavior had been observed preflight. Analyses of many areas of the guidance and navigation system is continuing, and the results will be reported in supplemental reports.

5.16.1 Mission Related Performance

Ascent/S-IVB coast. - The inertial measurement unit was inertially fixed at 0.42 second after lift-off upon receipt of the lift-off discrete from the launch vehicle instrument unit. Launch monitoring functions began immediately, with the display of inertial velocity, altitude rate, and altitude on the computer display and keyboard, and angular rate and attitude error on the flight director attitude indicator. The displayed data were nominal and reported to be adequate for abort monitoring purposes. The attitude errors displayed (fig. 5.16-1) are the difference between the actual gimbal angles and those computed by the computer based on stored ascent profile information. The normal delay in receipt of the lift-off discrete by the computer caused the apparent roll and pitch errors shown. As on previous flights, the maximum excursions occurred in the maximum dynamic pressure region and were not caused by this delay. A comparison of spacecraft and S-IVB gimbal angles for this period is contained in figure 5.16-2. Some evidence of flexure between the two platform mounts is indicated. The slope of the yaw axis difference was not caused by drift, but by crosscoupling of the initial azimuth misalignment as the vehicle pitched over to the horizontal. Although not shown on the figure, the yaw axis difference remained essentially constant from the end of the pitch program to orbital insertion.

The following table lists preliminary guidance system errors at insertion based on the difference between the spacecraft and S-IVB state vectors:

Axis	Position, ft	Velocity, ft/sec
X	-2 200.4	-5.16
Y	+15 818.2	+59.3
Z	+873.9	+0.08

The large out-of-plane error (Y-axis) was caused by an allowable gyrocompassing error at lift-off. All components indicate excellent inertial component performance.

Manual attitude control of the spacecraft/S-IVB combination was demonstrated satisfactorily. Rates in each axis were commanded using the rotational hand controller, the spacecraft computer, the S-IVB control computer, and the S-IVB attitude control engines. The following table

contains a comparison of the rates expected and achieved and shows that the performance was as expected:

Axis	Expected	Coupling display unit	Instrument unit	Spacecraft rate gyros
Pitch, deg/sec				
Minus	-0.3	-0.297	-0.290	-0.30
Plus	+0.3	+0.302	+0.301	+0.28
Roll, deg/sec				
Minus	-0.5	-0.460	-0.469	-0.44
Plus	+0.5	+0.505	+0.499	+0.50
Yaw, deg/sec				
Minus	-0.3	-0.33	-0.331	-0.32
Plus	+0.3	+0.33	+0.328	+0.30

Spacecraft/S-IVB separation.— The spacecraft/S-IVB separation dynamics are shown in figure 5.16-3. The largest transient was 1.35 deg/sec about the pitch axis. The 16-Hz oscillation shown in yaw is near the natural frequency of the gyro and is probably ringing in response to an impulsive input. The transposition and simulated docking after separation were satisfactorily controlled by the stabilization and control system.

Attitude reference system alignments.— The primary and backup attitude reference systems (inertial measurement unit and gyro display coupler) were satisfactorily aligned on many occasions. Table 5.16-I lists pertinent information about the inertial measurement unit alignments made with the sextant. The star angle differences were small in all cases. The differences provided a check of sighting accuracy because they were determined by the angle measured between stars used for the alignment and the angle calculated from ephemeris data. The gyro torquing angles also provided a measure of alignment accuracy and sighting repeatability in those cases where alignments were repeated within a short time. The capability of determining platform drift was demonstrated. A number of alignments with each of the three options were performed by all crew members, and there were no significant differences in results. Automatic star selection and optics positioning routines were successfully used, although an idiosyncrasy (no Apollo navigation star was in view) associated with the use of the automatic star selection routine (pick-a-pair) caused two computer restarts. At least one daylight alignment was made using the auto-optics

positioning. Spacecraft attitude control was used only to place stars within the optics drive limits, and no difficulty was reported.

Several backup techniques were demonstrated, including platform alignment with the crewman optical alignment sight, and gyro display coupler alignment with the telescope. A platform alignment using the sextant and backup alignment programs was also performed. This technique, although not scheduled for use, was satisfactorily used when the optics MARK circuit was suspected of malfunctioning. This apparent malfunction was later proved to be a procedural error.

Orientation determination and star visibility.- The inertial measurement unit was inertially oriented by use of the scanning telescope each time the guidance and navigation system was powered up. The telescope provided no operational problems at night; however, the one attempt in daylight was not successful because of star recognition problems. A number of star visibility tests were performed to establish how susceptible the optics were to stray light from outside the field-of-view and also to determine whether visibility degraded as the flight progressed. These tests required counting the number of stars observed in a known field of view, and from this count, the field luminance of the instrument could be determined. For each test, the telescope shaft axis was directed at a point in inertial space along the orbital track and separated from the sun by an angle of 120 degrees (best case) or 70 degrees (worst case). Further, the attitude was constrained to provide the maximum shielding of the optics from earthlight. Star counts were made at 4-minute intervals for 12 minutes, either starting at sunrise or starting 12 minutes before sunset and continuing until sunset.

Analyses of these tests are continuing. The preliminary indications are that in all cases, the star magnitude thresholds obtained from the counts were lower than anticipated, possibly because the Mylar-covered spacecraft structure may have intruded into the optics field of view; this consideration was not used in the preflight predictions. Evidence was also obtained that debris cloud effects were temporary.

The optic surfaces did not degrade significantly during the mission. This was verified by removing the eyepieces late in the mission and observing the moon through the optics outer surface. If the optics had been degraded, a glare would have existed around the moon, indicating the presence of an oily coating, and no glare existed. Finally, the test results indicate that the telescope is not usable for constellation recognition when the sun is within 60 to 70 degrees of the field center, but is usable at angles of 120 degrees or more.

A check was made of sunlight effects on the sextant. With the sextant pointed as shown in the two cases of figure 5.16-4, star counts were

attempted. In each case, the navigation star was sighted, but no additional stars were observed, even though plus-6 magnitude stars were in the field of view. This indicates that the luminance is too high to see adjacent stars.

Orbital navigation and landmark tracking.- The feasibility of the landmark tracking technique was demonstrated, and efficient crew procedures were developed. The initial difficulties were caused by lack of actual experience, minimum preflight training, and ground procedural problems such as selecting landmarks outside the automatic optics positioning limits and scheduling successive landmarks too close together. As the crew gained experience and the procedural problems were resolved, the crew were able to complete landmark tracking tasks with little difficulty. The Commander would establish an initial spacecraft pitch attitude and rate and, if the offset required it, an initial roll to allow easy acquisition. The landmarks were then tracked by the navigator with the optics controls, which proved to be adequate. The first series involved only updating of the landmark position. The second sequence utilized the onboard state vector update option, followed by automatic tracking on the next revolution. Both techniques were successful. Known and unknown landmarks were tracked, and sufficient data were obtained to allow assessment of navigation accuracy. The initial telescope trunnion angle was set at 38 degrees, which reduced the delay in the automatic acquisition sequence. This technique proved to be efficient and easy to complete.

Sextant tracking of the S-IVB.- The S-IVB was successfully tracked in all desired visibility conditions with the sextant before, during, and after the rendezvous, and out to a maximum range of 320 miles. Automatic optics positioning modes were used with excellent results. During post-flight crew debriefings, the crew reported sighting the S-IVB at a range of nearly 1000 n. mi.

Rendezvous.- Onboard rendezvous computations began after 28:00:00 with the selection of the computer rendezvous navigation program and the maneuver to the sextant acquisition attitude. No data are available from this sequence or the subsequent initiation of the pre-terminal phase initiation program; however, the crew reported that all operations were nominal. Table 5.16-II lists the computer-generated terminal phase initiation time and the actual terminal phase velocities for the four cycles through the targeting program. The number of sextant marks taken is also included. The computations were nominal. These mark data were also used to update the target state vector in the computer. All updates were small, the largest being 0.6 ft/sec on the first mark.

Approximately 8 minutes before terminal phase initiation, the crew reported that the sextant wandered off the target. This was caused by the inadvertent selection of the reaction control system firing program, in which automatic optics positioning capability is not available.

The maneuver to terminal phase initiate attitude was completed using a combination of manual and automatic control modes. Table 5.16-III contains pertinent ground and onboard data for the terminal phase initiate translation maneuver. The crew intended to apply the in-plane components of the onboard computer solution but only half the out-of-phase component in an attempt to move the location of the common node ahead of the rendezvous point. The low-bit-rate data available indicate that the actual velocity applied was very close to the computer solution but that the maneuver was 4 to 5 seconds early. Because of the limited data, an accurate reconstruction of the relative trajectory is not possible; however, the final ground solution, based on this reconstruction, indicates that the computer solution was accurate.

After terminal phase initiation, the midcourse correction program was selected, and the sextant marking schedule was resumed. Maneuver velocities for the first midcourse correction are shown in the following table. Because of the uncertainties in the actual state vectors, the onboard computer solution cannot be evaluated accurately; however, the difference from that applied was small and would have had little effect on the rendezvous.

Axis	Velocity to be gained, ft/sec		
	Computer	Backup	Applied
X	-3.7	-1.7	-2.0
Y	+0.4	--	0
Z	+0.2	+1.2	+0.5

Following the maneuver, the marking schedule was again resumed and the second midcourse solution computed. This time, the onboard and backup solutions were less than 1 ft/sec, and no correction was performed.

The braking phase (table 5.16-IV) started at 29:43:55 and lasted 11 minutes 48 seconds. The braking was started at a range of 1.2 n. mi. at 7 minutes 51 seconds prior to the time of theoretical intercept. Range-rate control was initiated at a range of 0.6 n. mi.

Attitude and translation control. - The attitude control modes used during the mission are listed in table 5.16-V. Although all significant modes were tested, the most commonly used were the stabilization and control system minimum-impulse and acceleration-command manual modes. Wide and narrow deadband attitude hold was demonstrated using both the digital autopilot and the stabilization and control system. Although body rates

were not established prior to the tests, and convergence to a minimum-impulse limit cycle was not demonstrated, sufficient activity occurred to insure the systems capabilities. The final portion of the maneuver to terminal phase initiate attitude was made automatically with the digital autopilot configured for a 0.5 deg/sec maneuver rate (fig 5.16-5). The figure is based on data obtained from a low-bit-rate dump with a sample rate of once every 5 seconds. The angle residuals appear to have been reduced within the attitude deadband with acceptable tolerances at the end of the maneuver. A number of manual attitude maneuvers were made with various mode configurations. The crew reported that control capability and flexibility were adequate.

Translation maneuvers with the reaction control system were performed in all axes. Figure 5.16-6 shows the Y-axis translations associated with the Y-accelerometer test early in the mission and indicates that significant cross coupling was present. The varying disturbance torque evident in the yaw rate is attributed to propellant motion. Plus X translations preceded each service propulsion system firing (figs. 5.16-7 through 5.16-14).

Several instances of aerodynamic torquing were noted after the perigee was reduced to approximately 90 n. mi. The disturbance was reported to be most noticeable near perigee with the longitudinal axis of the spacecraft perpendicular to the velocity vector. Further discussion is contained in section 5.2.

Thrust vector control.- Thrust vector control of service propulsion engine maneuvers was successfully demonstrated with both the digital autopilot and the stabilization and control system. Table 5.16-VI itemizes the maneuvers and pertinent parameters. Figures 5.16-7 through 5.16-14 contain appropriate dynamic parameters for each maneuver. The second, third, and fifth maneuvers show propellant slosh effects, while the first and eighth maneuvers show little or no slosh excitation. The minimum impulse maneuvers are shown in figures 5.16-4 and 5.16-6. The velocity-to-be-gained plots (fig. 5.16-15 through 5.16-22) indicate proper cross-product steering for the guidance-system controlled firings and acceptable pointing errors for the stabilization-and control-system controlled firings. In all cases, the impulse realized during tailoff was larger than predicted (12 000 lb-sec compared with 9599 lb-sec). Postflight analysis of the shutdown circuit showed a diode in parallel with the helium tank pressure relay; this diode contributed to the excess velocity accrued by causing a 100 to 150-millisecond lag in dropout of the relay which in turn controls the ball valve shutoff sequence. The allowance for tailoff was revised for the seventh and eighth maneuvers with more accurate results (table 5.16-VI). All engine gimbal trim estimates were within expectations. A manual takeover was successfully initiated during

the fifth service propulsion maneuver. Transients were small, as shown in figure 5.16-23, and manual control was adequately demonstrated. Velocity residuals were satisfactorily reduced to near zero with the reaction control system after the first, second, and eighth maneuvers.

Midcourse navigation/star horizon/landmark.- A number of star/earth horizon measurements were scheduled, but all attempts to perform these sightings were unsuccessful. This failure resulted partially from the difficulty of the control task at the relatively high earth-orbital rates, but primarily from the crew's inability to define a horizon locator, which was the primary purpose of these tests. The dichroic filter in the sextant landmark line-of-sight did not aid in land/sea definition and actually smoothed out the horizon such that it was impossible at earth orbital ranges to define a locator for repeatable sightings. The crew stated that at longer ranges, the sightings should be accomplished with ease. The capability for performing star/lunar landmark sighting was demonstrated using the star Alphard and lunar landmark 5 (crater Diophantus).

Passive thermal control.- The primary objective of the passive thermal control tests was to validate procedures for passive thermal control through examination of initial rate and attitude data. Figures 5.16-24 and 5.16-25 contain time histories of spacecraft attitude during the roll and pitch passive thermal control modes, respectively. Stability characteristics of each mode may be observed from the attitude time histories after attitude hold is relinquished in the two non-stabilized axes. The roll mode test stability characteristics were considered good with the pitch axis divergence attributable to aerodynamic disturbances. The roll axis divergence during the pitch mode test cannot be attributed to aerodynamics. These results indicate that the roll mode will be more stable in an environment in which aerodynamic moments are negligible.

Command module/service module separation.- The command module/service module separation dynamics were similar to those experienced on previous missions. Peak excursions in rate were minus 1.56, plus 0.84, and minus 0.22 deg/sec in pitch, roll, and yaw, respectively. The disturbances essentially disappeared after 1 second.

Entry.- A time history of dynamic parameters during entry is shown in figure 5.16-26. As noted, the spacecraft was controlled manually until 259:57:26 and automatically by the digital autopilot thereafter. The crew switched to dual reaction control system operation at 259:58:29 after reporting a large pitch disturbance and other visual observations (see section 11). The only abnormality visible in the data during this period occurred approximately 15 seconds before the crew switched to dual-system operation. At this time, sharp, but relatively small, amplitude changes were discernible in the pitch and yaw rate data. (See section 3.) Coupling of roll activity into both pitch and yaw axes occurred throughout the entry.

The proportion of the total fuel used to damp pitch and yaw rates was higher than predicted. All the excess was used in the 2-minute period before drogue deployment after the spacecraft entered the aerodynamically unstable transonic region. Simulations to reproduce flight results using transonic aerodynamic coefficients and gusting winds show fuel usage of this order is to be expected under these conditions with dual system operation.

The entry interface velocity and flight-path angle were greater than predicted by 2.2 ft/sec and 0.009 degree, respectively. The planned velocity at the entry interface altitude was 25 844.2 ft/sec with a planned flight-path angle of minus 2.063 degrees. The computer-calculated values were 25 846.4 ft/sec and minus 2.072 degrees for velocity and flight-path angle, respectively. These entry parameters compare favorably with the interface conditions obtained from the best estimated radar vector following the deorbit maneuver. Altitude and range during the entry are shown in figure 5.16-27.

The spacecraft reached the entry interface at 259:53:26 with the initial roll guidance program in operation, and the computer indicated an inertial range of 159 $\frac{1}{4}$ n. mi. to landing. The spacecraft, however, was being manually held at the entry trim conditions predicted for the 0.05g level. The computer switched to the entry post-0.05g program at 259:55:38. After 0.05g, the spacecraft was rate damped in pitch and yaw, and the crew maintained the lift vector up until shortly after 0.2g. The computer sensed 0.2g at 259:56:06 and change to the final phase program. The crew made the go/no-go check on the displayed downrange error against the ground predicted value after the computer changed to final phase. The difference was approximately 10 n. mi., well within the plus or minus 100 n. mi. tolerance set for the downrange error value. Simultaneously with the go/no-go check, the spacecraft was being manually rolled to a 55-degree roll-left lift vector orientation. This backup lift vector orientation was to be held for about 30 seconds while the computer go/no-go check was being completed. As soon as a GO decision was made, the entry could have been controlled from the computer commands. However, the crew maintained the backup bank angle until the first non-zero roll command (minus 15 degrees) was issued from the computer at about 202 000-foot altitude.

In figure 5.16-28, the computer commanded bank angle (roll command) and the actual bank angles are presented as a function of time. Comparison of the two parameters indicate very good response of the spacecraft to the bank angle commands after the spacecraft was turned over to the digital autopilot. Table 5.16-VII is a comparison of the telemetered navigation data and guidance commands with a reconstructed set, developed by calculating the navigation and guidance commands directly from accelerometer data. This comparison indicates that the computer correctly interpreted the accelerometer data.

A summary of the landing data is shown in figure 5.16-29. The computer display indicated an undershoot of 1 n. mi. The recovery forces estimate of landing point was 64.07 degrees west longitude and 27.54 degrees north latitude; this would result in a 7.78 n. mi. overshoot. Adequate radar tracking vector data were not obtained after communications blackout; therefore, no absolute navigation accuracy can be determined. However, a reconstructed trajectory has been produced by applying the platform errors (table 5.16-VIII) to the accelerometer data. The corrected accelerometer data trajectory indicated a landing at 64.15 degrees west longitude and 27.64 degrees north latitude for an overshoot of 1.9 n. mi. The comparison of the computer navigation data with this reconstructed trajectory (table 5.16-VII) shows that the computer had a downrange navigation error of approximately 2.2 n. mi. at drogue deployment. This error is within the 1-sigma touchdown accuracy predicted before the mission.

5.16.2 Guidance and Navigation System Performance

Inertial system.- Performance of the inertial system met all mission requirements. Parameter stability was maintained through nine system shutdown/power-up sequences. System accuracy during the ascent to orbit was satisfactory, based on preliminary analyses. Table 5.16-IX contains a summary of the important inertial parameter statistics taken from pre-flight data, including the measured data during countdown and the compensation values loaded in the computer erasable memory for flight.

Figure 5.16-30 shows the time history of velocity errors during the ascent phase. These comparisons show the difference between the space-craft data and the instrument unit data (launch vehicle guidance system measurements that have been corrected for known errors).

Table 5.16-X lists the error sources that have been identified during preliminary analysis of the launch phase. These sources were selected primarily on the criteria that they satisfy the observed errors in velocity. Secondary criteria were that the selected error sources be consistent with the prelaunch calibration histories and that they be consistent with in-flight measurements.

Early in the mission, observation of the Y-accelerometer register indicated that no accelerometer pulses were accumulating, although the preflight bias measurement showed 0.24 cm/sec². A small plus and minus Y-axis translation test verified that the accelerometer and associated electronics were functioning satisfactorily. Thus, it appeared the instrument bias had shifted from the preflight value to essentially zero. Subsequently, the onboard computer compensation for the bias term was updated to zero. Behavior such as this is called null coincidence and has been noted on a number of accelerometers in factory tests.

During free-flight phases, the accelerometer bias can be determined from the rate at which accelerometer pulses are accumulated in the accelerometer input registers. These results are degraded by external forces such as aerodynamic drag, venting, and waste water dump and by residual propulsive components from attitude maneuvers with the center of mass displaced from the center of rotation. The following table summarizes the data from selected checks of the inflight bias.

Time, hr:min		Bias, cm/sec ²		
From	To	X	Y	Z
4:39	4:52	0.275	0	0.215
142:55	144:20	0.318	0	0.209
144:20	145:05	0.294	0	0.208
142:55	145:05	0.309	0	0.208

A 13-minute check was performed after spacecraft separation from the S-IVB, but before any orbital maneuvers or system shutdowns. The latter series of checks determined the biases for essentially complete revolutions; using a complete revolution for bias determination tends to remove the influence of aerodynamic drag, but it does increase the effects of other disturbing forces. The results of these bias determination are considered to be satisfactory.

Successive (back-to-back) inertial system alignments determined the ability to measure zero-g bias drift. The inertial system was first aligned prior to the rendezvous maneuver. Several revolutions later, the system was aligned to the same desired stable member orientation. The gyro-torquing angles (the angles through which the stable member was moved to re-achieve the desired inertial attitude) were recorded. This test showed that the average stable member drift over that period was plus 0.7, minus 1.8, and minus 0.2 mERU, respectively, for the X, Y, and Z gyro axes. The results indicate that the inflight drift determination technique is satisfactory and that the stable member drift met mission requirements.

Guidance and navigation system temperatures were nominal throughout the mission. Although entry was performed using the environmental control system secondary cooling loop, which does not service the inertial measurement unit, no adverse effect was noted.

Computer system.- The performance of the computer hardware and software was satisfactory. The programs used are listed in table 5.16-XI. Although a number of alarms and restarts were recorded, the cause in each

case was isolated either to a procedural error or to transients resulting from one or more switching functions which had caused alarms in ground testing. Two of the noise sources were the cabin lights and the cryogenic fans. Both caused DOWNLINK TOO FAST alarms inflight as well as prior to flight. Procedural errors that caused restarts were associated with the inertial measurement unit alignment program, use of the external change-in-velocity program, and attempts to take horizon sightings with the landmark line-of-sight in the orbital navigation program.

Optical system.- The sextant and the scanning telescope properly performed their functions throughout the mission. When the optics dust covers were jettisoned after orbital insertion, 180 degrees of telescope shaft rotation was required, which is normal for counter-clockwise rotation. Clockwise rotation would have required only about 90 degrees. The crew reported that the optics drives operated smoothly in all modes and provided adequate control capability.

5.16.3 Stabilization and Control System Performance

The stabilization and control system performance was satisfactory. An attitude reference drift check of the gyro display coupler made early in the flight provided values smaller than expected. The drift values, accumulated over a period of 1 hour 15 minutes, were 2.96, 0.80, and 0.0 deg/hr in pitch, yaw, and roll, respectively.

Two hardware problems were noted. An inadvertent breakout switch closure was reported in the Commander's rotation hand controller, and flight director attitude indicator no. 1 did not operate properly in the pitch axis when the backup attitude reference was displayed (see section 11).

5.16.4 Entry Monitor System

The ΔV counter in the entry monitor system was used to measure changes in X-axis velocity for all maneuvers and to terminate the service propulsion system maneuvers controlled by the stabilization and control system. The X-axis accelerometer bias measurements made prior to each service propulsion maneuver exceeded preflight expectations. An intermittent malfunction in the counter occurred during the final countdown and also during the mission. The malfunctions appeared in the most significant digit on the counter, which indicated 9 at times during the setup procedures for the propulsion system firings. Another counter anomaly, detected and isolated preflight, concerned the entry range-to-go function. This malfunction was determined to have no adverse effect on the mission. Section 11 contains a discussion of both of these anomalies.

Figure 5.16-31 contains a reproduction of the g/velocity trace on the scroll retrieved postflight. Also shown are the pre-entry test patterns and a trace reconstructed in a postflight simulation. All indications are that the g/velocity function operated properly.

TABLE 5.16-I.- SUMMARY OF INERTIAL MEASUREMENT UNIT ALIGNMENTS

Time, hr:min	Crew member ^a	Program ^b	Option	Day or night	Star identification	Gyro torque angle, deg			Star difference, deg
						X	Y	Z	
2:12	CMP	52	3	N	2, Diphda; 4, Achunar	-00.012	+00.023	+00.186	00.002
5:16	CMP	52	1	N	1, Alpheratz; 3, Navi	00.000	00.012	00.001	00.000
12:40									
23:10									
25:16									
26:00									
39:40									
51:40	LMP	52	3	N	42, Peacock; 33, Antares	-00.420	-00.179	+00.149	00.001
51:51	LMP	52	3	N	42, Peacock; 33, Antares	+00.021	-00.044	+00.017	00.000
69:30									
72:30									
74:04									
90:30									
91:57	CMP	52	3	N	14, Canopus; 25, Acrux	00.044	00.019	00.001	00.000
97:45									
117:00									
118:36									
120:00									
121:45									
139:19	CMP	52	1	N	14, Canopus; 6, Acamar	-00.062	-00.008	-00.090	00.000
139:28	CMP	52	2	N	11, Aldebaran; 16, Procyon	+00.001	-00.021	-00.006	00.000
140:49	LMP	52	2	N	6, Acamar; 45, Fomalhaut	-00.080	+00.692	-01.378	00.001
145:16	CDR	52	3	N	2, Diphda; 45 Fomalhaut	-00.093	+00.042	-00.007	00.001

^aCMP - Command Module Pilot; LMP - Lunar Module Pilot; CDR - Commander.^bSee table 5.16-XV.

TABLE 5.16-I.- SUMMARY OF INERTIAL MEASUREMENT UNIT ALIGNMENTS - Concluded

Time, hr:min	Crew member ^a	Program ^b	Option	Day or night	Star identification	Gyro torque angle, deg			Star difference, deg
						X	Y	Z	
161:30									
164:20									
165:50									
193:20									
193:26	LMP	52	2	N	13, Capella; 11, Aldebaran	-00.199	+00.064	+00.093	00.001
205:30									
206:40	CDR	52	1	N	12, Rigel; 15, Sirius	+00.029	-00.006	-00.030	00.001
208:15									
211:10	LMP	52	2	N	12, Rigel; 11, Aldebaran	+00.001	-00.004	-00.012	00.000
212:31	CMP	52	1	D	12, Rigel; 11, Aldebaran	+00.780	+01.308	-03.096	00.001
214:10	CMP	51/52	2	N	12, Rigel; 15, Sirius	+00.724	+00.376	-01.690	00.000
233:47									
234:04	LMP	52	3	N	12, Rigel; 15, Sirius	+00.008	-00.024	+00.003	00.000
235:20									
238:10									
254:55									
256:20									
257:50									

^aCMP - Command Module Pilot; LMP - Lunar Module Pilot; CDR - Commander.^bSee table 5.16-XV.

TABLE 5.16-II.-- RENDEZVOUS SOLUTION COMPUTATIONS

Computation cycle	Ignition time, hr:min:sec	Velocity change, ft/sec		Number of marks (cumulative)
		TPI ^a	TPF ^b	
1. Ignition time load	29:23:00	--	--	--
2. First recycle	29:20:29.93	17.2	18.0	0
3. Second recycle	29:12:25.73	17.5	20.5	10
4. "Bonus" recycle	29:15:53.66	17.7	18.9	16
5. Final cycle	29:16:45.52	17.7	18.5	27

^aTerminal phase initiate.^bTerminal phase finalize (braking).

TABLE 5.16-III.- TERMINAL PHASE INITIATION

Quantity	Nominal	Ground-computed		Onboard computer	Intended	Actual	Best estimated trajectory
		Transmitted	Final				
Change in velocity (local horizontal), ft/sec							
X	14.2	15.0	15.1	15.6	15.6	15.7	15.5
Y	1.1	1.9	2.8	3.0	1.5	2.7	2.9
Z	-8.8	-7.5	-7.5	-7.9	-7.9	-7.7	-7.3
Total	16.7	16.9	17.1	17.7	17.5	17.7	17.4
Duration, sec	42.4		46.0				43.4
Time, hr:min:sec	29:23:05	29:18:34	29:17:36	29:16:46	29:16:46	29:16:33	29:16:27
Attitude (local horizontal), deg							
Roll	0.0	0.0	0.0	0.0	0.0	0.0	0.0
Pitch	32.6	26.3	26.1	26.4	26.8	26.8	24.9
Yaw	6.1	7.3	10.6	10.9	5.5	5.5	10.7
Velocity residual after cutoff, ft/sec							
X	0.0	0.0	0.0	0.0	0.0	0.1	0.0
Y	0.0	0.0	0.0	0.0	0.0	0.3	0.0
Z	0.0	0.0	0.0	0.0	0.0	-0.2	0.0

TABLE 5.16-IV.- TERMINAL PHASE BRAKING

Quantity	Nominal	Ground	Actual	Best estimate trajectory
Velocity change (vertical system), ft/sec				
Effective				
X	13.0	12.8	13.0	13.0
Y	0.2	2.0	3.7	4.6
Z	11.5	11.3	11.8	11.8
Total	17.4	17.2	18.0	18.2
Expended				
X	--	--	^a 14.2	--
Y	--	--	^a 14.7	--
Z	--	--	^a 32.0	--
Total	^b 18.2	^b 19.4	49.1	^b 19.4
Ratio (expended/effective)	1.05	1.13	2.73	1.07
Braking time, hr:min:sec				
Begin	29:55:01	29:49:08	29:43:55	29:42:33
End	30:00:36	29:55:19	29:55:43	29:54:00
Braking duration, min:sec	5:35	6:11	11:48	11:27
Time from theoretical intercept, min:sec	2:54	3:49	7:51	8:54
Range at beginning of braking, n. mi.	0.5	0.5	1.2	1.5
Time of theoretical intercept, hr:min:sec	29:57:55	29:52:57	29:51:45	29:51:27

NOTE: Effective ΔV is equivalent to theoretical ΔV for braking.

^aExpended ΔV is total along each axis; not vector-summed.

^bBased upon simulated braking with no errors; ΔV components not available.

TABLE 5.16-V.- CONTROL MODE USAGE

Control source ^a	Mode	Type of control	Verified by crew report	Verified by telemetry data
CMC	Automatic	Automatic maneuver at 4 deg/sec	X	
	Automatic	Automatic maneuver at 0.5 deg/sec	X	
	Automatic	Automatic maneuver at 0.2 deg/sec	X	
	Automatic	Automatic maneuver at 0.05 deg/sec	X	
	Hold	Manual maneuver at 4 deg/sec		
	Hold	Manual maneuver at 0.5 deg/sec	X	
	Hold	Manual maneuver at 0.2 deg/sec	X	
	Hold	Manual maneuver at 0.05 deg/sec	X	
	Hold	Limit cycle within 5-deg deadband	X	
	Hold	Limit cycle within 0.5-deg deadband	X	
	Free	Manual command with rotational hand controller	X	
	Free	Manual command with minimum impulse controller	X	
	Any mode	Manual translation	X	X
SCS	Rate command	Manual maneuver at high rates	X	
	Rate command	Manual maneuver at low rates	X	
	Rate command	Limit cycle within high rate, maximum deadband (8 deg)	X	
	Rate command	Limit cycle within high rate, minimum deadband (4 deg)	X	
	Rate command	Limit cycle within low rate, maximum deadband (4.2 deg)	X	
	Rate command	Limit cycle within low rate, minimum deadband (0.2 deg)	X	
	Accel. command	Manual commands	X	
	Minimum impulse	Manual commands	X	
	Any mode	Translation, manual	X	
	Any mode	Reaction control system direct, manual		X

TABLE 5.16-VI.- GUIDANCE AND CONTROL MANEUVER SUMMARY

Condition	Service propulsion maneuver and control mode ^a								
	1	2	3	4	5	6	7	8	
	DAP-TVC	DAP-TVC	SCS-AUTO	DAP-TVC	DAP-TVC	CCU-RTE CMD ^b	DAP-TVC	SCS-AUTO	DAP-TVC
Time									
Ignition, hr:min:sec	26:24:55.66	28:00:56.47	75:48:00.27	120:43:00.44	165:00:00.42	165:00:36.00	210:07:59.99	239:06:11.97	259:39:16.36
Cutoff, hr:min:sec	26:29:05.02	28:01:04.23	75:48:09.37	120:43:00.92	165:00:36.00	165:01:07.37	210:08:00.49	239:06:19.67	259:39:20.15
Duration, sec	9.36	7.76	9.10	0.48	--	66.95	0.50	7.70	11.79
Velocity, ft/sec									
Desired/actual									
X	206.1/208.7	175.0/178.1	211.0/214.8	13.0/15.3	--	1644.0/1693.0	15.3/18.6	225.0/226.3	349.4/349.6
Y	2.4/3.4	0.8/-0.2	3.3/3.2	0.1/0.1	--	22.4/20.3	-0.2/-0.4	0.0/1.4	-1.9/-2.7
Z	11.7/13.5	8.8/10.3	11.4/9.3	0.6/0.6	--	84.2/83.7	0.9/0.8	11.4/8.5	-18.6/-20.6
Pointing error, ft/sec									
Over/under velocity	+2.2	+3.1	+3.4	+2.3	--	--	+3.3	+1.3	-0.1
Lateral	2.1	1.8	2.1	0.0	--	--	0.2	3.2	2.3
Engine gimbal position, deg									
Initial									
Pitch	-0.81	-0.81	-0.98	-0.81	-0.64	-0.56	-0.68	-0.90	-0.68
Yaw	-0.27	-0.31	-0.56	-0.48	-0.44	-0.74	-1.19	-1.40	-1.24
Maximum excursion									
Pitch change	+0.30	+0.40	+0.30	+0.30	+0.66	-0.21	+0.30	+0.30	+0.31
Yaw change	-0.46	-0.52	-0.51	-0.67	-1.45	+0.21	-0.43	-0.45	-0.46
Steady-state									
Pitch	-0.77	-0.80	-0.70	--	-0.56	-0.64	--	-0.70	-0.64
Yaw	-0.27	-0.18	-0.27	--	-0.27	-0.61	--	-1.20	-1.11
Cutoff									
Pitch	-0.68	-0.64	-0.68	--	-0.56	-0.56	--	-0.55	-0.68
Yaw	-0.22	-0.31	-0.31	--	-0.74	-1.07	--	-1.20	-1.32
Rate excursion, deg/sec									
Pitch	-0.08	0.52	0.73	0.0	-1.04	0.40	-0.28	0.53	0.20
Yaw	-0.08	0.60	0.68	1.28	1.88	-0.48	-0.12	0.55	0.0
Roll	-0.08	0.0	0.08	0.0	-2.03	0.0	-0.38	0.15	0.0
Attitude error, deg									
Pitch	+0.28	-0.17	0.67	--	0.0	0.46	--	0.71	0.0
Yaw	+0.24	0.31	1.02	--	-0.35	-0.98	--	1.0	0.60
Roll	-3.61	-1.71	0.0	--	-5.0	0.0	--	0.0	-3.60

^aDAP TVC - digital autopilot thrust vector control

SCS - stabilization and control system

RTE CMD - rate command

^bManual takeover

TABLE 5.16-VII.- ENTRY NAVIGATION AND GUIDANCE RECONSTRUCTION

Condition	400 000 ft		0.2g		202 000 ft		Guidance termination	
	Computer	Simulated	Computer	Simulated	Computer	Simulated	Computer	Simulated
Time, hr:min:sec	259:53:28	259:53:28	259:57:06	259:57:06	259:57:26	259:57:26	260:02:20	260:02:20
Parameter								
X position, ft	20 314 447.0	20 314 648.0	18 583 873.0	18 584 252.0	17 491 316.0	17 491 782.0	15 006 438.0	15 007 346.0
Y position, ft	-126 287.1	-126 280.0	-109 069.5	-109 071.5	-88 281.6	-88 298.4	-115 586.3	-115 715.6
Z position, ft	6 430 460.7	6 430 423.6	10 134 454.0	10 134 452.0	11 825 984.0	11 826 015.0	14 661 135.0	14 661 311.0
X velocity, ft/sec	-8675.8	-8674.9	-13 095.5	-13 094.3	-13 743.4	-13 742.0	-1880.8	-1879.1
Y velocity, ft/sec	91.9	91.9	122.6	122.6	562.6	562.6	-150.9	-153.6
Z velocity, ft/sec	24 348.9	24 349.0	22 309.9	22 310.2	19 484.1	19 484.5	784.3	783.5

TABLE 5.16-VIII.- ONBOARD COMPUTER ENTRY NAVIGATION ACCURACY

Condition	400 000 ft		0.2g		202 000 ft		Drogue deploy	
	Computer	BET ^a	Computer	BET	Computer	BET	Computer	BET
Time, hr:min:sec	259:53:26	259:53:26	259:56:06	259:56:06	259:57:26	259:26	260:04:46	260:04:46
Parameter								
X position, ft	20 331 736.0	20 330 961.0	18 583 873.0	18 583 237.7	17 491 316.0	17 490 624.0	14 908 790.0	14 904 996.1
Y position, ft	-126 469.6	-126 616.2	-109 069.6	-109 396.8	-88 281.6	-88 704.8	-139 003.3	-139 668.7
Z position, ft	6 381 745.8	6 377 242.2	10 134 454.0	10 130 069.0	11 825 984.0	11 821 647.2	14 706 501.0	14 699 388.6
X velocity, ft/sec	-8616.7	-8615.2	-13 095.5	-13 095.2	-13 743.4	-13 744.8	-1229.4	-1242.6
Y velocity, ft/sec	91.5	90.4	122.6	121.6	562.6	561.6	-355.1	-355.5
Z velocity, ft/sec	24 367.6	24 368.0	22 309.9	22 310.8	19 484.1	19 484.0	740.5	724.9

^aBest estimate trajectory.

TABLE 5.16-IX.- INERTIAL COMPONENT PREFLIGHT HISTORY

Error	Sample mean	Standard deviation	No. samples	Countdown value	Flight load
Accelerometers					
X - Scale factor error, ppm Bias, cm/sec ²	-233.88 0.245	35.41 0.051	8 8	-306 0.24	-300 0.24
Y - Scale factor error, ppm Bias, cm/sec ²	-144.00 0.251	42.13 0.017	10 10	-235 0.25	-190 0.24
Z - Scale factor error, ppm Bias, cm/sec ²	-319.12 0.188	46.58 0.063	8 8	-408 0.16	-340 0.17
Gyroscopes					
X - Null bias drift, mERU Acceleration drift, spin reference axis, mERU/g Acceleration drift, input axis, mERU/g Acceleration drift, output axis, mERU/g	-0.843 6.52 8.64 3.13	1.17 9.02 4.15 0.71	10 10 7 10	1.44 11.95 6.7 3.88	-0.5 3.9 8.2 --
Y - Null bias drift, mERU Acceleration drift, spin reference axis, mERU/g Acceleration drift, input axis, mERU/g Acceleration drift, output axis, mERU/g	-0.21 -0.868 9.12 1.91	0.90 0.75 12.40 0.9	7 7 7 7	-0.43 -0.42 11.2 1.7	0.0 -0.4 11.6 --
Z - Null bias drift, mERU Acceleration drift, spin reference axis, mERU/g Acceleration drift, input axis, mERU/g Acceleration drift, output axis, mERU/g	-0.39 -11.53 21.11 2.49	2.13 7.14 2.13 0.58	7 7 7 7	-1.37 -16.2 16.2 2.4	-0.6 -8.8 20.8 --

TABLE 5.16-X.- INERTIAL SUBSYSTEM ERRORS USED
IN FIT OF BOOST VELOCITY ERRORS

Error	Observed	Specification
Z velocity offset, ft/sec	1.87	--
Bias, cm/sec ²		
X	0.04	0.2
Y	0.03	0.2
Z	0.01	0.2
Null bias drift, mERU		
X	0.9	2
Y	5.0	2
Z	0.1	2
Acceleration drift, input axis, mERU/g		
X	-12.1	8
Y	6.5	8
Z	-10.7	8
Acceleration drift, spin reference axis, mERU/g		
Y	-2.2	5

TABLE 5.16-XI.- COMPUTER PROGRAMS USED

No.	Description
01	Prelaunch initialization
02	Prelaunch gyrocompassing
03	Prelaunch verification of gyrocompassing
05	Guidance, navigation, and control system start-up
06	Guidance, navigation, and control system power down
11	Earth orbit insertion monitor
20	Rendezvous navigation
21	Ground track determination
22	Orbital navigation
23	Cislunar midcourse navigation
27	Computer update
30	External ΔV prethrust
34	Rendezvous terminal phase initiation
35	Terminal phase midcourse
40	Service propulsion thrusting
41	Reaction control thrusting
47	Thrust monitor
51	Inertial measurement unit orientation determination
52	Inertial measurement unit realignment
53	Backup inertial measurement unit orientation determination
54	Backup inertial measurement unit realignment
61	Entry maneuver to command module/service module separation attitude
62	Entry command module/service module separation and pre-entry maneuver
63	Entry initialization
64	Entry — post - 0.05g
67	Entry — final phase

NASA-S-68-6317

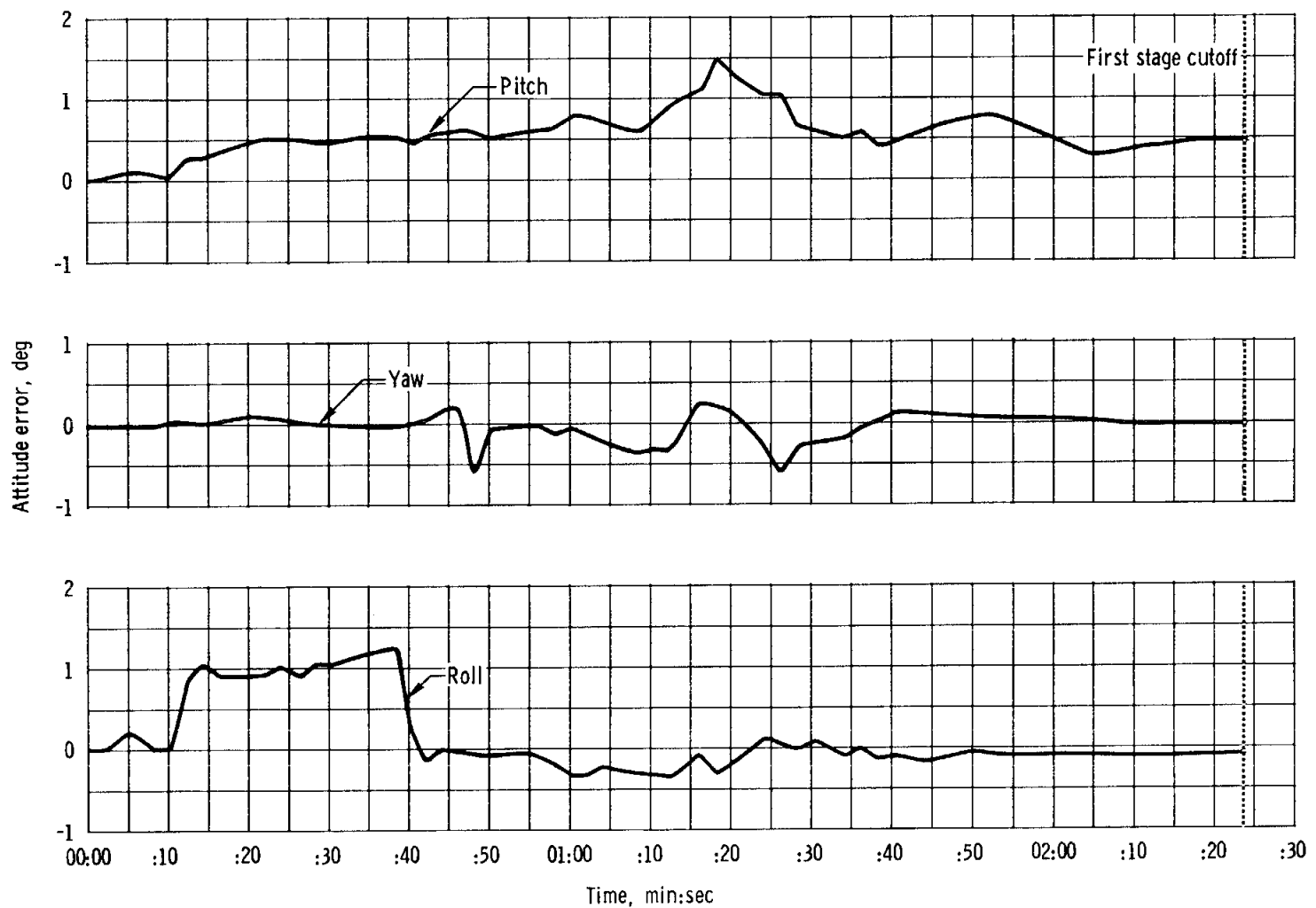


Figure 5.16-1. - Attitude error displayed during launch phase.

NASA-S-68-6318

5-116

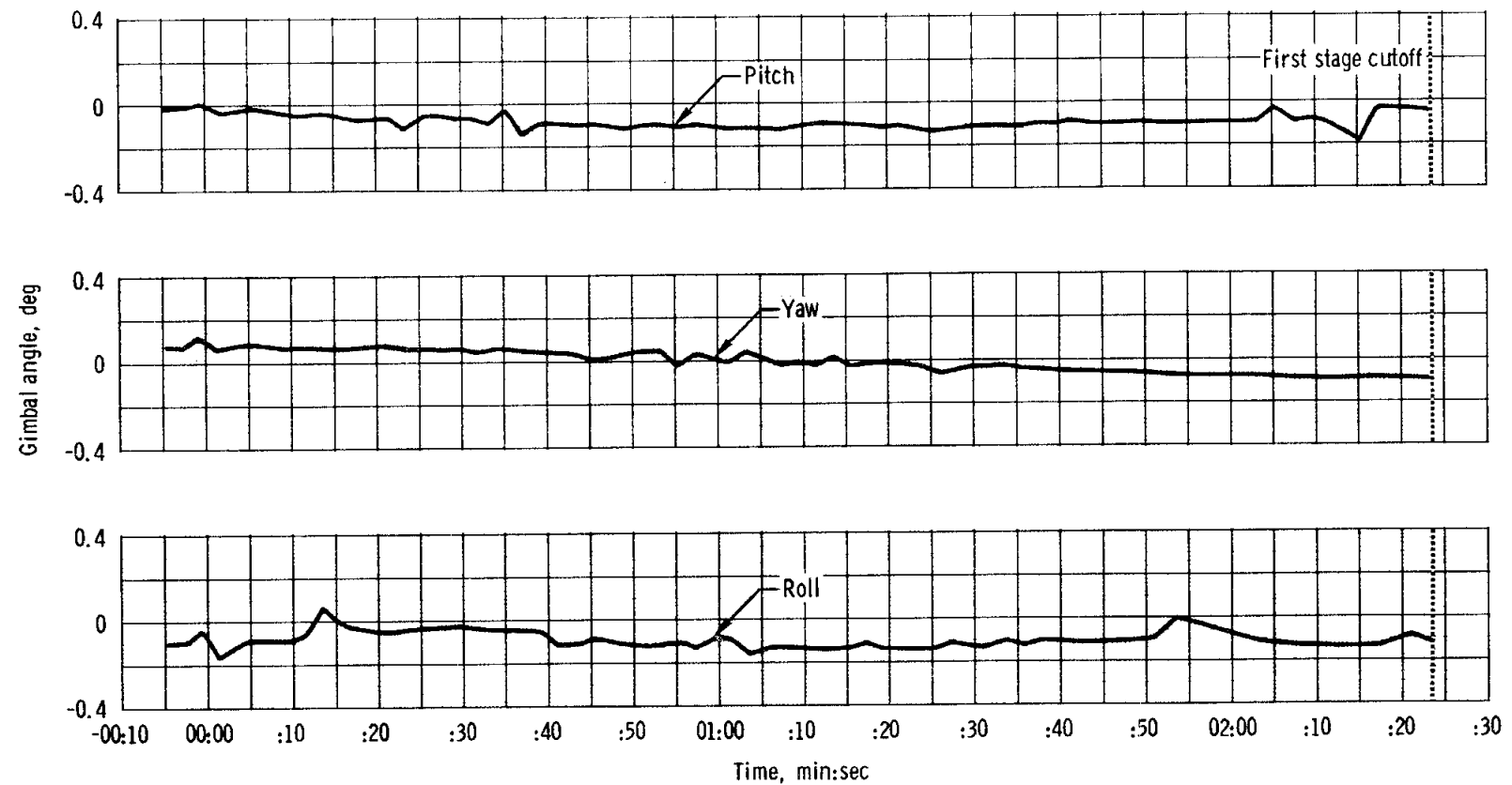


Figure 5.16-2. - Gimbal angle comparison during launch phase, instrument unit minus command module computer.

NASA-S-68-6319

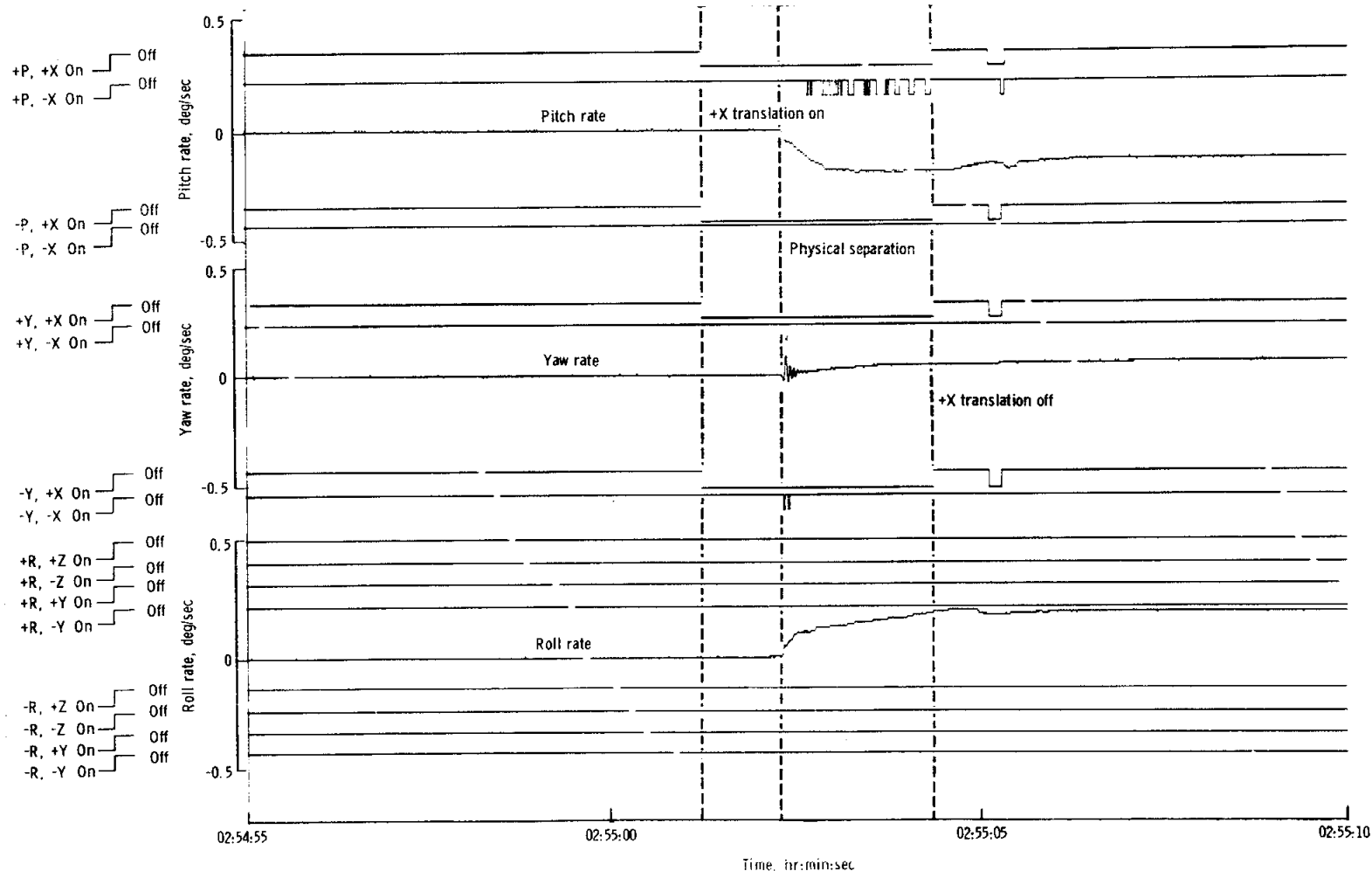


Figure 5.16-3. - Spacecraft dynamics during spacecraft/S-IVB separation.

NASA-S-68-6320

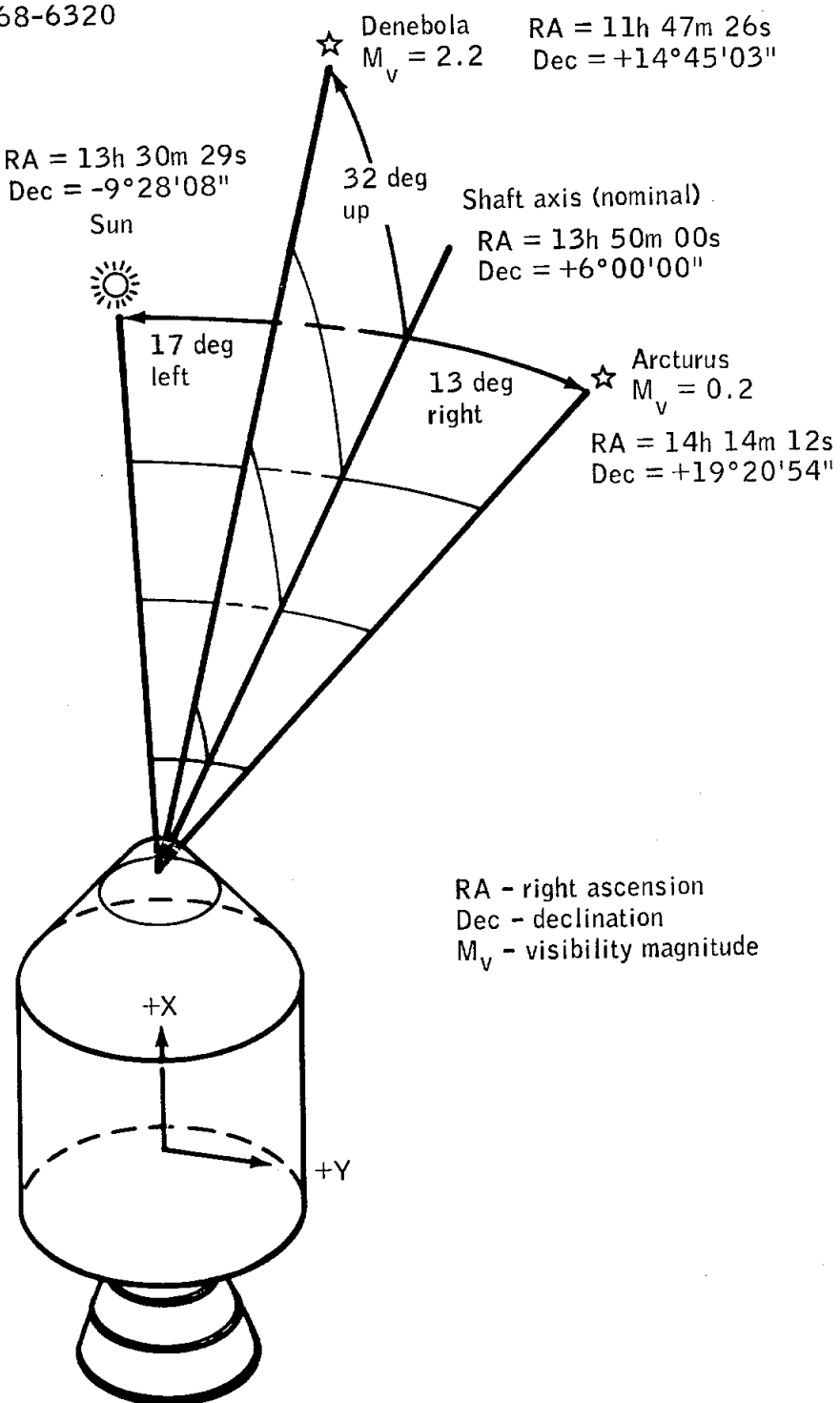


Figure 5.16-4.- Sextant star count geometry.

NASA-S-68-6331

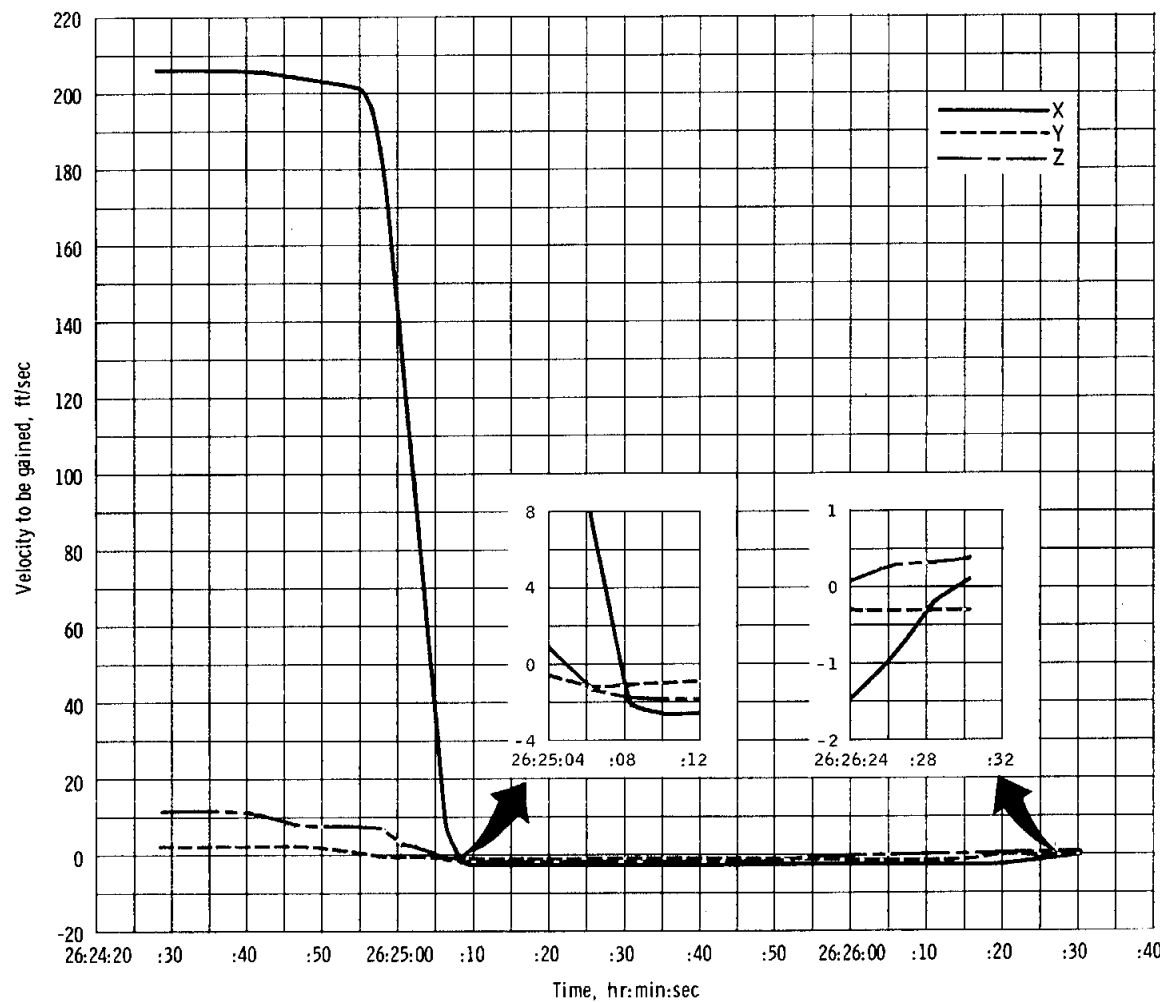


Figure 5.16-15. - Velocity to be gained during first service propulsion maneuver.

NASA-S-68-6332

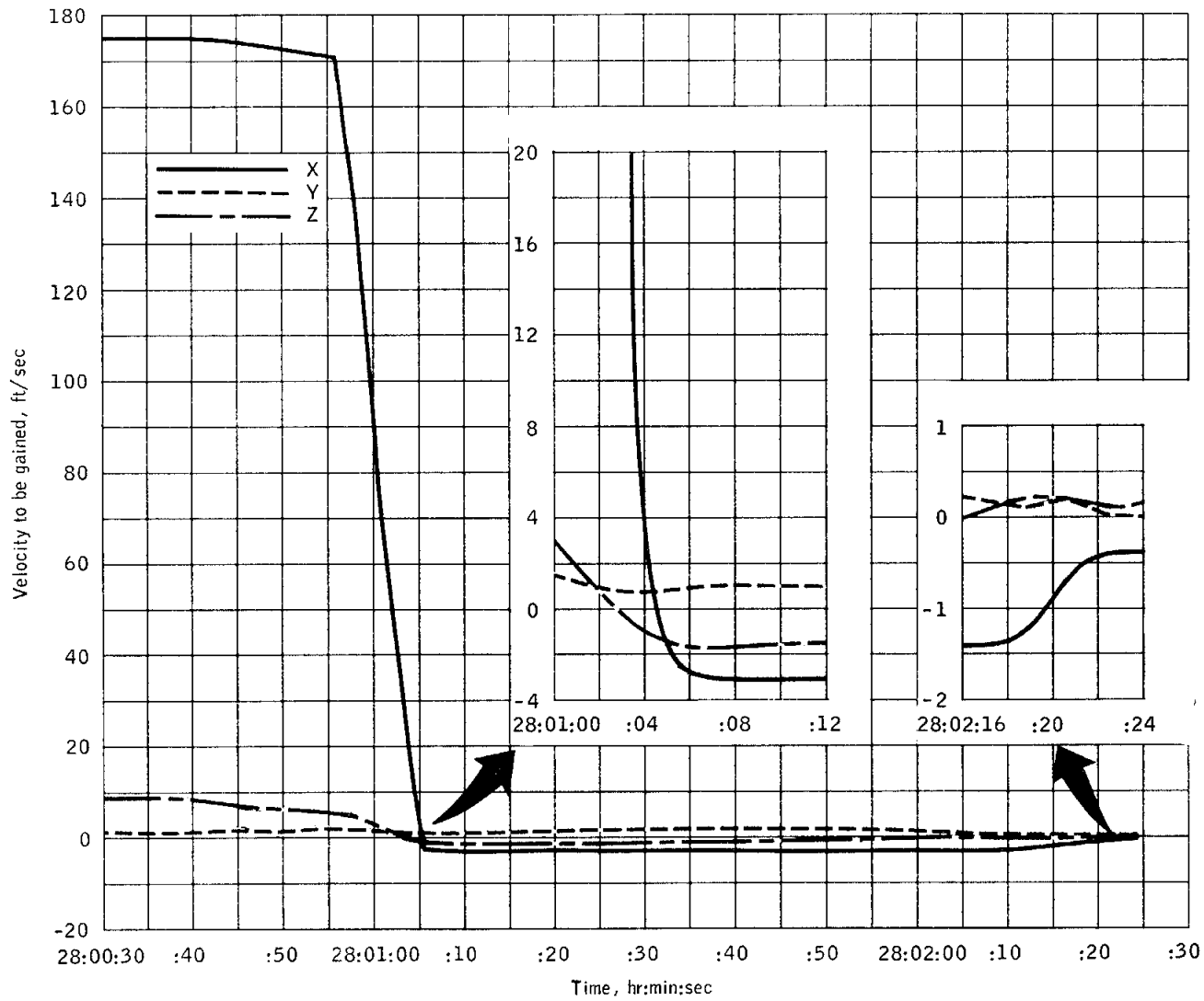


Figure 5.16-16.- Velocity to be gained during second service propulsion maneuver.

NASA-S-68-6333

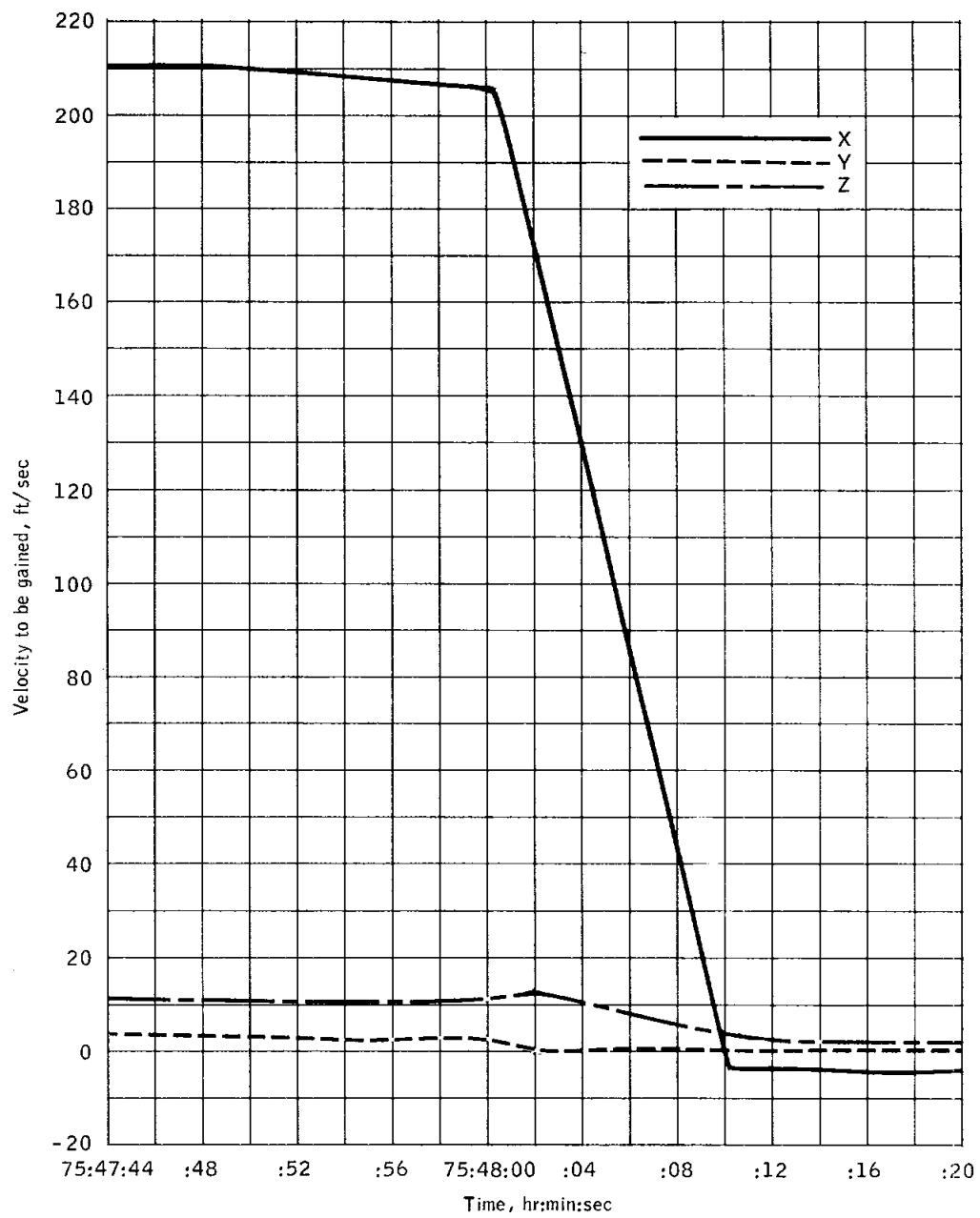


Figure 5.16-17.- Velocity to be gained during third service propulsion maneuver.

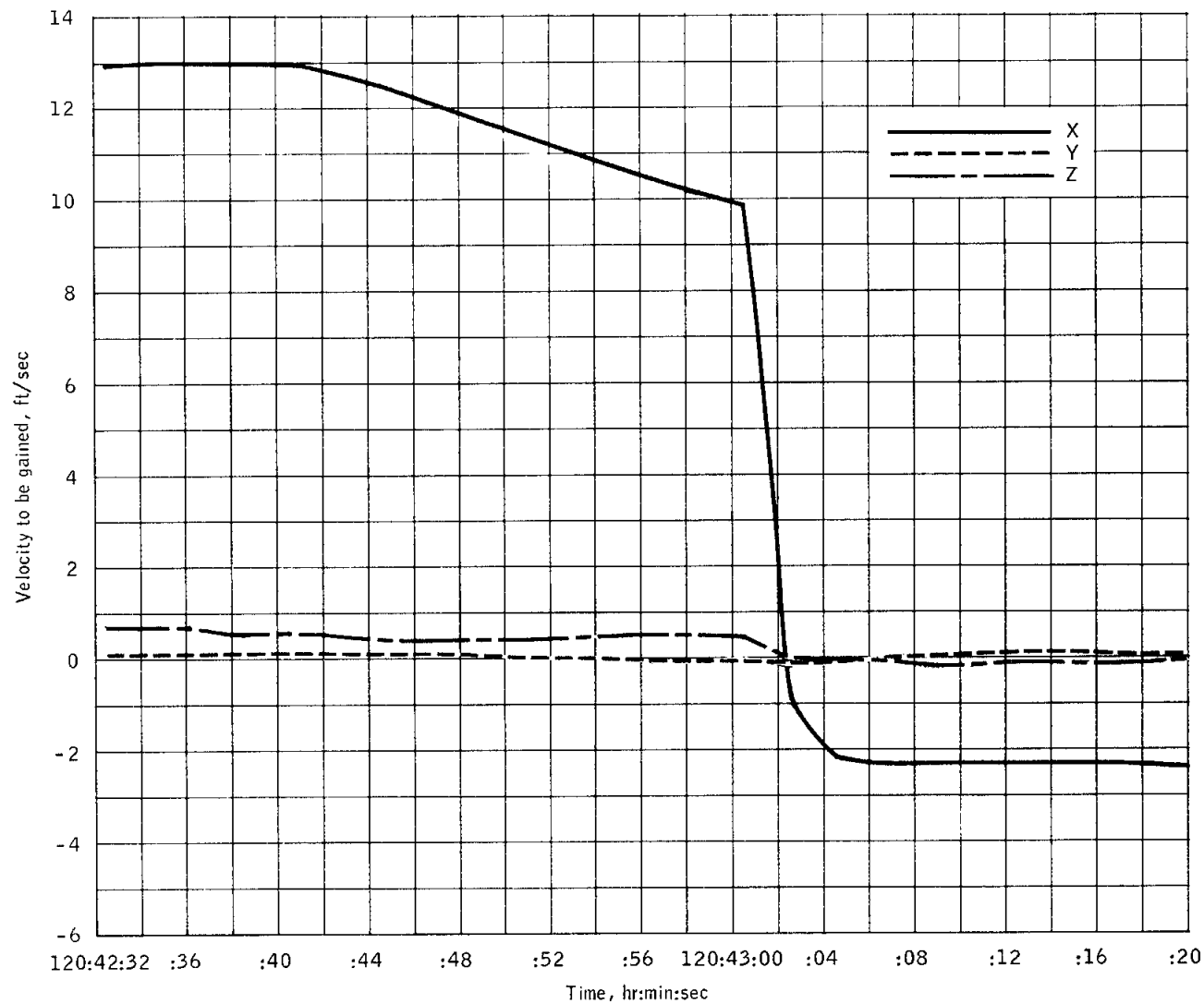


Figure 5.16-18.- Velocity to be gained during fourth service propulsion maneuver.

NASA-S-68-6335

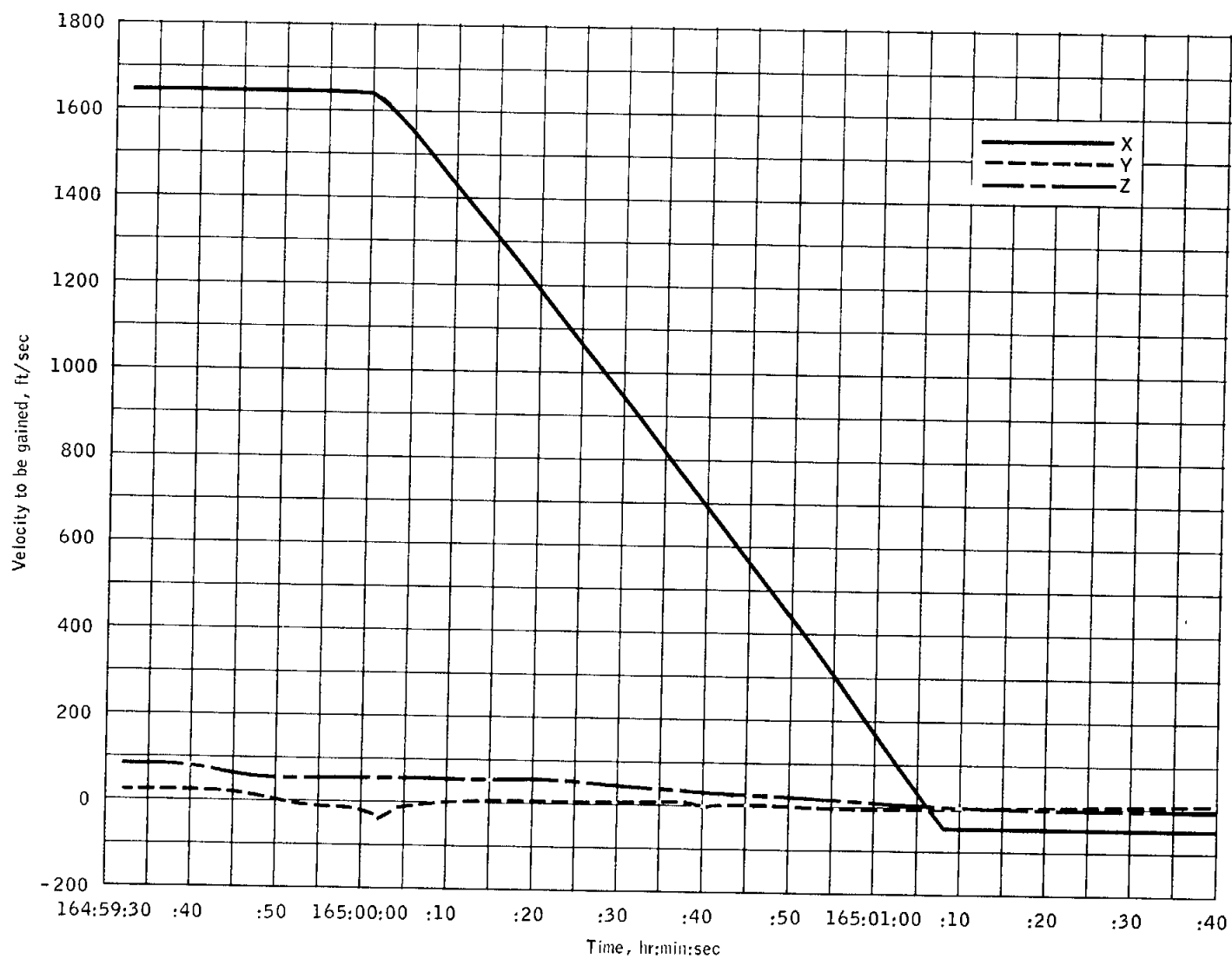


Figure 5.16-19.- Velocity to be gained during fifth service propulsion maneuver.

NASA-S-68-6336

45T-5

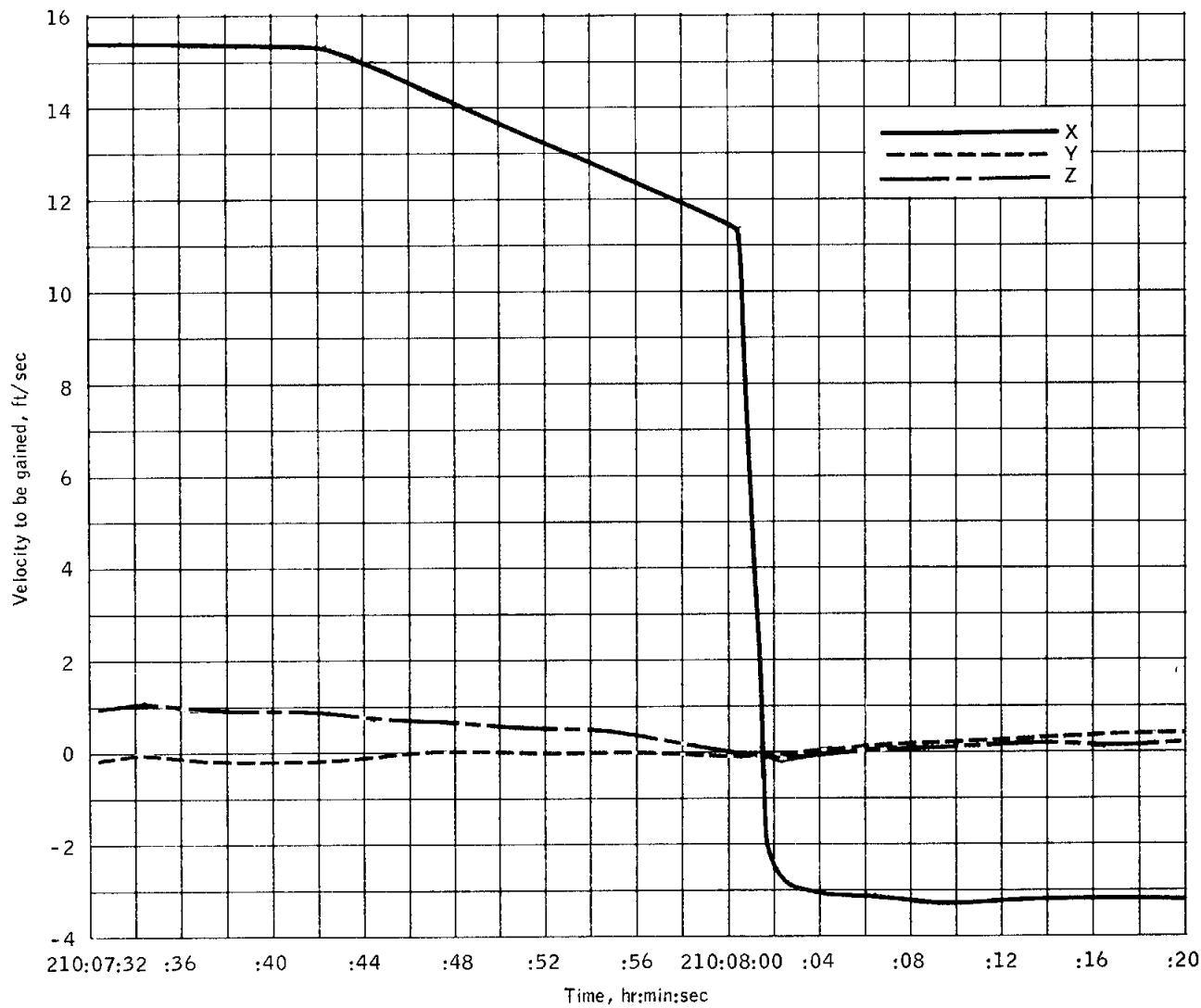


Figure 5.16-20.- Velocity to be gained during sixth service propulsion maneuver.

NASA-S-68-6337

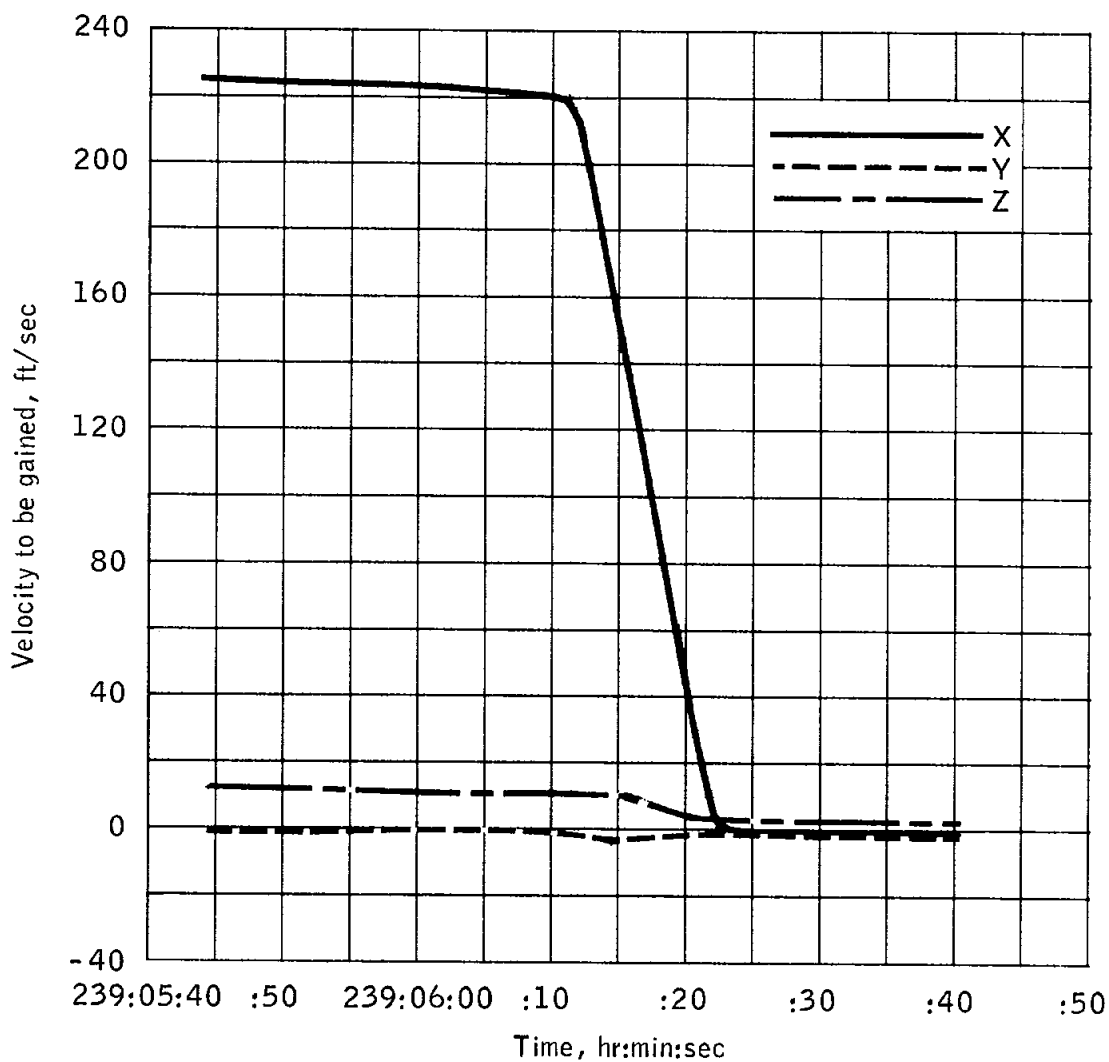


Figure 5.16-21.- Velocity to be gained during seventh service propulsion maneuver.

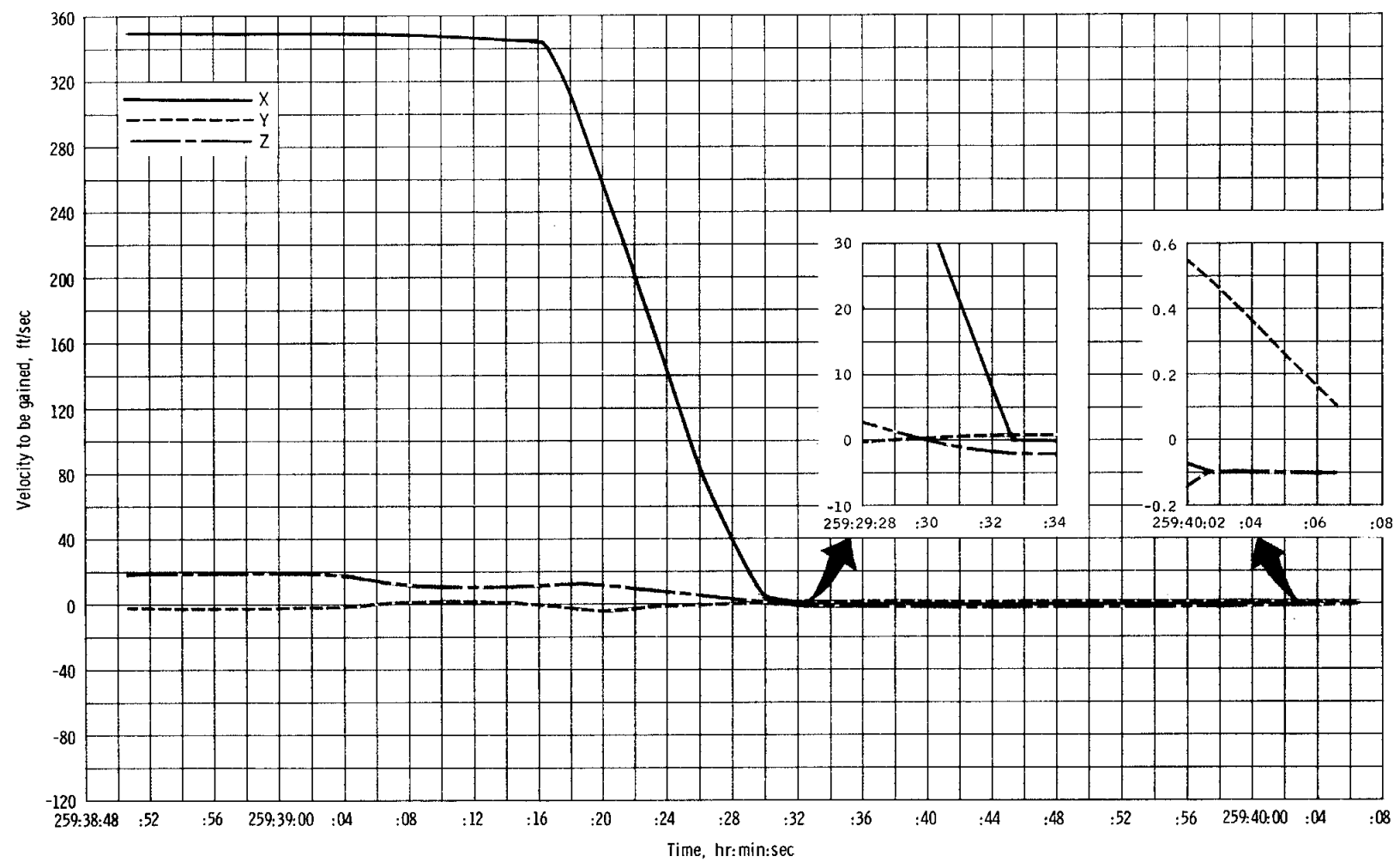


Figure 5.16-22. - Velocity to be gained during eighth service propulsion maneuver.

NASA-S-68-6339

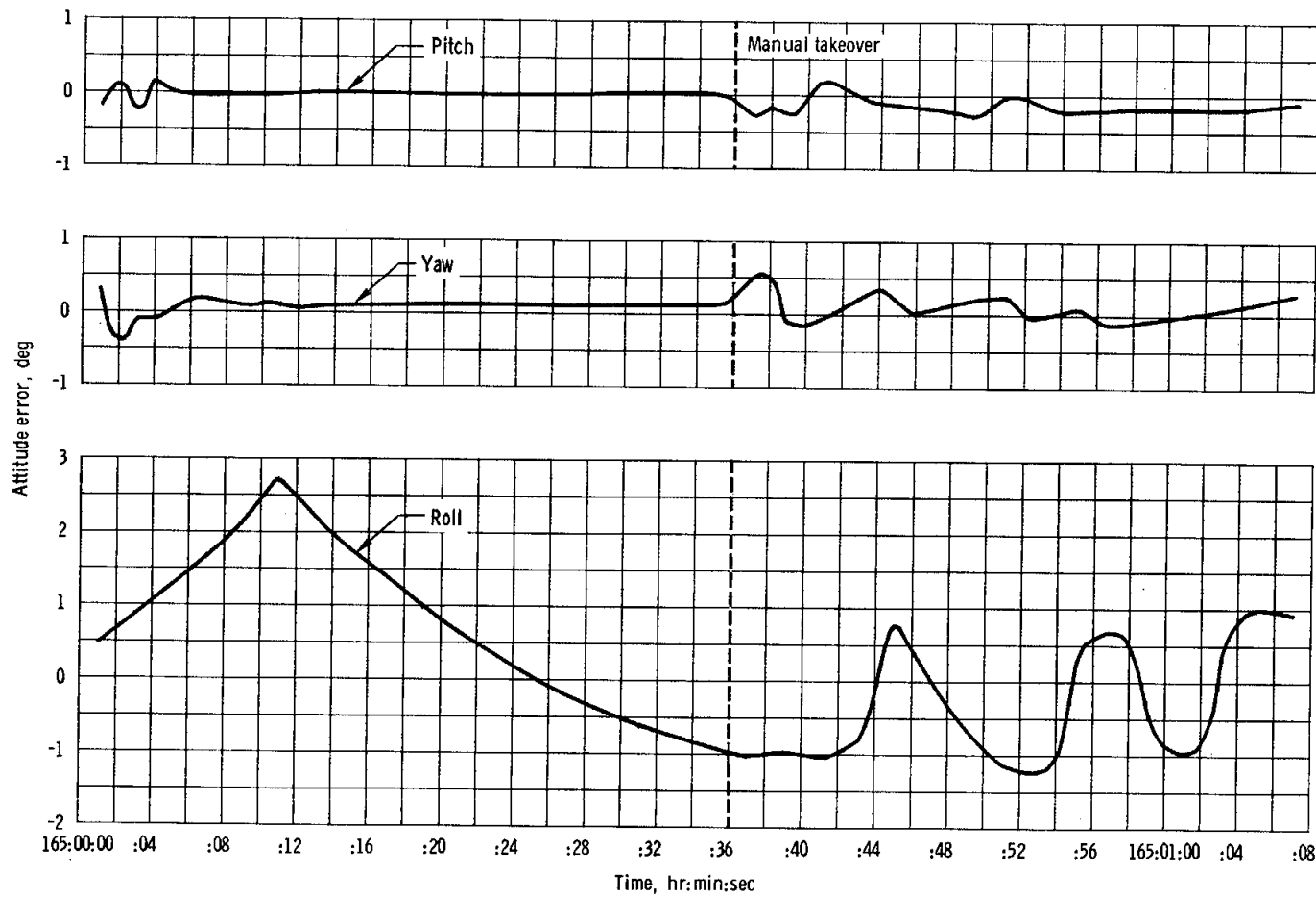


Figure 5.16-23. - Attitude errors during fifth service propulsion maneuver.

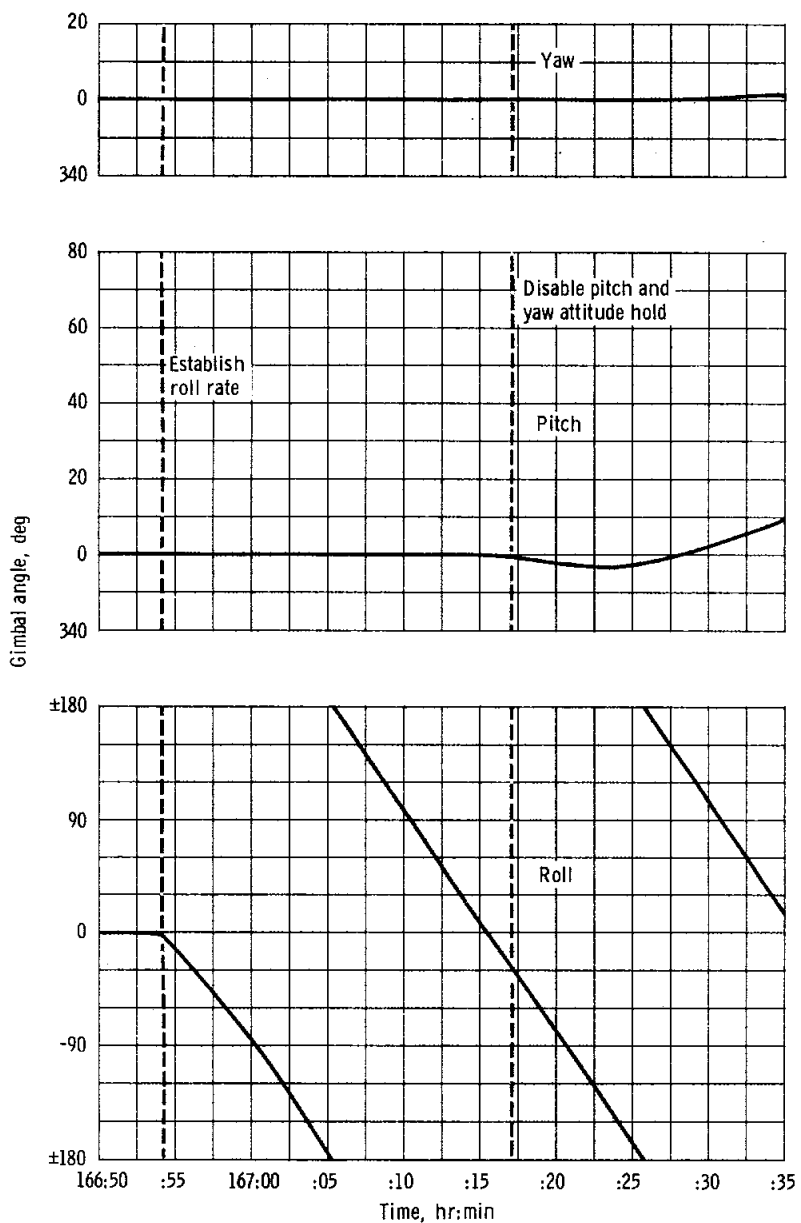


Figure 5.16-24. - Gimbal angles during roll passive thermal control test.

NASA-S-68-6347

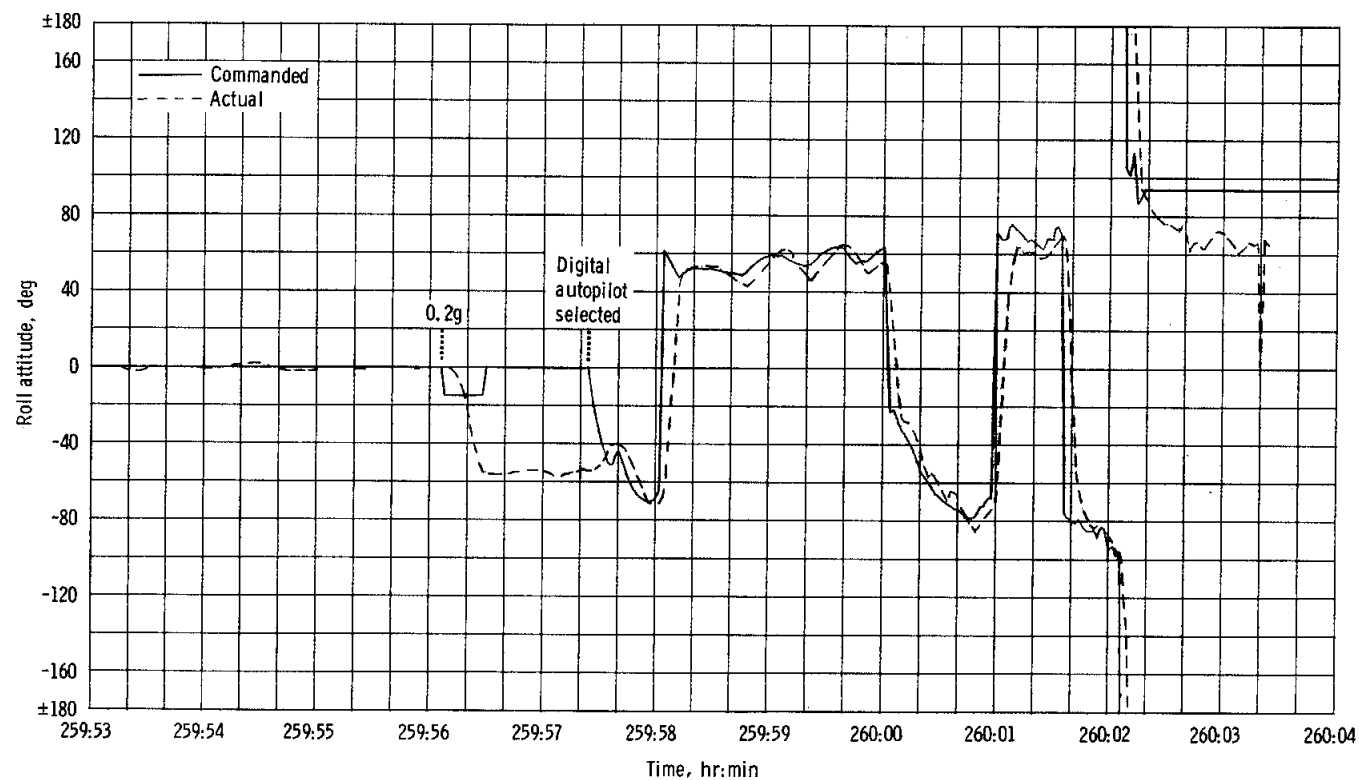


Figure 5.16-28. - Roll command plotted against actual roll.

NASA-S-68-6348

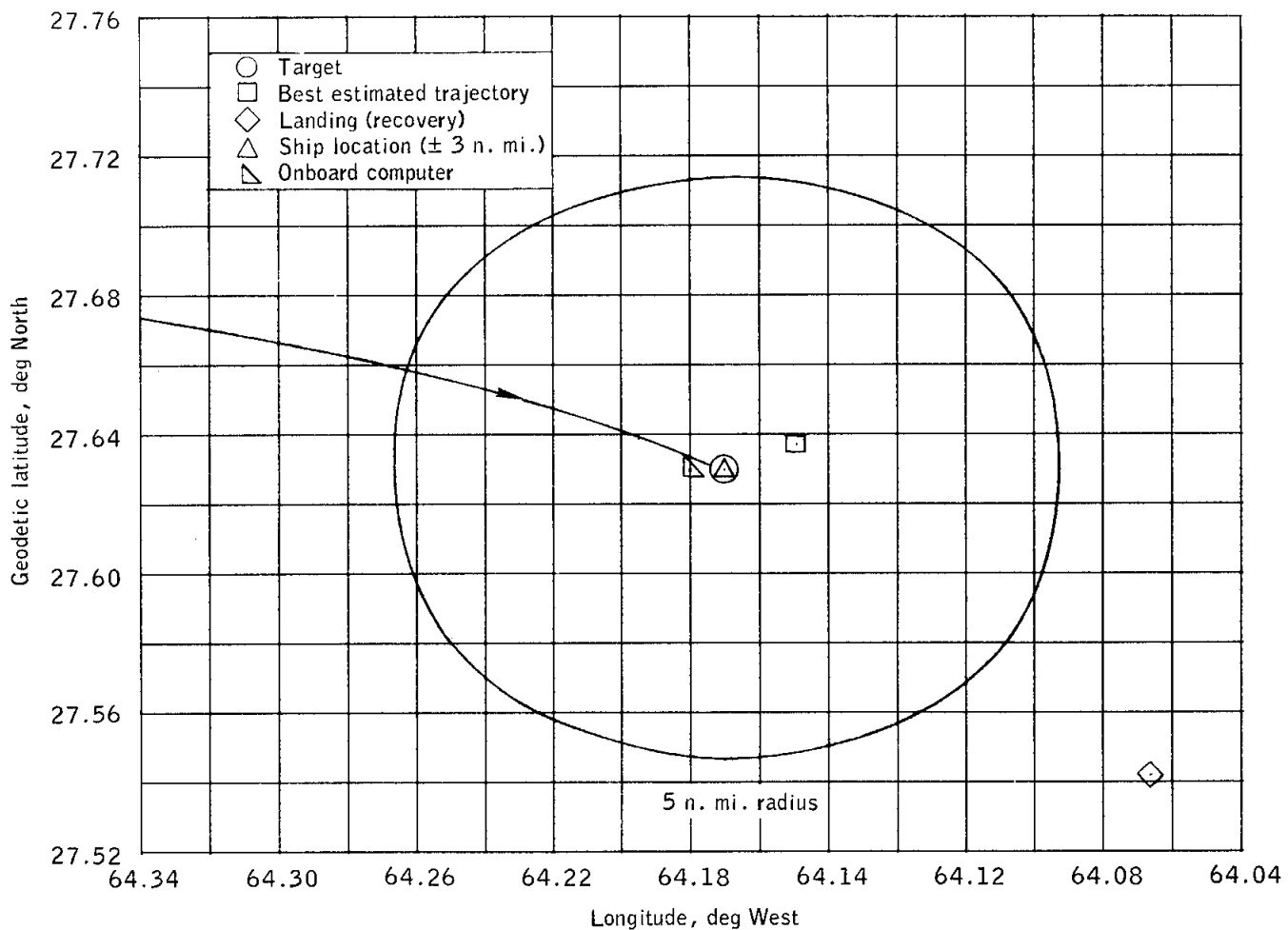


Figure 5.16-29.- Landing point data.

NASA-S-68-6349

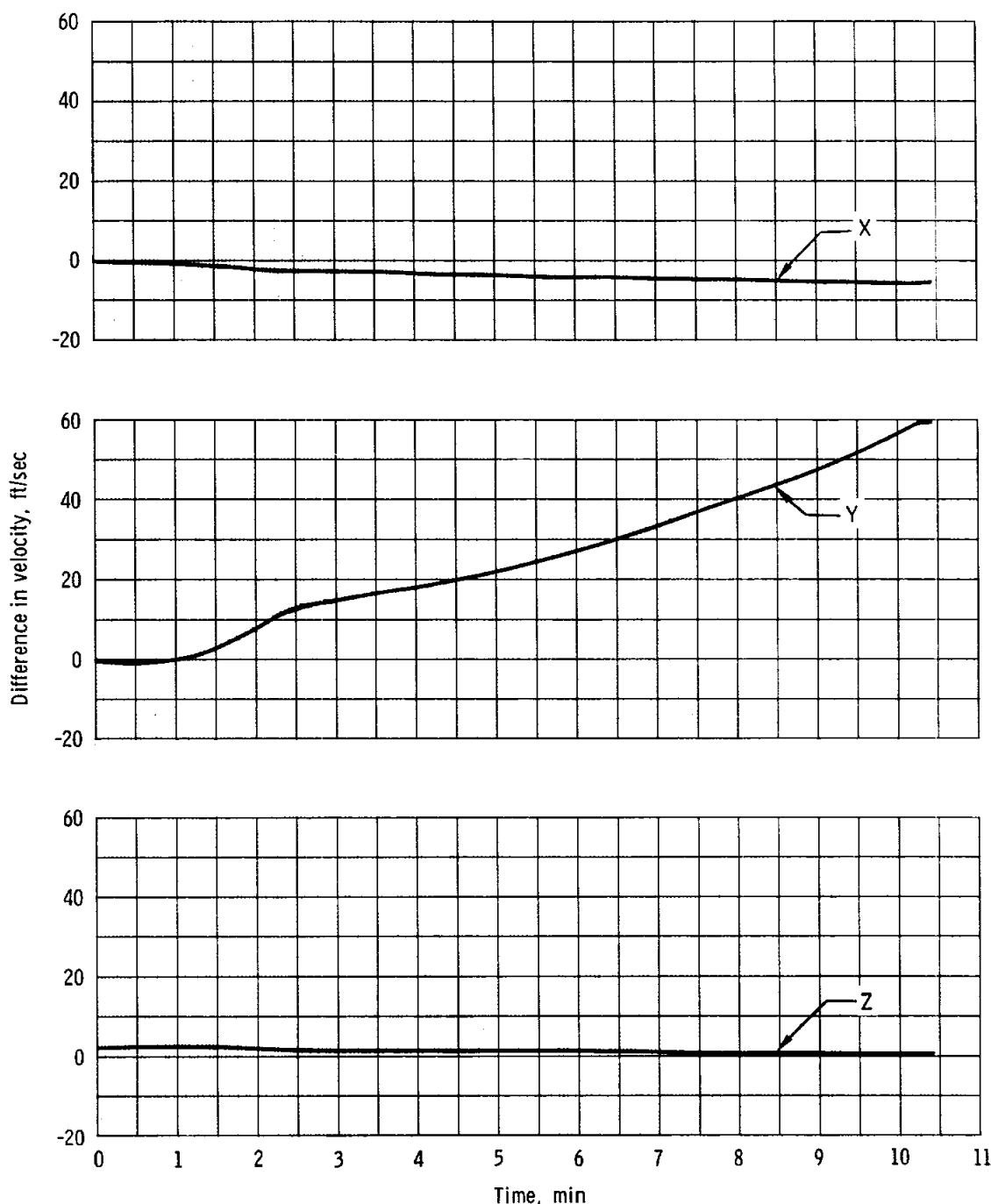
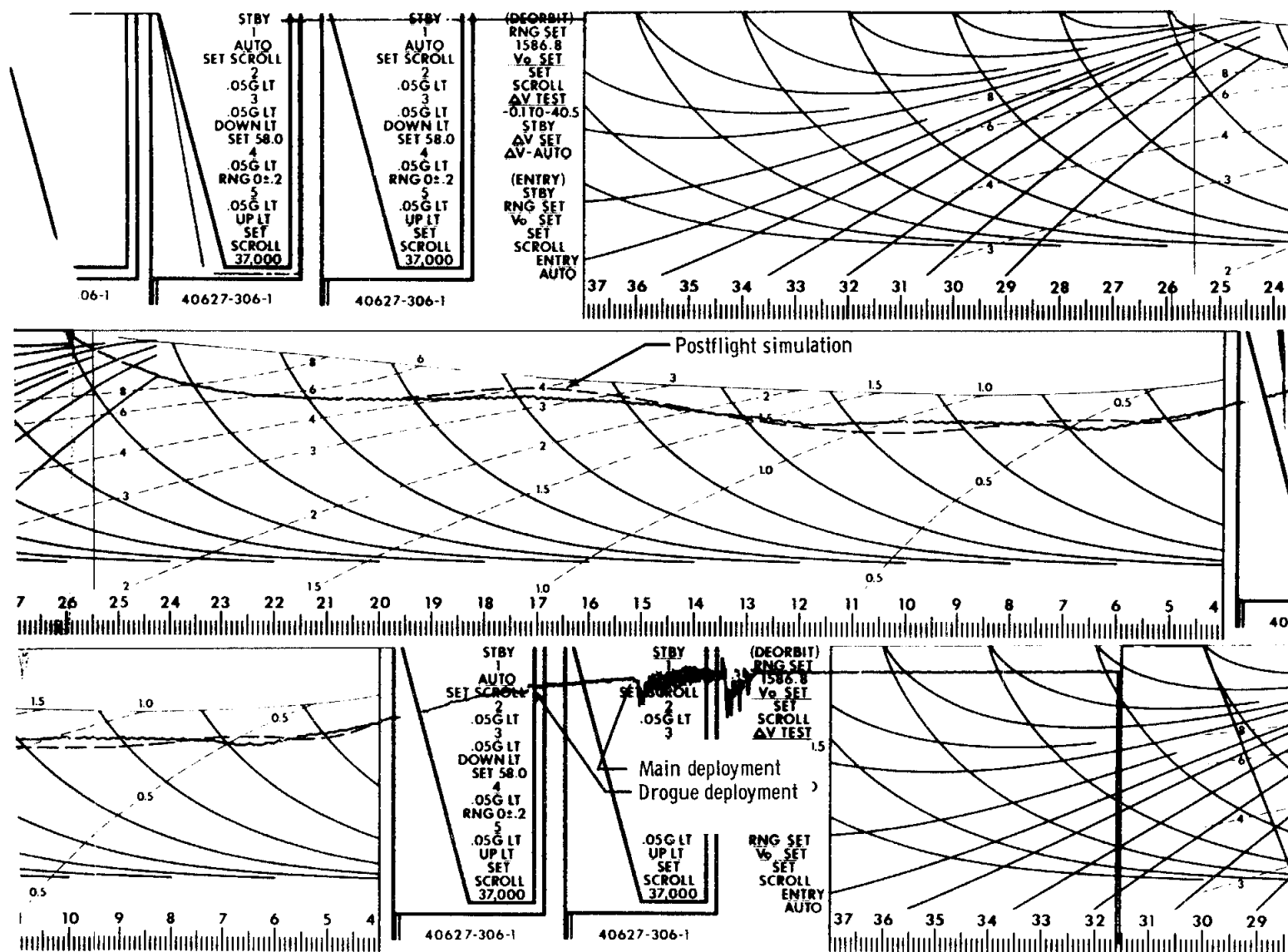


Figure 5.16-30. - Velocity comparison during launch phase, command module computer minus launch vehicle instrument unit.

NASA-S-68-6350



5-148

Figure 5.16-31. - Scroll from entry monitor system.

5.17 REACTION CONTROL SYSTEMS

All reaction control system parameters were normal throughout the mission except for measurements from one propellant quantity sensor that had failed prior to flight. The reaction control systems operated satisfactorily, and all test objectives were satisfied.

5.17.1 Service Module Reaction Control System

A 1-second static firing of the four plus X engines was performed 25 minutes prior to launch to purge the system of gas in the lines and to verify response of the system. The crew reported that they could audibly detect each firing.

The helium regulators for the service module reaction control system maintained the helium and propellant manifold pressures within nominal limits throughout the mission.

The total propellant consumption during the flight is shown in figure 5.17-1. With the major exception of rendezvous, propellant consumption approximated the predicted usage as adjusted for flight plan changes. The rendezvous required approximately 37 pounds or 11 percent more than predicted.

The propellant usage for each quad is shown in figure 5.17-2. The maximum mismatch in propellant quantity remaining among the four quads was maintained within 36 pounds by selectively varying combinations of one-, two-, and four-jet roll maneuvers and two- and four-jet plus X translations. A comparison of ground calculations with the onboard gage readings is shown in figure 5.17-2 for quads A, C, and D. The sensor for quad B failed before launch (see section 5.15). The telemetered gage readings have been converted from percent to weight of propellant remaining.

The fuel and oxidizer are each stored in two tanks, primary and secondary, with 38 percent of the total in the secondary tanks. Because of the uncertainty in the ground calculations (primary gaging system), the crew was requested to switch from the primary to the secondary tanks for each quad when the ground calculated quantity reached 43 percent remaining. This procedure precluded the possibility of supplying only oxidizer or only fuel to the engines, a condition which would be detrimental to the engines. To accomplish the switchover at 43 percent, the crew was instructed to switch at onboard gage readings of 46 to 54 percent, depending on the quad (as shown in table 5.17-1).

This variance from 43 percent was the correlation noted between ground calculations and the indication on the cabin gage. The major

contributing factor to this disparity was the selected helium pressure at propellant depletion used for the gage design. This and other factors are incorporated into a calibration nomograph, which was used to obtain corrected gage readings. The time of switchover, the telemetered and corrected gage readings, and the ground calculated quantity are also shown for comparison in table 5.17-1. As noted, the variance between ground calculations and corrected gage readings is 0.4 to 1.7 percent of full scale, whereas the differences for the uncorrected values are 2.4 to 8.7 percent. The cabin gage readings are then sufficiently accurate to be used as the primary gaging system by the crew, when corrected.

The primary quad heaters were activated at insertion and performed normally throughout the mission. During periods of low firing activity, all quad package temperatures were maintained between 117° and 141° F. The maximum quad package temperature resulting from aerodynamic heating during launch was 127° F on quad D. The maximum quad package temperature resulting from engine firing activity was 198° F on quad A after the rendezvous maneuvers. The quad package temperature limits are 70° F and 210° F.

The primary propellant tank outlet temperatures were initially at approximately 75° F, then decreased during the flight for all quads and reached a minimum of 33° F on quad A after 10-1/2 days. The helium tank temperatures closely followed the variations in primary propellant tank outlet temperatures; however, the helium tanks remained 5° to 10° F warmer.

5.17.2 Command Module Reaction Control System

No helium leakage was indicated prior to activation of the command module reaction control system. The system was activated prior to the deorbit maneuver at 259:39:02, the propellant isolation valves were opened shortly thereafter. Both manual and automatic control were used during entry in combinations of dual- and single-system firings, and the system performed normally.

A total of 50 pounds of propellant was used (29 and 21 pounds from systems A and B, respectively). The amount of propellant used during a particular event can be determined from figure 5.17-3. The momentary decreases in propellant expended after any usage are associated with system and instrumentation thermal stabilization. Consequently, the stabilized values indicate the amount of propellant consumed.

The helium tank temperatures remained between 77° and 59° F prior to activation of the system. The instrumented engine injectors remained above 46° F, eliminating the necessity for the valve warm-up procedure.

During postflight testing, an inadvertent opening of the oxidizer isolation valves was noted. It is suspected that the valves were damaged by hydraulic hammering during system activation. This is discussed further in section 11.

TABLE 5.17-I.- SECONDARY TANK SWITCHOVER

Condition	Quad			
	A	B	C	D
Time of switchover, hr:min	167:00	165:00	144:00	193:16
Required cabin gage readings for switchover, percent	46	49	54	49
Telemetered gage reading, percent	46	--	53	49
Corrected telemetered gage readings using fig. 5.17-2, percent . . .	41	--	46	43
Ground calculated propellant remaining at switchover, percent	43.6 (142 lb)	42.8 (140 lb)	44.3 (145 lb)	43.4 (142 lb)

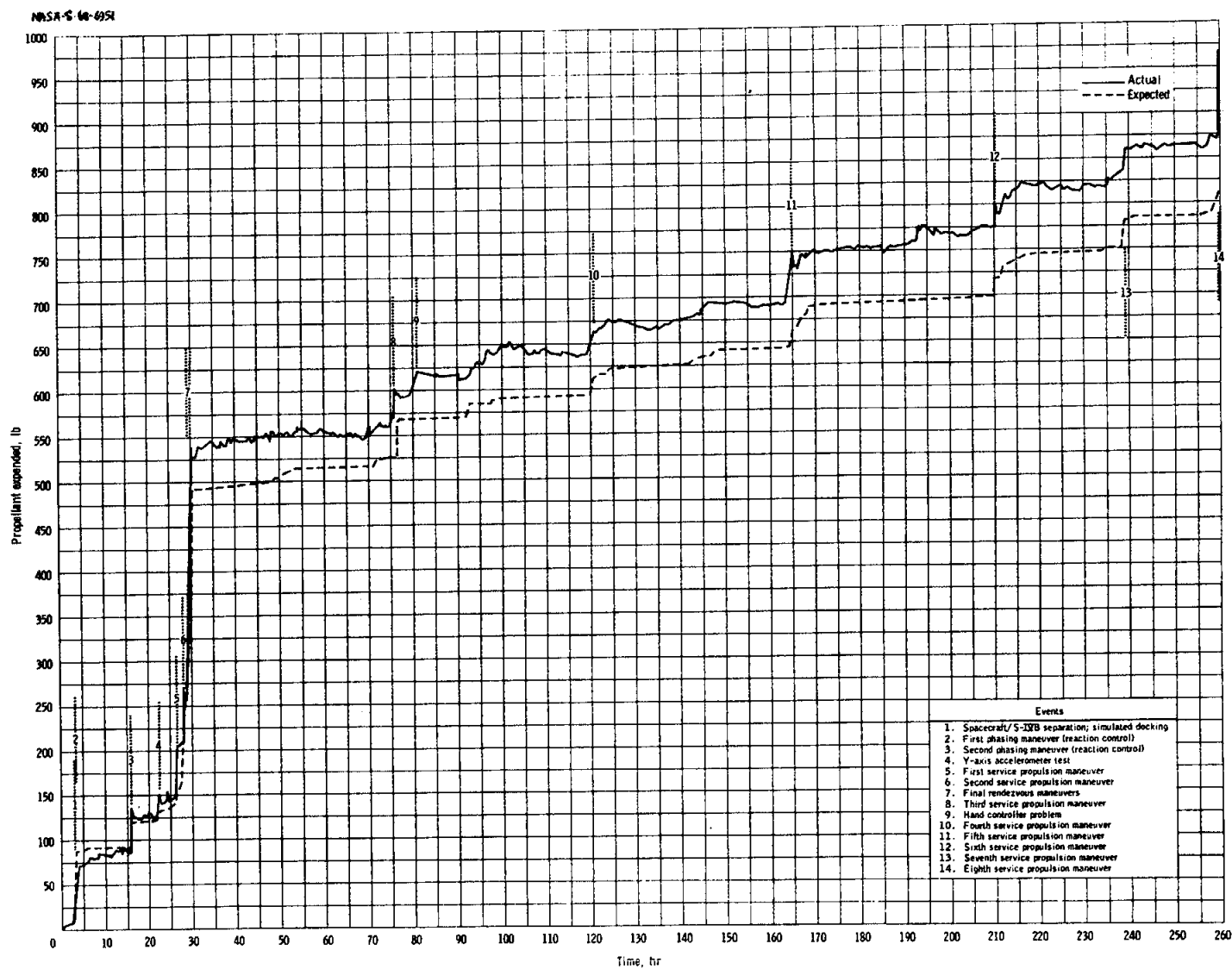
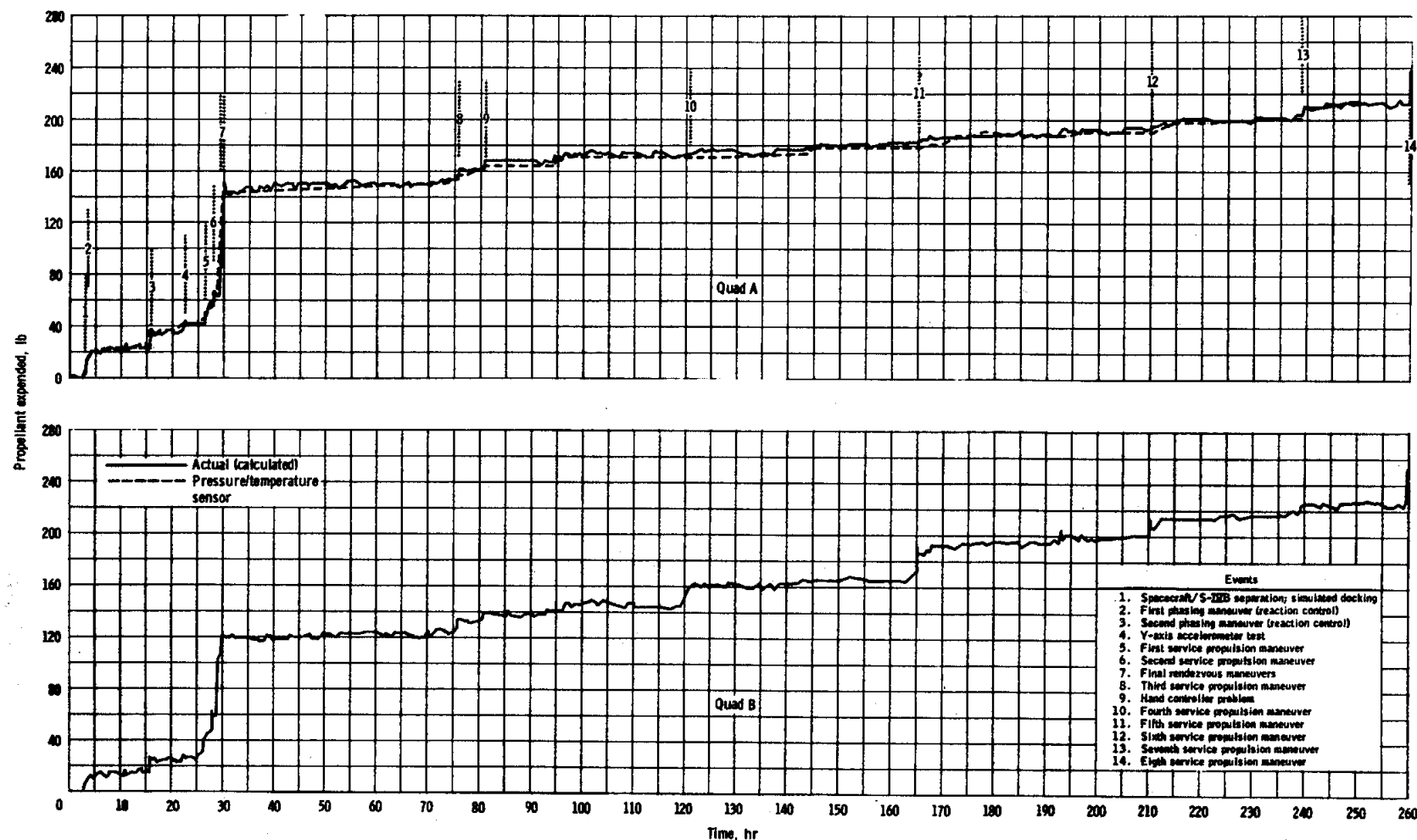


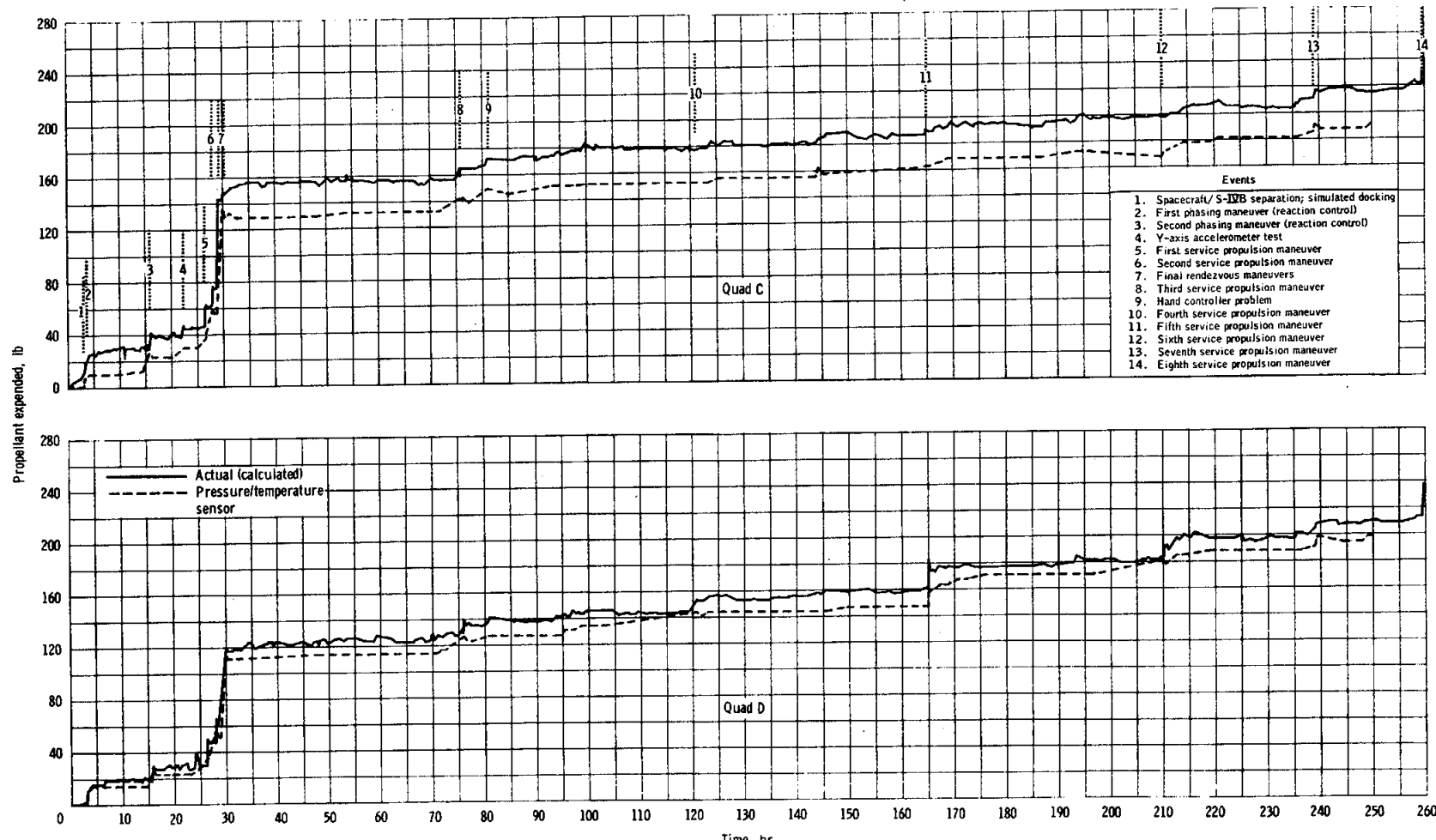
Figure 5.17-1. - Total propellant expended from service module reaction control system.



(a) Quads A and B.

Figure 5.17-2. - Propellant consumed from quads.

NASA-S-68-6353



(b) Quads C and D.

Figure 5.17-2. - Concluded.

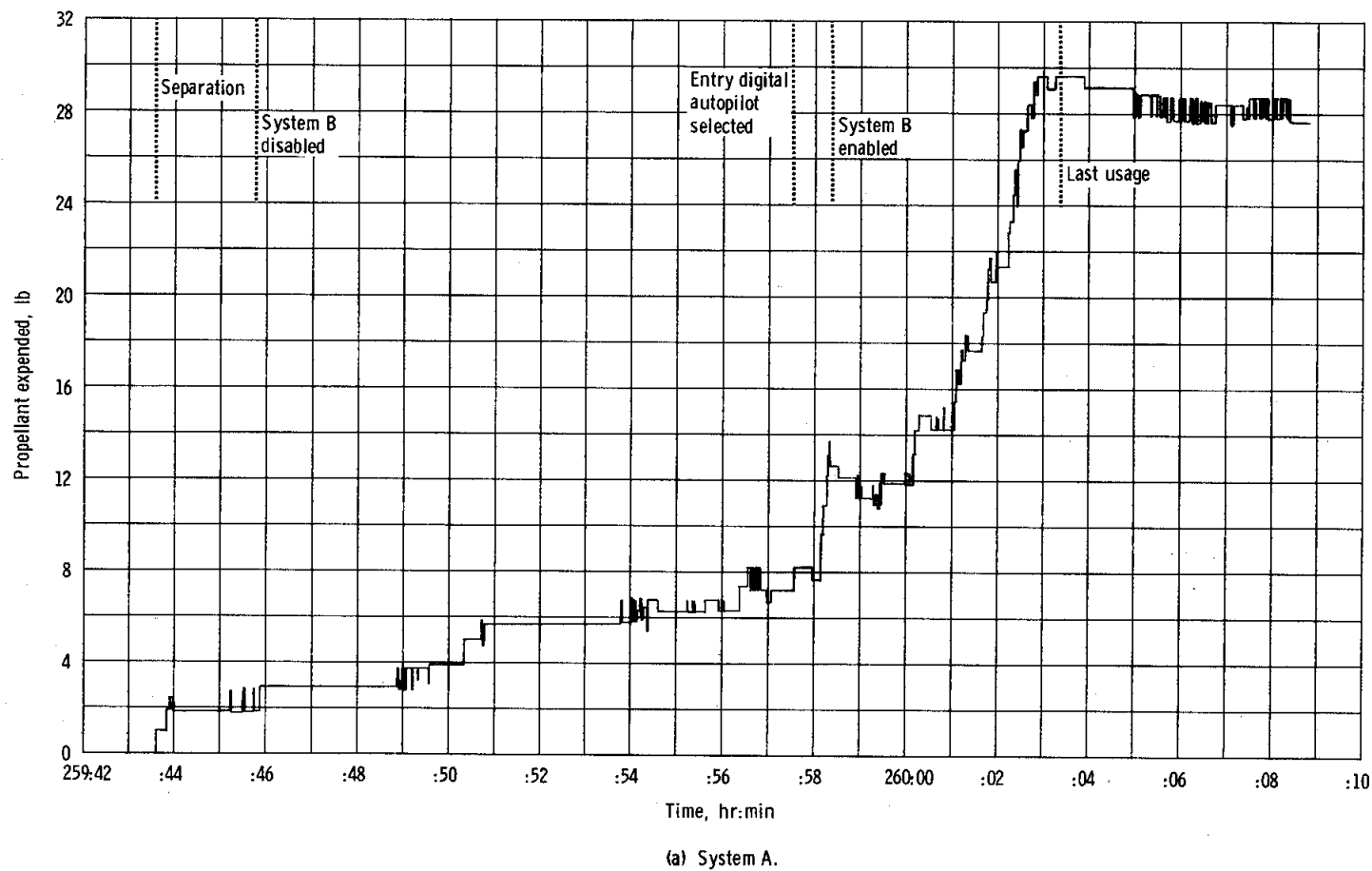


Figure 5.17-3. - Propellant expended from command module reaction control system.

NASA-S-68-6355

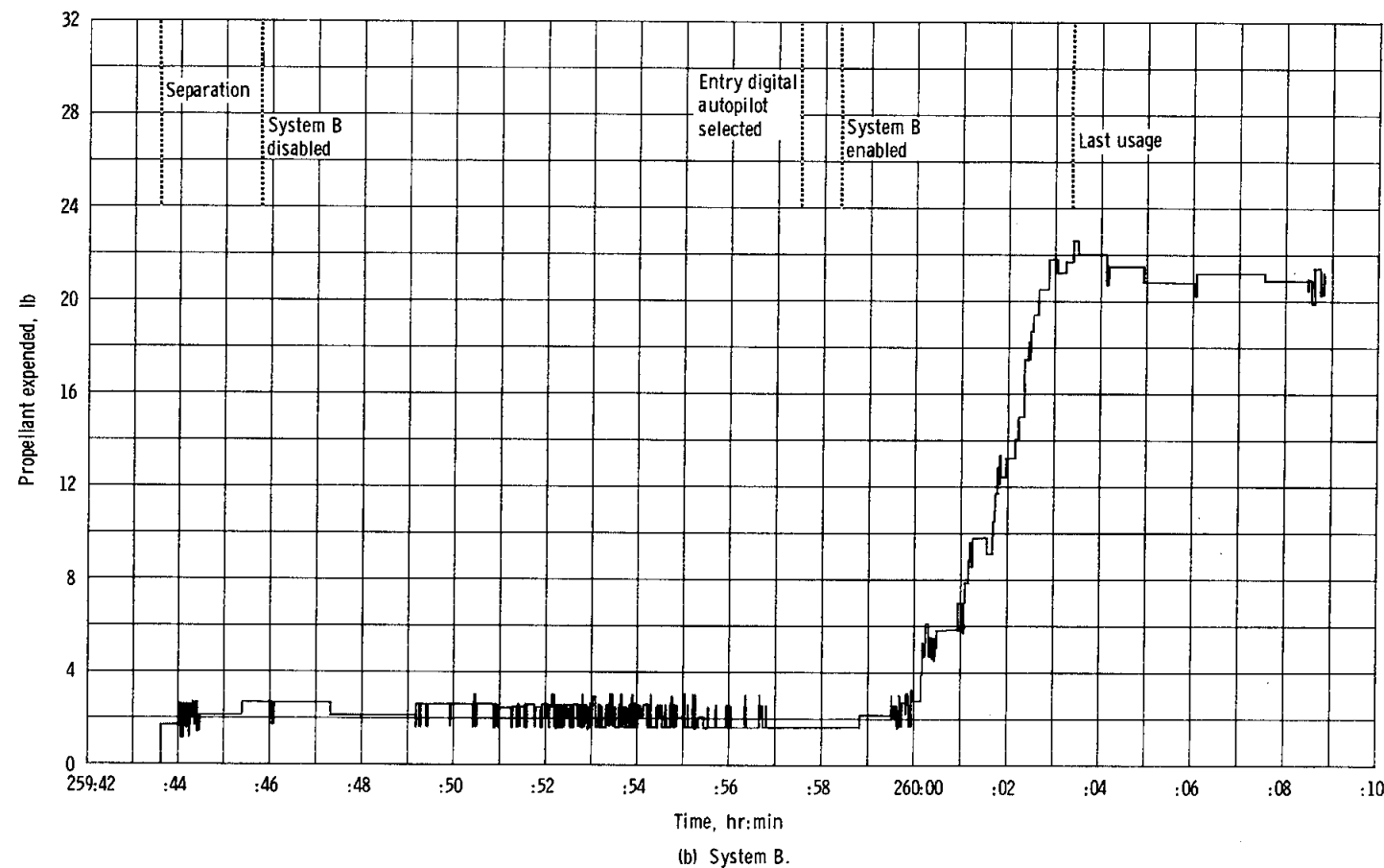


Figure 5.17-3. - Concluded.

5.18 SERVICE PROPULSION

Operation of the service propulsion engine during the eight planned maneuvers was satisfactory. A 3-hour cold-soak test was performed after the fifth maneuver without any notable decrease in propellant line temperatures. The propellant utilization and gaging system and the propellant thermal control system operated satisfactorily.

5.18.1 Engine Performance

A comparison of calculated and predicted steady-state values is shown in table 5.18-I. The calculated values were obtained from the simulation that best matched the command module computer acceleration data and provided the best estimate of the specific impulse (314.0 seconds). Measured chamber pressure during the fifth maneuver is shown in figure 5.18-1.

The flight performance adjusted to the standard inlet conditions yields a thrust of 20 721 pounds, a specific impulse of 314 seconds, and a propellant mixture ratio of 1.60; all values are within approximately 1 percent of the values for the acceptance tests of the engine.

The results of the relatively short first, second, third, seventh, and eighth engine operations are compared with the results of the fifth operation (long-duration) in table 5.18-II. The values shown were taken midway through each firing and all were nominal.

Operation of the pressurization system was satisfactory, without any indication of leakage. The helium supply pressure and the propellant ullage pressures indicated a nominal helium usage for the eight engine operations.

A summary of the shutdown transients for six engine operations (the minimum impulse firings are not included) is presented in table 5.18-III.

No start transient analysis is given, as recent ground tests have shown that the response of the flight-type chamber pressure transducer is thermally affected, thus giving erroneous indications during this period. The total impulse of shutdown transients (calculated from cutoff signal to zero-percent thrust) was nominal for the six full engine operations. The time from cutoff signal to 10-percent of steady-state thrust was within specification limits. The start and shutdown transients during the fifth operation are shown in figure 5.18-2.

The calculated total impulse from the two minimum-impulse operations (table 5.18-IV) was significantly higher than predicted utilizing either

chamber pressure or incremental velocity data. Chamber pressure during the two minimum impulse firings is shown in figure 5.18-3.

During the first engine operation, an oxidizer interface pressure spike of 250 psia occurred at ignition; however, this has been observed during ground tests and is considered normal for a dry start (no propellant between the ball valves).

5.18.2 Propellant Utilization and Gaging System

The onboard gaging system indicated 22.3 percent oxidizer and 22.2 percent fuel at propellant temperatures of 71° and 72° F, respectively. Analysis of one oxidizer sample yielded a density of 90.16 lbm/ft³ at the loaded temperature of 71° F and under a pressure of 190 psia. At 72° F and under a pressure of 190 psia, analysis of one fuel sample yielded a density of 56.42 lbm/ft³.

Calculated propellant loads utilizing the onboard gaging system and the densities obtained from the samples were as follows:

Propellant	Total mass loaded, lbm	
	Actual	Planned
Oxidizer	6026.7	6029.4
Fuel	^a 3710.6	3727.9
Total	9737.3	9757.3

^a Assumes 20 pounds inadvertently drained overboard prior to launch.

The propellant utilization and gaging system was operated in the primary mode for all service propulsion operations except the fifth, when it was switched to the auxiliary mode, which provided primary sump tank and total auxiliary (point sensors) propellant mass readings. Data from the fifth maneuver indicated that the auxiliary gaging system operated satisfactorily, with two point sensors being uncovered in both the oxidizer and fuel systems. The oxidizer primary gaging system operated as expected. The fuel primary system, however, exhibited shifts of approximately 0.5 percent between firings, and also unexpected upward shifts as large as 1.5 percent after the initial lockout. This upward shift was less evident in the fifth maneuver than the other seven. Only after 20 seconds into the fifth maneuver did the fuel primary probe operate as expected.

5.18.3 Propellant Thermal Control

The service propulsion thermal control system maintained the required temperature. The rate of temperature decrease of the propellant lines was better (less) than predicted. The minimum temperature was 55° F for the oxidizer and fuel engine feedlines and was 50° and 52° F for the oxizizer and fuel system feedlines, respectively. Most of the decrease in propellant line temperature resulted from the colder propellants moving into the lines from the tanks during each firing. The tank propellant temperatures decreased continually throughout the mission, as expected.

The bi-propellant valve temperature remained above 50° F prior to all firings, with heater operation necessary before the sixth and eighth firing to maintain the 50° F temperature. A 3-hour heater test of the A/B bank showed approximate temperature increases of 2° F/hr on the engine lines and 3° F/hr on the engine valve. This heating rate was about twice that observed during a previous 3-hour test using only the A-bank heaters. After the fifth firing, a 3-hour cold-soak test showed no notable decrease in propellant line or engine valve temperatures.

TABLE 5.18-I.- STEADY-STATE PERFORMANCE

Parameter	Predicted	Measured	Calculated
Instrumented			
Oxidizer tank pressure, psia	175	178	178
Fuel tank pressure, psia	175	175	176
Oxidizer interface pressure, psia	166	163	166
Fuel interface pressure, psia	173	171	174
Engine chamber pressure, psia	103	103	103
Calculated			
Oxidizer flow rate, lbm/sec	41.5		41.6
Fuel flow rate, lbm/sec	25.8		25.9
Propellant mixture ratio	1.61		1.61
Vacuum specific impulse, sec	312.5		314.0
Vacuum thrust, lbf	21 058		21 180

Note: Measured values taken from fifth maneuver (56 seconds after ignition).

TABLE 5.18-II.- STEADY-STATE PRESSURES

Maneuver no.	Oxidizer tank, psia	Oxidizer interface, psia	Fuel tank, psia	Fuel interface, psia	Chamber, psia
1	176	161	173	169	99
2	176	163	173	170	101
3	176	164	172	169	100
5	177	163	174	170	103
7	175	164	172	168	101
8	175	161	172	168	100

TABLE 5.18-III.- SHUTDOWN TRANSIENT SUMMARY

Parameter	First maneuver	Second maneuver	Third maneuver	Fifth maneuver	Seventh maneuver	Eighth maneuver	Acceptance test	Apollo 6 first maneuver	Specification value
Total vacuum impulse (cutoff to 0 percent steady-state thrust), sec	11 619	11 983	11 676	12 692	12 076	12 411	9650	11 905	8000 to 13 000
Time (cutoff to 10 percent steady-state thrust), sec	0.946	0.944	0.984	0.973	0.994	0.970	0.938	0.920	0.750 to 1.100

TABLE 5.18-IV.- MINIMUM IMPULSE FIRINGS

Parameter	Fourth firing	Sixth firing	Three-sigma for 0.5-sec commanded thrust
Time from ignition signal to cutoff signal, sec	0.5	0.5	--
Duration of thrusting, sec	2.67	2.82	--
Total impulse of firing, lbf-sec			
From chamber pressure	13 080	11 907	4800 to 7800
From acceleration	10 243	10 188	4800 to 7800

NASA-S-68-6356

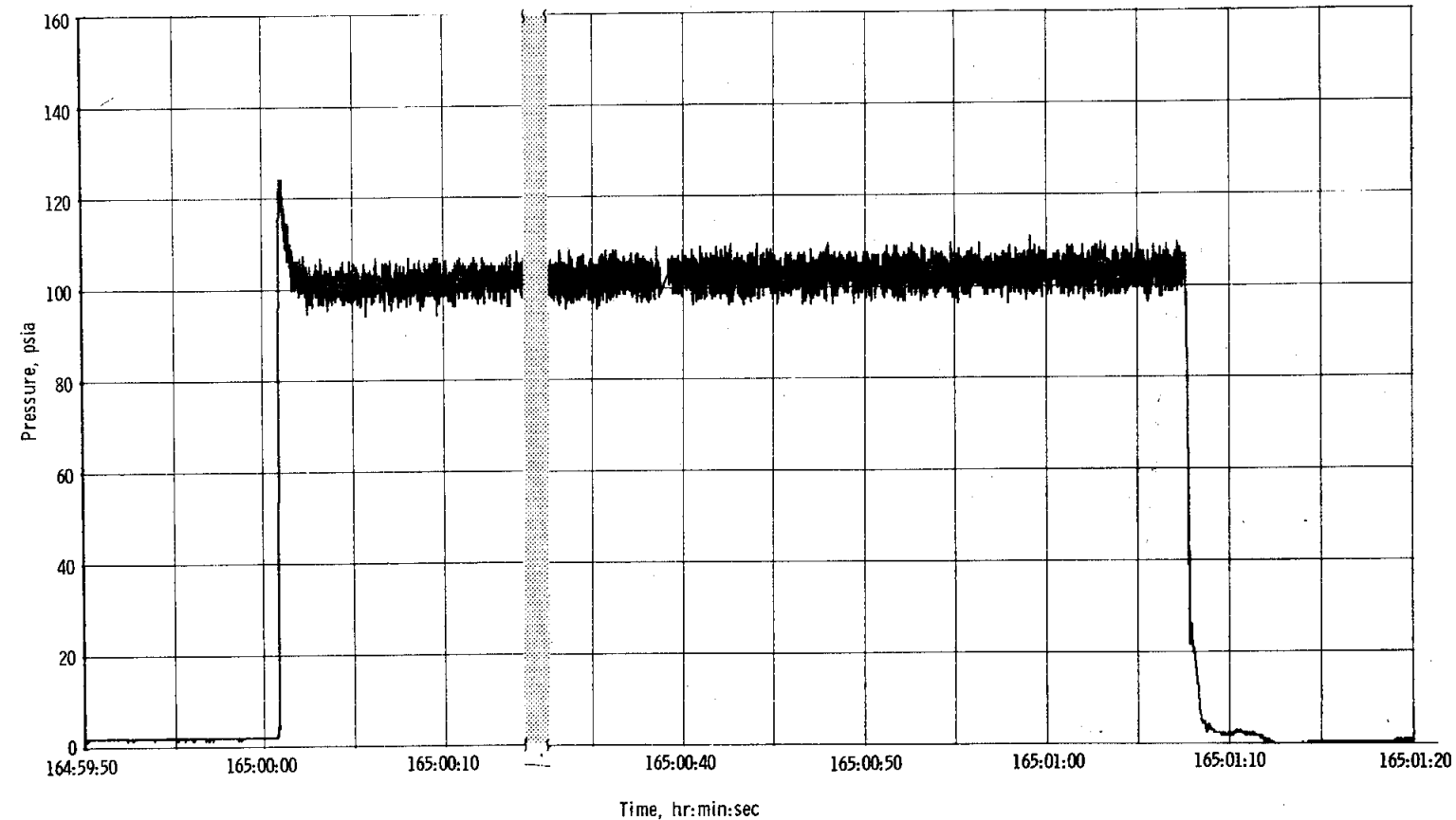


Figure 5.18-1. - Chamber pressure during fifth service propulsion maneuver.

5-165

NASA-S-68-6357

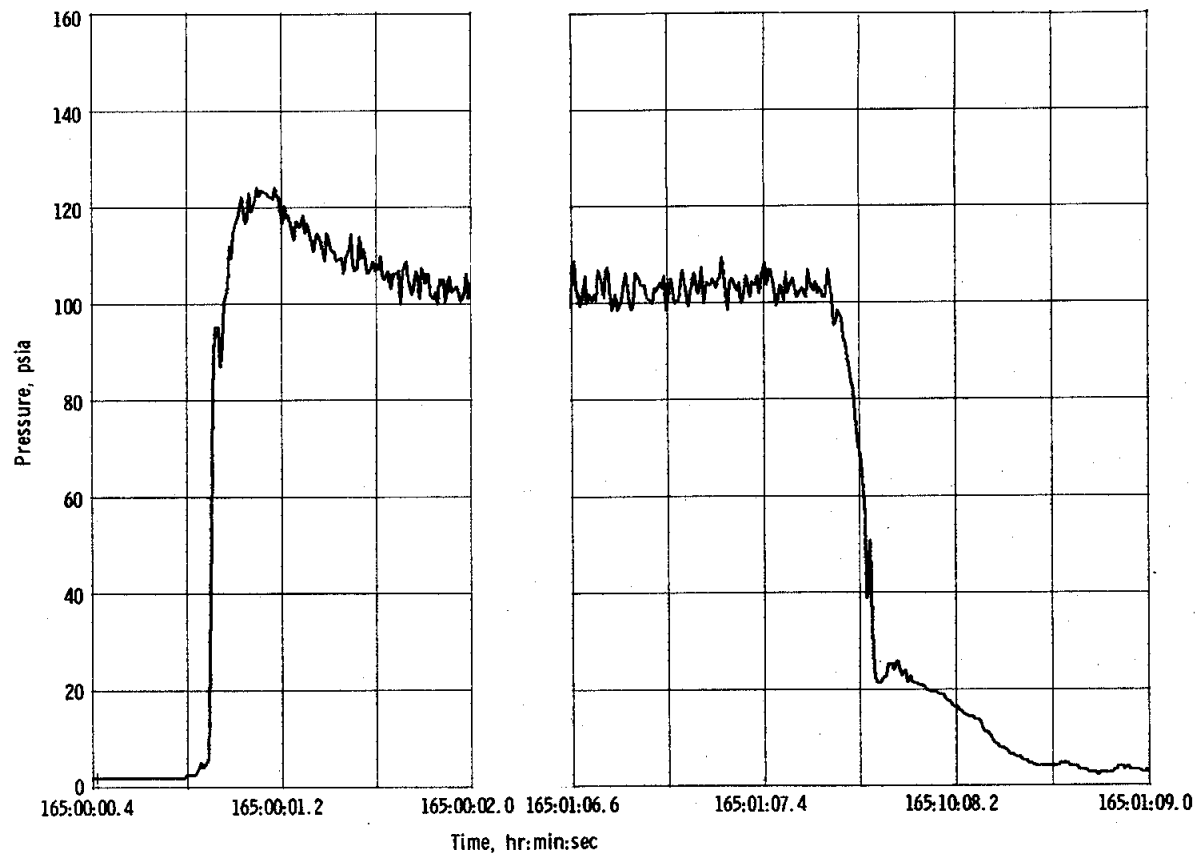
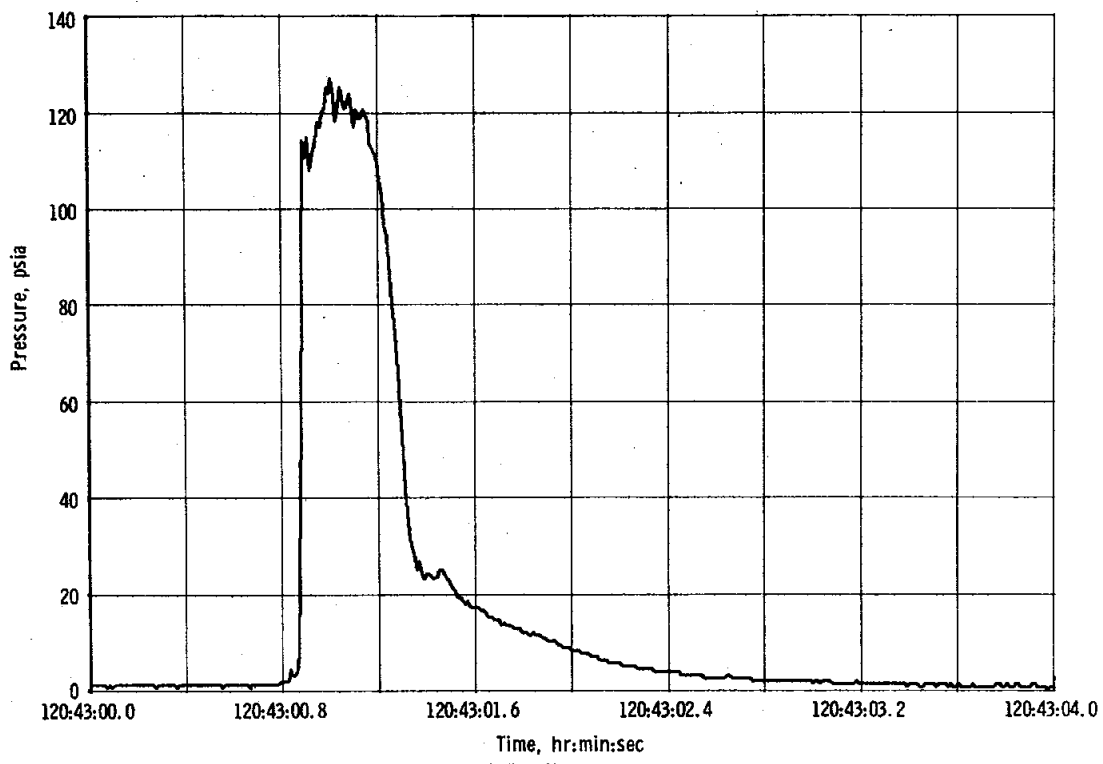
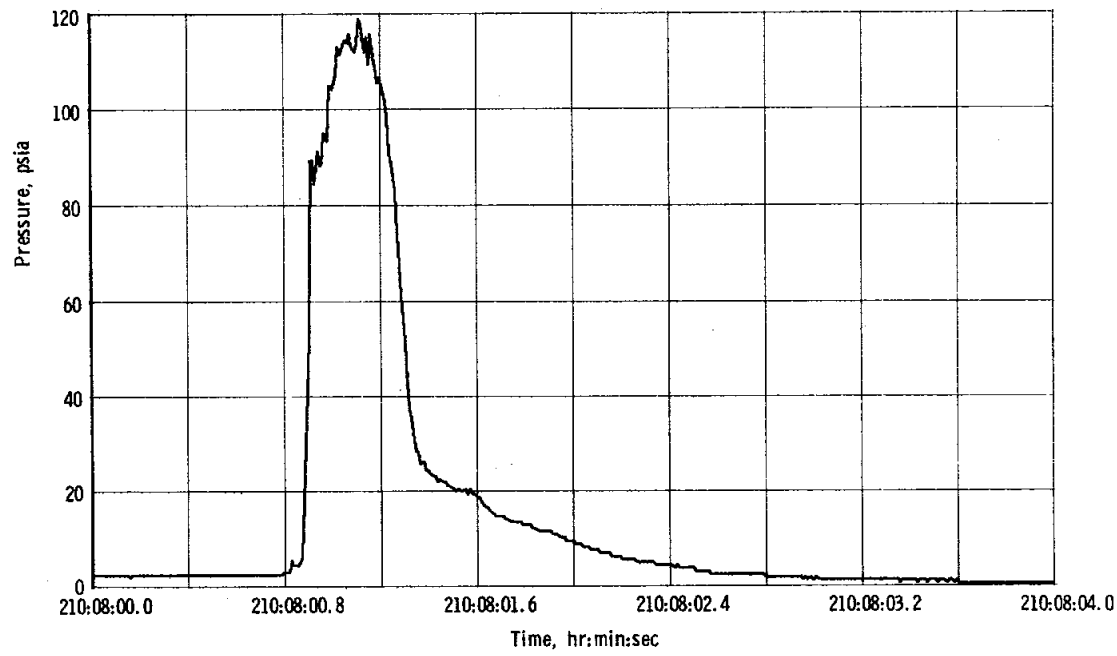


Figure 5.18-2. - Start and shutdown transients for fifth service propulsion maneuver.

NASA-S-68-6358



(a) Fourth maneuver.



(b) Sixth maneuver.

Figure 5.18-3. - Chamber pressure during minimum impulse firings.

5.19 CREW SYSTEMS

The performance of the environmental control system was, in general, satisfactory, with only minor difficulties. The crew was kept comfortable and the spacecraft equipment was maintained in an operable environment.

5.19.1 Pressure Suit and Cabin Circuits

The cabin pressure began relieving at 6.0 psid 48 seconds after launch. The relief valve sealed at 5.9 psig at about 5 minutes after launch, and the cabin pressure decreased fairly rapidly to cabin regulator operating pressure at about 02:40:00. The launch parameters for suit and cabin circuits are given in figure 5.19-1. The figure demonstrates the effect of launch vehicle acceleration the suit-to-cabin differential pressure; as acceleration is terminated, the suits tend to expand in volume, decreasing the differential pressure until the gas flow can compensate. A high cabin pressure decay rate was observed during the early phase of the mission because the waste management overboard dump valve was open to accelerate oxygen enrichment of the cabin gas. The oxygen enrichment cabin purge was ended at about 11:00:00, and the resulting oxygen partial pressure profile in the cabin gas is given in figure 5.19-2.

The cabin and suit circuits operated normally during entry (fig. 5.19-3).

Lithium hydroxide element usage.— Twenty-two lithium hydroxide elements were stowed onboard, including two installed in the environmental control unit canister. Each element is capable of absorbing 3.4 pounds of carbon dioxide with 93 percent lithium hydroxide utilization. The number of elements stowed was adequate for a 10.5-day mission, based on a 12-hour change interval. However, because of an accumulation of changes at less than 12-hour intervals, no new element was available for the change scheduled for 257:00:00, and element 1, which was only half used, was reinstalled for entry. The maximum allowable carbon dioxide pressure of 7.6 mm of mercury was never exceeded. Figure 5.19-4 shows typical and maximum cabin carbon dioxide partial pressures, and figure 5.19-5 presents a summary of chemical analysis of the lithium hydroxide cartridges. Most of the cartridges were used for 22 to 26 hours and indicate a lithium hydroxide utilization averaging 85 percent. Two cartridges (19 and 20) were left in the canister for longer than their useful life, as evidenced by lithium hydroxide utilization levels of 96 and 98 percent, respectively. The operational procedures provided good utilization of the lithium hydroxide.

Cabin fans.- The crew reported that the cabin fans were so noisy that first one fan and then both fans were turned off. The crew said they were comfortable without the fans operating. During postflight testing, the fans met all acceptance test requirements, but a washer and a nut were found between the cabin heat exchanger and fans, two washers were found between the exit screens and the downstream end of the fans, and the leading inlet edges of the fan blades were nicked. The noise is attributed to these foreign articles hitting the fan blades and moving back and forth between the fan and heat exchanger. It should be noted that the cabin temperature sensor is located at the inlet to the cabin heat exchanger, which is a relatively stagnant area without fan operation and thus not indicative of true cabin air temperature. The use of the cabin dry bulb temperature obtained during humidity surveys is, therefore, used as representative cabin temperature (fig. 5.19-6).

Cabin condensate.- A major problem associated with the cabin and suit circuits was condensation. This problem was anticipated in the cabin because the cold coolant lines from the radiator to the environmental control unit and from the environmental control unit to the inertial measurement unit were not insulated. The radiator return line temperature was as low as 16° F and normally was 34° to 45° F. The temperature for the inertial measurement unit was generally 40° to 50° F. These lines will be insulated on spacecraft 106.

Each time excessive condensation was noted on the coolant lines or in a puddle on the aft bulkhead after service propulsion maneuvers, the crew vacuumed the water overboard with the launch purge fitting connected to the waste management system hose.

On three occasions, the crew also reported gurgling and water droplets coming from the cold, or blue, suit ventilation hoses. Each time, two or three manual actuations of the cyclic accumulators corrected the problem. The manual operation could account for the fact that several automatic actuation indications are missing from PCM data. Postflight testing will be accomplished on the cyclic accumulators to determine whether a hardware malfunction occurred. It should be noted that the accumulators, cycled every 10 minutes, have a water collection capacity about twice that required for the estimated metabolic loads expected for the mission.

5.19.2 Oxygen Distribution Circuit

The oxygen system operated normally throughout the mission. The surge tank pressure followed the cryogenic system pressure but at a slightly lower level, as expected, because of the system flow and the

pressure drop of the restrictors. The calculated quantity of oxygen used during the mission for all environmental control functions was 99 pounds, including the 7 pounds of gaseous oxygen stored in the command module for use during entry.

5.19.3 Thermal Control System

The coolant system operation during the early phase of the mission was normal (fig. 5.19-7). The radiators were put on the line between 15 and 27 minutes after launch, and the outlet temperature rapidly decreased to less than the inlet temperature of 75° F.

During thermal mixing (that is, when the radiator outlet temperature is below 45° F), the evaporator inlet temperature sensor reads higher than the mixed temperature. The evaporator inlet temperature sensor was placed too close to the mixing valve and was influenced by the hot bypassed coolant, providing an erroneous reading.

The radiator system flow proportioning valve switched over to the redundant system three times. Each time, the system was reset to the primary system by the crew, indicating that no basic hardware problem existed. Each time the valve switched, the bus was noted to have dropped out. The logic circuitry of the valve controller should command a switch-over when the bus drops out for more than 12 milliseconds, and these switchovers are thus attributed to the electrical problem. The radiator control system in the primary coolant circuit operated normally, and the maximum observed temperature difference between the radiator panel was 16° F.

A radiator surface coating degradation test was performed from 92:30:00 to 97:00:00. A brief analysis of data obtained has been performed. Results indicate that the solar absorptivity of the radiator panel tested was 0.3, which is well within the predicted limits.

Glycol evaporator.- The only significant problem with the coolant system was associated with the glycol evaporator in the primary loop. At approximately 10:00:00, the evaporator steam pressure dropped to off-scale low, and the outlet glycol temperature increased above the control temperature, giving the appearance that the evaporator had dried out. The control system which commands water in-flow had failed to provide the required water for boiling. The evaporator was resurfaced by the crew but again dried out. The time between dryouts appeared to depend upon overall system heat load and the amount of water serviced by the crew. The thermal load on the system was low enough that when the evaporator was turned off, the radiators rejected all of the thermal load for about 1/2 revolution, and the peak outlet temperature on the radiators generally did not exceed 58° F during the remainder of the revolution. This failure to operate at the low-level thermal inputs did not have significant impact on the mission.

An 8-1/2 hour secondary coolant system test was performed from 183:40:00 to 191:00:00. The heat load at secondary loop activation was approximately 1400 watts and was increased to approximately 1800 watts at 187:01:00. As the evaporator began to operate, cycling was noted, with the steam pressure going as low as 0.07 psia and the evaporator outlet temperature going to 34° F. After five cycles, the evaporator was stabilized within the control band and maintained good control for the duration of the test, although some cycling occurred at each activation. Radiator outlet temperatures were 55° to 57° F during the day-light passes and decreased to 43° F during the night passes. The evaporator operated for 48 to 52 minutes on each revolution. Water usage rate was calculated to be 1.97 lb/hr at the higher heat load. Water generation rate during this period was calculated to be 1.88 lb/hr. No anomalous operation was experienced on the secondary system.

Because of the anomalous operation of the primary evaporator, the crew elected to enter on the secondary loop with the secondary evaporator operating (fig. 5.19-8). The primary pump also remained on, but the suit heat exchanger was bypassed and put on the secondary loop.

Glycol accumulator.- During preflight checkout, the primary pump accumulator bellows was found to stick at about 85 percent full. During countdown, a glycol quantity in the accumulator was established which would prevent the increase of coolant level to 85 percent from launch heating of the system, and no difficulty was experienced with the pump during the mission. The accumulator quantity at launch was 34.8 percent.

5.19.4 Water Management

About 2 hours prior to launch, the potable water was chlorinated with one ampule of chlorine. At lift-off, the potable and waste tank quantities were 56.3 and 72.3 percent, respectively. The potable tank, which is supplied by fuel cell water, became full at 13:00:00 and except for the small amount of crew consumption, remained full the entire mission. Post-recovery data show that 36.77 and 29.57 pounds of water were found in the potable and waste tanks, respectively. This compares with quantity readings of 101.8 percent potable water and 52.8 percent waste water quantity readings; at command module/service module separation, the quantities were 104.3 percent and 48.6 percent, respectively, indicating that free gas in the tanks was less than 3 percent. As expected, erratic readings of the waste system quantity were experienced during entry because of an effect of the g-loads on the partially filled tank and the gaging system. Waste water was not permitted to dump overboard automatically, and a total of approximately 265 pounds was dumped during the seven manual overboard dumps. During these dumps, the crew reported water leakage from the B-nut fitting which attached the transfer

hose mating quick disconnect to the water panel. A change to the water panel to recess the panel fitting for spacecraft 103 has resulted in a different configuration for the transfer fitting, which includes an O-ring seal.

The crew reported early in the mission that the water was unpalatable for 10 to 12 hours after each chlorination. The chlorination schedule was then changed from 24 hours to about 48 hours, as outlined in table 5.19-I. A test was made for chlorine concentration in the potable water after recovery, at an equivalent mission time of 266:55:00, and 0.13 ppm was found at the drink gun. Three lines which experienced chlorine concentration were sectioned and examined for corrosion. The level of corrosion found was acceptable.

Late in the mission, the crew reported that the cold water valve in the potable water supply assembly was becoming difficult to operate. Postflight testing showed that all actuation forces for operation of the valve were within specification limits. However, some epoxy which is used in the manufacture of the valve was found to be partially blocking a bleed flow channel. This blockage caused the valve to take 6 seconds to deliver the 1 ounce of water (specification is 3 seconds maximum).

5.19.5 Waste Management

The waste management system operated normally except for the leaking transfer fitting on the water system panel previously discussed. No indication of a freezeup of the dump system was experienced, and the auxiliary dump nozzle was not used. Urine was successfully dumped and no urine backup was experienced by the crew. The dump nozzle temperature ranged from 35° to 96° F during the mission.

Several times during the mission, a sustained high oxygen flow occurred, which was determined to be caused by the waste management system overboard valve inadvertently being left open after a urine dump.

The crew reported discomfort from odors during defecation. Since the suit loop charcoal bed is the only odor removal equipment, this situation can be expected during defecation until the suit loop flow sufficiently dilutes the odor to an acceptable level.

5.19.6 Postlanding Ventilation

At approximately 18 minutes after landing and after the crew uprighted the command module, the postlanding ventilation system was activated. The cabin temperature at landing was 70° F and the suit compressors were automatically turned off at landing. The crew had no cooling or circulation during this 18-minute period and started to become uncomfortable. When the postlanding ventilation system was turned on, the crew reported that operation was normal and that the outside air was cool and refreshing. The ambient air temperature in the landing area was 79° F. After recovery, about 50 gallons of sea water was found in the tunnel, indicating that the tunnel hatch check valve failed to perform its function. Postflight testing has shown that the valve leaked between 121 cc/min and 4 gal/min, depending on attitude conditions. This type valve is not used with the integrated tunnel hatch on subsequent spacecraft.

TABLE 5.19-I.-- WATER CHLORINATION

Scheduled time, hr:min	Performed	Omitted
11:30	X	
37:50	X	
57:50	X	
79:00		X
101:50	X	
126:00		X
149:50	X	
171:50		X
194:00	X	
217:40		X
242:40	X	

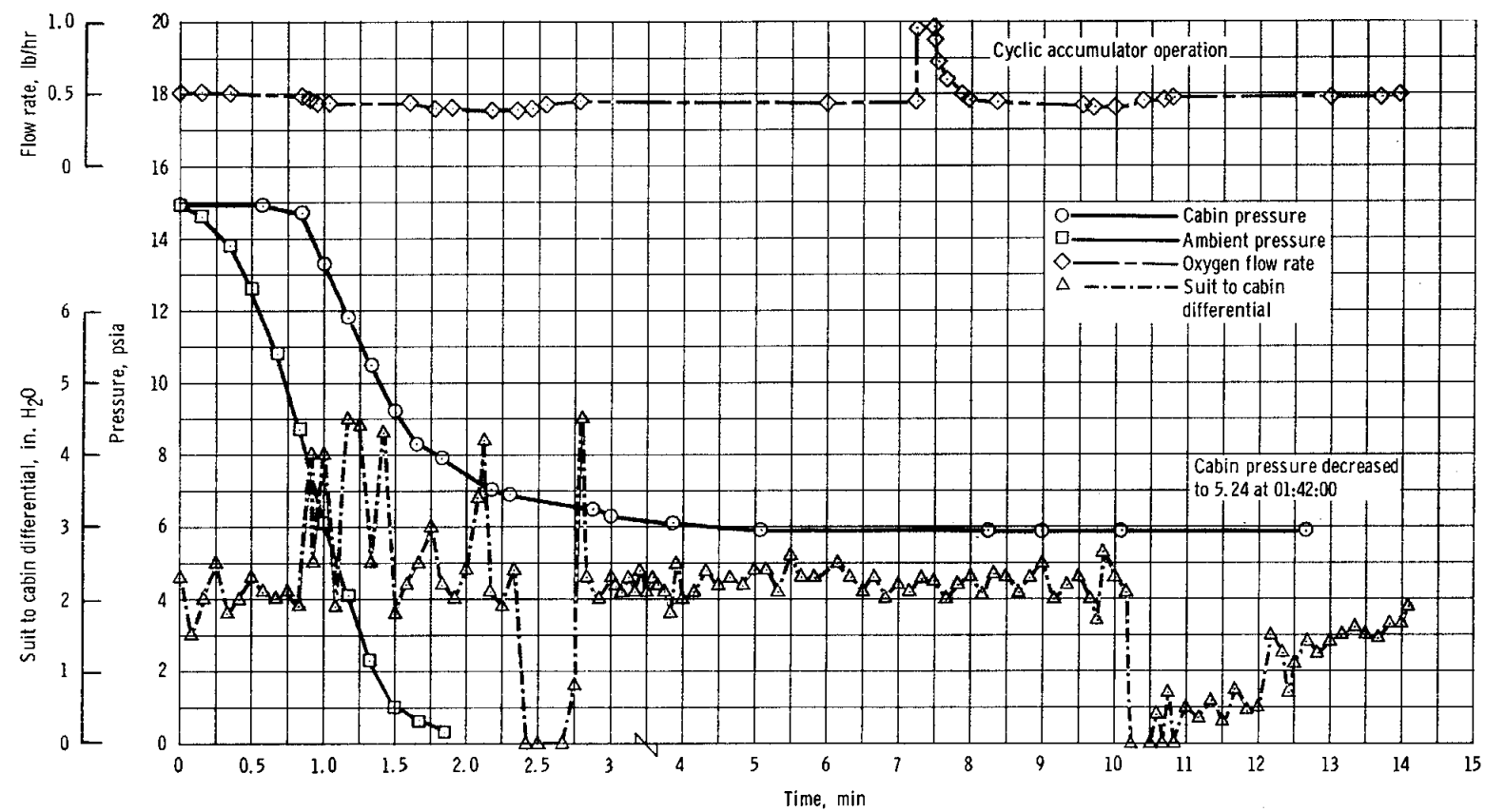


Figure 5.19-1. - Cabin and suit pressures and oxygen flow during launch phase.

NASA-S-68-6360

5-176

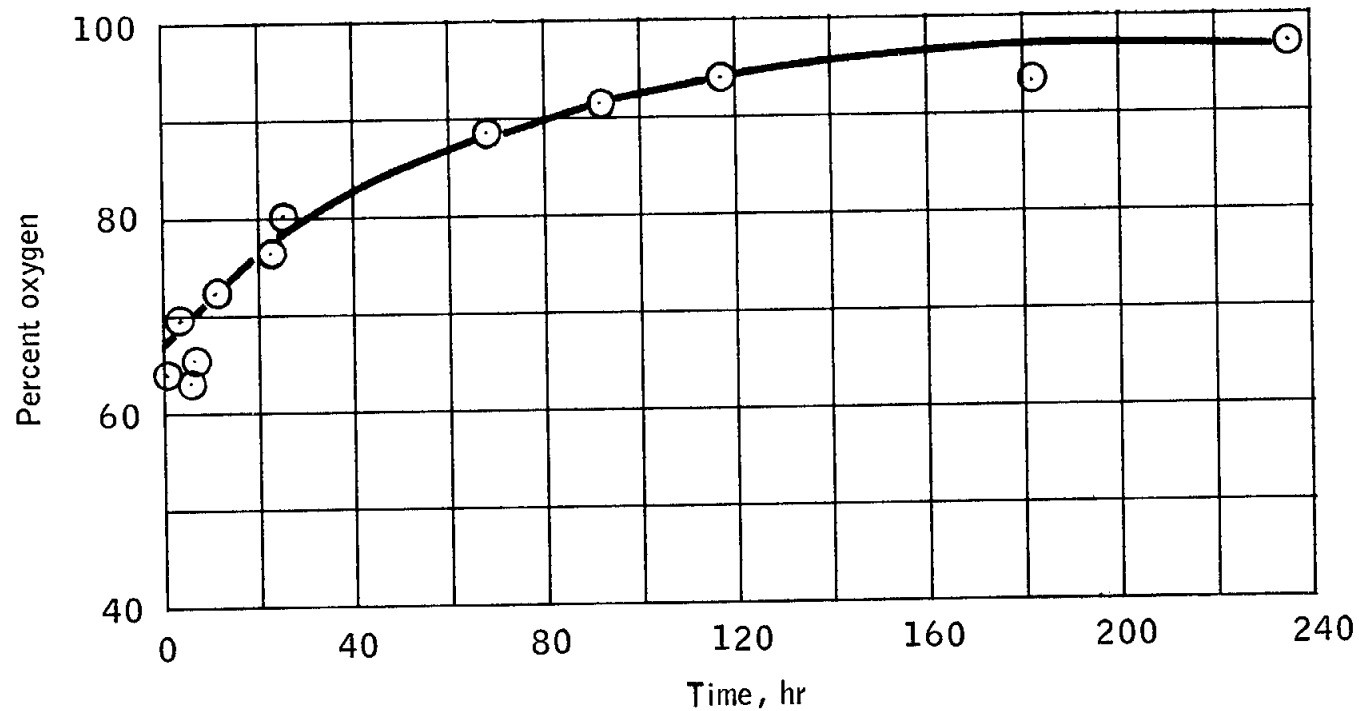


Figure 5.19-2.- Oxygen content of total cabin pressure.

NASA-S-68-6361

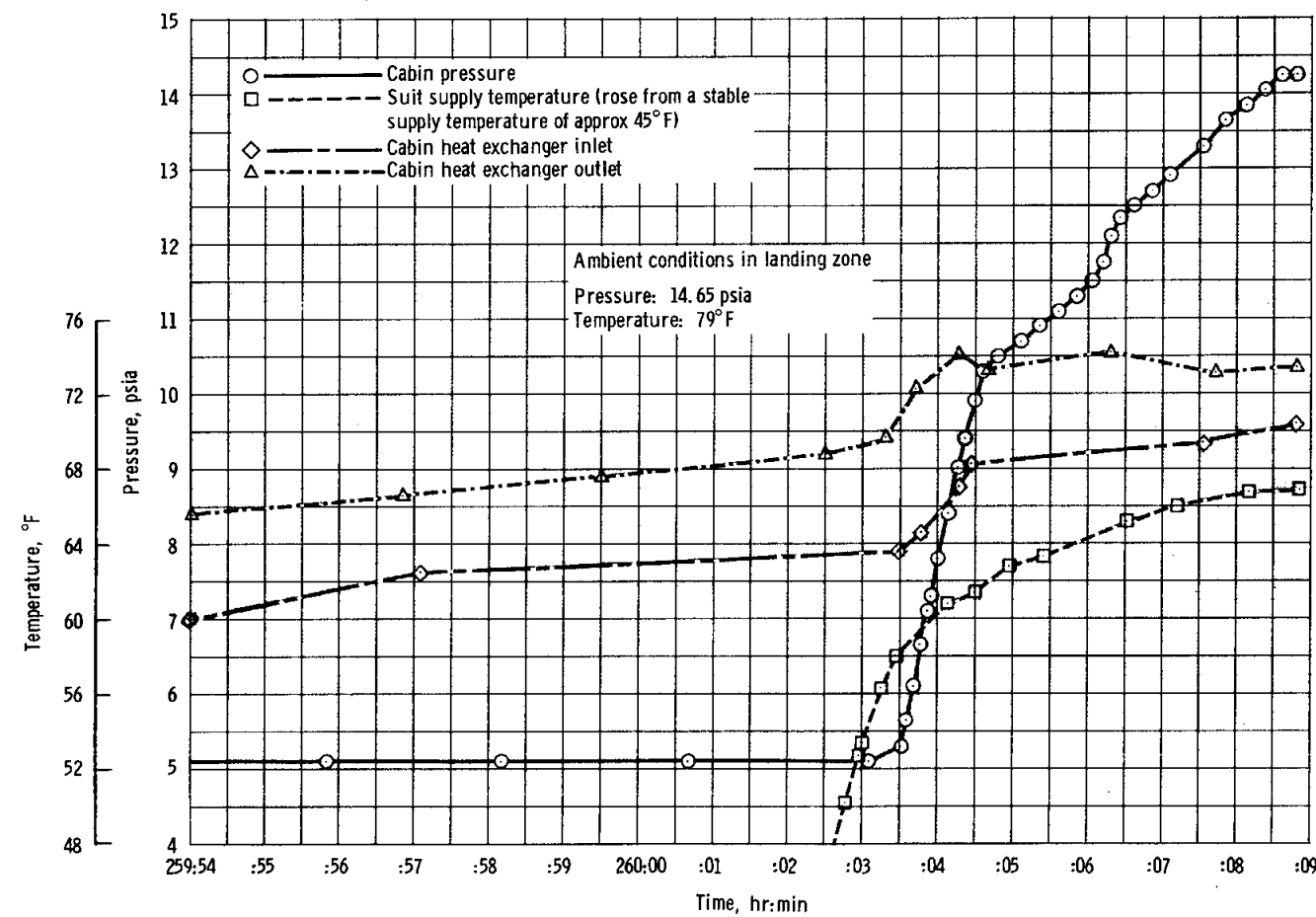


Figure 5.19-3. - Cabin pressure and temperature during entry.

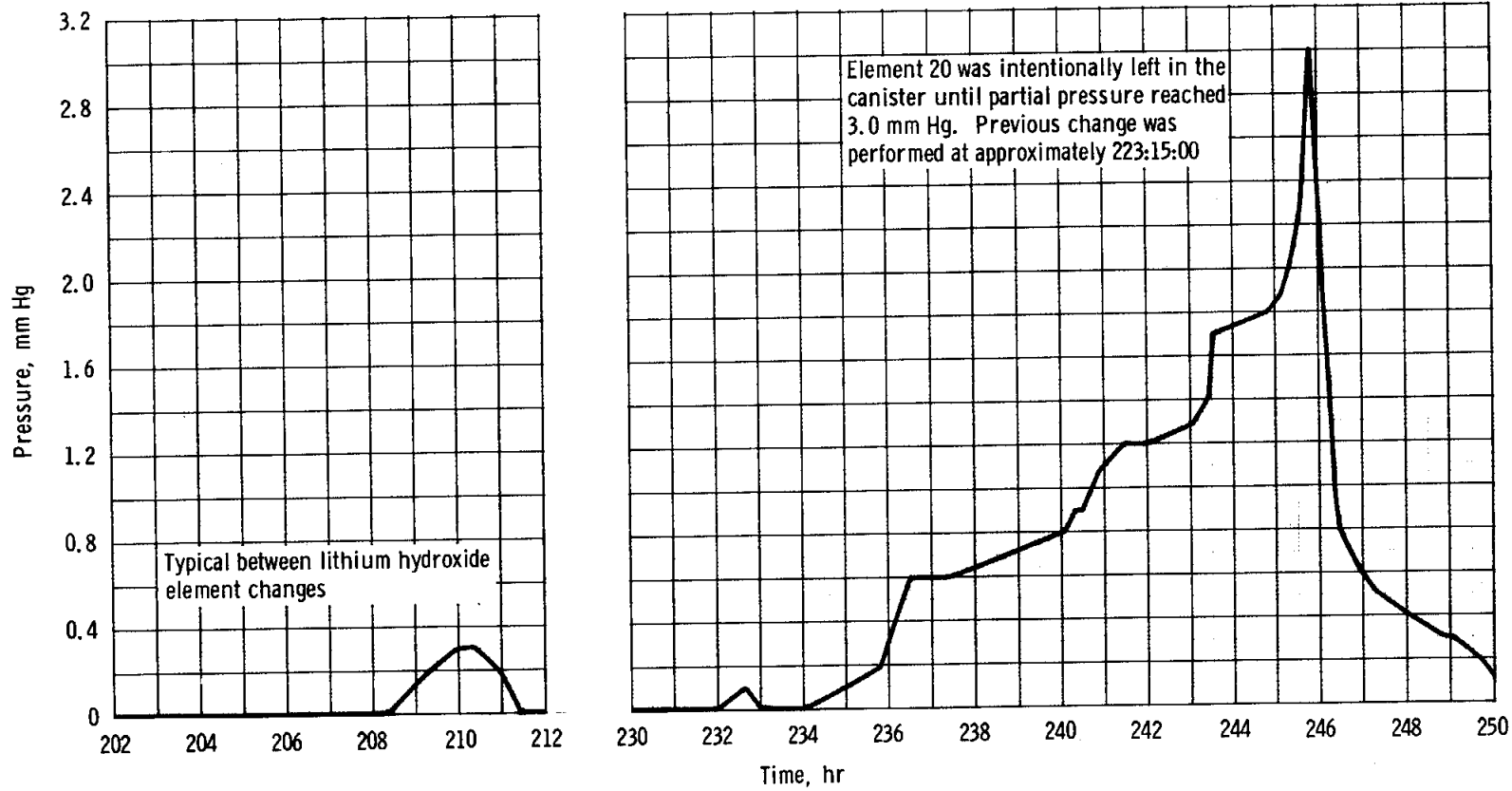


Figure 5.19-4. - Partial pressure of carbon dioxide.

NASA-S-68-6363

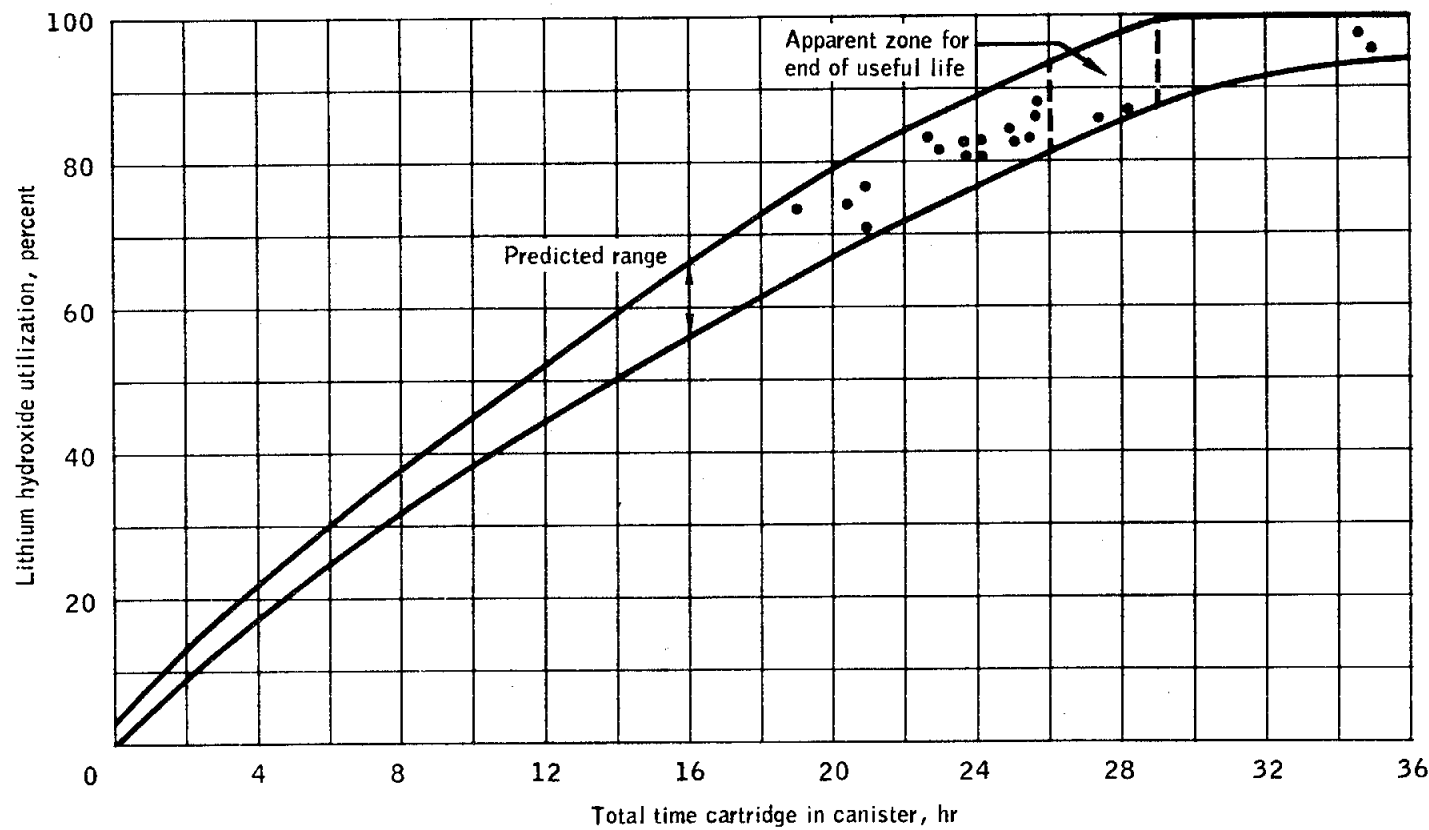


Figure 5.19-5.- Lithium hydroxide utilization.

NASA-S-68-6364

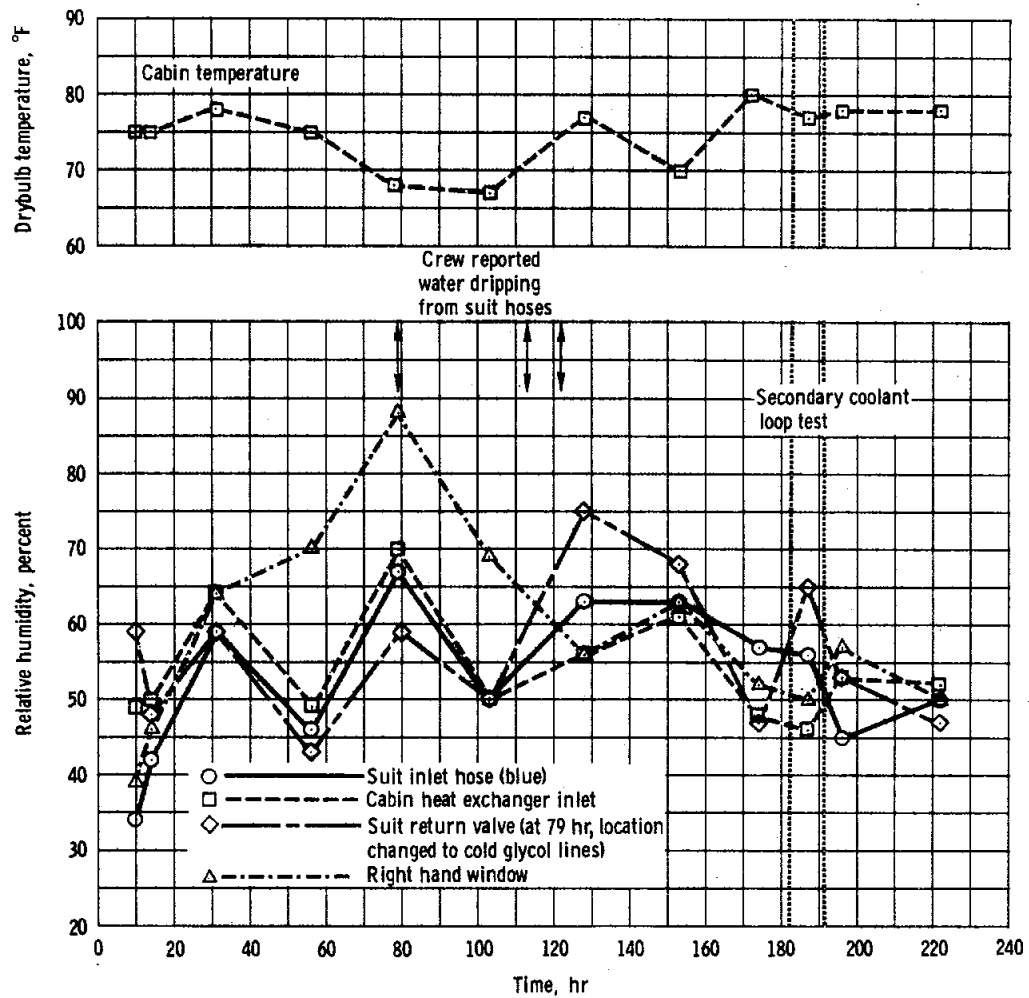


Figure 5.19-6. - Relative humidity survey.

NASA-S-68-6365

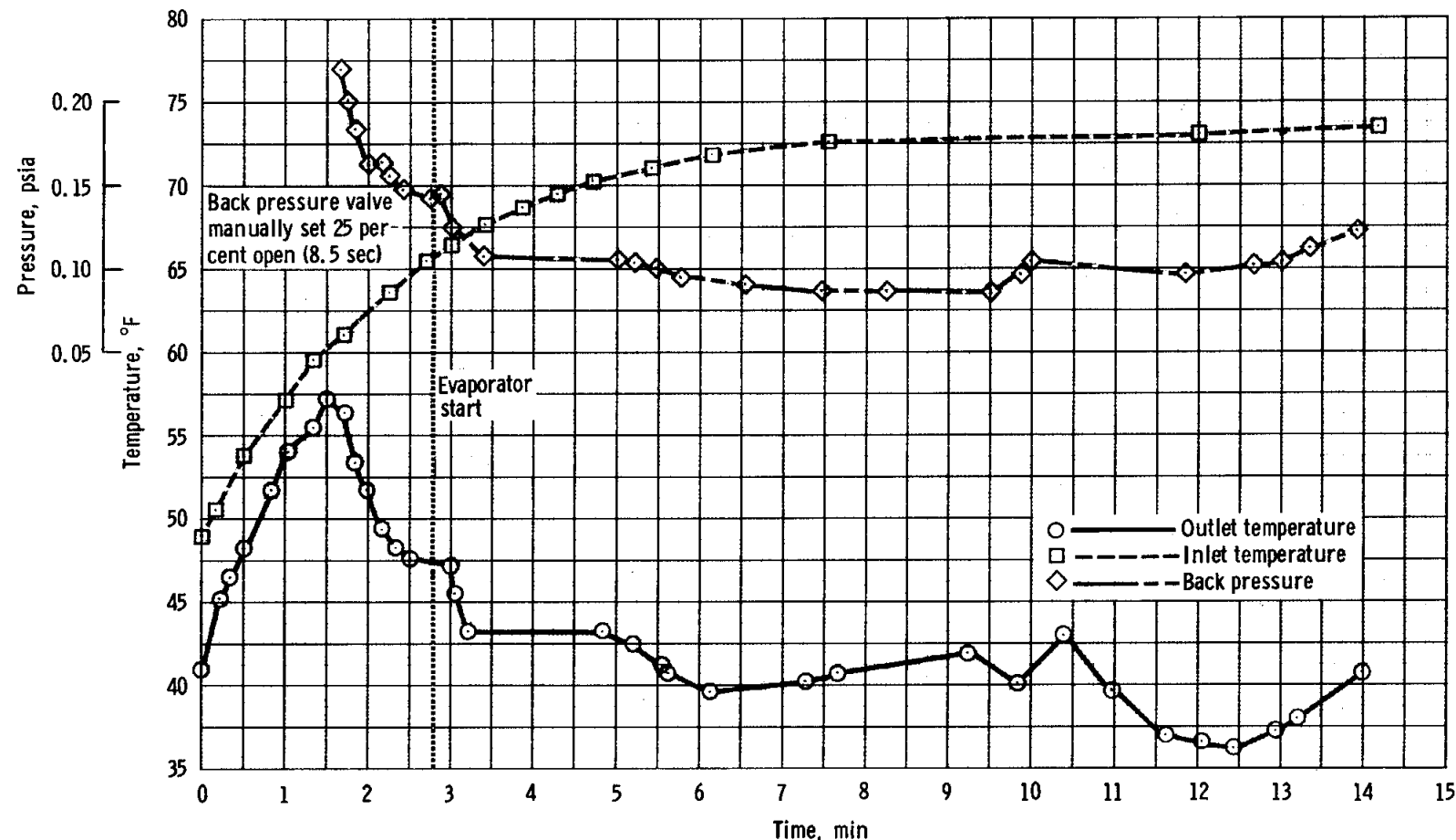


Figure 5.19-7. - Primary evaporator operation during launch.

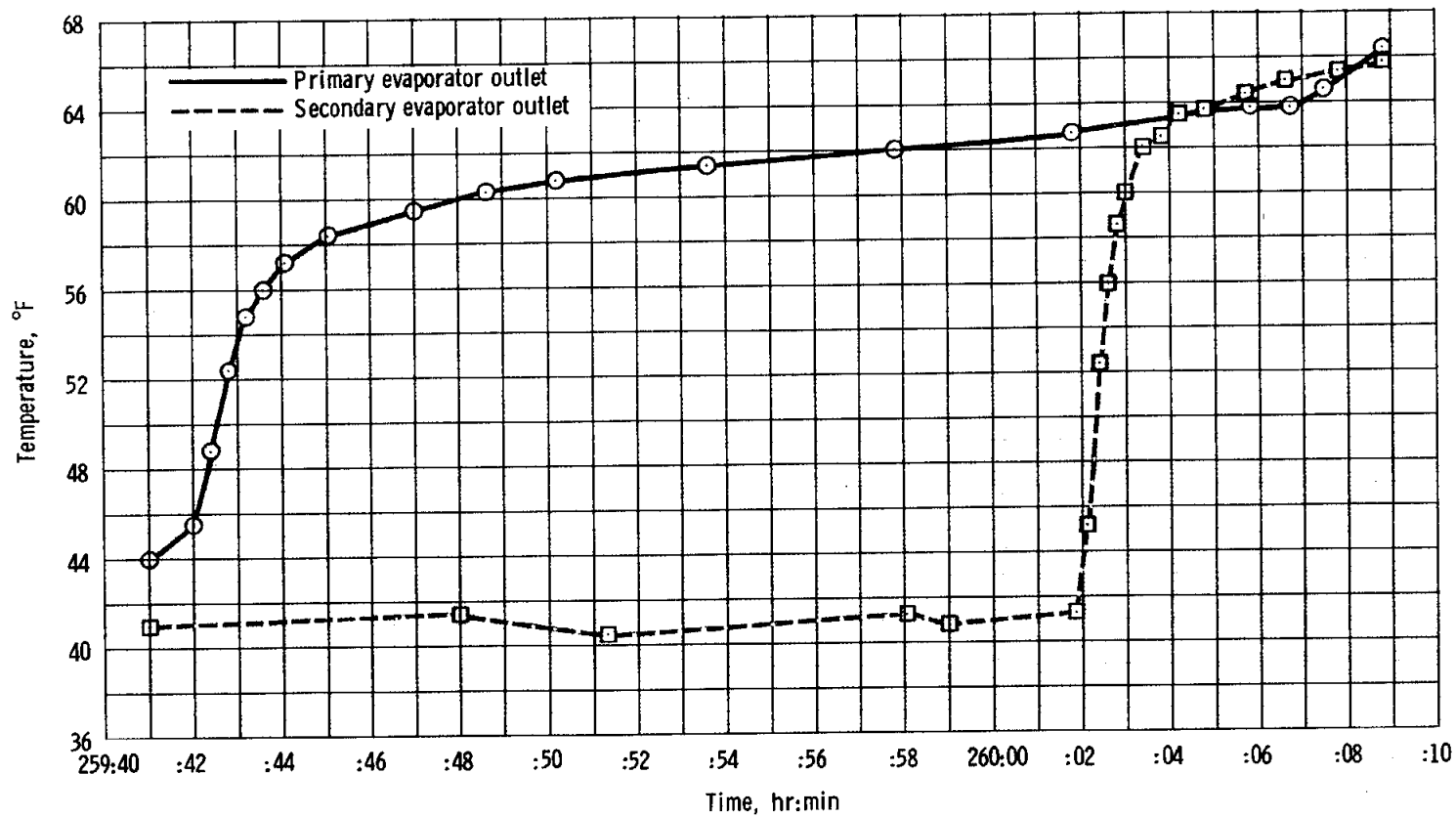


Figure 5.19-8. - Coolant loop operation during entry.

5.20 CREW STATION

This section contains an evaluation of major crew provisions, controls and displays, spacecraft windows and lighting, equipment stowage, and intravehicular activity.

5.20.1 Crew Provisions

A pressure suit was worn by each crewman during launch. The helmets and gloves were removed approximately 1 hour after launch, and the remainder of the suit was removed and stowed approximately 7-1/2 hours after launch. The performance of the pressure suits was satisfactory. The crew reported that ventilation in the suits was adequate during the orbital phase of the mission. Doffing and donning were much easier at zero-g than at one-g and created no problem for the crew. Because of the forces exerted by the crewman's communication and oxygen umbilicals, the Velcro on the boot soles and spacecraft cabin floor did not provide the optimum retention for body positioning. However, during the postflight analysis, the crew indicated body positioning caused little or no problem. The suits, without helmets and gloves, were worn during entry. Donning the suit (except for zipper closure, glove donning, and helmet installation) required approximately 2 minutes.

Postflight visual examination of the suits indicated wear areas on the shoulder turn-around ring and in the buttocks area. Suit leakage rates were not significantly different from those measured during acceptance testing prior to flight. Some of the interface areas, such as gloves and wrist rings, were binding prior to lubrication of the seals and O-rings.

The constant wear garments were satisfactory. However, the garment did not adequately restrain the biomedical belt; therefore, slack in the biomedical harness was critical. In addition, the size of the buttock port was too small to be useful. On future missions, the biomedical sensor leads will be custom-fitted to each crewman and the biomedical belt will be located vertically by crew preference. No other changes are being made to the garment.

A urine collection and transfer assembly was worn by each crewman during the suited portions of the mission, and the assemblies were satisfactory.

Intermittently throughout the flight, biomedical data were lost because the pin disconnects in the electrode biomedical harnesses repeatedly became dislodged by body movements. Both the Commander's and the Command Module Pilot's harnesses had broken wires at the signal conditioner connector; the breakage resulted from repeated flexing of the wire.

At approximately 180 hours, the dc-dc converter worn by the Command Module Pilot was overheating, and the biomedical system was subsequently removed. As a precautionary measure, the remaining two crewmen removed their biomedical systems at approximately 203 hours. Postflight evaluation of the entire biomedical/spacecraft system has shown that all components were operating properly with the exception of the broken electrode wires in the harness. (See section 11 for further discussion.)

The dual life vests, worn during the launch and entry phases, were inflated satisfactorily during the recovery operation.

The communications carriers performed satisfactorily during the mission. Only two problems were noted. The cup-type chin strap was found to be inferior to the under-the-chin type because of tenderness of the chin after beard growth. The cable from the communications carrier to the in-suit harness interferred with rotation of the head within the helmet and also pressed against the neck.

As the mission progressed, the water metering dispenser became increasingly difficult to operate, and by the ninth or tenth day, the trigger could be moved only with great effort. However, the crew were able to continue using the dispenser. The sticking trigger was caused by the metering O-ring swelling from extended exposure to the chlorine in the water. (See section 11 for details of this discrepancy.)

The dew point hygrometer was successfully used to perform eleven humidity surveys.

The Teflon inflight coverall garments were worn for most of the mission. The crew reported that the garments were comfortable.

The urine transfer system was acceptable. Each crewman developed his own technique for drying the cuffs after several uses. In addition, the cuffs developed pin-hole leaks; however, adequate spares were provided.

The two restraint bags for sleeping were located beneath the right and left couches and provided well-ventilated restraint enclosures. The foot portion of the bag, which restrained the knee area, permitted undesirable lower leg movement. For future spacecraft, the bag will be restrained by straps at the foot end.

During postflight inspection, one of the control heads on the crewman communications umbilicals had a bluish-green corrosive material at both electrical connectors of the control head and the mating half of the umbilical connector. The material was determined to be contamination and corrosion caused by salt water.

The crew reported that the emergency oxygen mask assemblies were satisfactory. During postflight testing, one of the masks was pressurized to 138 psi (normal operating pressure is 100 ± 10 psi) for approximately 6 minutes. A blister formed in the outer silicone layer, which subsequently split resulting in slight external leakage. This type failure has previously occurred in silicone rubber hose assemblies as a result of slight leakage around the end fitting nipple. For future missions, the silicone rubber hose will be replaced with hose more resistant to such a failure.

5.20.2 Displays and Controls

Based on crew reports, the displays and controls were satisfactory. Meters and dials were easily readable, even during periods of acceleration and vibration. After the fifth service propulsion maneuver, the crew noted a crack in the glass window of the mission elapsed timer on panel 2.

5.20.3 Windows

The visibility through the spacecraft windows ranged from good to poor. After the launch escape system was jettisoned, a residue was reported on the rendezvous windows, but this caused no appreciable degradation of visibility. As the mission progressed, deposits began to form on the interior surface of the outer pane of all windows. A postflight analysis identified this deposit as polymethyl silicates resulting from condensation of gases from the window sealant compound. The deposits progressed until the hatch window was almost unusable and the visibility through the side windows was seriously degraded. The rendezvous windows were least affected by these deposits. All windows were ineffective at certain sun angles. (See section 11 for details of this discrepancy).

The crew reported that the markings on the rendezvous window were good, but that the lines on the hatch window were too thick.

5.20.4 Lighting

Spacecraft interior lighting was satisfactory. Although the primary elements of both floodlights in the lower equipment bay failed, the secondary elements provided adequate lighting. See section 11 for further details on this failure. The electro-luminescent lighting for the optics switches on panel 122 also failed. Flashlights were used when work was required in dimly lit areas. The crew reported that the alpha-numeric

indications of the display keyboard, the delta-V counter, and the mission timer on the main display console were often unreadable because of sun glare.

At 215:59:00, the interior lights were dimmed to check the visibility of the exterior lights. When the display/keyboard lights were brightened, a program alarm from the computer was observed. The alarm was reset and the problem did not recur.

5.20.5 Equipment Stowage

Stowage of crew equipment within the command module was considered good. The Velcro provided in the cabin and on the loose equipment was adequate for inflight retention. A minor stowage deficiency was noted during the flight. Rubber retaining pads provided for the sequence camera bracket were not adequate. The cabin analyzer tended to float from the compartment each time the lid was opened since no retention was provided for its inflight stowage location.

5.20.6 Intravehicular Activity

Certain anticipated problems proved to be nonexistent, making many of the intravehicular provisions unnecessary. All areas of the cabin were readily accessible, and work could be performed without the use of restraints. The handholds, other than at the guidance-system station, were of no use. The hand controllers were reported to be susceptible to inadvertent activation during intravehicular activity.

5.21 CONSUMABLES

The usage of all liquid consumables, including cryogenics, is summarized in this section. Electrical power, often considered to be a consumable, is discussed in section 5.8.

5.21.1 Service Propulsion System Propellants

The total service propulsion system propellant loadings and consumption values are given. The loadings were calculated from gaging system readings and measured densities prior to lift-off.

	<u>Fuel, lb</u>	<u>Oxidizer, lb</u>
<u>Loaded</u>		
In tanks	3632.0	5903.0
In lines	<u>78.6</u>	<u>123.7</u>
	3710.6	6026.7
<u>Consumed</u>	2998.7	4812.4
<u>Remaining at separation</u>	711.9	1214.3

5.21.2 Reaction Control System Propellants

Service module.- The propellant utilization and loading data for the service module reaction control system are presented. Consumption was calculated from telemetered helium bottle pressure histories using the relationships between pressures, volume, and temperature.

	<u>Fuel, lb</u>	<u>Oxidizer, lb</u>
<u>Loaded</u>		
Quad A	111.3	223.7
Quad B	110.6	223.7
Quad C	110.8	225.9
Quad D	<u>110.6</u>	<u>225.1</u>
	443.3	898.4
<u>Consumed</u>	943.8	
<u>Remaining at separation</u>	397.9	

Command module.- The propellant loading and utilization data for the command module reaction control system are tabulated. Consumption was calculated from pressure, volume, and temperature relationships.

	<u>Fuel, lb</u>	<u>Oxidizer, lb</u>
<u>Loaded</u>		
System A	44.4	87.6
System B	<u>44.4</u>	<u>87.5</u>
	88.8	175.1
<u>Consumed</u>		
System A	10.2	18.3
System B	<u>7.4</u>	<u>13.2</u>
	17.6	31.5
<u>Remaining at landing</u>		
System A	34.2	69.3
System B	<u>34.0</u>	<u>74.3</u>
	68.2	143.6

5.21.3 Cryogenics

The cryogenic hydrogen and oxygen quantities loaded and consumed are given in the following table.

	<u>Hydrogen, lb</u>	<u>Oxygen, lb</u>
<u>Loaded</u>		
Tank 1	26.2	318.4
Tank 2	<u>25.7</u>	<u>317.1</u>
	51.9	635.5
<u>Consumed</u>		
Tank 1	22.7	227.9
Tank 2	<u>22.0</u>	<u>226.3</u>
	44.7	454.2

5.21.4 Water

The water quantities loaded, consumed, produced, and expelled during the mission are summarized in the following table.

	<u>Water, lb</u>
<u>Loaded</u>	
Potable water tank	21
Waste water tank	40
<u>Produced inflight</u>	
Fuel cells	394
LiOH	59
<u>Dumped overboard</u>	359
<u>Evaporated</u>	77
<u>Remaining postflight</u>	
Potable water tank	37
Waste water tank	30

6.0 FLIGHT CREW

6.1 FLIGHT CREW PERFORMANCE

The Apollo 7 flight crew members were: Commander, W. Schirra; Command Module Pilot, D. Eisele; and Lunar Module Pilot, W. Cunningham. This section presents a training summary, discusses crew activities in accomplishing the flight plan, evaluates human factors briefly, and discusses major operational equipment use.

6.1.1 Training

The Apollo 7 crew completed their training program essentially as planned and were well prepared for the mission. The effectiveness of the overall crew training is indicated by the satisfactory flight crew performance during the mission and by flight crew comments during the postflight debriefing. Crew performance during network simulations (phase III) was excellent.

6.1.2 Flight Activities

A summary flight plan of the mission activities is presented in figure 6-1, and a description of the mission is given in section 2. The only significant alteration to the flight plan was the rescheduling of the third service propulsion maneuver from approximately 91-1/2 to 75-1/2 hours. This maneuver was performed earlier than scheduled so that the orbit would be lowered to a 90 n. mi. perigee, thereby improving the backup deorbit capability using the service module reaction control system. This change had been agreed to prior to flight, but its implementation was deferred to a real-time decision. The rescheduling of the third service propulsion maneuver caused other changes in the sequence of the planned activities and system tests.

Crew performance was satisfactory throughout the mission, even though all three crewmen had minor colds and head congestion. All assigned detailed test objectives were achieved. Toward the end of the mission, several new test objectives were added (see section 10).

Powered flight.- The crew monitored launch-vehicle performance during the powered flight phase and reported that all required events occurred as scheduled. The crew did not receive the Mode IV voice call due to a

communications difficulty at that time. The lack of this transmission could have presented a problem in the event of an onboard computer malfunction. The S-IVB manual control takeover following orbital insertion was successfully performed. The Commander reported that the exercise was easier to perform in flight than during simulations.

Rendezvous operations.- Rendezvous and station keeping were successfully accomplished. The rendezvous activities began at approximately 22 hours with preparation for the first service propulsion maneuver. During the night period about three revolutions before this first maneuver, the inertial measurement unit was fine-aligned in the nominal mode corresponding to the planned conditions at terminal phase initiation (TPI). The maneuver was initiated at 26:24:56, with the velocity residuals reduced to negligible values using the service module reaction control system. The first service propulsion maneuver was so precise that a second maneuver was unnecessary. During this period, the rendezvous navigation computer program was exercised, with the Command Module Pilot using the sextant to track the S-IVB. During this period, the S-IVB was visible in reflected sunlight. Auto-optics tracking was performed, but no navigation marks had been incorporated into the state vector.

The circularization maneuver for the rendezvous was accomplished at 28:00:54 using the service propulsion engine; the residuals were reduced to 0.1 ft/sec. After this maneuver, the S-IVB was tracked using the auto-optics pointing feature of the sextant. The target was reported to have been visible in reflected light in the sextant but not in the scanning telescope. The terminal phase initiation program was then activated and a preliminary maneuver was computed. The crew determined that the computation required 4 to 5 minutes, as compared with about 3 minutes during training in the simulator. The final onboard solution was obtained at 14 minutes prior to maneuver initiation to allow for the computation delay. The onboard computation compared favorably with the ground-computed solution, and the onboard value was executed with the plus-X reaction-control thrusters. The spacecraft was automatically oriented to the maneuver attitude, resulting in a final attitude approximately 10 degrees out of the orbit plane in yaw. The crew believed that this value was excessive and reduced the yaw angle by about one-half before executing terminal phase initiation.

Following this maneuver, the computer was used to acquire the target in the sextant so that the state vector could be updated in preparation for the first midcourse correction. The crew reported that in the dark period at terminal phase initiation the flashing lights on the S-IVB were not visible in either the telescope or front window until the range had decreased to less than 15 miles. At that point, the S-IVB image in

the telescope could be resolved as four discrete spots of light. Because the target was tumbling, the center could not be consistently identified. However, the displayed range and velocity changes were small; therefore, the navigation updates were accepted as valid. After the first midcourse maneuver, the polar plot indicated a near nominal approach trajectory, and no second midcourse was required.

Sunrise occurred during the rendezvous when the S-IVB was 2 to 3 miles from the spacecraft, and the Commander was able to estimate the range using the S-IVB diameter subtended angle in the crewman optical alignment sight. Very little thrusting was required to control the in-plane line-of-sight rate, but some thrust was required in the yaw direction to control the out-of-plane drift. The rendezvous was completed within the propellant budget at the nominal time of approximately 30 hours. After the rendezvous, the crew easily maneuvered the spacecraft around the S-IVB in order to inspect and photograph the vehicle.

The subsequent orbital operations were performed as noted in figure 6-1.

Entry.- Crew comments regarding deorbit preparation indicate that the flight plan allowed adequate time, and all activities were successfully accomplished. The deorbit maneuver and subsequent events were normal and performed as planned.

Landing and recovery.- Spacecraft landing loads were reported as light with a rotation to the stable II (apex down) flotation attitude immediately after touchdown. The crew believed that the parachutes were instrumental in pulling the spacecraft over to the stable II attitude. Although the parachutes were released as soon as possible, by that time the command module was oriented with the X-axis horizontal. The Lunar Module Pilot turned off the VHF transceiver and beacon as soon as it was determined that the spacecraft would remain in the stable II position. At this point, the crew began a 8-minute cooling period before activating the uprigthing system. During this period, the crew could determine a drift rate by observing the parachutes sinking below the command module. They also noticed that water was entering the area between the outer glass panes in the windows and that the undeployed dye marker had been normally activated through sea-water contact.

The Command Module Pilot released his restraints and went into the lower equipment bay to open the pyrotechnic circuit breakers. Eight minutes after landing, the Commander activated the compressors which inflate the uprigthing bags, and a rotation to normal flotation attitude was accomplished in about 4 1/2 minutes. The compressors were left on for an additional 2 minutes after uprigthing. As a result, the Commander did

not hear the Lunar Module Pilot advise him to turn on the postlanding vent switch. After the uprighting, the Lunar Module Pilot turned on the recovery beacon and VHF transceiver A. The crew then removed their space suits and put on their constant wear garments. The postlanding vent switch was turned on, and just prior to egress, the battery circuit breakers were opened to power down the command module. Helicopter pickup of the crew was nominal.

6.1.3 Human Factors

The crew station was adequately configured for this mission and presented no compromise to crew performance of their required duties. The crew encountered no difficulties in moving about the cabin and no obstructions to motion. The crew did report that the hand controllers were somewhat susceptible to inadvertent actuation during intravehicular motion and that some improvement in the sleeping-bag restraints and shielding of some main display panel instruments from sun glare would be helpful. Additional discussion of crew-station effectiveness, major crew provisions, and certain operational equipment is presented in section 5.20.

6.1.4 Operational Equipment Evaluation

After the third day of the mission, the 70-mm camera malfunctioned because of a bent interlock blade, which prevents photography with the dark slide in the magazine. This metal blade protrudes from the camera housing to sense the dark slide only during shutter activation and then slides back into the housing. The Commander returned the blade to the original position, and the camera operated satisfactorily thereafter.

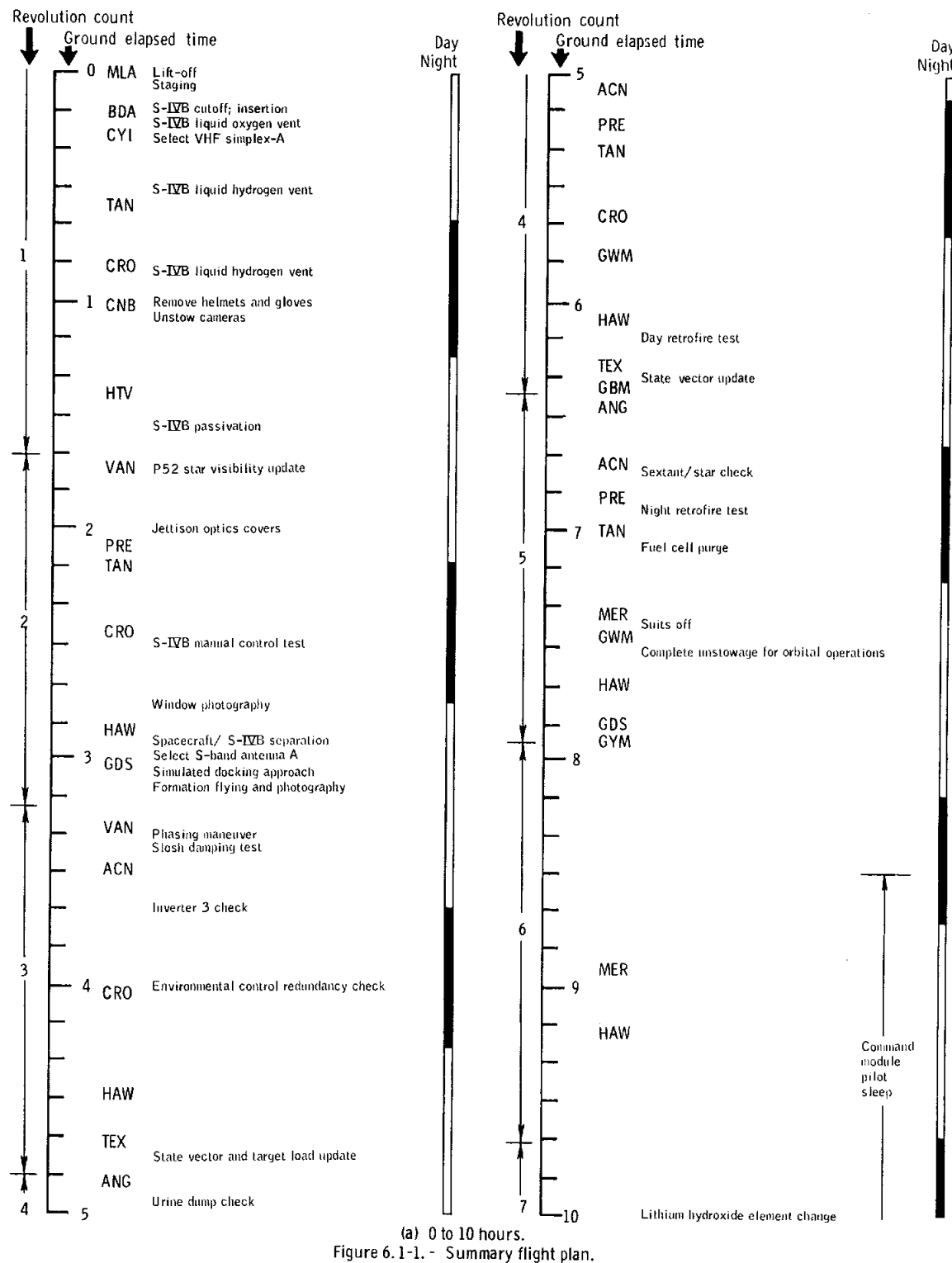
The type of 70-mm film magazines used on this mission were of the same type as those used in the last Gemini flights and could be put on an uncocked camera. This occurred during the Apollo 7 flight with the resultant loss of the first exposure after magazine assembly. The magazines also had no positive indication of end of film, and the crew took several exposures after the film was depleted. Several more exposures were lost when photography was attempted with the dark slide still in the magazines. The configuration of these magazines was such that, when inserting the dark slide, it hit a detent or hard spot at about the last 1/8-inch of travel. This detent was assumed by the crew to have indicated full travel, which is required to activate the shutter interlock.

The glareshield and eyeglasses used during rendezvous and during alignment with the crew optical alignment sight, proved very helpful in reducing glare for out-the-window activity.

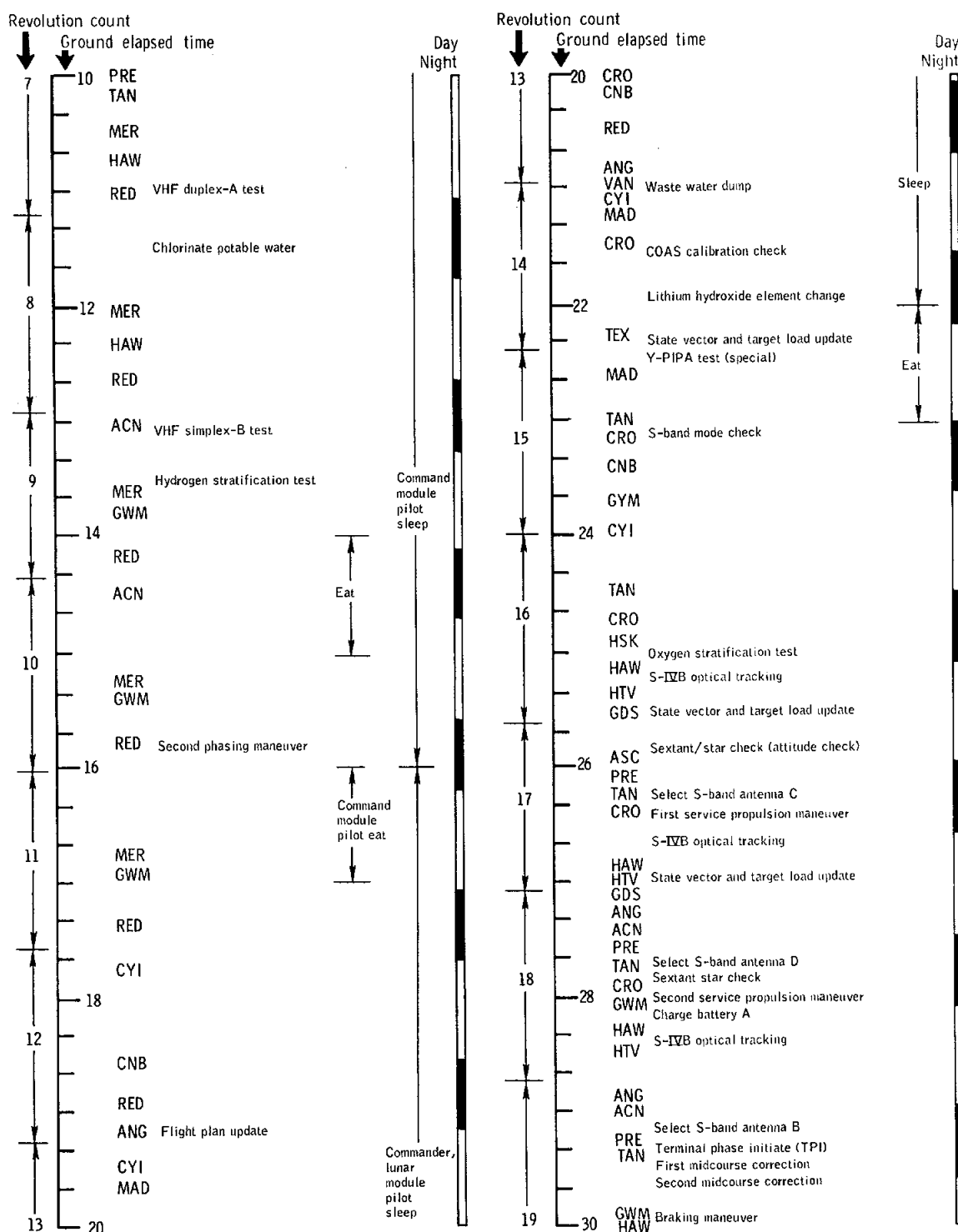
The lightweight headsets were worn as necksets by the crew. These units were placed so that the microphone electronics were below the throat, with the boom positioned in front of the mouth. A minor failure occurred when the eartube adapter separated from one headset, resulting in loss of communication to the crewman involved.

All other operational equipment performed satisfactorily.

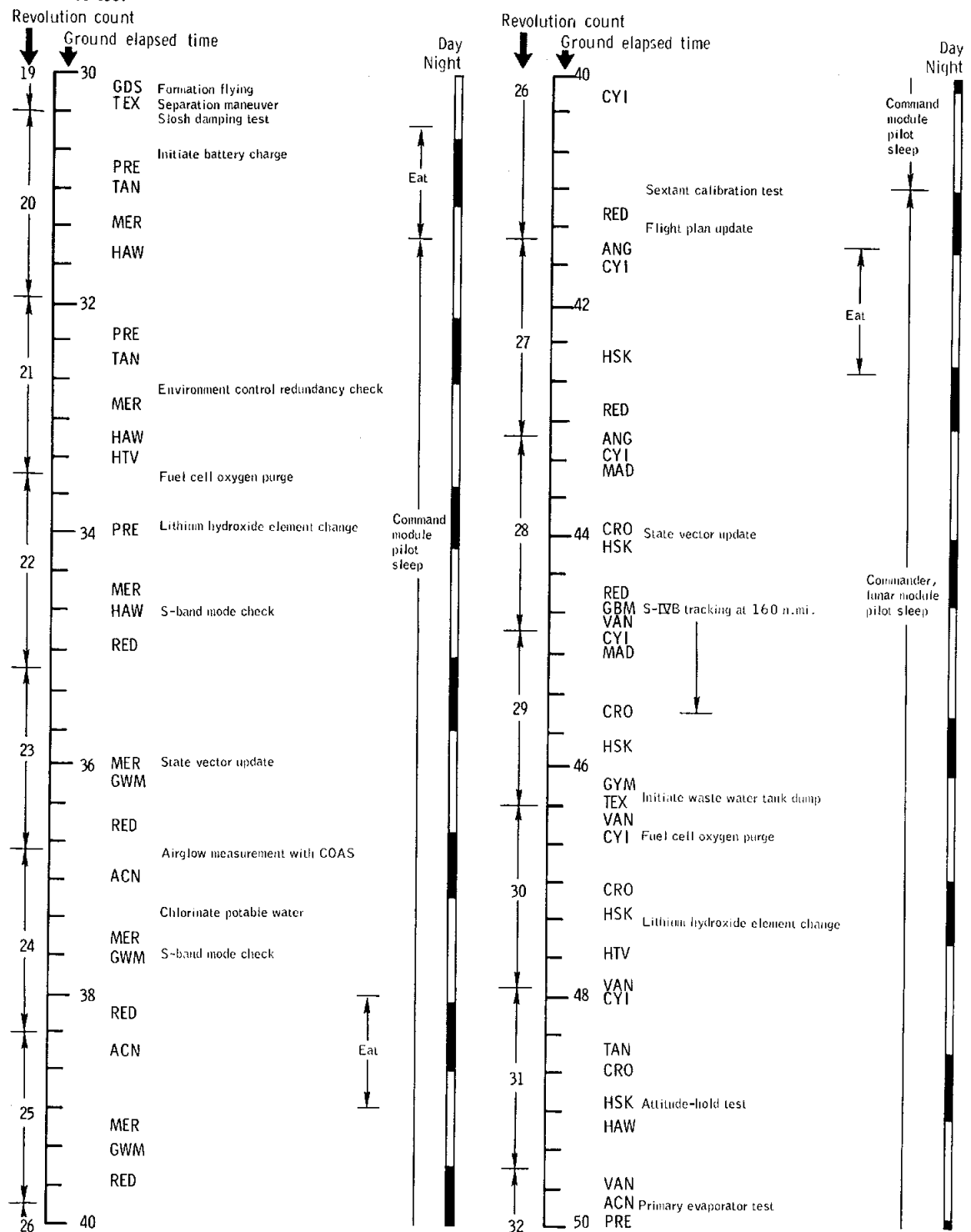
NASA-S-68-6367

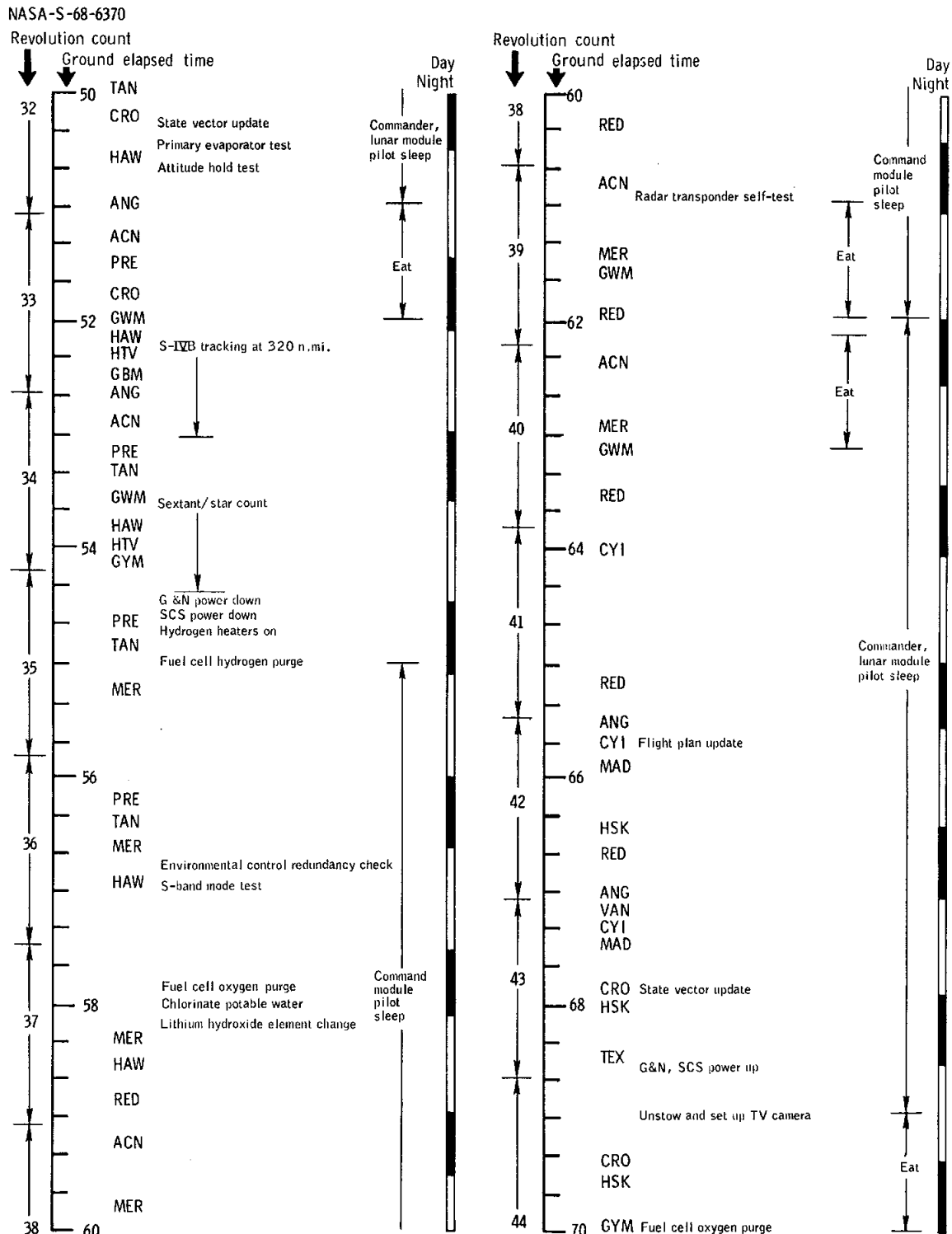


NASA-S-68-6368

(b) 10 to 30 hours.
Figure 6.1-1. - Continued.

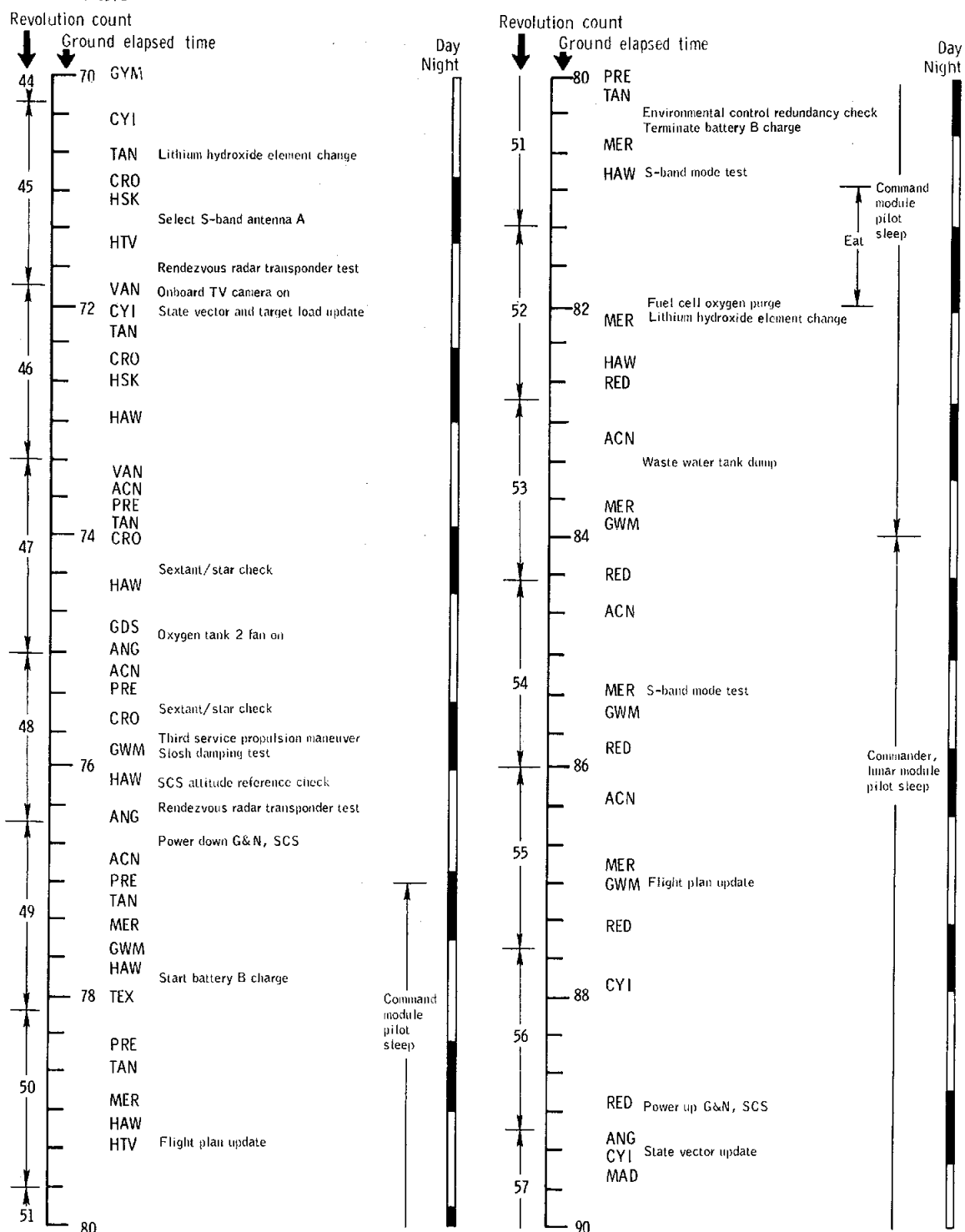
NASA-S-68-6369

(c) 30 to 50 hours.
Figure 6.1-1. - Continued.



(d) 50 to 70 hours.
Figure 6.1-1. - Continued.

NASA-S-68-6371

(e) 70 to 90 hours.
Figure 6.1-1. - Continued

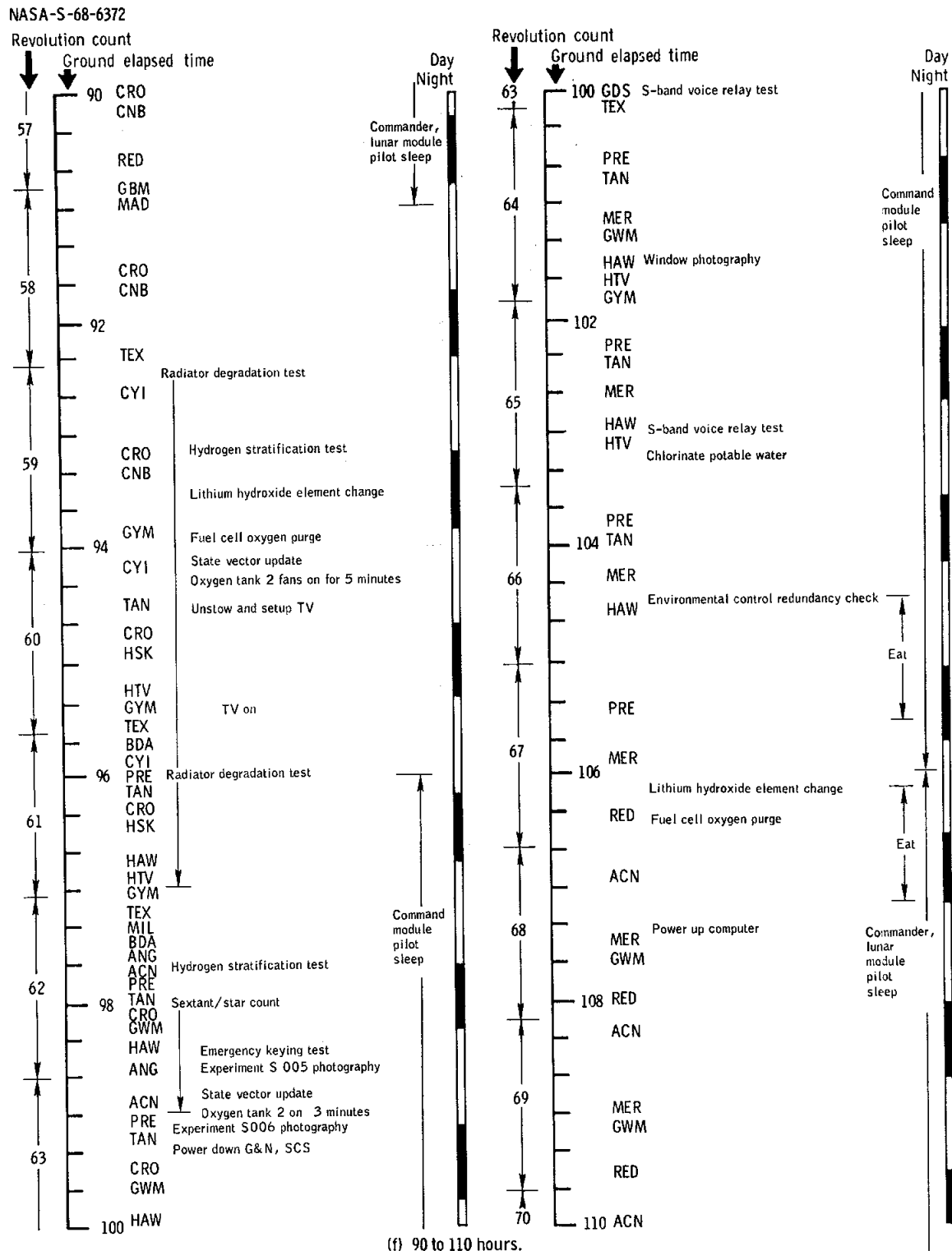


Figure 6.1-1.- Continued.

NASA-S-68-6373

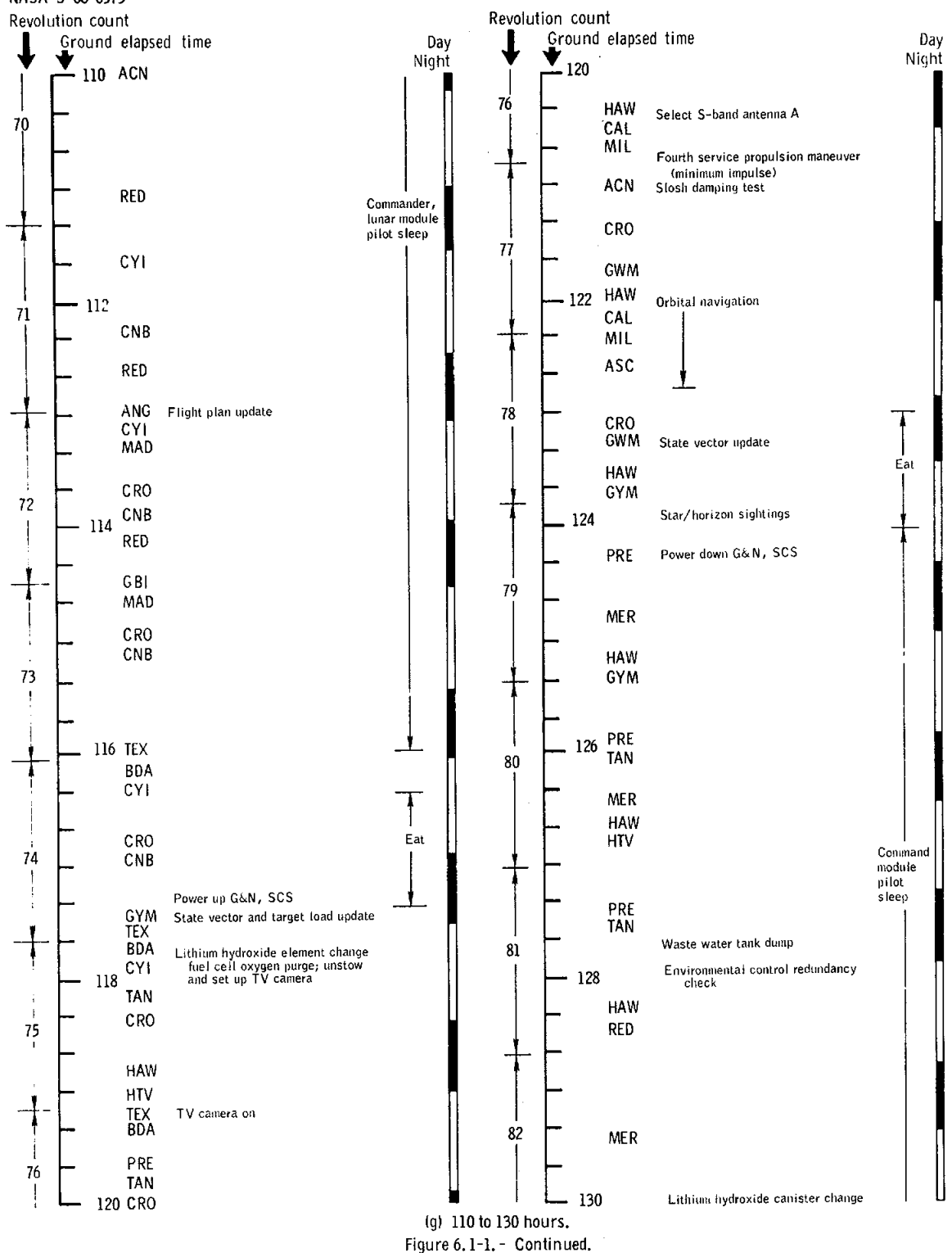
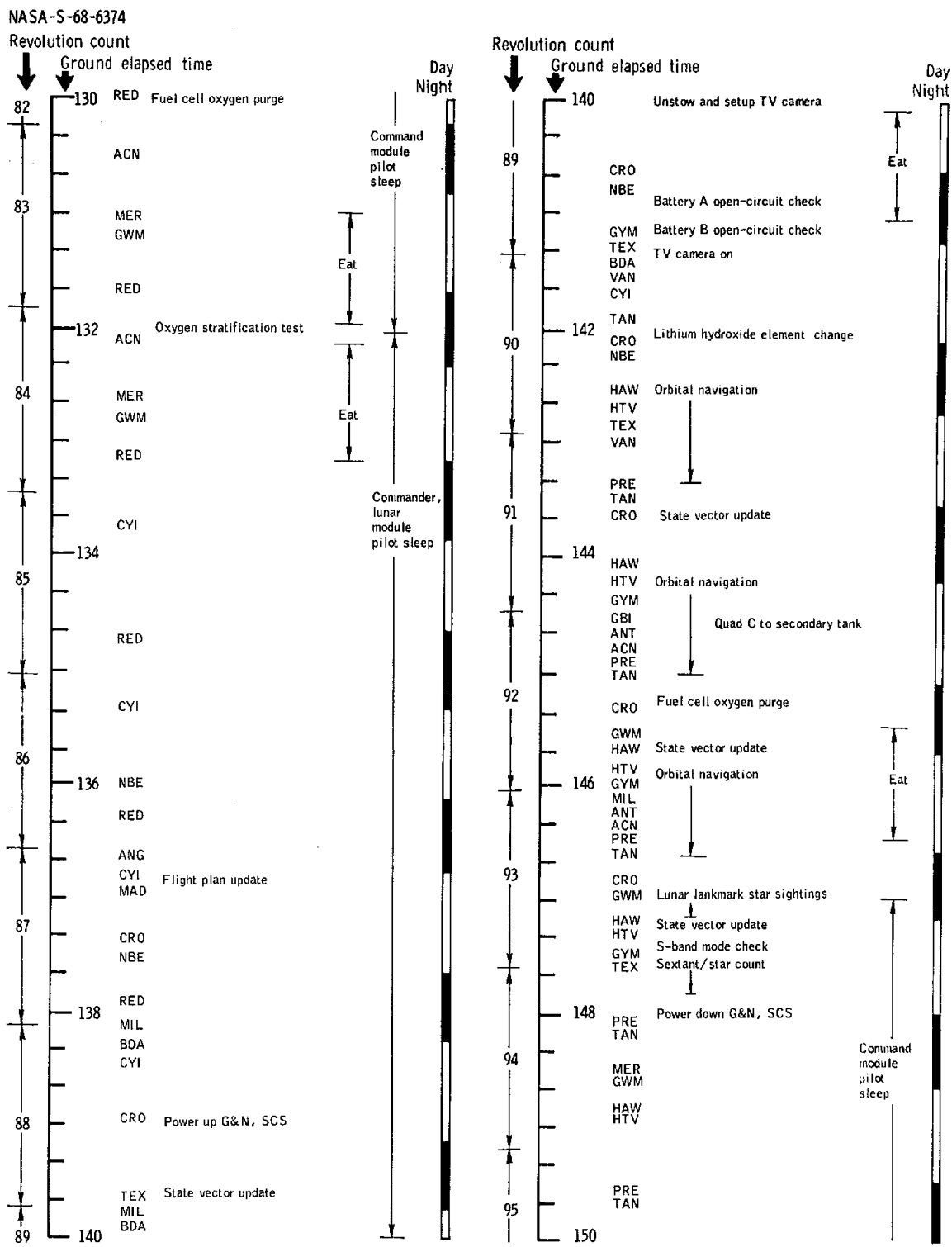
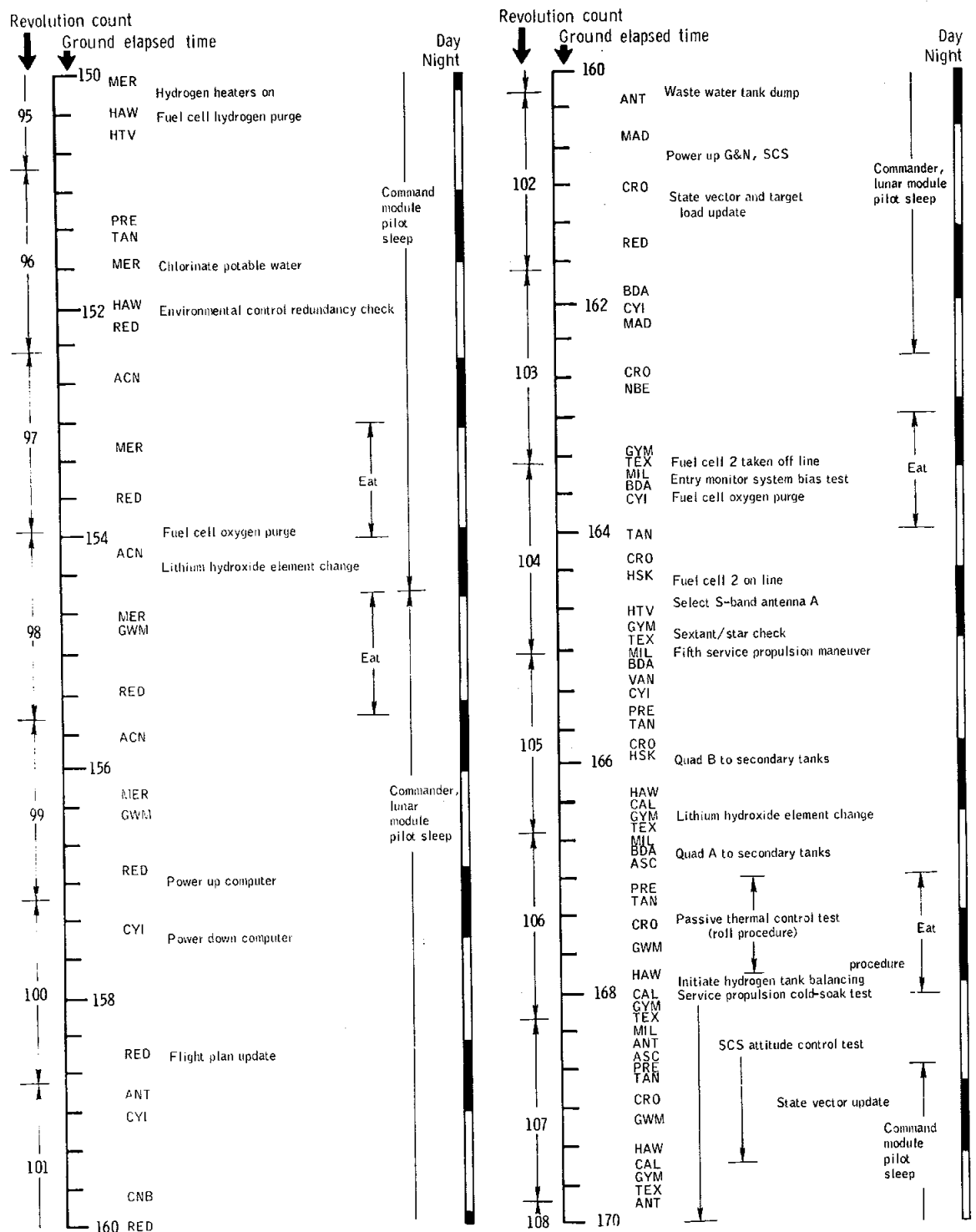


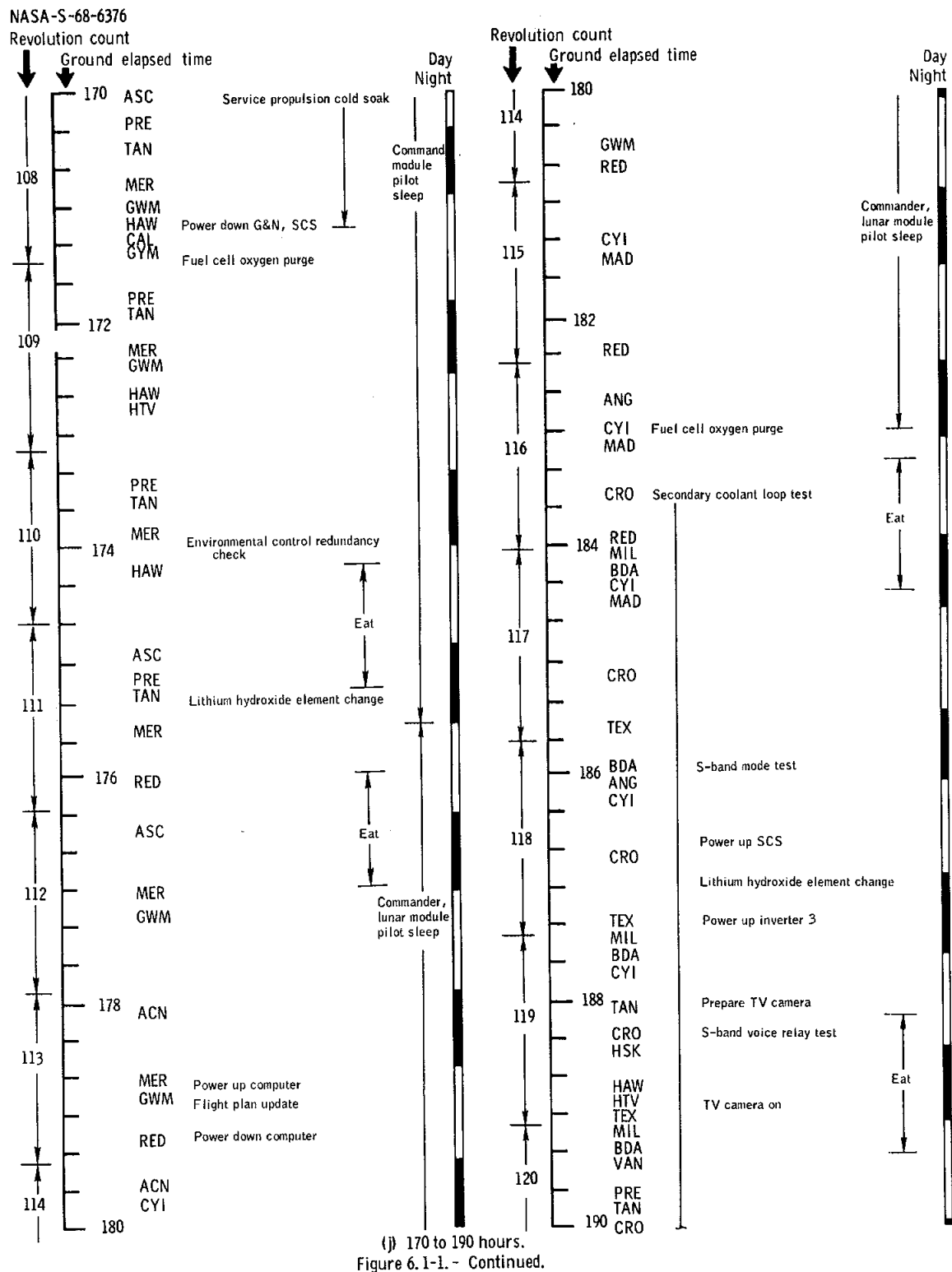
Figure 6.1-1. - Continued.



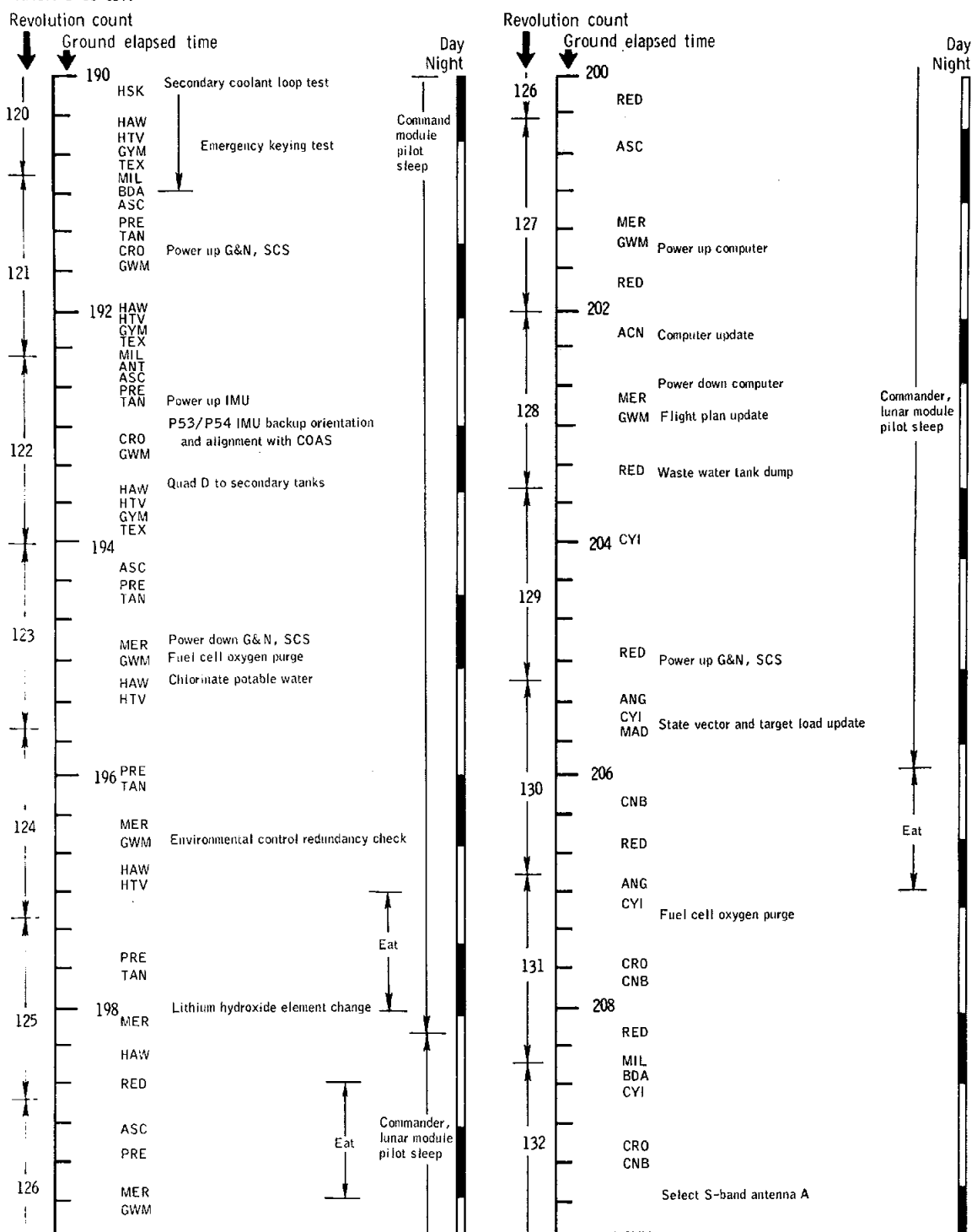
(h) 130 to 150 hours.
Figure 6.1-1. - Continued.

NASA-S-68-6375

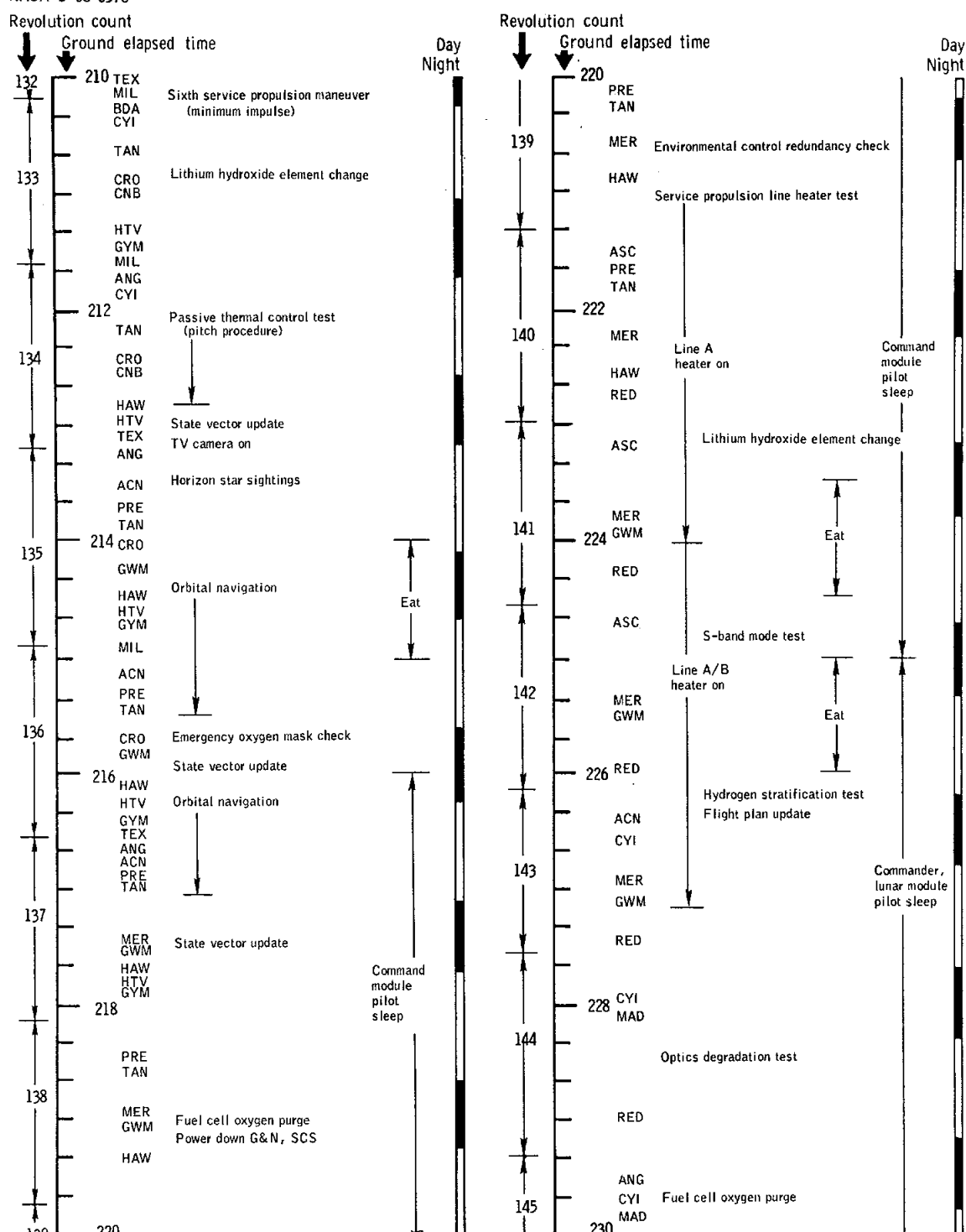
(i) 150 to 170 hours.
Figure 6.1-1. - Continued.



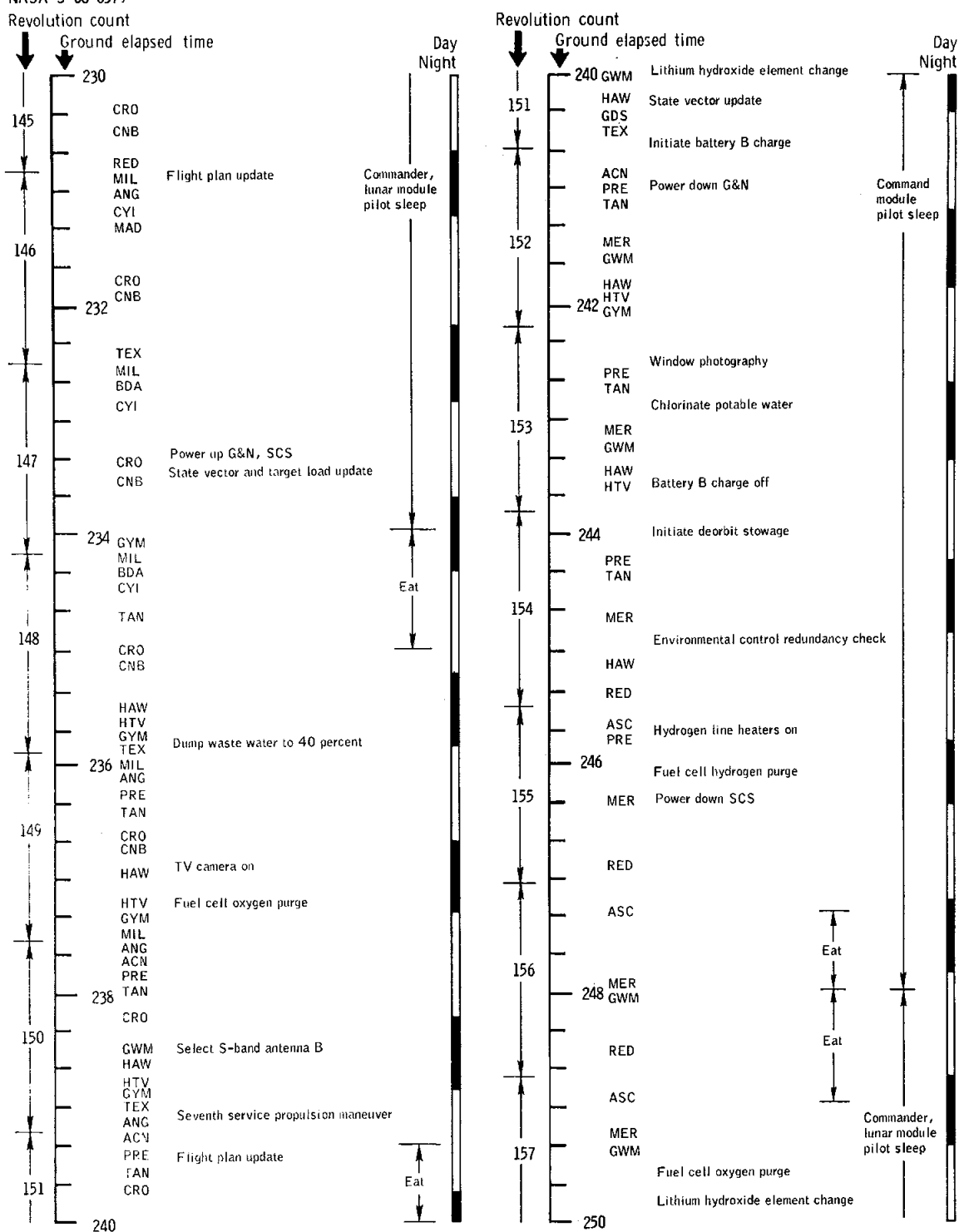
NASA-S-68-6377

(k) 190 to 210 hours.
Figure 6.1-1. - Continued.

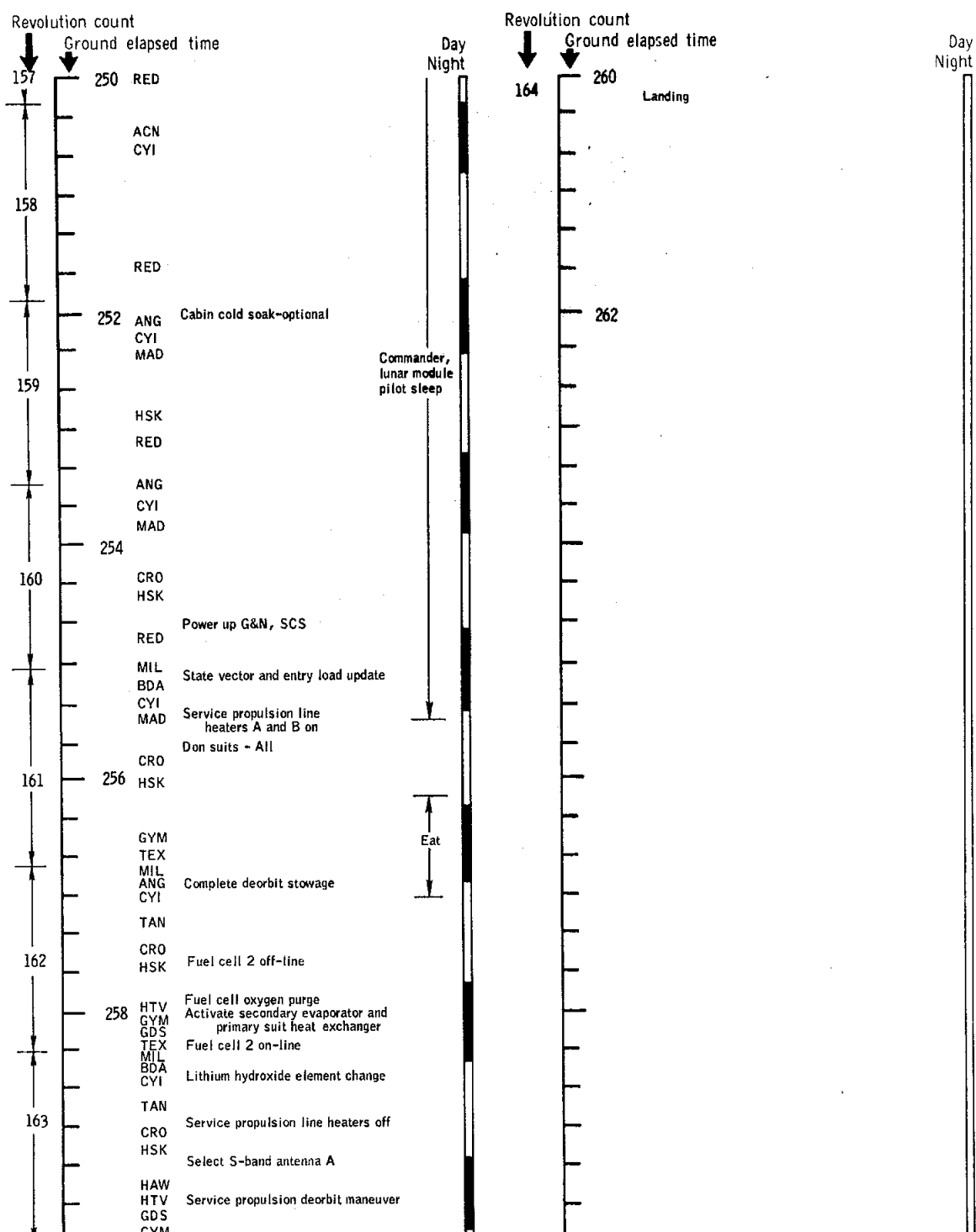
NASA-S-68-6378

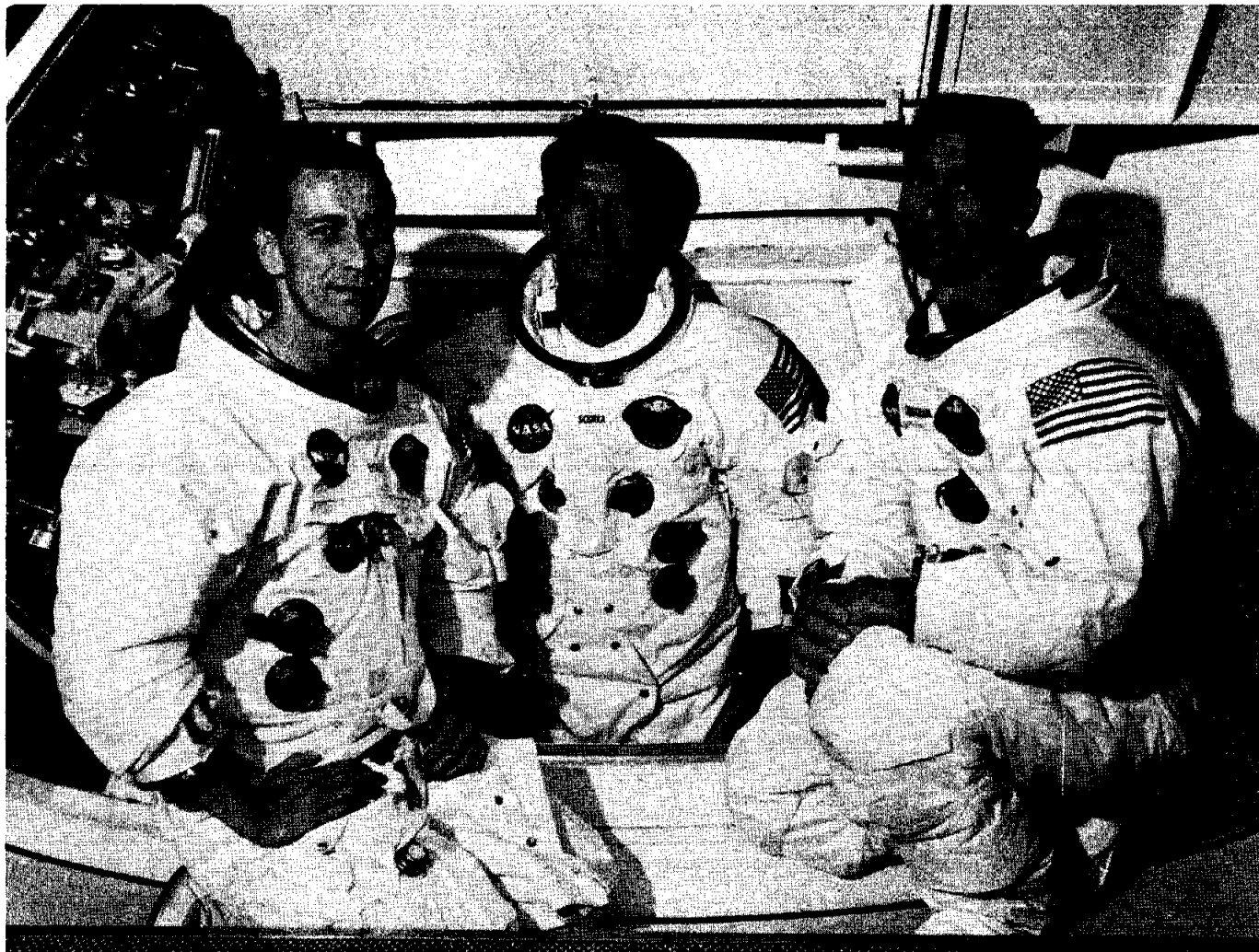
(II) 210 to 230 hours.
Figure 6.1-1. - Continued.

NASA-S-68-6379

(m) 230 to 250 hours.
Figure 6.1-1. - Continued.

NASA-S-68-6380

(n) 250 to 262 hours.
Figure 6.1-1. - Concluded.



Apollo 7 flight crew
Command Module Pilot D. Eisele, Commander W. Schirra, Lunar Module Pilot W. Cunningham.

6.2 FLIGHT CREW REPORT

The flight of Apollo 7 was the culmination of more than 3 years of intensive work by the flight crew. It was also proof that the design concepts of the command and service module system were, in fact, sound. The crew's confidence in this system was very high, but this confidence had not been achieved by casual or recent observation. A tremendous amount of time had been devoted to testing, to checkout, to simulation, to studying, to reviewing, to meetings, all to accumulate confidence in each area of concern.

6.2.1 Mission Description

Powered flight was uneventful; the launch vehicle (the S-IB and the S-IVB) performed in an excellent manner. At orbital insertion, the spacecraft remained attached to the S-IVB, which maintained orbital attitude, or local vertical, with the flight crew in a heads-down position. Separation was conducted at the appropriate time, and transposition was followed by the simulated docking exercise. Even though the total mass of the spacecraft was much less than will be experienced on some subsequent missions, the great mass was still most noticeable during the docking exercise when the spacecraft was being positioned in relation to the target adapter. One of the adapter panels had deployed and then retracted, thereby decreasing the volume for maneuvering. The spacecraft performed very well. No thruster problems were noted either in attitude or in translation throughout the flight.

Rendezvous with the S-IVB was commenced with a phasing maneuver at the completion of station keeping. It would have been more comforting if the terminal phase maneuver had been done in line of sight, but all solutions were accurate and procedures normal. The suggested out-of-plane correction was believed to be somewhat high, so only half that amount was introduced. Subsequent solutions justified this conservatism. The braking maneuver was very discomforting because there was no reliable backup ranging information available to compare with computer solutions. Judging S-IVB diameter and interpreting optical variations in the alignment scope were very difficult. With a smaller target like the lunar module, a better backup visual ranging system must be devised. Of course, there is no reason to expect on lunar missions that both the VHF and LM radar system will fail, but the optical backup system must work to lend confidence.

One of the more pleasant aspects of the flight was the quick and apparently complete adjustment which the crew made to weightlessness. The Command Module Pilot unstrapped and began moving around at about

40 minutes elapsed time and the Commander and Lunar Module Pilot loosened all restraints but kept the seat belt loosely fastened until after the transposition and simulated docking exercise. At no time was intra-vehicular activity a problem although movement while suited was awkward when compared with unsuited motion. Movement within the spacecraft was documented by onboard 16-mm film. There were no disorientation problems associated either with movement inside the spacecraft or looking out the windows at the earth. At one time, the Lunar Module Pilot attempted to induce vertigo or motion sickness by movement of the head in all directions at rapid rates with negative results.

One problem during the flight was the extreme discomfort caused by head colds. All three crewmen contracted head colds in fairly rapid order. The major problem was that in one-g conditions, the mucus is drawn vertically from the head through the throat to the lungs or stomach; in zero-g, the mucus does not leave the head area, where it congests and fills the cavities. It was therefore very difficult to clear the ears, nose, and sinuses. The Commander began taking two aspirin every 4 hours and one decongestant tablet every 8 hours. The result was an increase in congestion of mucus that became much thicker. This medication was terminated on about the third day, and after a period of time, the Commander resumed the process of blowing the mucus out through the nostrils frequently, in preference to not being able to clear his head at all because of the thickened mucus. During this same period, the Command Module Pilot developed a similar head cold and had slight flecks of blood in his mucus. Finally, the Lunar Module Pilot had a continual cold starting on about the fourth or fifth day. Collectively, the crew were concerned for the entry period as to whether they could clear their throats sufficiently to avoid gagging on mucus that might be withdrawn during the increase of gravity. The final consideration was whether the Valsalva maneuver (inflating the middle ear by closing the mouth and nostrils and blowing so as to puff out the cheeks) could be performed. The Valsalva maneuver would be appropriate only if the sinuses and the eustachian tubes were clear, and the problem was to clear these passages of fluid so that the pressure at the eardrums could be relieved. As a result of the head colds, a technique was developed of stowing cleaning tissues on the aft bulkhead in a Beta cloth box and putting the used tissues in an empty stowage compartment. On a regular basis, the tissues in the compartment were emptied into a used Beta cloth tissue compartment and restowed.

The most significant effect discerned on the flight, from an aerodynamic standpoint, was the unexpected phenomenon noted as perigee torquing. When the perigee was as high as 120 miles, this effect was possibly masked by the water boiler causing a yaw to the right at rates of up to 0.2 to 0.3 deg/sec, but it was very obvious when the perigee was at 90 miles.

Each of the service propulsion firings proceeded as scheduled. The residuals for the deorbit firing were reduced to less than 0.1 ft/sec in each axis, and as a result, retargeting for landing point was not required. This technique was developed by the crew during the final phases of simulation and has proved to be an optimum method of handling an earth orbit entry when a propulsion system is available for reducing these residuals.

It was elected to make the entry with helmets and gloves removed primarily to provide a means of clearing the sinus and inner ear cavities. The crew would have preferred to remove the suits as well for entry, but no other means of restraining leg motion was available. The head area was padded to provide support and bring the spine approximately straight during entry deceleration. Based on Apollo 7, suits-off entry or even an entire unsuited mission is recommended for future flights from the standpoint of crew comfort and reduction in crew fatigue. There should be no compromise to safety from a possible rapid decompression since the cabin structural integrity is well checked out before flight.

The entry was normal and provided no great surprises. The headrests were padded and were custom-fitted during flight so that head injury was precluded. The suits were donned to provide heel restraint.

The weather conditions for the recovery area deteriorated rapidly from the first briefing while the spacecraft was still in orbit and not yet committed to entry until the final observation at landing. The landing site was totally obscured; the local ceiling was approximately 80 to 100 feet.

6.2.2 Systems Operation

From a crew standpoint, all spacecraft systems operated within nominal limits except as indicated in the following paragraphs.

Guidance and navigation system.- In general, the guidance and navigation system performed flawlessly for the entire 11 days of flight. The alignments were quite accurate and star difference angles were negligible. The gyro torque angles were quite small for fine alignment, and the only time the angles exceeded 0.1 or 0.2 degree was during the realignment procedures. When a crewman first looked through the telescope, one of the big surprises was the excessive loss of light. Several minutes were required for the crewman's eyes to become adapted to the dark before any use could be made of the stars for position orientation. However, this did not pose a great problem. Sextant operation was quite satisfactory, and usually there were many stars in the field of view. The auto-optics feature performed very well and was quite useful in bringing selected stars into the sextant field of view. The pick-a-pair routine was useful; however, in some instances, pick-a-pair did not function, although

there were two or more stars available in the telescope field of view. Inertial measurement unit alignment using the calibrated optical sight was not difficult to perform except that attitude control of the spacecraft was a bit tedious. The pulse mode provides very satisfactory attitude control for this type of alignment. Although the motion of a star could not be stopped exactly in the center of the reticle pattern, it was possible to use the pulse control mode to make the star drift directly through the center of the reticle. The alignment accuracy was a quarter of a degree. The backup alignment procedure was a similar task. The minimum impulse controller was used to position the spacecraft and entailed flying with all three axes in free drift, a tedious but not difficult task. Accuracy was half a degree on the backup alignment.

The orbital navigation program, which required landmark tracking, was interesting. The ground provided as much information as possible regarding the relative location of landmark targets, that is, the time at which they would come into the field of view and the distance north or south of track. This permitted the trunnion angle to be adjusted to about 30 degrees or greater before proceeding into the auto-optics portion of the program, and as the target came into the field of view, the auto-optics placed the center of the reticle pattern very close to the target.

The midcourse navigation program, which was to use the earth horizon and a star, could not be accomplished because the earth horizon was very indistinct and variable. The air glow was about 3 degrees wide and had no distinct boundaries or lines when viewed through the sextant. This problem seemed to be associated with the spacecraft being in a low earth orbit. However, using this same program on lunar landmarks and a star was a very easy task to perform. Lunar landmarks showed up just about as well as earth landmarks. Stars could be seen 10 or 15 degrees, and greater, from the moon.

The ground track determination program was used extensively throughout the flight for onboard navigation. It was useful for keeping track of the spacecraft position around the earth.

At low sun angles, ice crystals formed by vented water and waste reflected into the optics and obliterated the star field. These crystals dispersed during the course of a night pass.

From a hardware standpoint, the onboard computer worked flawlessly through the entire mission. There were two anomalies involving the computer, but both were the result of procedural errors.

The two biggest problems confronting the crew during rendezvous were the inability to see the S-IVB flashing lights beyond 10 to 15 miles through the telescope or the rendezvous window and the lack of a direct range measurement.

Service propulsion system.- Throughout the flight, the temperatures of the service propulsion propellant tanks remained between 65° and 72° F and eliminated the requirement for manual cycling of the line heaters. The maximum temperature (72° F) was reached during a test of the line heaters late in the flight.

Reaction control system.- The propellant quantity meter for quad B of the service module reaction control system failed at the 92 percent level prior to launch and remained there throughout the flight. A significant deviation existed between the ground-calculated quantities and the onboard quantity readouts for all four quads; this difference was not the same from quad to quad. Ground calculations of propellant quantity were considered to be most accurate. For future space programs, an accurate onboard gaging system would be a great asset.

The command module reaction control system was not checked prior to the deorbit maneuver, but satisfactory pressurization and activation were obvious from the audible cues. The thruster temperatures were above 46° F throughout the flight, and no heater operation was required. After separation, the spacecraft was configured for system A operation only but was reconfigured for a two-system operation after a loud noise and a suspected thruster malfunction. The portion of the entry controlled by the digital autopilot was flown in the two-system configuration.

Electrical power.- The failure of ac buses 1 and 2 was attributed to simultaneously switching off the fans in both oxygen tanks. Thereafter, the tank 1 fans were left on automatic operation and the tank 2 fans were turned off and used for only about 5 minutes of every 8 to 12 hours. No further occurrences of the AC BUS FAIL lights occurred during the subsequent 200 hours.

The electromagnetic interference from the oxygen tank fans was verified later in the flight when a switch actuation of the oxygen tank 2 fans started the digital event timer in the lower equipment bay.

The dc power system showed transient undervoltage indications on both main buses for several minutes following open-circuiting of fuel cell 2. Indications were normal after the other two fuel cells warmed up. The last undervoltage occurred at command module/service module separation and was directly attributable to batteries A and B being in a much lower state of charge than had been expected for the entry phase.

At separation, bus voltages dropped to approximately 25.2 volts, but slowly increased to more than 26 volts during entry. From a crew standpoint, this situation is unsatisfactory, and appropriate action should be taken for future spacecraft.

The open-circuit voltage for the pyro batteries was 37 volts midway in the flight and 36.8 volts prior to the deorbit maneuver.

Fuel cells and cryogenics.- After 160 hours, when the spacecraft was powered up, fuel cell 2 was unable to maintain its condenser exit temperature within normal operating limits. This fuel cell performed properly when the spacecraft loads were 1400 watts and responded appropriately to the malfunction procedures when powered up. Fuel cells 1 and 3 each had one instance when condenser exit temperature was outside the nominal operating range. Throughout the mission, fuel cell 2 carried 10-percent higher loads than either of the other two fuel cells. The fuel cells were purged at scheduled intervals, and there was a noticeable increase in performance after oxygen purges.

The hydrogen appeared to be free of stratification, but the oxygen was subject to stratification at high densities. Manual balancing of the hydrogen tanks was initiated at 168 hours when a differential of 3.4 percent was indicated. After 10 hours, the two tanks were balanced to within 0.2 percent. Cryogenic usage was less than expected because less electrical power was required than had been predicted before flight.

Environmental control.- Chlorination of the water system was started at 11 hours and was continued as scheduled for 3 subsequent days. At the end of this time, the water had a very strong chlorine taste which persisted for 10 to 12 hours after the third chlorination. A water chlorination schedule of alternate days was then followed, and the chlorine aftertaste was eliminated.

The water gun operated satisfactorily for the first 8 days, but by the 10th day, the trigger was almost too stiff to operate. There was always sufficient hot water to prepare meals simultaneously for all three crewmen, and the food bags maintained the heat for the necessary 10 to 15 minutes.

The primary evaporator was off the line for most of the flight because of evaporator dryout. Throughout the mission, at random times, the evaporator would dry out, be reserviced, and be placed back on the line when convenient or required. When the evaporator was off the line, the glycol evaporator outlet temperature approached 60° F, but the cabin remained comfortable. The last time the evaporator dried out, it was serviced with water but was not placed on the line for entry.

Twice in the first 48 hours, the radiator flow control switched automatically to the no. 2 controller. In both cases it was reset to no. 1 and placed to AUTO. After the second occurrence, the no. 1 flow controller operated for the remainder of the mission.

The secondary evaporator was operated satisfactorily for each redundancy check and for 7-1/2 hours during the secondary coolant loop test. The secondary radiator flowed only during the first redundancy check and the secondary coolant loop test.

On at least three occasions when the crew were in the shirt-sleeves mode, the hoses supplying cold air to the cabin accumulated internal globules of water; these globules eventually were blown out of the hoses and impacted the walls of the spacecraft.

The temperature and humidity in the suits and cabin remained within a comfortable range throughout the flight, although the electrical power varied between 1400 and 2200 watts. The relative humidity varied from approximately 45 to 80 percent. The lithium hydroxide cartridges performed well. The carbon dioxide partial pressure indication was always less than 1 mm of mercury until late in the flight, when one cartridge was used for nearly 35 hours because the stowage was one cartridge short; the partial pressure approached 3 mm of mercury. The last change was accomplished about 3 hours prior to the deorbit maneuver, at which time the cartridge used during launch was reinstalled.

The oxygen flow meter was one of the most frequently used, but its usefulness would have been enhanced if the range had been extended to 2 lb/hr. Flow rates during normal purges and dumps frequently exceeded the full-scale reading of 1 lb/hr.

The fitting which attached to the waste water panel for waste water dumping extended too far from the panel and interferred with access to one stowage compartment.

Waste management system.- The urine dump system was satisfactory, although its use was complex. The urine dump heater A was used throughout the mission, and there were no problems with urine dump line freezing. The fecal bags were utilized on 11 occasions with no significant problems.

Communications.- The VHF communications system was operated almost entirely with the left antenna. On several occasions, switching between the left and right antennas was initiated during voice contact to determine the effect on communications; there was no discernible difference. The signal from the VHF recovery beacon apparently was not received by the recovery forces until just prior to spacecraft landing. During entry,

the antennas were selected in accordance with the check list, and the VHF-AM was in the simplex A mode. The VHF beacon was turned on at 9000 feet altitude, but the antenna may not have deployed properly until just before landing. VHF voice communications were adequate while the spacecraft was descending on the parachutes. After landing, the spacecraft assumed the stable II (apex down) position, and the radios were turned off. As soon as the spacecraft was uprighted, the radios were turned on again and all voice and beacon contact was normal.

The S-band omnidirectional antenna patterns were significantly larger than those on the crewman simulator. Throughout the mission, the S-band was operated in the high-power mode and utilized two opposing omnidirectional antennas as much as possible. Antenna switching, performed manually on request from the flight controllers, was required so frequently as to be a continuous task, but no other means of switching was available. To the flight crew, the voice quality of the S-band and VHF systems seemed comparable. Of the audio center controls, the only position not normally utilized was the VOX circuit; however, this was utilized for the relay mode tests.

The data storage equipment was frequently not available for recording onboard voice; this situation was always caused by problems associated with dumping the tape. For example, when a full tape of high-bit-rate data were recorded during rendezvous, 8 hours was required to dump the tape. Without a voice recording capability, a large amount of paper and additional work was required to maintain data.

Premission planning.- The flight plan did not account for normal habit patterns of having a breakfast shortly after waking, lunch part-way through the work day, and then dinner several hours prior to retiring. The flight plan had at least two of the crew eating a dinner at breakfast time every day past the fourth. Since the meals were eaten by the normal schedule mentioned, no meal was available for breakfast on the 11th day.

7.0 BIOMEDICAL EVALUATION

This section contains a summary of specific Apollo 7 medical findings and anomalies. The complete and comprehensive Apollo 7 biomedical evaluation is to be published as a separate report and will contain details of any special medical studies.

During Apollo 7, the crew accumulated more than 780 hours of space flight experience. For the first time, the crew experienced unrestricted movement in the weightless state (intravehicular activity). Apollo 7 was also the first spacecraft to be launched with a mixed cabin atmosphere of 64-percent oxygen and 36-percent nitrogen.

The real-time operational medical support was limited to biomedical monitoring on a time-shared basis in contrast to the Gemini flights in which both crewmen were continuously monitored. The Apollo 7 crew participated in a series of special pre- and postflight medical studies designed to assess the changes incident to the mission and to further the understanding of human capabilities and limitations in the space environment.

The preliminary analysis of the data indicates that the Apollo command module does provide a habitable environment which will permit the objectives of the Apollo Program to be attained without compromise to crew health and safety. The physiological changes observed postflight were generally consistent with those noted and reported in earlier manned space flights. However, comparison of the Apollo 7 mission with previous long-duration missions must be accomplished before the full significance of the Apollo 7 medical data can be fully recognized and understood.

7.1 INFLIGHT

This section documents the principal mission events of medical significance from lift-off to landing.

7.1.1 Bioinstrumentation Performance

Problems with the Apollo 7 bioinstrumentation harnesses began prior to lift-off. At 2 hours and 9 minutes prior to launch, soon after crew ingress, the Command Module Pilot's sternal electrocardiogram (EKG) was lost. The appearance of the EKG signal indicated that the sternal lead was disconnected. The same type of electrical noise pattern had been demonstrated by disconnecting the pin connector of the sternal lead. Since this failure was something that could probably be corrected inflight

after the crew got out of their suits, the decision was made to continue the countdown. At 2 hours before launch, the Lunar Module Pilot's EKG signal was also lost. As in the previous case, the electrical noise pattern indicated that the failure was caused by a disengaged pin connector. Valid impedance pneumograms (ZPG) were, however, still being received from these crewmen. The crewmen were able to restore their EKG signals inflight. However, after the first 24 hours of flight, the bioinstrumentation problem began to recur and progressed in magnitude as the flight continued. The Command Module Pilot stated that during his duty watch on the seventh day, he noted that the dc-dc converter in his bio belt was becoming progressively warmer and he elected to remove his bioharness. All three bioharnesses were subsequently removed and stowed. A chronological summary of the bioinstrumentation problems experienced during the flight is presented in table 7-I. See section 11 for discussion of this problem.

7.1.2 Physiological Data

In general, the ground support worked well and demonstrated that the systems are capable of supporting bioenvironmental data monitoring during Apollo missions.

A total of only 27 hours of inflight physiological data was collected during the 11-day mission because of the instrumentation problems; 8 hours were collected for the Commander, 13 hours for the Command Module Pilot, and 6 hours for the Lunar Module Pilot. About 10 hours of the 27 were average-to-good physiological data.

Descriptive statistics describing the heart and respiration rates calculated from telemetered data are given in tables 7-II and 7-III.

The baseline heart and respiration rates for the orbital phase of the mission are also shown in tables 7-II and 7-III. These data reflect normal variations, but because of the limited data quality, no conclusions can be made regarding extremes. The high and low rates throughout the Apollo 7 flight are omitted since they were most frequently noise spikes.

Perhaps the most striking results shown in the tables are the magnitude of the standard deviations. For heart rates, these ranged from a low of 8 to a high of 47 with the majority in the 13-17 range. A reasonable expected range for these standard deviations is from 4 to 13. The spuriously high values obtained are probably a function of 64 percent noisy data, as well as isolated grounding and exercise artifacts in the remaining 36 percent of the data. No filtering of the data other than that provided by the cardiotachometers was done.

The objective of accurately quantifying physiological changes associated with crew activity could not be completed because of the lack of both physioloical data and recorded detailed knowledge of crew activities. However, an attempt was made to fit the collected data to a sine wave that would describe the daily physiological variations in an attempt to validate the conclusions made. Because of the amount of distribution of the data, the results might be misleading. The method involved taking a sample of the data approximately equally distributed throughout the mission and calculating the best-fit sine wave for these points. These results, presented in table 7-IV, show that the samples extracted for this analysis are representative of the entire flight except that the variability for the sample was less than that for the flight. Assuming no error, the calculated results from the model indicated that the Commander, Command Module Pilot, and Lunar Module Pilot operated on a daily circadian cycle of 23.4, 21.3, and 29.0 hours, respectively. The results also indicated that the rhythmic variations in heart rate for the Commander, Command Module Pilot, and Lunar Module Pilot (8, 13, and 19 percent, respectively) can be accounted for by daily variations predicted by the model.

7.1.3 Medical Observations

Lift-off and powered flight.- The physical sensation of lift-off was perceptible to the crew, and instrument cues served to confirm this sensation. The maximum g-loading experienced by the crew during powered flight was 4.3. The Commander's prelaunch baseline heart rate was approximately 68 beats per minute and ranged from 68 to 90 beats per minute during powered flight. No vertigo or disorientation was experienced by the crew. This phase of flight was completely normal.

Weightlessness and intravehicular activity.- The Apollo 7 spacecraft was large enough to permit intravehicular activity. The Lunar Module Pilot performed somersaults and other unrestrained body movements with no symptoms of motion sickness or sensory illusions. He remained oriented at all times with respect to the spacecraft. Each crewman experienced the characteristic feeling of fullness of the head which had been observed and reported by previous flight crews to occur shortly after orbital insertion. How long this sensation lasted in the Apollo 7 crew was undeterminable because of the early onset of head colds.

Adaptation to the weightless state was readily accomplished. Learning to relax the muscles appeared to be a particular problem and perhaps takes the longest period of time.

The crew also reported some soreness of their back muscles in the costovertebral angle (kidney area); this soreness was relieved by exercise and hyperextension of the back. The Apollo 7 results tend to confirm all previous space flight observations regarding weightlessness and

at the same time to add new understanding as well as identify problems for future observations.

Inflight illness. - Three days prior to launch, the Command and Lunar Module Pilots experienced symptoms of slight nasal stuffiness. They were both successfully treated for these symptoms, and since the launch-day physical examinations on the crew demonstrated no manifestations of any illness, they were medically certified fit for flight.

Approximately 15 hours after lift-off, the crew reported that the Commander had developed a bad head cold. In addition to the aspirin taken by the Commander for symptomatic relief, the Flight Surgeon recommended that one decongestant tablet (60 mg pseudoephedrine hydrochloride/ 2.5 mg triprolidine hydrochloride) be taken every 8 hours. The Commander reported he would remain on this dosage schedule until he felt better or exhausted the onboard supply of decongestant. He also reported that his temperature was normal and that he had no symptoms of sore throat, cough, or lung congestion. Twenty-four hours later, the Command and Lunar Module Pilots also began experiencing head cold symptoms. The treatment schedule instituted was the same as for the Commander. Approximately 2 days later, the crew expressed concern about developing middle ear blocks and rupturing their eardrums on entry. At that time, however, it was still too early to recommend a course of action for entry. They might or might not have a problem at time of entry depending on the results obtained from the medication and the stage of progression of their illness.

Later, the Lunar Module Pilot asked the advisability of taking antibiotic medication for his cold. He was advised that it was not indicated at that time and would be prescribed only in the event of secondary bacterial infection.

After the midway point in the flight was reached, the crew became more concerned about their entry configuration (shirt sleeves versus suits). A Valsalva maneuver, used to equalize the pressure within the middle ear cavity and prevent rupture of the eardrum, could not be performed satisfactorily in a pressure suit with the helmet on. The crew were advised that the pressure garment had to be worn for entry because there was no leg restraint in the unsuited mode. At forty-eight hours prior to entry, the crew made the decision not to wear helmets or gloves. They were then given a medication schedule for the last 24 hours of flight. The last nine decongestant tablets were taken at 8-hour intervals. The times for taking the tablets were selected so as to obtain the maximum benefit at the time of the deorbit maneuver and entry.

During entry, none of the crewmen had any difficulty in ventilating his middle ears. No Valsalva maneuvers were required nor did any rupture of the eardrums occur. In the postflight physical examinations, the two

crewmen who had reported the most distressing symptoms inflight had cleared completely and showed no obvious evidence of their colds. The other crewman did exhibit a slight amount of fluid in the middle ear.

The Commander stated postflight that his cold symptoms began about 1 hour after lift-off (6 hours after his prelaunch physical examination). He also observed that in this environment, the drainage of nasal and sinus secretions ceases. The body's normal means of eliminating such secretions is lost because of the absence of gravity. Forceful blowing is the only method available for purging these secretions from the nose, but blowing the nose is ineffective in removing mucoid material from the sinus cavities. The Commander also observed that in the weightless state, there is no postnasal drip. The secretions do not reach the lower respiratory tract and thus do not produce coughing.

Work/rest cycles.- Based on previous flight experience, a medical recommendation was made to program simultaneous crew rest periods during the mission, referenced to the crew's normal Cape Kennedy sleep cycle. Flight plan and crew constraints, however, precluded simultaneous sleep. The ac bus failure, which occurred unexpectedly and required immediate action, demonstrated the wisdom of having at least one crewman on watch on the first flight of a new spacecraft.

The large departures from the crew's normal circadian periodicity caused problems during the mission. The wide dispersions of the work/rest cycles are given in figure 7-1. A "practical shift" of 5 hours before or 5 hours after start of the Commander's and Lunar Module Pilot's usual Cape Kennedy sleep period is shown. The Command Module Pilot experienced a "practical shift" of 5 to 14 hours before his assumed Cape Kennedy sleep time.

The crew reported poor sleep for about the first 3 days of the flight and experienced both restful and poor sleep after that period of time. The Command Module Pilot reported that fatigue and exhaustion caused him to fall asleep once on his watch and that he took 5 mg of d-amphetamine on another occasion to stay awake during his work cycle.

The amount of sleep each crewman obtained was indeterminable.

Crew status reporting procedures.- Difficulties associated with on-board voice recording and subsequent dumping procedures (see section 5.15) resulted in significant loss of time in recovering data relayed to the remote ground stations. In fact, some food and water usage data were not recovered at all.

7.1.4 Oxygen Enrichment Procedure

The spacecraft was launched with a 64-percent oxygen, 36-percent nitrogen cabin gas atmosphere. The flight crew denitrogenated for 3 hours prior to launch and remained isolated in the 100-percent oxygen environment of the suit loop until helmets and gloves were doffed at 59 minutes after launch. The waste management overboard dump valve was left open to facilitate the cabin oxygen enrichment procedure, and the onboard gas analyzer was used to verify the cabin oxygen enrichment. Figure 7-2 shows the oxygen enrichment profile obtained during the first 24 hours, and figure 7-3 shows the enrichment curve by days. The oxygen enrichment curve followed the predicted curve fairly well, but it did not increase as fast as predicted because of the slow spacecraft cabin leak. The maximum cabin oxygen concentration measured during the flight was 97 percent (255 mm Hg) at 236 hours. The altitude equivalency was never above sea level (i.e., oxygen partial pressure was always greater than that at sea level). The cabin oxygen enrichment technique was thus verified by the Apollo 7 flight.

7.2 PHYSICAL EXAMINATIONS

The preflight physical examinations were accomplished for certification of the crew's physical qualifications for the mission; and to detect and treat, or correct, any minor physical problems which might compromise mission completion, crew health, safety, or comfort. A preliminary examination was performed 4 days prior to flight; and a cursory physical examination was performed on the morning of the flight. A comprehensive physical examination was done immediately after recovery so as to document any physical effects of the mission upon the crew and to detect any medical problems that might need treatment. A detailed discussion of the preflight and postflight physical findings will be reported later; but in summary, definite residuals of an inflight upper respiratory infection were noted in only one crew member. Excessive fatigue was evident in the Command Module Pilot immediately postflight, and one crew member had a rash which apparently was caused by contact with the Velcro watchband.

TABLE 7-I.-- SUMMARY OF BIOMEDICAL INSTRUMENTATION PROBLEMS

Time, hr:min	Crewman	Problem	Solution
09:18	LMP	Upper sternal EKG pin connector disconnected 2 hours prior to launch	Reconnection made at this time
24:51	CDR	Sternal EKG pin connector disconnected	Reconnection performed at 32:55
41:48	CMP	No sternal EKG since 2 hours prior to launch; suspect pin connector	Unknown repair performed at this time; ZPG poor quality
70:08	CDR	No sternal EKG; suspect pin connector	Reconnection made at 74:38
75:46	CMP	No sternal EKG; pin connector disconnected	Reconnected prior to 84:17
125:20 130:33	CDR LMP	Sternal EKG leads broken at signal conditioner Sternal EKG lost; suspect pin connector	ZPG leads transferred to EKG signal conditioner; conversion to axillary EKG with deletion of ZPG at 126:43 for CDR and 170:49 for LMP
171:19	LMP	Sternal EKG unsatisfactory for waveform due to absent P- and T-waves	Sternal sensors relocated to original position
174:00	CMP	Sternal EKG leads broken at signal conditioner	ZPG leads transferred to EKG signal conditioner; axillary EKG obtained at 176:33
180:53	CMP	Report that dc-dc converter hot to touch	Entire biomedical harness removed
199:00	CDR, LMP	Biomedical harnesses considered possible electrical hazard	Harnesses removed and stowed at 207:07

TABLE 7-II.- DESCRIPTIVE STATISTICS OF HEART RATES

Crewman	Statistic	Pre-launch	Launch	Orbit									
				7-day total	Daily totals								
					0	1	2	3	4	5	6	7	
CDR	No. of minutes	79	16	467	102	7	39	59	30	39	136	55	
	Heart rates				72	76	90	68	68	70	66	68	71
	Mean	66	94		--	74	88	65	65	69	64	64	67
	Median	62	82		19	16	13	16	16	11	13	18	17
CMP	No. of minutes	5		775	7	80	148	43	145	199	101	52	
	Heart rates				79	112	79	76	80	78	81	85	77
	Mean	84			--	107	76	74	77	76	78	73	72
	Median	74			19	47	13	13	16	13	17	34	21
LMP	No. of minutes	10		370	40	129	16	19	88	44	3	31	
	Heart rates				70	62	70	61	75	71	75	63	68
	Mean	98			--	59	66	59	72	68	65	65	66
	Median	96			20	18	16	12	15	15	30	10	21

TABLE 7-III.- DESCRIPTIVE STATISTICS OF RESPIRATION RATES

Crewman	Statistic	Pre-launch	Launch	Orbit									
				7-day total	Daily totals								
					0	1	2	3	4	5	6	7	
CDR	No. of minutes		16	467	102	7	39	59	30	39	136	55	
	Respiration rates				12.9	17	12	15	12	6	8	12	9
	Mean	17	17		--	17	12	14	12	4	7	12	8
	Median	18	17		8	6	4	6	7	5	6	7	5
CMP	No. of minutes	5		775	7	80	148	43	145	199	101	52	
	Respiration rates				13.6	18	8	13	16	14	14	15	11
	Mean	25			--	27	6	13	15	14	14	15	11
	Median	25			8	13	7	7	7	6	7	7	10
LMP	No. of minutes	10		370	40	129	16	19	88	44	3	51	
	Respiration rates				14.5	14	15	14	17	16	12	10	12
	Mean	30			--	14	15	15	16	16	12	10	11
	Median	19			6	5	6	5	8	6	5	5	6

TABLE 7-IV.- CIRCADIAN VARIATION IN HEART RATES

	Gemini VII		Apollo 7		
	Command Pilot	Pilot	Commander	Command Module Pilot	Lunar Module Pilot
<u>Sampled data</u>					
No. points	600	506	216	216	216
Mean, beats/min	73.1	66.3	72.8	80.7	70.7
Standard deviation, beats/min	9.3	10.9	16.9	16.2	15.2
<u>Calculated model</u>					
Fitted curve parameters					
Period (biological day), hr	23.5	23.5	23.4	21.3	29.0
Amplitude of variation, beats/min	7.3	8.2	5.7	11.2	8.6
Phase of variation, hr*	20.2	19.8	18.7	11.2	15.3
Baseline, beats/min	71.2	64.3	69.9	84.2	73.7
Circadian ratio**	0.10	0.13	0.08	0.13	0.12
Standard error					
Period, hr	2.98	3.18	7.08	4.40	5.23
Amplitude, beats/min	0.69	0.85	8.39	3.40	1.57
Phase, hr	0.35	0.40	2.80	0.99	0.19
Baseline, beats/min	0.35	0.44	5.90	1.90	3.35

*Referenced to local launch time (Gemini VII - 2:30 p.m. e.s.t.; Apollo 7 - 10:02 a.m. e.s.t.).

**Amplitude/baseline, or variation due to circadian effects.

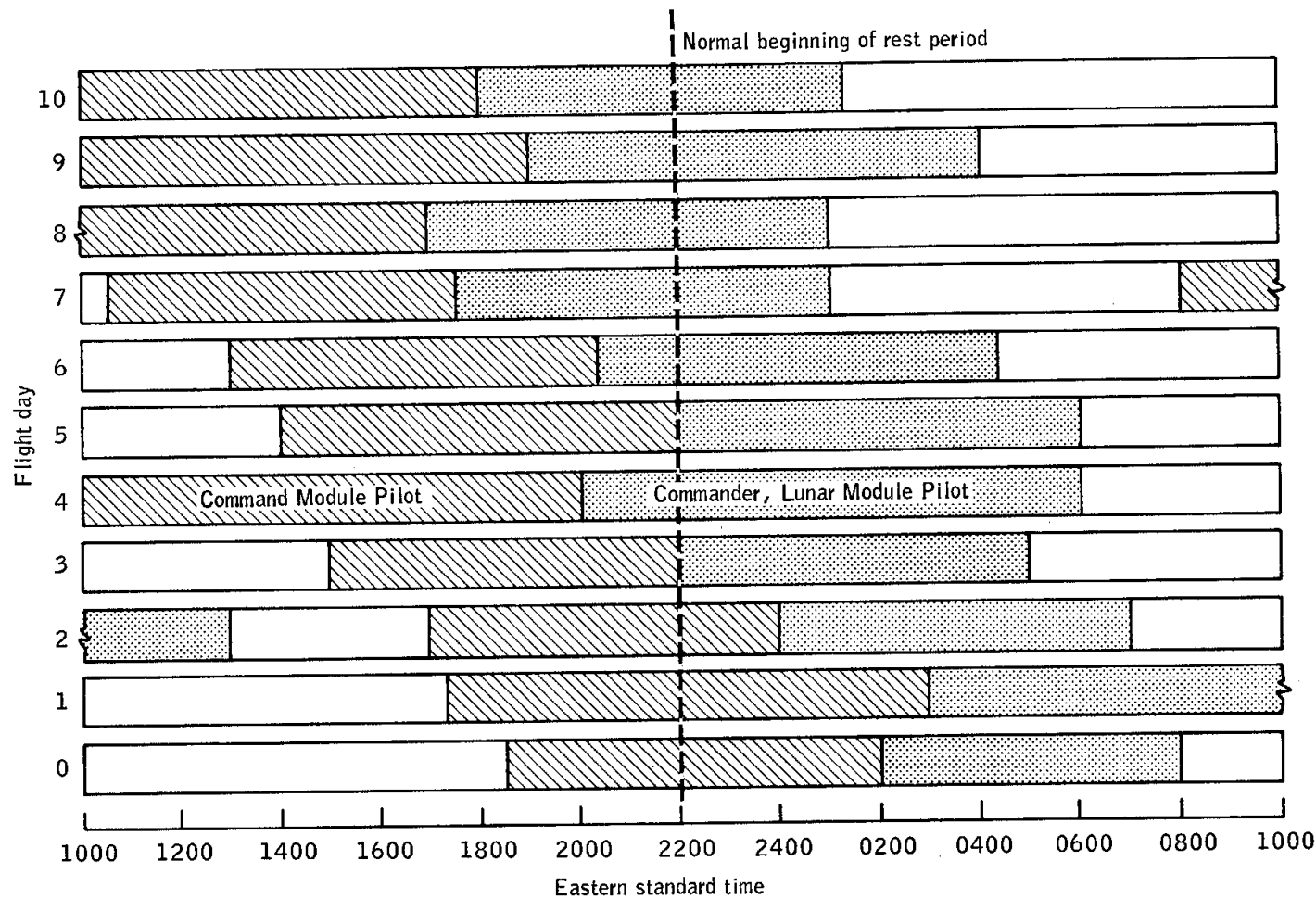


Figure 7-1.- Crew rest cycles.

NASA-S-68-6382

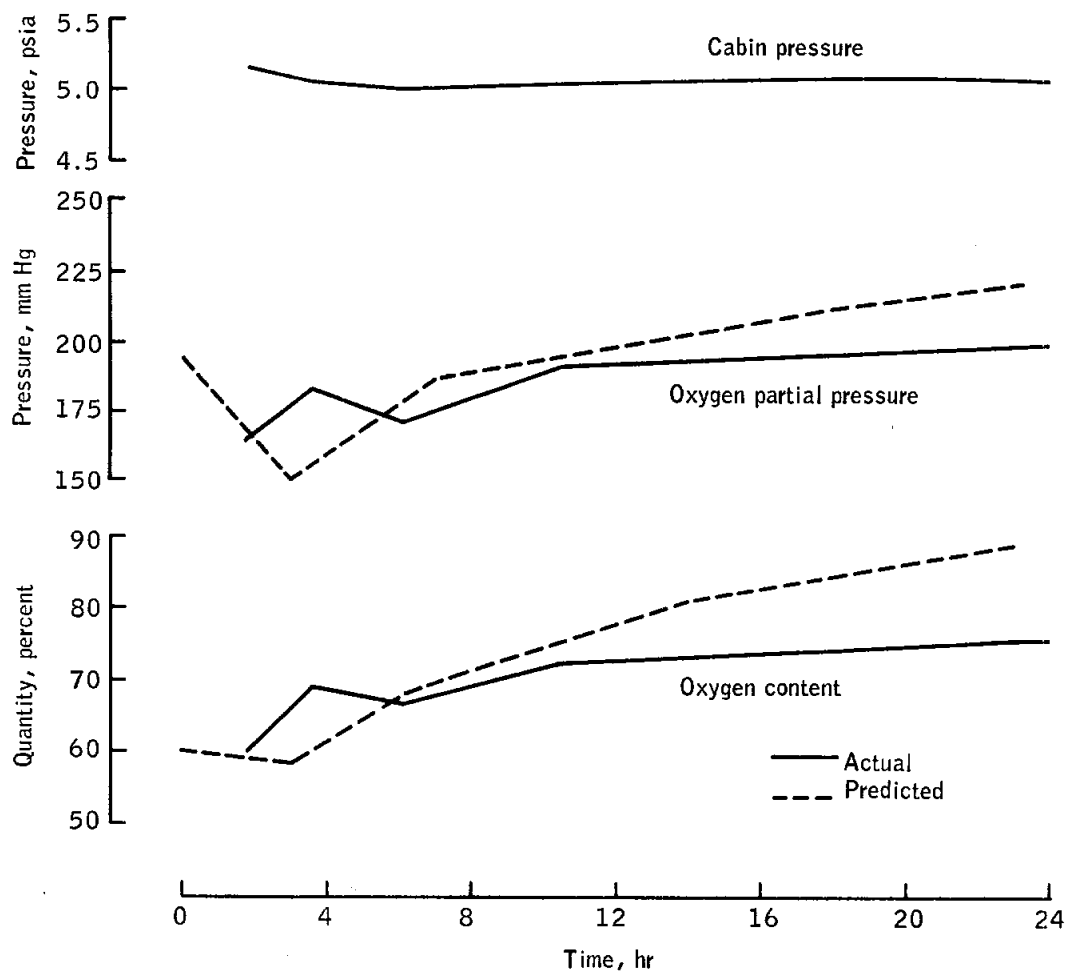


Figure 7-2.- Oxygen enrichment sequence for 24 hours.

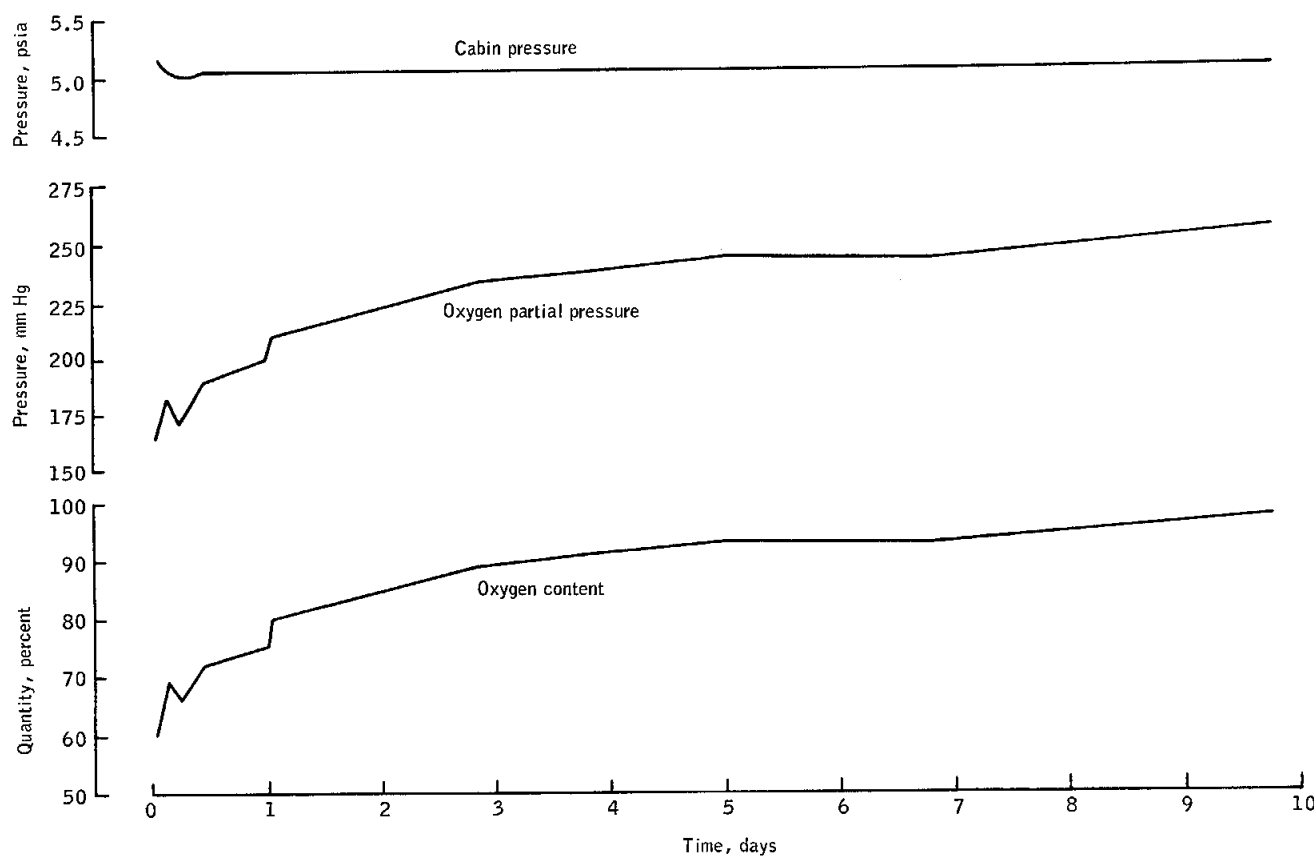


Figure 7-3.- Oxygen enrichment sequence for 10 days.

8.0 MISSION SUPPORT PERFORMANCE

8.1 FLIGHT CONTROL

This section of the report is based upon real-time observations unless otherwise noted and may not agree with the final data analysis in other sections of the report.

8.1.1 Prelaunch Operations

The Mission Control Center began flight operational support of the terminal countdown 15 hours before lift-off, and the prelaunch command checks with the launch vehicle were successfully completed 2 hours later. The crew ingress commenced 2 hours 27 minutes before lift-off. At 6 minutes 15 seconds before lift-off, the count was held for 2 minutes 45 seconds to complete the propellant chilldown. At 4 minutes 50 seconds before lift-off, all elements were GO for the automatic sequencing operation leading to lift-off. At 2 minutes prior to lift-off, the telemetry computer status was questionable, causing the 2 kB data to not be used. Alternate 40.8 kb data were available and the count was continued.

8.1.2 Powered Flight

The guidance reference release and S-IB ignition were nominal with lift-off occurring at 15:02:45 G.m.t. During the S-IB boost phase, the hydrogen-vent-valve-closed indication was lost several times. The non-propulsive vent line pressures confirmed the vent was closed, and the problem was diagnosed as a telemetry transducer problem. At 00:00:30, the onboard-computer state vector had a large range error; however, all guidance platform attitude indications and the other state vector indications all appeared nominal. At 00:04:30 the error disappeared after the time bias was corrected in the Real Time Computer Complex. Both S-IB staging and S-IVB ignition were nominal.

Beginning at approximately 00:08:00, air-to-ground communications became garbled. However, the launch phase was continued because it was believed that adequate communications could be restored when the spacecraft was in orbit. The loss of communications appeared to be a network problem and not a spacecraft anomaly. The spacecraft was configured for VHF duplex-B as the prime mode and S-band as the backup mode during the launch phase. At Canary Island, the spacecraft was switched to simplex-A mode in accordance with the flight plan, and communications quality was good. During the launch phase, intermittent data dropouts were caused by either noise bursts or station handovers.

8.1.3 Orbital Flight

The insertion orbit was 151.1 by 122.5 n. mi., with apogee occurring at 00:54:19. The Carnarvon tracking data updated the orbit to 153.3 by 122.7 n. mi. The change was attributed to S-IVB venting after insertion. At approximately 01:18:34, a 2-minute power failure occurred in the Mission Control Center. Air-to-ground communications were not lost during this period, and the failure had no significant effect on the control of the mission. Passivation of the S-IVB stage commenced at 01:34:27, and liquid oxygen dump was successfully completed, although the predicted flow rates were not achieved, as evidenced by the extended time required to achieve this dump. This probably resulted from the two-phase flow (liquid and gas) through the engine. The orbit-safing maneuver (passivation) produced a 23.5 ft/sec change in velocity instead of the predicted 32 ft/sec. The discrepancy was probably caused by the two-phase venting (liquid and gas). At adapter separation, the right panel only opened 30 degrees as compared with the normal 45 degrees.

The reaction control system was used to perform a phasing maneuver at 03:20:00. This maneuver was intended to result in a separation of 76.5 n. mi. between the spacecraft and S-IVB at the beginning of the rendezvous period; however, it became obvious that the required separation distance would not be achieved because of the S-IVB venting, and a second phasing maneuver was executed at 15:52:00. The second phasing maneuver set up the desired rendezvous conditions.

The crew reported at 06:00:00 that a HIGH O2 FLOW light was on. They completed the malfunction procedures and found no problems. The cabin pressure remained at 5.0 psia and the surge tank remained at 858 psi, indicating that no oxygen flow problem existed. The light went out at 07:24:18. (Editor's note: Light went out when waste management overboard dump valve was closed.)

Rendezvous maneuvers.- In preparation for rendezvous with the S-IVB, the first service propulsion maneuver was performed at 26:24:53 and was so accurate that an additional backup maneuver was not required. The planned second service propulsion maneuver was completed at 28:00:56.

The ground-computed terminal phase initiation maneuver was performed at 29:18:34 (compared with 29:16:45 computed by the crew). The first midcourse correction occurred at 29:37:48 and the second midcourse maneuver was not required. The rendezvous was completed at 29:52:00, with the spacecraft approximately 70 feet from a tumbling S-IVB; one S-IVB acquisition light was not operating properly. After a short period of station-keeping, a separation maneuver of 2 ft/sec was performed with the reaction control system and the resultant orbit was 161.5 by 122.0 n. mi.

The complete rendezvous phase was very close to premission predictions; terminal phase initiation occurred 4 to 5 minutes early because of S-IVB position prediction errors.

Fuel cell purging.- A total of 21 oxygen and four hydrogen fuel cell purges were performed during the mission. The first oxygen and hydrogen purges were as scheduled in the flight plan. Subsequent purges were initially based on prelaunch cryogenic purities. The second oxygen purge demonstrated excessive fuel cell degradation since the first purge, the oxygen purity was determined to be 99.92 percent, rather than the pre-launch value of 99.995.

The second hydrogen purge, scheduled 48 hours after the first, did not noticeably improve fuel cell performance. Therefore, subsequent hydrogen purge intervals were extended to 96 hours. The only other deviation from purge schedule was to purge oxygen 2 hours prior to each service propulsion maneuver, thus increasing the load sharing of the fuel cell and conserving battery energy.

Onboard computer restart.- At 07:24:21, the crew reported an onboard computer restart, along with a program alarm light, while in the inertial measurement realignment program using the pick-a-pair routine (see section 5.16). The alarm code readout on the display/keyboard was 120, which indicated the computer had requested optics drive with the optics not zeroed. All computer functions appeared normal so an eraseable memory octal dump was not requested. The restart was later duplicated with identical conditions during a ground simulation; basically, the problem involved the use of the computer to drive the optics to an illegal or nonexistent star. Playback of the data storage equipment recording during the restart period was attempted. However, the playback was terminated prior to reaching the activity causing the restart; thus, data verification of the explanation was never obtained.

Eight other major restarts of the onboard computer were observed during the mission, and all were associated with the same type of conditions.

Primary evaporator dryout.- Automatic start-up and operation of the primary evaporator was performed during the launch phase. Although the evaporator outlet temperature and the steam pressure decreased as low as 34° F and 0.087 psi, respectively, the evaporator recovered and was operating normally at the time of Canary Island loss of signal. Over Carnarvon, the evaporator was still operating with the radiator outlet temperature reaching a maximum of 55° F, but by the time of loss of signal at Canberra, the temperature had decreased to 49° F. Primary evaporator operation was observed whenever the radiator outlet temperature equaled 50.8° F during this time period.

The crew reported at 10:10:00 that the secondary coolant loop was activated when the primary evaporator outlet temperature exceeded 50° F and the steam pressure went off scale low. Manual start-up of the evaporator proved successful. Automatic operation was then resumed, and the evaporator operated properly for a short period of time. The previous symptoms recurred, and at 14:40:00, the crew was instructed to accomplish the following:

- a. Close the back pressure control valve.
- b. Service the evaporator and discontinue its operation.
- c. Activate the secondary coolant loop if the primary evaporator outlet temperature exceeded 60° F.

At that time, the steam pressure rose higher than normally expected for the evaporator and then varied with the evaporator outlet temperature. Between 14:40:00 and 48:43:00, primary evaporator operation was not observed, even though radiator outlet temperatures of 57° F were observed. Steam pressure varied with evaporator outlet temperature but was higher than water vapor pressure at those temperatures. Thereafter, the crew used various procedures for manually controlling the evaporator until automatic operation resumed. The primary evaporator was operated intermittently for the remainder of the mission.

Y-Axis PIPA Anomaly.- At 13:36:00, the Guidance, Navigation, and Control Officer reported the absence of Y-axis accelerometer counts. The output should have been 160 pulse/hr. In drifting flight, accelerometer outputs resulting from drift are accumulated; however, the Y-axis was not indicating any output. The computer average "g" integration was monitored during the plus X translation for the second rendezvous maneuver. A Y-axis velocity change was observed, with no Y-axis translation input, thus indicating that the Y-axis accelerometer compensation was being interpreted as actual acceleration. A procedure was executed at 17:25:00 to determine if the accelerometer was being zeroed during each computer cycle. The noncompensated output had been zero. The procedure loaded all 1's as the accelerometer accumulated output. The result was a constant accumulation of 11111; therefore, the output was not being zeroed, indicating one of two conditions existed. First, the accelerometer interface was dead, or second, the accelerometer was a perfect no zero-g bias instrument. After discussion of the alternatives or the impact of the accelerometer not operating, another test was attempted. The procedure was to translate along the minus Y axis for 7 seconds. The thrusting was 2-jet and monitored by the computer. The test was successful, thus proving that the accelerometer had not failed, but was a perfect no zero-g bias instrument.

AC bus dropout.- The crew reported that ac inverter 1 in the electric power system disconnected from ac bus 1 at approximately 19:47:00, but that the inverter had been reset to the same bus in the original configuration with no problem. The only condition for an ac bus disconnect is an overvoltage condition of 130 (± 5) V ac on any phase of the ac bus. The same inverter disconnected from ac bus 1 again at 57:00:00, and then both inverters 1 and 2 disconnected from buses 1 and 2 at 61:05:00. Analysis of the data showed a relationship between bus disconnects and cycles of the cryogenic heaters and fans. After the third ac bus disconnect, the oxygen tank 2 fans were cycled manually, and no subsequent bus disconnect problems were noted.

Main A and B undervoltage.- At 32:28:58, the crew reported that a main A/B bus undervoltage warning light came on during the suit compressor check. It had been 25.5 hours since the fuel cells had been purged and both main buses were operating slightly below the 26 V nominal. At the time of the redundant suit compressor check, the cryogenic heaters (approximately 15 amperes) were activated. This action, combined with the heavy surge of current (13 to 14 amperes) resulting from both suit compressors being turned on at the same time, caused the undervoltage.

To prevent undervoltage conditions during the remainder of the mission, fuel cell purges were adjusted to maintain high performance during heavy load conditions, and care was exercised to prevent applying high surges to the buses when the fuel cells were degraded or already supplying high demands.

Battery charging.- During the mission, three battery charge cycles were attempted. To insure that the batteries were fully charged, but not overcharged, the premission plan was to charge the batteries one at a time until the amp-hours replaced equaled the amp-hours removed or until the battery charger current reached the 0.6-amp cut-off point. In the first charge attempt on battery A, the charger current of 0.6 amp was reached much quicker than expected, and it was determined that the battery had not had as much energy replaced as had been removed by the battery loads. Previous to the flight, a new cut-off point of 0.4 amp was established and was implemented at this time. The estimated amp-hours replaced in the battery from this charge was approximately 4.5 amp-hours, considerably less than the estimated depletion of 9.3 amp-hours. The second battery charge performed during the flight was on battery B. This charge differed from the battery A charge in that the charge was started approximately 2 hours after a service propulsion maneuver instead of immediately after a maneuver. The results were essentially the same as the first charge. An estimated 2.30 amp-hour was replaced in the battery during this charge. The estimated depletion prior to the charge was 11.55 amp-hours. An additional battery charge was also made on battery B to determine the repeatability of the charge characteristics.

This charge was started approximately 1.5 hours after a service propulsion maneuver, and the results were essentially the same as the two previous charges. It was estimated that 16 amp-hours had been removed from the battery, but only 2.4 amp-hours were replaced.

Proportional control valve switchover.- At 57:00:00, the crew reported a proportional control valve switchover during the environmental control system component check. They advised that this problem had also occurred earlier, at 21:47:00, and was believed to have been caused by an ac bus 1 disconnect. The switchover occurred once more during the flight. All three switchovers were a normal result of ac bus disconnects discussed previously.

S-band transponder.- The USNS Redstone reported at 65:11:00 that they were not receiving PCM telemetry from the spacecraft. Further investigation disclosed that the station had lost the phase modulation (PM) telemetry subcarrier. The crew was advised to switch the premodulation processor from normal to auxiliary at 65:41:00 to provide telemetry on the FM downlink. Over Carnarvon, at 66:20:00, the crew switched from the secondary transponder to the primary transponder. All PM downlink functions were restored with no further problems.

Computer MARK button.- At 70:09:00, the crew reported that depression of the MARK button had no effect on the onboard computer when the computer was in the platform orientation program. A computer self-check was performed, and all data appeared normal. A check on the MARK button/computer interface was performed, and the procedures failed to create an alarm, thus indicating that the malfunction was in the interface.

A bypass for the MARK button failure was accomplished by utilizing the backup alignment programs, which use the ENTER button input. Subsequently, it was discovered that bit 14 of flagword 2 was erroneously set. This bit is normally set to indicate to the computer that the MARK data is to be processed for a tracking target instead of a star or landmark. Bit 14 is automatically reset when rendezvous tracking sightings are terminated. The termination of the previous rendezvous tracking was incorrect, and the computer could not respond to the MARK button depression. The crew was given a procedure to verify the interface. This procedure was executed and the MARK button interface was verified.

Water in the command module.- At various times, the crew reported water in the cabin from three sources: the glycol lines in the environment control unit, the suit hoses, and the quick disconnect fitting on the water control panel.

At 79:02:00, the crew reported water on the aft bulkhead. They removed a panel on the environmental control unit, and discovered the source to be condensation of the cold glycol lines. Approximately

1 pint of water was reported to have collected in this area by 80:39:00. At 106:53:00, the crew described large "globbs" of water collecting on the unit, but they added that there was no apparent problem; the relative humidity was 70 percent and cabin temperature was 68° F, while the dew point was 58° F. Since the temperature of water/glycol returning from the radiators varied between 25° and 50° F during periods of low power levels, condensation on cold glycol lines could be expected.

At 79:30:00, the crew reported water coming from the suit supply hoses. The crew indicated that both accumulators functioned properly in AUTO mode during malfunction procedure evaluation. However, it was concluded that water in the suit hoses was condensation that was not removed from the suit heat exchanger because the cyclic accumulator did not operate automatically.

The crew reported that water leaked from the quick disconnect fitting in the waste water tank port on the water control panel each time the tank was dumped. This was found to be the result of a missing washer that is required for a seal between the fitting and the panel.

Rotational hand controller.- At 82:11:00, the crew reported an anomaly with the rotational hand controller no. 2, causing a loss of minimum impulse control in the minus pitch direction. This was diagnosed as a breakout switch problem. The crew proceeded through the malfunction procedures, and verified that there was definite thrust in the minus pitch direction. At 91:04:00, the problem solved itself, with no explanation.

Radiator degradation test.- The radiator degradation test began at 92:37:00, about 1 hour and 43 minutes earlier than planned. The test was moved up to allow landmark tracking over the United States on the last revolution of the day. An updated set of recorder operating times was relayed to the crew to augment the ground coverage during the test. An analysis has indicated that the test was successful, and the radiator degradation was not as severe as suspected. Thus the radiator is adequate for a lunar mission.

Mission event timer.- The crew reported at 102:46:50 that the digital event timer started running without any crew action. The oxygen tank 2 fan cycled on coincidently with the timer start. It is believed that electromagnetic interference caused by the cycling of the cryogenic fans caused the event timer to start.

Biomedical harness.- At 126:07:00, the Commander reported problems with the signal conditioner leads on his biomedical harness; however, signal conditioner leads were exchanged and adequate data were obtained. At 180:52:00, the Command Module Pilot reported that his biomedical signal conditioner was hot to the touch. There was a possibility of a shorted resistor between the 28 V dc power source and the dc-dc converter

on the harness. If this were the case, the wiring downstream of the resistor might ignite the cotton padding in the biomedical harness. Because of numerous problems throughout the mission with the biomedical harnesses and the potential danger, it was decided that the harnesses should be removed and stowed for the remainder of the flight.

Battery bus A and B voltage drop.- A drop of approximately 1 to 2 volts in battery buses A and B was detected between 137:30:00 and 139:00:00 hours. The crew performed open-circuit voltage checks with all loads removed; battery A indicated 36.1 volts and battery B, 35.9 volts, as expected. The batteries were then returned to the normal configuration. The analysis indicated that the voltage drop was caused by a normal transition of the peroxide level to the monoxide level in the batteries. Battery voltage should shift from approximately 1.85 volts per cell to 1.6 volts per cell at the time of the peroxide/monoxide shift, which occurs after approximately 9 to 11 A-h have been used from each battery.

Chlorine injector anomaly.- At 152:02:00, the commander reported a brown substance at the base of the chlorine injector. The crew were advised that this substance had been observed in preflight testing, and was a mixture of water, chlorine, and lubricant, and that it was not harmful to the crew.

Fuel cell condenser exit temperature.- Between 161:19:00 and 161:39:00, coincidentally with spacecraft power-up, the condenser exit temperature on fuel cell 2 began increasing and failed to stabilize at the normal power-up level. No other abnormal indications were observed during this period. The temperature increased to 180° F at 163:32:00 (normal is 155° to 165° F). At this time fuel cell 2 was open-circuited and allowed to cool down so that it would be available for the next service propulsion maneuver. Fuel cell 2 was placed back on line 30 minutes prior to the maneuver and remained on line through the maneuver and subsequent scheduled powered-up activities. Prior to spacecraft power-down at 171:20:00, the condenser exit temperature reached a maximum of 184° F and appeared to have stabilized. Subsequent to powering down, the temperature decreased to a level comparable with the exit temperature on fuel cells 1 and 3. Thereafter, when the spacecraft was powered up, the temperature on fuel cell 2 increased to 185° to 190° F but the fuel cell was not open-circuited again until just prior to entry, when it appeared that the temperature would not stabilize below 200° F. The increased load on fuel cell 1, caused by the first open-circuiting of fuel cell 2, resulted in an abnormal increase in fuel cell 1 condenser exit temperature which reached 175° F just prior to fuel cell 2 being placed back on line. This temperature then returned to normal. During all powered-down operations, the condenser exit temperature on fuel cell 3 dropped below the expected operating level. At 232:57:00, the

temperature dropped to 149° F, causing a master alarm indication. The anomalies associated with all three fuel cells are indicative of malfunctioning coolant bypass valves.

Flight director attitude indicator anomaly.- At 169:40:00, the crew reported that when the gyro display coupler was switched for display on flight director attitude indicator no. 1, the indicator switched about 180 degrees in pitch. Analysis indicated a possible relay problem and a test was suggested for making additional analysis. The test was not performed because it could result in the complete loss of indicator no. 1. At 192:10:00, the crew was advised they should not switch the gyro display coupler to indicator no. 1.

Solar flare.- At 231:08:00, the Solar Particle Alert Network facility at Carnarvon reported a Class 1B solar flare. The data were analyzed and it was confirmed that the flare would have no effect on the space-craft or crew. However, this solar flare exercise proved to be an excellent checkout of the systems and procedures that will be used in the event of a solar flare during a lunar flight.

Entry preparations.- At 239:06:11, the seventh service propulsion maneuver was performed satisfactorily in the stabilization and control system AUTO mode. This maneuver was performed to shape the orbit for the deorbit maneuver on the final day. The crew was advised at approximately 259:19:00 that a reaction control system/digital autopilot deorbit capability was available and that all the necessary equipment for a hybrid deorbit was working properly. Therefore, two backup deorbit techniques were available in the event of any malfunction of the primary deorbit system (service propulsion system). These two backup deorbit techniques existed throughout the entire mission.

8.1.4 Entry Phase

The deorbit computations appeared to be normal. The landing time based on tracking data from the last station (Carnarvon) prior to the deorbit maneuver, was about 0.7 second later than the loaded (computer) time. At the Honeysuckle site during the previous pass, the times were 0.11 second different. Part of the landing error is attributed to accumulated small errors in the state vectors that were loaded into the computer at approximately 4 hours before landing. At the last revolution over Merritt Island, the onboard computer indicated a position error of 4138 feet and a velocity error of 0.24 ft/sec. At Carnarvon, the errors were 3278 feet and 0.03 ft/sec. Such a close agreement occurred earlier than expected, and it was decided not to update the onboard computer load prior to deorbit. The deorbit maneuver was performed at 259:39:16, and the residuals were nulled to ± 0.1 ft/sec.

At command module/service module separation, the main bus voltage dropped to 25.9 volts on telemetry. The crew reported 25.5 volts onboard indication just after separation. Factors which contributed to this low voltage were that the batteries were relatively cold, and loads were 6 to 8 amperes higher than predicted entry loads. The batteries were also in a relatively depleted state.

The batteries were not fully charged because of the limitation on the number of charges and because the battery charger could not replace the energy removed from the batteries. The main bus voltage was observed to increase as the batteries warmed up under load and satisfactory voltage levels were supplied.

Only limited post-blackout radar data were received; however, antenna angles (azimuth) indicated that the spacecraft was very close to the target point. The pre-blackout radar data indicated the footprint to be about 8 miles uprange of the nominal.

Onboard computer target point	Landing point (onboard computer)	Landing point (recovery ship)
27° 37.8' N	27° 37.8' N	27° 32.5' N
64° 10.2' W	64° 10.8' W	64° 04.0' W

The recovery ship landing point data may have been as much as ± 7 n. mi. in error, and the indications are that the actual landing was very close to the target point.

8.2 NETWORK

The Mission Control Center and the Manned Space Flight Network were placed in operational status September 28, 1968, for the Apollo 7 mission.

Operation of the facilities and support by the personnel in the Mission Control Center were excellent, and only minor problems were encountered. On launch day, a facilities electrical power problem occurred at the Mission Control Center when a relay/circuit breaker was tripped. The breaker was immediately reset and power was restored in approximately 7 minutes. A short-circuit in the wiring to a cooling tower fan is suspected.

Air-to-ground communication quality was acceptable with variances depending on the mode, the spacecraft attitude, and the quality of the circuits to the ground stations. Communication support by the Satellite

Communications Agency was successful. The greatest cause for loss of air-to-ground capability was in the communications link between the Mission Control Center and a remoted site. In particular, HF communications to the network ships and to the Tananarive station were marginal throughout the mission. The VHF communications were usable but had the expected audio distortion. S-band communications were good. Support by the network aircraft (ARIA) using S-band communications was very good.

A high level of telemetry playback activity occurred during the mission; the only significant problem was that high-sample-rate contingency playbacks required more time than expected. The network sites appeared to have some difficulty in obtaining the necessary configuration for performing this operation. Almost 4000 commands were transmitted during the mission, and a spacecraft reject, ground reject, or loss of the command occurred on less than 1 percent of the commands attempted. The C-band and S-band tracking operations were conducted with no significant problems.

8.3 RECOVERY OPERATIONS

8.3.1 Landing Areas and Recovery Force Deployment

The Department of Defense provided recovery forces commensurate with the probability of a spacecraft landing within a specified area and with any special problems associated with such a landing (table 8.3-I). The location of the elements are shown in figure 8.3-1 and 8.3-2.

8.3.2 Command Module Location and Retrieval

After communications blackout, the first contact with the command module by recovery forces was an S-band signal received by airborne direction finding equipment. A VHF voice position report from the flight crew after main parachute deployment was the first indication that the spacecraft would near the planned target point. Voice contact was maintained until command module landing; however, the recovery beacon signals were not received until 13 minutes later.

Landing (fig. 8.3-3) occurred at 1112 G.m.t. on October 22, 1968, at latitude 27 degrees 32.5 minutes north and longitude 64 degrees 4 minutes west (approximately 290 n. mi. south of Bermuda). Landing time was based on the flight crew's voice report that the command module was descending through the 300-foot altitude level. The distance from the target point to the landing point was 7.7 n. mi. on a heading of 136 degrees from true North. Landing coordinates were determined onboard the primary recovery ship, USS Essex, by dead reckoning based on a loran fix.

at 0945 G.m.t.; during the preceding 10 days, loran fixes between 1000 and 1230 G.m.t. had been unreliable.

According to flight crew reports, the command module went to the apex down (stable II) position after landing and was uprighted 12 minutes later. During this period, the recovery aircraft received intermittent and erratic signals on the recovery beacon. When the command module was again upright (stable I), strong signals from the recovery beacon were received and voice contact was reestablished by the aircraft. The recovery 3 helicopter arrived 7 minutes later and deployed the flotation collar and swimmers. When the flotation collar was inflated, the flight crew began their egress from the command module and were then hoisted aboard the recovery helicopter. The flight crew arrived aboard the primary recovery ship 56 minutes after spacecraft landing. The command module was hoisted aboard 1 hour 51 minutes after landing (figures 8.3-4 and 8.3-5).

An aircraft carrying the flight crew departed the recovery ship at 1256 G.m.t. on October 23, 1968, and arrived at Cape Kennedy at 15⁴⁵ G.m.t.

The following is a chronological listing of significant events during recovery operations:

October 22, 1968

<u>G.m.t.</u>	<u>Event</u>
1105	S-band contact by recovery aircraft
1107	VHF (296.8 MHz) voice reception by recovery forces
1112	Command module landed (went to stable II position)
1120	Initiation of inflation of flotation bags
1124	Command module uprighted to stable I position
1125	Recovery beacon (243.0 MHz) reception by recovery aircraft
1126	Reestablished VHF (296.8 MHz) voice communications
1132	Visual sighting of command module from recovery helicopter
1134	Swimmers and flotation collar deployed
1143	Flotation collar installed
1147	Command module hatch opened
1200	Flight crew aboard recovery helicopter
1208	Recovery ship arrived at command module
1303	Command module hoisted aboard recovery ship

Weather conditions, as recorded onboard USS Essex at the time of command module retrieval, were as follows:

Wind direction, deg true	260
Wind speed, knots	16
Air temperature, °F	74
Water temperature, °F	81
Cloud cover	600 ft overcast
Visibility, n. mi.	2
Light rain showers	
Sea state	
Height, ft	Waves Swells
3	3
3	3
Direction, deg true	260 110

All recovery equipment except the flotation collar and the recovery hook performed normally. The flotation collar appeared not to fit correctly around the command module. An investigation of this problem has been initiated. Prior to retrieval, an auxiliary recovery loop had been attached to the command module in order to increase the safety factor of the command module recovery loop. The cable of the auxiliary recovery loop and the command module recovery loop were taped together before the hoisting operation. The size of the resulting cable made it difficult to properly engage the recovery hook from the ship.

8.3.3 Direction Finding Equipment

The following table summarizes the signal reception of the S-Band (2287.5 MHz) and recovery beacon (243.0 MHz) reception equipment.

S-Band Equipment				
Aircraft	Initial time of contact, G.m.t.	Initial reception range, n.mi.	Type receiver	Aircraft position
Kindley	1105	135	AN/ARD-17	26°46'N
Rescue 1 (HC-130H)				68°10'W
Kindley	1106	215	AN/ARD-17	28°10'N
Rescue 2 (HC-130H)				60°07'W

VHF Recovery Beacon Equipment

Aircraft	Initial time of contact, G.m.t.	Initial reception range, n.mi.	Type receiver	Aircraft position
Kindley Rescue 2 (HC-130H)	1125	168	AN/ARD-17	27°29'N 60°55'W
Recovery 2 (SH-3A)	1128	21	SARAH	27°23'N 63°45'W
Recovery 1 (SH-3A)	1129	72	SARAH	27°49'N 64°39'W
Air Boss (SH-3A)	1129	12	SARAH	27°29'N 63°52'W
Recovery 3 (SH-3A)	1130	4	SARAH	27°34'N 64°04'W

8.3.4 Command Module Postrecovery Inspection

The following is a summary of observations made during the recovery and postrecovery operations:

- a. The uprighting bags remained inflated and the command module remained in the stable I position after uprighting. When the command module was retrieved, the plus Y bag was partially inflated and the minus Y and plus Z bags were fully inflated. One of the swimmers reported that he fell against the plus Y bag during installation of the auxiliary recovery loop. A small amount of water was found in the plus Z bag.
- b. The toroidal bay was full of water.
- c. The flashing light was erected but was activated only briefly by the flight crew to verify that it would operate satisfactorily.
- d. The fluorescein sea dye was not deployed.
- e. Both VHF antennas were deployed properly. The blade and whiskers on antenna number 1 were bent during the retrieval operation.
- f. The main parachute disconnect operated properly.
- g. The apex cover was not sighted; however, a piece of recovered insulation material was believed to be from this cover.
- h. The drogue disconnects operated properly.

- i. Approximately 2 gallons of liquid was found inside the command module. A sample of the liquid was taken for future analysis.
- j. All windows were fogged between the panes but cleared within approximately 4 hours. The outer pane of the rendezvous windows had a very thin iridescent residue that had not cleared before the window covers were installed.
- k. A hole was punctured in the aft bulkhead when a camera pack (not a flight item) was dropped while the command module interior was being photographed.
- l. Gouges in the aft heat shield were apparently made by the retention rings on the flotation collar.

8.3.5 Command Module Deactivation

The command module was off-loaded from USS Essex at the Norfolk Naval Air Station on October 24, 1968. The Landing Safing Team started evaluation and deactivation at 1400 G.m.t. Inspection of the command module pyrotechnics indicated that all of the normally activated pyrotechnics had fired. The remainder of the pyrotechnics were safed by removal of the initiator from the squib valve body. The reaction control system propellants were expelled into the ground support equipment and measured; system A had approximately 2.8 gallons of fuel remaining and system B had approximately 4.8 gallons. The amount of oxidizer could not be accurately measured because of the high boil-off rate. No leakage was detected in the engine injection valves. Deactivation was completed at 0130 G.m.t. on October 27, 1968. The command module was transported to Long Beach, California, and delivered to the contractor's facility.

Table 8.3-I-- RECOVERY SUPPORT

Landing area	Max retrieval time, hr	Max access time, hr	Support	Remarks
Launch site	-	1/2	LCU(1) CH-3C(1) HH-3E(1) HH-53C(2) K-501(2) LVTR(2)	Landing craft utility (landing craft with command module retrieval capabilities) Helicopter with 3-man rescue team Helicopter with 3-man swim team Helicopter capable of lifting the command module; each with 3-man swim team Fire suppression fits, each with 3 firemen Landing vehicle tracked retriever (tracked amphibious vehicles with command module retrieval capabilities)
Launch abort	24 (Area A)	4	CVS(1)	Primary recovery ship, aircraft carrier, USS Essex
	48 (Area B)		AKA(1) AIS(1) APA(1) HC-130H(3)	Attack cargo ship, USS Arneb Apollo Instrumentation Ship, USNS Vanguard Attack transport, USS Cambria Fixed wing search and rescue aircraft, each with 3-man pararescue team

Table 8.3-I.- RECOVERY SUMMARY - Concluded

Landing area	Max retrieval time, hr	Max access time, hr	Support	Remarks	
Secondary	12 (Zone 1)	6 (Zone 1)	AKA(1)	USS Arneb, redeployed from launch abort area	
	24 (Zone 2)	6 (Zone 2)	APA(1)	USS Cambria, redeployed from launch abort area	
	24 (Zone 3)	6 (Zone 3)	DD(2)	Destroyers, USS Rupertus and USS Tucker	
	12 (Zone 4)	6 (Zone 4)	DD(2)	Destroyers, USS Cochran and USS Nicholas	
Primary	12	2	HC-130H(8) (2 each zone)	Fixed wing search and rescue aircraft, each with 3-man pararescue team (includes 3 used supporting launch abort areas)	
			CVS(1)	USS Essex, redeployed from launch abort area	
			SH-3A(5)	Helicopters, three recovery with 3-man swim teams, one photographic, one air traffic control	
Contingency		18	E-1B(1)	Fixed-wing aircraft, communications relay	
			HC-130H(18)	Fixed wing search and rescue aircraft, each with 3-man pararescue team (includes 8 supporting the four recovery zones)	
 Totals:					
Fixed-wind aircraft		19			
Helicopters		9			
Ships		8	(excluding Vanguard)		

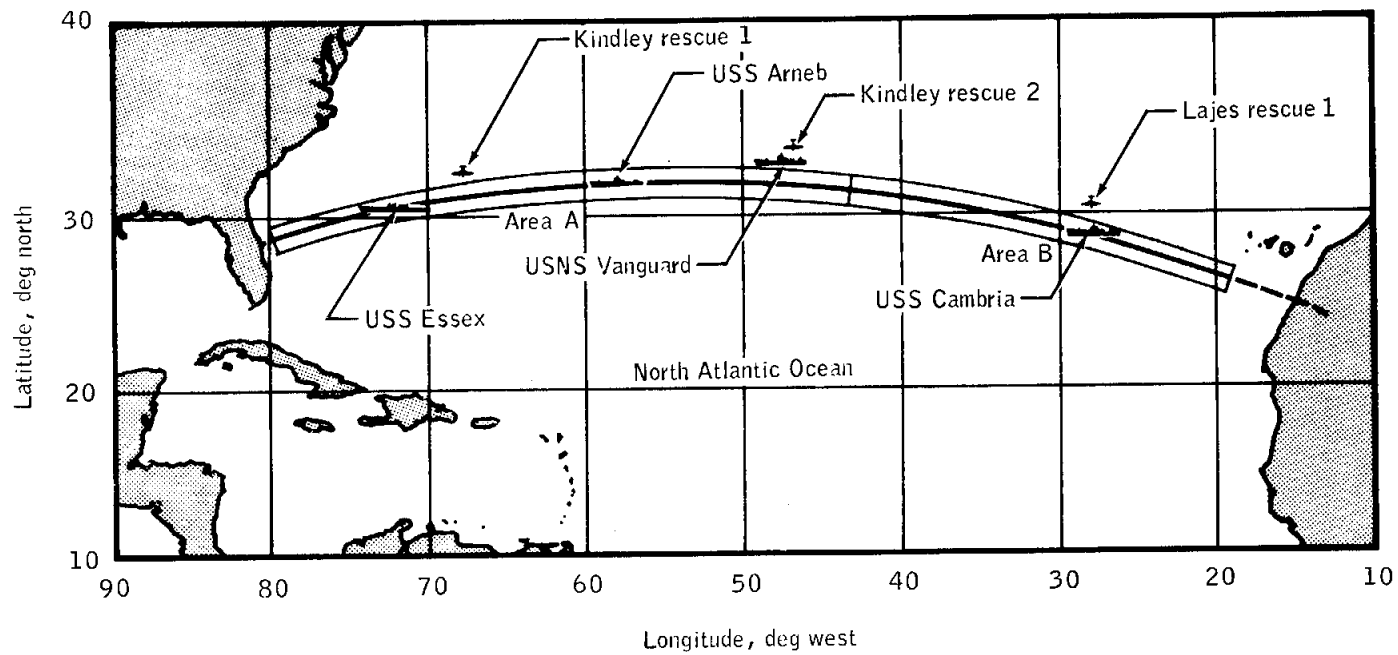


Figure 8.3-1.- Launch abort areas and recovery force deployment.

NASA-S-68-6385

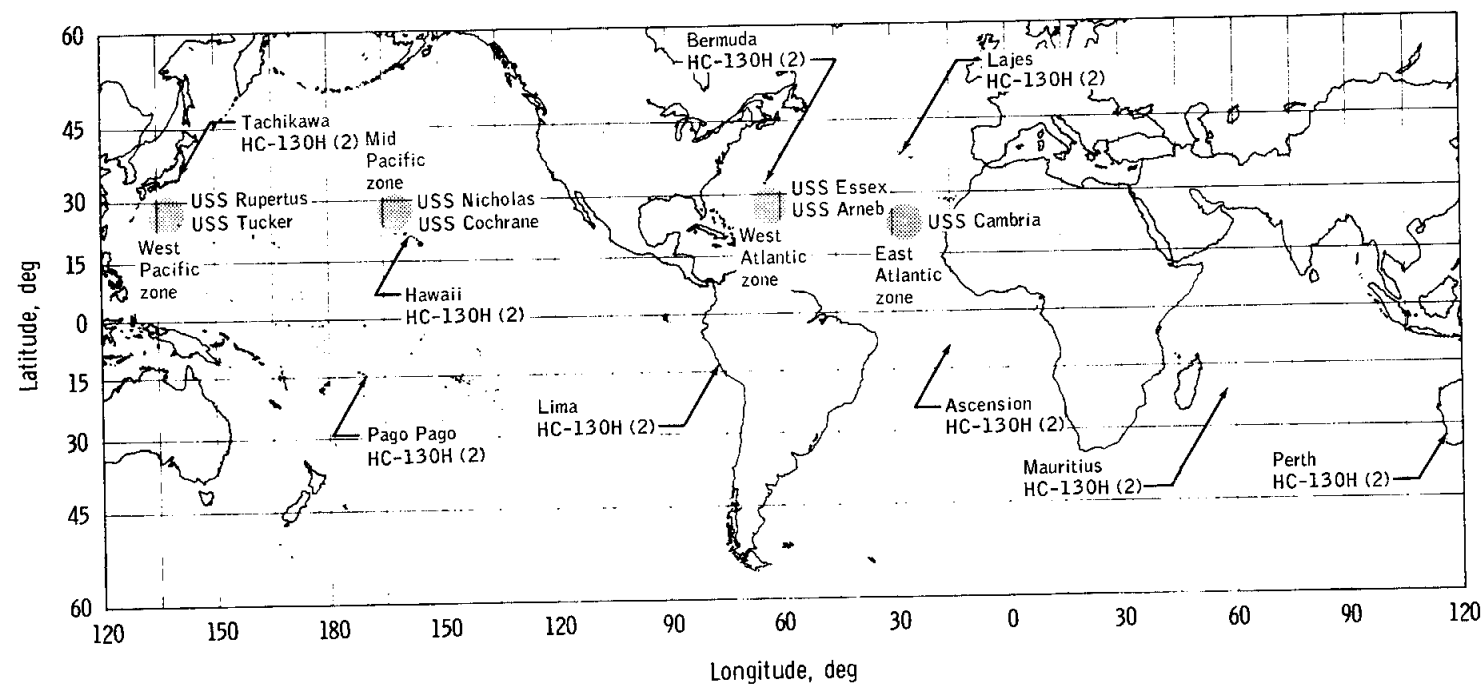


Figure 8.3-2. - Recovery zones, aircraft staging bases, and recovery force deployment.

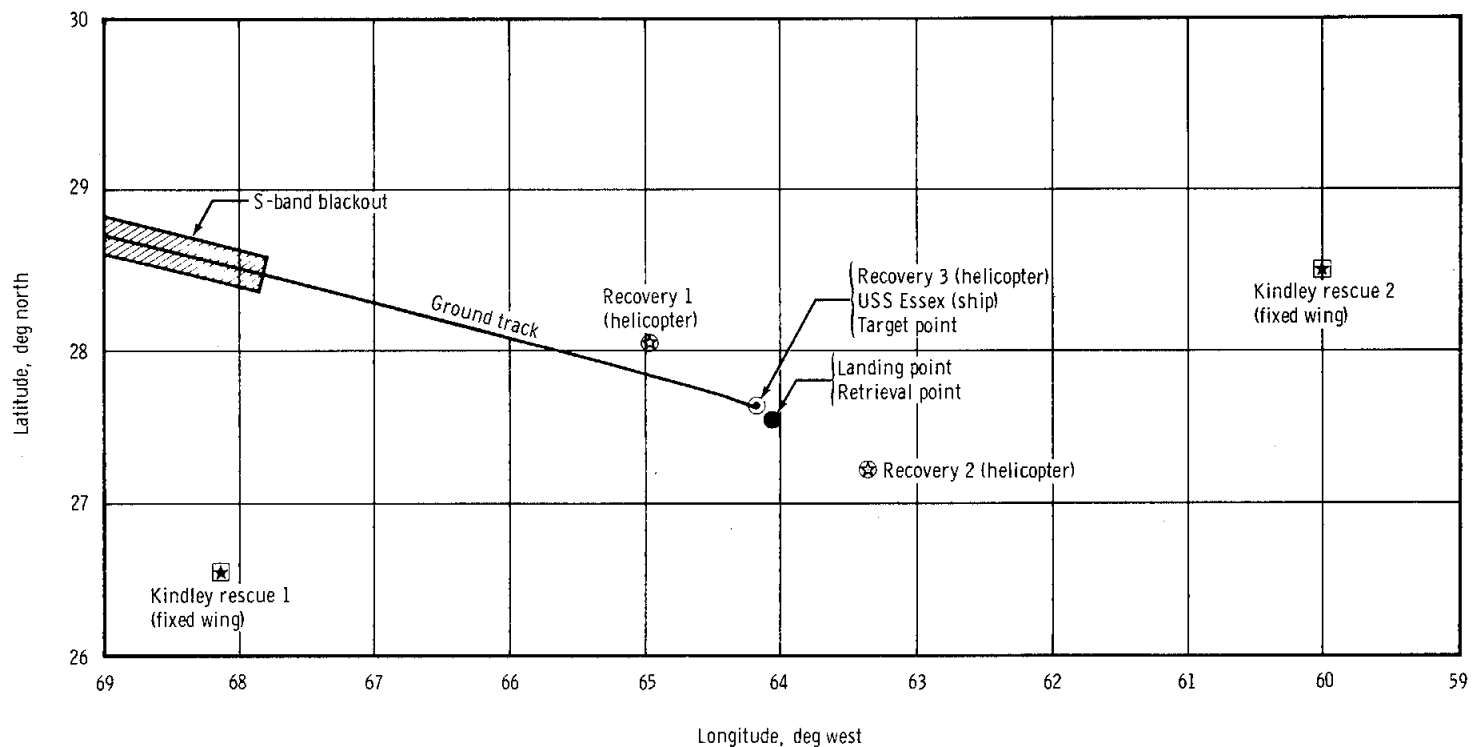


Figure 8.3-3. - Predicted entry trajectory and recovery force deployment.

NASA-S-68-6387

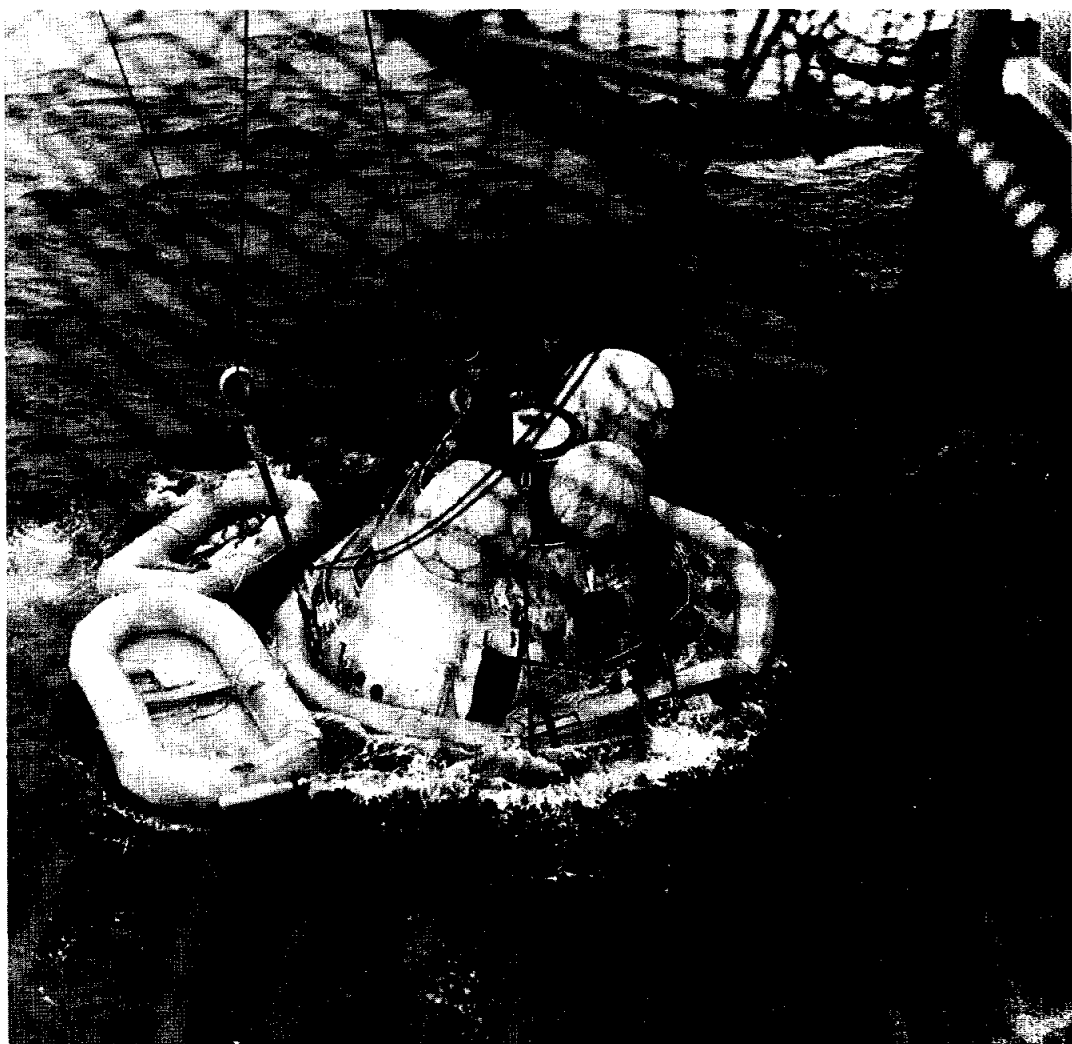


Figure 8.3-4.- Command module in flotation collar.

NASA-S-68-6388

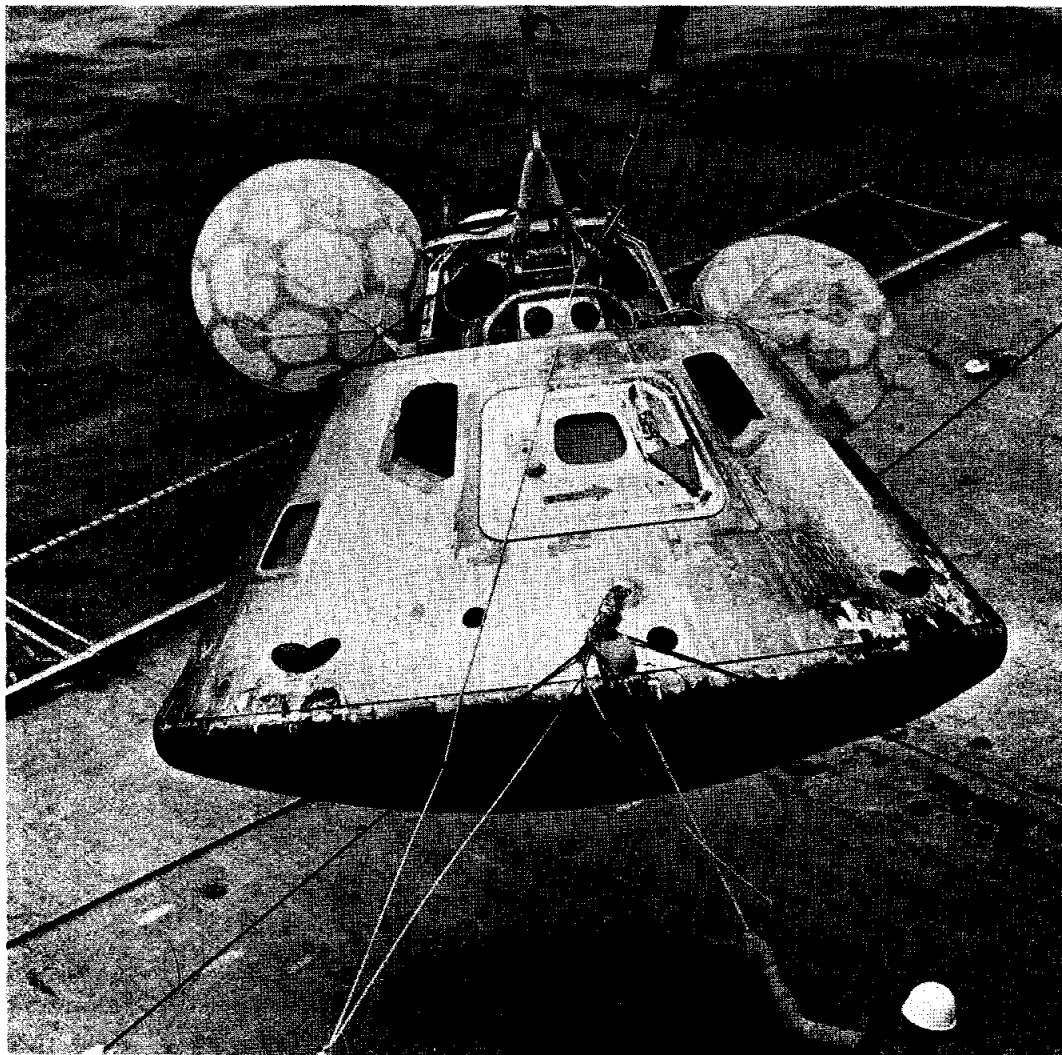


Figure 8.3-5.- Command module aboard recovery ship.

9.0 EXPERIMENTS

Specific experiments included on the Apollo 7 mission were experiments S005 (Synoptic Terrain Photography) and S006 (Synoptic Weather Photography). The photography was also reviewed by a cross section of disciplines in the scientific community. Comments regarding the general applicability of the photography to scientific uses are as follows:

- a. Geography - The two major areas of use in geography are in urban analysis and in land use and regional planning. A land use study of the internal structure of New Orleans can be made, as well as continuing land use and regional planning studies from space photography of the Imperial Valley and the California coast.
- b. Cartography - The additional coverage of this photography is of some value for photographic mosaic preparation, including extension of the coverage of mosaics and photographic maps compiled from Gemini and Apollo 6 photography. Certain areas covered by previous space photography as a means of detecting changes for purposes of updating existing maps.
- c. Meteorology - There are sufficient "cloud street" views in this photography, over known locations and at known times, to provide useful information for the study of this phenomenon. Hurricane dynamics can be studied from the views of Gladys and Gloria. Additional characteristics of sea breeze effect, clearing over lakes and rivers, and structure over mesoscale systems can be also gained.
- d. Oceanography -- The repetition of this photography over certain areas, as the Gulf of California, affords the opportunity for view of specific areas under different camera angles, sun angles, and atmospheric conditions and also provides a record of dynamic feature changes. As an example, sea surface patterns in the Gulf of California are enhanced by the sun's glint on this photography and were not evident on previous space photography showing no sun glint.
- e. Geology - The photography is closer to Gemini than to Apollo 6 photography, which was better for geologic uses. Because most of the views in Gemini and Apollo 7 are oblique, true shapes of surface features tend to be distorted or obscured. In geology, the main use of oblique photography is to show an introductory or complementary view to vertical photography, which is preferred.
- f. Hydrology - For hydrologic purposes, the Apollo 7 photography will be of use, though limited, for three purposes. They are (1) general descriptive hydrology of river basins, lakes, irrigated land uses,

et cetera; (2) qualitative analysis of bottom topography and sediment transport using the more oblique views and near sun glint areas; and (3) semi-quantitative measurements of bottom topography and sediment transport using the near-vertical photography where sun glint is not too close to the area of interest.

g. Agriculture/forestry - In the southwestern United States, brushlands, timberlands, grasslands can be differentiated fairly well on some of the views. A few of the photographs, although they are oblique views, can be useful for evaluation of vegetation and related resource features.

9.1 EXPERIMENT S005 — SYNOPTIC TERRAIN PHOTOGRAPHY

The objectives of the Synoptic Terrain Photography experiment were to obtain high-quality photographs of selected land and ocean areas for geologic, geographic, and oceanographic study and to evaluate the relative effectiveness of color versus black-and-white film. Nadir photographs were desired, particularly in sequences of three or more overlapping frames.

Of the more than 500 photographs obtained during the Apollo 7 mission, approximately 200 are usable for the purposes of this experiment. In particular, a few near-vertical, high sun angle photographs of Baja California, other parts of Mexico, and portions of the Middle East will be very useful for geologic studies. Pictures of New Orleans and Houston are generally better for geographic urban studies than those obtained on previous missions. The first extensive photographic coverage of northern Chile, Australia, and other areas was obtained. A number of areas of oceanographic interest were photographed for the first time, particularly islands in the Pacific Ocean.

The objective of comparing color with black-and-white photography of the same areas was not successful because of problems with focus, exposure, and filters.

A hand-held modified 70-mm Hasselbald 500C camera with 80-mm focal length lens was used for this photography experiment. S0-121 film was used for the synoptic weather and terrain experiments, and S0-368 was used for both operational and experiment photography. A type 2A filter was used with all but one of the magazines containing the S0-121 film, and no filter was used with the S0-368 film.

In general, the color and exposure quality of the pictures on the S0-368 film was excellent. Some problems were encountered in exposing the S0-121 film, and many frames were either underexposed or overexposed.

The need to change the film magazines, filters, and exposure settings hurriedly when a target came into view probably accounts for the improper exposure of many frames. Another factor contributing to underexposure was the use of a 1-degree field of view spot-meter to determine settings of the camera that has a field of view of approximately 52 degrees. By using corrective photographic processing techniques, many of the exposure problems can be corrected.

Sharpness ranged from fair to excellent on both films, with a problem in holding the camera steady a probable factor in those frames containing blurred images. Swells on the sea surface were resolved on both films.

The following regional areas and problems are now under study using the Apollo 7 photographs, as well as Gemini and Apollo 6 photography.

Geologic mapping of Baja California. - Apollo 7 photography of Baja California is considered, for geologic studies, superior in several ways to Gemini and Apollo 6 photography (fig. 9.1-1). The higher sun angle on the Apollo 7 imagery appears low enough to prevent wash-out and still retain an adequate shadow pattern from the topography which is necessary for geologic structural mapping.

Structural geology of the Middle East. - Several of the Apollo 7 photographs were taken over areas in the Middle East previously photographed during the Gemini flights (fig. 9.1-2). The Apollo 7 photography again shows the amount of detail that can be observed of the topographic and geologic features for the purpose of regional mapping.

Origin of the Carolina bays, United States. - A number of elliptical bays can be observed on the Apollo 7 photographs of southeast Brazil (fig. 9.1-3) and of Louisiana. Comparisons of these bays with the Carolina bays add further knowledge regarding the origin of these striking features, suggesting that they were not formed by the impact of meteorites but by terrestrial processes.

Wind erosion in desert regions. - Again the Apollo 7 photography complements the Gemini photography of large arid regions affected by natural forces (fig. 9.1-4). Extensive areas of abraded rock knobs and ridges, sculptured and formed by wind containing the erosion agents, and areas of great sand plains and dunes can be further studied on the Apollo 7 photography to determine the actual importance and character of wind erosion in desert regions.

Coastal morphology. - Apollo 7 photography covers a number of new shorelines and coastal features not previously photographed from space, as well as several areas previously shown on the Gemini and Apollo 6 photographs (fig. 9.1-6). Studies will be made of changes in shorelines,

river deltas, and submarine topography by comparing space photographs with maps, charts, and hydrologic information currently available.

Rift valley tectonics.- Photography taken at different oblique views, altitudes, and sun angles of the highlands bordering the Red Sea and the Gulf of Aqaba reveal structural conditions that may help determine the origin of the African rift valley (fig. 9.1-6) Preliminary study reveals no evidence of lateral displacement along the Dead Sea rift.

NASA-S-68-6389

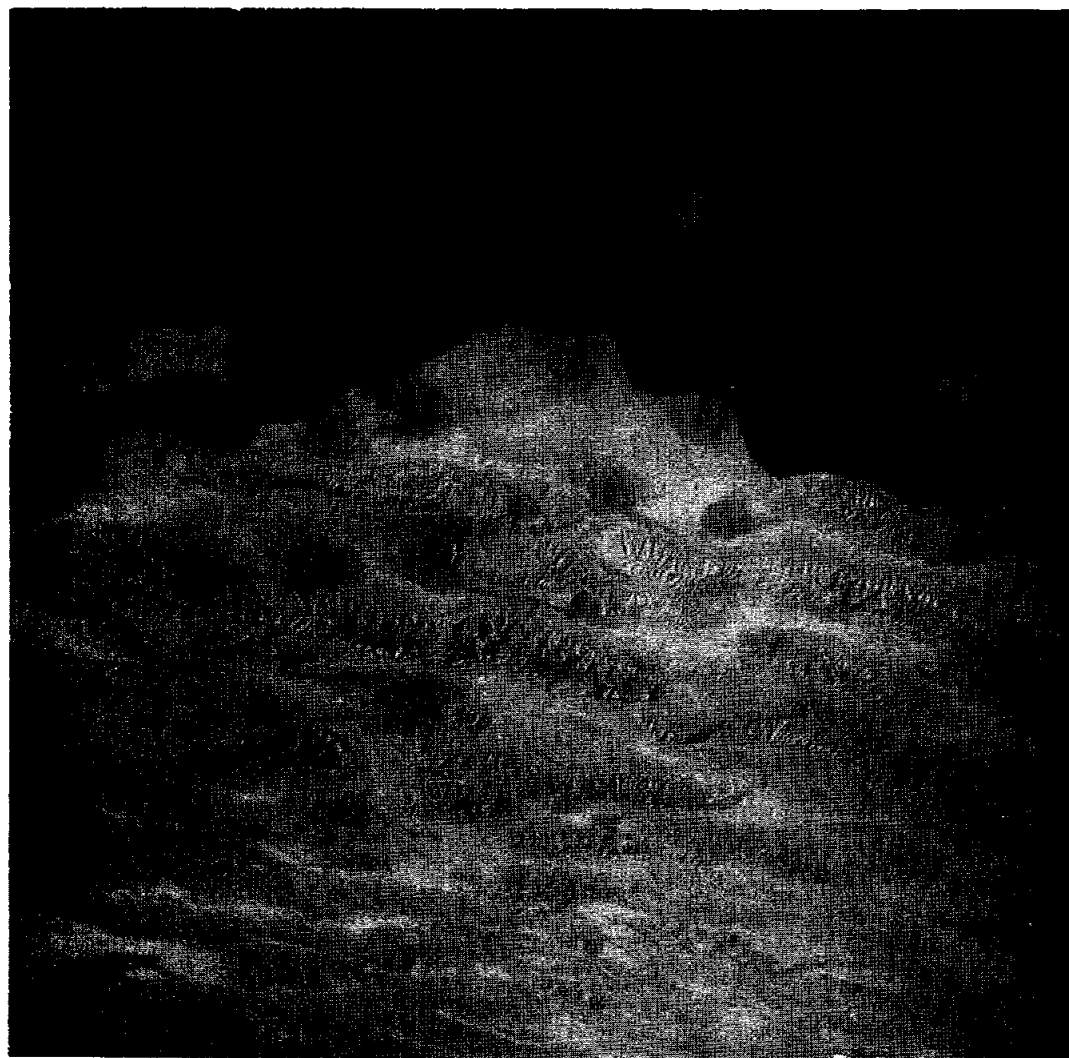


Geologic features show very well, partially because of a good sun angle.

Figure 9.1-1.- Mexico, Gulf of California, central Baja California,
mainland north of Guaymas.

9-6

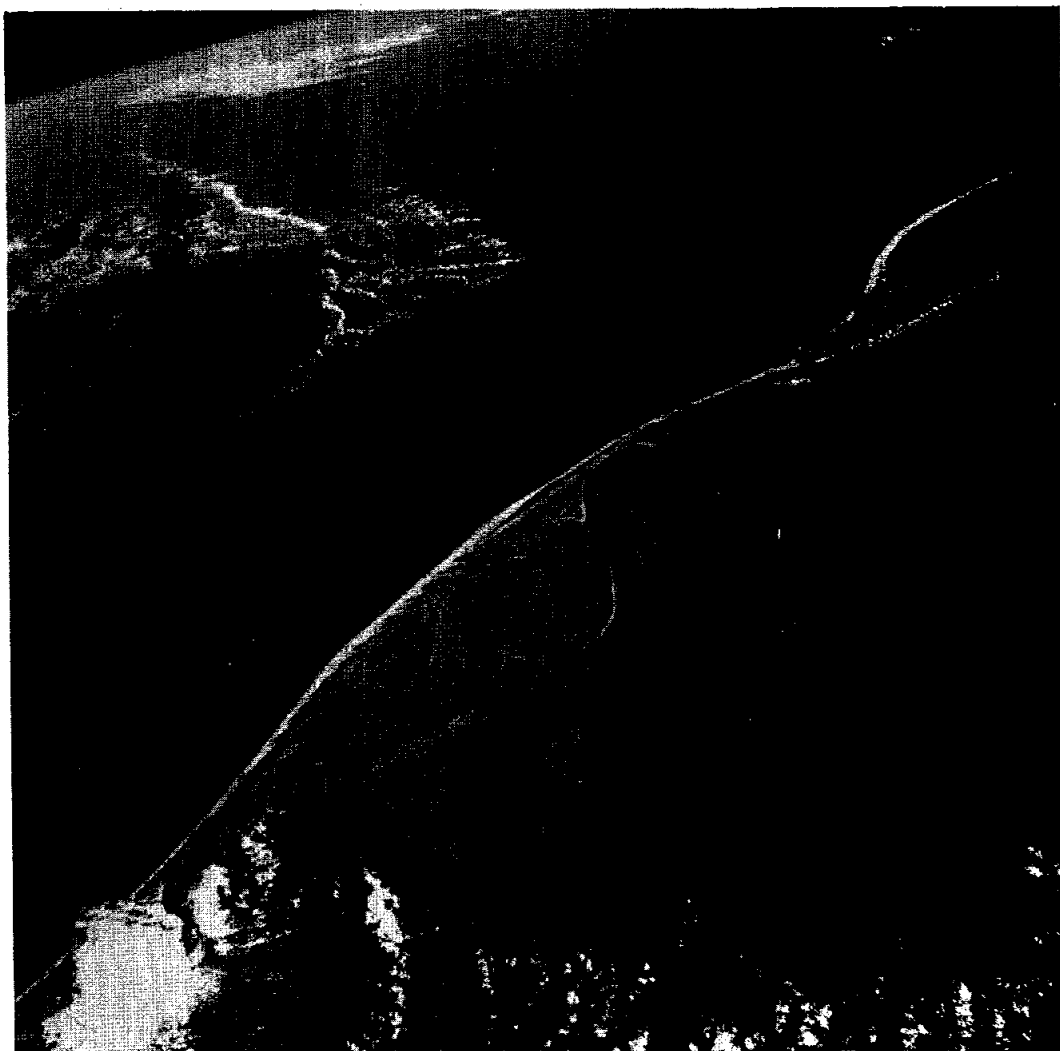
NASA-S-68-6390



Photograph taken almost vertically shows great amount of detail for topographic and geologic mapping.

Figure 9.1-2.- Iran, Persian Gulf coast.

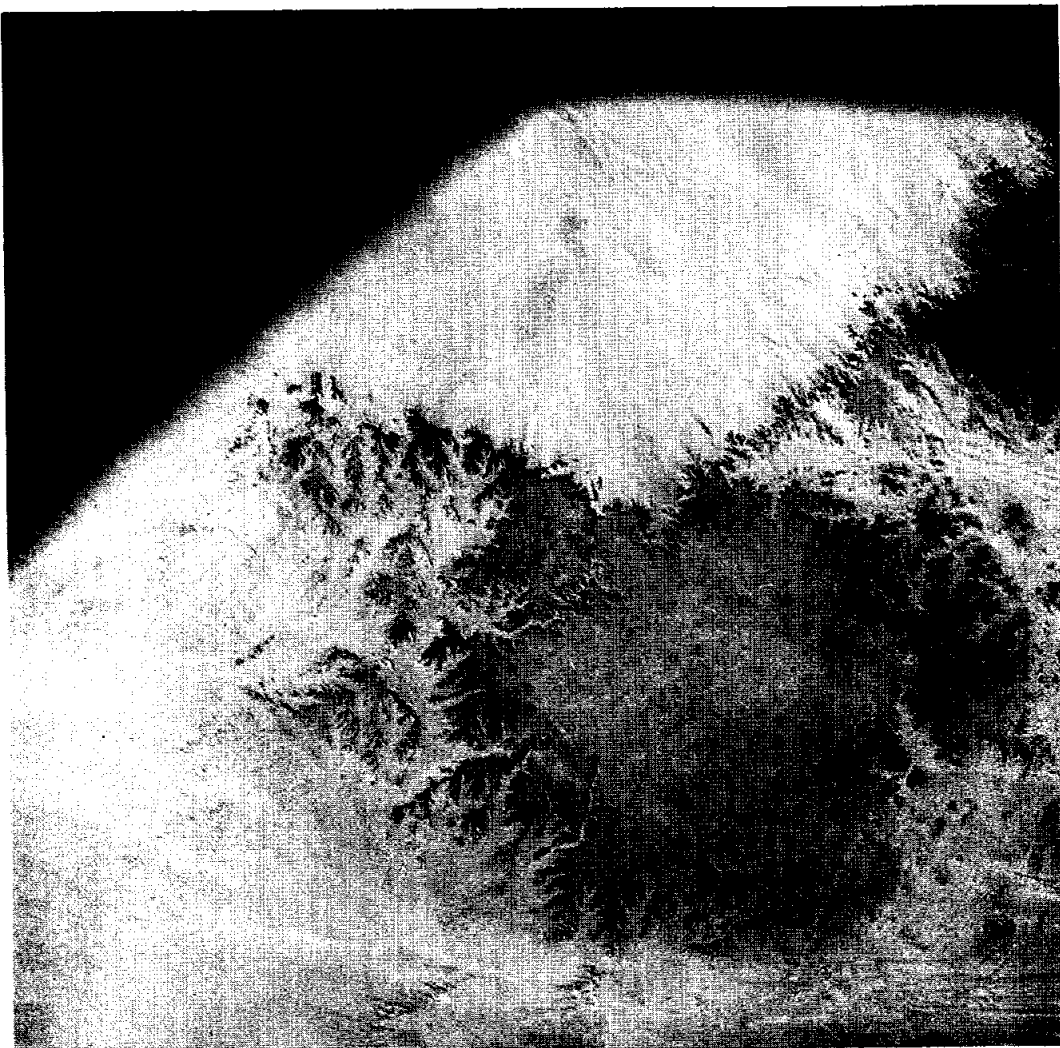
NASA-S-68-6391



These elliptical bays can be compared with those found on the Carolina and Louisiana coasts.

Figure 9.1-3.- Brazil, Uruguay, Atlantic coast, Lagoa dos Patos, Lagoa Mirim.

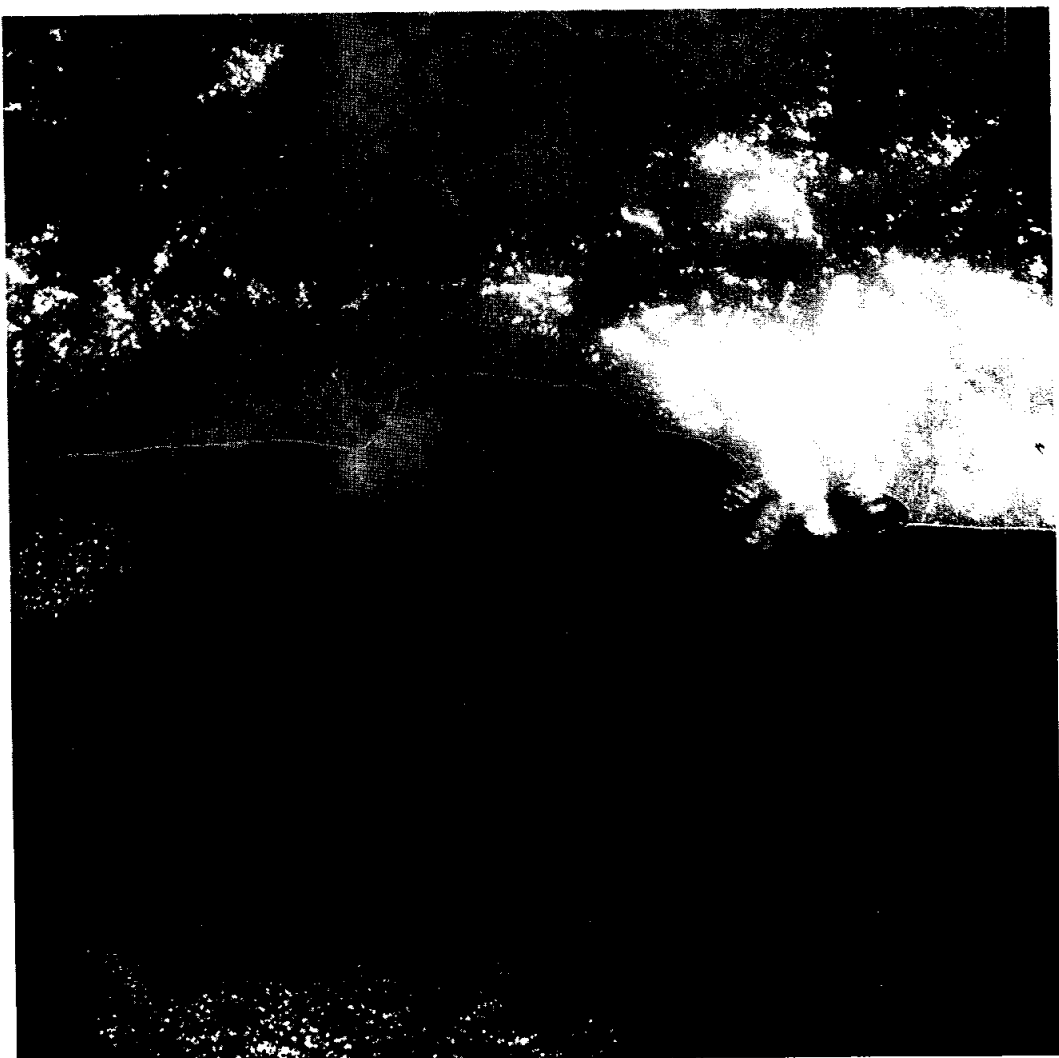
NASA-S-68-6392



This example of a desert shows the effects of wind and water erosion.

Figure 9.1-4.- United Arab Republic, Gilf Kebir Plateau.

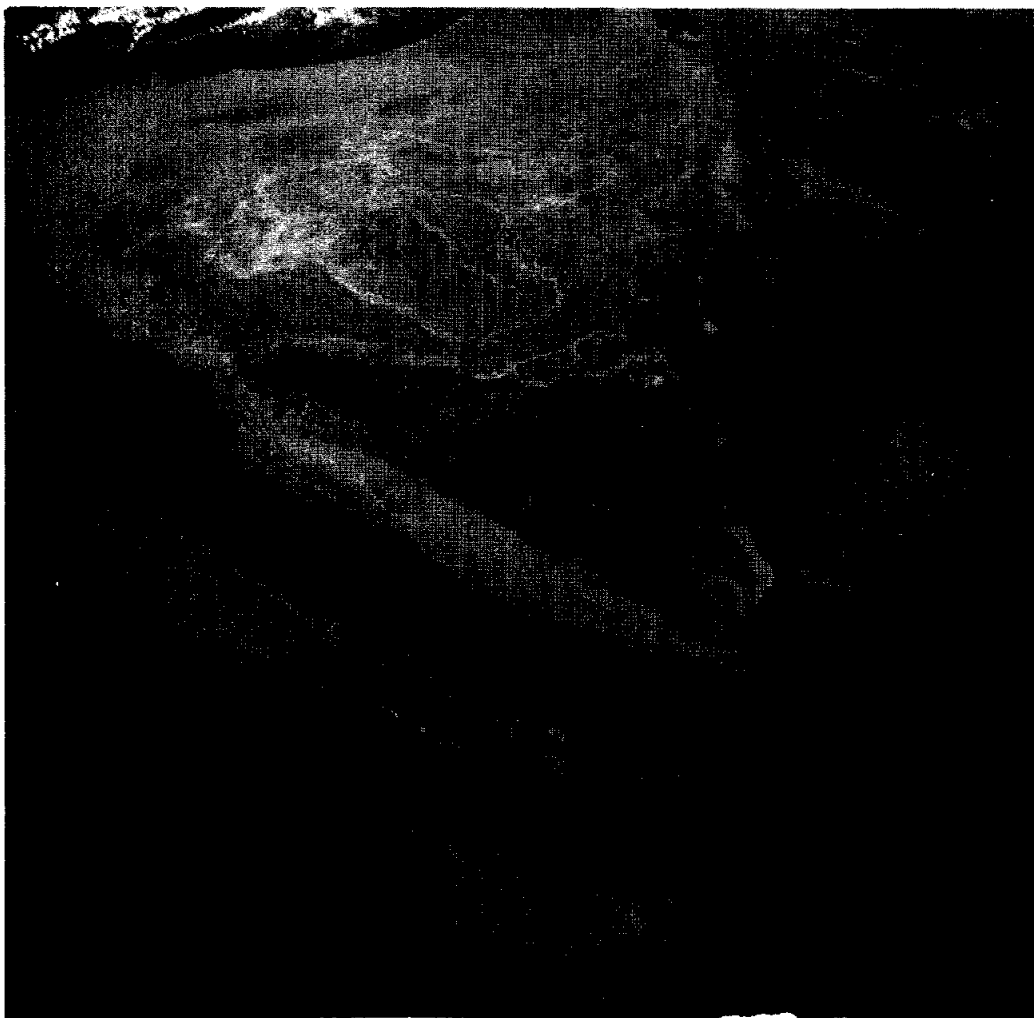
NASA-S-68-6393



Coastline and coastal features, as well as the sediment outflow of the Balsas River, can be seen.

Figure 9.1-5.- Mexico, Bahia de Petacalco, Balsas River.

NASA-S-68-6394



The African Rift Valley system can be seen in this photograph.

Figure 9.1-6.- Sinai Peninsula, Gulf of Suez, Gulf of Aqaba.

9.2 EXPERIMENT S006 — SYNOPTIC WEATHER PHOTOGRAPHY

The objective of the Synoptic Weather Photography experiment was to secure photographic coverage of as many as possible of 27 basic categories of weather phenomena. Of the approximately 500 70-mm color pictures obtained, approximately 300 show clouds or other items of meteorological interest and approximately 80 contained features of interest in oceanography. In addition to the many photographs of ocean areas, a number of pictures were obtained over the following geographic areas: southern United States, northern Mexico, northeastern Africa, southern and eastern Asia, western and northern Australia, and the Hawaiian Islands. A general summary of the phenomena which are considered worthy of further study are shown in table 9.2-I.

Two types of film, SO-121 and SO-368, were used in a modified 70-mm Hasselblad camera. Many frames of the SO-121 film were overexposed or underexposed. Even when properly exposed, the SO-121 film exhibited an excessive magenta coloration in the highlights. By using corrective processing techniques, many of the exposure problems can be eliminated. Image sharpness ranged from fair to excellent on both films, with steadiness in holding the camera a probable factor in those frames tending to contain blurred images. Ocean swells could be resolved on both films from altitudes near 100 n. mi.

Excellent views of Hurricane Gladys and Typhoon Gloria were obtained. Figure 9.2-1 shows one of a series of views taken of Hurricane Gladys at 1531 G.m.t. on October 17, 1967. This view, and others taken during this revolution, are the best color photographs of a tropical storm circulation taken from space. Views of tropical storms taken during other space flights typically included only part of the storm area or were dominated by a high cirrus deck. In this view, when the storm was just west of central Florida, the spiral bands of shower activity, characteristic of tropical storms, are easy to detect. There is a typical, although relatively small, deck of cirrus over the storm, but the circular cap near the eye is unusual. Such clouds are normally formed when the rising air from a very active cumulonimbus cloud is retarded by the stable air above the tropopause and, in the absence of wind shear, spreads out in all directions. Sometimes the outflow appears to be in a wavelike motion, creating concentric rings of more prominent clouds.

For comparison, figure 9.2-2 shows the ESSA-7 weather satellite picture of Hurricane Gladys taken about 4 hours after the exposure in figure 9.2-1. Such operational satellite pictures routinely are used to show the locations and gross features of meteorological systems. The color photograph enables the meteorologist to ascertain much more accurately the types of clouds involved.

Figure 9.2-3 is a photograph of Typhoon Gloria taken at 0026 G.m.t. on October 20, 1968, and is one of the best views from space of the eye of a tropical storm. Again for comparison, the ESSA-7 view (fig. 9.2-4) taken about 5 hours later shows the large well formed eye of this storm.

The effects of islands on the cloud distribution and on the wind field, as shown by cloud patterns, is well illustrated by photographs of the scale and quality of those obtained on the Gemini and Apollo 7 flights. One example is the picture of Oahu, Hawaii (fig. 9.2-5). Here the trade wind flow from the east has apparently been split by the island resulting in convergence and cloud lines on the lee side of the island.

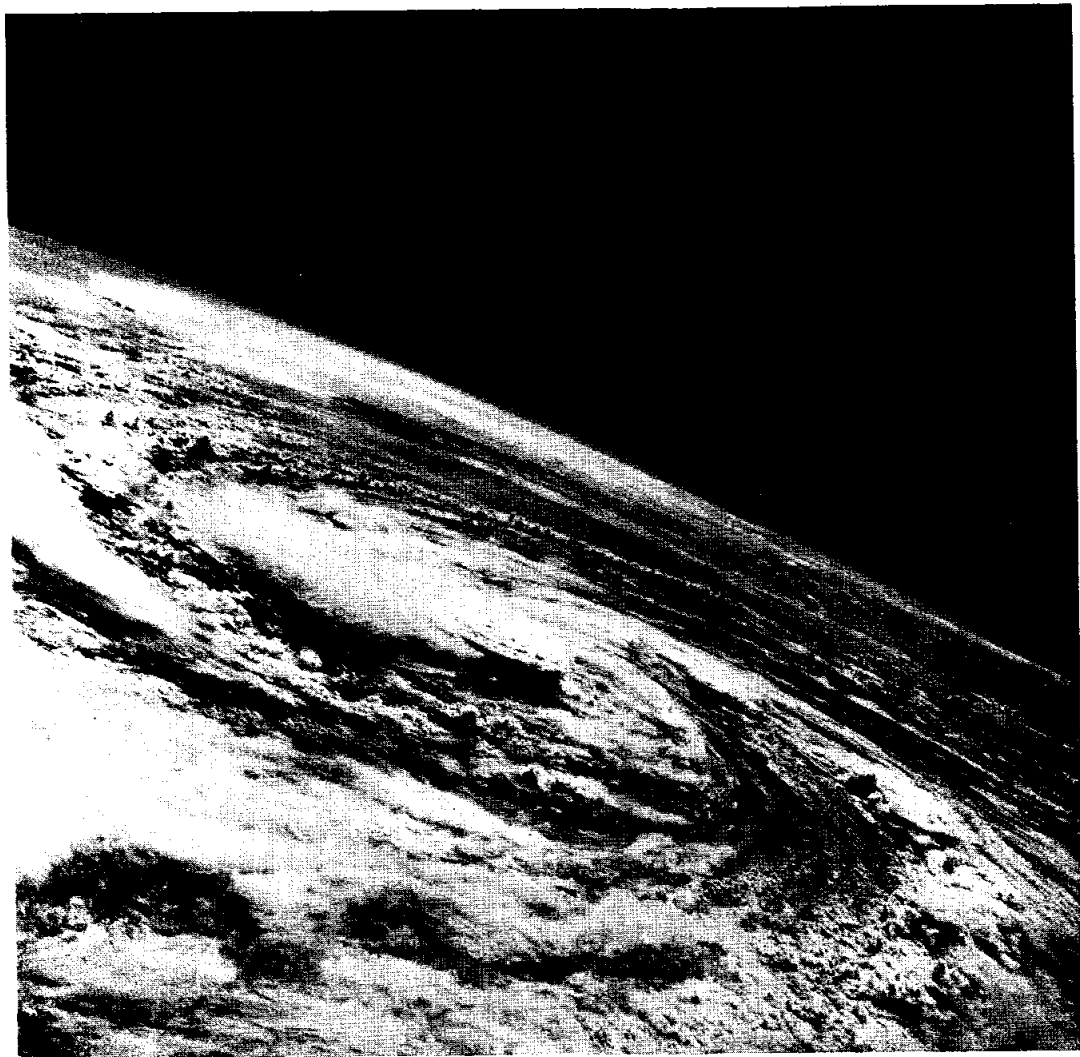
Oceanographic surface features have been revealed more clearly in the photographs from this mission than in any of the preceding manned flights. Phenomena such as eddies, slicks, swells, and other lines are indicators of surface water motion. One of the most remarkable photographs from space is given in figure 9.2-6. This view, featuring the Indonesian Islands of Biak and Supiori, shows a faint but definite pattern of ocean waves — more properly swells — north of the islands. The wave spacing is about 1000 feet. Also, the surf line appears brighter and wider on the northern reefs and beaches than on the southern coast. It is probable that the swells originated from the winds of Typhoon Gloria, which for several days was located some 1200 to 1500 miles to the north.

The various patterns on the sea surface are especially evident when the sun's reflection is photographed. Sediment discharged from rivers into the sea discolors the water, making it possible to see the movement of coastal waters by currents. A careful study and interpretation of these phenomena can produce information on wind direction and on slicks, which frequently show the presence of internal waves. Marine meteorology is strongly influenced by the interaction between the air and the sea. Sun glint photographs showing large areas of the sea surface can be a most useful tool in studying marine weather.

TABLE 9.2-I.- EXPERIMENT 5006 PHOTOGRAPHY

General category	Phenomena	Location
Weather systems	1. Tropical storms	Florida, Pacific Ocean
	2. Thunderstorms	United States, S.E. Asia, South America
	3. Frontal zones	United States
	4. Cellular stratocumulus	Eastern Pacific Ocean, Eastern Atlantic Ocean
Winds	1. Cumulus cloud lines	United States
	2. Sea swells	Biak, Socotra
	3. Sea breeze zone	United States, Brazil
	4. Cirrus anvil clouds	United States, Africa, Australia
	5. Jet-stream cirrus clouds	Africa, Australia
	6. Billow clouds	United States
	7. Smoke plumes	Australia, Southern U.S., Hawaii
	8. Sand dune alignment	Africa, Asia
	9. Surf zone	Coasts, islands
Ocean surface	1. Vortices	Biak, Socotra, Persian Gulf, Gulf of California
	2. Sea swells	Biak, Socotra
	3. Slicks and lines	Gulf of California, Persian Gulf
Underwater zones	1. Ocean bottom configuration	Australian reefs, Pacific atolls, Bahama banks, Cuba
	2. Turbid water patterns	Coastlines, gulfs
Landform effect	1. Mountain lee clouds	Sierra Nevada, Hawaiian Islands, Canary Islands
	2. Eddy clouds	California coast, Cape Rhir
Climatic zones	1. Snow line and cover	Asian mountains
	2. Vegetation boundary	Africa, mountain slopes
Hydrology	1. Snow cover	Asian mountains
	2. Streams and lakes	Lake Chad, United States

NASA-S-68-6395



Spiralling cloud bands in this southeasterly view are especially clear.
In other tropical storms, they are typically obscured by high cirrus clouds.

Figure 9.2-1.- Hurricane Gladys, centered off the West Coast of Florida, at 1531 G.m.t.
on October 17, 1968.

NASA-S-68-6396

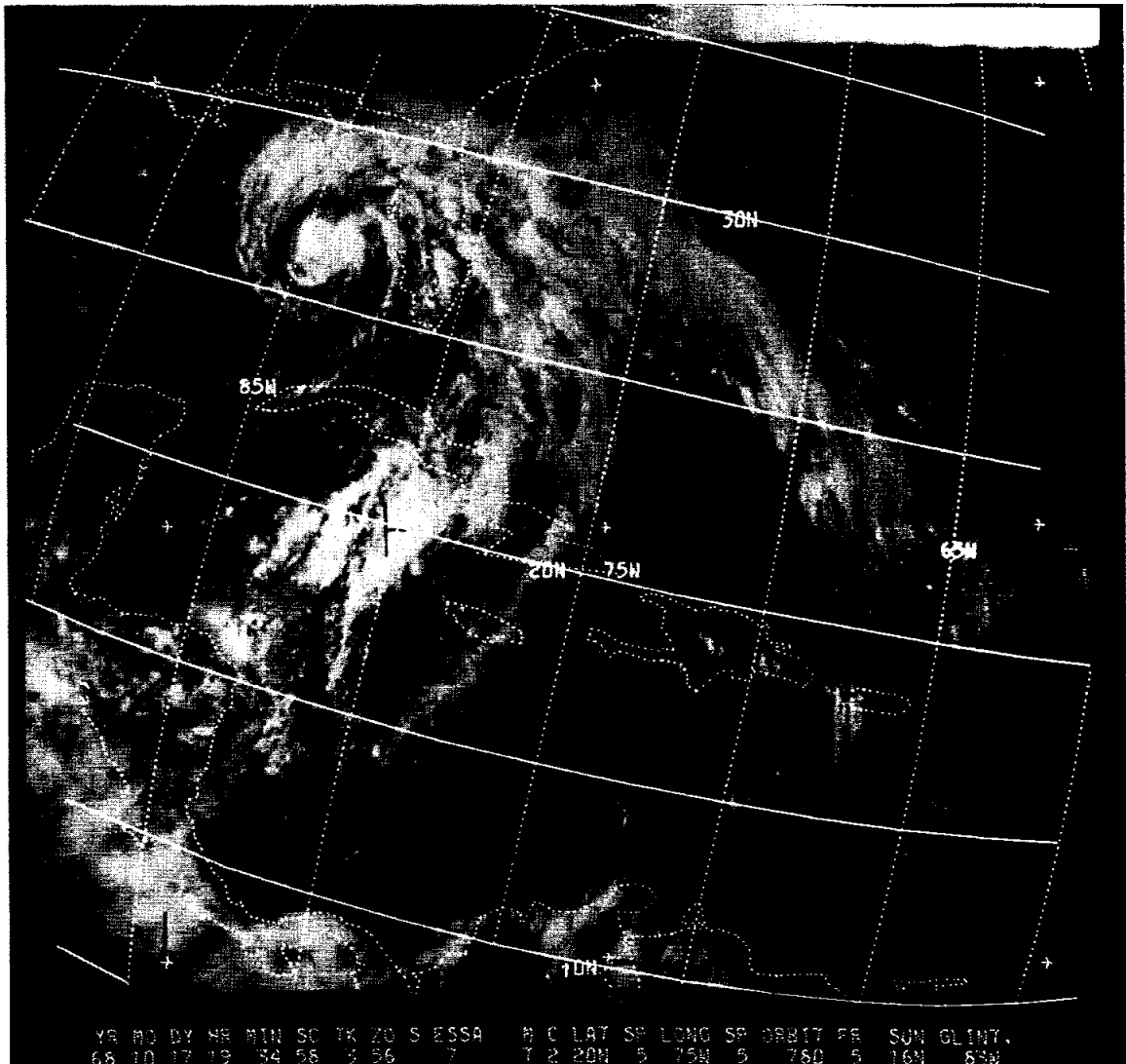


Figure 9.2-2.- Hurricane Gladys photographed from ESSA-7
(meteorological satellite) on October 17, 1968.

NASA-S-68-6397



Figure 9.2-3.- Eye of typhoon Gloria (western Pacific Ocean) taken at 0026 G.m.t.
on October 20, 1968.

NASA-S-68-6398

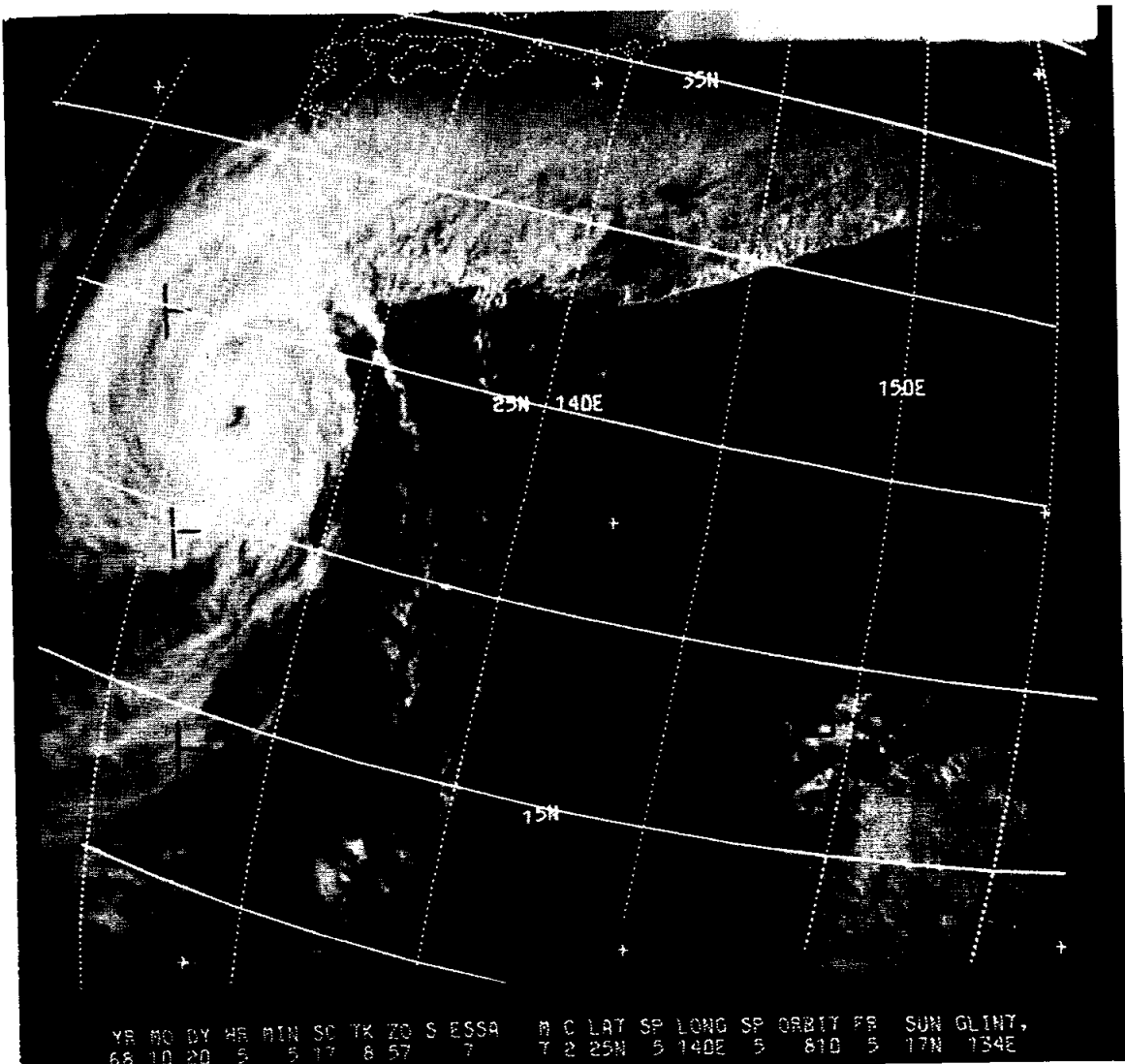
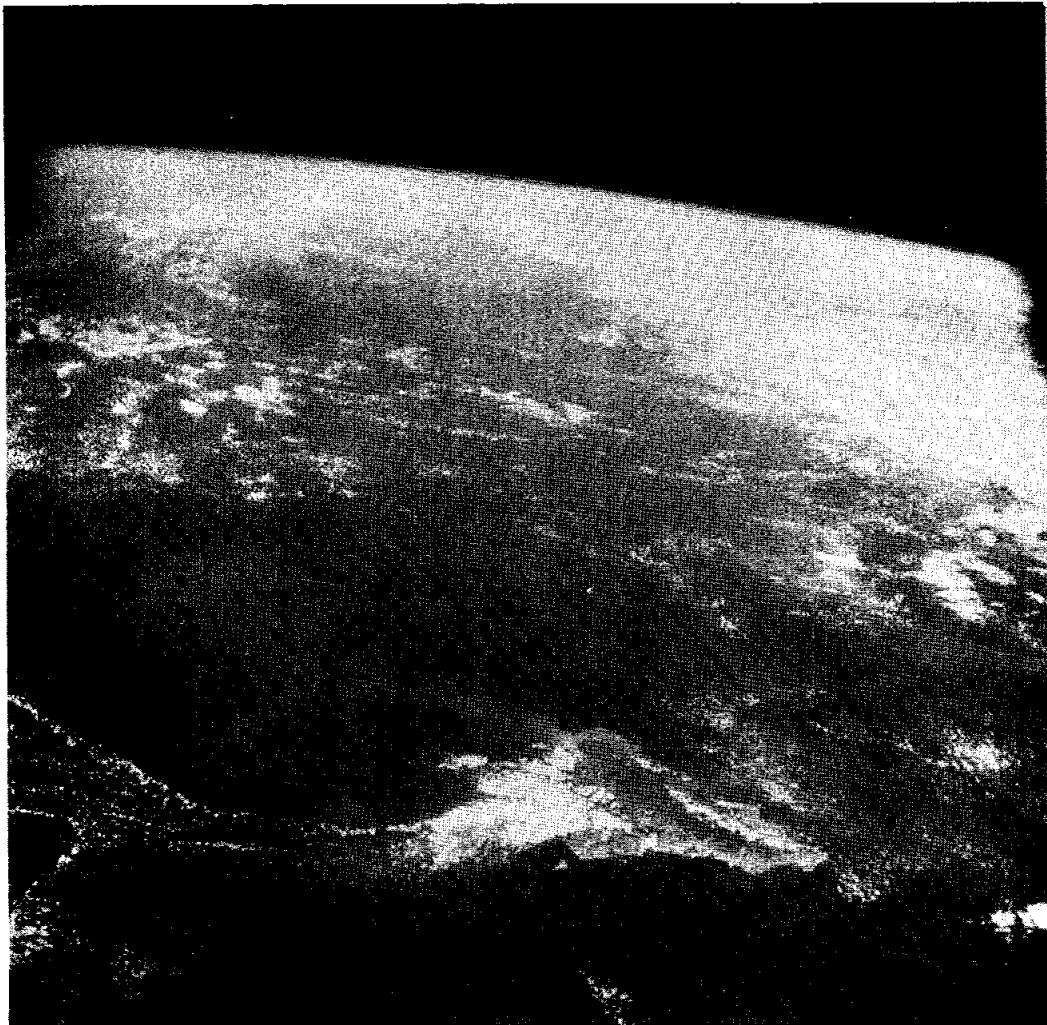


Figure 9.2-4.- Typhoon Gloria photographed from ESSA-7 at 0505 G.m.t. on October 20, 1968.

9-18

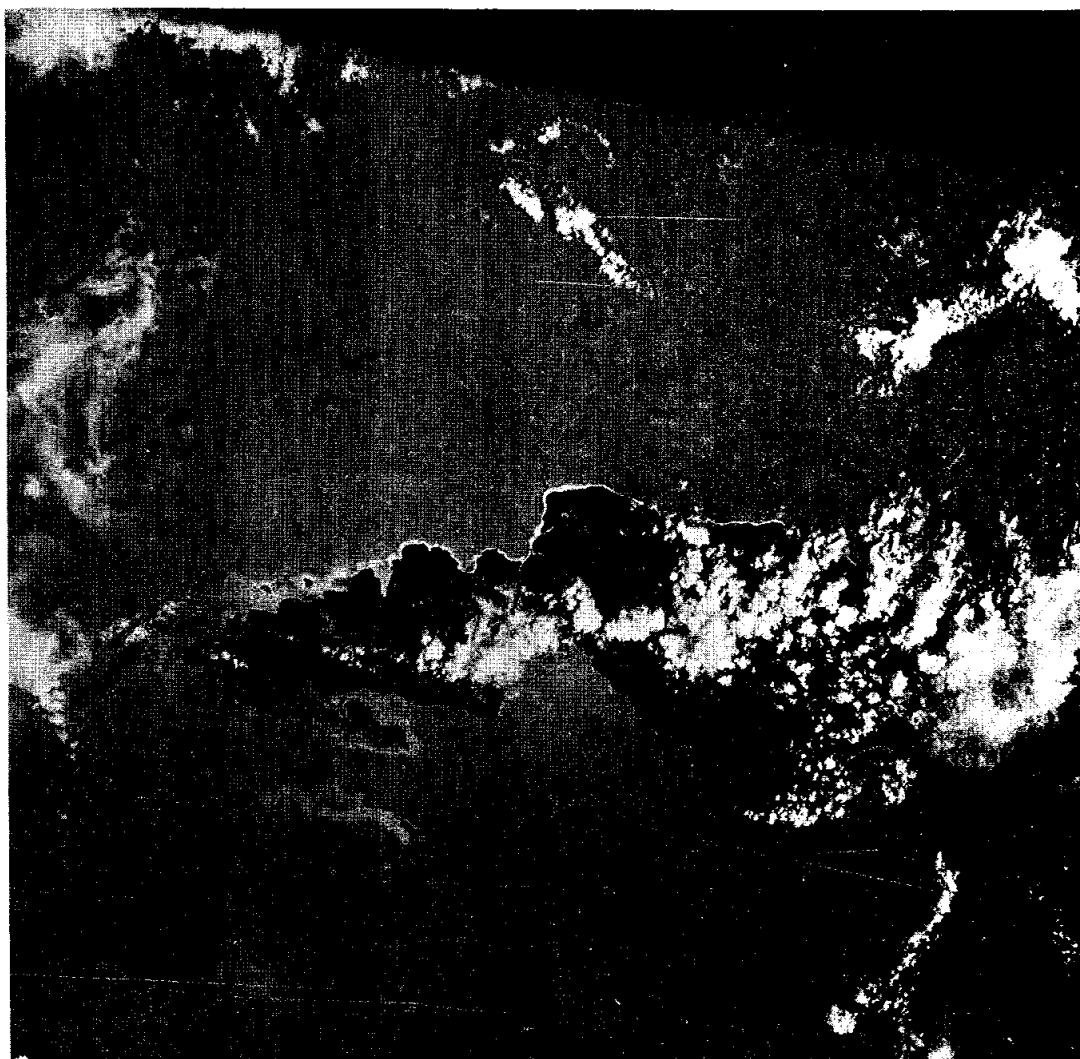
NASA-S-68-6399



Easterly trade winds are disturbed by the island and cloud lines form in its lee.

Figure 9.2-5.- Northerly view of Oahu in the Hawaiian Islands taken at 0001 G.m.t.
on October 15, 1968.

NASA-S-68-6400



Sea swells and eddies are prominent features in the sun glint pattern.
(Swell visible through magnifying glass.)

Figure 9.2-6.- Supiori and Biak Islands in Indonesia are surrounded by the sun's reflection on October 22, 1968, 0219 G.m.t.

10.0 ASSESSMENT OF MISSION OBJECTIVES

The mission objectives for Apollo 7 are defined in reference 3. The primary objectives for the mission were to:

1. Demonstrate command and service modules/crew performance
2. Demonstrate crew/space vehicle/mission support facilities performance
3. Demonstrate command and service module rendezvous capability.

Detailed test objectives defining the tests required to fulfill the primary mission objectives are defined in reference 4. These detailed test objectives are listed in table 10-I.

The data obtained and presented in other sections of this report are sufficient to verify that all the primary mission objectives were met. However, in isolated cases, portions of detailed test objectives were not completely met. These objectives and their significance are discussed in the following paragraphs.

10.1 GUIDANCE AND NAVIGATION ATTITUDE CONTROL (P1.12)

The intent of objective P1.12 was to demonstrate the ability of the digital autopilot to correctly perform automatic and manual attitude control and translation control in both maximum and minimum deadband modes at various maneuver rates.

All required modes were demonstrated; however, all rates were not checked. Those were automatic maneuver capability at the maneuver rates of 0.5 and 4.0 deg/sec, and manual attitude control using the rotation hand controller at maneuver rates of 0.05 and 4.0 deg/sec.

Based upon the successful accomplishment of the primary modes, the logic and operation of the systems were demonstrated. These modes are not normally used in any mission and do not represent different logic of the system.

10.2 MIDCOURSE NAVIGATION (P1.15)

The intent of objective P1.15 was to accurately define parameters required for the earth horizon locator model, test the lighting constraints, and determine crewman skills in coordinating attitude and optics tasks in obtaining good marks for computer inputs.

When viewed through the sextant, the earth horizon was indistinct and variable, with no defined boundaries or lines, thus precluding obtaining the necessary data.

The inability to obtain the required data on this mission has no significant impact on future Apollo missions. This technique of obtaining navigation information is one of a number of backup techniques to the primary Manned Space Flight Network means of midcourse navigation. Sufficient information was obtained on this mission to verify procedures required for another of the backup techniques (star/lunar landmark).

The inability to obtain the required data was attributed to the low altitude of the mission profile. The objective has been implemented into the flight plan for the next Apollo mission.

10.3 STABILIZATION AND CONTROL ATTITUDE DRIFT CHECKS (P2.7)

The attitude reference system in the stabilization and control system is required during the lunar mission coast periods when the guidance and navigation system is powered down or as a backup in the event the guidance and navigation system fails.

The intent of this objective was to verify predicted attitude reference system performance in the flight environment. The areas of interest are the boost phase and the zero-g coast phase. In addition, an assessment of the ORDEAL-orbit rate check was made.

The drift check was accomplished during the coast phase, early in the mission, with better than expected values. Although the boost phase comparison was not specifically done, the zero-g check was sufficient to demonstrate the drift characteristics.

10.4 SEXTANT/HORIZON SIGHTINGS

An objective was added to the mission in real time in an attempt to obtain some data for earth horizon definition as an alternate method to the star/earth horizon technique (reference paragraph 10.2). This objective was not satisfied because erroneous procedures were given to the crew.

TABLE 10-I.- DETAILED TEST OBJECTIVES

No.	Description	Primary objectives supported ^a	Completed
P1.6	Inflight alignment of inertial measurement unit	1	Yes
P1.7	Determination of inertial measurement unit orientation		Yes
P1.8	Orbital navigation/landmark tracking	1	Yes
P1.10	Sextant tracking	1 and 2	Yes
S1.11	Launch phase monitoring	--	Yes
P1.12	Guidance and navigation attitude control	1	Yes ^b
P1.13	Guidance and navigation velocity control	1	Yes
P1.14	Guidance and navigation entry monitoring	1	Yes
P1.15	Midcourse navigation	1	No
P1.16	Inertial measurement unit performance	1	Yes
P2.3	Entry monitor system performance	1	Yes
P2.4	Stabilization and control attitude control	1	Yes
P2.5	Stabilization and control velocity control	1	Yes
P2.6	Manual takeover of thrust vector control	1	Yes
P2.7	Stabilization and control drift checks	1	Yes ^b
P2.10	Backup alignment procedure for stabilization and control	1	Yes
P3.14	Service propulsion minimum impulse firing	1	Yes
P3.15	Service propulsion performance	1	Yes
P3.16	Primary/auxiliary propellant gaging system	1	Yes
S3.17	Service module reaction control system performance	--	Yes
P3.20	Thermal control of service propulsion propellants	1	Yes
P4.4	Environmental control life support function	1	Yes
P4.6	Waste management system	1	Yes
P4.8	Secondary coolant loop	1	Yes
P4.9	Water management system	1	Yes
P4.10	Postlanding ventilation	1	Yes
P5.8	Zero-g effects on cryogenics	1	Yes
P5.9	Cryogenic pressure control	1	Yes
P5.10	Water separation and potability	1	Yes
P6.7	S-band updata link	2	Yes
P6.8	Rendezvous radar transponder	1	Yes
P7.19	Primary radiator degradation	1	Yes
P7.20	Flat apex thermal protection	1	Yes
S7.21	Adapter panel deployment	--	Yes
S7.24	Passive thermal control	--	Yes
S7.28	Structural performance	--	Yes
P20.8	Separation/transposition/simulated docking	1 and 2	Yes
S20.9	Manual deorbit attitude orientation	--	Yes
P20.10	S-band communications performance	2	Yes
P20.11	Consumables usage	1	Yes
S20.12	Manual spacecraft/S-IVB attitude control	--	Yes
P20.13	Command and service module active rendezvous	3	Yes
S20.14	Launch vehicle propellant pressure displays	--	Yes
P20.15	Crew activities evaluation	1	Yes
S20.16	Environment-induced window deposits	--	Yes
S20.17	Propellant slosh damping	--	Yes
S20.18	Communications through Apollo Range Instrumented	--	Yes
S20.19	VHF voice communications	--	Yes
S20.20	Evaluation of crew optical alignment sight	--	Yes
S005	Synoptic terrain photography	--	Yes
S006	Synoptic weather photography	--	Yes
c ₁	Pitch about Y axis	--	Yes
2	Optics degradation evaluation	1	Yes
3	Sextant/horizon sightings	1	No
4	Three additional S-band communication modes	2	Yes

^aSee page 10-1 for primary objectives.^bPrimary objective met; minor portion of detailed test objective not attempted.^cAdded during the mission.

11.0 ANOMALY SUMMARY

11.1 LOSS OF S-BAND SUBCARRIERS

The PCM and voice subcarriers were lost at approximately 65:00:00 on the secondary S-band transponder. Real-time telemetry, data storage equipment playback, and television were time-shared on the downlink S-band FM mode until the crew manually switched to the alternate transponder. Downvoice was transmitted by modulation of the PM carrier (backup downvoice).

The failure was characterized by:

- a. Drop in the ground-received PM signal strength
- b. Loss of PM subcarriers
- c. Lower than expected transponder-received signal strength.

No other abnormalities were detected. The only components within the S-band system which could have failed and caused all these symptoms are the panel switch for selecting the primary or secondary transponder and the wiring which controls this function. The switch was X-rayed and functionally tested postflight with no abnormalities noted. The transponder was tested in the command module and on the bench, including vibration and temperature acceptance testing, and the results were all negative.

When the select switch is changed from one transponder to the other, a momentary hesitation in the OFF position is required to allow latching relays to reset. Switching without this hesitation can cause both transponders to be ON and will create all the symptoms of the failure.

The transponder select switch, directly above the antenna select switch, may have been inadvertently thrown during one of the frequent antenna switchings, and both transponders may have been activated. Although the crewmember on duty cannot remember inadvertently throwing the wrong switch, he does not discount the possibility.

No further action is required, and this anomaly is closed.

11.2 BIOMEDICAL INSTRUMENTATION

Some leads on the biomedical instrumentation were broken and some became disconnected inflight. One dc-dc converter, used to supply power to the biomedical signal conditioner on the suit harness, was reported to be physically hot.

To correct the lead breakage, insulation for the wiring has been changed from Teflon to polyvinyl chloride, which is more flexible and, therefore, reduces susceptibility to wire breakage. Also, the potting at the harness connectors has been changed to a softer, more pliable material to reduce concentrated stresses. The inline connectors from the sensor to the signal conditioners have been eliminated to prevent the disconnects. A ground test of a dc-dc converter was conducted during the flight and indicated that for the worst case failure, the temperature would reach only 120° F. Postflight tests of the flight dc-dc converter, biomedical harness, and spacecraft circuits showed no abnormal operation. However, the electrical connections on each end of the control head of the biomedical/communications cable were corroded with salt deposits.

The Apollo 8 crew have participated in tests with dc-dc converters at 120° and 135° F and have been instructed to inspect connector ends for cleanliness before mating the connectors. If the overheating condition happens again inflight, the crew will remove the harness, as was done on Apollo 7. This anomaly is closed.

11.3 WATER GUN TRIGGER STICKING

The trigger on the water metering dispenser (water gun) became sticky and was difficult to operate. Postflight, the trigger activation forces were measured at 11 pounds as compared to the specification value of 4 pounds. The forward (metering) O-ring was 0.004 to 0.013 inch oversize. The O-ring was replaced, and activation forces were measured and were normal. Sodium hypochlorite in the drinking water caused the O-ring to swell.

The O-ring material has been changed to ethylene propylene for all future missions. This material is compatible with water chlorination, and the modification to the Apollo 8 water gun has been made. This anomaly is closed.

11.4 SHIFT ON FLIGHT DIRECTOR ATTITUDE INDICATOR

The total attitude displayed on flight director attitude indicator no. 1 changed approximately 160 degrees in the pitch axis when the attitude source was switched from the guidance and navigation system to the stabilization and control system. The first shift was noted by the crew approximately 1 minute after switching. On subsequent switching attempts, the shift was immediate. Operation was nominal in the normal attitude display configuration (guidance and navigation system attitude on indicator no. 1 and stabilization and control system attitude on indicator no. 2).

During ground tests on another system, the condition was reproduced by inhibiting the transfer of one of a pair of switching relays which select the sine and cosine resolver outputs from the respective attitude sources. In this situation, the resolver in the flight director attitude indicator resolver is driven with 400-cycle sine information from the stabilization and control system and 800-cycle cosine information from the guidance and navigation system.

The malfunction could not be reproduced with the flight hardware in the spacecraft or at the subsystem and component level. The electronic display assembly, which contains the relays, was subjected to acceptance temperature and vibration tests, with nominal results. The module containing the relay was then removed, and a life cycle test was successfully performed on the relay. Finally, the relay was opened and visually inspected. A tin/silver solder ball was found, and it was large enough to have caused the condition noted, except the 1-minute delay reported by the crew.

The relay is of a type which was the subject of an extensive switching logic analysis in 1967. One of the failure modes of concern at that time was a failure of the relay to transfer. As a result of this and other failures, all relays involved in critical switching functions were made redundant. No further action is required and this anomaly is closed.

11.5 MOMENTARY FAILURE OF ROTATION HAND CONTROLLER

Rotation hand controller no. 2 failed to generate the second of a series of minus pitch, minimum impulse commands. The minus pitch reaction control engines fired with no rotation controller movement when the control mode was subsequently switched to acceleration command. After several hours, the controller was checked and operated properly, and it continued to perform correctly for the remainder of the mission.

The symptoms reported would occur if a hand controller breakout switch temporarily failed to open when the controller was returned within the detent. In the minimum impulse mode, one pulse or short firing command is generated for each closure of a breakout switch. In the acceleration command mode, a continuous switch is closed.

The condition has not been reproduced postflight. The controller has been successfully subjected to acceptance temperature and vibration tests and to visual and mechanical checks at successive stages of disassembly. The microswitch has been opened, and no evidence of contamination or other abnormality was found.

Rotation hand controllers of this design have exhibited a tendency for sticky cam operation in the past. This condition could have caused the reported symptoms. The controllers on spacecraft 103 and subsequent are of a more recent design; among other things, the later design contains an improvement that will reduce the likelihood of a breakout switch problem. Two hand controllers are carried onboard, and sufficient redundancy and switching flexibility is available to prevent loss of system capability for a single failure of this type. No further action is required, and this anomaly is closed.

11.6 ENTRY MONITOR SYSTEM MALFUNCTIONS

Both the delta V and the range counter circuits in the entry monitor system malfunctioned prior to lift-off; no other problems with the system were encountered during the mission. The first preflight failure involved the range counter performance during a self-test. In this test, the counter is preset and then counts down in response to a known stimulus for a preset period of time, finally reaching a value near zero miles. The system repeatedly failed this test, both preflight and inflight. The condition was simulated preflight by opening the input to the range integrator, and a poor solder connection was suspected. Despite this condition, the unit was accepted for flight because of its lack of influence on crew safety or mission success.

Following the mission, the malfunction was still present in spacecraft and inertial subsystem tests but disappeared during thermal cycling. All attempts to cause the problem to reappear have failed.

A delta V counter malfunction, totally independent of the range counter failure, was noted just prior to lift-off, during the prelaunch setup of the delta V counter. A "nine" appeared in the most significant digit of the counter when the crew switched the function selector to the

delta V set position. The setup was normal during a repeat of the procedure; therefore, no alarm was issued. The malfunction occurred several times in flight, in all but one instance coincident with a switching operation.

The malfunction has been repeated twice postflight by applying pressure to an internal wire crimp connection. The applied pressure apparently cleared the poor connection because subsequent attempts to cause the problem have failed. A laboratory analysis of the crimp has also been inconclusive, possibly because the condition was corrected by the applied pressure.

The failures encountered appear to be quality problems and have not generally been experienced on other units. In addition, all units have now been subjected to more extensive acceptance testing including thermal cycling. Therefore, unless a material or manufacturing deficiency is discovered, no further action is required. This anomaly will be closed by December 18, 1968.

11.7 ADAPTER PANEL DEPLOYMENT

Photographs taken during the second revolution showed that three of the adapter panels were opened to about 45 degrees, but the remaining panel (+Y) was open only about 25 degrees. Photographs taken during revolution 19 showed all four panels open at the normal angle of about 45 degrees.

At separation of the command and service modules from the launch vehicle, the four adapter panels are deployed by pyrotechnic actuators. The energy of the opening panels is absorbed by attenuators, which consist of a tube filled with honeycomb. Still photographs taken during the second revolution show that the two attenuator cables attached to the lower corners of the panels were slack on the panel which was not fully deployed, indicating the panel had gone to the full-open position and returned to the observed position. The outside retention cable, designed to prevent panel rebound after opening, is visible on three panels but not on the +Y panel in the photograph from revolution 2; however, the cable on the +Y panel is visible in the revolution 19 photographs.

For cable vibration control during launch, each outside retention cable is wrapped with cork and aluminized tape for a 10-inch length at the hinge line, providing a snug or possibly force fit in the slot (about 1/4 inch wide) of the retention cable channel. Each retention cable is attached to a spring-driven reel at the lower end of the cable, which automatically reels in slack cable when the panels open.

The roll rate of about 7 deg/sec during the 19th revolution was not sufficient to compress the honeycomb in the attenuators (a roll rate of about 120 deg/sec would be required). Therefore, as indicated by the slack attenuator cables in the first photographs, the panel did fully deploy initially but then rebounded because the retention cable was caught in the channel. The roll rate was, however, sufficient to move the panel to the full open position. When the retention cable later released, prior to revolution 19, the slack was properly reeled in, and the panel was then retained open.

All four panels are to be jettisoned on future missions and do not have the retention cable which caused the problem. No hardware changes are required, and this anomaly is closed.

11.8 COMMAND MODULE WINDOW FOGGING

The crew reported window fogging by a film which built up on the glass surface during the mission.

Postflight examination showed the film to be a product of the outgassing of the room-temperature-cured RTV used in the window area on the edges of the insulation between the heat shield and the pressure vessel. This window surface contamination was the same as experienced on Gemini flights. The outgassing product has been duplicated in ground tests at altitude and elevated temperature.

The room-temperature-cured parts are to be replaced on future spacecraft by parts which have been pre-cured in vacuum at elevated temperatures (similar to the Gemini modification). The change is being verified by ground tests and will be implemented on command module 104. This anomaly is closed.

11.9 FLIGHT QUALIFICATION COMMUTATOR FAILURE

The high-level commutator in the command module failed approximately 5 minutes after it was turned on prior to command module/service module separation.

Approximately 15 minutes of entry data cannot be recovered. The commutator exhibited a loss of time-sequencing and was cycling through only 18 of the 90 channels of data. The unit performed satisfactorily during postflight testing on the command module and was returned to MSC for additional testing. All additional testing to date has not duplicated

the flight anomaly or caused abnormal operation. This testing has included abnormal voltage, vibration, acceleration, temperature, corona, vacuum (7 days at 100 000 to 300 000 feet) and electromagnetic interference acceptance tests. An adverse electromagnetic interference test is planned which will subject the commutator to noise spikes of 50 to 300 volts, at a frequency of 1 to 200 pps and a duration of 2 milliseconds. This test is scheduled for completion by December 18, 1968.

The high-level commutator is not used on any future command and service modules but is used on lunar module 3. The anticipated close-out date is pending completion of analysis and postflight tests.

11.10 WATER NEAR WASTE WATER DISCONNECT

A water leak was observed at the B-nut connection to the quick disconnect during overboard dumps. The leak was the result of a poor metal-on-metal seal at the B-nut connection to the waste water overboard quick disconnect. The design on Apollo 8 and subsequent has an O-ring instead of the metal-on-metal seal where the leak occurred. This anomaly is closed.

11.11 MOMENTARY LOSS OF AC BUSES

The crew reported two ac bus 1 failure indications and one ac bus 1 and 2 failure indication early in the mission.

The loss of voltage was verified by the onboard meter, and the voltage was restored to normal by resetting the ac bus sensors. The occurrences were coincident with automatic cycles of the cryogenic oxygen tank fans and heaters. The only condition under which an ac bus can be automatically disconnected is an overvoltage being sensed by the ac sensing unit. After a procedural change was made to prevent the fans in both tanks from cycling simultaneously, the problem did not recur for the remaining 200 hours of flight.

Postflight tests indicate that the cause was associated with corona arcing of the ac power within the motor-operated cryogenic fan switch located in the service module. A leak in the environmental seal caused the pressure to drop to the threshold for corona arcing when the controls were opened to turn off fan power. Both individual dropouts of ac bus 1 and ac bus 2 and simultaneous dropouts of both buses have been reproduced with the interior of the motor switch exposed to low pressure. One of two switches that were manufactured at approximately the same time as the Apollo 7 switch had a leak rate seven times the specification limit.

Manual switching of the fans eliminates the condition, because this technique bypasses the service module motor switch and confines the opening and closing of contacts to the pressurized area of the cabin. For subsequent missions, manual operation of the fans will be used. No hardware changes will be made, and this anomaly is closed.

11.12 BATTERY CHARGING

The inflight charges on entry batteries A and B returned 50 to 75 percent less energy to the batteries than expected.

The resistance of the spacecraft charging circuit greatly affects the energy returned to the batteries, in that the charging potential is reduced by the line losses in the circuit. This resistance was determined analytically on Apollo 7. Preflight tests on the battery charging circuits were conducted on a functional basis, and an integration to determine energy returned was not accomplished.

Preflight, inflight, and postflight tests on the spacecraft and ground tests during the mission, all conducted using the actual spacecraft circuit resistances, showed the same characteristics and resulted in a low energy return to the battery.

On future spacecraft, individual charger characteristics with the associated line drop will be checked for satisfactory battery charging. This anomaly is closed.

11.13 UNDERVOLTAGE INDICATION ON DC BUSES A AND B

At command module/service module separation, the crew reported caution and warning undervoltage indications and voltages of 25.0 and 25.1 volts on main buses A and B, respectively.

The main bus voltages at command module/service module separation were as much as 4.5 volts lower than expected. The voltage slowly increased to above the alarm level (26.2 volts) on both buses in approximately 5 minutes and to 27.0 volts in 20 minutes. The low voltage condition resulted from the mid-range state of charge, low temperature, and displacement of electrolyte from contact with the plates because of the zero-g environment.

For Apollo 8, the batteries will be warmed by placing them on the main buses about 12 minutes prior to command module/service module separation. The service propulsion gimbal motors will be turned on, and fuel

cell 2 will be removed from the buses to provide higher battery loads prior to separation and to lessen transient loads at separation. Also, present plans for subsequent missions include changing the battery separator material to an absorptive cellophane material to preclude electrolyte displacement in the zero-g environment. This anomaly is closed.

11.14 FUEL CELL EXIT TEMPERATURE INCREASE

Prior to the fifth service propulsion maneuver, the condenser exit temperature of fuel cell 2 increased to 180° F (nominal is 155° to 165° F). The electrical load was removed from the fuel cell for approximately 5½ minutes to permit cooling prior to the service propulsion maneuver. During this period, the fuel cell 1 condenser exit temperature increased to 175° F; however, the temperature returned to the normal operating level after fuel cell 2 was returned to the bus. Fuel cell 1 operated satisfactorily for the remainder of the mission.

Four days later, the electrical load was again removed from fuel cell 2 for a short period of time to insure proper performance during the deorbit maneuver. After the fifth service propulsion maneuver, every time the fuel cell loads were increased, the fuel cell 2 exit temperature increased to a level between 180° and 190° F.

Flight data indicate that the abnormal operation was caused by malfunctions in the respective secondary bypass valves. After the flight, similar erratic operation of the shuttle valve has been demonstrated with contaminants intentionally introduced into the system.

On Apollo 8, the radiator half of the cooling system has now been drained, flushed, and reserviced as a precautionary measure. Additionally, studies are being made concerning the necessity of adding a filter upstream of the bypass valve or modifying the system such that the valve is afforded better protection. The outcome of the study will determine what can be done practically to alleviate the contamination problem on subsequent spacecraft. This anomaly is closed.

11.15 INADVERTENT PROPELLANT ISOLATION VALVE SWITCHING

During postflight testing of the relief valves for the command module reaction control system, a high amount of leakage was observed through the closed oxidizer propellant isolation valves. When voltage was removed, the oxidizer isolation valves opened, and the position indicator switch verified the change.

The propellant isolation valve is spring-loaded closed with a bellows preload and should remain closed when voltage is removed. The bellows was damaged from hydraulic hammering during system activation, thus causing the valve to open when the voltage was removed. The propellant isolation valves were in the closed position at system activation, a condition for which the valves have not been qualified.

Use of the proper procedure — opening the isolation valves before activation of the command module reaction control system — will preclude recurrence of the problem. The checklist and the Apollo Operations Handbook have been changed accordingly, and the crews will also be instructed. This anomaly is closed.

11.16 VOICE COMMUNICATIONS DURING LAUNCH PHASE

About 7 minutes after lift-off, voice communications became garbled and erratic.

Both Grand Bahama and Bermuda were patched to air-to-ground 1 from 7 minutes to about 8 minutes; this is an improper procedure. From 8 to 10 minutes, VHF downlink was remoted to the Mission Control Center through Bermuda only, and the voice was still garbled. At 10 minutes, S-band downlink voice was patched to network 1, and quality was good. However, uplink voice was not transmitted by VHF, another improper procedure. Consequently, transmissions which the crew expected on VHF were not received. From 12 to 13 minutes, USNS Vanguard was remoting VHF voice to the Mission Control Center and the transmission was readable. At 13 minutes, Vanguard was requested to remote S-band, and no voice was received. Voice quality was also garbled after handover to Canary Islands. Simplex-A was then selected at 19 minutes, and the quality was satisfactory. Duplex-B was successfully reverified at about 07:20:00.

These problems resulted from improper procedures and/or malfunctioning receivers at the ground stations. Patching of voice to the Mission Control Center during Apollo 7 was effected by the network sites. To preclude the procedural problems associated with this technique, patching of the voice to the Mission Control Center will be accomplished at a single point at Goddard Space Flight Center during future Apollo missions. This anomaly is closed.

11.17 ERRATIC OPERATION OF WATER EVAPORATOR

Under the low, variable heat loads which existed, the primary evaporator operated erratically in the automatic mode, causing what appeared to be wick drying and subsequent flash freezing. The evaporator was frequently serviced with water in an attempt to keep it operating under these conditions, but it was subsequently turned off.

The automatic control thermodynamics are such that this situation can be expected, as was demonstrated with a similar evaporator operating under simulated flight conditions. Postflight tests with the flight evaporator verified the characteristics observed in flight. Removal of some of the sponge material in the area of the sensors which control operation of the evaporator prevented dryout under the low, cyclic heat loads. This modification has already been employed on the evaporators for command module 106 and subsequent. In effect, the removal of the sponge material from the temperature sensors located in the boiler wicks increases the response of the sensors to the conditions in the wick by eliminating the influence of the wet sponge. Under higher heat loads, when the evaporator is actually required, the system did not dry out in the postflight test. This anomaly is closed.

11.18 CONDENSATION IN CABIN

Moisture condensed on approximately 200 inches of coolant lines which were not thermally insulated. These lines ran from the radiator to the environmental control unit and from the environmental control unit to the inertial measurement unit.

The condensation was anticipated, and it was dumped overboard by the crew using the urine transfer hose and cabin enrichment purge assembly. The same condition is expected to occur on Apollo 8. The urine transfer hose is acceptable for removing free water. On spacecraft 106 and subsequent, the lines are insulated and this condition should not occur. This anomaly is closed.

11.19 FOOD

A seam on three food bags split, and the crew reported that some of the food crumbled badly.

For future missions, the menu will be changed and the food bags will be inspected for defects. This anomaly is closed.

11.20 BATTERY MANIFOLD LEAK

The entry battery manifold pressure increased to cabin pressure of 5 psia, indicating a leak from the cabin into the battery manifold.

The leak rate during postflight tests was within specification (B-nut fittings to the battery cases were not included, since the batteries had been removed). Similar leakage noted on spacecraft 2TV-1 was caused by undertorqued B-nuts (below specification value). On future spacecraft, the B-nuts will be torqued to the specification values.

No hardware change is required since the crew has manual control of the manifold overboard vent. This anomaly is closed.

11.21 FAILED FLOODLIGHTS

Sometime during the mission, both of the primary lamps failed in the lower equipment bay floodlights. Postflight investigations revealed that the lamp filaments (cathodes) had completely vaporized, which caused a diode to short in each lamp driver.

A new lamp has a start-up voltage of about 500 volts. As the lamp ages, the cathode deteriorates, thus increasing the start-up voltage, which can go as high as 1800 volts. The diode is rated at 700 volts; therefore, it would burn out. The rate of cathode deterioration is dependent on the operating voltage. Maximum deterioration rate occurs when the dimming rheostat is halfway between the full-dim and full-bright positions.

Tests are in progress to establish lamp life at the critical operating voltage. Normally, these lamps should operate 2000 hours.

Procedural changes are being made to use only the secondary lamp on full bright during ground tests, and consideration is being given to installing flight lamps just prior to the countdown demonstration test. No hardware changes are planned. This anomaly is still open.

11.22 CRACKED GLASS ON MISSION EVENT TIMER

The glass on both mission timers cracked during the mission, but the operation of the timers was not affected. For Apollo 8, transparent tape will be placed over the glass. The mission effectiveness of any additional corrective action is pending the results of the failure analyses.

11.23 WATER IN DOCKING TUNNEL

Approximately 290 pounds of water was found in the docking tunnel. Postflight tests show that the upper hatch vent valve leakage rate with the hatch in the stable I position was between 0.5 and 3.0 gal/min. The leakage rate with the hatch rotated 100 degrees from the stable I position was 120 cc/min. It should be noted that all of the structure and seals were in satisfactory condition to prevent any leakage other than through the makeshift ball check valve which was installed in the top hatch. The normal valve which controls pressure in the tunnel had been rendered inoperative. No other spacecraft has this peculiarity. This anomaly is closed.

11.24 VHF RECOVERY BEACON OPERATION

Recovery forces reported that the VHF recovery beacon signal was not received while the spacecraft was descending on the main parachutes. The crew reported that the beacon was turned on at about 9000 feet, turned off while the spacecraft was in stable II after landing, and turned on again when stable I was achieved. The recovery forces reported reception of the beacon when the spacecraft returned to stable I position.

The beacon and antenna system operated properly during postflight testing. However, the antenna was bent and may not have deployed properly until after return to stable I. There is no conclusive evidence as to why the beacon was not received from 9000 feet to landing. This anomaly is closed.

11.25 APPARENT FREE WATER IN SUIT SUPPLY HOSE

The crew reported hearing a gurgling sound in the suit supply hoses and observed droplets of water at the hose endings. The problem was not severe enough to cause any discomfort to the crew or hazard to the mission.

This gurgling sound and free water could have been caused by either the water separator not operating properly or the cyclic accumulator not being cycled properly. Tests have been conducted on the heat exchanger, concentrating on the water separation function. The water flow capacity was measured at 0.8 lb/hr, which is approximately the same as that measured during the servicing in countdown. Although this flow rate is lower than normally expected, there is no indication concerning whether the flow rate changed during the flight. A decrease in flow rate below 0.6 lb/hr

would cause excess water in the system. Postflight tests of the separator have shown the flow rate to vary from 0.2 to 15 lb/hr. The cause of this erratic flow rate is unknown at this time and is being studied.

During the mission, the cyclic accumulator was frequently in the manual rather than the automatic mode; the automatic mode provides accumulator cycling every 10 minutes. From 79:30:00 through 87:30:00, no automatic actuations were identified and four actuations were missed. The gurgling sound was noted at about this time period. It is believed that, at times, accumulator operations took place for periods in excess of 10 minutes. Also, if manual operation was conducted at intervals of less than 10 minutes, a decrease in efficiency would have resulted. At 2-minute intervals, no water is removed because once the accumulator has stroked, approximately 2 minutes will elapse before the piston begins to retract. This time is a function of the relationship between the characteristics of the piston spring and the pressure bleed orifice. Improper cycling in the manual mode would cause excess water in the system.

On future flights, the procedure will be to operate accumulators in the automatic mode, and the manual mode will be used only if the automatic system fails. The closure of this anomaly is awaiting the outcome of the separator flow rate study.

11.26 ELECTROMAGNETIC INTERFERENCE PROBLEMS

Electromagnetic interference problems have been experienced during ground tests, and the nature of these problems do not warrant hardware changes.

The mission event timer started inadvertently, coincident with an oxygen fan cycle. Timer starts have occurred in ground tests, usually associated with voltage transients. These conditions are a nuisance for the crew but do not degrade system performance.

The interior lights were dimmed during the mission to check the visibility of the exterior lights. When the lights were brightened, a computer program alarm existed. The alarm was reset without incident. Alarms resulting from electromagnetic interference have been observed previously during ground tests and are not significant.

The central timing equipment read 00:42:09 at 12:07:26, indicating that it had been reset at 11:25:17. The central timing was updated and operated satisfactorily for the remainder of the mission.

These problems are closed.

12.0 CONCLUSIONS

The Apollo 7 mission was successful in every respect, and all mission objectives were effectively accomplished. The following conclusions are drawn from the analyses contained in this report.

1. The results of the Apollo 7 mission, when combined with results of previous flights and ground tests, demonstrate that the command and service modules are qualified for operation in the earth orbital environment. The command and service modules are now ready for flight tests in the cislunar and lunar orbital environments.
2. The concepts and operational functioning of the crew/spacecraft interfaces, including procedures, provisioning, accommodations, and displays and controls, are acceptable.
3. The overall thermal balance of the spacecraft, for both active and passive elements, was more favorable than predicted for the near-earth environment.
4. The endurance required for systems operation on a lunar mission was demonstrated.
5. The capability of performing rendezvous using the command and service modules, with only optical and onboard data, was demonstrated; however, ranging information would be extremely desirable for the terminal phase.
6. Navigation techniques in general were demonstrated to be adequate for lunar missions. Specifically -
 - a. Onboard navigation using the landmark tracking technique proved feasible in earth orbit.
 - b. The earth horizon is not usable for optics measurements in low earth orbit with the present optics design and techniques.
 - c. A debris cloud of frozen liquid particles was identified following venting. While this cloud obscured star visibility with the scanning telescope, it can be expected to dissipate rapidly in earth orbit without significantly contaminating the optical surfaces.
 - d. Star visibility data with the scanning telescope indicate that in cislunar space, with no venting and with proper spacecraft orientation to shield the optics from sun and earth or moon light, constellation recognition will be adequate for platform inertial orientation.

e. Sextant star visibility was adequate for platform realignments in daylight using Apollo navigation stars as close as 30 degrees from the sun line-of-sight.

7. The rendezvous radar acquisition and tracking test demonstrated the capability of performance at ranges required for rendezvous between the command and service modules and the lunar module.

8. Mission support facilities, including the Manned Space Flight Network and the recovery forces, are satisfactory for earth orbital missions.

APPENDIX ASPACE VEHICLE DESCRIPTION

The Apollo 7 space vehicle (fig. A.0-1) comprised a block-II configuration Apollo spacecraft (101) and a Saturn-IB launch vehicle (AS-205). The spacecraft consisted of a launch escape system, a command module, a service module, a spacecraft/launch-vehicle adapter, and a structural member that replaced the lunar module in the adapter. The Saturn IB launch vehicle consisted of an S-IB stage, an S-IVB stage, and an instrument unit. The following sections provide a more detailed description of the combined space vehicle and its systems.

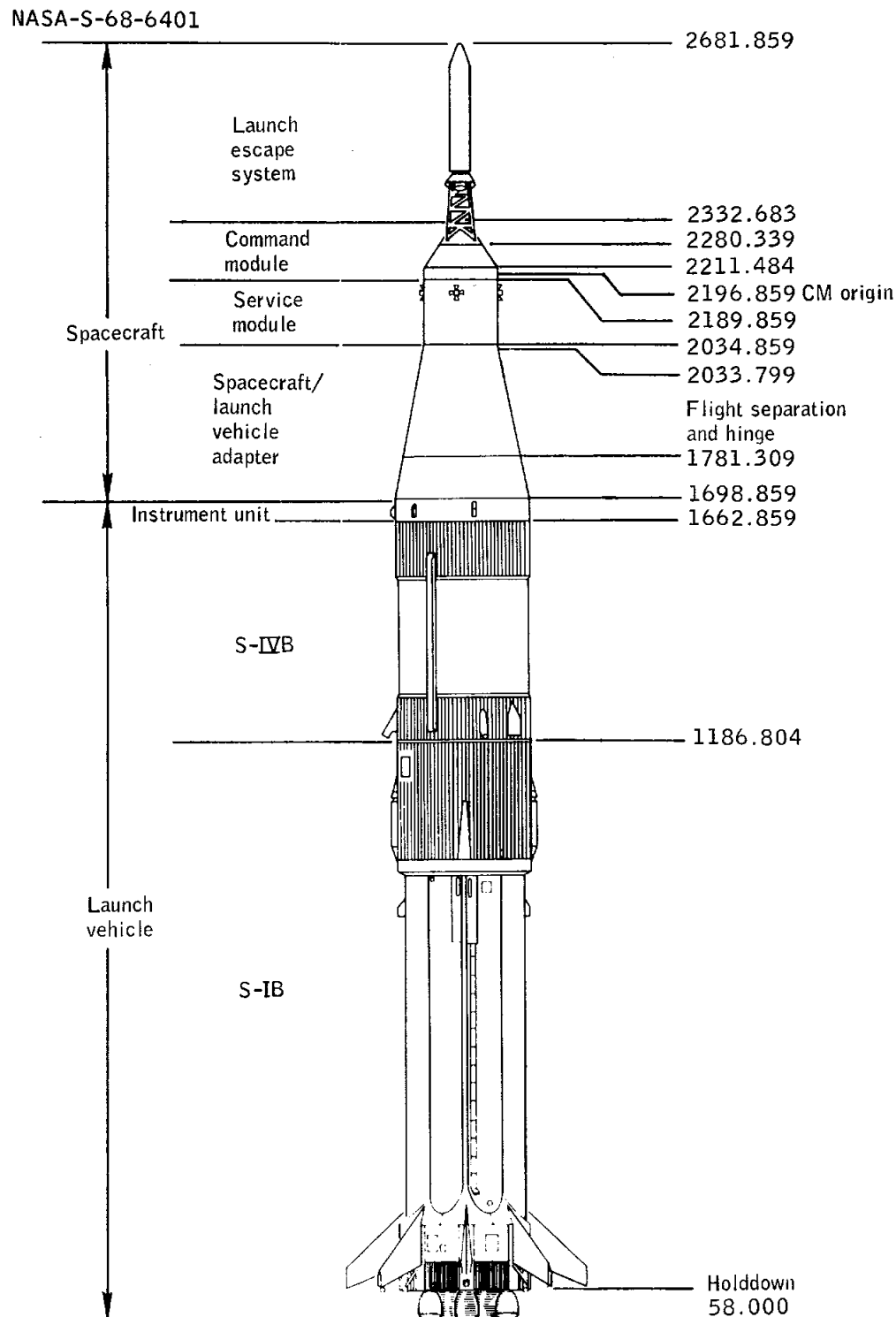


Figure A.0-1.- Apollo 7 space vehicle.

A.1 COMMAND AND SERVICE MODULES

A.1.1 Structures

The major structural components of the spacecraft discussed in the following paragraphs are shown in figure A.1-1.

Command module.- The command module is composed of an inner pressure vessel (shown in figure A.1-2) and a conical outer heat shield. The inner structure is fabricated from aluminum longerons and stiffeners with a shell of aluminum honeycomb panels. The outer structure of stainless-steel honeycomb is covered with an ablator of varying thickness and forms a thermal barrier to protect the pressurized crew compartment. The heat shield, shown in figure A.1-3, is composed of three sections; a forward heat shield, a crew compartment heat shield, and an aft heat shield.

Access to the crew compartment is through an outward-opening hatch assembly and adapter frame mounted in the crew compartment heat shield. The hatch can be latched or unlatched manually. A counterbalance assembly uses pressurized nitrogen as the stored energy to provide a quick-opening capability in a one-g environment. The unpressurized volume between the forward heat shield and the crew compartment contains components of the earth landing system and related recovery aids. The unpressurized annular volume between the bottom of the crew compartment, the crew compartment heat shield, and the aft heat shield houses a major portion of the command module reaction control system.

A laminated fiberglass and Teflon boost protective cover encloses the command module ablator to protect it from launch-phase aerodynamic heating. This cover is attached to the tower legs and is removed when the launch escape system is jettisoned.

Service module.- The service module, shown in figure A.1-4, is a cylindrical structure fabricated from aluminum and aluminum-honeycomb panels and houses the systems and consumables for the service propulsion system, the fuel cells and cryogenic fluids, and the service module reaction control system. The interior volume between the forward and aft bulkheads of the service module is divided into sectors by six radial beams or webs. These sectors, or bays, are arranged in three diametrically opposed pairs around a central cylindrical section. The service propulsion engine is attached to, and extends below, the aft bulkhead.

A.1.2 Emergency Detection System

The launch vehicle emergency detection system monitors certain critical parameters of the launch vehicle guidance, propulsion, and attitude control systems, as depicted in figure A.1-5. If the monitored parameters exceed certain predetermined limits, the crew can initiate an abort utilizing the launch escape system or, after tower jettison, the crew can command a service propulsion system abort. Also included are provisions for the initiation of an automatic abort in the event of loss of thrust on two or more engines during first-stage flight; excessive vehicle angular rates in the pitch, yaw, or roll plane; or loss of electrical continuity between the spacecraft and launch vehicle.

An abort request light is provided to inform the crew that ground control is advising an immediate manual abort. Prior to lift-off, the light can be illuminated by the Launch Director through a hardline via the instrument-unit umbilical. After lift-off, the light would be illuminated if the Range Safety Officer armed the launch vehicle destruct system or by command from the Flight Director through the spacecraft updata link.

The following variables are monitored by the emergency detection system with appropriate displays in the command module:

- a. Launch vehicle engine status
- b. Launch vehicle guidance
- c. Launch vehicle attitude rates
- d. Angle of attack
- e. Vehicle lift-off
- f. S-IVB stage fuel and oxidizer tank pressures

A.1.3 Sequential Events Control System

The purpose of the sequential events control system is to control the sequential operation of crew-safety-related functions during the ascent and entry portions of the mission or, in the event of an abort, to perform the normal separation functions. A functional flow diagram of the sequential system is shown in figure A.1-6.

The sequential events control system consists of redundant controllers, or functions, which provide automatic, semi-automatic, and manual control for initiation and termination of various mission events. These

controllers include those for the master events sequence, earth landing sequence, the reaction control system, and the service module jettison, as well as the pyrotechnic continuity verification box. Each controller contains relays, timers, and other components to control systems operation and automatic timing of events.

A.1.4 Communications System

The communications system (fig. A.1-7) includes the spacecraft communications and data equipment required for the following functions: voice communications; acquisition, processing, storage, and transmission of operational and flight-qualification telemetry data; reception of updata; appropriate tracking and ranging signals; onboard television transmission; special communications tests, and postlanding recovery transmissions. The system includes both VHF and S-band antennas to accommodate the various RF frequencies used in air-to-ground transmissions.

Voice communications include spacecraft intercommunications between crewmen, hardline two-way voice communications with the Launch Control Center through the service-module umbilical during the prelaunch period, inflight two-way voice communications with the Manned Space Flight Network by VHF-AM and S-band systems, and postlanding voice communications with recovery ships and aircraft.

Data operations include time-correlated voice tape recording of flight crew comments and observations; acquisition and processing of on-board telemetry data for monitoring the operation of spacecraft systems and crew performance; telemetry data storage; S-band transmission of real-time or stored telemetry data; and S-band reception of updata (guidance and navigation data, timing data, and real-time commands) from the Manned Space Flight Network.

The tracking and ranging capability includes retransmission of S-band pseudo-random noise codes received from the Manned Space Flight Network uplink, and the maintaining of downlink carriers in phase coherence for ranging and tracking of the spacecraft. The recovery beacon transmissions are also included in this category.

A.1.5 Environmental Control System

The environmental control system is functionally depicted in figure A.1-8 and includes the following circuits:

- a. Pressure suit and cabin
- b. Oxygen distribution and pressure control
- c. Heat transport
- d. Water management
- e. Waste management
- f. Postlanding ventilation

Pressure control of the suit circuit, spacecraft cabin, and fluid storage tanks is accomplished by the oxygen control system. The primary oxygen supply is the cryogenic gas storage system in the service module; in addition, 7 pounds of gaseous oxygen, stored in the command module, is available during periods of high system flow requirements, such as after command module/service module separation, and to provide a cabin represurization capability of from 0 to 3 psia in 1 minute.

The heat transport system contains a primary and a partial secondary heat-transport loop. The transport fluid is a water/ethylene glycol mixture. The temperature of the heat-transport fluid is controlled either by radiator heat rejection to space or by water evaporation.

The water management system provides water for food reconstitution, drinking, and evaporator boiling. Potable water is supplied as a by-product from the fuel cells, and waste water is primarily perspiration condensed by the suit heat exchanger. If the water production rate should exceed the usage rate, the water is dumped overboard through the dump nozzle after both the potable-water tank (36 pounds) and waste-water tank (56 pounds) are full. Urine is also dumped through this nozzle. An auxiliary dump nozzle is installed in the unified-hatch purge fitting.

After spacecraft landing, the postlanding ventilation system provides fresh air into the cabin, and active cooling is no longer required. This ventilation system is composed of an inlet valve, an outlet valve, and a selectable 100 to 150 cfm fan. A ball check valve is provided to vent the tunnel section but to preclude entry of water should the command module assume a stable II (apex down) position in the water.

A.1.6 Guidance and Control System

Guidance and control of the spacecraft is provided by the primary guidance, navigation, and control system and by two backup systems, the stabilization and control system and the entry monitor system. Either the primary system or the combination of the two backup systems is capable of accomplishing the following major functions:

- a. Maintain an attitude reference frame from which any desired attitude can be established and maintained
- b. Perform any desired attitude and/or translation maneuver
- c. Generate stabilization commands to control the thrust vector during powered flight
- d. Measure velocity changes along the spacecraft longitudinal axis
- e. Display system status information and spacecraft dynamic data to the crew

The primary system provides the following additional capabilities that are not available with the two backup systems:

- a. Determine spacecraft position and velocity
- b. Compute and automatically execute maneuvers necessary to change the spacecraft trajectory
- c. Generate steering commands to cancel any cross-axis velocities during service propulsion maneuvers
- d. Automatically guide the spacecraft to a specific landing point during entry

The primary and backup systems were interconnected to the extent that the rotation and translation hand controllers, the electronics that provided control engine on-off signals, and the flight director attitude indicator are part of both the stabilization and control system and the guidance, navigation, and control system.

Guidance, navigation, and control system.- A functional diagram of the guidance, navigation, and control system is shown in figure A.1-9. This system consists of inertial, optical, and computing equipment.

The inertial equipment, which includes an inertial measurement unit and inertial coupling data units, senses spacecraft acceleration and changes in attitude and provides velocity and attitude information to the

computer equipment. The inertial measurement unit consists of a stable platform mounted in a three-degree-of-freedom gimbal system. Mounted on the stable member are three accelerometers and three gyroscopes to provide velocity and attitude information.

The optical equipment, which consists of a sextant, a scanning telescope, optical coupling data units, MARK and REJECT switches, and a minimum-impulse hand controller, provides directional data to the command module computer. Visual sightings are made and precision measurements are taken on celestial objects by using the sextant and the telescope. The optics data are used in the command module computer to calculate spacecraft position and trajectory and to align the inertial measurement unit to an inertial reference.

The computing equipment, which consists of digital computer and two display/keyboard assemblies, provides data processing, data storage, information displays to the crew, and a limited malfunction diagnosis capability. It also provides a time standard for the guidance and navigation computations and for the central timing equipment. Stored within the computer's memory is a series of instructions forming various programs and routines used to navigate, guide, and control the spacecraft through its various flight phases. Of special interest are those routines that make up the three digital autopilot systems:

- a. The reaction control system autopilot, which provides attitude control
- b. The thrust-vector-control autopilot, which processes steering commands and generates gimbal drive signals for the stabilization and control system during service propulsion maneuvers
- c. The entry autopilot, which provides rate damping and lift vector control during entry.

Stabilization and control system.- The stabilization and control interface with other systems is shown in figure A.1-10. This system consists of an attitude reference system, attitude control system, thrust vector control system, mode switching logic, and crew displays.

The attitude reference system includes body-mounted attitude gyros, a gyro display coupler, an electronic display assembly, an attitude-set control panel, and two flight director attitude indicators. The system senses spacecraft changes in attitude and rate to provide an attitude reference for the stabilization and control system. An attitude reference frame, established with the gyro display coupler, is used for effecting desired attitude changes. The redundant body-mounted attitude gyros provide attitude and rate data to the electronic display assembly,

which in turn displays this information on the flight director attitude indicator.

The attitude control system utilizes information from the body-mounted attitude gyros and the attitude and translation hand controllers to generate firing commands to the control engines. The system provides for manual-direct, minimum-impulse, and attitude-hold types of rotation and direct translation control.

Thrust vector control equipment generates commands to change the position of the gimbal actuators such that the thrust vector is through the spacecraft center-of-gravity. Three modes of control are provided for the redundant gimbal system: fully automatic, and manual with and without rate compensation.

Entry monitor system.- The entry monitor system provides a backup method for monitoring both the entry and any midcourse correction maneuvers. For major thrusting phases, the desired change in velocity is preset into the system, which then integrates the acceleration during the firing, decrements the change-in-velocity display, and automatically issues a service-propulsion system cutoff command when the change in preset velocity is reduced to zero.

During entry, the entry monitor system is initialized with a predicted horizontal range from the point at which 0.05g acceleration is sensed to the landing point. After the 0.05g point is reached, the system provides a continuous display of spacecraft acceleration, velocity, roll attitude, and range-to-go. The entry monitor displays permit the crew to evaluate the entry trajectory such that a decision can be made for manual takeover at any time to complete a safe landing.

A.1.7 Electrical Power System

The electrical power system consists of the equipment and reactants, which provide energy storage and power generation, conversion, and distribution for the spacecraft. A functional schematic of the system is shown in figure A.1-11. Primary electrical power is provided by three fuel cells which combine cryogenic hydrogen and oxygen to produce electrical energy and water.

Energy storage.- Cryogenic oxygen in the fuel cells is stored in two identical tanks at a pressure of 900 psia. Each tank nominally holds 320 pounds of usable oxygen and contains two heaters and two circulating fans which automatically control tank pressure and maintain the oxygen in single-phase thermodynamic condition. The automatic control can be overridden by the crew. A schematic of the oxygen storage system is shown in

figure A.1-12. Cryogenic hydrogen is stored in two identical tanks at a pressure of 245 psia. Each tank nominally holds 28 pounds of usable hydrogen and contains heaters and circulating fans similar to those in the oxygen tanks.

Electrical energy is stored in five silver-oxide/zinc batteries located in the command module. Three of these five are entry batteries which are rated at 40 ampere-hours each and are rechargeable. The remaining two are pyrotechnic batteries which supply power for pyrotechnic ignition and are isolated from all other electrical circuits. These batteries are not rechargeable. If one or both pyrotechnic batteries fail, power is available from the entry batteries through a normally open circuit breaker which connects the entry batteries to the pyrotechnic buses. Two of the entry batteries are placed on-line in parallel with the fuel-cells during peak-power loads, such as service propulsion maneuvers, to augment the fuel cell capability to accept transient load conditions. After the command module is separated from the service module, the entry batteries provide all spacecraft power.

Power generation.- Each of the three Bacon-type fuel cells can supply up to 1420 watts of primary dc power at 29 volts under normal operating conditions. All three fuel cells are activated before lift-off. In the event of failure of one fuel cell, the remaining two can provide sufficient power for safe return of the crew from a lunar mission with nonessential loads removed. Each fuel cell uses a glycol/radiator cooling system and uses potassium hydroxide as the electrolyte. A schematic of the fuel cell power-plant system is shown in figure A.1-13.

Power conversion.- Conversion of dc to ac is provided by three solid-state inverters that provide 115-volt, 400-Hz, 3-phase power of up to 1250 volt-amperes each. A single inverter could supply all ac power requirements. Each inverter may be connected to either or both of the ac buses, but the inverters cannot be connected in parallel because they are not phase-synchronized. A solid-state battery charger can use either primary dc power or ac power to provide current at a constant voltage of 40 V dc for entry-battery recharging during the flight.

Power distribution.- Both dc and ac power distribution is accomplished through two main buses in each system. A single-point ground on the spacecraft structure eliminates ground-loop effects. Sensing and control circuits provide for the monitoring and protection of each system. Distribution of dc power is accomplished through a two-wire system and a series of interconnected buses, circuit breakers, isolation diodes, and switches. The dc negative buses are connected to a single-point ground. Distribution of ac power is accomplished with a four-wire system and a pair of isolated buses. The ac neutral bus is connected to the single-point ground.

A.1.8 Service Propulsion System

The service propulsion system provides the primary impulse for all major velocity changes, including the capability for launch abort after the launch escape system has been jettisoned. Control of the system is primarily automatic, but a manual override is provided. The service propulsion system incorporates a helium pressurization system, a propellant feed and gaging system, and a rocket engine. The oxidizer is nitrogen tetroxide, and the fuel is a blend of approximately 50 percent unsymmetrical dimethyl hydrazine and 50 percent anhydrous hydrazine. Displays and sensing devices are included to permit ground-based stations and the crew to monitor system operation. Functional flow diagrams are presented in figures A.1-14 and A.1-15.

The propellant supply includes storage and sump tanks for both the oxidizer and fuel. The storage and sump tanks for each propellant system are connected in series by a single transfer line. Propellant quantity is measured by both a primary and auxiliary sensing system. The sensing systems are active only during thrusting periods because the capacitance and point-sensor measuring techniques do not provide accurate quantity indications under zero-g conditions. A propellant utilization valve is installed in the oxidizer line but is powered only during thrusting periods. This valve provides for optimum depletion of both propellant fluids. The bipropellant valve distributes the propellants to the engine injector during thrusting periods and isolates the propellants from the injector during non-thrusting periods.

The engine assembly is gimbal mounted to the aft bulkhead of the service module to permit thrust-vector alignment through the center of mass prior to thrust initiation and to provide thrust-vector control during thrusting periods.

A.1.9 Reaction Control Systems

The two reaction control systems are those of the service module and the command module. After the spacecraft has separated from the launch vehicle, the service module reaction control system controls space-craft rotation about all three axes and can perform minor translation maneuvers, including separation from the launch vehicle, service-propulsion-system ullage maneuvers, and the command module/service module separation maneuver. After the command module is separated from the service module, the command module reaction control system controls space-craft rotation about all three axes. This system does not possess direct translation capability, but with specialized techniques, it may be used to provide a backup deorbit capability. Diagrams of the two systems are shown in figures A.1-16 and A.1-17.

The propellants for both reaction control systems consists of nitrogen tetroxide as the oxidizer and monomethyl hydrazine as the fuel. Pressurized helium gas is the propellant-transfer agent. The reaction control engines are capable of being fired in either a pulse mode to produce small impulses or continuous mode to produce a steady-state thrust of 100 lbs each. Each engine includes electrically operated fuel and oxidizer valves using an automatic coil excited by signals from the stabilization and control system or a direct coil excited by commands from the hand controller.

Service module reaction control system.- The service module reaction control system consists of four functionally identical packages, or quads, located 90 degrees apart around the forward section of the service module periphery and offset from the Y-axis and Z-axis by approximately 7 degrees. Each quad configuration is mounted such that the reaction-control engines are on the outer surface of the vehicle and the remaining components are inside the vehicle. The engine combustion chambers are canted approximately 10 degrees away from the panel structure, and the two roll engines on each quad are mounted in an offset fashion to accommodate engine plumbing. Each quad package incorporates a pressure-fed, positive-expulsion, pulse-modulated, bipropellant supply system to produce engine thrust. The operating temperature of each quad is maintained by internally mounted, thermostatically controlled electric heaters.

Command module reaction control system.- The command module reaction control system is designed to provide the thrust control necessary to orient the command module to a predetermined entry attitude and to maintain the proper orientation and stabilization during the entry phase of the mission. This system actually consists of two identical and independent systems. One system can be manually selected for entry operations, and the other system reserved for backup. Although either system can provide the impulse necessary to perform the required entry maneuvers, both systems are normally activated and pressurized just prior to command module/service module separation. Both systems are totally contained within the command module, and each of the 12 engine nozzles are ported through the vehicle surface in a sector predominantly on the minus Z side. The propellant and pressurizing tanks are located in the aft compartment on the plus Z side.

A.1.10 Instrumentation System

The instrumentation system provides for monitoring spacecraft system status, crew biomedical functions, flight events, and certain scientific activities. These data are transmitted in real time to ground receiving stations of the Manned Space Flight Network and may also be recorded onboard the spacecraft for later playback.

The instrumentation system is divided into two major groups: operational and flight qualification instrumentation systems (fig. A.1-18). Operational instrumentation is required for preflight checkout of the spacecraft, inflight monitoring of the spacecraft and crew, and postflight evaluation of system performance. Flight qualification instrumentation is required for evaluation of vehicle test objectives relative to the qualification and verification of engineering design. This instrumentation is separable and related to a specific mission, and most flight qualification data are stored on a separate recorder.

The operational instrumentation system is primarily composed of sensors, signal conditioning equipment, pulse code modulation, central timing, and data storage equipment. Information processed includes analog and digital signals from the guidance and navigation system and data from the central timing equipment, the sensors, and the transducers located throughout the spacecraft systems and from the biomedical sensors worn by the crewmen. These signals are either conditioned within integrated instrumentation pickups or conditioned by central signal-conditioning equipment for onboard handling. The PCM equipment converts the analog and event functions and computer and central-timing-equipment words into time-sequenced digital output signals. These digital data are transferred to the premodulation processor for transmission over RF communication equipment.

Time correlation of instrumentation parameters is provided by the central timing equipment, which also provides timing and synchronization signals to other systems requiring time-sensitive functions.

For Apollo 7, biomedical instrumentation was limited to one crewman at a time, and no scientific instrumentation parameters were monitored.

Specific flight-qualification instrumentation equipment required for this mission was two constant bandwidth modulation packages, two 90 by 10 high-level commutators, one 90 by 10 low-level commutator, a flight qualification tape recorder with an internal time code generator, and sensors and transducers located throughout the spacecraft. Time correlation was also provided by time code word which was recorded on the flight qualification tape recorder.

The flight qualification instrumentation data were recorded during three mission phases: launch, fifth service propulsion maneuver, and entry. The data were processed by the high-level commutator located in the service module and were also redundantly transmitted via the operational PCM system.

A.1.11 Pyrotechnics

Certain spacecraft events and operations are initiated or accomplished by pyrotechnic devices. Nearly all these devices are actuated electrically by means of a standard hotwire initiator. In most applications, the initiator is boosted by another explosive charge to perform the required function, and redundant hotwire initiators or cartridges are provided. The electrical signal that activates pyrotechnic devices generally comes from the sequential events control system, but manual backup initiation is available to the flight crew. The following is a list of functions initiated or accomplished by pyrotechnic devices:

- a. Launch escape system
 - 1. Canard deployment
 - 2. Escape-tower leg separation
 - 3. Pitch-control-motor ignition
 - 4. Launch-escape-motor ignition
 - 5. Jettison-motor ignition
- b. Earth landing system
 - 1. Apex-cover jettison
 - 2. Apex-cover parachute deployment
 - 3. Drogue deployment
 - 4. Drogue jettison
 - 5. Pilot parachute deployment
 - 6. Main-parachute deployment and drogue disreef (hotwire initiator not used)
 - 7. Antenna deployment release (hotwire initiator not used)
- c. Command module/service module separation
 - 1. Command module/service module tension tie separation
 - 2. Command module circuit interruption

3. Command module/service module umbilical separation
 4. Command module reaction control system pressurization
 5. Service module circuit interruption
- d. Adapter separation
1. Adapter/service module umbilical disconnect
 2. Adapter separation
 3. Adapter panel deployment
- e. Command module reaction control propellant dump and burnoff

A.1.12 Crew Provisions

The Apollo 7 crew provisions consisted of various removable equipment (listed in table A.1-I) required for crew support. The couch and restraint system provide support and restraint to the crew during launch, inflight thrust maneuvers, entry, and landing. The couches are also the normal station for most crew operations during zero-g portions of the flight.

The function of the waste management system is to control and dispose of fecal and urine wastes. The fecal material is collected, contained, and stowed in flexible bags, with a germicide added, and placed in protective outer bags. The urine is either collected in the urine collection transfer assembly in the suit or ported overboard through the urine dump line and nozzle.

Metal compartments and fabric containers provide stowage for the crew equipment. For example, a Beta fabric bag located beneath the hatch is used to store the three emergency oxygen masks. The food boxes, made of formed polyamide material, are removable to allow for packaging and refrigerated stowage prior to final installation.

The crewman electrical umbilicals transmit biomedical data to the telemetry system and the biomedical tape recorder and transmit voice signals to and from the spacecraft communication system.

The crewman oxygen umbilical ducts oxygen from the environmental control system to the space suit and circulates the return flow to the spacecraft system. These umbilicals are utilized when the flight crew are in their space suits in either a pressurized or unpressurized cabin.

The inflight tool set contains an emergency wrench, adapter handle, adjustable end wrench, U-joint driver, and torque set driver. These tools can be used to operate environmental control system valves, to unlatch or latch fasteners of access panels and cover caps, and other similar adjustments.

The internal and external metal viewing mirrors were located on adjustable arms above the crew couches. The internal viewing mirrors were used by the flight crew to aid in attaching and releasing the restraint system and for viewing the couch adjustment levers. The external viewing mirrors were used to verify launch escape tower jettison and parachute deployment.

The purpose of the crewman optical alignment sight is to provide range, range rate, and line-of-sight information during the docking maneuver. This sight can also be used to verify proper spacecraft attitude by sighting selected stars as a backup to the inertial measurement unit. The sight was a collimator device, similar to an aircraft gunsight, and consisted of a lamp with an intensity control, a reticle, a barrel-shaped housing, a mount, a combiner assembly, and a power receptacle. The normal location of the sight is at the left window, but it can be positioned at the right window. The unit is stowed near the left window for launch and entry.

The pressure-suit assemblies consist of a basic torso-limb pressure vessel with removable helmet and gloves. The suits are provided in an extravehicular and intravehicular configuration, both of which provide flame and abrasion protection to the crewman. The Commander and the Lunar Module Pilot wear the extravehicular version, which includes an integral outer thermal-meteoroid protective garment. The Command Module Pilot wears an integral outer cover layer garment, which is light weight by comparison to the thermal-meteoroid garment. The pressure garments are designed to provide sufficient mobility when pressurized to allow the crew to perform required tasks for a safe return to earth.

The inflight coverall garment is a three-piece suit consisting of a jacket, trousers, and boots and is worn over a constant wear garment during flight when the pressure suit is not required. This garment is entirely fabricated from Teflon fabric, and restraint tabs are incorporated to hold the communications adapter cable in place.

The sleep restraint assembly provides a crewman with a zero-g environment enclosure for use during rest periods. Two bags are provided, one each located under the left and right couches. These bags are made of Teflon Beta fabric restrained at each end to the bulkhead by straps, have a full-length zipper opening for the torso, and are perforated for ventilation. Straps are provided at the middle of the bag to secure the crewman if he is lying on the bag, rather than inside.

A.1.13 Recovery System

The recovery system includes the earth landing system, the uprighting system, the impact-attenuation system, and various recovery aids.

Earth landing system.- The purpose of the earth landing system is to attitude-stabilize the command module and decelerate it after entry to a safe velocity for landing. The system consists of two mutually redundant sequence controllers, two drogue parachutes, three pilot parachutes, three main parachutes, and associated devices such as mortars, reefing-line cutters, and parachute disconnects.

After activation by the flight crew, the earth landing sequence controller initiates the deployment of the drogues through closure of baroswitches at a pressure altitude of approximately 25 000 feet during descent. A second set of baroswitches in the sequence controller closes at a pressure altitude of approximately 11 000 feet to initiate drogue release and pilot-parachute deployment, which subsequently deploy the main parachutes. This sequence can be inhibited by the flight crew should they elect to perform the deployment manually.

The conical-ribbon drogues have a nominal diameter of 16.5 feet. The drogue riser consists of 16.7 feet of fabric line and 15 feet of steel cable. The steel portion consists of 4 strands of 1/4-inch stainless-steel cable which is dry-film-lubricated and is potted in foam for storage in the mortar. The drogues are deployed by two separate mortars initiated by the sequence controller and immediately restrained to 42.8 percent of nominal diameter by two active reefing lines. Approximately 10 seconds after line stretch, the reefing lines are severed by dual sets of pyrotechnically operated cutters, enabling the drogues to inflate fully. At a velocity low enough for safe deployment of the main parachutes, the drogues are disconnected and the pilot-parachute mortars are fired.

The three ringsail main parachutes decelerate the vehicle to a final descent velocity safe for landing. These parachutes have a nominal diameter of 83.5 feet. The main parachutes are initially reefed to 8.4 percent of the nominal diameter for approximately 7 seconds by two reefing lines, each having two reefing-line cutters. The second stage of reefing is 24.8 percent of the nominal diameter and uses two 10-second delay cutters on a single reefing line. The drogues and main parachutes are attached to the command module at the disconnect housing to give the command module a resulting hang angle of 27.7 degrees. A manual switch is provided to initiate the parachute-disconnect sequencer after landing.

Impact-attenuation system.- The impact-attenuation system is designed to reduce the landing shock, to maintain vehicle structural integrity, and to maintain crew deceleration at an acceptable level. The

external energy absorption is provided by the heat shield and inner structure and by crushable aluminum ribs in the aft compartment. The internal attenuation is provided by eight crushable aluminum honeycomb struts which support the crew couches and can absorb energy at predetermined rates in three different axes.

Uprighting system.- The purpose of the uprighting system is to insure an apex-up (stable I) flotation attitude of the command module after water landing. The system, shown in figure A.1-19, consists of three inflatable bags stowed in canisters on the parachute deck. Should the command module assume an apex-down (stable II) attitude after landing, the three bags can be simultaneously inflated by two compressors electrically operated on command from the crew. The crew can then shut off the compressors after the command module has rotated to an apex-up attitude.

Recovery aids.- Recovery aids for Apollo 7 consisted of the VHF antennas, a flashing light, and a sea-dye-marker/swimmer-umbilical, all located in the forward compartment.

During main parachute deployment, a lanyard attached to the parachute riser initiates an 8-second time delay in a pyrotechnic cutting device. This action releases the spring-operated mechanisms which deploy the two VHF antennas and the flashing light. The flashing light has an independent power source and can be turned on by the crew when required.

The sea-dye-marker/swimmer-umbilical deployment mechanism can be activated when the spring-loaded restraining pin is manually released. The sea dye canister is deployed overboard by springs, but remains attached to the command module by a cable that includes the swimmer telephone umbilical.

TABLE A.1-I.- EQUIPMENT LIST

<u>Couch pads and restraints</u>	<u>Crew accessories and operational equipment -</u> <u>continued</u>
Back pads (3)	Driver U-joint
Headrest pad	End wrench
Sleep restraint assembly (2)	Oxygen umbilical
Restraint harness, couch	Oxygen screen caps
<u>Waste and water management</u>	Oxygen coupling assembly
Hose, flex	Communications control cable
Water dispenser assembly	Control head
Fecal collection assembly	Electrical adapter
Outer fecal bag	<u>Carry-on equipment</u>
Inner fecal bag	Pressure suit assemblies
Germicide pouch	Constant wear garments
Wrapper	Penlights (3)
Wet wipe	Urine collection and transfer assemblies
<u>Containers and compartments</u>	Scissors
Strap, cable	Bioinstrumentation assemblies
Food container (2) and cover (2)	Dual life vests
Container, stowage	Bio-belt assemblies
Oxygen interconnect container	Communications carriers
Sanitation box (2)	<u>Stowed equipment</u>
Container, hose screen caps	Medical accessories kit
Window shade container	Survival rucksack kits 1 and 2
Pressure garment container (L-shape	Metering water dispenser
Temporary storage bag	Tissue dispensers
Storage bag (2)	Utility towel assemblies
Bag, oxygen mask	Helmet stowage bags
Constant wear garment adapter container	Extra vehicular mobility unit maintenance kit
<u>Crew accessories and operational equipment</u>	Constant wear garments
Optical sight and mount	O ₂ masks and hoses
Handhold, MDC-2 (monkey bar)	Dew point hygrometer
Straps, handhold	Inflight coverall garments
Handhold, MDC-2	Cabin O ₂ analyzer
Handhold strut	Penlights (5)
Mirrors	Urine transfer system and receiver
Tool set, inflight	Roll-on cuff stowage bags
Pouch	Neck dam assemblies
Tool tether	
Adapter handle	
Torque set drive	

NASA-S-68-6402

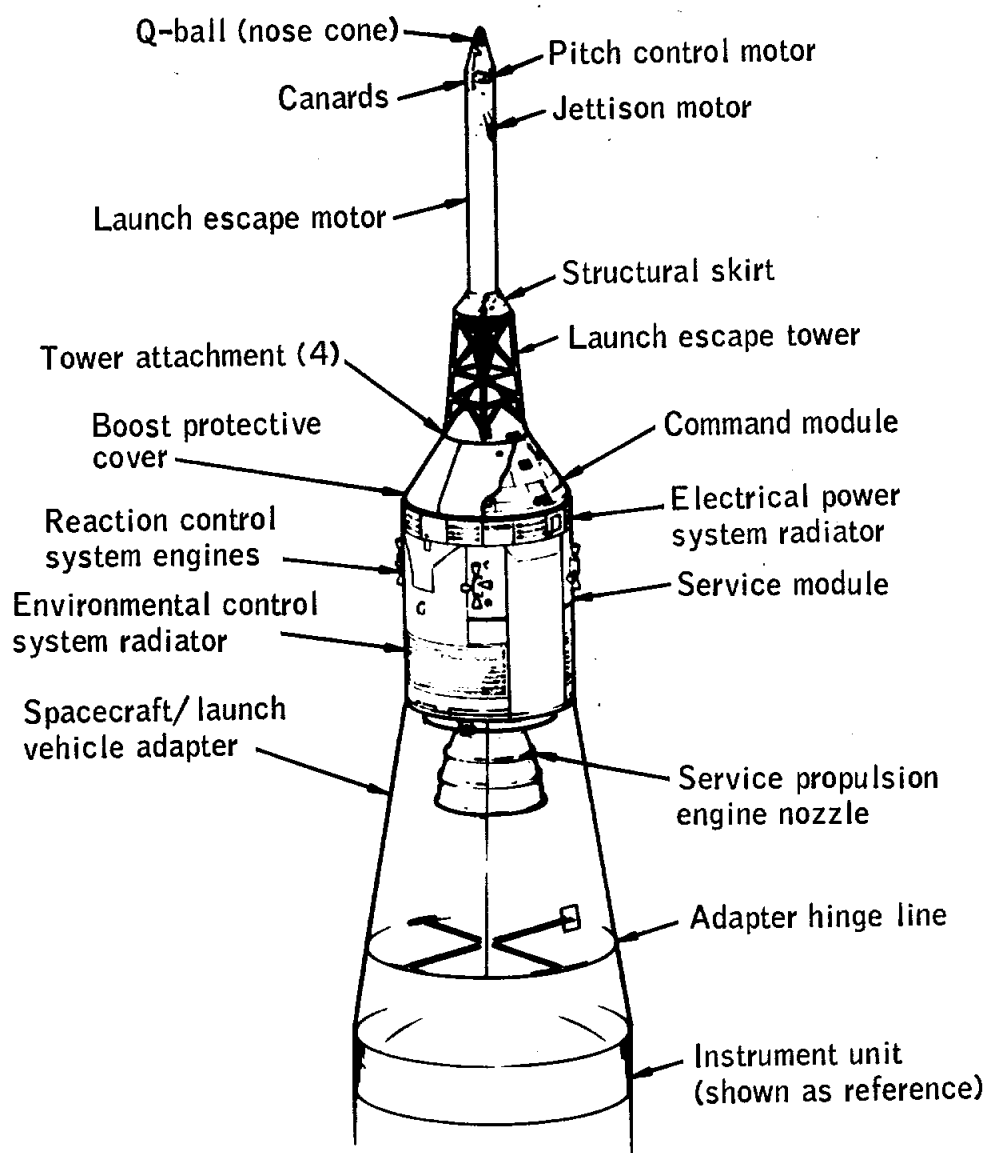


Figure A.1-1.- Spacecraft 101 configuration.

NASA-S-68-6403

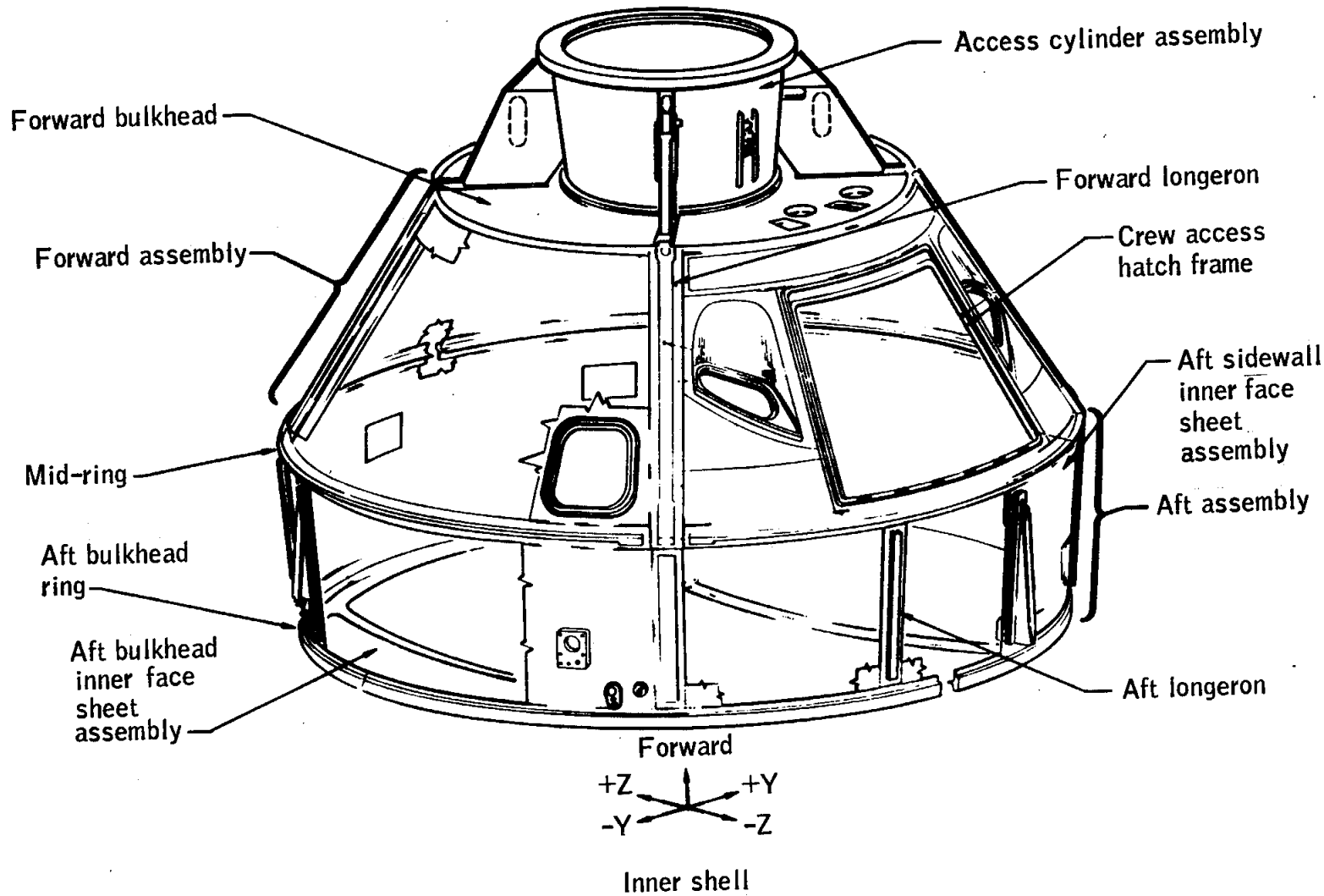


Figure A.1-2.- Inner structure.

NASA-S-68-6404

A-22

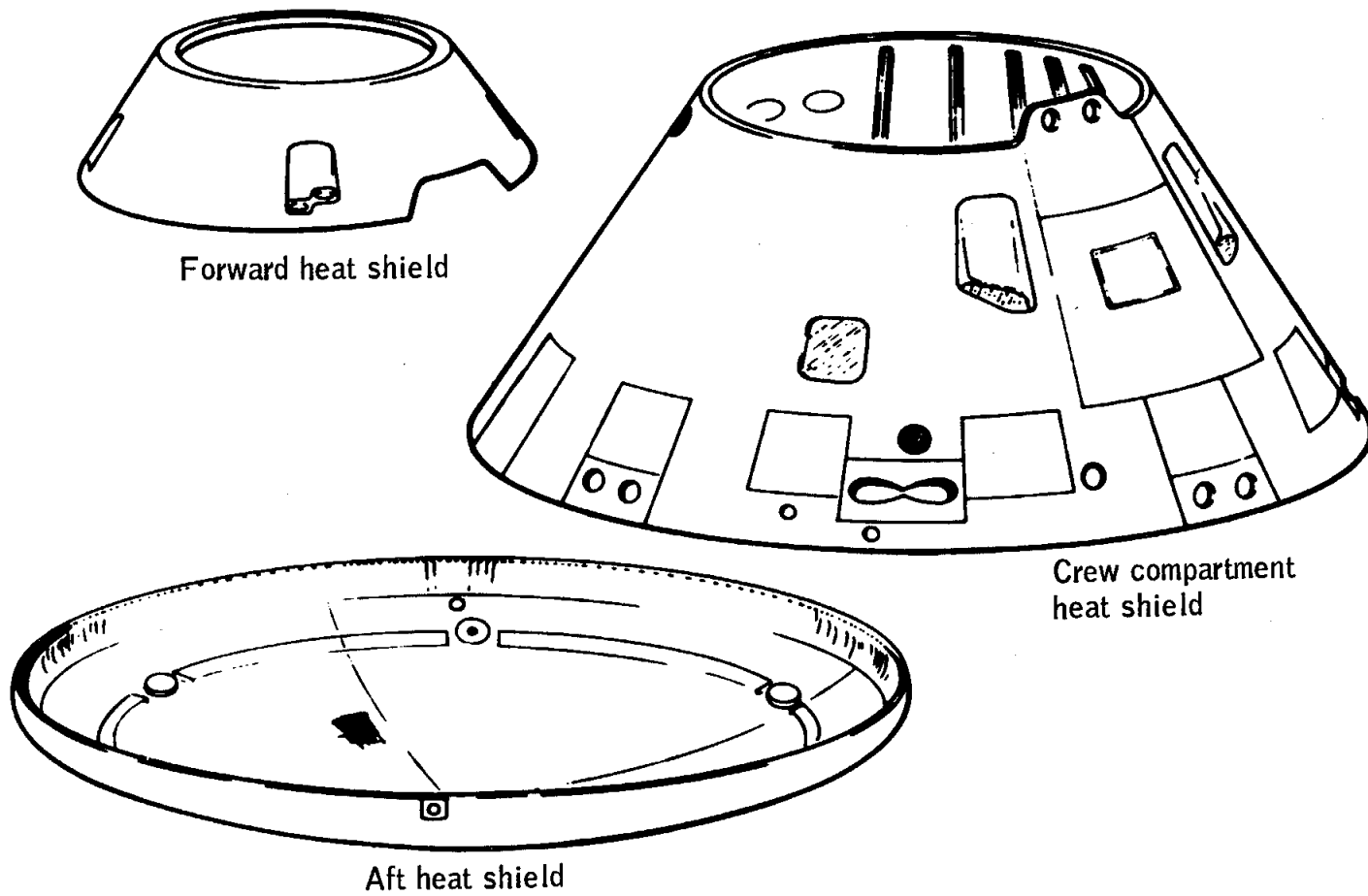


Figure A.1-3.- Command module heat shields.

NASA-S-68-6405

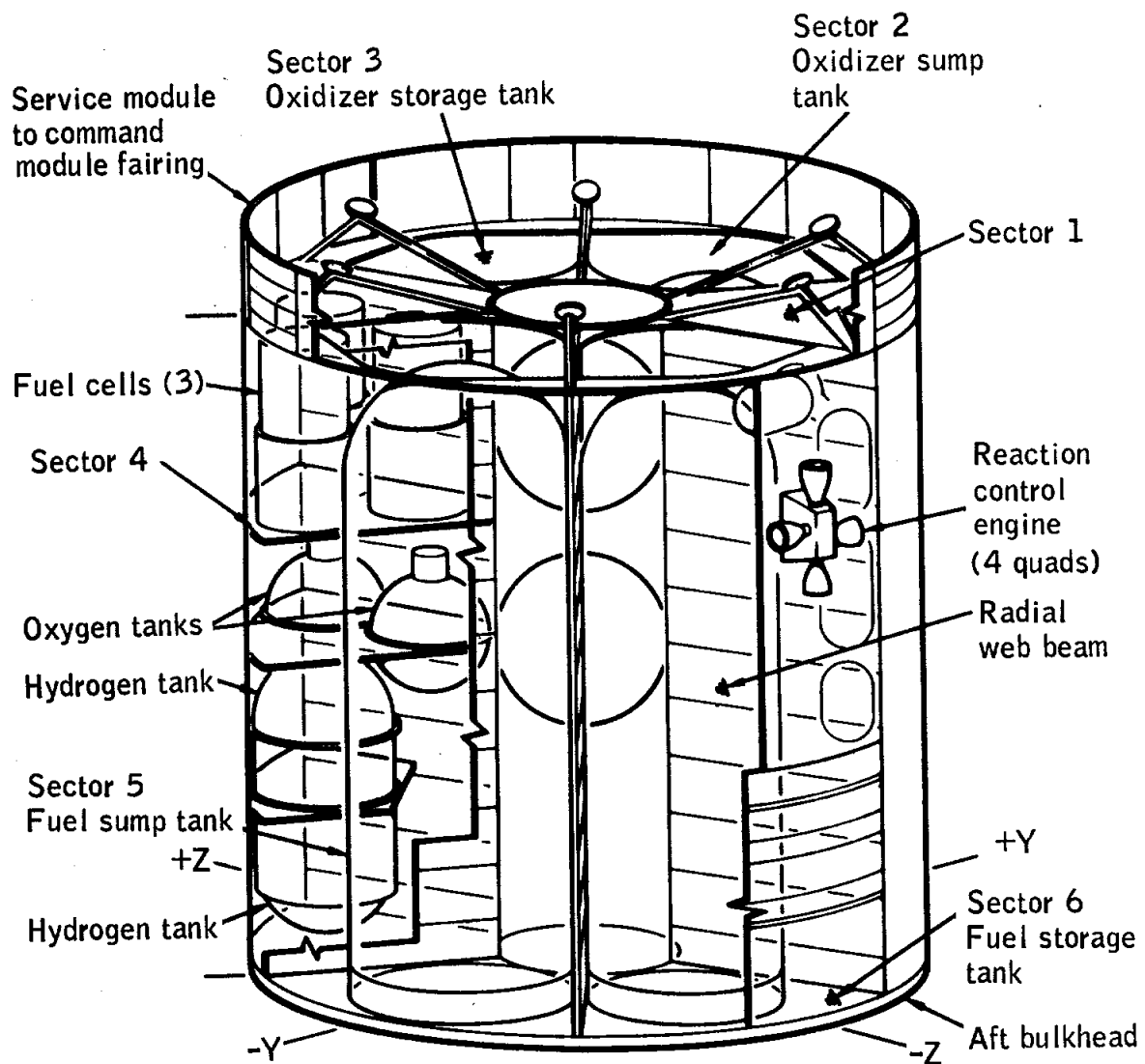


Figure A.1-4.- Service module.

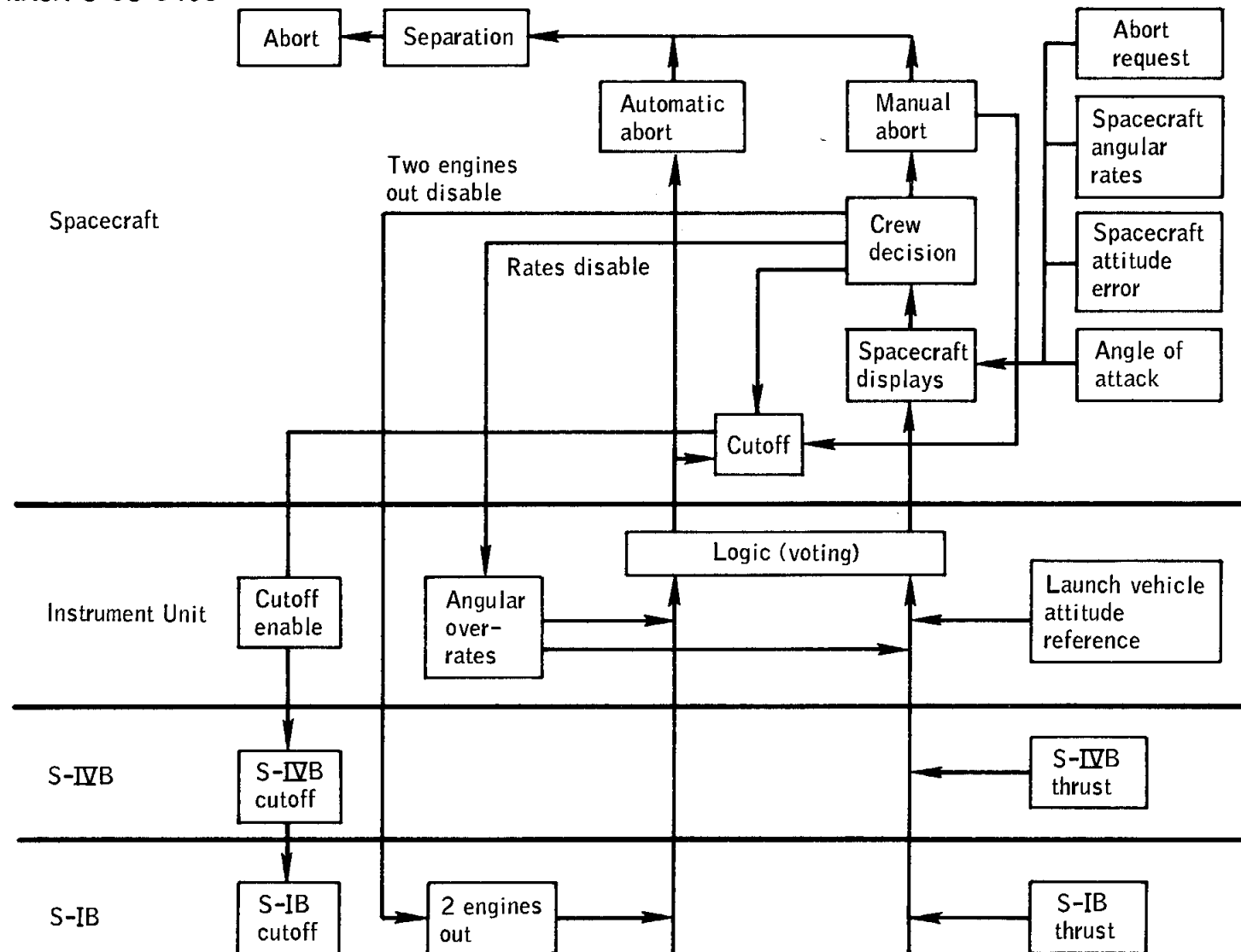


Figure A.1-5.- Emergency detection system.

NASA-S-68-6407

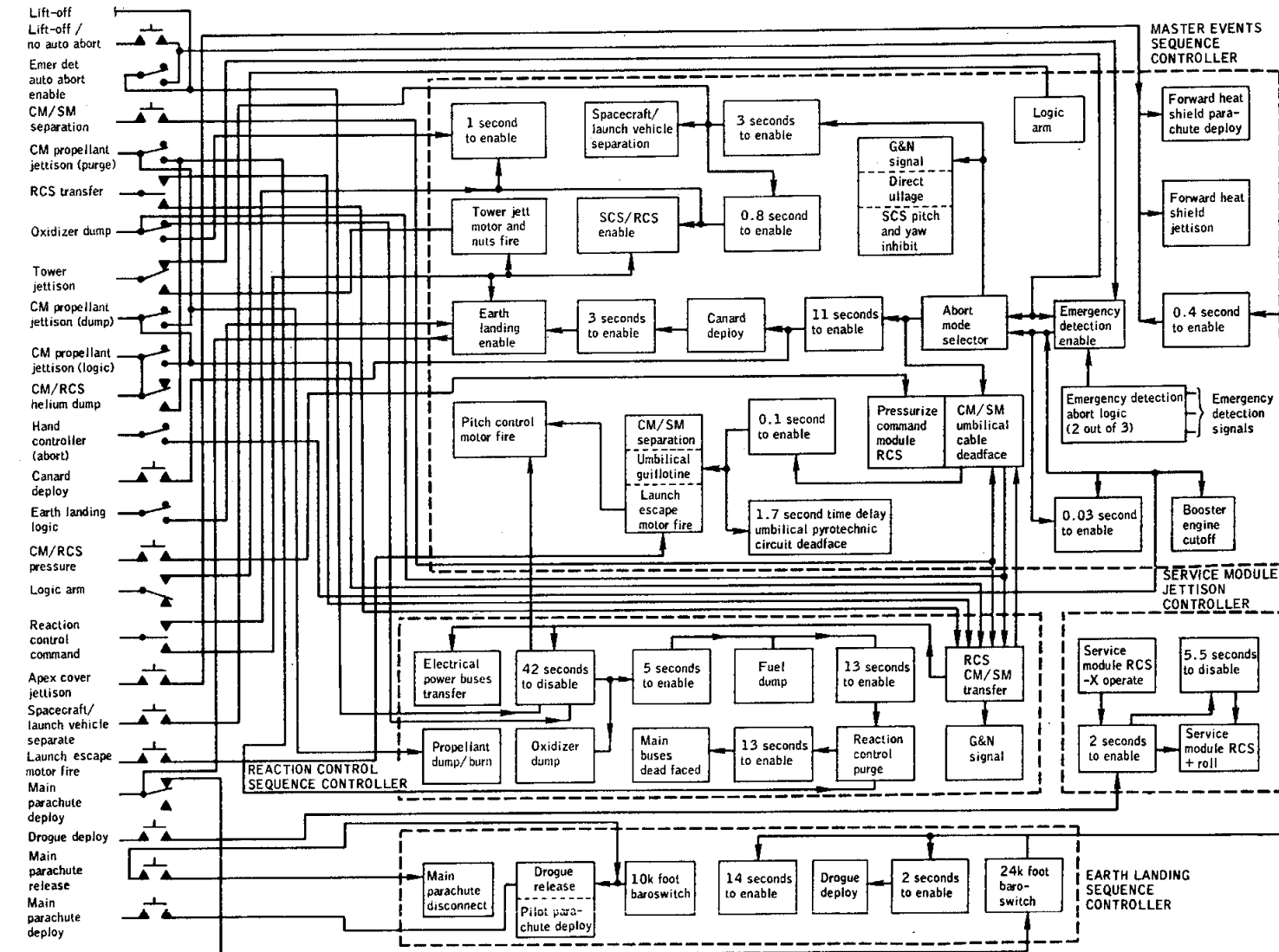


Figure A.1-6. - Sequential events control system.

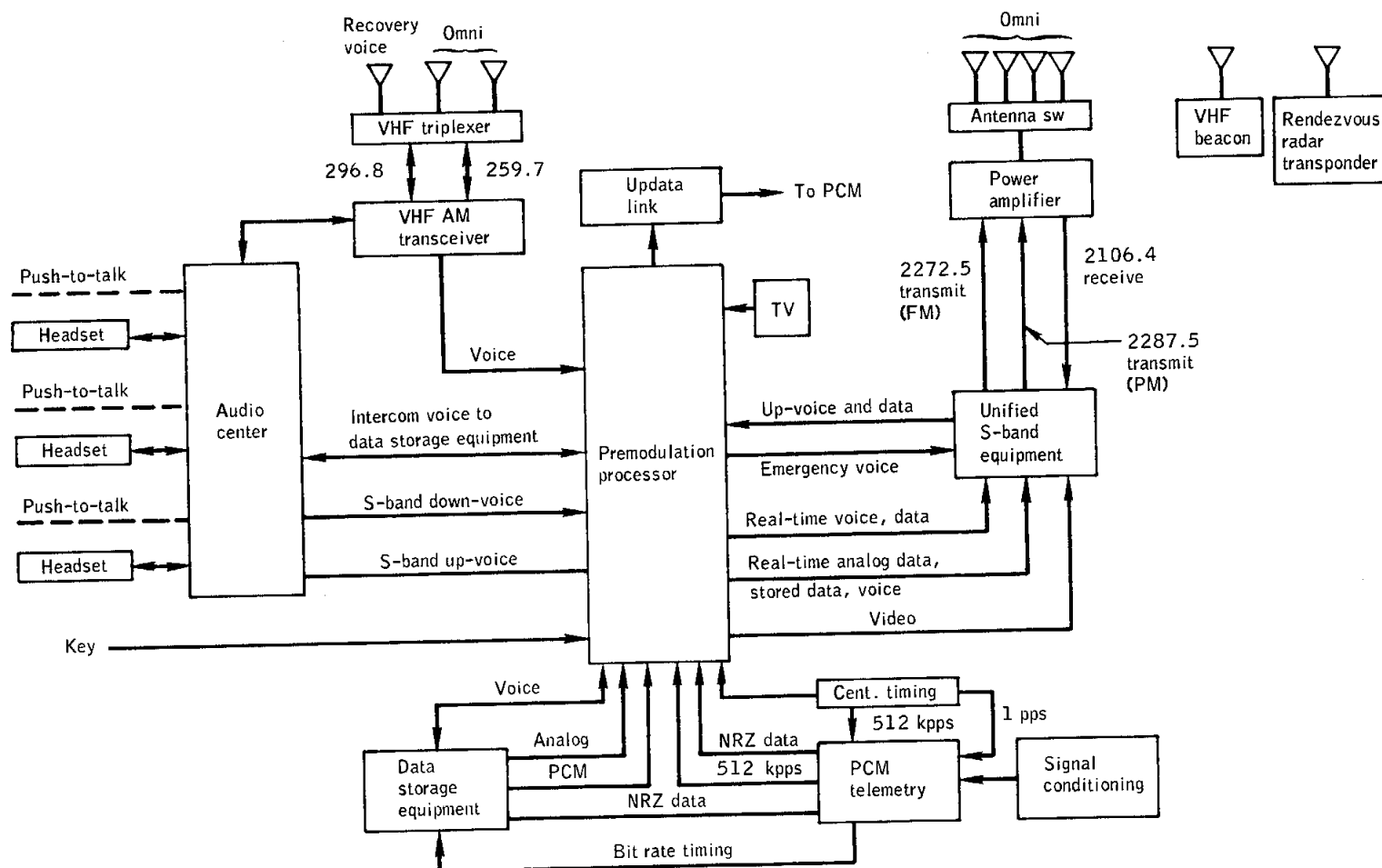
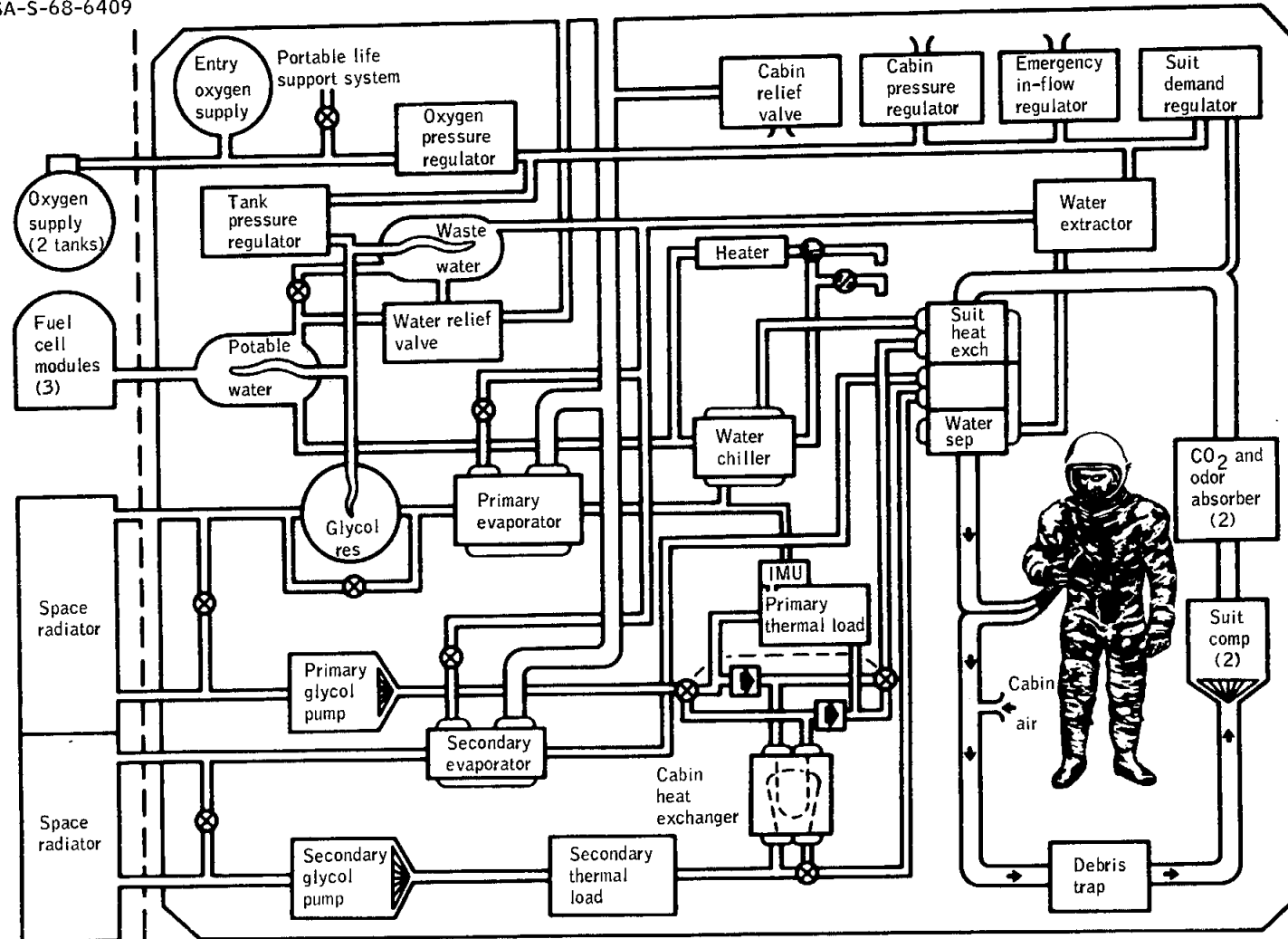


Figure A.1-7.- Communications.

NASA-S-68-6409



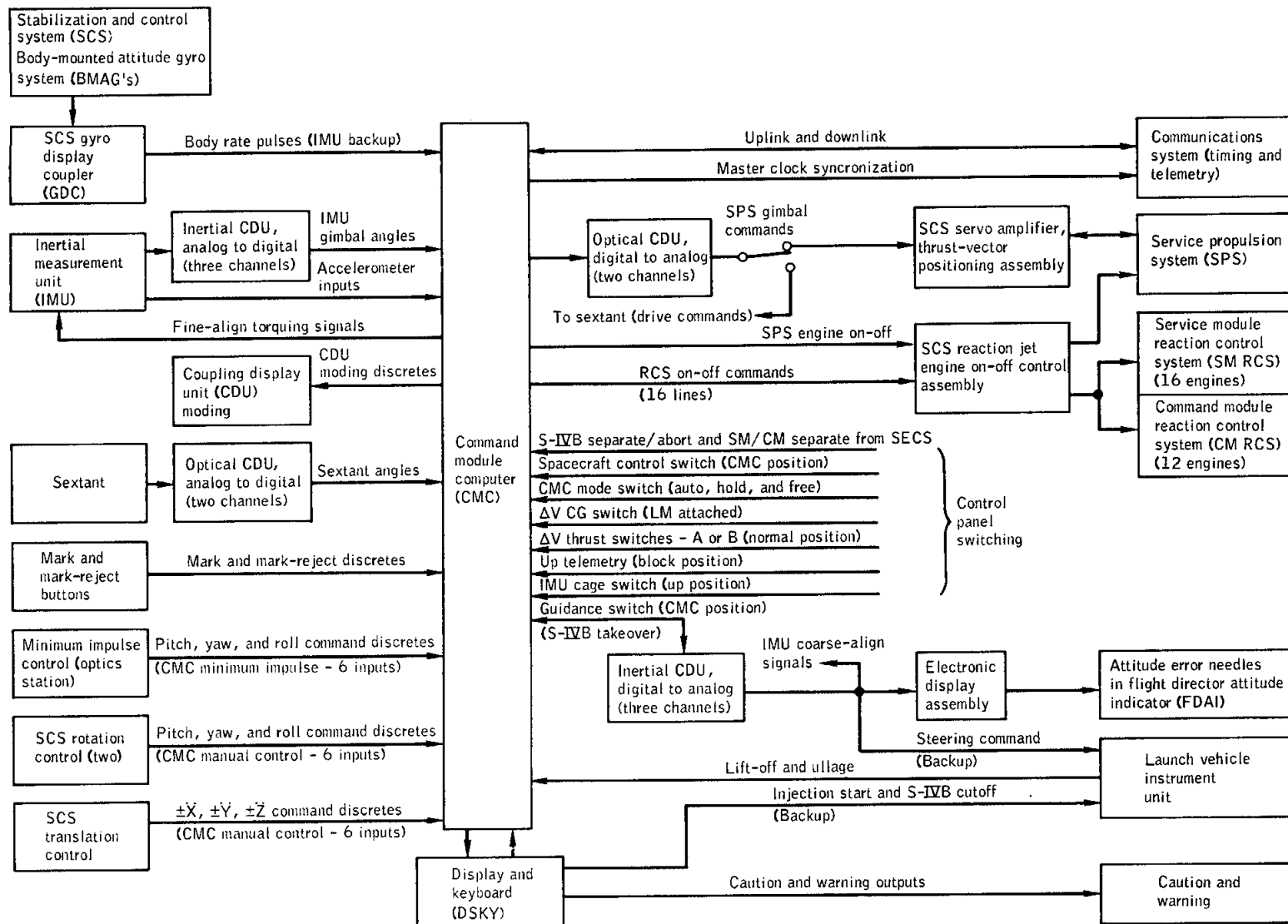


Figure A.1-9.- Guidance and navigation.

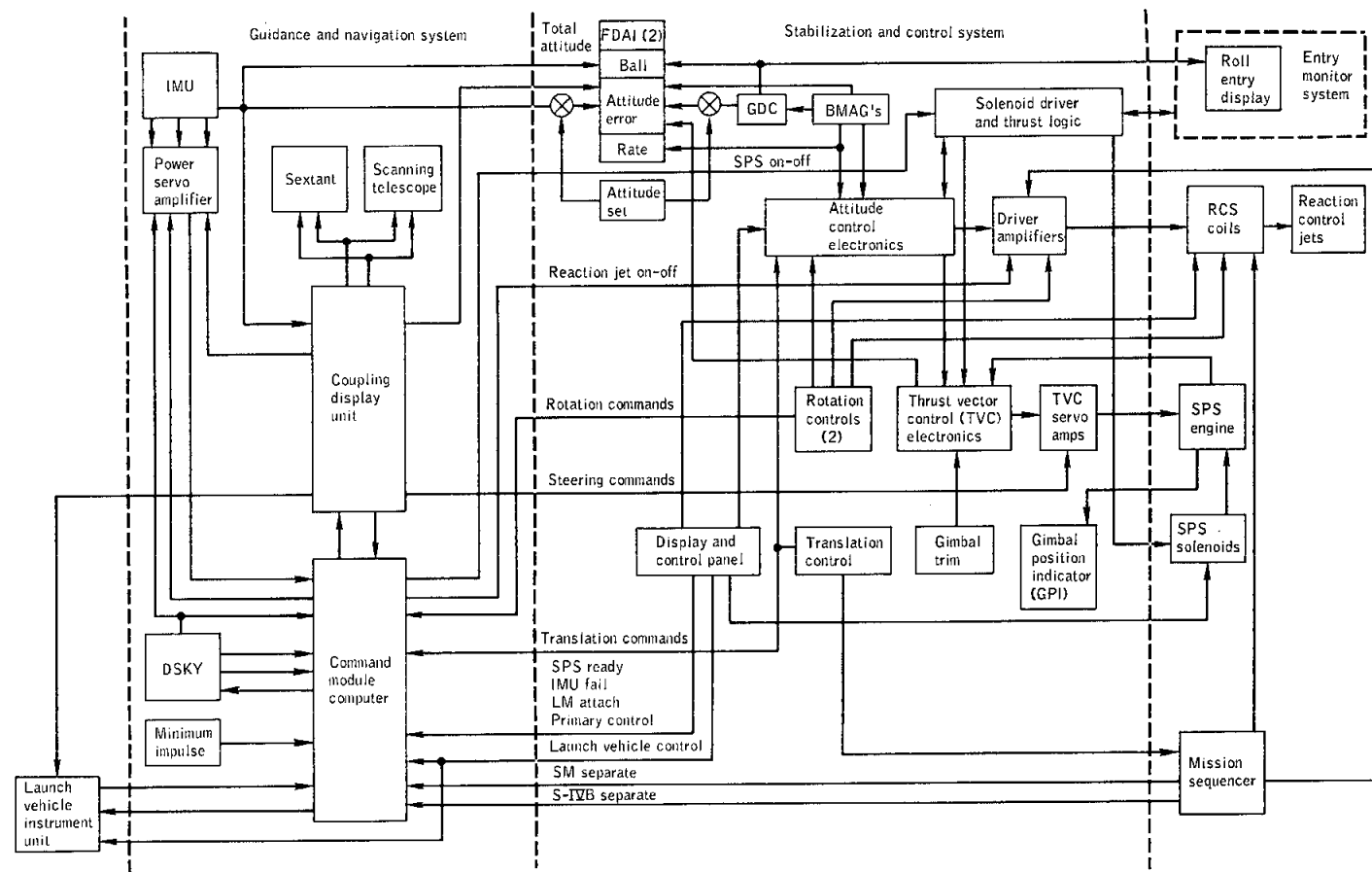
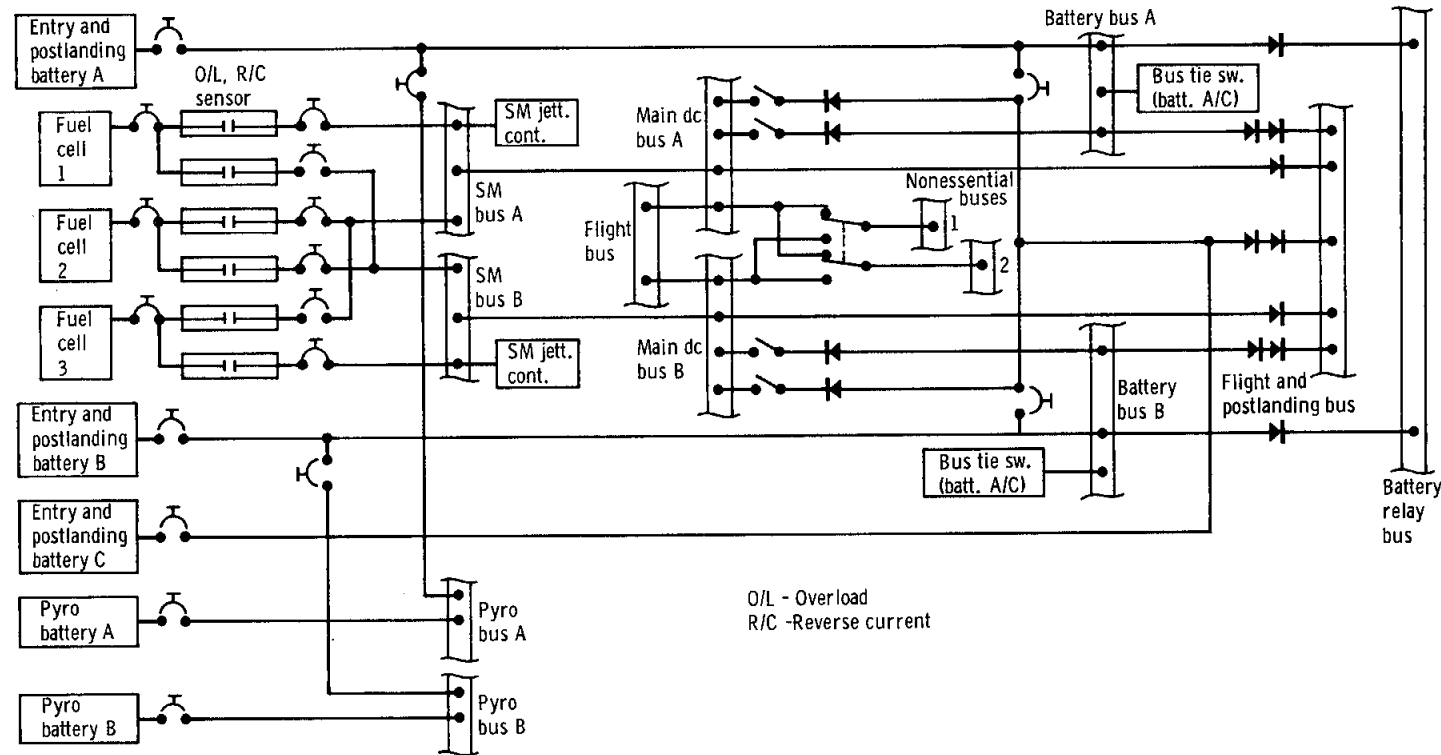


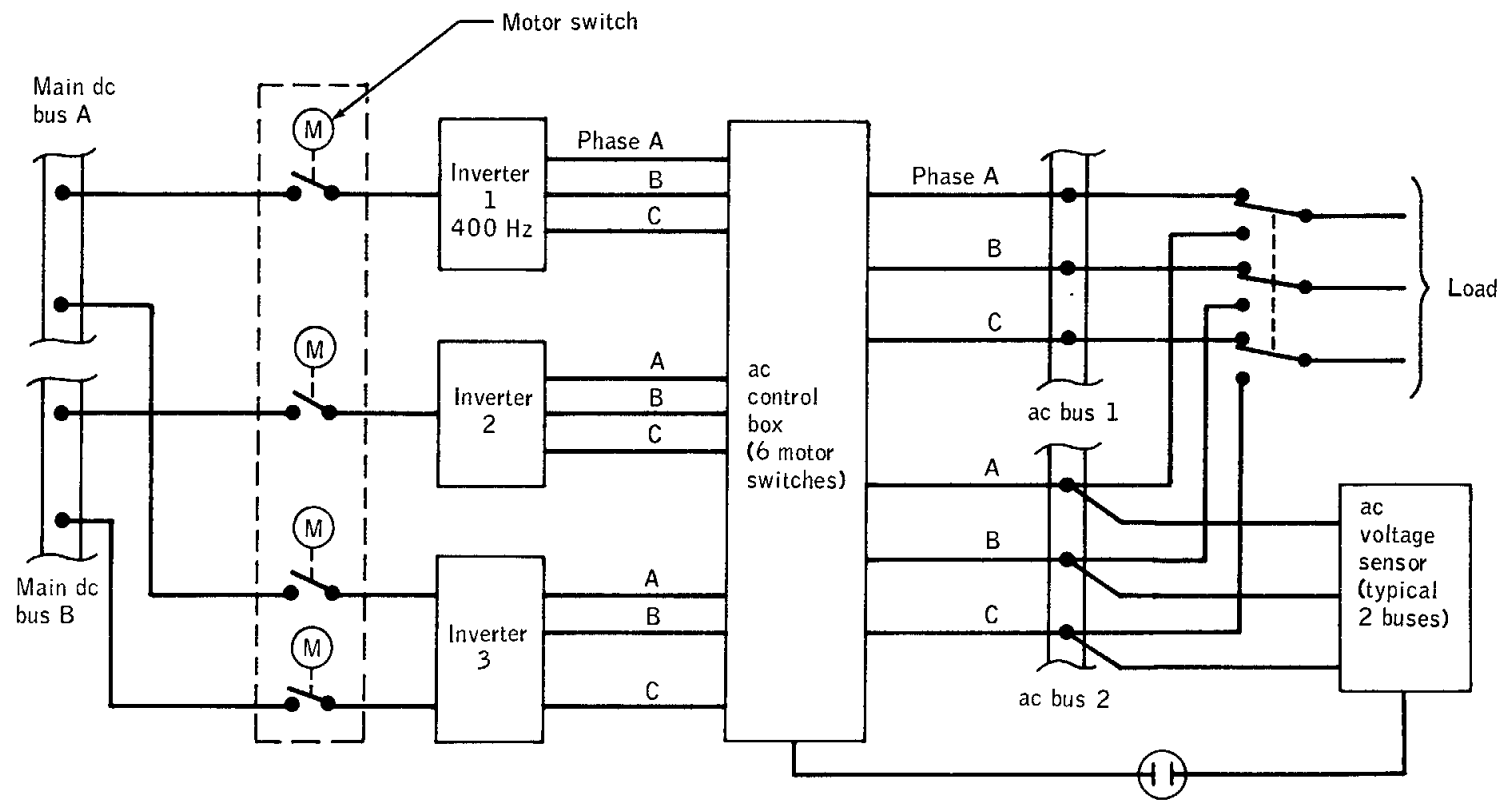
Figure A.1-10.- Stabilization and control system.



(a) dc

Figure A.1-11. - Electrical power system.

NASA-S-68-6413



(b) ac.

Figure A.1-11.- Concluded.

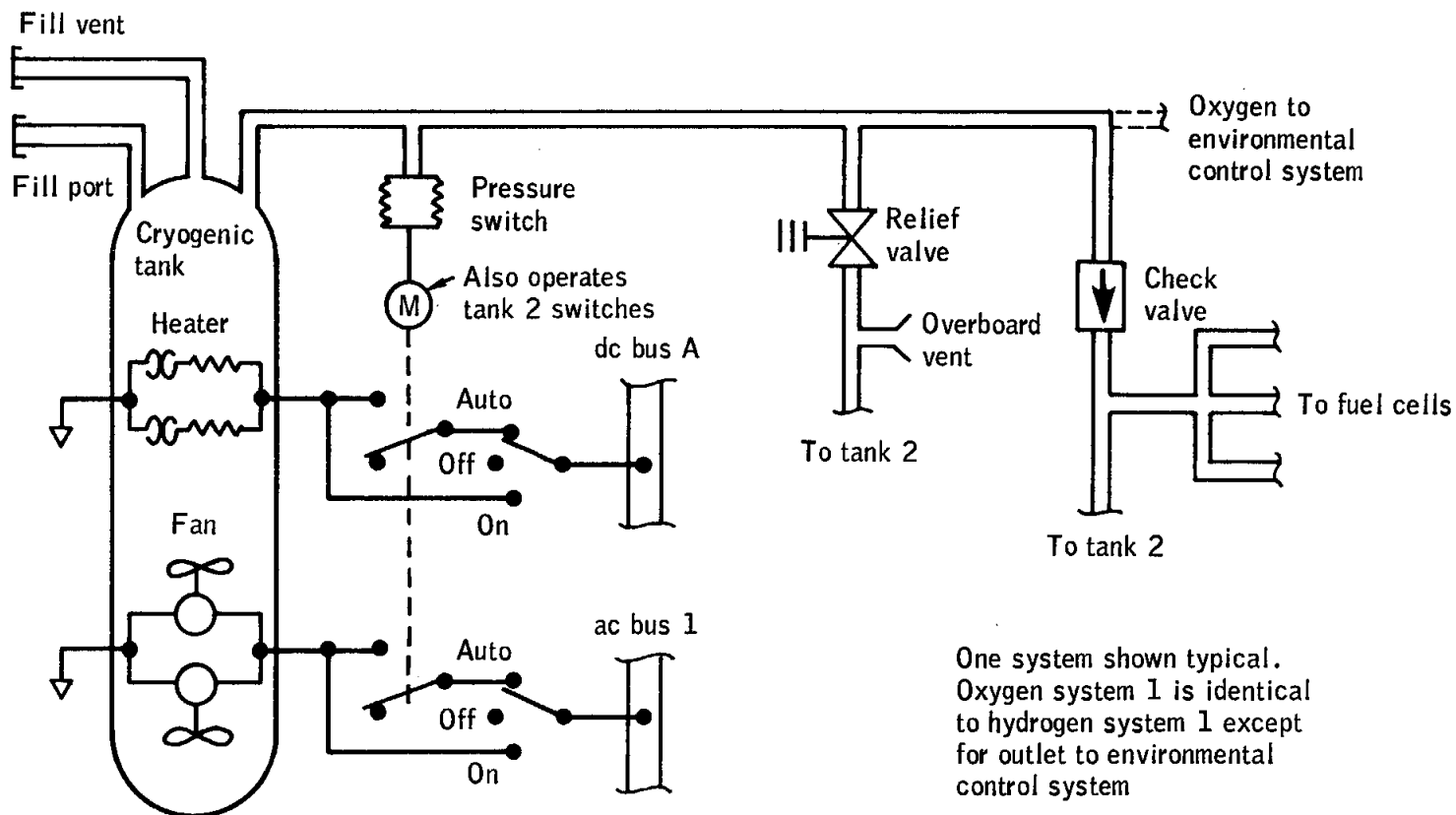


Figure A.1-12.- Cryogenic oxygen storage system.

NASA-S-68-6415

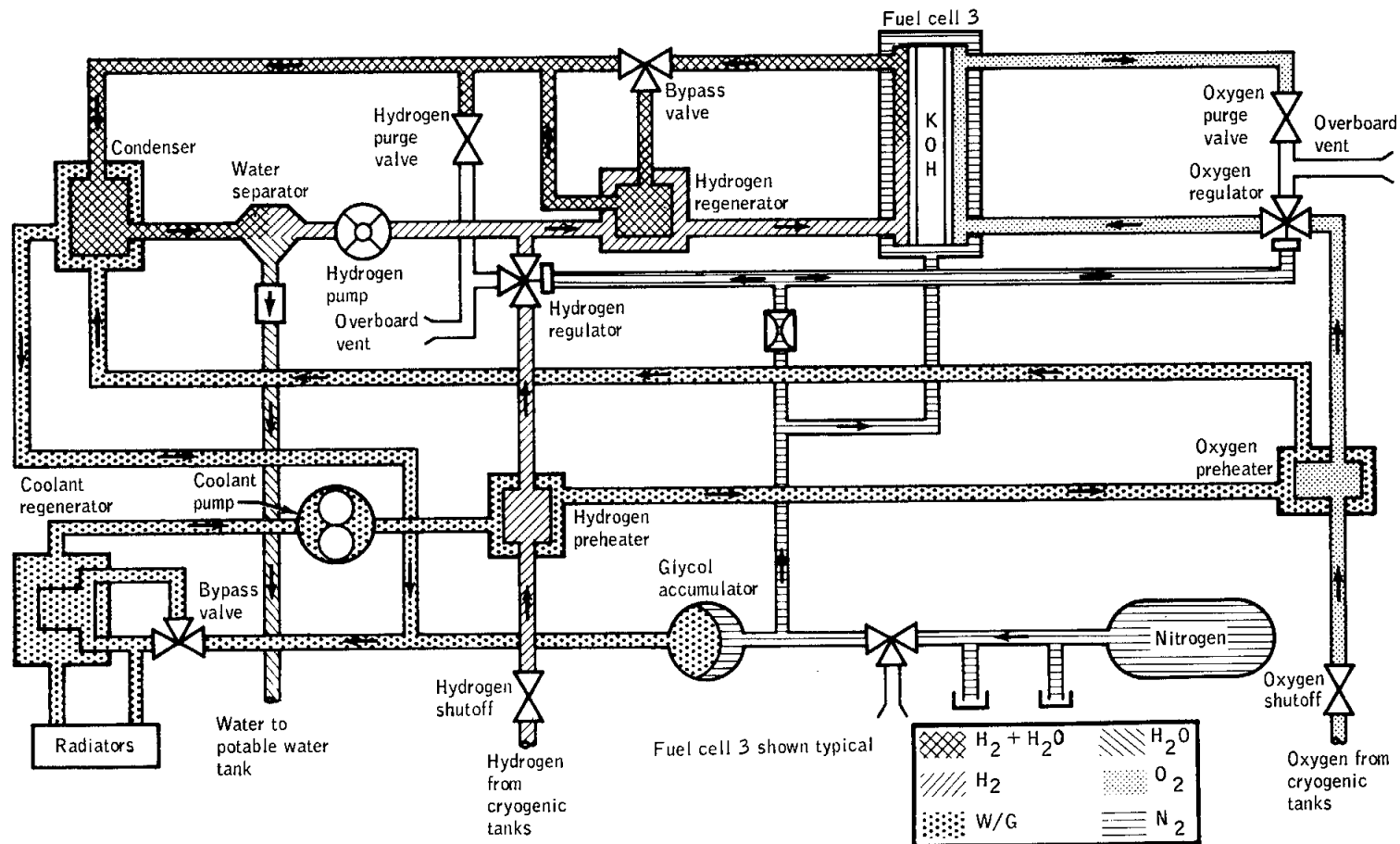


Figure A.1-13.- Fuel cell schematic.

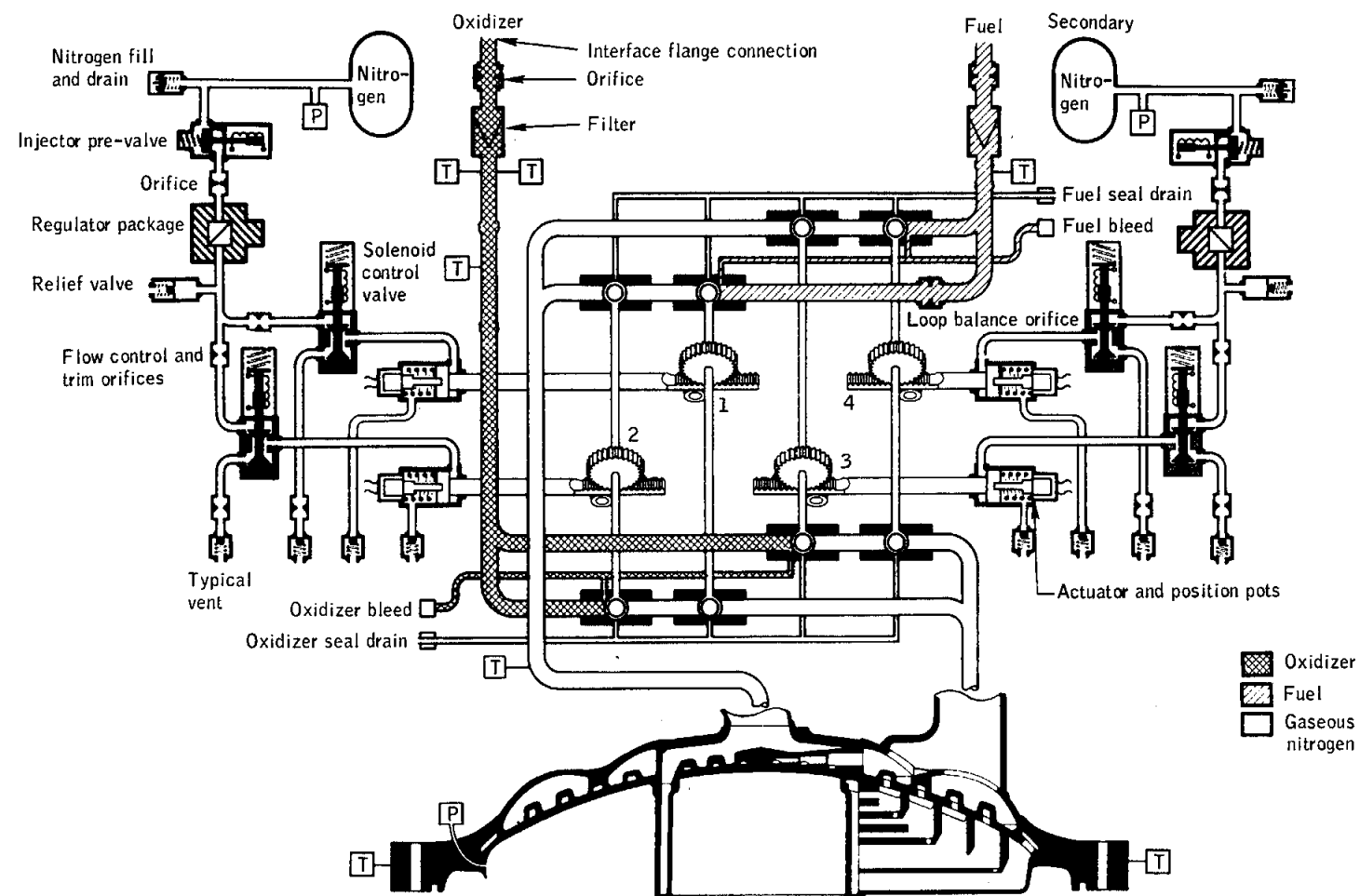


Figure A.1-14.- Control for service propulsion propellants.

NASA-S-68-6417

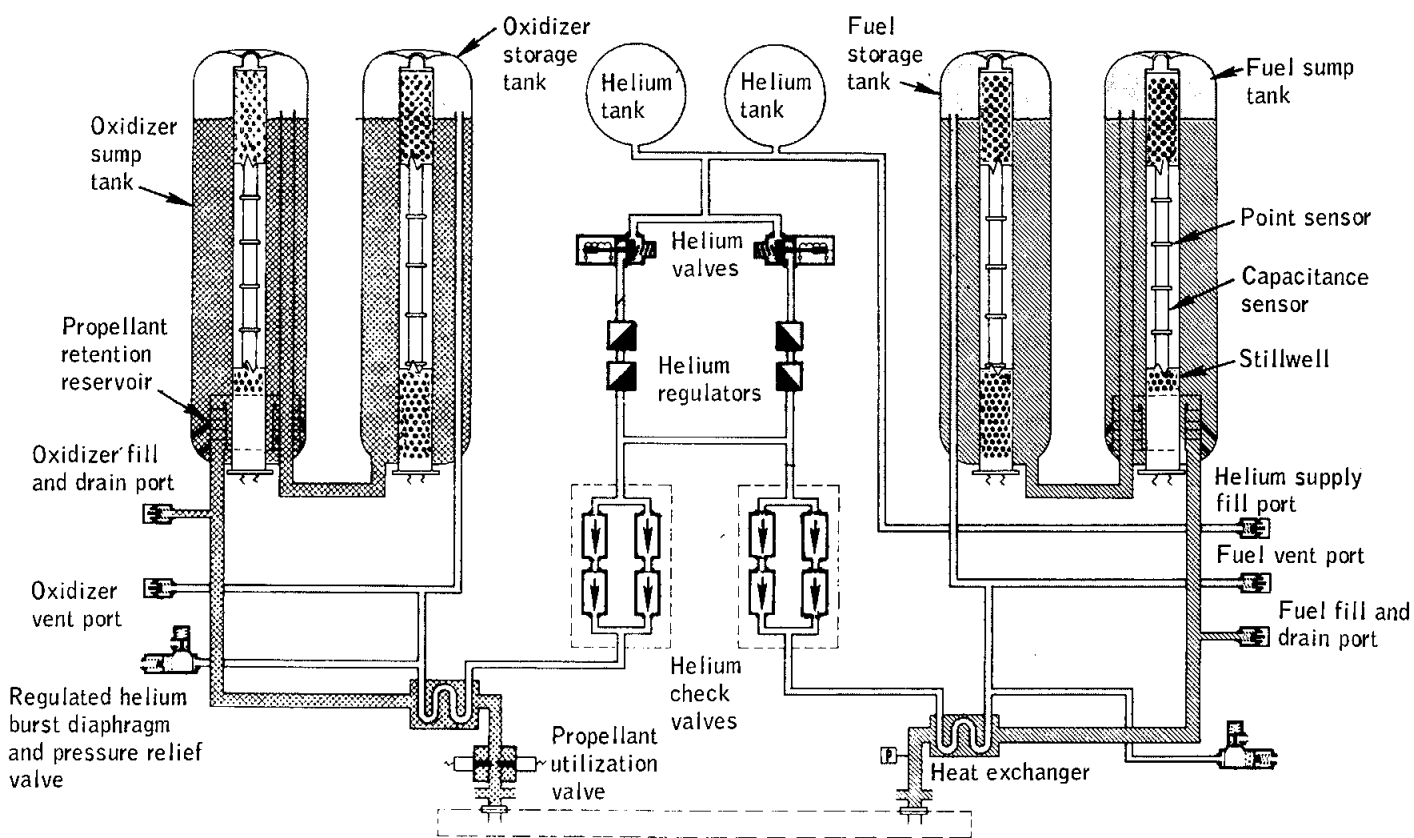


Figure A.1-15.- Flow of service propulsion propellants.

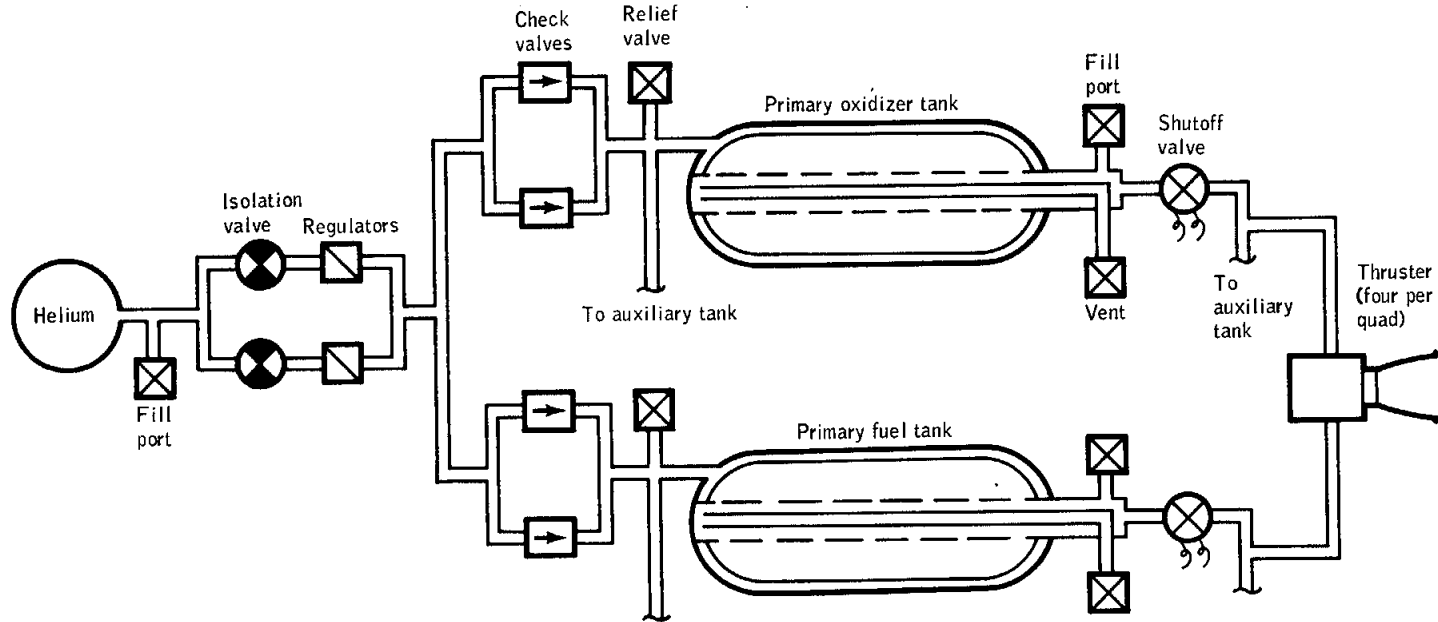


Figure A.1-16.- Service module reaction control system.

NASA-S-68-6419

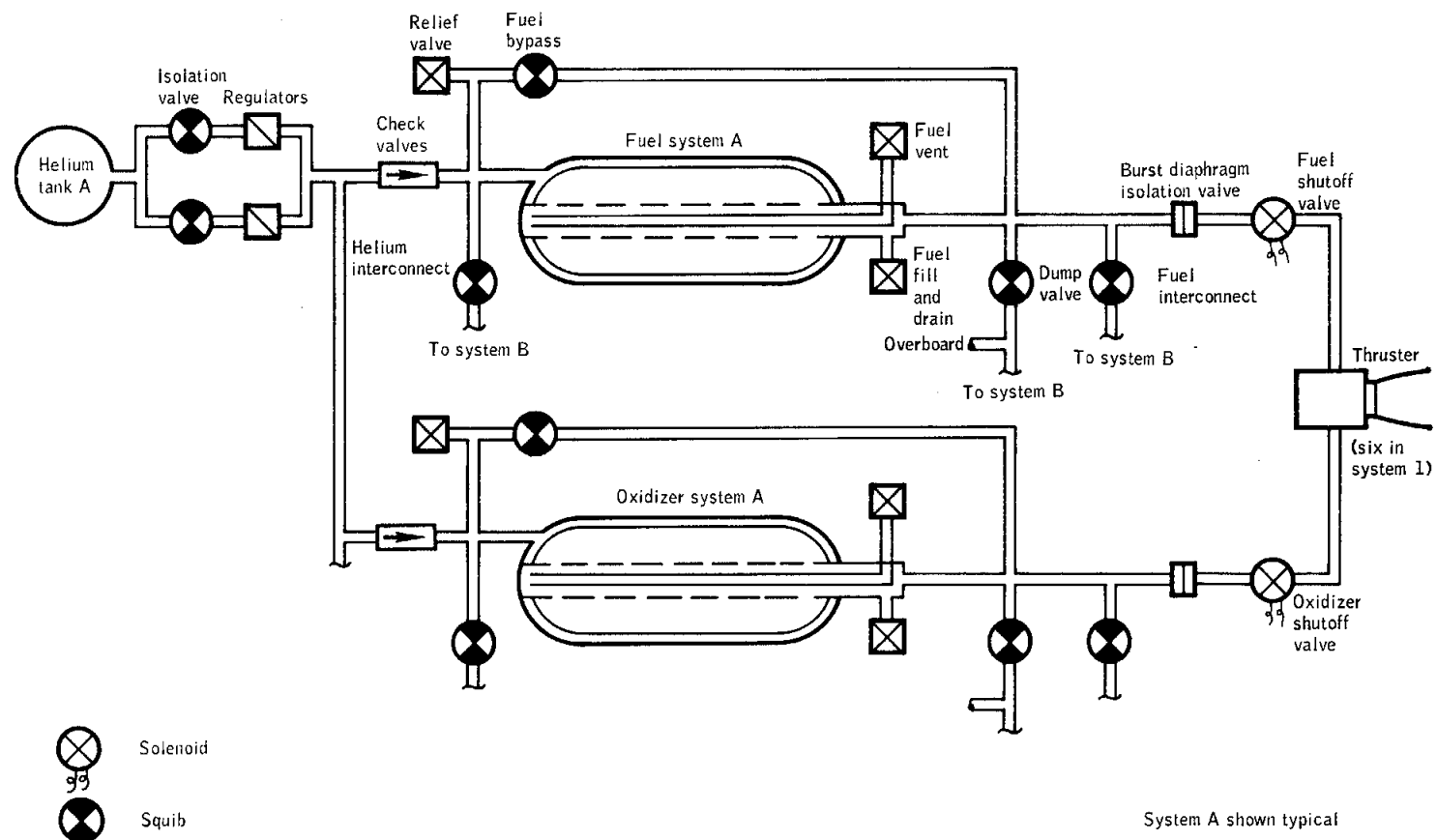
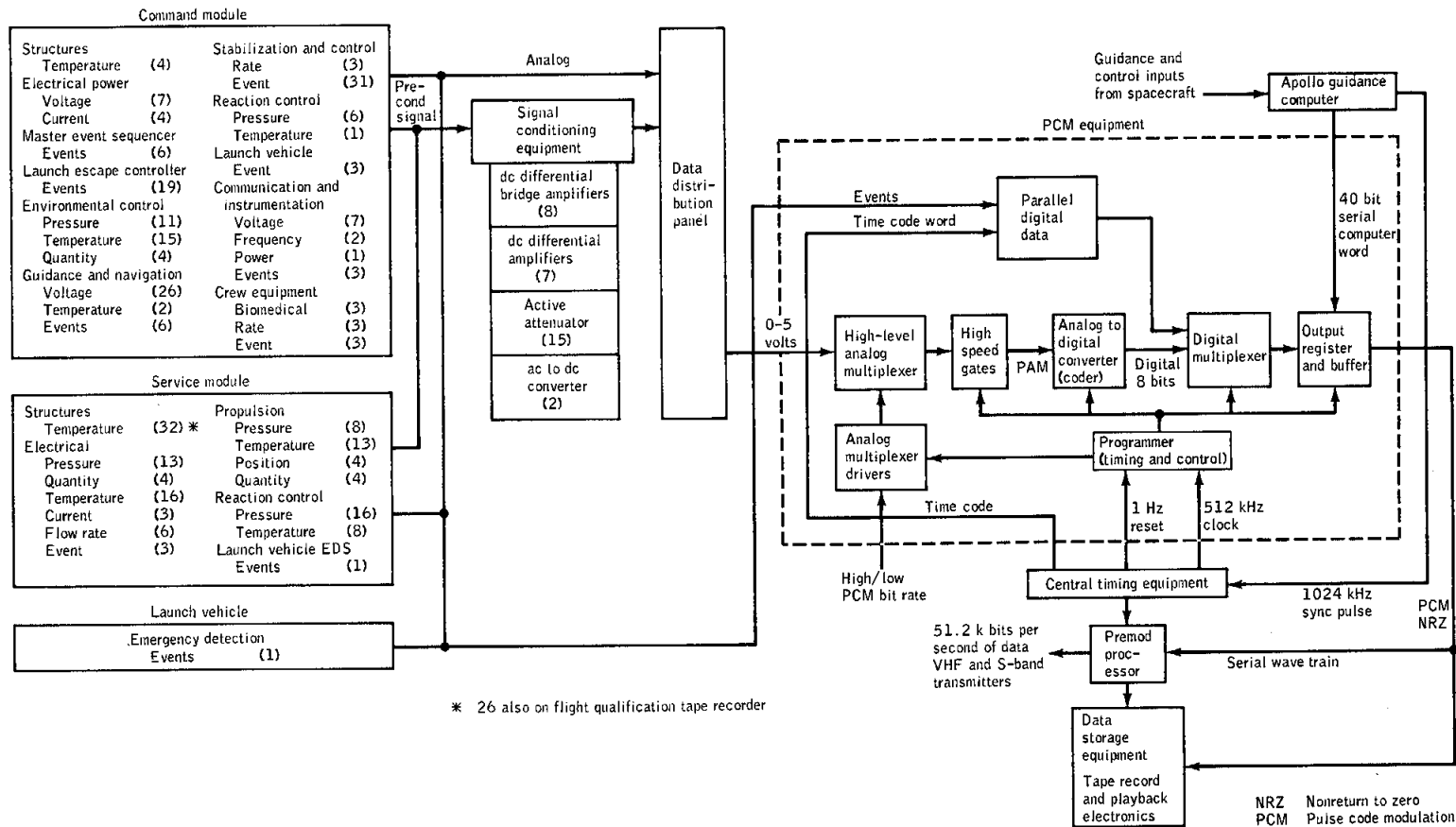


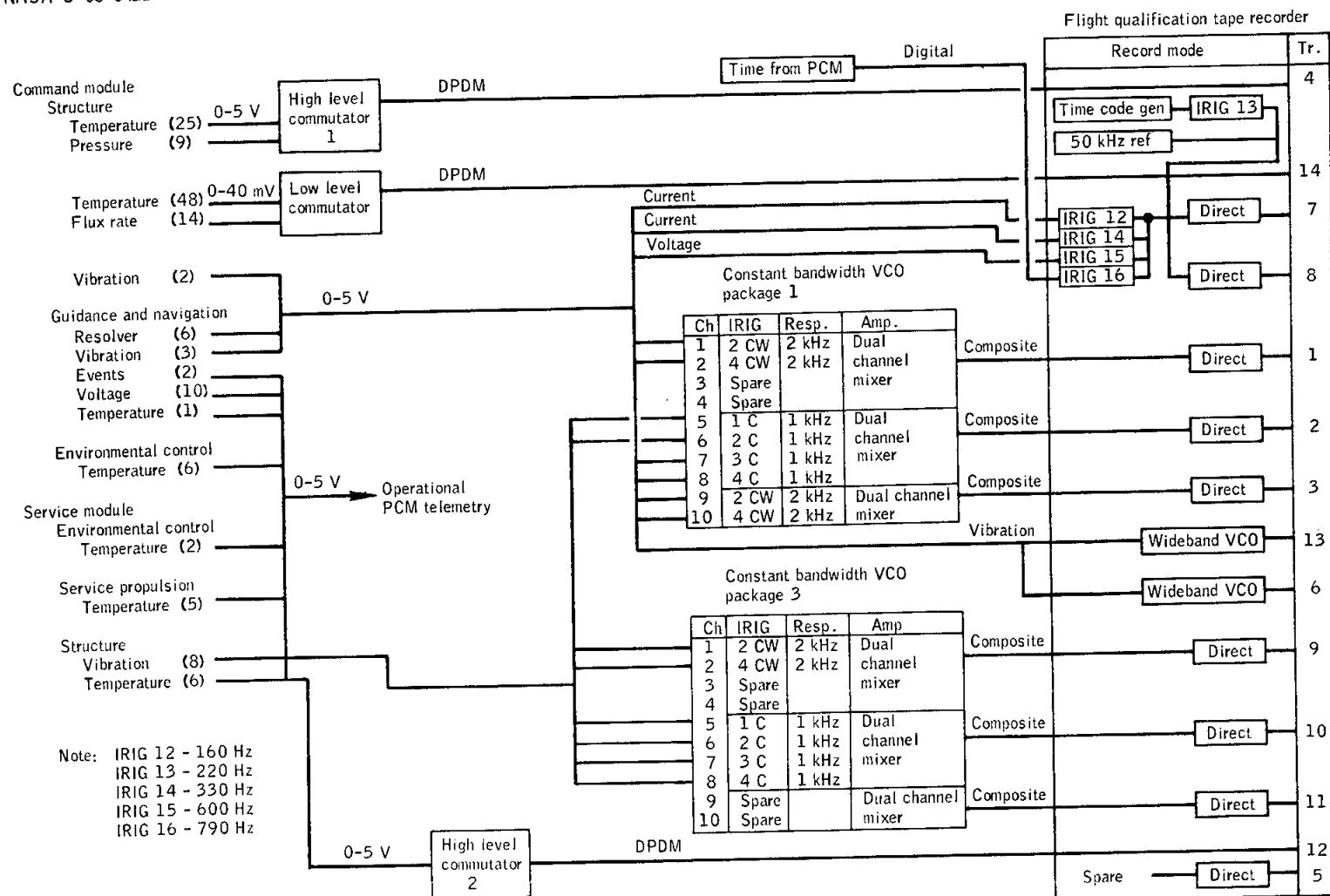
Figure A.1-17.- Command module reaction control system.



(a) Operational.

Figure A.1-18.- Instrumentation.

NASA-S-68-6421



(b) Flight qualification.
Figure A.1-18. - Concluded.

NASA-S-68-6422

A-40

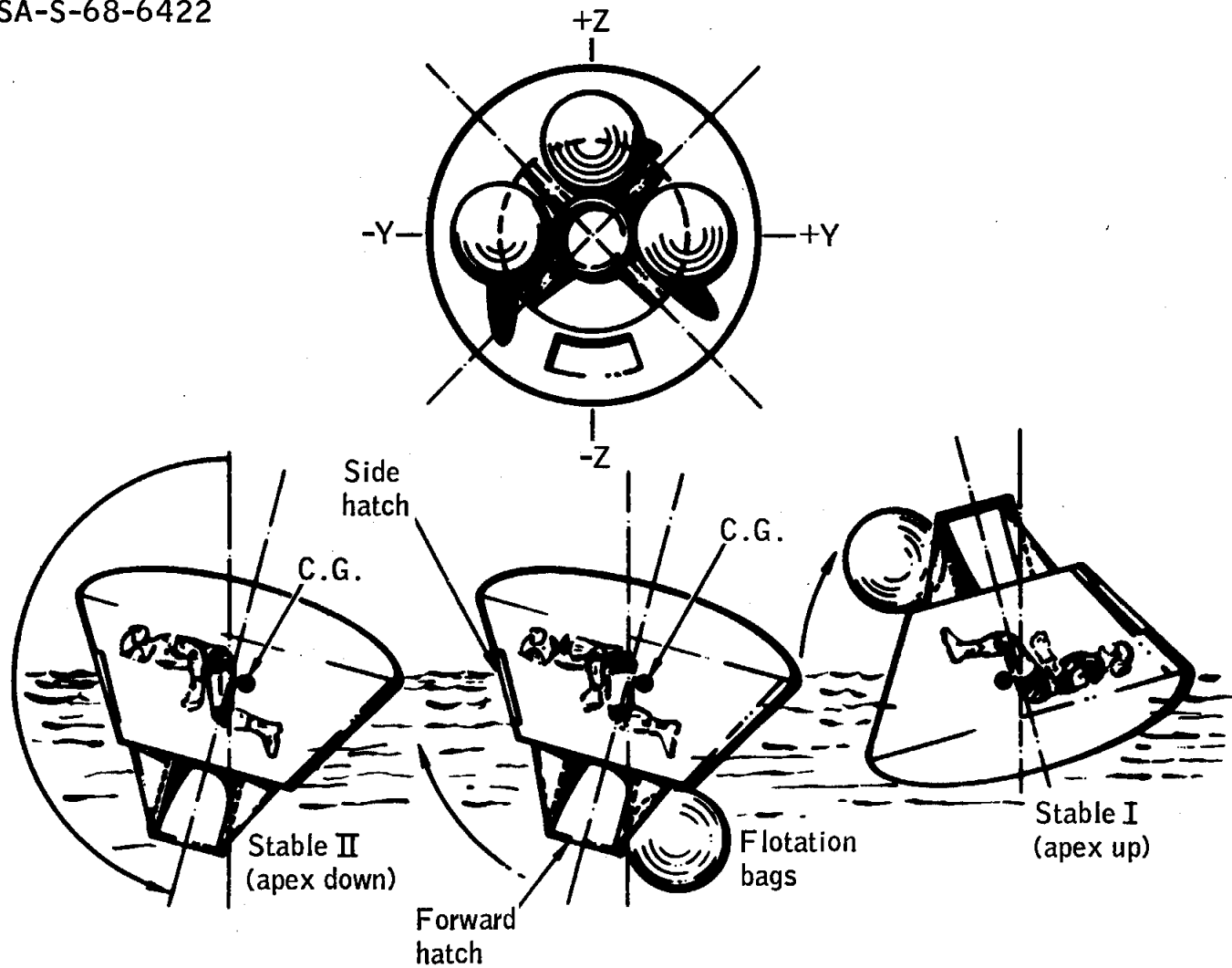


Figure A.1-19.- Uprighting system.

A.2 LAUNCH ESCAPE SYSTEM

The launch escape system (fig. A.2-1) is composed of a nose cone with an integral dynamic pressure measurement (q-ball), a canard system, three rocket motors (for launch escape propulsion, pitch control, and tower jettison), a structural skirt, and a titanium-tube tower structure (fig. A.2-1). The function of the escape system is to propel the command module away from the launch vehicle in the event of an atmospheric abort. The escape system is armed to provide this function from just prior to lift-off until the system is jettisoned after S-IVB ignition and guidance stabilization. In the event of an abort, the launch escape system would be jettisoned prior to parachute deployment.

NASA-S-68-6423

A-142

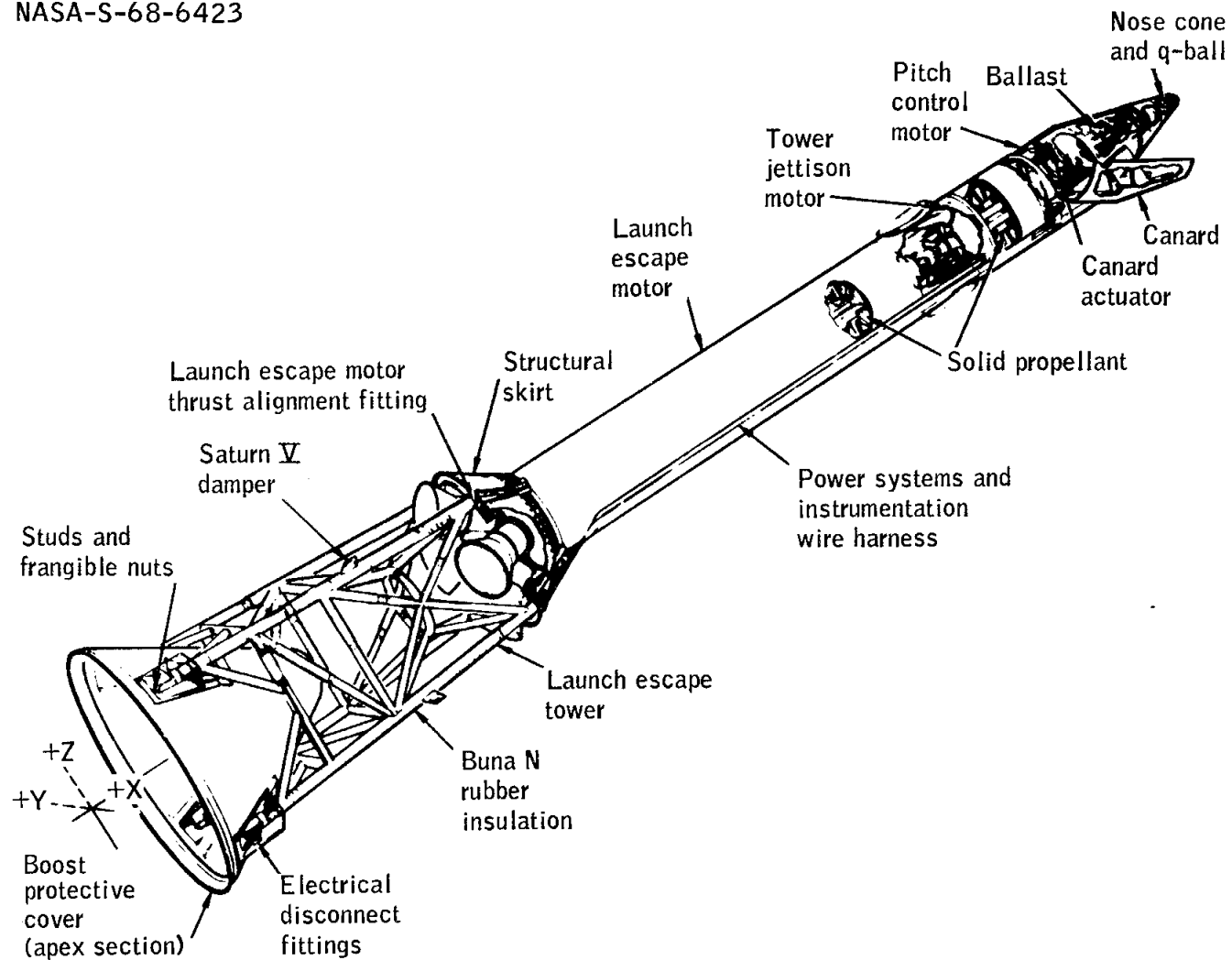


Figure A.2-1.- Launch escape system.

A.3 SPACECRAFT/LAUNCH-VEHICLE ADAPTER

The spacecraft/launch-vehicle adapter houses the lunar module and consists of a 28-foot long truncated conical structure of aluminum honeycomb shell and ring frames. The Apollo 7 adapter had a structural stiffener that was substituted for the lunar module. The adapter has a forward section consisting of four panels connected to an aft assembly. At separation of the adapter from the service module, the four panels are separated from one another by an explosive train. A gas-operated thruster cylinder at the hinged edge of each panel rotated the panels to the open position, which is approximately 45 degrees with respect to the longitudinal axis. The panels are normally retained in the open position by a spring/cable attenuation system.

A.4 LAUNCH VEHICLE

A.4.1 S-IB Stage

The S-IB stage is 80.3 feet long and 21.4 feet in diameter. A cluster of eight uprated H-1 engines power the S-IB stage and produce a total sea-level thrust of 1 600 000 pounds. Each of the four outboard engines gimbal in a plus or minus 8-degree square pattern to provide pitch, yaw, and roll control. The inboard engines are canted 3 degrees and the outboard engines 6 degrees outward from the vehicle longitudinal axis.

A kerosene-type fuel and liquid oxygen are supplied to the engines from nine propellant tanks arranged in a cluster. Oxidizer and fuel tank pressurization modules regulate the tank pressures during ground operation and S-IB stage flight. The nominal stage propellant loading capacity is 884 000 pounds.

Eight fins attached to the base of the S-IB stage provide vehicle support and hold-down points prior to launch and provided inflight aerodynamic stability. The area of each fin is 53.3 square feet. Each fin extends radially approximately 9 feet from the outer surface of the thrust structure.

Additional systems on the S-IB stage include flight control; hydraulic, which gimbal the outboard engines; electrical; environmental control, which thermally condition the aft compartment of instrument canisters F1 and F2; data acquisition; range safety; propellant utilization; and four solid-propellant retrograde motors. Guidance and control commands for the S-IB stage are initiated from the instrument unit.

A.4.2 S-IVB Stage

The S-IVB stage is 21.7 feet in diameter and 59.1 feet long, including an 8-inch protrusion of the liquid hydrogen container beyond the S-IVB stage and instrument unit mating surface. A single gimbal-mounted J-2 engine powers the vehicle during the S-IVB stage portion of powered flight. The engine is mounted on the thrust structure and can be gimbaled in a plus or minus 7-degree square pattern. The engine provides 200 000 pounds total thrust at vacuum conditions when the propellant mixture ratio is a nominal 5:1.

The propellant tanks (fuel forward and oxidizer aft) are separated by a common bulkhead. The liquid-hydrogen fuel tank consists of a cylindrical container with a bulkhead at each end. The liquid oxygen tank

consists of the section between the common bulkhead and an adjacent bulkhead and enclosed by the structural skin.

Oxidizer-and fuel-tank pressurization modules regulate the tank pressures during both ground operations and powered flight. The pneumatic control system uses ambient helium to operate the control valves. Nominal propellant loading capacity is 228 500 pounds.

The auxiliary propulsion system of the S-IVB stage provides roll control during S-IVB powered flight and attitude stabilization and control during orbital coast. The modules are mounted on opposite sides of the S-IVB aft skirt.

Additional systems on the S-IVB stage include flight control, which provide auxiliary attitude control and thrust vector control; hydraulic, which gimbal the J-2 engine; electrical; thermoconditioning, which thermally controls the electronic modules in the forward skirt area; data acquisition and telemetry, which acquires and transmits data for the evaluation of stage performance and environment; ordnance used for rocket ignition and stage separation; and three ullage motors. Guidance and control commands for S-IVB powered flight are also initiated from the instrument unit.

A.4.3 Instrument Unit

The instrument unit, located just forward of the S-IVB stage, is a three-segment, cylindrical, unpressurized structure 21.7 feet in diameter and 3 feet long. The cylinder forms a part of the vehicle load-bearing structure and interfaces with the S-IVB stage and the adapter. Various launch vehicle telemetry and tracking antennas are mounted on the instrument unit. The instrument unit houses electrical and mechanical equipment that guides, controls, and monitors the launch vehicle from lift-off until conclusion of orbital lifetime, normally 4.5 hours.

A.5 MASS PROPERTIES

Spacecraft mass properties for the Apollo 7 mission are summarized in table A.5-I. These data represent the conditions as determined from postflight analyses of expendable loadings and usage during the flight. Variations in spacecraft mass properties are determined for each significant mission phase from lift-off through landing. Expendables usage are based on reported real-time and postflight data as presented in other sections of this report. The weights and center of gravity of the individual command and service modules were measured prior to flight and the inertia values were calculated. All changes incorporated after the actual weighing were monitored, and the spacecraft mass properties were updated. Spacecraft mass properties at lift-off did not vary significantly from the preflight predicted values.

TABLE A.5-I.- SPACECRAFT MASS PROPERTIES

Event	Weight, lb	Center of gravity, in.			Moment of inertia, slug-ft ²			Product of inertia, slug-ft ²		
		X _A	Y _A	Z _A	I _{xx}	I _{yy}	I _{zz}	I _{xy}	I _{xz}	I _{yz}
1. Lift-off	45 295	992.1	1.0	4.4	28 874	393 235	396 846	-2035	84	-324
2. Insertion	36 419	917.3	1.2	5.4	28 036	141 839	145 517	-1397	2196	-333
3. Service propulsion maneuver 1	32 356	950.4	1.4	6.0	18 129	56 210	59 982	-1747	595	-32
4. Coast	31 711	951.6	1.2	6.1	17 774	55 638	59 073	-1628	550	-67
5. Service propulsion maneuver 2	31 595	951.7	1.2	6.2	17 781	55 655	59 084	-1633	560	-69
6. Coast	31 057	952.7	1.1	6.2	17 470	55 112	58 246	-1550	521	-103
7. Service propulsion maneuver 3	30 671	953.0	1.1	6.2	17 446	55 085	58 219	-1578	559	-90
8. Coast	30 050	954.4	0.9	6.3	17 096	54 373	57 175	-1475	511	-127
9. Service propulsion maneuver 4	29 780	954.5	1.0	6.3	17 057	54 309	57 123	-1495	531	-110
10. Coast	29 731	954.7	1.0	6.3	17 032	54 253	57 044	-1487	527	-113
11. Service propulsion maneuver 5	29 607	954.7	1.1	6.1	16 978	54 159	56 973	-1500	531	-90
12. Coast	25 077	969.7	-0.7	7.0	14 632	45 675	46 274	-505	77	-330
13. Service propulsion maneuver 6	24 975	969.9	-0.7	6.8	14 599	45 594	46 202	-532	111	-314
14. Coast	24 927	970.1	-0.7	6.9	14 574	45 459	46 044	-518	105	-316
15. Service propulsion maneuver 7	24 864	970.2	-0.6	6.8	14 556	45 412	46 000	-535	128	-308
16. Coast	24 295	972.9	-0.9	6.9	14 268	43 773	44 090	-368	54	-336
17. Service propulsion maneuver 8	24 262	973.0	-0.9	6.9	14 262	43 748	44 062	-383	77	-331
18. Command module/service module separation	23 453	977.2	-1.3	7.1	13 829	40 971	40 878	-110	-45	-373
19. Command module after separation	12 364	1040.8	-0.2	6.0	5 799	5 213	4 745	42	-423	30
20. Entry interface (400 000 feet)	12 356	1040.8	-0.2	6.0	5 795	5 208	4 744	41	-421	30
21. Mach 10	12 277	1041.0	-0.2	5.9	5 735	5 144	4 687	42	-417	30
22. Drogue deploy	11 936	1039.7	-0.1	5.9	5 649	4 901	4 467	42	-392	32
23. Main parachute deploy	11 855	1039.4	-0.1	6.1	5 633	4 841	4 424	42	-366	32
24. Landing	11 409	1037.4	-0.1	6.1	5 567	4 567	4 131	40	-371	33

APPENDIX B

SPACECRAFT HISTORY

A checkout history of the command and service modules at the contractor facility in Downey, California, is shown in figure B-1. Spacecraft history at Kennedy Space Center, Florida, is shown in figure B-2.

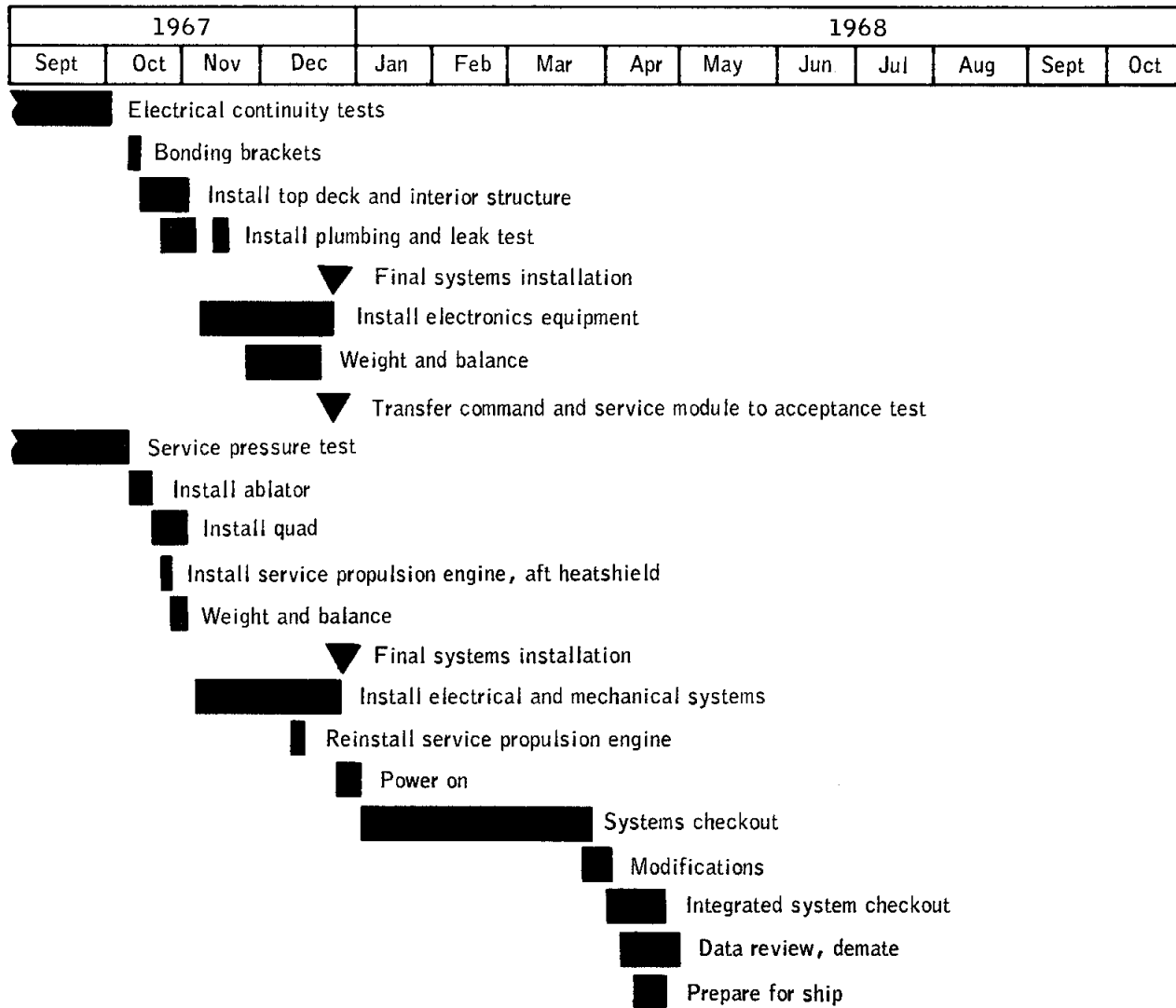


Figure B-1.- Command and service module checkout at contractor facility.

NASA-S-68-6425

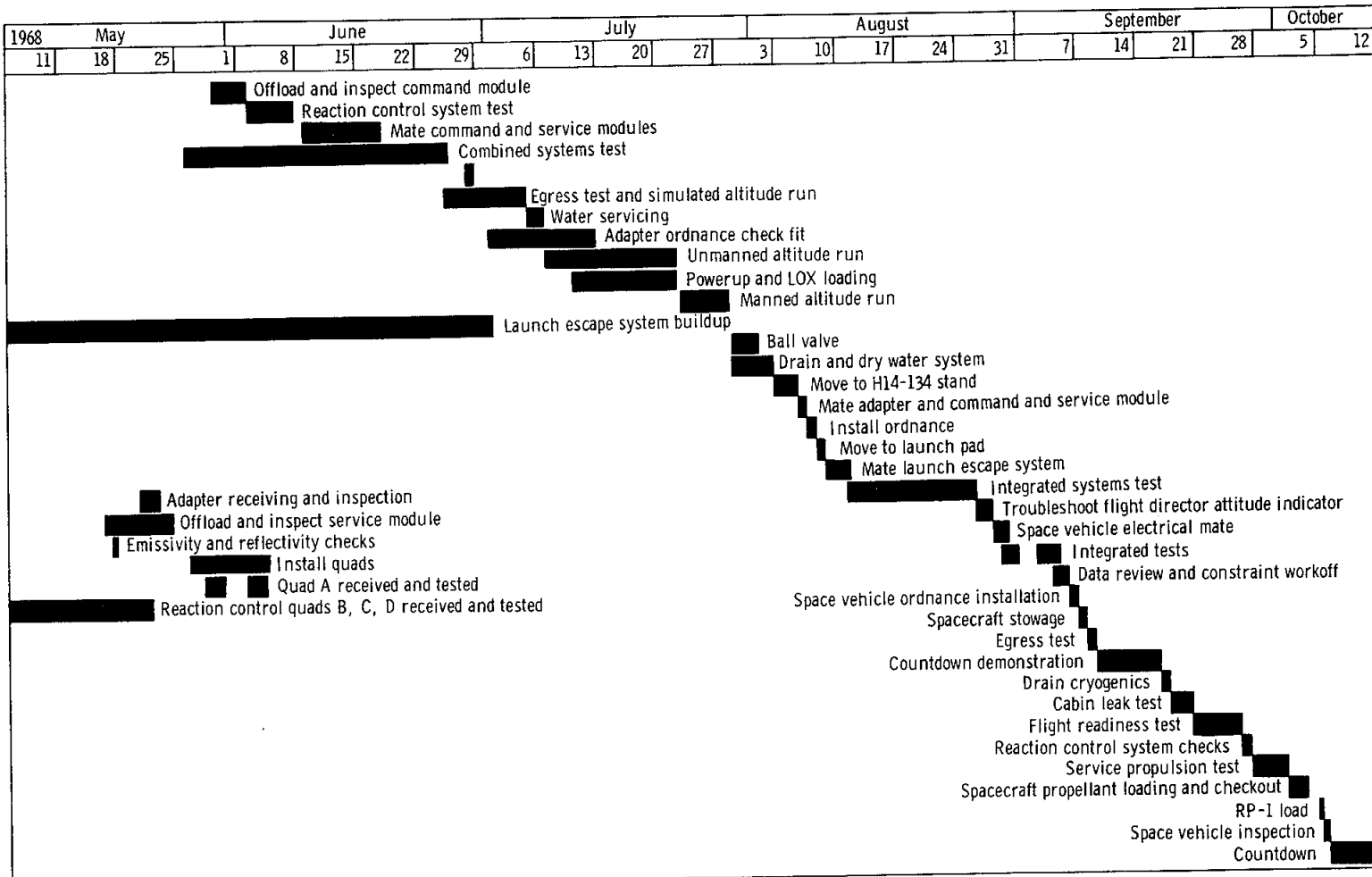


Figure B-2. - Spacecraft checkout history at Kennedy Space center.

APPENDIX CPOSTFLIGHT TESTING

The command module arrived at the contractor's facility in Downey, California, on October 27, 1968, after reaction control system deactivation and pyrotechnic safing at Norfolk, Virginia. Postflight testing and inspection of the command module for evaluation of the inflight performance and investigation of the flight irregularities are being conducted at the contractor's and vendors' facilities and at the Manned Spacecraft Center. The testing is being conducted in accordance with approved Apollo Spacecraft Hardware Utilization Requests (ASHUR's). The tests performed as a result of flight problems are described in table C-I and discussed in the appropriate systems performance sections of this report. Tests being conducted for other reasons are not included in the table. However, they are covered by ASHUR's or are basic contractual requirements.

TABLE C-I.- POSTFLIGHT TESTING SUMMARY

C-2

ASHUR no.	Purpose	Tests performed	Results
Environmental control			
101007	To investigate extent of corrosion in the potable water system	Water panel functional and leakage tests. Lines analyzed for corrosion. (Test complete)	Water panel satisfactory. Minor corrosion found in lines.
101019	To investigate extent of corrosion in potable water system and cause of strong chlorine taste	Potable tank inlet and outlet check valves and tank inlet nozzle removed for leak check and corrosion analysis. (Test complete)	Check valves leaked excessively due to accumulation of corrosion products (from lines). Nozzle was in satisfactory condition. Minor corrosion found in valves and nozzle
101021	To investigate high noise level of cabin fans reported by crew	Cabin fans operated in CM and removed for inspection and acceptance tests. (Test complete)	Fans sounded normal in CM and operated properly. Leading edges of fan blades had chipping damage. Three loose washers and a nut found in vicinity of fans.
101022	To investigate anomalous inflight operation of environmental control unit primary glycol evaporator, cause of "gurgling" sound, and condensation in a suit hose	Environmental control unit removed and subjected to acceptance testing and corrosion analysis. Teardown and analysis of suit heat exchanger underway	Water/glycol temperature sensor resistance found below specification. Primary evaporators performed as inflight in component malfunctions found. Flow through the separator plates of the suit heat exchanger was below normal.
101023	To investigate difficult operation of the potable cold water supply valve	Assembly subjected to acceptance testing, teardown, and inspection. (Test complete)	Valve performed within specification. Epoxy found in air vent.
101024	To obtain loose fibers and debris from the cabin for analysis	CM was vacuumed and collected material is being analyzed.	Analysis not complete.
101043	To perform a leakage test on the battery vent valve, which appeared to leak in flight	Valve leak checked. (Test complete)	Leakage was within specifications.
101044	To perform a leak test of the forward tunnel hatch check valve to determine if it allowed water to enter the tunnel	Valve leak rates determined for different CM attitude. (Test complete)	Leak rates: Stable II - 1.0 cc/min Stable I - 0.5 to 3.0 gal/min
101506	To analyze the brown contaminant found on the chlorine ampule needle assembly	Contaminant analyzed. (Test complete)	Carbonized Teflon, sodium hydroxides and phosphates found on needle assembly, as expected.
Electrical power			
101017	To determine the cause of the low battery inflight-charging rates	Batteries were charged in CM with flight charger. Charger was recalibrated. Batteries were removed and subjected to load tests. Circuit resistance measured. (Test complete)	Charger operated properly. Output voltage low but within specification. Batteries were satisfactory.

TABLE C-I.- POSTFLIGHT TESTING SUMMARY - Continued

ASHUR no.	Purpose	Tests performed	Results
Electrical power - continued			
101027	To perform power-up tests and determine the cause of the ac bus dropouts	Power-on tests performed with simulation of service module cryogenic fan with a leaky motor switch. (Test complete)	Cycling of the motor switch at altitude produced the ac bus dropout problem experienced in flight.
101510	To perform continuity checks on wiring associated with the flight director attitude indicator, hand controller, and PM subcarriers anomalies	Continuity checks performed. (Test complete)	No abnormal conditions found.
101514	To obtain output characteristics of the battery charger outside the spacecraft	Charger was removed and recalibrated. (Test complete) Guidance and control	Normal operations.
101011	To investigate the entry monitor system range integrator and delta V counter anomaly	Functional testing, vibration thermal cycling, E&I, power dropout, thermal shock and module analysis. (Test complete)	A bad crimp joint was found in the delta V ranging submodule which caused a voltage drop and the delta V problem. The ranging discrepancy was verified but disappeared during thermal testing.
101012	To perform a functional test of the entry monitor system scroll assembly	Functional test performed. (Test complete)	Normal operations.
101018	To investigate the rotational hand controller breakout switch malfunction (both controllers checked)	Functional tests, thermal tests, vacuum tests, switch activation tests, teardown and analysis. (Test complete)	All functions on components operated normally.
101026	To determine the cause of the abnormal shift of the flight director attitude indicator no. 1	Power up tests in CM. Electronic display assembly tests at vendor: functional, environmental, vibration, relay cycling. (Test complete)	Solder ball found in suspected relay.
Communications			
101029	To determine the cause of the loss of PM subcarriers during operation of the secondary transponder	Secondary S-band transponder functionally tested in CM. S-band equipment tests at vendor: functional, thermal, vibration. (Test complete)	No abnormal operation found.
101032	To determine if the S-band transponder switch contributed to the loss of PM data	Switch X-rayed, vibration, contact and insulation resistance. (Test complete)	No contaminations or abnormalities in switch.
101036	To investigate light weight headset failures (broken boom and eartube)	Functional test. Failure analysis. (Test complete)	Earpiece inadequately bonded to eartube. Broken boom caused by improper usage in flight.

TABLE C-I.- POSTFLIGHT TESTING SUMMARY - Continued

C-
4

ASHUR no.	Purpose	Tests performed	Results
Communications - continued			
101507	To perform a functional test of the VHF recovery beacon to investigate the report that no beacon signal was received by recovery forces	The beacon was functionally tested in the CM and bench tested for frequency. (Test complete)	No abnormal operation found.
Instrumentation			
101034	To determine the cause of the high-level commutator no. 1 failure during entry	Performance checked during CM power up. Commutator removed and vibration, temperature, and vacuum tested. Voltage spike tests to be performed.	No improper operation found at this time.
Reaction control			
101512	To determine the cause of the propellant isolation valve malfunctions experienced during postflight operations	Oxidizer valves are undergoing teardown and analysis. (Test complete)	Valve bellows were sprung.
Displays and controls			
101014	To X-ray toggle switches for internal solder balls and contaminants	Switches removed and X-rayed. Contaminated switches undergoing: contact and insulation resistance, operating force, vibration tests, X-ray, teardown and analysis.	No contamination.
101015	To investigate the cracked glass on the two mission timers	Glass examined and shock tests performed. (Test complete)	Cracks attributed to internal stress created during bake for bonding glass to facing.
101511	To perform failure analysis of the two inoperative floodlights (primary system)	Circuits checked in CM. Functional tests and teardown at vendor. Tests to determine cause for diode failures are underway	Primary circuits in floodlights inoperative as result of a shorted diode in each of the two failed lights.
Crew station			
101010	To investigate reported 70-mm camera malfunction	Functionally tested and inspected. Failure mode analysis being performed.	Inflight problem could not be duplicated. No abnormal conditions found.
101013	To perform analysis of heat shield window contamination	Heat shield windows removed for infrared emission and chemical analysis of surface contamination. (Test complete)	Products of outgassing from RTW found on inside of heat shield windows. No organic products found on outside of windows. Transmission through the windows had decreased up to 20 percent.

TABLE C-I.- POSTFLIGHT TESTING SUMMARY - Concluded

ASHUR no.	Purpose	Tests performed	Results
Crew station - continued			
101020	To reinstall bioinstrumentation in the spacecraft and perform a systems test to verify spacecraft circuits as a result of the in flight report of an overheating dc-dc converter	Systems test in CM using flight biomedical equipment. Spacecraft continuity checks. Bench test of biomedical circuit current limiter assembly. Bench test of control head connectors which were corroded. (Test complete)	Limiting resistor and spacecraft wiring were normal. O-ring was found missing from umbilical end of control head. Salt corrosion found in connectors of the control head
101031	To analyze the water metering dispenser for cause of difficult operation	Teardown and analysis. (Test complete)	Caused by a swollen O-ring.
101030	To perform bioinstrumentation component tests for cause of broken sensor wires and dc-dc converter overheating	Preinstallation test performed on signal conditioners and dc-dc converters. Bioinstrumentation functionally checked on a subject. (Test complete)	No malfunction found.
101033	To investigate food bag failures	Failure analysis. (Test complete)	Three bags had seam failures due to improper heat sealing. One bag was sealed completely closed and was cut open by crew.

APPENDIX D

DATA AVAILABILITY

The data reduction for the Apollo 7 mission evaluation was accomplished by processing the data needed for analysis of anomalies and systems performance. The telemetry station coverage used to process data and the data reduction effort are presented in table D-I.

TABLE D-I.- DATA AVAILABILITY

Time		Rev	Site						Site						Site							
Start	Stop		Band			Events			Band			Events			Band			Events				
			pass	pass	pass	comps	events	charts	spec	pass	pass	comps	events	charts	spec	pass	pass	comps	events	charts	spec	
00:00	00:10	1	MIL	X	X	X	X	X		27:57	28:08	18	CRO	X	X	X	X		65:10	65:19	41	RED
00:00	00:03	1	FQR	X	X	X	X	X		28:11	28:16	18	GWM	X	X	X	X		65:40	65:48	42	CYI
00:02	00:13	1	BDA	X	X	X	X	X		28:23	28:31	18	HAW	X	X	X	X		67:59	68:07	43	HSK
00:07	00:20	1	VAN	X	X	X	X	X		28:32	28:36	18	HTV	X	X	X	X		68:34	68:37	43	TEX
01:30	01:36	1	GDS	X	X	X	X	X		28:33	28:41	18	GDS	X	X	X	X		68:36	68:43	44	MIL
01:36	01:44	2	MIL	X	X	X	X	X		28:46	29:46	18	TEX	X	X	X	X		69:25	69:33	44	CRO
02:27	02:35	2	CRO	X	X	X	X	X		29:42	28:49	19	MIL	X	X	X	X		70:10	70:18	45	MIL
02:52	03:04	2	HAW	X	X	X	X	X		29:51	30:00	19	D/T	X	X	X	X		70:29	70:33	45	CYI
03:03	03:10	2	GDS	X	X	X	X	X		29:54	29:37	19	CRO	X	X	X	X		71:56	72:06	46	CYI
03:07	03:15	2	TEX	X	X	X	X	X		29:44	29:52	19	GWM	X	X	X	X		72:17	72:32	46	D/T
03:11	03:19	3	MIL	X	X	X	X	X		29:59	30:05	19	HAW	X	X	X	X		75:44	75:51	48	CRO
03:19	03:24	3	VAN	X	X	X	X	X		30:04	30:11	19	HTV	X	X	X	X		75:56	76:04	48	GWM
03:22	03:28	3	CRO	X	X	X	X	X		30:09	30:17	19	GWM	X	X	X	X		76:30	76:34	49	MIL
03:28	03:31	3	D/T	X	X	X	X	X		30:13	30:20	19	TEX	X	X	X	X		76:00	79:02	50	D/T
04:18	04:20	3	GWM	X	X	X	X	X		32:51	32:59	21	MER	X	X	X	X		80:53	81:02	51	HAW
04:27	04:35	3	HAW	X	X	X	X	X		33:00	21	D/T	X	X	X	X		82:12	82:29	52	MER	
04:37	04:45	3	GDS	X	X	X	X	X		33:08	33:16	21	HAW	X	X	X	X		85:24	85:31	54	GWM
04:42	04:50	3	TEX	X	X	X	X	X		34:43	34:50	22	HAW	X	X	X	X		88:58	89:07	56	RED
04:45	04:53	4	MIL	X	X	X	X	X		35:25	35:31	23	ACN	X	X	X	X		90:05	90:39	57	CRO
04:56	06:04	4	D/T	X	X	X	X	X		36:00	36:07	23	MER	X	X	X	X		90:12	90:19	57	HSK
05:03	05:13	4	ACN	X	X	X	X	X		36:33	36:42	23	RED	X	X	X	X		90:17	90:33	57	RED
05:38	05:44	4	CRO	X	X	X	X	X		36:59	37:08	24	ACN	X	X	X	X		90:50	90:58	58	ANG
05:49	05:56	4	GWM	X	X	X	X	X		37:41	37:48	24	GWM	X	X	X	X		91:02	91:09	58	CYI
06:02	06:13	4	HAW	X	X	X	X	X		39:40	39:53	25	RED	X	X	X	X		92:19	92:24	58	TEX
06:12	06:19	4	GDS	X	X	X	X	X		42:51	43:00	27	RED	X	X	X	X		92:22	92:28	59	MIL
06:21	06:25	5	MIL	X	X	X	X	X		43:55	44:07	28	CRO	X	X	X	X		92:25	92:32	59	BDA
07:21	07:26	5	MER	X	X	X	X	X		44:17	45:32	28	D/T	X	X	X	X		92:30	92:43	59	CYI
07:25	07:33	5	GWM	X	X	X	X	X		44:28	44:32	28	RED	X	X	X	X		93:10	93:19	59	CRO
07:37	07:45	5	HAW	X	X	X	X	X		44:43	44:49	29	MIL	X	X	X	X		93:19	93:29	59	HSK
09:13	09:21	6	HAW	X	X	X	X	X		44:46	44:53	29	BDA	X	X	X	X		93:37	93:40	59	D/T
09:19	09:26	6	HTV	X	X	X	X	X		44:56	45:04	29	CYI	X	X	X	X		94:09	94:19	60	GYM
10:46	10:58	7	HAW	X	X	X	X	X		45:31	45:40	29	CRO	X	X	X	X		94:37	94:40	60	TEX
10:56	12:00	7	D/T	X	X	X	X	X		45:40	45:48	29	HSK	X	X	X	X		94:43	94:53	60	CRO
12:38	12:46	8	RED	X	X	X	X	X		46:13	46:16	29	GWM	X	X	X	X		95:35	94:39	60	MIL
13:04	13:12	9	ACN	X	X	X	X	X		46:16	46:24	30	MIL	X	X	X	X		95:39	94:42	60	BDA
13:12	14:13	9	D/T	X	X	X	X	X		46:20	46:28	30	D/T	X	X	X	X		95:59	94:36	60	CYI
13:40	13:48	9	MER	X	X	X	X	X		48:13	49:01	31	D/T	X	X	X	X		96:09	96:19	60	D/T
13:47	13:53	9	GWM	X	X	X	X	X		48:41	48:50	31	CRO	X	X	X	X		96:47	96:50	61	CYI
14:12	14:21	9	RED	X	X	X	X	X		49:08	49:15	31	HAW	X	X	X	X		96:51	95:00	61	HSK
14:39	14:47	10	ACN	X	X	X	X	X		49:13	49:21	31	HTV	X	X	X	X		96:58	95:12	61	D/T
14:47	15:15	10	D/T	X	X	X	X	X		49:18	49:26	31	GDS	X	X	X	X		97:15	95:22	62	HTV
15:15	15:23	10	MER	X	X	X	X	X		49:19	49:27	31	GYM	X	X	X	X		97:22	95:30	62	GYM
15:21	15:29	10	GWM	X	X	X	X	X		49:26	49:33	32	MIL	X	X	X	X		97:25	95:32	62	TEX
15:48	15:56	10	RED	X	X	X	X	X		49:29	49:37	32	BDA	X	X	X	X		97:29	95:36	62	MIL
17:22	17:31	11	RED	X	X	X	X	X		50:16	50:25	32	CRO	X	X	X	X		97:35	95:42	62	BDA
18:15	19:36	13	D/T	X	X	X	X	X		50:42	50:50	32	HAW	X	X	X	X		97:44	95:50	62	CYI
18:58	20:03	13	D/T	X	X	X	X	X		50:48	50:55	32	HTV	X	X	X	X		97:03	96:37	62	D/T
19:27	19:35	13	CYI	X	X	X	X	X		50:52	51:00	33	GDS	X	X	X	X		96:19	96:27	62	CRO
20:03	20:11	13	CRO	X	X	X	X	X		50:57	51:04	32	TEX	X	X	X	X		96:45	95:52	62	HAW
21:31	21:46	14	CRO	X	X	X	X	X		51:00	51:08	33	MIL	X	X	X	X		96:50	96:58	62	HTV
21:46	21:58	14	HSK	X	X	X	X	X		51:06	51:13	33	ANG	X	X	X	X		96:55	97:02	61	GDS
22:20	22:26	14	TEX	X	X	X	X	X		51:21	51:28	33	ACN	X	X	X	X		96:55	97:03	61	GYM
22:23	22:30	15	MIL	X	X	X	X	X		51:21	51:59	33	CRO	X	X	X	X		97:00	97:06	61	TEX
22:26	22:33	15	EDDA	X	X	X	X	X		52:03	52:11	33	GWM	X	X	X	X		97:03	97:10	62	MIL
22:55	23:47	15	CYI	X	X	X	X	X		52:17	52:24	33	HAW	X	X	X	X		97:09	97:15	62	ANG
23:20	23:50	15	HSK	X	X	X	X	X		52:23	52:30	33	HTV	X	X	X	X		97:22	97:29	62	ACN
23:50	24:01	15	TEX	X	X	X	X	X		52:27	52:33	33	GDS	X	X	X	X		97:26	99:19	62	D/T
23:57	24:05	16	MIL	X	X	X	X	X		52:35	52:42	34	MIL	X	X	X	X		98:18	98:26	62	HAW
24:02	24:10	16	BDA	X	X	X	X	X		52:41	52:47	34	ANG	X	X	X	X		98:25	99:31	62	HTV
24:10	24:21	16	CYI	X	X	X	X	X		52:45	53:08	34	D/T	X	X	X	X		98:30	98:37	62	GWM
24:48	25:04	16	CRO	X	X	X	X	X		52:49	53:01	34	ACN	X	X	X	X		98:34	98:40	62	TEX
25:55	25:02	16	HSK	X	X	X	X	X		53:36	53:46	34	GWM	X	X	X	X		98:37	98:43	63	MIL
25:15	25:53	16	HAW	X	X	X	X	X		53:53	53:59	34	HAW	X	X	X	X		98:42	98:49	63	ANG
25:25	25:28	16	HTV	X	X	X	X	X		53:56	54:08	34	D/T	X	X	X	X		98:46	99:17	63	D/T
25:25	25:31	16	GDS	X	X	X	X	X		53:59	54:03	34	HTV	X	X	X	X		98:56	99:03	63	ACN
25:28	25:36	16	TEX	X	X	X	X	X		54:03	54:09	34	GWM	X	X	X	X		102:03	102:53	65	D/T
25:32	25:40	17	MIL	X	X	X	X	X		54:07												

TABLE D-1-- DATA AVAILABILITY - Concluded

Time				Rev	Site	Band	Events	Spec	Trip	Spec	Prog	Time				Rev	Site	Band	Events	Spec	Trip	Spec	Time				Rev	Site	Band	Events	Spec	Trip	Spec		
Start	Stop	Start	Stop									Start	Stop	Start	Stop								Start	Stop	Start	Stop									
118:34	118:40	75	HSK	X								167:50	167:59	106	HAW	X							237:22	237:30	150	MIL				X					
118:55	118:57	75	HAW	X								168:03	168:10	106	GYM	X	X	X					238:11	238:22	150	CRO				X	X	X			
118:57	119:05	75	HTV	X								168:10	168:16	107	MIL	X	X	X					238:25	238:33	150	GWM				X	X	X			
119:14	119:20	76	BDA	X								168:15	168:22	107	ANG	X	X	X					238:50	238:58	150	GYM				X	X	X			
120:02	120:08	76	CRO	X								169:12	169:22	107	GWM	X	X	X					238:58	239:04	151	MIL				X	X	X			
120:25	120:33	76	HAW	X	X	X	X	X				169:27	169:34	107	HAW	X	X	X					239:04	239:10	151	ANG	X	X	X	X	X				
120:36	120:43	76	ODS	X	X	X	X	X				169:33	169:40	107	HTV	X	X	X					239:17	239:24	151	ACN	X	X	X	X	X				
120:37	120:44	76	GYM	X	X	X	X	X				169:37	169:43	107	GDS	X	X	X					239:48	239:56	151	CRO				X	X	X			
120:40	120:47	76	TEX	X	X	X	X	X				169:42	169:48	107	TEX	X	X	X					240:00	240:10	151	GWM				X	X	X			
120:44	120:51	77	MIL	X	X	X	X	X				169:52	169:56	108	ANG	X	X	X					240:15	240:22	151	HAW				X	X	X			
120:51	120:55	77	ANG	X	X	X	X	X				170:57		108	D/T	X	X	X					240:30	240:35	151	TEX				X	X	X			
121:32	121:42	77	CRO	X	X	X	X	X				171:09	171:16	108	HTV	X	X	X					248:27	248:36	156	RED				X	X	X			
121:59	122:07	77	HAW	X	X	X	X	X				171:15	171:20	108	GYM	X	X	X					248:53	249:03	157	ACN	X	X	X	X	X				
122:14	122:21	77	TEX	X	X	X	X	X				171:27		110	D/T	X	X	X					254:50	254:58	160	RED	X	X	X	X	X				
122:37	122:43	78	ACH	X	X	X	X	X				178:45	178:51	113	MER	X	X	X					255:06	255:13	161	MIL				X	X	X			
123:09	123:14	78	CRO	X	X	X	X	X				186:11	186:16	118	CYI	X	X	X					255:20	255:28	161	CYI				X	X	X			
123:19	123:28	78	GWM	X	X	X	X	X				186:45	186:55	118	CRO	X	X	X					256:37	256:45	161	TEX				X	X	X			
123:44	123:49	78	GDS	X	X	X	X	X				188:21	188:31	119	CRO	X	X	X					259:33	259:41	163	HAW				X	X	X			
123:49	123:54	78	TEX	X	X	X	X	X				192:33	191:44	121	CRO	X	X	X					259:38	259:47	163	HTV				X	X	X			
124:51	124:58	79	MER	X	X	X	X	X				192:12	192:19	121	GYM	X	X	X					259:48	259:56	163	TEX				X	X	X			
128:32	128:39	82	RED	X	X	X	X	X				192:38	192:45	122	ACH	X	X	X					259:52	259:59	164	MIL				X	X	X			
130:31	130:39	83	ACH	X	X	X	X	X				192:42	193:21	122	D/T	X	X	X					259:56	260:02	164	BEA				X	X	X			
130:38	130:46	83	MER	X	X	X	X	X				193:10	193:17	122	CRO	X	X	X					259:39	260:02	Entry	FQR	X	X	X	X	X				
130:46	131:00	83	D/T	X	X	X	X	X				193:21	193:31	122	GWM	X	X	X					259:39	260:11	Entry	DSE	X	X	X	X	X				
131:39	131:47	83	RED	X	X	X	X	X				194:30	194:52	122	D/T	X	X	X																	
132:41	132:47	83	MER	X	X	X	X	X				194:57		122	HAW	X	X	X																	
132:47	132:53	83	GWM	X	X	X	X	X				193:47	193:52	122	GDS	X	X	X																	
133:13	133:21	84	RED	X	X	X	X	X				193:58	193:54	122	GYM	X	X	X																	
138:59	139:07	86	CRO	X	X	X	X	X				197:33	198:21	125	D/T	X	X	X																	
139:08	139:16	86	HAW	X	X	X	X	X				198:06	198:14	125	MER	X	X	X																	
139:15	139:40	86	D/T	X	X	X	X	X				198:25	198:34	125	HAW	X	X	X																	
139:41	139:47	86	TEX	X	X	X	X	X				201:49	201:59	127	RED	X	X	X																	
139:59	140:08	89	CYI	X	X	X	X	X				202:15	202:26	130	ACN	X	X	X																	
140:42	140:51	89	HSK	X	X	X	X	X				205:21	205:28	130	ANT	X	X	X																	
141:14	141:21	89	TEX	X	X	X	X	X				205:32	205:40	130	CYI	X	X	X																	
141:18	141:25	90	MIL	X	X	X	X	X				206:55	207:05	131	ANG	X	X	X																	
142:45	142:52	90	GYM	X	X	X	X	X				208:13	208:21	131	RED	X	X	X																	
142:48	142:55	90	TEX	X	X	X	X	X				210:00	210:09	134	TEX	X	X	X																	
143:02	144:07	91	D/T	X	X	X	X	X				210:04	210:12	133	MIL	X	X	X																	
143:41	143:50	91	CRO	X	X	X	X	X				210:19	210:26	133	CYI	X	X	X																	
144:07	144:15	91	HAW	X	X	X	X	X				211:56	212:01	134	CYI	X	X	X																	
144:19	144:26	91	GYM	X	X	X	X	X				211:59	212:13	134	D/T	X	X	X																	
144:26	144:33	92	MIL	X	X	X	X	X				212:29	212:40	134	CRO	X	X	X																	
144:45	144:52	92	ANG	X	X	X	X	X				212:38	212:45	134	HSK	X	X	X																	
144:50	145:30	92	D/T	X	X	X	X	X				212:56	213:05	134	HAW	X	X	X																	
145:15	145:24	92	CRO	X	X	X	X	X				213:11	213:19	134	TEX	X	X	X																	
145:28	145:35	92	GWM	X	X	X	X	X				213:36	213:41	135	ACN	X	X	X																	
145:57	145:58	92	GDS	X	X	X	X	X				214:39	214:05	135	D/T	X	X	X																	
146:10	146:43	93	D/T	X	X	X	X	X				214:30	214:41	135	HAW	X	X	X																	
146:19	146:25	93	ACK	X	X	X	X	X				214:44	214:52	135	GYM	X	X	X																	
147:01	147:09	93	GWM	X	X	X	X	X																											

REFERENCES

1. Marshall Space Flight Center: Apollo 7 Mission Report, Launch Vehicle. (This report has not yet been released; therefore, no report number can be cited.)
2. Smithsonian Institute: Special Report No. 170. 1964.
3. Office of Manned Space Flight: Apollo Flight Mission Assignments. M-D MA 500-11 (SE 010-000-1), December 4, 1968.
4. Manned Spacecraft Center: Mission Requirements, SA-503/CSM 103, C' Type Mission, (Lunar Orbit). SPD 8-R-027, November 16, 1968.

APOLLO SPACECRAFT FLIGHT HISTORY

(Continued from inside front cover)

<u>Mission</u>	<u>Spacecraft</u>	<u>Description</u>	<u>Launch date</u>	<u>Launch site</u>
Apollo 4	SC-017 LTA-10R	Supercircular entry at lunar return velocity	Nov. 9, 1967	Kennedy Space Center, Fla.
Apollo 5	LM-1	First lunar module flight	Jan. 22, 1968	Cape Kennedy, Fla.
Apollo 6	SC-020 LTA-2R	Verification of closed-loop emergency detection system	April 4, 1968	Kennedy Space Center, Fla.
Apollo 7	SC-101	First manned flight earth-orbital	Oct. 11, 1968	Cape Kennedy, Fla.